

UNIVERSITY OF OKLAHOMA

GRADUATE COLLEGE

DESIGN AND GENERATION OF PEPTIDOMIMETIC CLPP
ACTIVATOR AND N-PHENYL-1-NAPHTHYLAMINE
LIBRARIES AS TOOLS FOR UNDERSTANDING
PHYSICOCHEMICAL PROPERTIES THAT INFLUENCE
GRAM-NEGATIVE ACCUMULATION

A THESIS

SUBMITTED TO THE GRADUATE FACULTY

in partial fulfillment of the requirements for the

Degree of

MASTER OF SCIENCE

By

QUENTIN M. R. GIBAUT

Norman, Oklahoma

2020

DESIGN AND GENERATION OF PEPTIDOMIMETIC CLPP
ACTIVATOR AND N-PHENYL-1-NAPHTHYLAMINE
LIBRARIES AS TOOLS FOR UNDERSTANDING
PHYSICOCHEMICAL PROPERTIES THAT INFLUENCE
GRAM-NEGATIVE ACCUMULATION

A THESIS APPROVED FOR THE
DEPARTMENT OF CHEMISTRY AND BIOCHEMISTRY

BY THE COMMITTEE CONSISTING OF

Dr. Adam S. Duerfeldt, Chair

Dr. Helen I. Zgurskaya

Dr. Robert H. Cichewicz

Dr. Isabelle Ripoche

Dr. Isabelle Thomas

Acknowledgements

First, I would like to express my sincere appreciation to all those that made this great experience possible. I would like to offer my special thanks to Dr. Adam Duerfeldt, my Principal Investigator during my time at the University of Oklahoma. He is the best mentor a graduate student could ever wish for, and I am extremely happy to have been in his lab, especially for my first time in the US. I thank him for his support, the motivation he gave me and everything he taught me in medicinal chemistry. I am also very grateful for his help during this year, which has been quite intense and challenging. Not enough words could describe how thankful I am to him.

I also would like to thank the Department of Chemistry and Biochemistry for giving me the great opportunity of studying at OU as well as my committee members, Dr. Zgurskaya and Dr. Cichewicz for allowing me to start, what I hope will be, an interesting scientific career. The OU-Blaise Pascal program is a wonderful opportunity for any student willing to discover new ways of thinking or ways of doing things. I sincerely thank everyone involved in this program. You are the initiators of great things, past, present and I hope future. I wish to thank and express my sincere gratitude to Dr. Ripoché and Dr. Thomas, my French committee members, as well as every faculty member at Sigma-Clermont for their help, their kindness, their support and for transmitting me their passion for science.

I wish to acknowledge the Duerfeldt lab and especially Quentin Avila who helped me a lot when I arrived. Ines Forrest has been a great friend and the best roommate I could ever wish for. Your support has meant a great deal to me and I am extremely happy to

have shared this experience with you, which will continue next year. Finally, I would like to thank my friends and family in France who can make me forget sometimes that I am on another continent. You are the best and I love you.

Table of Contents

Acknowledgements	IV
List of Figures	IX
List of Schemes	XI
List of Tables.....	XII
Abstract.....	XIV
Chapter 1.....	1
<i>An Introduction to Gram-negative Accumulation, Acyldepsipeptide Antibiotics and the Fluorescent Probe N-Phenyl-1-Naphthylamine</i>	1
1. Antibiotic Permeation in Gram-negative Bacteria.....	3
1.1. Gram-negative bacteria VS Gram-positive bacteria	3
1.2. Current state of Permeation.....	5
2. ClpP and Acyldepsipeptides, An Emerging Target and Chemotype for Antibacterial Discovery.....	12
2.1. ClpP, a promising new antibacterial target	12
2.2. ADEP, a ClpP activating chemotype.....	14
3. N-Phenyl-1-Naphthylamine, a Hydrophobic Fluorescent Probe	17
3.1. Fluorescent probes	17
3.2. N-Phenyl-1-Naphthylamine	19
Chapter 2.....	23

<i>Design and Synthesis of Small Molecule ClpP Activators</i>	23
1. Introduction	23
2. Synthesis of Small Molecule N-Acyl-difluorophenylalanine Derivatives	27
2.1. Synthesis of amides 1	30
2.2. Synthesis of ureas	33
2.3. Synthesis of sulfonamides	35
2.4. Synthesis of amides 2	37
3. Compound Activity Against Select Gram-negative Strains	41
4. Conclusions and Future Directions	46
<i>Chapter 3</i>	49
<i>Design, Synthesis and Preliminary Assessment of N-Phenyl-1-Naphthylamine</i>	
<i>Derivatives</i>	49
1. Introduction	49
2. Synthesis of the Library	51
2.1. Synthesis of amides	52
2.2. Synthesis of ureas	54
2.3. Synthesis of sulfonamides	55
2.4. Synthesis of alkyl amines	60
2.5. Synthesis of aryl amines	67
3. Fluorescence and Growth Inhibitory Profiles of Library Members	69
3.1. Excitation and emission optima.....	69

3.2.	Emission coefficient determination.....	73
3.3.	MICs.....	80
4.	Conclusions and Future Directions.....	81
	<i>Experimental Section and Spectral Characterization</i>	<i>84</i>
1.	Biochemical Procedures	84
2.	Compound Synthesis and Characterization.....	87
	<i>References.....</i>	<i>176</i>
	<i>Spectral Data for All Identified Compounds and Starting Materials.....</i>	<i>187</i>

List of Figures

Figure 1. Gram-positive and Gram-negative membrane architectures.⁷	4
Figure 2. (A) Gram-positive selective antibiotics converted into broad spectrum agents following the “eNTRy Rules”; (B) An example of an exception to the “eNTRy Rules”⁷	10
Figure 3. Structures of the main E. coli proteases in distal and apical views. (A) ClpP (PDB: 1YG6), (B) Lon (PDB: 1RR9), (C) FtsH (PDB: 4V0B) and (D) HslUV (PDB: 5JI3). Software used: PyMOL.	13
Figure 4. A cartoon of the ClpP protease associated to ClpA/ClpX complex	14
Figure 5. Structures of representative ADEP derivatives (1, 2, and 3) and small molecules based on the ADEP pharmacophore (4 and 5).	15
Figure 6. Typical excitation and emission spectrum showing the Stokes shift, the difference between the excitation and the emission optima	18
Figure 7. Chemical structure of NPN	20
Figure 8. Chemical structure of ADEP 4 and its pharmacophore (red)	24
Figure 9. Representative ACP molecules	24
Figure 10. Selected scaffolds for the linear small molecule ADEP analogues library	26
Figure 11. ¹³C-NMR, spectral characterization of SM1 in CDCl₃, 300 MHz	29
Figure 12. Comparison of ¹H-NMR spectra in CD₃OD between two urea analogues made with different equivalents of isocyanates. (A) 1.5 equivalents; (B) 1.0 equivalent	34
Figure 13. Summary of the NPN project	50

Figure 14. Structures of compounds 79 and 80.....	62
Figure 15. Structures of compounds 83, 85, 86, 88, 90 and 92.....	64
Figure 16. Structures of compounds 84 and 94.....	64
Figure 17. Excitation and emission spectra for compounds 52, 77, 92 and 101 (NPN) at a gain of 100 using the TECAN Infinite M200	70
Figure 18. Structures of compounds 50, 53, 54, 58 and 69.....	71
Figure 19. Emission coefficient graphs for analogues 48, 68, 92 and 101 (NPN) at a gain of 65.....	74
Figure 20. Structures of compounds 59, 88, 61 and 90.....	76
Figure 21. Structure of compound 47	78
Figure 22. Optimization of the emission coefficient of compound 47 at a gain of 65	79
Figure 23. Structures of compounds 47, 69 and 92.....	81

List of Schemes

Scheme 1. Synthetic route for the synthesis of the starting material 2 (SM2)	28
Scheme 2. Reaction conditions for the synthesis of amide 1 analogues. 1) reaction between an amine and a carboxylic acid; 2) reaction between an amine and an acyl chloride	30
Scheme 3. Synthetic procedure for the generation of urea analogues	33
Scheme 4. Hydrolysis of isocyanates⁵⁵	35
Scheme 5. Synthetic procedure for the generation of sulfonamide analogues	36
Scheme 6. Synthetic route for the synthesis of the starting material 7 (SM7)	39
Scheme 7. Synthetic procedure for the generation of amide 2 analogues	40
Scheme 8. Synthetic procedure for the generation of amide analogues	52
Scheme 9. Synthetic procedure for the generation of urea analogues	54
Scheme 10. Aluminum complex (DABAL-Me₃) formation.....	57
Scheme 11. Suggested mechanism of the sulfonamide formation using DABAL-Me₃	58
Scheme 12. Synthetic procedure for the generation of sulfonamide analogues	59
Scheme 13. Synthetic procedures for the generation of alkyl amine analogues. 1) N-Alkylation; 2) Reductive amination; 3) Ullmann coupling reaction; 4) Amide reduction	65
Scheme 14. Mechanism of the Buchwald-Hartwig⁷⁷⁻⁷⁸ and Ullmann reactions⁷⁹	67
Scheme 15. Synthetic procedure for the generation of aryl amine analogues	68

List of Tables

Table 1. Accumulation study showing relative fluorescence units using the hydrophobic fluorescent probe NPN in <i>A. baumannii</i>, <i>B. cepacia</i> and <i>B. thailandensis</i> after 600 seconds. A greater fluorescence means a better intracellular uptake.....	6
Table 2. Amide 1 analogue structures. (An.: analogue number, (X): reaction type, (D): Boc deprotection)	32
Table 3. Urea analogues. (An.: analogue number)	33
Table 4. Sulfonamide analogues. (An.: analogue number)	36
Table 5. Amide 2 analogues. (An.: analogue number, (D): Boc deprotection)	40
Table 6. MICs (μM) of select derivatives in <i>E. coli</i>	43
Table 7. MICs (μM) of select derivatives in <i>A. baumannii</i>	44
Table 8. MICs (μM) of select derivatives in <i>P. aeruginosa</i>	46
Table 9 Amide analogues of the NPN library. (An.: analogue number, (D): deprotection,)	53
Table 10. Urea analogues of the NPN library. (An.: analogue number, (D): deprotection)	54
Table 11. Optimization of reaction conditions for the synthesis of sulfonamides ...	56
Table 12. Sulfonamide analogues of the NPN library. (An.: analogue number, (D): deprotection)	60
Table 13. Optimization of reaction conditions for the synthesis of alkyl amines. (reaction 1: N-alkylation, reaction 2: reductive amination, reaction 3: coupling reaction, reaction 4: amide reduction).....	62

Table 14. Alkyl amine analogues of the NPN library. (An.: analogue number, (X): reaction type).....	66
Table 15. Aryl amine analogues of the NPN library. (An.: analogue number).....	68
Table 16. Excitation and emission optima of the NPN derivatives (50 µmol/L) in lipids (50 µg/ml) at a gain of 100 using the TECAN Infinite M200. (FI: fluorescence intensity of the emission optimum)	72
Table 17. Emission coefficients of the NPN derivatives (50 µmol/L) in lipids (6.25-100 µg/mL) using the TECAN Spark 10M. Green = satisfies emission coefficient, Yellow = does not satisfy emission coefficient.	75
Table 18. Physicochemical property comparison between NPN derivatives that gave correct emission coefficients (S-NPN) and the ones that did not (F-NPN)	77
Table 19. MICs (µM) of active NPN derivatives in <i>E. coli</i>	80
Table 20. MICs (µM) of active NPN derivatives in <i>A. baumannii</i>	80
Table 21. MICs (µM) of active NPN derivatives in <i>P. aeruginosa</i>	81
Table 22. Parameters used for the excitation and emission determination.....	85
Table 23. Parameters used for the emission coefficient determination	86

Abstract

Gram-negative bacteria pose a major threat to human health as they demonstrate low sensitivity to most antibiotics. This lack of sensitivity to antimicrobials is largely due to the amphipathic membrane architecture and efficient efflux pumps. Additionally, antibiotics have been overused, which increases the prevalence of multidrug-resistant pathogens and thus, less efficient antibiotics. For these reasons, the need for broad-spectrum antibiotics has never been more important. In the early 1980s, a new class of antibiotics based on the natural product acyldepsipeptide (ADEP) was discovered. ADEPs target the well-conserved bacterial protease caseinolytic protease P (ClpP). Overactivation of this protease leads to uncontrolled protein degradation and, in many cases, cell death. However, the membrane-permeability and susceptibility to efflux preclude the use of ADEPs to target Gram-negative bacteria. Unfortunately, a lack of understanding exists for how to rationally “design in” Gram-negative activity and thus it remains very difficult to improve the spectrum of known chemotypes.

Related to the aforementioned challenges, we have a research program focused on elucidating which physicochemical properties of small molecules influence Gram-negative membrane-permeation and, in turn, intracellular small molecule accumulation. As part of this initiative, we synthesized two libraries, 1) a peptidomimetic library of putative ClpP activators based on the ADEP pharmacophore and 2) a library based on the fluorescent probe *N*-phenyl-1-naphthylamine (NPN). In total, 46 new peptidomimetic analogues and 57 NPN derivatives were synthesized. During the construction of these libraries two new applications for the reagent DABAL-Me₃ were developed. In addition, all compounds were assessed for minimum inhibitory concentrations against wild-type

and compromised Gram-negative bacterial strains. The 103 compounds synthesized in this work represent an important component of a larger collaborative effort to determine molecular features and species-specific biology that dictate small molecule accumulation. Completion of these libraries sets the stage for incorporation into larger scale cheminformatics, accumulation assessments, and kinetic modelling of permeation and accumulation parameters.

Chapter 1

An Introduction to Gram-negative Accumulation, Acyldepsipeptide Antibiotics and the Fluorescent Probe N-Phenyl-1-Naphthylamine

“I have no idea what's awaiting me, or what will happen when this all ends. For the moment I know this: there are sick people and they need curing.”

« Je ne sais pas ce qui m'attend ni ce qui viendra après tout ceci. Pour le moment il y a des malades et il faut les guérir. »

The Plague (“La Peste”), 1947, Albert Camus – Nobel Laureate 1957 in Literature

In his novel *The Plague*, Albert Camus, the famous French writer, describes the consequences of a plague appearing in Oran, Algeria in the 1940s. A deep analysis and a perspective through the eyes of his characters allow Camus to show us what could become of society when a tragedy like a plague strikes. This book should be read by everyone interested not only in medicinal chemistry but also in the social consequences of disease.

Today, we are facing a serious and urgent global health crisis. Until 2020, many of us have wondered what would happen if an extremely contagious viral or bacterial infection propagated throughout society and no treatment existed. Unfortunately, we are living this first-hand, as COVID-19 is currently sweeping the globe. No longer do we need to

speculate about the consequences if new anti-infectives are not developed – the current situation illustrates the urgency and importance very clearly.

Throughout history, this scenario has played out multiple times as new threatening diseases have emerged. One can think of the Justinian's Plague (542-546 AD), the first recorded plague which claimed approximately 100 million lives. Another plague, in the Middle Ages commonly known as the "Black Death" (1347-1351 AD), was caused by *Yersinia Pestis* and killed 50 – 200 million people.¹ Smallpox, since its initial appearance ~3000 years ago, has produced more than 300 million deaths; more than every war in history combined.²⁻³ Cholera, another famous disease dating from 5th century BC, spread across Europe from 1817-1923 killing millions. This disease, caused by *Vibrio cholerae*, still impacts humans today, but to a lesser extent and only significantly affects specific regions, such as Haiti, Madagascar and Bangladesh.⁴⁻⁵ More recently, humanity has faced newer more modern viruses during the 20th and 21st centuries, such as the Spanish influenza (1918-1920), the more recent H1N1 influenza, which is derived from the 1918 virus⁶ and the ongoing Coronavirus (COVID-19). Humans have always and will always face newly evolved infectious diseases, whether they have viral or bacterial origins.

Although COVID-19 is a virus and thus cannot be treated by antibiotics, the same parallels can be drawn for infectious resistant bacteria. Antibiotics represent the only weapon at our disposal against bacteria and because of the appearance of multi-drug resistant pathogens, this weapon loses efficiency every day. As history demonstrates, a new bacterial pandemic or the resurgence of an old plague could very well happen, and humanity should be prepared when that time comes. As such, the search for new anti-infectives will always be an important and urgent endeavor.

1. Antibiotic Permeation in Gram-negative Bacteria

1.1. Gram-negative bacteria VS Gram-positive bacteria

The need for new antibacterials has never been so important, given the significant and rapid rise of multi-drug resistance in pathogenic bacteria. In particular, Gram-negative bacteria represent a serious challenge, as they inherently demonstrate low sensitivity to most antibiotic classes. This lack of sensitivity is largely due to the complex membrane architecture of these bacteria, which poses an amphipathic environmental barrier to molecules and contains protective efflux pumps. Many antibiotic classes can neither permeate nor accumulate inside Gram-negative bacteria species, limiting their use to Gram-positive pathogens.⁷⁻⁸ In hospitals, the most common infections which escape the lethal action of antibiotics are known as the “ESKAPE bugs” comprised of *Enterococcus faecium*, *Staphylococcus aureus*, *Klebsiella pneumoniae*/*Escherichia coli*, *Acinetobacter baumannii*, *Pseudomonas aeruginosa*, and *Enterobacter* species.⁹ Four of the six are Gram-negative bacteria (*K. pneumoniae*/*E. coli*, *A. baumannii*, *P. aeruginosa*, and *Enterobacter* species), rendering them extremely difficult to treat.

Unlike Gram-positive bacteria, Gram-negative species possess two cellular membranes (**Figure 1**) composed of an outer membrane coated with lipopolysaccharides. Lipopolysaccharides are comprised of lipids (lipid A) and saccharide polymers (oligosaccharides).¹⁰ The oligosaccharides are different from one strain to another but are typically negatively charged and are attached to lipid A.¹⁰ Lipid A is made up of negatively charged phosphorylated disaccharides consisting of 4 to 7 acyl chains.¹⁰ Due to stabilization effects among the lipopolysaccharide units, the outer membrane is packed very tightly, making it difficult for most small molecules to enter through passive

diffusion.¹⁰ The Gram-negative bacterial outer membrane is also composed of porins, narrow water-filled membrane-protein channels that allow some hydrophilic molecules to diffuse rapidly through the channel and enter into the cell.¹¹ The inner membrane is a symmetrical phospholipid bilayer responsible for various metabolic and physiological functions and is surrounded by a thin peptidoglycan cell wall.¹²⁻¹³ The latter is composed of repeating disaccharide units cross-linked by pentapeptide side chains, forming a rigid exoskeleton and giving the cell its shape.¹²⁻¹³ The space between the inner and the outer membrane is called the periplasm. This compartment is a viscous environment filled with proteins and degradative enzymes that threaten the integrity of antibiotics.¹²⁻¹³ In addition to the complex membrane architecture, bacteria have developed another mechanism of defense called efflux pumps that pump out substances such as antibiotics (**Figure 1**).

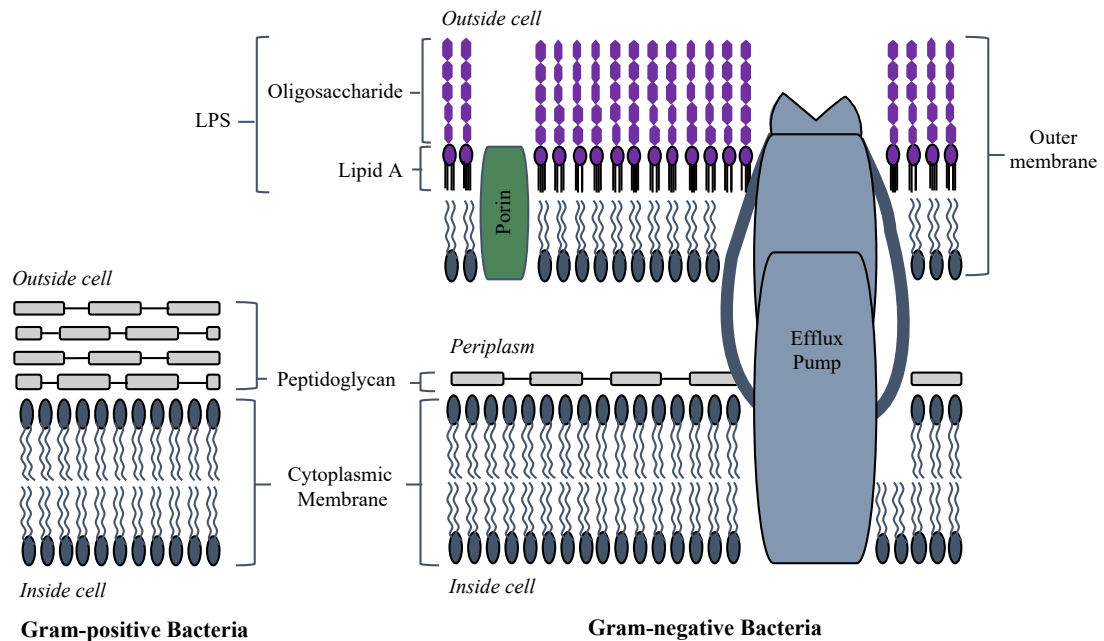


Figure 1. Gram-positive and Gram-negative membrane architectures.⁷

1.2. Current state of Permeation

Due to widespread overuse of antibiotics spanning decades, bacteria have developed efficient mechanisms of defense. The fear of returning to a time period resembling the pre-antibiotic era has never been so present. Currently, the evolution of bacterial resistance outpaces our ability to develop new antibiotics, especially against Gram-negative pathogens. One major reason for our inability to keep pace with resistance is our lack of knowledge about what physicochemical properties a molecule must exhibit to accumulate in Gram-negative bacteria, an attribute often required to interact with the target. Understanding molecular properties that influence small molecule accumulation would not only enable the rational design of new antibiotics from hits identified in screening campaigns, but also the ability to broaden the scope of chemotype that only exhibits activity against Gram-positive bacteria due to problems with accumulation in Gram-negatives.

As mentioned previously, it is difficult for molecules to cross the outer membrane in Gram-negative bacteria through passive diffusion. Most small molecules utilize one of two different mechanisms to permeate the outer membrane. These two mechanisms of permeation are 1) porins/specific channel mediated entry or 2) self-promoted uptake.⁷ Porins such as OmpF in *E. coli* are the main entry points of most polar antibiotics. OmpF is a well-studied porin that has a cylindrical shape characterized by a narrow central region comprised of a negatively charged loop. This region is approximately 7 Å by 11 Å, and prevents the entry of larger molecules (MW >600 Da)^{13, 7, 14} Certain channels are species specific and typically exhibit some level of selectivity, such as the uptake of sugar by the OprB porins or the diffusion of basic amino acids and peptides by the OprD porins both

in *P. aeruginosa*.¹⁵ The self-promoted uptake pathway is typically observed for polycationic molecules, which destabilize the lipopolysaccharide layer to enable penetration of the outer membrane.¹⁵

A study in 2017 using the fluorescent probe N-phenyl-1-naphthylamine (NPN), demonstrated that permeation in Gram-negative bacteria is even more complicated than initially thought, as permeability barriers (i.e., membrane and efflux pump composition) are significantly different between bacterial strains. For example, hyperporination induces more efficient accumulation of NPN in *A. baumannii* ATCC 17978 than in *B. cepacian* ATCC 25416 (**Table 1**). The same kind of observations were also noticed between efflux deficient strains, suggesting that accumulation is strain dependent.¹⁶

<i>Bacterial strains</i>	Wild Type	Hyperporinated	Efflux Deficient
<i>A. baumannii</i> ATCC 17978	~3,000	~18,000	~28,000
<i>B. cepacian</i> ATCC 25416	~2,900	~5,000	-
<i>B. thailandensis</i>	~3,000	~5,000	~8,000

Table 1. Accumulation study showing relative fluorescence units using the hydrophobic fluorescent probe NPN in *A. baumannii*, *B. cepacian* and *B. thailandensis* after 600 seconds. A greater fluorescence means a better intracellular uptake.

Studies indicate that antibiotics that have Gram-negative activity are usually smaller (MW < 600 Da) and more polar than antibacterials only active against Gram-positive bacteria. This observation was initially reported by O’Shea and Moser in 2008, and has been supported in further studies.¹⁰ This observation laid the foundation for researchers

starting to think about rules or designing principles that can be used to guide the conversion of antibiotics into broad spectrum agents. However, it is important to note that this observation and numerous others (e.g., polarity, size, pKa) have been controversial, as not all small molecules that exhibit these properties permeate and accumulate in Gram-negative bacteria.¹⁶ This indicates that identified parameters are likely not universal and more investigations are needed to understand not only the molecular properties that influence accumulation, but also the species-specific trends.¹⁶ Contrary to the outer membrane, the inner membrane of Gram-negative bacteria is permeable to most molecules.¹⁶ However, drugs that successfully cross the outer membrane and then the inner membrane are subjected to efflux pumps that protect the cell by exporting substances from both environments out of the bacteria. There are two main types of efflux pumps that interfere with drug accumulation 1) efflux transporters that are present in the inner membrane and affect cytoplasmic accumulation and 2) efflux transporters settled in the periplasm and the outer membrane that belong to the resistance-nodulation-cell division.¹⁶ Therefore, in order for a small molecule to achieve robust accumulation in Gram-negative bacteria, the rate of permeation (influx) must exceed that of efflux.¹⁰

Multiple strategies have been investigated to increase the accumulation of drugs into Gram-negative bacteria. One of them is the development of efflux pump inhibitors. However, the task of identifying and then developing a good efflux pump inhibitor is not trivial, as it needs to meet the same clinical parameters as a drug such as potency, pharmacokinetics, toxicity. It is also important to know the exact mechanism of action for the efflux inhibition and this should be compatible with the pharmacological properties of an antibiotic to avoid any undesired drug/drug interactions. Multiple efflux pump

inhibitors have been discovered in the literature but have failed to reach clinical development, mainly due to toxicity issues.^{17,15} While the discovery and development of efflux pump inhibitors is a promising avenue to enhance our antibiotic arsenal it is a complex process and much more research is required. Furthermore, the inhibition of efflux pumps would only be effective for enhancing the activity of substrates known to permeate Gram-negatives.

Another interesting and arguably more versatile strategy attempts to convert Gram-positive specific antibiotics into broad spectrum agents. In 2017, Richter et al. established the “eNTRY rules” for converting select Gram-positive specific antibacterial compounds into agents also active against the Gram-negative pathogen *E. coli*. This study assessed more than 100 rationally designed compounds for accumulation in *E. coli* and identified compelling evidence for three essential properties of molecules that accumulate, including 1) the presence of a non-sterically encumbered ionizable nitrogen such as a primary amine, 2) high rigidity (<5 rotatable bonds), and 3) low three-dimensionality (i.e., globularity, ≤ 0.25).¹⁰ Globularity is an interesting parameter that describes the spherical nature of a molecule. While the concept of this feature is intuitive, especially with regard to porin-mediated uptake, three-dimensionality has long been known to be an important factor in molecular recognition between a ligand and its target.¹⁸ Thus, more investigation is needed to determine the relationship between manipulating globularity and the subsequent effect on target selectivity. Based on the authors’ findings, they successfully converted the natural product deoxynybomycin (DNM, **Figure 2**) into a broad-spectrum agent 6DNM-NH₃. This molecule inhibits mutant DNA gyrase but is only active against Gram-positive bacteria. As it already possesses the right rigidity and globularity, the team

simply added an amine to a position that did not alter its antibacterial activity. First, they demonstrated that accumulation of the new compound in *E. coli* considerably improved when the amine was added (6DNM: 298 nmol per 10^{12} colony-forming units (CFUs), 6DNM-NH₃: 1,114 nmol per 10^{12} CFUs). Second, the authors showed that MICs for different Gram-negative pathogens also improved for the aminated compound. 6DNM-NH₃ was active not only against Gram-positive *S. aureus* but also against Gram-negative *E. coli*, *A. baumannii*, *K. pneumoniae*, *E. cloacae* except *P. aeruginosa*. This strategy was then employed on other chemotypes to demonstrate scope.¹⁰ (**Figure 2**)

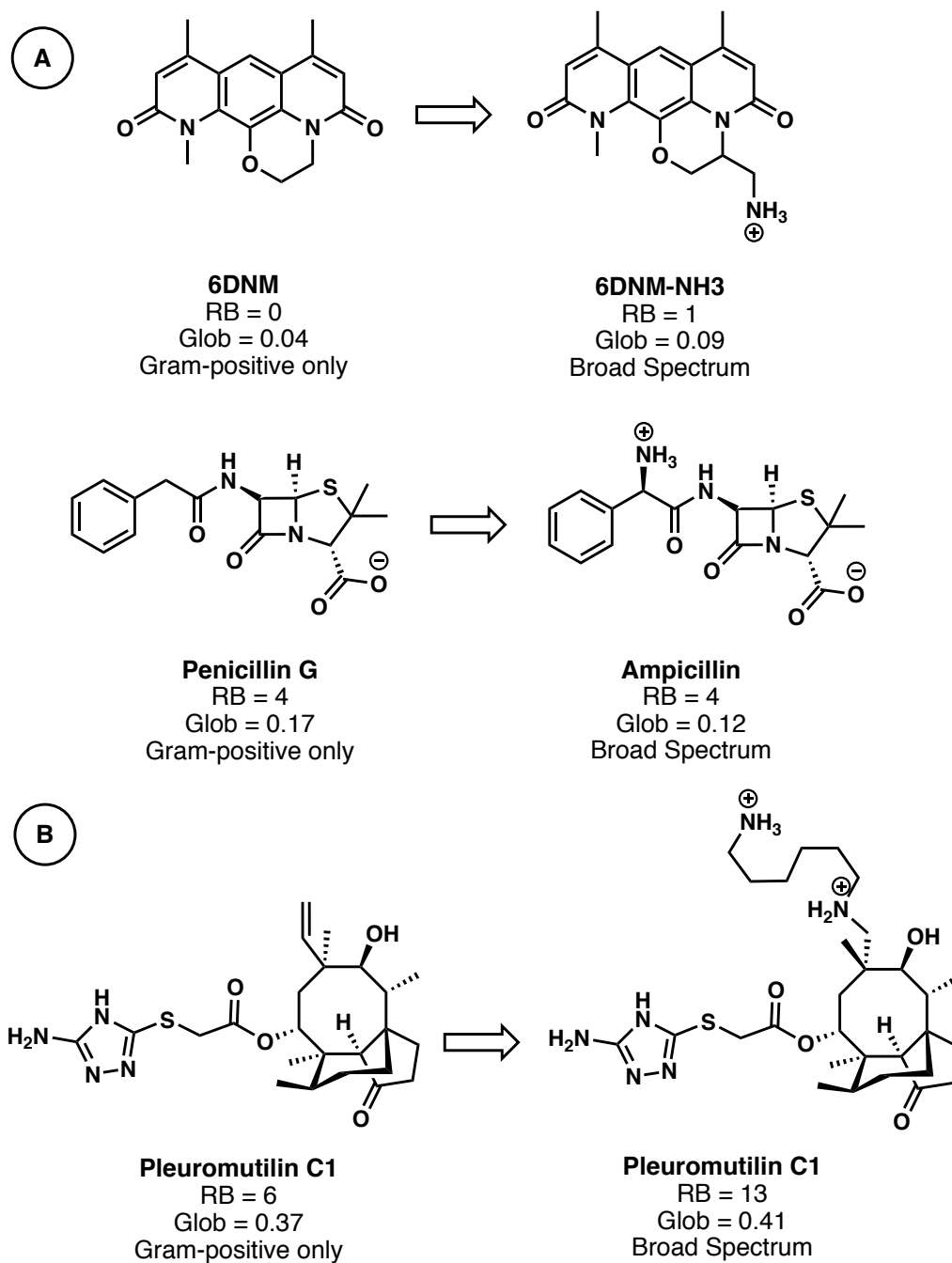


Figure 2. (A) Gram-positive selective antibiotics converted into broad spectrum agents following the “eNTRy Rules”; (B) An example of an exception to the “eNTRy Rules”⁷

These rules have been studied in more detail and employed in several instances since the initial publication.^{11, 19} In 2020, researchers developed a web application to calculate the

“eNTRy rule” compatibility of any compound simply by evaluating the SMILES string.¹⁹ However, these three guiding principles only give a glimpse of the physicochemical properties needed for broad-spectrum antibiotics. These parameters taken one by one were only studied in accumulation assays in *E. coli* and even if MICs were performed against other Gram-negative strains, the underlying effect on accumulation in the other strains was not reported. In addition, more information is needed as to which form of positive charge is accepted regarding the ionizable nitrogen.⁷ The study focused on primary amines, but other nitrogen-based functionalities could also be employed (e.g., anilines, heterocycles, secondary amines).⁷ This information would be important knowing that most porin channels have juxtaposed positively and negatively charged regions, which suggest that zwitterionic compounds might also interact favorably within the porin cavity.⁷ Finally, the major question regarding the role of self-promoted uptake in compound accumulation will have to be answered, as it is difficult to deconvolute what physicochemical features of compounds plays a role in self-promoted versus the porin-mediated pathways.⁷

As demonstrated previously, the major limitation in the discovery of broad-spectrum antibiotics is the Gram-negative permeability as we know that many Gram-positive antibiotics also exhibit activity against Gram-negative pathogens if the outer membrane is compromised. Determining rules that enable rational design of antibiotics or early hit molecules, like the ones that we are going to discuss next, into broad-spectrum agents would address a major limitation in antibiotic drug development.

2. ClpP and Acyldepsipeptides, An Emerging Target and Chemotype for Antibacterial Discovery

2.1. *ClpP, a promising new antibacterial target*

To date, every antibiotic class is limited by the evolution of drug resistance. In addition to innate mechanisms, bacteria can acquire resistance through natural processes, including spontaneous target mutation, gene mutation/regulation, and/or horizontal gene transfer.²⁰ Improper exposure to antibiotics enhances natural selection, resulting in the survival and propagation of resistant cells that produce recalcitrant progeny. As such, the discovery of new antibiotic chemotypes and new targets are continuous and urgent needs.

One example of a new target class is bacterial proteases, which play important roles in intracellular regulatory mechanisms for homeostasis and virulence. Proteases are capable of degrading obsolete or denatured polypeptides by hydrolyzing peptide bonds between amino acids, which is essential for cellular homeostasis bacteria viability. The major proteases that are responsible for the turn-over of cellular proteins include ClpP, Lon, FtsH and HslUV (**Figure 3**), which comprise the broad class of AAA⁺ enzymes (ATPases associated with various cellular activities).²¹ Each protease can be described as having two main components, one component responsible for recognition and binding (i.e., cochaperones), and the other that hydrolyzes peptide bonds (i.e., protease).

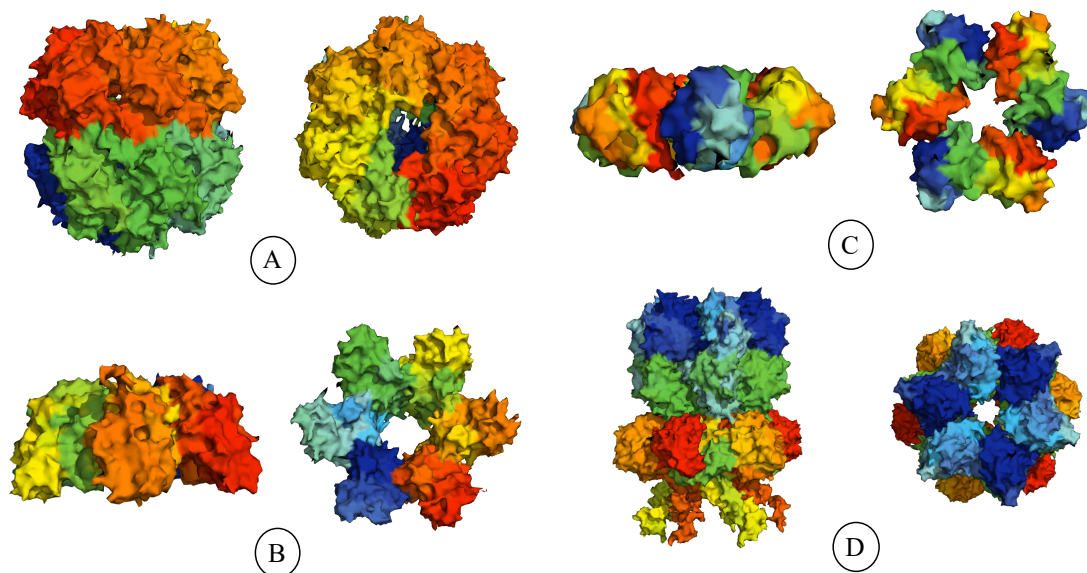


Figure 3. Structures of the main *E. coli* proteases in distal and apical views. (A) ClpP (PDB: 1YG6), (B) Lon (PDB: 1RR9), (C) FtsH (PDB: 4V0B) and (D) HslUV (PDB: 5JI3).

Software used: PyMOL.

Caseinolytic protease P (ClpP) has been the focus of many studies over multiple decades. ClpP is an interesting target due to the ability to induce antibacterial activity through the inhibition or activation of this protease. ClpP is composed of 14 subunits forming two heptameric rings arranged in a cylindrical-like shape. The protease is composed of an internal chamber containing the active sites responsible for peptide hydrolysis.²² ClpP on its own can only degrade small peptides composed of less than 5-6 amino acids and requires the association of Clp-ATPase chaperones (e.g., ClpA or ClpX) to degrade larger substrates. ClpA and ClpX belong to the AAA⁺ protein family and form hexameric rings that can bind coaxially to each side of ClpP, providing an enhanced substrate selectivity (**Figure 4**).²³⁻²⁵

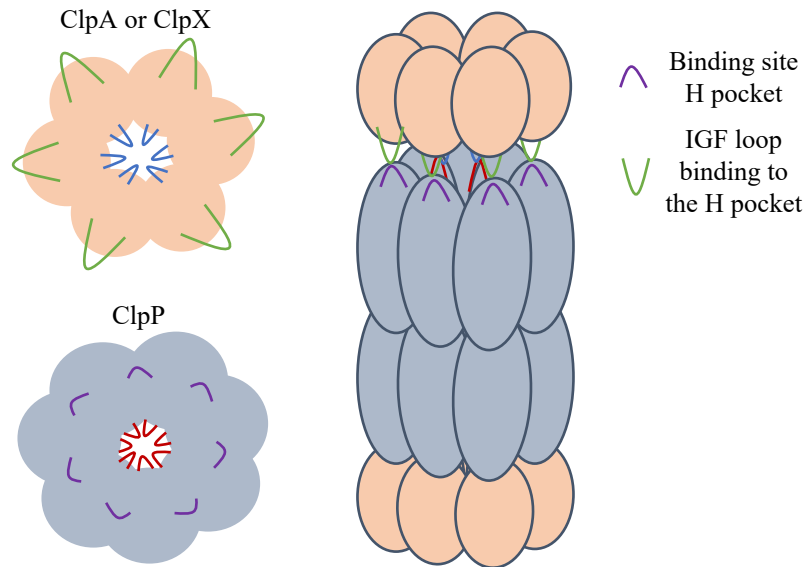


Figure 4. A cartoon of the ClpP protease associated to ClpA/ClpX complex

In the past, researchers have developed multiple small molecules that activate or inhibit ClpP. Antibiotics that exhibit their antibacterial property through activation rather than inhibition is a new paradigm that has captured the interest of researchers. By competitively engaging the co-chaperone docking sites with small molecules, it is possible to artificially stimulate ClpP activity, essentially turning ClpP into an unregulated “garbage disposal” that unselectively degrades polypeptides. This dysregulation results in cell death making ClpP a formidable target.

2.2. ADEP, a ClpP activating chemotype

The first class of ClpP-activators to be discovered was found by Eli Lilly when they isolated eight A54556 cyclic acyldepsipeptides (ADEPs) from *Streptomyces hawaiiensis* (**Figure 5**).²⁶ ADEP molecules demonstrated high activity against a broad range of Gram-positive bacteria but lacked efficacy against Gram-negative bacteria, determined to be due

to low membrane permeability and active efflux.²⁷⁻²⁸ Interestingly, ADEPs possess bactericidal properties, not by inhibiting the activity of ClpP protease but by over-activating it. In addition, ADEPs not only activate the serine protease but also disrupt its interaction with its co-chaperones. In other words, ADEPs possess two mechanisms of action, they induce uncontrolled degradation of unfolded proteins and nascent polypeptides and competitively prevent co-chaperone binding. The binding of ADEPs to ClpP results in an opening of the axial pores and exposure of the catalytic residues.²⁹⁻³⁰

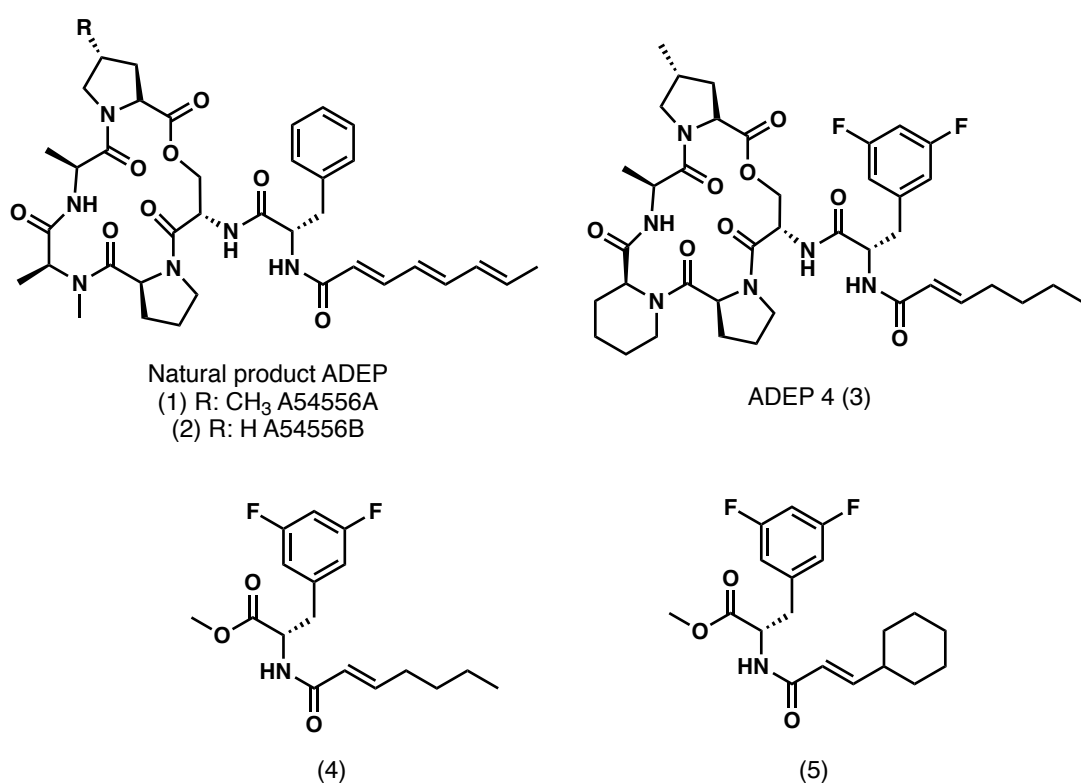


Figure 5. Structures of representative ADEP derivatives (1, 2, and 3) and small molecules based on the ADEP pharmacophore (4 and 5).

The structure of ADEP A54556A (1) and B (2) has been determined by Brötz-Oesterheltz and co-workers and >50 analogs have been derived to date. An initial structure-activity relationship (SAR) study of (1) and (2) led to the development of

ADEP4 (**Figure 5**), which exhibits better chemical stability and activity against Gram-positive bacteria, such as *S. aureus*.³¹ Small molecule derivatives based on the ADEP pharmacophore have also been identified (**4** and **5**, **Figure 5**) and show good MIC activity against *B. subtilis*.³² The development of ADEP4 and new analogs provides proof-of-concept that rational design of this scaffold can lead to very potent activity. Unfortunately, the constraint of this chemotype to Gram-positive bacteria remains a serious limitation to further development. In 2005, however, Brötz-Oesterheltz et al. published a paper in Nature Medicine stating the following:²⁵

« Gram-negative bacteria were only affected [by ADEP compounds] when efflux pumps were deleted or permeabilizing agents were added to the culture broth, indicating that penetration across the outer membrane is hampered, as expected for molecules of that size. »

This offers major new perspectives as it suggests that derivatives of this family retaining on-target activity but also addressing Gram-negative limitations could treat infections caused by these pathogens. Herein, we report a library of small molecule derivatives based on the ADEP pharmacophore designed to exhibit different physicochemical properties with an aim to provide a better understanding of the “rules” required to attain accumulation and might lead to active compounds against Gram-negative bacteria.

3. *N*-Phenyl-1-Naphthylamine, a Hydrophobic Fluorescent Probe

3.1. *Fluorescent probes*

Fluorescent probes are molecules capable of absorbing light at a specific wavelength and emitting light at a different wavelength. Molecules that exhibit such a profile are useful as chemical tools, especially for tracking properties like permeability, accumulation, and cell localization. Each molecule is unique and offers a different absorption and emission profile depending not only on molecular structure but also on environmental queues (e.g., temperature, pH, solvent, interactions).³³ Once a molecule absorbs an excess of energy, its electrons are promoted from the ground state to the excited singlet states (e.g., from S_0 to S_1 or above).³³ The electrons do not stay in the excited state long and eventually recede back to ground state. In order to release this energy, the excited fluorophore can undergo vibrational relaxation, collide with other molecules, experience internal conversion (non-radiative processes) or release photons, also called fluorescence (radiative process) to return to ground state energy.³³ In the case of fluorescence, the release of a quantum of energy will always be from the lowest excited singlet state S_1 to the ground state.³³ Thus, in theory, the emission wavelength will always be longer (less energy released) than the excitation wavelength. This difference between the two maxima can be seen on an excitation - emission spectrum and is called the Stokes shift (**Figure 6**).³⁴

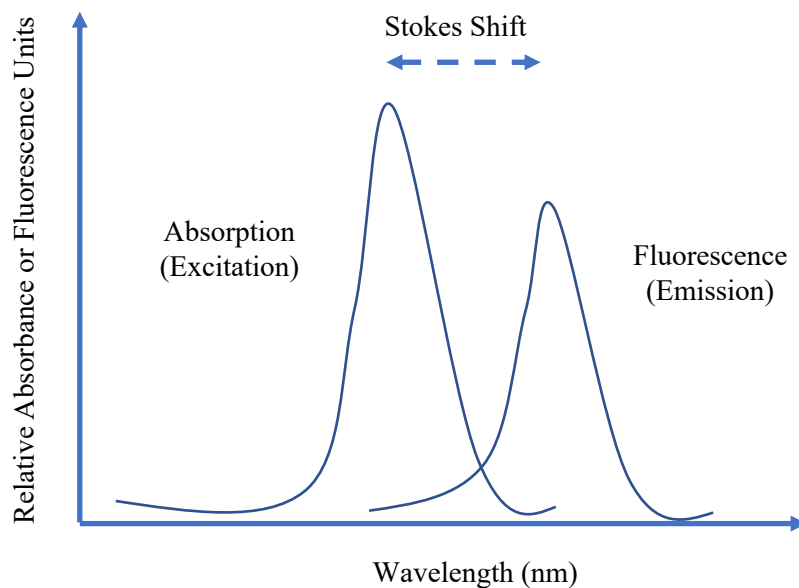


Figure 6. Typical excitation and emission spectrum showing the Stokes shift, the difference between the excitation and the emission optima

Fluorescent probes and more generally fluorescent methods have been widely used in the biological and medicinal field.³⁵⁻³⁶ They are employed for numerous applications such as medical imaging for cancer diagnostics or bioimaging for specific immune responses, proteins, or live-cells, and tissue labeling and imaging.³⁷ Fluorescent probes are also used in drug discovery with, for example, the use of fluorescence polarization in HTS (High-Throughput Screening) assays.³⁷

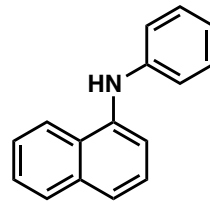
Fluorescent molecular probes have found utility in the study of cell membranes. Common fluorescent probes can be classified into three main categories. The first, includes fluorescent probes capable of identifying specific components of the membrane, such as cholesterol.³⁸ The second class is composed of probes that partition specifically into the liquid-ordered or the liquid-disordered phase of the membrane. Finally, the last

class comprises probes that are sensitive to their environment and can directly distinguish the liquid-ordered from the liquid-disordered phase.³⁸

With the rise of multi-drug resistant bacteria, fluorescent probes have become a powerful tool to assess the overall composition, integrity, and/or fluidity of the bacterial membrane.³⁵ The bacterial membrane is the first rampart that must be surpassed by molecules. As previously mentioned, Gram-negative bacteria possess a very complex membrane and efflux defense system, which work in parallel to keep molecules out. As one might expect, fluorescent probes have been grafted to antibiotics to follow their accumulation and activity in Gram-positive and Gram-negative bacteria.³⁹ Fluorescent probes are extremely advantageous to work with as they do not require highly specialized equipment and they are quite affordable. Numerous probes have been reported but in the context of our work we will focus on one in particular, *N*-phenyl-1-naphthylamine.

3.2. N-Phenyl-1-Naphthylamine

N-Phenyl-1-naphthylamine, also called NPN (**Figure 7**), is a hydrophobic probe that exhibits high fluorescence emission in phospholipid environments but a weak emission in aqueous environments.⁴⁰ Therefore, this molecule is a useful tool to assess the properties of biological membranes.⁴⁰ NPN should, however, be manipulated carefully since it is a toxic and carcinogen compound.⁴¹



Chemical Formula: C₁₆H₁₃N
Molecular Weight: 219.29

NPN

Figure 7. Chemical structure of NPN

NPN has been utilized throughout decades for mainly one reason, to assess the permeability of Gram-negative bacteria under different conditions. For instance, previous work utilized NPN to determine the effect of different environmental conditions on the integrity Gram-negative bacterial membranes. Boziaris et al. demonstrated that thermal stress improves transient sensitivity to nisin, a bacteriocin produced by acid lactic bacteria,⁴² in *Pseudomonas aeruginosa* and *Salmonella* Enteritidis PT4, PT7. In addition, the authors assessed the damage on the outer membrane caused by the thermal shock using among other methods, NPN uptake. Significant outer membrane damage was demonstrated by a better permeation of NPN, which allowed NPN to accumulate in the inner-membrane and fluoresce. The authors noticed an increase in fluorescence intensity when bacteria were stressed, confirming that the outer membrane was damaged.⁴³ Another paper written by Cao-Hoang et al. investigated nisin sensitivity under rapid and slow chilling of *E. coli*. In this work, the correlation between nisin sensitivity and the permeability of the outer membrane induced by cold stress was evaluated the same way as before, by measuring the fluorescence of NPN in stressed bacteria.⁴²

Another principal use of NPN is to evaluate the permeability of Gram-negative bacteria when incubated with antibiotics. Numerous case studies report the use of NPN to

assess the effect of various small molecules on outer membrane integrity. In the journal *Acta Biomaterialia*, Tang and al. ran fluorescent probe-permeability assays using NPN to investigate and demonstrate the mode of action of chitosan-arginine on *P. fluorescens* and *E. coli*. Chitosan is a carbohydrate biopolymer found in crustacean exoskeletons that has interesting antimicrobial properties. NPN fluorescence assays were used to demonstrate the permeabilization effect of chitosan-arginine in this paper.⁴⁴ Another article published in the *Journal of Bioscience and Bioengineering*, also assessed the antibacterial action of chitosan (kojic acid-grafted-chitosan oligosaccharides) on the cell membrane of bacteria. The authors used NPN to investigate the permeabilization of the outer membrane by measuring the fluorescence of NPN after the antibacterial agent was added to a suspension of *E. coli*.⁴⁵ Many other studies have utilized NPN in order to determine the mode of action of new antimicrobial agents and to verify permeabilization effects on Gram-negative bacteria.^{40, 46, 47, 48, 49}

Herein, we report a library of new NPN derivatives designed to exhibit different physicochemical properties. This library is expected to exhibit a wide range of permeation in Gram-negative bacteria, not due to an alteration of the outer membrane, but due to the molecular properties of the derivatives themselves. Successful development of such a library is expected to provide new fluorescent probes that will find utility in permeation and accumulation assessments.

Understanding the properties of small molecules that influence accumulation has never been so important. Such an accomplishment will enable medicinal chemists to develop new antibiotics able to treat Gram-negative bacteria and more particularly the ESKAPE pathogens. From the data collected from our small molecule ADEP and NPN

libraries (in combination with other libraries under development), we hope to discover new physicochemical trends that will allow for the elaboration of guiding principles and design strategies for antibiotics.

Chapter 2

Design and Synthesis of Small Molecule ClpP Activators

1. Introduction

The first part of our work centered on the synthesis of ClpP activator derivatives. As stated previously, ClpP and AAA+ cochaperones play important roles in maintaining protein homeostasis.⁵⁰ Disruption of ClpP activity results in severe consequences to bacterial viability and virulence. Acyldepsipeptides (ADEPs), isolated from *Streptococcus hawaiiensis*, comprise a new family of antibiotics that target the highly conserved ClpP and thus exhibit a novel mechanism of action. Previous works demonstrate that ADEPs exhibit bactericidal activity by activating ClpP, leading to uncontrolled protein degradation and preventing natural co-chaperones from binding.²⁵ While rationally designed ADEPs (**Figure 8**) exhibit remarkable antibacterial activities against Gram-positive bacteria, they fail to kill Gram-negative bacteria due to low accumulation.^{25, 51} However, Gram-negative pathogens are affected when efflux pumps are deleted or if ADEPs are co-administered with a permeabilizing agent,²⁵ suggesting that broad spectrum activity of ClpP activators can be attained if permeation is improved and/or sensitivity to efflux pumps is lowered.

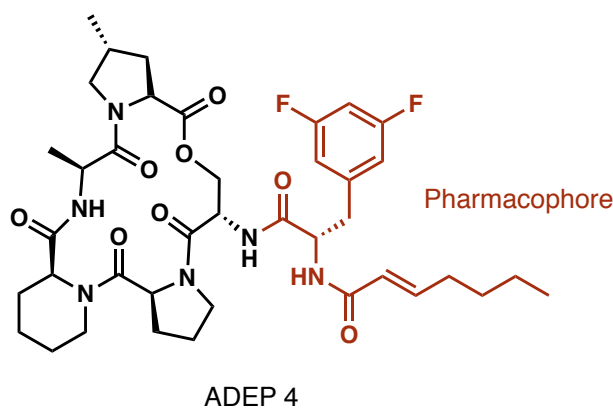


Figure 8. Chemical structure of ADEP 4 and its pharmacophore (red)

Several SAR studies have elucidated the effect of ADEP structural alteration on ClpP activation and concomitant antibacterial properties. For example, various studies have investigated the impact of macrocycle and acyl chain alteration by synthesizing analogues with various substituents to induce structural rigidities or constraints.^{27, 52-53} MICs on Gram-positive bacteria, and to a lesser extent Gram-negative bacteria, are performed with hopes of discovering a more potent ADEP. These studies are always challenging due to the complexity of analog synthesis.

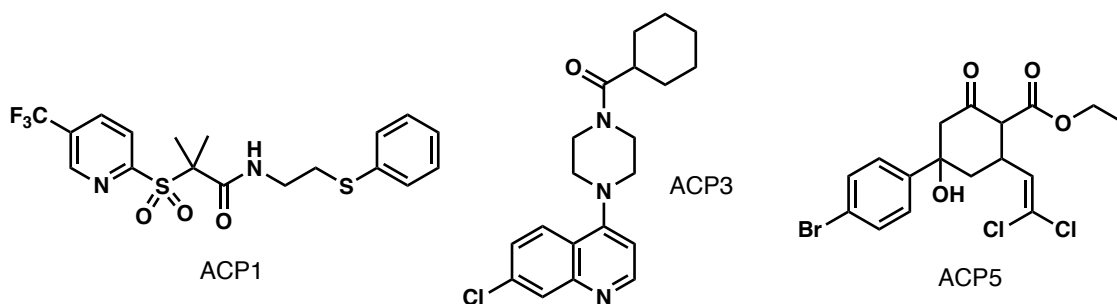


Figure 9. Representative ACP molecules

In attempts to identify simplified small molecule ClpP activators, the Houry group conducted a high-throughput screen with commercially available libraries. New ClpP activators with unique scaffolds (**Figure 9**) and promising activities were identified and

termed Activators of Self-Compartmentalizing Proteases (ACPs).²³ These molecules demonstrated that simplified, smaller and unique molecules could also activate ClpP, allowing new opportunities in research.

In order to define the relative contributions of each part of ADEP4 in the ClpP binding and activation, Sello et al. evaluated the MICs for multiple fragments of the ADEP structure in *B. subtilis*. They discovered that the *N*-acyl-difluorophenylalanine motif retains most of the bioactivity and should be considered the ADEP4 pharmacophore (MIC pharmacophore 8 $\mu\text{g}\cdot\text{ml}^{-1}$; MIC macrocycle >128 $\mu\text{g}\cdot\text{ml}^{-1}$) (**Figure 9**).³² However, a year later it was revealed that this fragment is recognized by efflux pumps and it is likely what causes ADEP to be pumped out of Gram-negative bacteria.²⁸

Our library will be based on the ADEP4 pharmacophore motif as it is an attractive scaffold for multiple reasons: 1) it ensures a chemically tractable synthesis allowing the production of sufficient amounts of material, 2) it can be rapidly derivatized in 2-4 steps from scalable intermediates, 3) it allows direct comparisons not only within the analogues of the library but also among derivative scaffolds studied by our collaborators to interrogate the role of structural variations on penetration and efflux, and 4) the scaffold provides an opportunity to probe the effects of structural modification on permeation, efflux susceptibility, and accumulation.

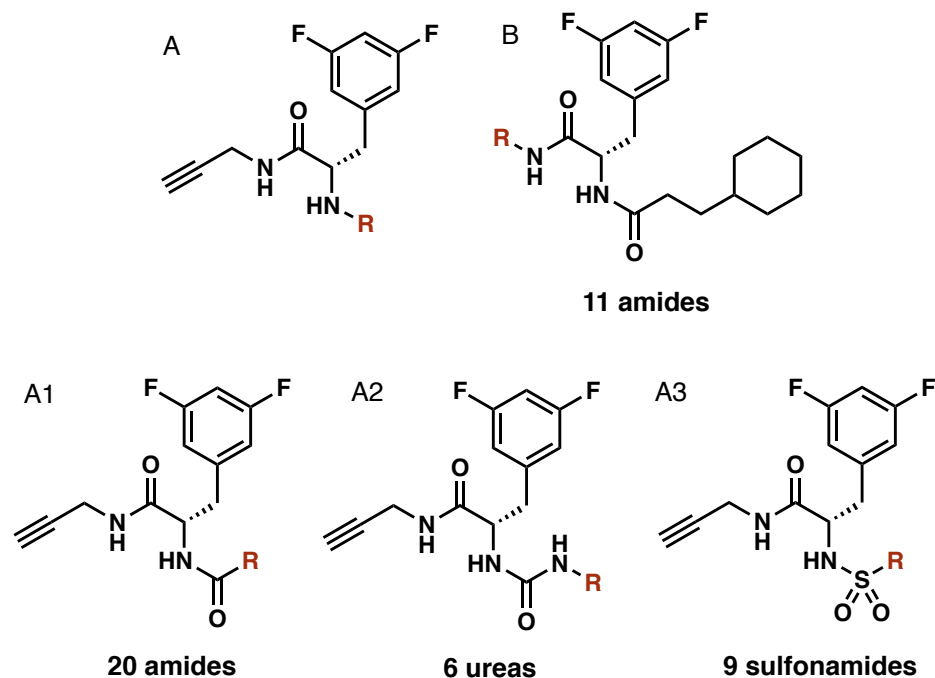


Figure 10. Selected scaffolds for the linear small molecule ADEP analogues library

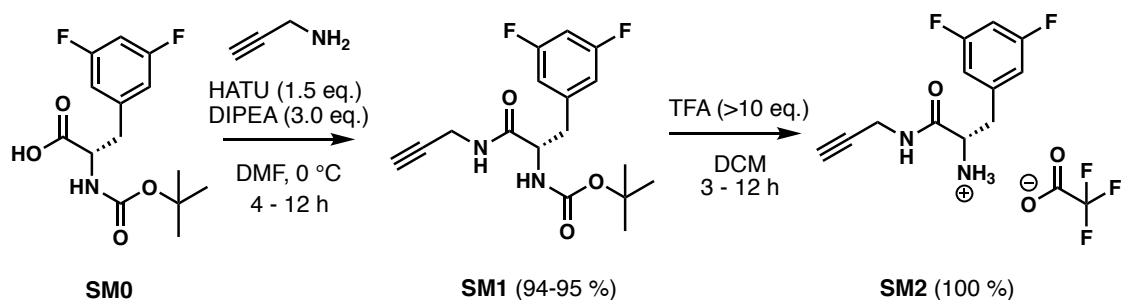
We chose two *N*-acyl-difluorophenylalanine scaffolds (**A** and **B**, Figure 10) for the synthesis of the library, as well-established chemistry can be utilized to functionalize the indicated positions (**R**). The functionalization of **A** and **B** was determined through a collaboration with MERCK after a rigorous computational study to provide a library with diverse physicochemical properties. From these two fragments, we synthesized analogues comprising three different molecular connectivities: amides (**A1** and **B**), ureas (**A2**) and sulfonamides (**A3**).

The overall project aims to define physicochemical properties leading to accumulation into Gram-negative bacteria. We will collect data on physicochemical properties, MIC values against 3 species (*E. coli*, *A. baumannii*, *P. aeruginosa*) including 4 different strains for each (ranging in levels of membrane or efflux compromise), and mass spectrometry accumulation data. In combination with other work being done in our lab

and our collaborator's all the data will then be compiled and analyzed using multi-component analyses in attempts to extract meaningful trends correlating physicochemical properties induced by scaffold and structural modifications with: 1) the activity against ClpP, 2) the effect on bacterial permeation, 3) the effect on efflux susceptibility. We hope to derive rules or trends that can be applied to new hit molecules or existing classes to enhance their Gram-negative activity.

2. Synthesis of Small Molecule *N*-Acyl-difluorophenylalanine Derivatives

To synthesize starting material **SM2**, a required component for the first part of the small molecule ClpP activator library, we began with an amidation reaction between Boc-3,5-difluoro-L-phenylalanine (**SM0**) and propargylamine to form **SM1**. This amidation reaction leverages HATU (Hexafluorophosphate Azabenzotriazole Tetramethyl Uronium), a common reagent used in peptide couplings and DIPEA (N,N-Diisopropylethylamine), an organic base, in DMF. Although other peptide coupling reagents could have been used (e.g., HOBT, HBTU or DCC), HATU was chosen due to the availability in lab. This peptide coupling procedure was used frequently to form amide analogues in the *N*-acyl-difluorophenylalanine and NPN libraries, as it is reliable, scalable, and straightforward to execute.



Scheme 1. Synthetic route for the synthesis of the starting material 2 (SM2)

In the ¹³C-NMR spectrum, we observed that the two fluorine atoms on the phenyl ring couple with the proximal carbons; each carbon in the ring appears as a triplet or as a doublet of doublets (**Figure 11**; A/A': dd, $J = 212.5, 11.1$ Hz; B: t, $J = 21.5$ Hz; C/C': dd, $J = 15.6, 6.5$ Hz; D: t, $J = 7.8$ Hz). This phenomenon can be seen on the ¹³C-NMR spectrum of each analog for the ADEP library, especially when sufficient sample amounts were used in NMR analysis. This coupling was particularly useful as a diagnostic tool to determine if a reaction and/or a purification was successful.

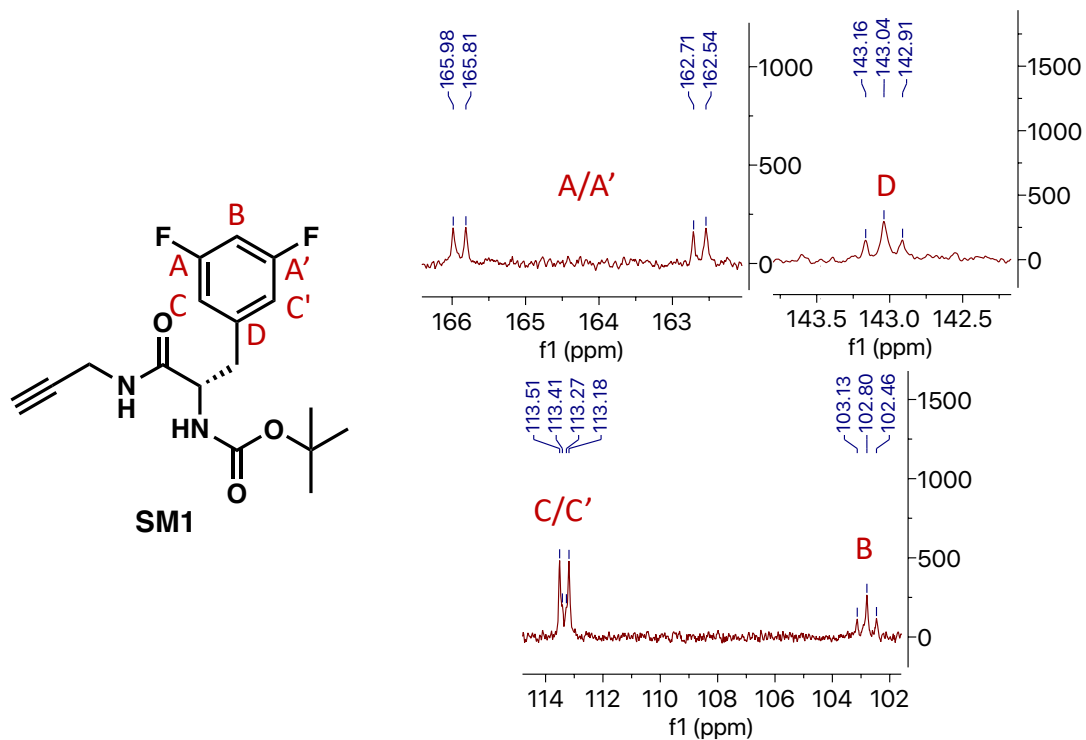
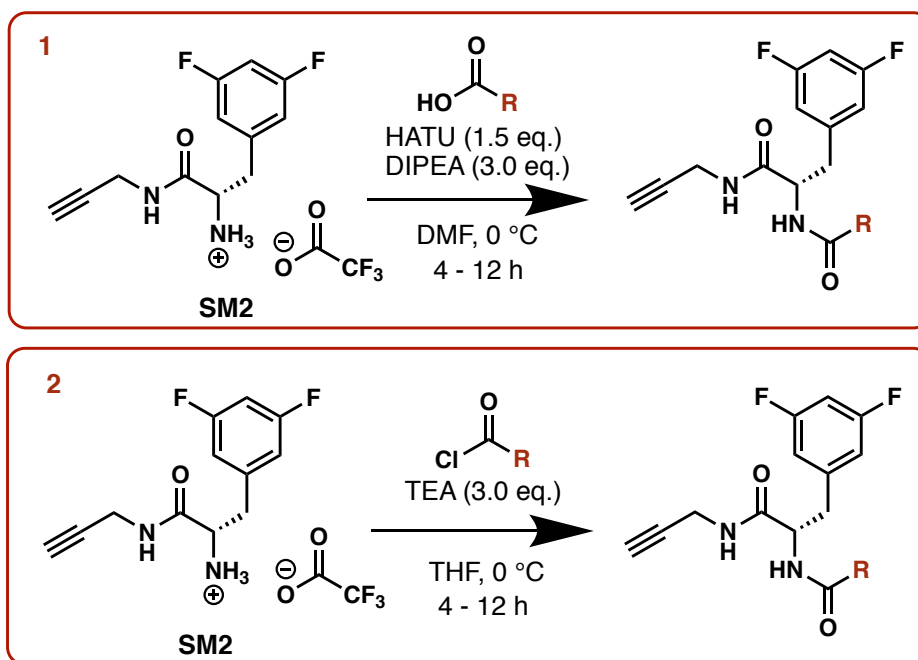


Figure 11. ^{13}C -NMR, spectral characterization of SM1 in CDCl_3 , 300 MHz

The next and final step to generate **SM2** is Boc (tert-butoxycarbonyl) removal to free the primary amine. To do so, **SM1** was stirred in a solution of excess TFA (trifluoroacetic acid) in DCM to form the TFA salt of **SM2**. The key to this step was to wash the salt multiple times with DCM prior to drying to completion under vacuum to ensure complete removal of residual TFA. Failure to remove all TFA resulted in a brown sticky oil that presented difficulties in handling and stability issues. This reaction gave a quantitative yield. The product **SM2** was typically used as a salt without any further purification for the synthesis of analogues (**Scheme 1**).

2.1. Synthesis of amides 1

The synthesis of amides 1 is based on the reaction between the free amine of **SM2** with a carboxylic acid or an acyl chloride. In the case of the carboxylic acid, the same HATU and DIPEA reaction that provided **SM1** was used (**Scheme 2.1**). For acyl chlorides, the use of 3 equivalents of TEA (triethylamine) was sufficient to form the desired amide (**Scheme 2.2**). Both reactions could be stirred overnight or longer without any issues.



Scheme 2. Reaction conditions for the synthesis of amide 1 analogues. 1) reaction between an amine and a carboxylic acid; 2) reaction between an amine and an acyl chloride

Amide Structure 1	An.	-R	An.	-R
	1 (1)	 71 %	11 (1)	 56 %
	2 (1)	 80 %	12 (1)	 79 %
	3 (1)	 100 %	13 (2)	 97 %
	4 (1)	 91 %	14 (2)	 71 %
	5 (1)	 48 %	15 (2)	 45 %
	6 (1)	 64 %	16 (1)	 98 %
	7 (1)	 63 %	17 (D)	 89 %
	8 (1)	 86 %	18 (1)	 71 %
	9 (1)	 26 %	19 (D)	 95 %

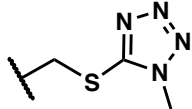
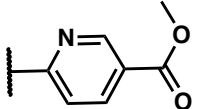
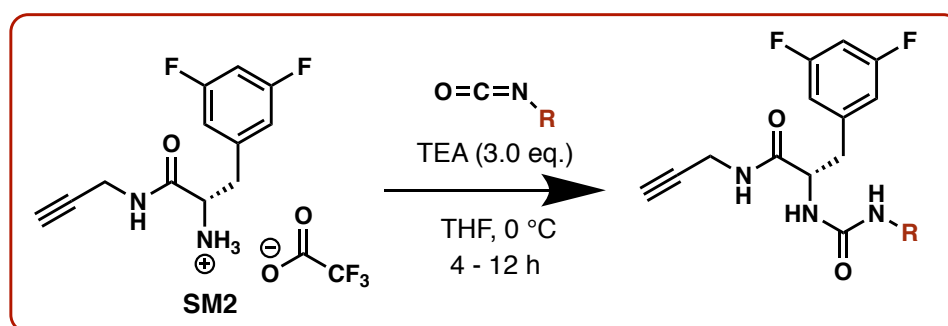
	10 (1)	 66 %	20 (1)	 83 %
--	-------------------------	---	-------------------------	---

Table 2. Amide 1 analogue structures. (An.: analogue number, (X): reaction type, (D): Boc deprotection)

Most derivatives were obtained in good yields as indicated in **Table 2**. The most challenging part of these reactions was purification. Compounds **1 – 8**, **12 – 16**, **18** and **20** were purified by flash column chromatography (SiO₂). Final compounds were typically quite polar and suffered from poor UV activity or failed to stain with common TLC stains (e.g., CAM, KMnO₄, Ninhydrin, *p*-anisaldehyde, phosphomolybdic acid). Two compounds (**9**, **10**) exhibited high polarity and low solubility in most organic solvents, and thus could not be purified by standard flash column chromatography. Instead, another purification technique called pTLC (Preparative Thin Layer Chromatography) was employed with a mixture of co-solvents as eluents. A mix of MeOH:DCM (10:90) for **9** and a MeOH:DCM:Toluene (5:70:25) for **10** was used to isolate sufficient amounts of each derivative for structural characterization and evaluation in biological assays. Compound **11** was also not amenable to typical chromatographic methods, as stability issues were observed upon exposure of **11** to silica. However, due to the insolubility of **11** in most organic solvents, the crude product could be washed with diethyl ether and methanol. Finally, **17** and **19** were obtained after Boc removal from **16** and **18**, respectively, after treatment with a solution of 4 M HCl in dioxane. The crude products were washed with acetone to remove any impurities.

2.2. Synthesis of ureas

Urea analogues were synthesized by treating **SM2** with an isocyanate in the presence of a base, TEA (**Scheme 3**). This reaction, inspired by the procedure of the work of Ouyang and co-workers,⁵⁴ was typically conducted in a cold bath at 0 °C but could also be run at room temperature without complications. Isocyanates are highly sensitive to water and thus this reaction required the use of anhydrous THF in order to avoid any complications.



Scheme 3. Synthetic procedure for the generation of urea analogues

Urea Structure	An.	-R	An.	-R
	21	 51 %	24	 100 %
	22	 45 %	25	 65 %
	23	 88 %	26	 94 %

Table 3. Urea analogues. (An.: analogue number)

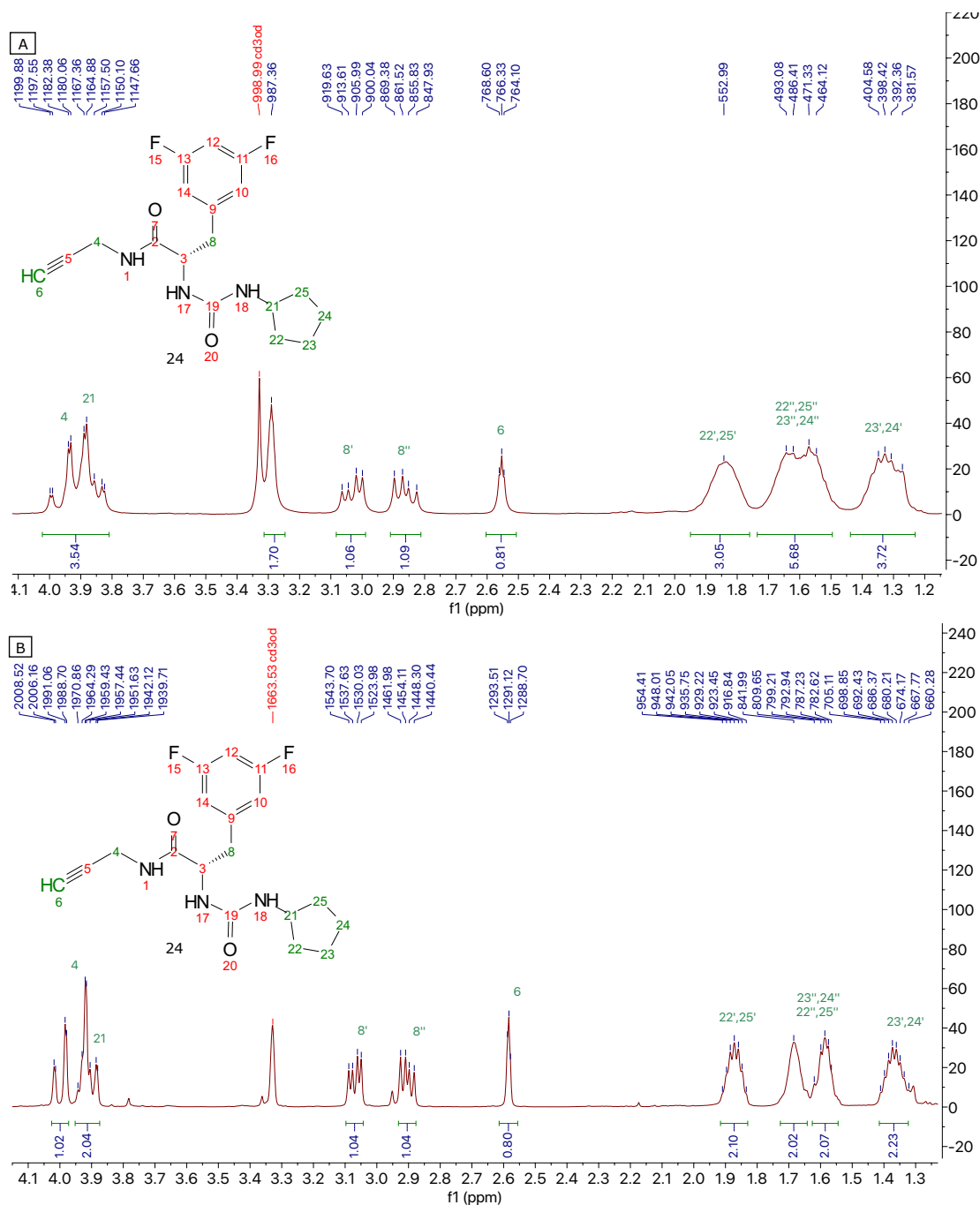
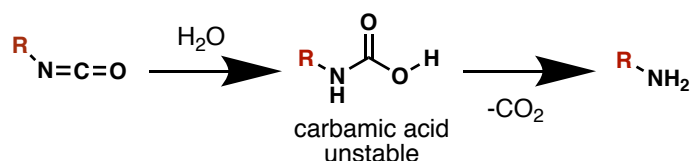


Figure 12. Comparison of ^1H -NMR spectra in CD_3OD between two urea analogues made with different equivalents of isocyanates. (A) 1.5 equivalents; (B) 1.0 equivalent

Although the urea formation proceeds rapidly due to the high reactivity of isocyanates, we found that an excess of isocyanate led to the formation of the corresponding amine

during the workup, which complicated purification (**Scheme 4**). The resulting amine often eluted at the same time as the desired product and could not be separated by flash column chromatography, pTLC, organic solvent wash or acidic workup. The only indication that co-elution of the amine by-product and desired product occurred was via analysis of the NMR spectrum, wherein the integration is higher than expected (e.g., **Figure 12**). Formation of the undesired amine by-product could be avoided by utilizing ≤ 1.0 equivalent of the requisite isocyanate.



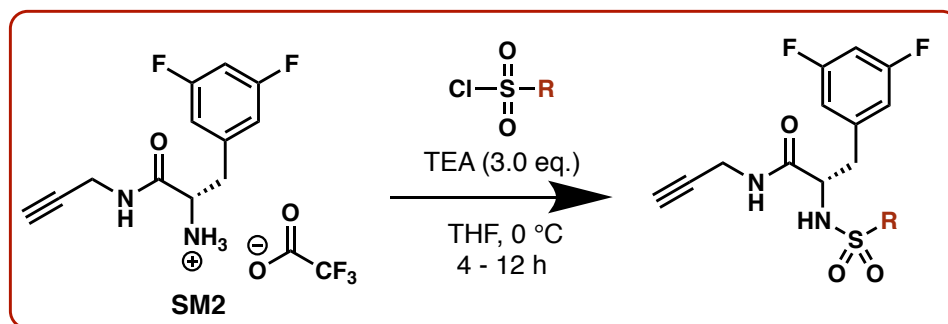
Scheme 4. Hydrolysis of isocyanates⁵⁵

Yields for these compounds were expected to be excellent, but again, the purification proved challenging. As with many of the amides, the ureas exhibited high polarity and insolubility in most solvents. Moreover, the small amount of product (scale of 15 mg) precluded recrystallization methods. Fortunately, compounds **21**, **23**, **24** and **25** were purified by standard chromatography methods with a high percentage of either ethyl acetate or methanol in the eluent. For compounds **22** and **26** crude products were washed with an organic solvent to remove impurities.

2.3. Synthesis of sulfonamides

Sulfonamides were prepared by reacting **SM2** with sulfonyl chlorides in presence of TEA (**Scheme 5**). Sulfonamide analogues are polar molecules, thus, purification using silica column was not always trivial. Indeed, solvents used during silica flash

chromatography or pTLC usually involved methanol/DCM to elute the compounds. Similar to formation of the amides and ureas, the reaction was usually placed in a cold bath, but reactions run at room temperature also proceeded without problems.



Scheme 5. Synthetic procedure for the generation of sulfonamide analogues

Sulfonamide Structure	An.	-R	An.	-R
	27	 99 %	32	 51 %
	28	 49 %	33	 49 %
	29	 27 %	34	 89 %
	30	 53 %	35	 35 %
	31	 72 %		

Table 4. Sulfonamide analogues. (An.: analogue number)

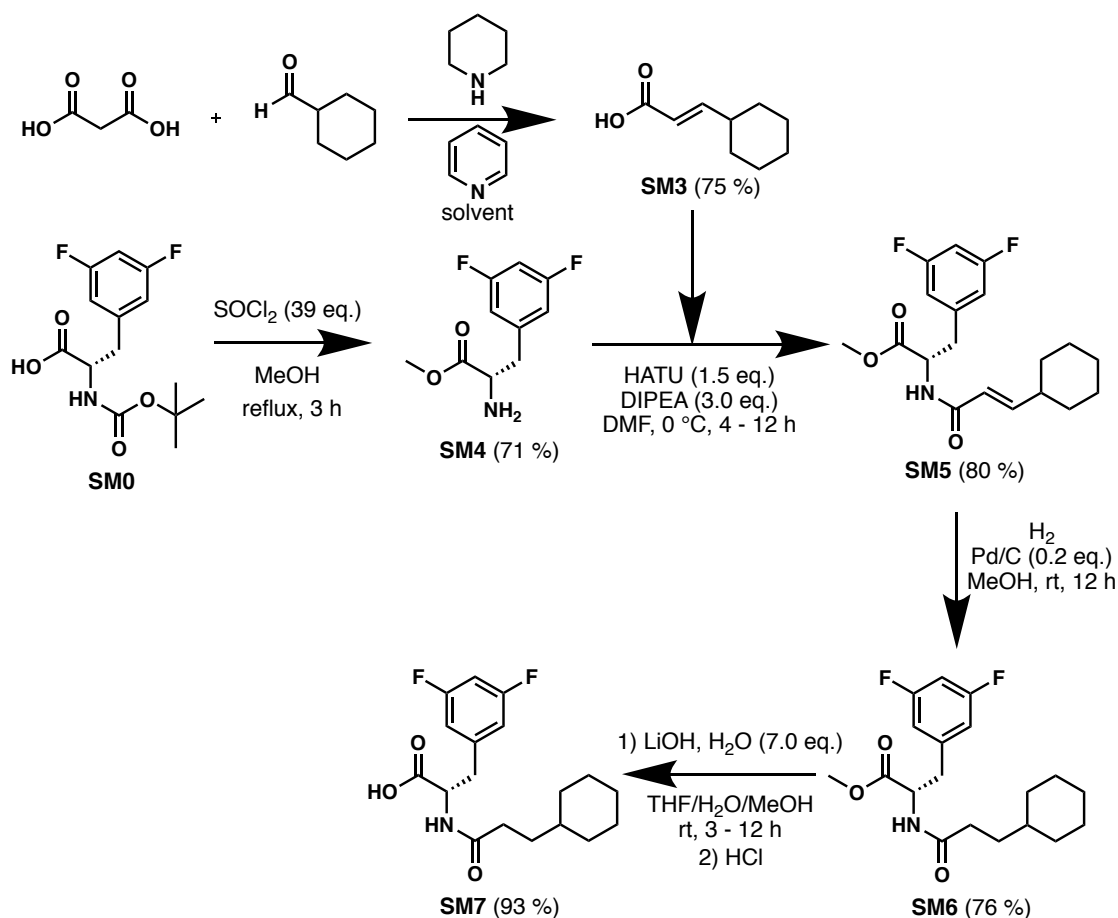
As indicated in **Table 4**, lower yields were obtained for the sulfonamides than for amides and ureas. This is likely caused by the need for multiple purifications for each derivative to obtain the pure product. For example, **29** and **35**, produced in 27% and 35%, respectively, were purified by column chromatography (SiO₂) followed by an organic solvent wash to remove impurities that could be seen by NMR. Indeed, an impurity persisted through chromatography and could only be removed by a carefully selected solvent wash. Compounds **27** and **31** were purified via flash column chromatography (SiO₂) without any particular difficulties. For analogue **33**, the crude product was an insoluble solid and a wash with DCM was sufficient to remove impurities and obtain a clean NMR spectrum. Compounds **28**, **30** and **32** could not be purified by typical chromatographic methods due to high polarity or impurity coelution with the desired product. Additionally, the crude products were oils, and thus organic solvent wash was not feasible. In these cases, pTLC was used to obtain the pure products. Interestingly, the reactant used to form **28** contained a *tert*-butyl group on the oxygen that was cleaved during the reaction or the work up to provide the free hydroxyl. The 2-hydroxypyridine group is subject to tautomerization to form the 2-pyridone.⁵⁶ The same *t*-butyl cleavage was also observed when the same reactant was used for the NPN library. Finally, analogue **34** was generated without the need of purification as determined by NMR.

2.4. Synthesis of amides 2

The second subset of the library was generated from starting material **SM7** (**Scheme 6**). To generate **SM7** a Verley–Doebner modification with malonic acid and cyclohexanecarboxyaldehyde in the presence of piperidine and pyridine provided

cinnamic acid **SM3** in good yield.⁵⁷ This reaction requires the use of relatively fresh cyclohexanecarboxyaldehyde, as this reactant is prone to air-mediated oxidization to the corresponding carboxylic acid. In parallel, **SM4** is prepared by a two-step, one pot reaction. Esterification of **SM0** and Boc removal occurs in the same step, as the use of thionyl chloride produces HCl during the reaction. However, the resulting product from this procedure is the HCl salt, requiring the use of a dilute base at 1M such as NaOH or K₂CO₃ to obtain the free amine, while avoiding saponification of the ester.

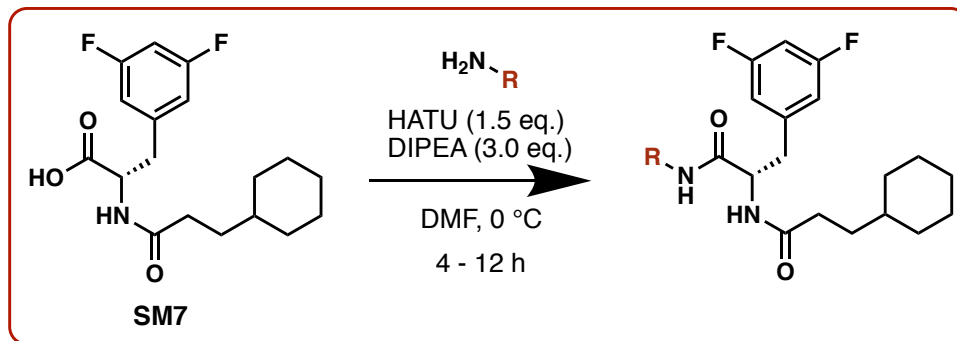
The next step in the sequence was to generate **SM5** by coupling **SM3** and **SM4** using HATU and DIPEA to afford a dark orange crude product. As expected, this reaction worked well and provided (**SM5**) in 80% yield. Due to the orange color of the crude product, it was noticed that during purification, column (internal diameter: ½ inch) became “visually” saturated. Consequently, a larger column (internal diameter: 1-inch) was required to get the pure product in the form of a white powder.



Scheme 6. Synthetic route for the synthesis of the starting material 7 (SM7)

The subsequent step to generate **SM6** employed hydrogen and Pd/C to catalytically hydrogenate the alkene in **SM5**. Finally, using lithium hydroxide in a mixture of THF/H₂O/MeOH, ester saponification provided the key intermediate **SM7**, which was used without further purification.

SM7 was then utilized to generate amide 2 analogues through reaction with select amines in the presence of HATU and DIPEA in DMF at 0 °C, as shown in **Scheme 7**.



Scheme 7. Synthetic procedure for the generation of amide 2 analogues

Amide Structure 2	An.	-R	An.	-R
	36	 46 %	42	 88 %
	37	 34 %	43	 60 %
	38	 40 %	44	 90 %
	39	 97 %	45	 85 %
	40	 56 %	46	 69 %
	41 (D)	 53 %		

Table 5. Amide 2 analogues. (An.: analogue number, **(D)**: Boc deprotection)

Similar to previous derivatives, these compounds were particularly polar, exhibited low UV activity and/or poor stainability, which complicated purification. Compounds **37** – **40** and **43** – **46** were obtained via typical flash column chromatography (SiO₂) but required significant fraction pooling and concentration to observe product spots on TLC. Analogues **36** and **37** arise from the same reaction, as the boronic acid **36** decomposed to the resulting hydroxyl derivative **37** during column chromatography. Thus **37** was obtained through column chromatography, whereas **36** was isolated after organic solvent wash with DCM. Finally, analogue **41** was generated by Boc removal from compound **40** and was purified with an acetone wash, as the resulting salt was insoluble in this solvent.

3. Compound Activity Against Select Gram-negative Strains

Minimum inhibitory concentrations (MICs) are defined as the lowest antimicrobial concentration that prevents visible growth of an organism after 24 hours of incubation. MICs were performed by the Zgurskaya lab for each compound against select Gram-negative bacteria. Three different bacteria were chosen to conduct this assessment: *Escherichia coli* (BW), *Acinetobacter baumannii* (AB) and *Pseudomonas aeruginosa* (PAO). These bacteria were chosen in particular because they are part of the “ESKAPE” pathogens mentioned in chapter 1.

To evaluate MICs, we utilized strains of bacteria differing in membrane permeability and efflux efficiencies for each species. Wild-type (WT) bacteria refers to the typical form or phenotype that can be found in nature. Pore cells are hyperporinated cells that exhibit arabinose induced permeabilization of the outer membrane but still contain the wild-type

repertoire of efflux pumps.⁵⁸ Δ TolC cells are efflux-deficient derivatives that lack the outer membrane channel TolC used by most of the efflux pumps of *E. coli*. For *A. baumannii* and *P. aeruginosa*, different efflux pumps have been suppressed (Δ 3: AdeABC, AdeIJK, AdeFGH; Δ 6: Δ mexAB-oprM, Δ mexCD-oprJ, Δ mexXY, Δ mexJKL, Δ mexEF-oprN, Δ triABC). The final strain for each bacterium has been compromised both through hyperporination and efflux-deficiency. MIC values collected from these studies are expected to reveal which bacterial features (i.e., membrane integrity or efflux) present the biggest barrier to compound activity.

For each compound the MIC was determined using the 2-fold broth dilution method described by Clinical and Laboratory Standards Institute⁵⁹ with minor modifications. Bacterial cells were grown to 0.5 McFarland standard and stock solutions of compounds were prepared in DMSO. Serial dilutions were made in 96 well plates and the total volume was brought up to 100 μ l with modified M9 medium. Antibiotics such as azithromycin and ciprofloxacin were used as positive controls. The bacterial cells were inoculated and incubated at 37 °C for 24 h.

Category	Analogue	BW WT	BW Pore	Δ TolC MCS	Δ TolC Pore
Amide 1	1	>100	>100	>100	100
	2	>100	>100	>100	100
	3	>100	>100	>100	100
	4	>100	>100	>100	100
	5	>100	>100	>100	>100
	6	>100	>100	>100	>100
	7	>100	>100	>100	>100
	8	>100	>100	>100	>100
	9	>100	>100	>100	100
	10	>100	>100	>100	100
	11	>100	>100	>100	>100
	12	>100	>100	>100	100
	13	>100	>100	>100	>100

	14	>100	>100	>100	>100
	15	>100	>100	>100	>100
	16	>100	>100	>100	100
	17	>100	>100	>100	>100
	18	>100	>100	>100	100
	19	>100	>100	>100	>100
	20	>100	>100	>100	>100
Urea	21	>100	>100	>100	>100
	22	>100	>100	>100	>100
	23	>100	>100	>100	>100
	24	>100	>100	>100	>100
	25	>100	>100	>100	>100
	26	>100	>100	>100	>100
Sulfonamide	27	>100	>100	100	100
	28	>100	>100	>100	100
	29	>100	>100	>100	>100
	30	>100	>100	>100	>100
	31	>100	>100	>100	>100
	32	>100	>100	>100	>100
	33	>100	>100	>100	>100
	34	>100	>100	>100	>100
Amide 2	35	>100	>100	>100	>100
	36	>100	>100	>100	25
	37	>100	>100	>100	100
	38	>100	>100	100	100
	39	>100	>100	>100	25
	40	>100	>100	>100	>100
	41	>100	>100	>100	>100
	42	>100	>100	>100	>100
	43	>100	>100	>100	>100
	44	>100	>100	>100	>100
	45	>100	>100	100	100
46	>100	>100	>100	>100	

Table 6. MICs (μM) of select derivatives in *E. coli*

Category	Analogue	AB WT	AB Pore	$\Delta 3$ MCS	$\Delta 3$ Pore
Amide 1	1	>100	>100	>100	100
	2	>100	>100	>100	>100
	3	>100	>100	>100	>100
	4	>100	>100	>100	>100
	5	>100	>100	>100	>100
	6	>100	>100	>100	>100
	7	>100	>100	>100	>100

	8	>100	>100	>100	>100
	9	>100	>100	>100	100
	10	>100	>100	>100	100
	11	>100	>100	>100	>100
	12	>100	>100	>100	100
	13	>100	>100	>100	>100
	14	>100	>100	>100	>100
	15	>100	>100	>100	>100
	16	>100	>100	>100	100
	17	>100	>100	>100	>100
	18	>100	>100	>100	100
	19	>100	>100	>100	>100
	20	>100	>100	>100	>100
Urea	21	>100	>100	>100	>100
	22	>100	>100	>100	>100
	23	>100	>100	>100	>100
	24	>100	>100	50	25
	25	>100	>100	>100	>100
	26	>100	>100	100	100
Sulfonamide	27	>100	>100	>100	>100
	28	>100	>100	>100	>100
	29	>100	>100	>100	>100
	30	>100	>100	>100	>100
	31	>100	>100	>100	>100
	32	>100	>100	>100	>100
	33	>100	>100	>100	>100
	34	>100	>100	>100	>100
	35	>100	>100	>100	>100
Amide 2	36	>100	>100	100	50
	37	>100	>100	>100	>100
	38	>100	>100	100	100
	39	>100	>100	>100	>100
	40	>100	>100	>100	>100
	41	>100	>100	>100	>100
	42	>100	>100	>100	>100
	43	>100	>100	>100	>100
	44	>100	>100	>100	>100
	45	>100	>100	100	100
46	>100	>100	>100	>100	

Table 7. MICs (μM) of select derivatives in *A. baumannii*

Category	Analogue	PAO WT	PAO Pore	$\Delta 6$ MCS	$\Delta 6$ Pore
Amide 1	1	>100	>100	>100	>100
	2	>100	>100	>100	>100
	3	>100	>100	>100	>100
	4	>100	>100	>100	>100
	5	>100	>100	>100	>100
	6	>100	>100	>100	>100
	7	>100	>100	>100	>100
	8	>100	>100	>100	>100
	9	>100	>100	>100	100
	10	>100	>100	>100	100
	11	>100	>100	>100	100
	12	>100	>100	>100	>100
	13	>100	>100	>100	>100
	14	>100	>100	>100	>100
	15	>100	>100	>100	>100
	16	>100	>100	>100	100
	17	>100	>100	>100	>100
	18	>100	>100	>100	>100
	19	>100	>100	>100	>100
	20	>100	>100	>100	>100
Urea	21	>100	>100	>100	>100
	22	>100	>100	>100	>100
	23	>100	>100	>100	>100
	24	>100	>100	>100	100
	25	>100	>100	>100	100
	26	>100	>100	>100	50
Sulfonamide	27	>100	>100	>100	>100
	28	>100	>100	>100	>100
	29	>100	>100	>100	>100
	30	>100	>100	>100	>100
	31	>100	>100	>100	>100
	32	>100	>100	>100	>100
	33	>100	>100	>100	>100
	34	>100	>100	>100	>100
	35	>100	>100	>100	>100
Amide 2	36	>100	>100	>100	100/50
	37	>100	>100	>100	>100
	38	>100	>100	>100	100
	39	>100	>100	>100	25
	40	>100	>100	>100	>100
	41	>100	>100	>100	>100
	42	>100	>100	>100	100
	43	>100	>100	>100	100

	44	>100	>100	>100	>100
	45	>100	>100	>100	50
	46	>100	>100	>100	100

Table 8. MICs (μM) of select derivatives in *P. aeruginosa*

The first thing that can be noticed from **Tables 5-7** is that there is no activity against wild-type bacteria. This can mean one of three things, 1) the compounds do not have activity against the target, 2) the compounds fail to accumulate in bacteria with sufficient concentration or 3) a combination of poor target engagement and accumulation. Comparison between WT and mutant strain data suggests that the compounds are sensitive to efflux since strains having efflux deficiency are the only susceptible strains. This confirms the previous work on this chemotype that revealed this fragment to be an efflux substrate.²⁸ *P. aeruginosa* shows a very interesting profile as only when bacteria are efflux deficient and permeabilized are they susceptible. Nonetheless this preliminary data demonstrates antibacterial activity of this scaffold if analogs can be designed that accumulate in Gram-negative bacteria.

4. Conclusions and Future Directions

In conclusion, we developed and synthesized a library of *N*-acyl-difluorophenylalanines as putative activators of the bacterial caseinolytic protease P (ClpP). ClpP is an attractive target as it has diverse regulatory roles in bacteria and its disruption is detrimental to bacterial survival and/or virulence. The natural product acyldepsipeptides (ADEPs), on which our library is based, demonstrate bactericidal properties by artificially stimulating ClpP activity. This chemotype demonstrates

promising activity against Gram-positive bacteria but is inactive against Gram-negative bacteria due to permeation barriers and efflux pump recognition.

With our collaborators, our team designed different scaffolds based on the ADEP pharmacophore that were expected retain pharmacological activities but provide a chemotype amenable to rapid library development and physicochemical analysis goals. I was charged with synthesizing one of these libraries comprised on a linear scaffold inspired from the ADEP4 pharmacophore.

I synthesized 46 putative ClpP activators to generate a complete library. To synthesize these molecules a wide range of reactions involving the formation of amides, ureas and sulfonamides was performed. In addition, the compounds were assessed in MIC assays against Gram-negative bacteria to get an insight of the bacterial activity as well as the effects membrane integrity and efflux exhibit on this chemotype. We discovered that some of the simplified ADEP analogues exhibit activity if efflux recognition can be eliminated.

While the analysis of this 46-membered library represents a good start, the data set is too small to extract meaningful trends at this point. Overall, this library represents one of many that will comprise the total collection of compounds evaluated in this project in order to develop guiding principles for rational design of Gram-negative active compounds.

This library is the foundation of further research that is expected to have a significant impact on antibacterial drug discovery. In combination with parallel studies on unrelated chemotypes, this work and future studies will provide new insights towards the aim of

finding efficient antibiotics and developing a better understanding of Gram-negative accumulation.

Chapter 3

Design, Synthesis and Preliminary Assessment of *N*-Phenyl-1-Naphthylamine Derivatives

1. Introduction

As explained previously, *N*-phenyl-1-naphthylamine (NPN) is a hydrophobic fluorescent probe commonly used to assess the effect an external stressor (e.g., environmental changes, presence of antibiotic) has on the integrity of the bacterial outer membrane. If the bacterial membrane is compromised, NPN accumulates in phospholipid-based inner membrane resulting in a fluorescent signal. An intact outer membrane precludes NPN entry and thus binding to phospholipids, resulting in only a background fluorescent signal.

This property of NPN to give a fluorescence signal only in a lipophilic environment is a limitation to its use as general fluorescent probe but is an ideal characteristic for our interests in identifying molecular features that influence permeability. In the context of Gram-negative bacteria, the NPN fluorescence properties provide a very simple way to assess accumulation of derivatives of this chemotype. The overall idea was to generate a library of NPN derivatives with diverse functionalities in hopes of identifying analogues that permeate the outer membrane without the need of external stressors and avoid being recognized and extruded by efflux pumps. An accumulation of NPN analogues in the inner membrane of Gram-negative bacteria would provide insight into molecular features that influence outer membrane permeation and/or efflux pump recognition. Typically,

accumulation in bacteria is measured using mass spectrometry. Successful completion of this library and identification of derivatives that accumulate in the inner membrane phospholipid bilayer without compromised membranes and/or efflux pumps would provide yet another tool for elucidating features that influence permeation and accumulation.

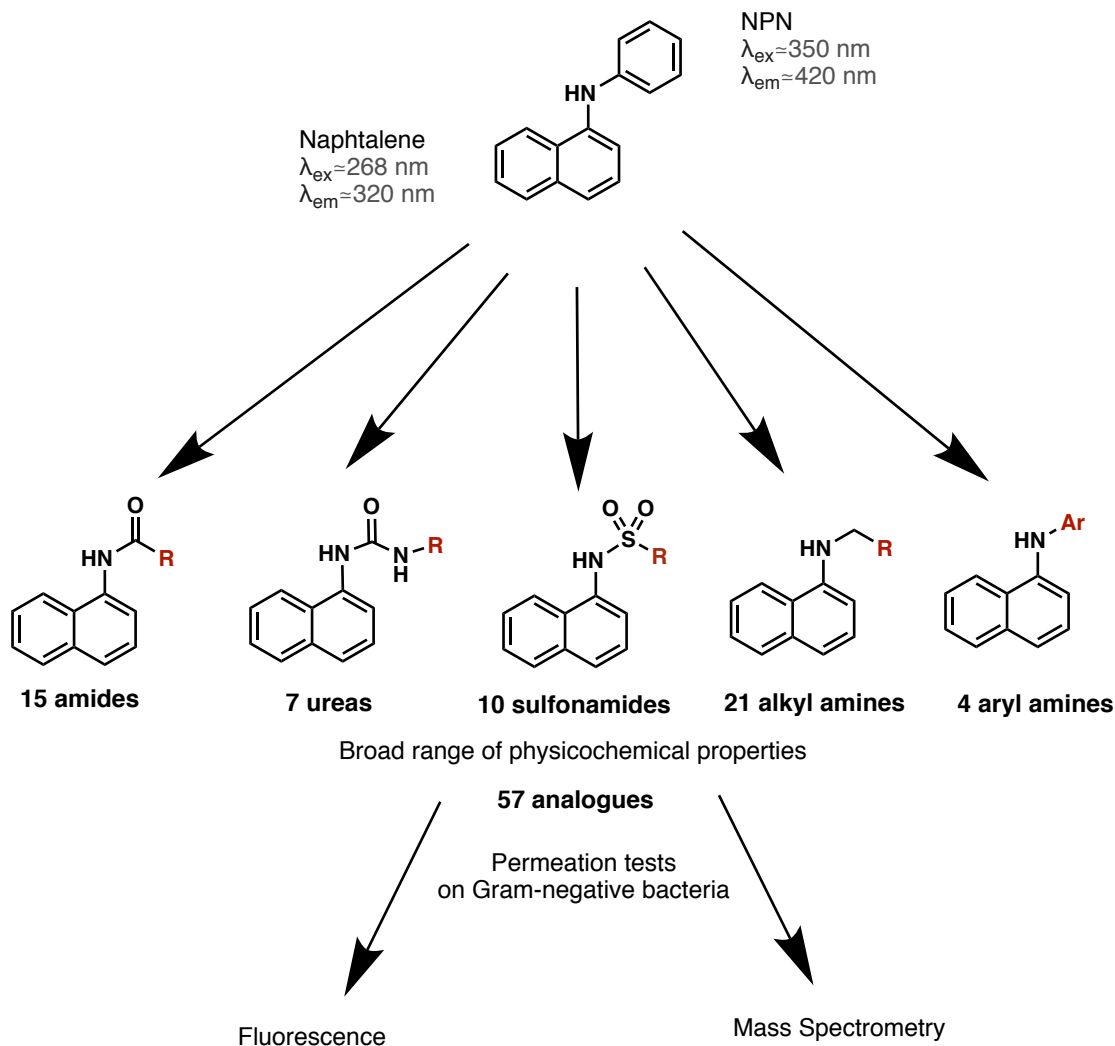


Figure 13. Summary of the NPN project

The NPN library was designed to use reagents already in hand (from the generation of other libraries) or reagents that could be obtained from others in the department. The

fluorescence characteristics of NPN are mainly due to the naphthalene group.⁶⁰ Therefore, that motif was maintained in our library and we chose to diversify the amine. Target analogues were classified into 5 categories: amides, ureas, sulfonamides, alkyl amines and aryl amines (**Figure 13**), comprising 57 analogues in total. The fluorescence profiles were determined for all derivatives. In addition, compound MICs against the same bacteria as in chapter 2, on three different species of bacteria (*E. coli*, *A. baumannii* and *P. aeruginosa*) including 4 different strains for each were determined. After future studies reveal accumulation profiles for each derivative, all data will be combined with the global library comprised of 200-500 compounds spanning 5-6 chemotypes in addition to 200+ known antibiotics for a large data analysis including cross-chemotype comparisons of physicochemical properties, MICs, accumulation data, and kinetic data. In the end, this NPN library was prepared as part of a larger effort to identify physicochemical properties that influence accumulation.

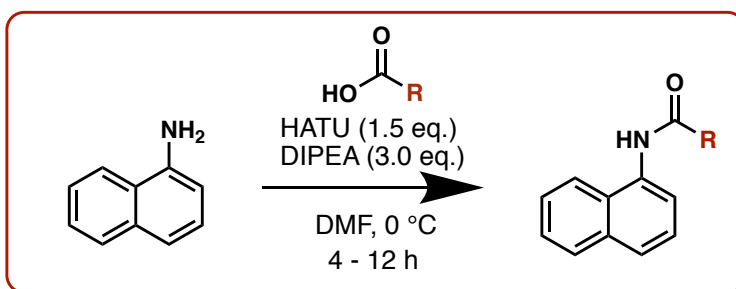
2. Synthesis of the Library

The synthesis of the NPN library proved to be more straight-forward than the ADEP pharmacophore library presented in chapter 2. First, the starting material used for most of the reactions, 1-naphthylamine, is commercially available. Therefore, reactions could be run without any requisite modifications to the starting material. NPN analogues are highly UV active, independent of the appendage attached, making reaction tracking and identification on TLC more feasible. Finally, NPN derivatives are relatively nonpolar, making them amenable to traditional flash column chromatography. In generating the

library, the only limiting factor originated from the attenuated reactivity of the 1-naphthylamine, which made some reactions quite challenging.

2.1. Synthesis of amides

The first subset of NPN derivatives comprised of amides. Target analogues (**Table 9**) were synthesized by exposing 1-naphthylamine to a variety of carboxylic acids in the presence of HATU and DIPEA in DMF at 0 °C (**Scheme 8**).



Scheme 8. Synthetic procedure for the generation of amide analogues

Amide Structure	An.	-R	An.	-R
	47	 52 %	55	 68 %
	48	 79 %	56	 37 %
	49	 97 %	57	 65 %

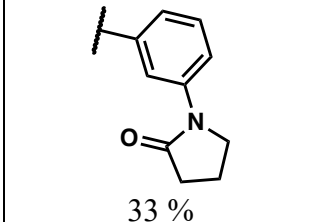
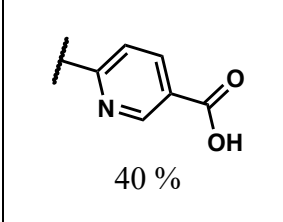
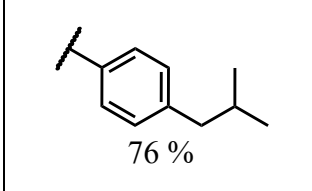
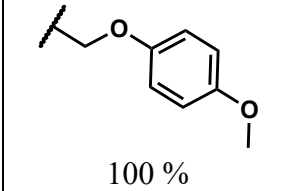
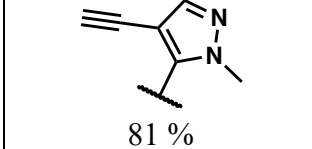
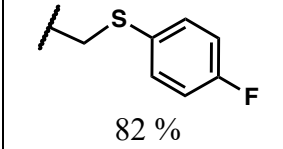
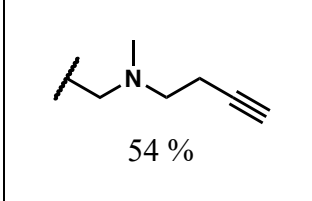
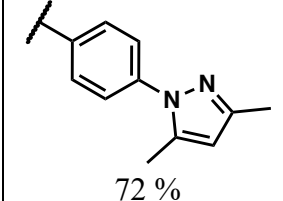
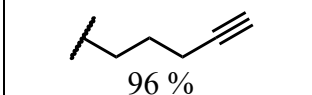
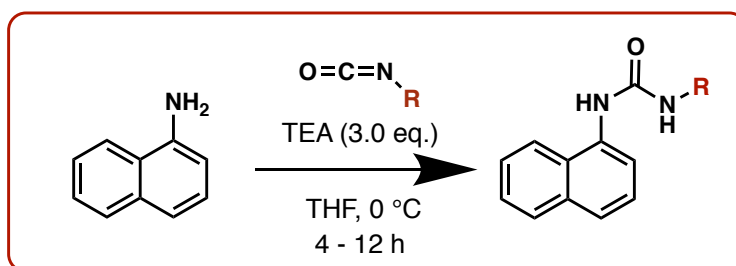
	50	 33 %	58 (D)	 40 %
	51	 76 %	59	 100 %
	52	 81 %	60	 82 %
	53	 54 %	61	 72 %
	54	 96 %		

Table 9 Amide analogues of the NPN library. (An.: analogue number, (D): deprotection,)

Desired compounds were obtained in modest to good yield, as shown in **Table 9**. Compounds **48**, **49** and **50** exhibited low solubility in organic solvents and thus were purified either with a methanol or acetone wash. Analogue **53** was first purified by flash column chromatography (SiO₂) but because of similar polarity to 1-naphtylamine, **53** could not be obtained in pure form using this purification method. Enough compound for evaluation, however, was obtained by pTLC. Every other compound, except for **58**, was purified through silica flash chromatography. Compound **58** was generated by the hydrolysis of **57** and did not require further purification as determined by NMR. In total, 15 amide-linked analogues were generated and characterized.

2.2. Synthesis of ureas

Urea derivatives (Table 10) were generated employing the same reaction methodology described in chapter 2, except that 1-naphthylamine was utilized instead of SM2 (Scheme 9). No particular issues were encountered for this reaction, as side products were rarely observed. However, from what we learned in chapter 2 regarding the formation of undesired amine products, we used ≤ 1 equivalent of each reactant.



Scheme 9. Synthetic procedure for the generation of urea analogues

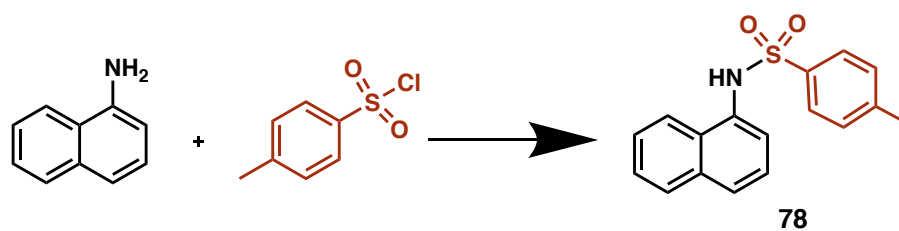
Urea Structure	Ref	-R	Ref	-R
	62	 40 %	66	 59 %
	63	 70 %	67 (D)	 100 %
	64 (D)	 52 %	68	 74 %
	65	 33 %		

Table 10. Urea analogues of the NPN library. (An.: analogue number, (D): deprotection)

The method of purification for each compound was determined depending on their solubility profile in organic solvents. Most of the analogues are insoluble in organic solvents. Therefore, compounds **62**, **63**, **65** and **68** were simply purified by a quick organic solvent wash. Compound **66** is soluble in dichloromethane and ethyl acetate and was purified by silica flash chromatography. Finally, analogues **64** and **67** were generated by the hydrolysis of **63** and **66**, respectively. To do so, we used lithium hydroxide and no further purification was needed, as determined by NMR. In total, 7 urea-linked analogues were generated and characterized.

2.3. Synthesis of sulfonamides

The third subset of the NPN library is comprised of sulfonamides. Initially, we attempted to utilize the same reaction conditions used in chapter 2 between an amine and a sulfonyl chloride with TEA in THF. However, under these reaction conditions numerous substrates revealed little to no conversion. We hypothesized that the poor nucleophilicity of the 1-naphthylamine was the culprit for poor conversion and thus investigated a number of conditions in attempts to push the reaction to the desired sulfonamides (**Table 11**).

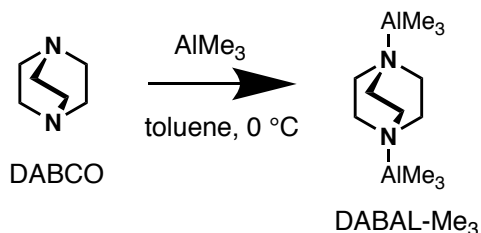


Entry	Base	Catalyst	Solvent	T (°C)	Yield
1	TEA (3 eq.)	-	THF	0 °C-rt	0
2	pyridine	DMAP (0.1eq)	pyridine	60 °C	0
3 ⁶¹	K ₂ CO ₃ (1 eq.)	-	solvent free	rt	0
4 ⁶²	Cs ₂ CO ₃ (0.1 eq.)	-	MeCN	25 °C	0
5	KOtBu (1.5 eq.)	DMAP (0.2eq)	THF	reflux	0
6 ⁶³	-	CuO (0.05eq)	MeCN	rt	0
7	NaH (1 eq.)	-	DCM	rt	0
8	<i>n</i> -BuLi (1 eq.)	-	THF	rt	0
9	<i>n</i> -BuLi (1 eq.)	-	toluene	rt	37 %
10	<i>n</i> -BuLi (1 eq.)	-	DMF	rt	0
11	<i>n</i> -BuLi (1 eq.)	DMAP (0.5eq)	DMF	0 °C	0
12	<i>n</i> -BuLi (1 eq.)	-	THF	-78 °C	0
13	LDA (1.1 eq.)	-	THF	-78 °C	0
14 ⁶⁴	-	DABAL-Me ₃	THF	40 °C-reflux	82%

Table 11. Optimization of reaction conditions for the synthesis of sulfonamides

Due to limited reagent availability, trial reactions were conducted with *p*-toluene sulfonyl chloride, a simple and affordable surrogate, to identify conditions. First, we tried to make the sulfonyl chloride more reactive by treatment with DMAP.⁶⁵ We postulated that we could overcome the poor reactivity of 1-naphthylamine by further activating the sulfonyl chloride. However, no conversion was observed under these conditions. Other reaction conditions that found success in the literature (e.g., reactions **3**, **4** and **6**) were attempted

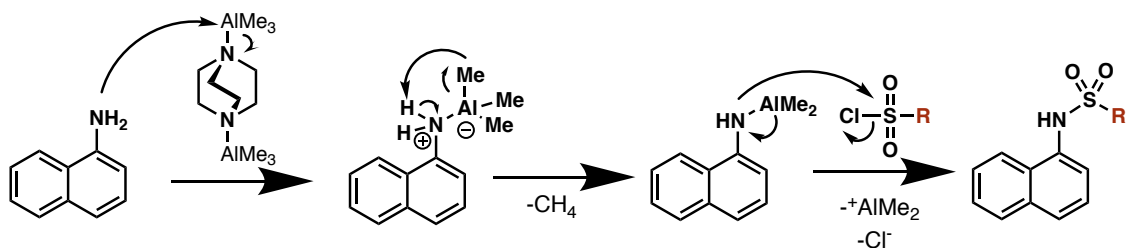
but failed to produce any desired product in our hands. It is worth noting that even though we used the exact same reaction conditions and reactants, reactions **3** and **4** failed to demonstrate any conversion of the starting material. Additionally, we tried to experiment with base mixtures, including KO*t*Bu with DMAP at reflux in THF (reaction **5**), but no desired product was formed. We hypothesized that the nucleophilicity of the naphthylamine nitrogen may be enhanced if it was deprotonated first. However, we failed to isolate any product with NaH, LDA or *n*-BuLi in a variety of solvents. However, when employing *n*-BuLi in toluene, the desired product was obtained in 37% yield. Unfortunately, these conditions proved to be unpredictable and difficult to reproduce. Finally, we attempted to activate the amine of 1-naphthylamine utilizing a DABCO aluminum complex (DABAL-Me₃), methodology developed by Novak and co-workers.⁶⁴ Under these conditions we were pleased to find a reproducible and high yielding conversion to the desired product.



Scheme 10. Aluminum complex (DABAL-Me₃) formation

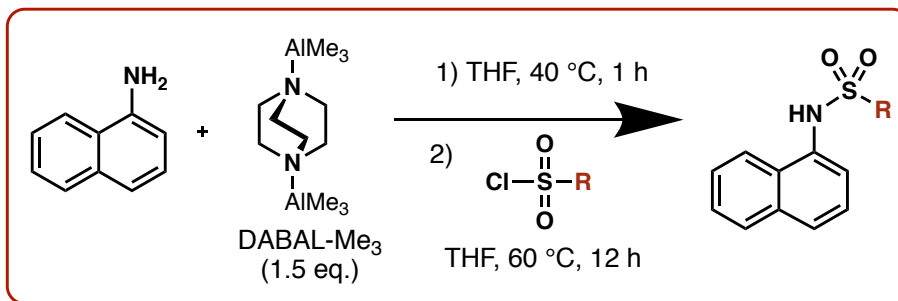
The aluminum complex functions similarly to the activation of amines observed with methyl aluminum. However, the DABAL-Me₃ complex provides several advantages compared to the traditional AlMe₃. For example, contrary to AlMe₃, DABAL-Me₃ is a non-pyrophoric solid that is air stable and can be easily manipulated. It provides all the properties of a strong Lewis acid, like AlMe₃, but in a safer and more controlled manner.

DABAL-Me₃ was generated following the guidelines of Biswas and co-workers⁶⁶ (**Scheme 10**) by adding methyl aluminum to a solution of DABCO in toluene at 0 °C, resulting in instantaneous formation of the desired product as a white precipitate. The purification and isolation of the complex was completed by washing with diethyl ether to ensure no AlMe₃ remained. In the literature, evidence demonstrates DABAL-Me₃ to be a versatile reagent that can be used to perform methyl cross coupling,⁶⁷⁻⁶⁹ alkylation of aldehydes,⁶⁶ form amide bonds^{64, 70} or ureas⁷¹⁻⁷³ but no evidence exists (that we can find) for the use of this complex to generate sulfonamides. In fact, we were surprised to find that few examples exist to sulfonylate aryl amines in general, presumably due to their lack of reactivity. Considering the importance of sulfonamides, especially in medicinal chemistry, we expect this DABAL-Me₃ sulfonylation methodology to find broad utility.



Scheme 11. Suggested mechanism of the sulfonamide formation using DABAL-Me₃

Because the reactivity of DABAL-Me₃ is expected to be similar to the reactivity of AlMe₃, the aluminum complex likely activates the amine after transferring from DABCO to the less sterically hindered 1-naphthylamine, resulting in the release of methane. Because of the difference of electronegativity between the nitrogen and the aluminum, the amine exhibits enhanced nucleophilicity and thus is poised to react with an eventual electrophile as depicted in **Scheme 11**.



Scheme 12. Synthetic procedure for the generation of sulfonamide analogues

The DABAL-Me₃ mediated sulfonylation conditions were then employed to generate the targeted analogues for the NPN library (**Scheme 12**).

Sulfonamide Structure	An.	-R	An.	-R
	69	 77 %	74 (D)	 59 %
	70 (D)	 83 %	75	 91 %
	71	 77 %	76	 44 %
	72	 93 %	77	 92 %

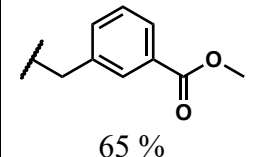
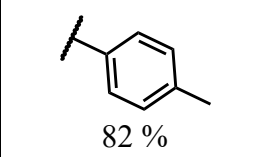
	73		78	
--	----	--	----	---

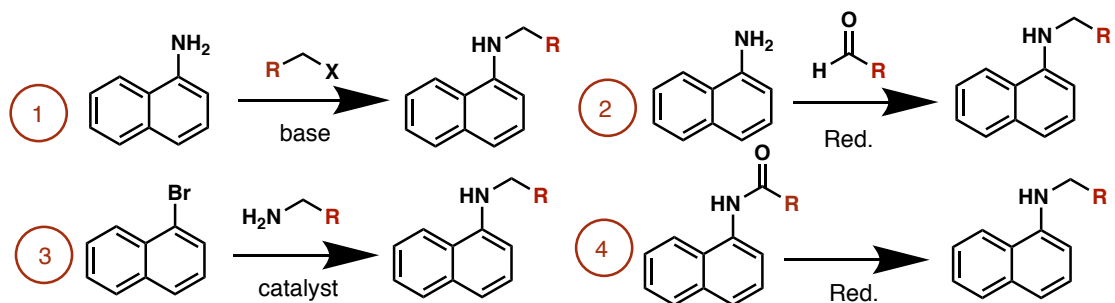
Table 12. Sulfonamide analogues of the NPN library. (An.: analogue number, (D): deprotection)

Desired compounds were obtained in good to modest yields and the reactions conditions provide broad scope and high reproducibility (**Table 12**). As typical, various purification techniques were employed depending on the substrate. Compounds **72**, **73**, **75**, **77** and **78** were isolated by flash column chromatography (SiO₂). Compound **72** had to be washed with diethyl ether after chromatographic separation due to an unidentified co-eluting impurity. Analogue **69** was purified using pTLC, as residual 1-naphthylamine co-eluted with the desired product. Compounds **71** and **76** were obtained by a simple wash due to low solubility in organic solvents. However, as seen before in chapter 2, the -*Ot*Bu in compound **71** cleaved during the reaction or the workup to give the free alcohol, which is likely in equilibrium with the pyridone tautomer.⁵⁶ Finally, analogue **70** and **74** were generated from the hydrolysis of **69** and **73**, respectively. After the deprotection, no further purification was needed, as determined by NMR. In total, 10 sulfonamide analogues were generated and characterized.

2.4. Synthesis of alkyl amines

This subset of the library was the most challenging. At the onset of our studies, we decided to preview a number of reaction conditions, ranging from alkylations to reductive aminations. While reductive amination is the typical method chosen to alkylate amines,

due to the formation of polyalkylated products under typical alkylation conditions, 1-naphthylamine exhibits attenuated nucleophilicity and thus we were uncertain what to expect.



Entry	Reaction	Base or Red.	Catalyst	Solvent	T (°C)	Yield
1	1	Cs ₂ CO ₃ (1.5 eq.)	-	DMF	50 °C	10 %
2	1	TEA (3 eq.)	-	DMF	80 °C	12 %
3	1	Cs ₂ CO ₃ (1.5 eq.)	TBAB (0.2 eq.)	DMF	80 °C	14 %
4	1	Cs ₂ CO ₃ (1.5 eq.)	TBAI (0.2 eq.)	DMF	80 °C	42 %
5 ⁷⁴	1	KOtBu (1.5 eq.)	TBAB (0.05 eq.)	DMSO	130 °C	5 %
6	1	Cs ₂ CO ₃ (1.5 eq.)	TBAI (0.5 eq.)	DMSO	130 °C	6 %
7	1	KOtBu (1.5 eq.)	TBAI (0.5 eq.)	toluene	80 °C	8 %
8	1	-	DABAL-Me ₃	THF	40 °C-reflux	0
9	1	-	DABAL-Me ₃ NaI (1 eq.)	THF	40 °C-reflux	0
10	1	Cs ₂ CO ₃ (1 eq.)	-	THF	25 °C (1 h) 60 °C (5 h)	0-81 %
11	2	LiAlH ₄ (1.2 eq.)	DABAL-Me ₃	THF	40 °C-reflux	77 %
12 ⁷⁵	3	K ₂ CO ₃ (1 eq.)	TBAB (0.75 eq.) (Ph ₂ P) ₂ Py (0.05 %) Pd(OAc) ₂ (0.025 %)	DMF	135 °C	0
13 ⁷⁶	3	K ₂ CO ₃ (2 eq.)	CuI (0.1 eq.) L-proline (0.2 eq.)	DMSO	75 °C	22 %
14	1	Ag ₂ CO ₃ (1.2 eq.)	-	DMF	25 °C (1 h) 60 °C (5 h)	0-60 %
15	4	LiAlH ₄ (3 eq.)	-	THF	rt	16-39 %

Table 13. Optimization of reaction conditions for the synthesis of alkyl amines. (reaction 1: N-alkylation, reaction 2: reductive amination, reaction 3: coupling reaction, reaction 4: amide reduction)

As shown in **Table 13**, 4 different methods were investigated to generate the desired disubstituted amines. We attempted classic alkylation conditions using alkyl halides and a base, but every attempt provided extremely low yields, regardless the base (e.g., Cs₂CO₃, TEA, KO^tBu, Ag₂CO₃), the solvent (e.g., DMF, THF, toluene, DMSO) or the temperature employed. Eventually, we investigated order of addition and the overall experimental method in attempts to improve the yield. For **entry 10**, 1-naphthylamine was stirred with cesium carbonate (or silver carbonate, **entry 14**) for an hour at 25 °C, at which time the alkyl halide was added prior to heating at 60 °C for 5 h (longer time points induced polyalkylation). Interestingly, the results from this approach proved to be very substrate specific. We obtained an excellent yield to generate analogue **80** but observed no conversion in attempts to generate analogue **79** (**Figure 14**). Consequently, we concluded that this reaction was narrow scope and relied on this method for only six derivatives.

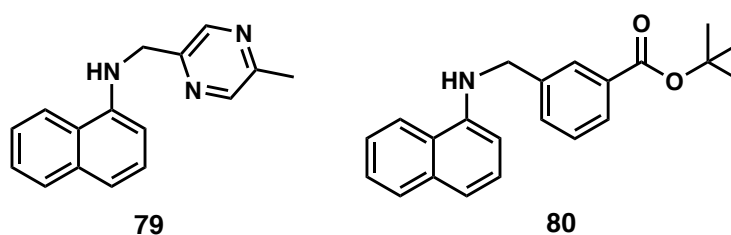


Figure 14. Structures of compounds 79 and 80

As mentioned previously, reductive amination was another method employed to generate target analogs. The power of reductive amination is that it avoids complications arising from over alkylation. We first attempted this approach to generate compound **92**

(**entry 11**) with a small amount of acetic acid to catalyze the imine formation. Acetic acid is commonly used as a catalyst in this reaction because it activates the aldehyde and thus often results in more rapid conversions. However, when monitoring the reaction by TLC, it was noticed that the reaction failed to progress to complete conversion even after heating and stirring overnight. At this point we hypothesized that a stronger Brønsted–Lowry or Lewis acid might result in more complete conversion. Drawing on previous results, we utilized the DABAL-Me₃ complex, which in theory would not only activate the aldehyde but also our amine. This would also represent a completely new use (i.e.; catalyst for reductive amination) of the aluminum complex and we were very pleased to see that the starting material was completely converted into the imine by TLC. Following addition of the reductive agent (i.e., LiAlH₄ or NaCNBH₃), without workup we obtained the desired amine. Interestingly, compounds **85** and **86** (**Figure 15**) come from the same reaction type except that **85** was obtained upon the use of NaCNBH₃ as the reductant, whereas **86** was generated using LiAlH₄. Even though this reaction works very well for several substrates, we have not been able to use it for all of target compounds because not all requisite aldehydes are commercially available. Based on our experience with these reaction conditions however, we are optimistic that this method is broadly applicable, as long as desired aldehydes can be generated or purchased. It is also worth noting that typical reductive amination conditions (i.e., without DABAL-Me₃) worked well enough for **83**, **88**, and **90** (**Figure 15**) to provide sufficient amounts of final compound for biological testing.

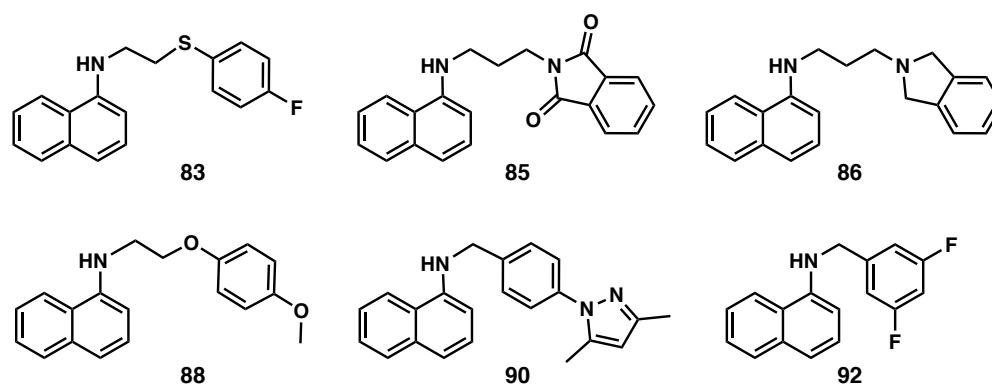


Figure 15. Structures of compounds 83, 85, 86, 88, 90 and 92

The third method we employed for the formation of target analogues was to couple an aryl halide (1-bromonaphthalene) to an alkyl amine. Initially, the Buchwald-Hartwig reaction, which uses palladium acetate (**entry 12**) was employed in attempts to generate analogue **94** (**Figure 16**) but was unsuccessful. Ullmann conditions (**entry 13**), which utilize copper instead of palladium provided a low yield, but enough product was produced for future biological studies. Due to the complexity of these conditions and inconsistency, it was only used to generate two derivatives, **84** and **94** (**Figure 16**), which could not be accessed through other means. In total, 22 amine-linked analogues were generated and characterized thanks to the combination of these four reactions (**Scheme 13**).

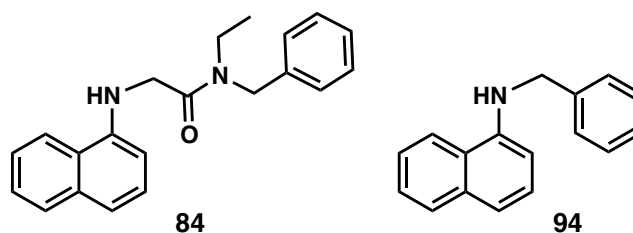
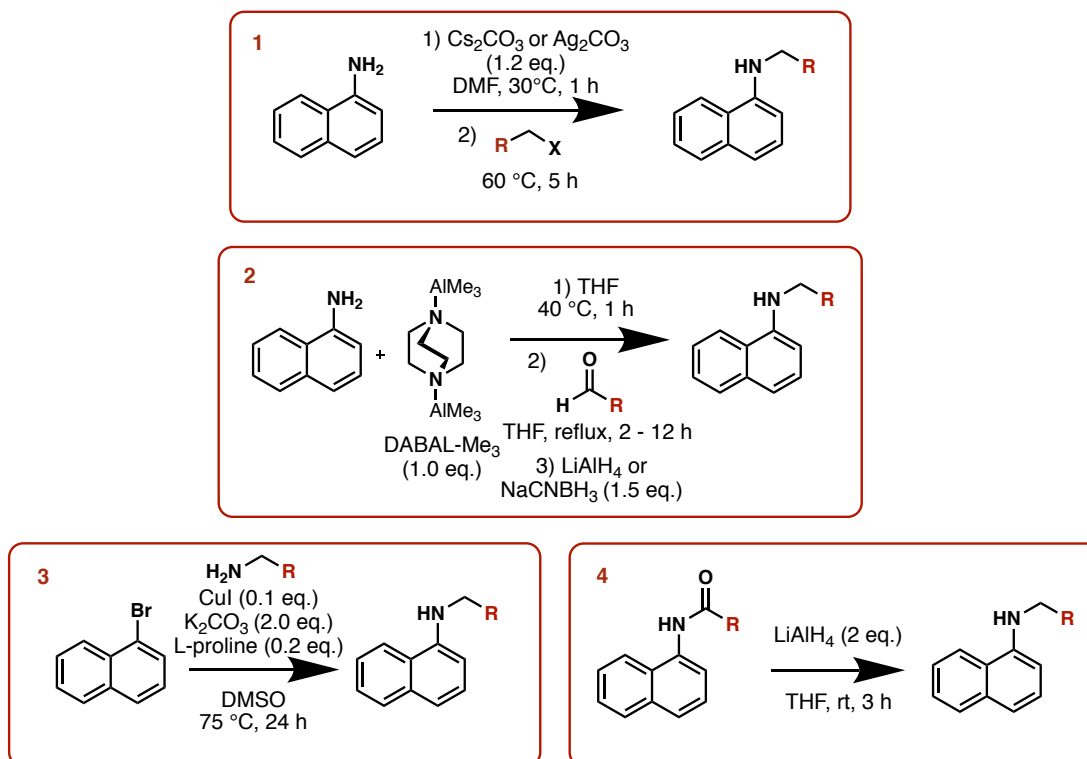


Figure 16. Structures of compounds 84 and 94



Scheme 13. Synthetic procedures for the generation of alkyl amine analogues. 1) N-Alkylation; 2) Reductive amination; 3) Ullmann coupling reaction; 4) Amide reduction

Alkyl Amine Structure	An.	-R	An.	-R
	79 (2)	 24 %	91 (1)	 51 %
	80 (1)	 81 %	92 (2)	 77 %
	81 (1)	 26 %	93 (1)	 60 %

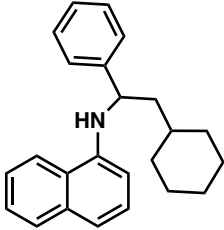
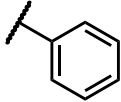
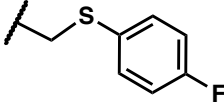
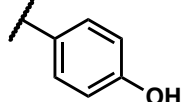
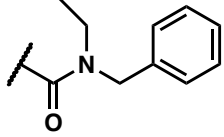
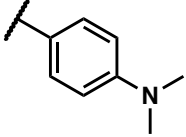
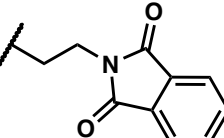
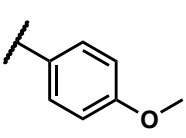
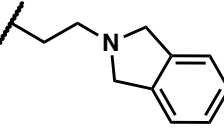
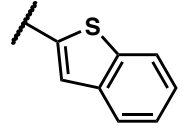
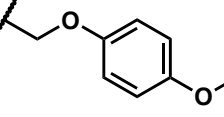
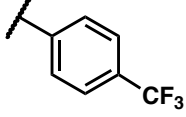
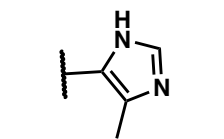
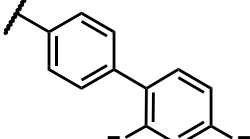
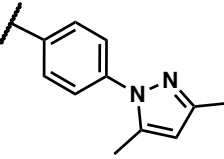
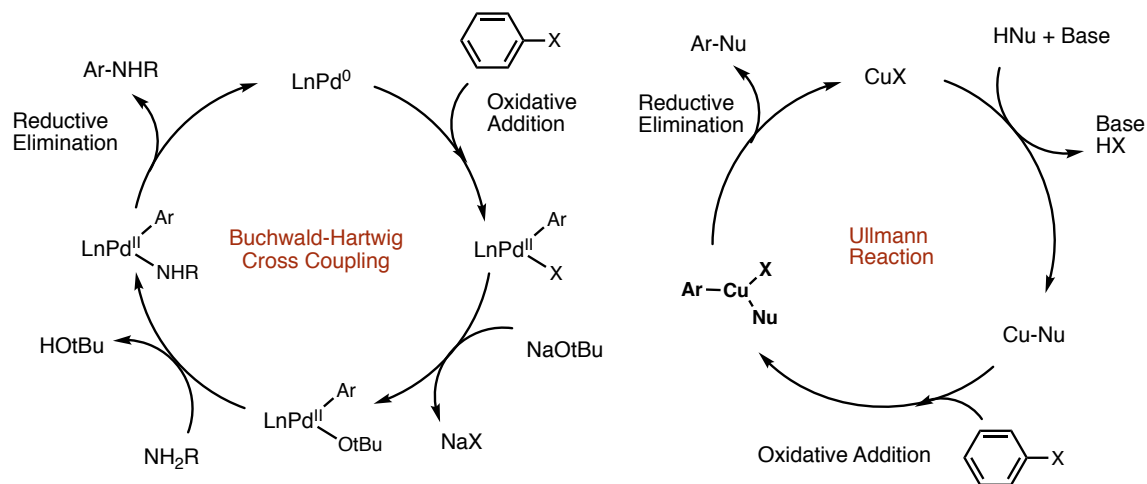
	82 (1)  34 %	94 (3)  22 %
	83 (4)  39 %	95 (2)  77 %
	84 (3)  16 %	96 (2)  54 %
	85 (2)  57 %	97 (2)  62 %
	86 (2)  20 %	98 (2)  65 %
	88 (4)  16 %	99 (2)  77 %
	89 (2)  52 %	100 (2)  66 %
	90 (4)  23 %	

Table 14. Alkyl amine analogues of the NPN library. (An.: analogue number, (X): reaction type)

Most of the amine-linked analogues exhibit good solubility in organic solvents and could be purified with standard flash column chromatography. Compounds **85**, **94** and **96**, however, were purified by pTLC due to co-eluting impurities that could only be separated through this small-scale purification method. Compound **89** is surprisingly a solid and was purified with an acetone wash.

2.5. Synthesis of aryl amines

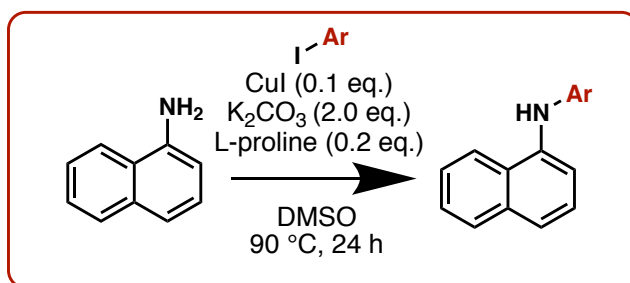
The final subset of the NPN library comprises disubstituted aryl amines, more truly mimicking the true NPN chemotype. Typically, one must employ metal-catalyzed (e.g., Pd or Cu) methods to couple two aryl subunits through a nitrogen linkage.



Scheme 14. Mechanism of the Buchwald-Hartwig⁷⁷⁻⁷⁸ and Ullmann reactions⁷⁹

The two best known synthetic methods for the arylation of amines are the Buchwald-Hartwig and the Ullmann coupling reactions. As mentioned previously, the Buchwald-Hartwig reaction employs palladium as the metal whereas Ullman conditions utilize copper (Scheme 14). For all substrates attempted, the Buchwald-Hartwig reaction

(reaction conditions: **Table 13, entry 12**) failed to provide any desired compound. However, we obtained low, albeit sufficient, yields for target compounds when the Ullmann reaction was employed with L-proline as the ligand and the aryl halide provided as the iodide. The procedure for the Ullmann reaction was taken from the 2003 work of Ma and co-workers⁷⁶ and allowed for the generation of four aryl amine derivatives, including NPN itself.



Scheme 15. Synthetic procedure for the generation of aryl amine analogues

Aryl Amine Structure	An.	-Ar	An.	-Ar
	101	 9 %	103	 10 %
	102	 9 %	104	 10 %

Table 15. Aryl amine analogues of the NPN library. (An.: analogue number)

The Ullmann reaction (**Scheme 15**) gave many colorful impurities that were difficult to remove from the desired product. In addition to the low yields, the purification of these compounds was challenging. The products have good solubility in organic solvents; thus, purification was performed either by flash column chromatography (SiO₂, **101** and **102**)

or pTLC (**103** and **104**). Even though the yields were low (**Table 15**), sufficient amounts of final compounds for biological evaluation were isolated. Future works on the synthesis of aryl amines should be based on the optimization of this reaction or the formation of more diverse analogues.

3. Fluorescence and Growth Inhibitory Profiles of Library Members

3.1. Excitation and emission optima

Prior to assessment for antibacterial and accumulation properties, the excitation and emission profile for each analog was determined. Because the parent molecule, NPN, exhibits enhanced fluorescence in lipophilic environments, the fluorescence profile of each analogue was assessed in the presence of bacterial lipids. To do this, an *E. coli* polar lipids extract, which forms unilamellar vesicles in aqueous solution, was utilized to mimic the inner membrane of *E. coli*. The assay was performed in a 96-well black microplate format. Each well contained a 100 μ L solution of NPN derivative (50 μ mol/L) and *E. coli* lipids (50 μ g/mL) in HMG buffer (5.0 % of HEPES-KOH (pH 7.0) solution; 0.1 % of 1 M MgSO₄ solution; 1.0 % of 40 % Glucose solution). Fluorescence measurements were obtained using a TECAN Infinite M200. The excitation and emission spectra were recorded with careful consideration of minimal distances to prevent any excitation light from the flash lamp reaching the detector.⁸⁰ For each compound, the excitation spectrum was recorded from 250 to 430 nm with the emission wavelength held constant at 464 nm and the emission spectrum was recorded from 284 to 550 nm with the excitation wavelength held constant at 250 nm. The blank signal (i.e., buffer and lipids) was

subtracted from the signal obtained by the NPN derivatives in the presence of lipids, and the data was normalized by dividing them by their highest RFU (Relative Fluorescence Signal) value to allow for the plotting of the excitation and emission spectra on a same graph with a Y-scale of 0 to 1. For each compound, the optimum excitation and emission wavelength was determined and the non-normalized highest emission fluorescence intensity (FI) is reported in **Table 16**. We used non-normalized values to compare each compound with their ability to give a fluorescent signal.

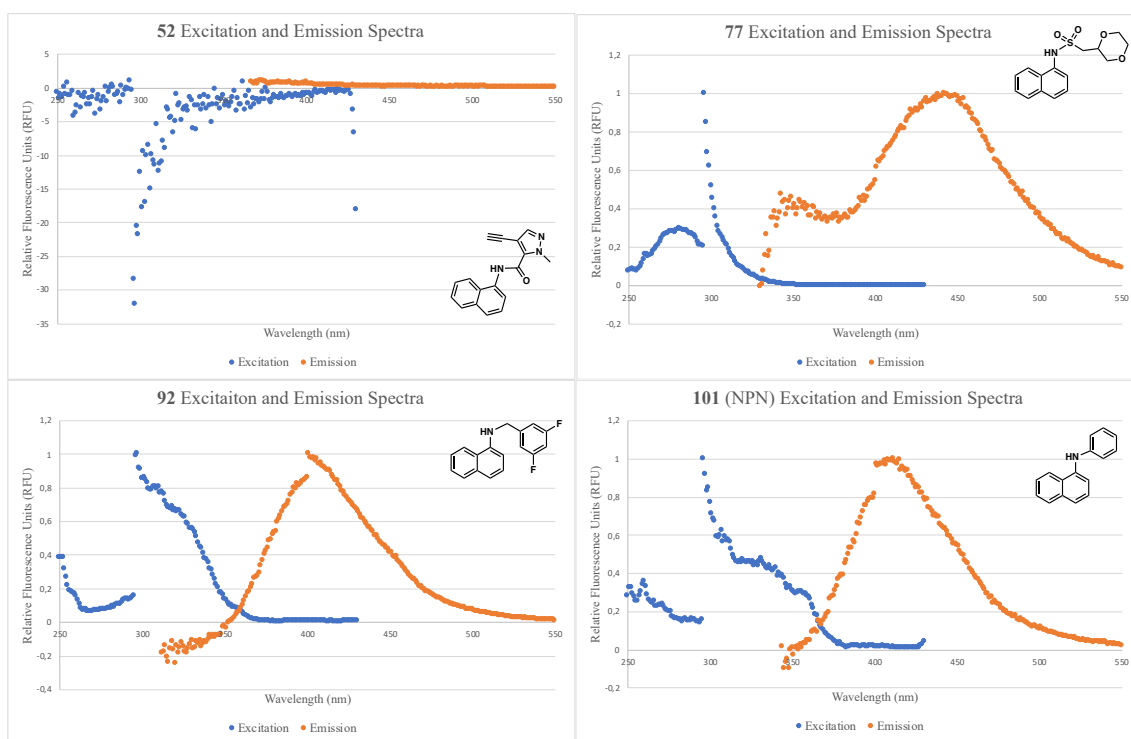


Figure 17. Excitation and emission spectra for compounds 52, 77, 92 and 101 (NPN) at a gain of 100 using the TECAN Infinite M200

Among the 55 NPN analogues evaluated, 46 compounds exhibited fluorescence in the presence of lipids by giving a signal higher than the background. Four examples of excitation and emission spectra where the blue and orange plots reference excitation and

emission measurements, respectively, are shown in **Figure 17**. Compound **52** exhibited no excitation and emission optima meaning that either it does not sequester in lipids, or it fails to exhibit detectable fluorescence properties in the wavelengths tested. Surprisingly, with compounds **50**, **53**, **54**, **58** and **69** (**Figure 18**) negative values for the excitation spectrum after blank subtraction were recorded, signifying lower fluorescence than the blank.

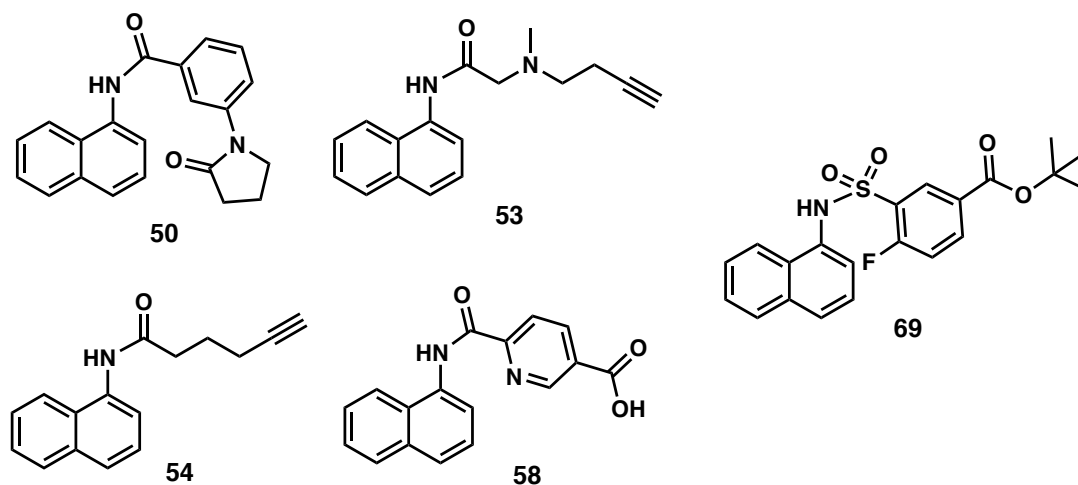


Figure 18. Structures of compounds **50**, **53**, **54**, **58** and **69**

Analogue	λ_{exc} max (nm)	λ_{em} max (nm)	FI	Analogue	λ_{exc} max (nm)	λ_{em} max (nm)	FI
47	364	397	17	76	296	417	148
48	295, 350	385, 387	44, 44	77	296	343, 442	162, 342
49	274, 350	422, 438	70, 67	78	296	428	23
50	0	0	0	79	296	447	248
51	310	374	43	80	296	401	49
52	0	0	0	81	296	421	2970
53	0	0	0	82	296	401	1102
54	0	0	0	84	296	411	1070
55	330	400	33	85	284	456	8
56	299	397	46	86	296	423	1948
57	0	0	0	88	296	406	832
58	0	0	0	89	296	424	2985

59	294	339	260	90	296	405	2269
61	282	453	8	91	296	406	1355
62	275	374	269	92	297	401	859
63	296	362	321	93	296	447	65
64	295	387	45	94	296	406	1054
65	296	354	804	95	296	441	1459
66	296	369	181	96	296	414	1088
67	296	377	1244	97	296	411	1301
68	300	357	368	98	296	402	1015
69	0	0	0	99	296	401	842
70	296, 364	422, 463	7, 6	100	296	401	1145
71	310	0	0	101 (NPN)	296	411	308
72	298	422	13	102	296	0	0
73	298	451	8	103	297	404	30
74	296	413	22	104	296	406	421
75	296	381	26				

Table 16. Excitation and emission optima of the NPN derivatives (50 $\mu\text{mol/L}$) in lipids (50 $\mu\text{g/ml}$) at a gain of 100 using the TECAN Infinite M200. (FI: fluorescence intensity of the emission optimum)

Interestingly and for reasons that still need to be explored, compound **77** and others (e.g., **48**, **49**, and **70**) in **Table 16** exhibit more than one optimum. Most of the NPN derivatives exhibit well-behaved spectra, for example **92** (**Figure 17**). Closer inspection of the data in **Table 16** reveals that the compounds exhibiting the highest emission fluorescence intensities recorded by the spectrofluorometer are typically amines, indicating either a better accumulation into lipid vesicles or enhanced fluorescence properties for this chemotype compared to others. Conversely, compounds that have the lowest fluorescence values tend to be amides, which suggests that this molecular functionality could dramatically attenuate fluorescent properties and/or decrease the ability of derivatives to sequester in lipophilic environments.

3.2. Emission coefficient determination

After determining which of the derivatives provided well-behaved fluorescence profiles, the emission coefficient was determined for each. This coefficient is representative how well a compound accumulates into lipids and this parameter is required for a mathematical model developed by Westfall and al.⁸¹ that will be employed for future accumulation studies of this NPN library. The model describes drug uptake into Gram-negative bacteria using two important kinetic parameters, the efflux and permeation constants, and is useful for calculating the rate of compound accumulation. In order to obtain this emission coefficient, a standard curve was determined for the fluorescent signal of each analogue in the presence of different lipid concentrations. Optimal excitation and emission wavelengths for each compound were utilized to maximize the fluorescence intensity and thus signal. For these studies we used a concentration of 50 $\mu\text{mol/L}$ for the NPN derivatives, as it demonstrated the best results (best reproducibility and best R^2) during preliminary trials with NPN and a range of lipid concentrations (100-6.25 $\mu\text{g/mL}$). The average blank signal (buffer + lipids at their respective concentration) was subtracted from each well and experiments were conducted in triplicate. Relative Fluorescence Units (Y-axis) were plotted in function of the respective lipid concentration (X-axis) in a scatter graph. Finally, the emission coefficient was determined by calculating the slope of the line of linear regression. A positive slope with a R^2 close to 1.0 signifies a quality curve indicating a predictable and concentration dependent accumulation of the compound into lipids. A negative slope and R^2 close to 0 signifies that there is no

correlation between the fluorescence signal and the accumulation of the compound into lipids under the conditions employed.

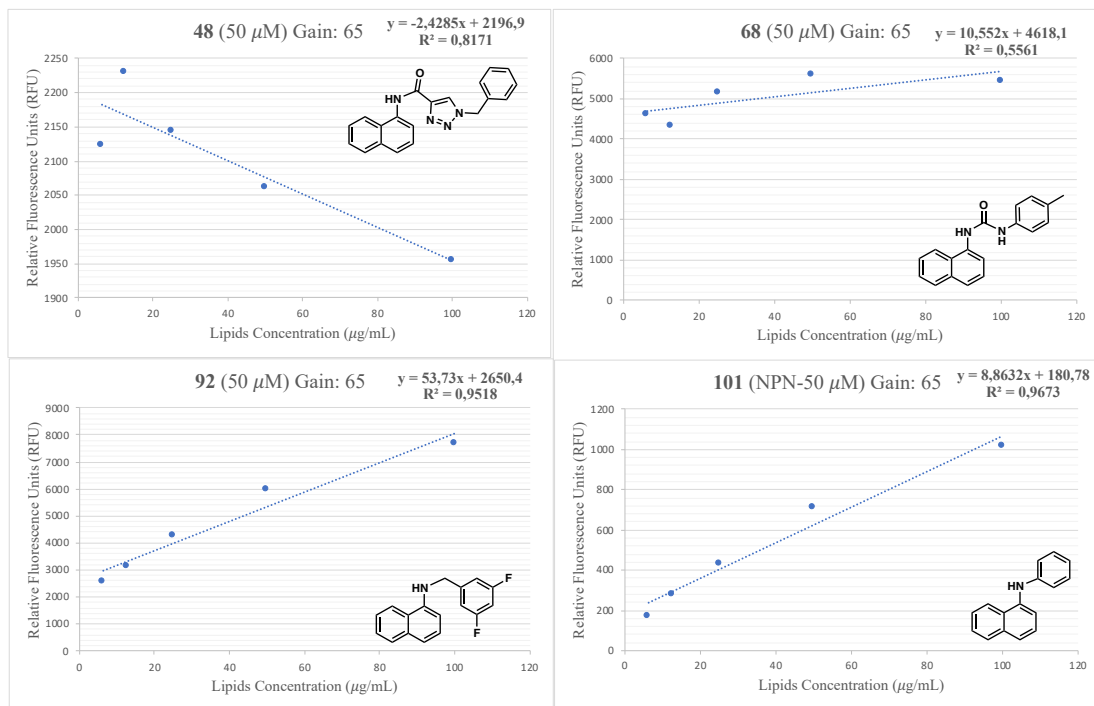


Figure 19. Emission coefficient graphs for analogues 48, 68, 92 and 101 (NPN) at a gain of

65

Mole. Funct.	Ref	λ_{exc} (nm)	λ_{em} (nm)	Emission coefficient	R^2	Gain	Emission coefficient	R^2	Gain
Amide	47	330	400	0.0323	0.6116	65	0.0907	0.8369	75
	48	295	385	-2.4285	0.8171	65	-11.559	0.5674	75
	49	274	422	32.1970	0.9375	65	88.237	0.9297	75
	51	310	374	-0.0481	0.6621	65	-0.1667	0.7659	75
	55	330	400	-0.0191	0.0381	65	-0.0353	0.116	75
	56	299	397	0.4441	0.9353	65	1.1969	0.9518	75
	59	294	339	-8.6946	0.4665	65	-28.841	0.8170	75
	61	282	453	-0.0829	0.5940	65	-0.1568	0.7766	75
Urea	62	275	374	0.1447	0.0919	65	0.1828	0.0053	75
	63	296	362	5.3053	0.3137	65	15.411	0.3765	75
	64	295	387	0.9805	0.9702	65	2.651	0.918	75
	65	296	354	-34.7460	0.9862	65	-102.3	0.9811	75
	66	296	369	-12.2750	0.7708	65	-33.969	0.7737	75

	67	296	377	-48.9840	0.5599	65	-41.488	0.1754	75
	68	300	357	10.5520	0.5561	65	34.333	0.7617	75
Sulfona.	70	296	422	0.2207	0.3916	65	0.5017	0.3452	75
	72	298	422	-0.1689	0.6560	65	0.2782	0.3983	75
	73	298	451	0.2044	0.8682	65	0.4157	0.8699	75
	74	296	413	-0.5485	0.0915	65	1.2265	0.5888	75
	75	296	381	0.1780	0.9130	65	0.5753	0.9813	75
	76	296	417	1.3243	0.0583	65	3.0957	0.0382	75
	77	296	422	-27.8160	0.9817	65	-72.295	0.9904	75
	78	296	428	2.1779	0.7646	65	8.0263	0.7570	75
Alkyl Amine	79	296	447	-3.0450	0.9319	65	-8.6262	0.9509	75
	80	296	401	1.6072	0.9989	65	4.4926	0.9983	75
	81	296	421	-0.9941	0.0121	65	-9.6586	0.0705	75
	82	296	401	28.2460	0.9915	65	76.857	0.9901	75
	84	296	411	34.5300	0.9970	65	91.009	0.9979	75
	85	284	456	-0.1975	0.9924	65	-0.5119	0.9723	75
	86	296	423	-25.7980	0.9154	65	-66.697	0.9234	75
	88	296	406	71.8640	0.9948	65	196.16	0.9935	75
	89	296	424	-52.2970	0.9902	65	-101.03	0.993	75
	90	296	405	44.5080	0.9964	65	119.46	0.9958	75
	91	296	406	40.7800	0.9998	65	110.19	0.9996	75
	92	297	401	53.7300	0.9518	65	147.1	0.9486	75
	93	296	447	-1.1236	0.9830	65	-2.6913	0.9281	75
	94	296	406	41.8230	0.9674	65	115.23	0.9674	75
95	296	441	-11.0550	0.9479	65	-27.113	0.9594	75	
96	296	414	45.9930	0.9949	65	118.23	0.9957	75	
97	296	411	54.5420	0.9912	65	143.62	0.9898	75	
98	296	402	62.8230	0.9955	65	166.14	0.9963	75	
99	296	401	25.4760	0.9721	65	69.682	0.9703	75	
100	296	401	26.4570	0.9923	65	73.19	0.9921	75	
Aryl Amine	101 (NPN)	296	411	8.8632	0.9673	65	25.801	0.9836	75
	103	297	404	-3.2658	0.5418	65	-15.578	0.4472	75
	104	296	406	20.9530	0.9530	65	58.661	0.9581	75

Table 17. Emission coefficients of the NPN derivatives (50 $\mu\text{mol/L}$) in lipids (6.25-100

$\mu\text{g/mL}$) using the TECAN Spark 10M. Green = satisfies emission coefficient, Yellow = does not satisfy emission coefficient.

Among the 46 fluorescent NPN derivatives analyzed, only 23 demonstrated a reasonable linear trend with a positive slope and a R^2 close to 1. The other half, such as compound 48 exhibited a negative slope and/or a poor R^2 value. Compound 92 is a good example of a nice linear trend, comparable to that obtained with 101 (NPN). Compounds highlighted

in green in **Table 16**, follow this well-behaved trend and accumulate in lipids in a concentration dependent fashion. Upon further analysis of the data in **Table 17** it becomes apparent that alkyl amines (13 out of 20) represent the most well-behaved subset, while the amides (3 out of 14) tend to exhibit the poorest profiles, similar to what was observed in the excitation/emission optima assay. It is worth noting that comparison of directly related derivatives only differing in linkage units (e.g., **59** to **88** and **61** to **90**) confirm that the amide linkage is enough to dramatically alter the fluorescent profile (**Figure 20**).

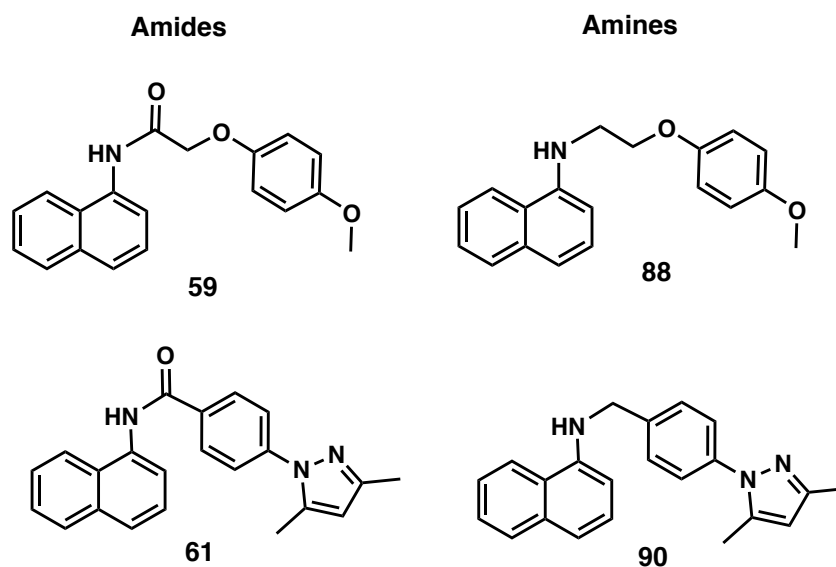


Figure 20. Structures of compounds **59**, **88**, **61** and **90**

The reason why some compounds fail to present expected fluorescent behavior still needs to be determined. The size of our library does not allow us to make final conclusions and more analogues need to be generated. The NPN library, however, provides an interesting compound set that will be evaluated for accumulation assays in future research.

➤ **Preliminary physicochemical property assessment of NPN derivatives**

Using QikProp within the Schrödinger Drug Discovery Suite, (Maestro 12.1.013) we calculated basic physicochemical properties (rotatable bonds, dipole, number of H-bond donors and acceptors, three-dimensionality/globularity, LogP, and subscription to Lipinski's rules of five) of the NPN derivatives with hopes of uncovering features that may influence the behavior in the lipid accumulation assay. All compounds were classified into two categories: successful NPN derivatives (S-NPN) and the NPN derivatives that failed to produce a reasonable emission coefficient, failed NPN derivatives (F-NPN).

	Rotatable Bonds ≤ 5	Dipole (Average)	Donor H Bonds (Average)	Acceptor H Bonds (Average)	Globularity (Average)	LogP < 5	Rules of 5
S-NPN	91%	3.93 $\sigma = 2.7$	1.24 $\sigma = 0.7$	2.77 $\sigma = 1.9$	0.83 $\sigma = 0.02$	61%	61%
F-NPN	96%	4.61 $\sigma = 2.1$	1.50 $\sigma = 0.6$	3.88 $\sigma = 1.7$	0.83 $\sigma = 0.02$	91%	91%

Table 18. Physicochemical property comparison between NPN derivatives that gave correct emission coefficients (S-NPN) and the ones that did not (F-NPN)

As seen in **Table 18**, and as expected, the physicochemical properties between the two classes (at least the ones calculated) are likely not the reason for dramatically different fluorescence profiles. The problem is likely more related to the unique fluorescent properties of each compound and more work is needed to identify the features that provide predictable lipid accumulation. However, it should be noted that this assessment of physicochemical properties is very limited and more detailed analyses with 20+ molecular features are underway.

➤ **Optimization trial**

Because emission coefficients are important to evaluating the accumulation of molecules in Gram-negative pathogens using fluorescence, we attempted to optimize the assay in hopes that the condition alteration could improve compound performance. To begin, we selected compound **47** (**Figure 21**), which has a positive but non-ideal R^2 value. We assessed compound and lipid concentrations in hopes of identifying a better proportionality between fluorescence and lipid concentrations. Experiments were completed in triplicate and, as before, the fluorescence emission from the blank (lipids at the respective concentration + buffer) was subtracted from the fluorescence emission of the NPN analogue in the presence of lipids. Results were plotted as before and the slope of the line of linear regression was calculated along with the R^2 values.

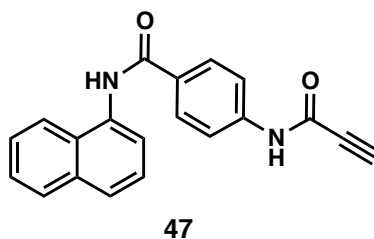


Figure 21. Structure of compound 47

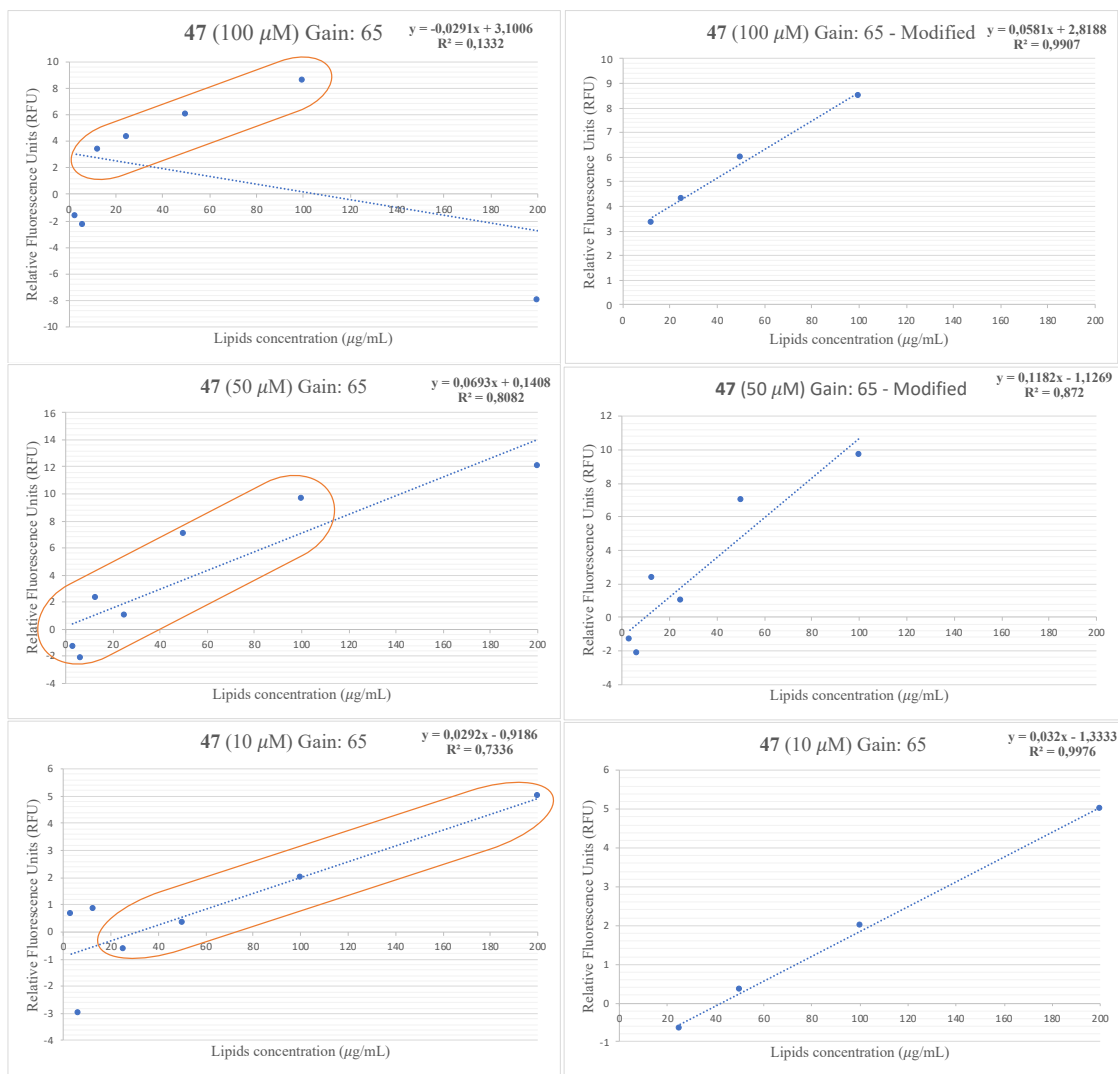


Figure 22. Optimization of the emission coefficient of compound 47 at a gain of 65

As seen in **Figure 22** with compound **47**, alteration of lipid and compound concentrations, dramatically improved the performance in the assay as we obtained a better R^2 . These results suggest that this optimization approach should be taken for all previous analogs that failed to provide reasonable fluorescence profiles. A lower concentration of NPN derivative could improve the data for these compounds and the whole study might be performed again under these conditions. However, initial attempts to employ this

optimization approach failed to improve the performance of compound **51**, which exhibited a negative slope in the initial conditions.

From our initial optimization assays, it seems to be that compounds that have a positive slope but an unacceptable R^2 can be improved. However, for reasons that still need to be determine, preliminary studies suggest that compounds that initially exhibited negative slopes in the emission coefficient studies cannot be improved through this approach.

3.3. MICs

As with the ClpP activator series, the Zgurskaya lab performed MIC assays for the NPN analogues against three different Gram-negative bacteria (*E. coli* - BW, *A. baumannii* - AB and *P. aeruginosa* - PAO) each of which consisted of four strains: wild-type (WT), a hyperporinated mutant (Pore), an efflux deficient mutant (Δ TolC MCS, Δ 3 MCS, or Δ 6 MCS), and a severely compromised mutant containing hyperporination and efflux deficiencies (Δ TolC Pore, Δ 3 Pore, or Δ 6 Pore).

Analogue	BW WT	BW Pore	Δ TolC MCS	Δ TolC Pore
NPN	>200	>200	50-100	50-100
47	>200	>200	25	12.5-25
69	>200	>200	>200	~ 25
92	>200	>200	50	25-50

Table 19. MICs (μ M) of active NPN derivatives in *E. coli*

Analogue	AB WT MCS	AbPore	Δ 3 MCS	Δ 3 Pore
NPN	>200	>200	>200	50
47	>200	>200	>200	6.25-12.5
69	>200	>200	>200	~ 50
92	>200	>200	>200	25

Table 20. MICs (μ M) of active NPN derivatives in *A. baumannii*

Analogue	PAO WT	PAO Pore	$\Delta 6$ MCS	$\Delta 6$ Pore
NPN	>200	>200	>200	50-100
47	>200	>200	>200	100
69	>200	>200	>200	>200
92	>200	>200	>200	50

Table 21. MICs (μM) of active NPN derivatives in *P. aeruginosa*

Among 55 NPN-derivatives tested, only 3 exhibited MICs (47, 69, and 92, Figure 23) in the concentration range tested. No obvious correlation between growth inhibition and molecular structure is obvious at this point. It is most likely that these hydrophobic compounds can diffuse and saturate the outer membrane leading to the cell death.

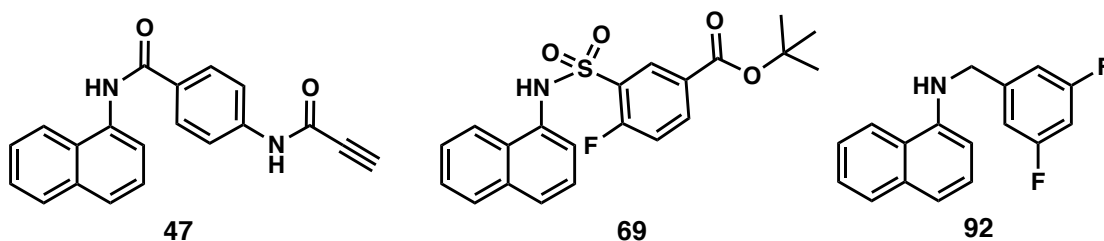


Figure 23. Structures of compounds 47, 69 and 92

4. Conclusions and Future Directions

In conclusion, a library of diverse NPN analogues was synthesized for ongoing initiatives aimed at determining molecule features that influence accumulation in Gram-negative bacteria. This library is unique in that it is comprised of a chemotype that exhibits fluorescence and thus is expected to provide an opportunity to monitor accumulation via fluorescence in parallel to mass spectrometry. We successfully designed and synthesized 57 NPN derivatives.

The primary challenge encountered in the synthesis of this library resulted from the low reactivity of 1-naphthylamine, making the formation of specific chemotypes difficult (e.g., sulfonamides and alkylamines). However, we successfully employed an aluminum-DABCO complex (DABAL-Me₃) to develop conditions for sulfonylation and reductive amination of 1-naphthylamine. As far as we can tell, these methodologies are vastly underexplored and/or utilized for the formation of sulfonamides and alkylated products. We believe this methodology will find broad utility in the functionalization of amines that exhibit attenuated nucleophilicity and further studies are ongoing to broaden the scope of this work.

The excitation and emission profile of each NPN derivative was determined and for compounds that demonstrated linear dose response fluorescence profiles in the presence of ligands, an emission coefficient was calculated. Among the 46 compounds that exhibited acceptable excitation/emission profiles, only 23 showed a positive linear trend line and a R² close to 1.0, allowing the emission coefficient to be determined. More work will need to be done in order to determine the issues facing the additional 23 analogs. Finally, we subjected the NPN library to MIC determinations against four Gram-negative bacteria (12 strains total) and surprisingly discovered 3 analogues that exhibited growth inhibitory activity against efflux deficient and/or hyperporinated strains.

Future studies for this library include finishing the determination of the emission coefficients and ensuring that the fluorescence profiles of this family are correctly characterized. Then, accumulation studies using both fluorescence and mass spectrometry will be performed with this library in collaboration with the Zgurskaya lab. Resulting data will be combined with that from other libraries and paired with kinetic models and

cheminformatic analyses with an aim of identifying physicochemical properties that influence Gram-negative accumulation.

Experimental Section and Spectral Characterization

1. Biochemical Procedures

Lipid preparation and micelle formation

E. coli Polar Lipid Extract (CAS: 1240502-50-4) from Avanti was received in chloroform (100 mg in 4 mL, 25 mg/mL) and stored at -20 °C. The lipid solution was split equally into 5 vials and the chloroform was evaporated under vacuum overnight at room temperature to provide 20 mg of lipids in each vial. Into each vial was added 1 mL of HEPES-KOH buffer (pH 7) and the vials were sonicated for 10 minutes. Finally, each vial was purged with nitrogen before being sealed and stored at -20 °C.

Excitation and Emission Spectra Recording

Excitation and emission spectra were recorded using 96-well black microplates and a TECAN Infinite M200 microplate reader. In triplicate, into each well was added 100 µL of a solution of 50 µmol/L NPN derivative and 50 µg/mL lipids (*E. coli* Polar Lipid Extract, Avanti) suspended in HMG buffer (2.5 mL HEPES.KOH (1 M pH 7.0), 0.5 mL 40 % Glucose, 0.05 mL 1 M MgSO₄ adjusted to 50 mL). A blank consisting of 100 µL of 50 µmol/L lipids in HMG buffer was also incorporated in triplicate in each plate. The excitation spectrum was recorded from 250 to 430 nm with the emission wavelength held constant at 464 nm. A minimal distance (MD) of 34 nm (9 nm excitation bandwidth + 20 nm emission bandwidth + 5 nm safety factor) was carefully maintained between the end of the excitation spectrum and the emission wavelength. The emission spectrum was recorded from 284 to 550 nm for each derivative with the excitation wavelength kept at

250 nm. An MD of 34 nm was also maintained between the excitation wavelength and the beginning of the emission spectrum. For both spectra, a step size of 1 nm, top mode and a gain of 100 was chosen. Data were processed with Microsoft Excel. The average relative fluorescence unit (RFU) of the blank was subtracted from the average RFU obtained by each NPN derivative in lipids and XY (scatter) plots representing RFU as a function of the wavelength were plotted. Excitation and emission optima were then determined.⁸⁰

	Excitation Spectrum	Emission Spectrum
Instrument	Tecan Infinite M200	Tecan Infinite M200
Excitation	250 – 430 nm	284 – 550 nm
Emission	464 nm	250 nm
Minimal Distance (MD)	Tecan Infinite M200 : 34 nm	Tecan Infinite M200 : 34 nm
Step size	1 nm	1 nm
Gain	100	100
Flash scan	25	25
Mode	Top mode	Top mode

Table 22. Parameters used for the excitation and emission determination

Emission Coefficient Determination

Extinction coefficients were determined using 96-well black microplates and a TECAN SPARK 10M microplate reader. In triplicate, each well was added 100 μ L of a solution of 50 μ mol/L NPN derivative and a gradient of lipid (*E.coli* Polar Lipid Extract, Avanti) concentrations: 6.25, 12.5, 25, 50 and 100 μ g/mL in HMG buffer (2.5 mL HEPES.KOH (1 M pH 7.0), 0.5 mL 40 % Glucose, 0.05 mL 1 M MgSO₄ adjusted to 50 mL). Blank wells consisted of 100 μ L lipids at each concentration in HMG buffer. Fluorescence values were recorded at the excitation and emission optimum of each compound at a gain of 65 and 75 with the top mode. Data were processed on Microsoft Excel. The average relative fluorescence unit (RFU) of each blank was subtracted from the average RFU obtained for each NPN derivative in the respective lipid concentration. XY (scatter) plots representing RFU as a function of lipid concentration were generated and the extinction coefficient was extracted as the slope of the corresponding linear regression line.

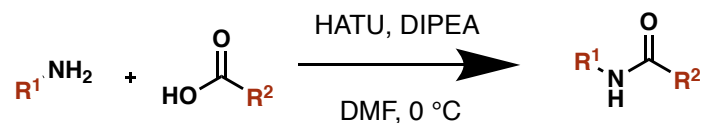
Parameters	
Instrument	Tecan Spark 10M
Excitation	Compound optimum
Emission	Compound optimum
Gain	65 and 75
Z-Position	20000 μ m
Flashes	30
Mode	Top mode

Table 23. Parameters used for the emission coefficient determination

2. Compound Synthesis and Characterization

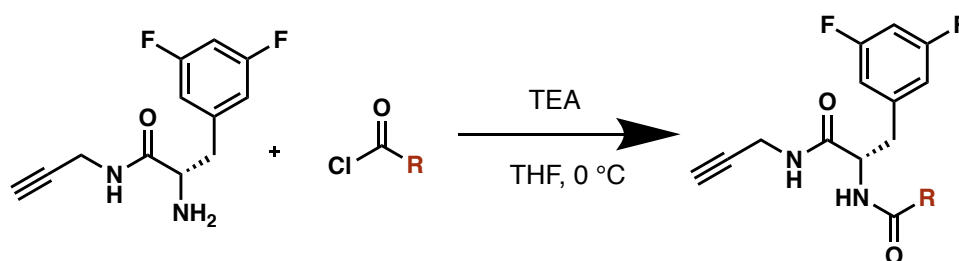
General synthetic information

All commercial reagents were used without further purification. Distilled water was used for all water necessities in synthetic procedures (e.g., reagent, solvent, work-up). All reactions were run with anhydrous solvents. Flash column chromatography was performed with silica gel 60. TLC analyses were completed with EMD Millipore silica gel coated (250 μ M) F254 glass plates and visualized with UV light (254 nm) or alkaline KMnO_4 solution, followed by gentle heating. NMR data were all collected on a 300, 400, or 500 MHz (specified below) Varian VNMRS Direct Drive spectrometer equipped with an indirect detection probe. Data was collected at ambient temperature unless otherwise stated using standard pulse methods as supplied by Varian VNMRJ 4.2 software. Coupling constants are quoted to the nearest 0.1 Hz and multiplicities are given by the following abbreviations and combinations: m (multiplet), s (singlet), d (doublet), dd (doublet of doublets), ddd (doublet of doublet of doublets), t (triplet), td (triplet of doublets), tt (triplet of triplets), q (quartet). All NMR data was processed in MestreNova v12.0.2. Peak positions are reported after reference centering on deuterated solvent of relevance.



General Procedure 1: Synthesis of amide analogues using carboxylic acids

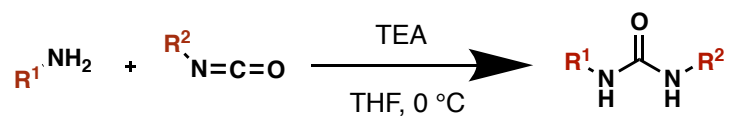
To a solution of amine (1.0 eq.), carboxylic acid (1.5 eq.) and HATU (1.5 eq.) in dry DMF at 0 °C was added DIPEA (3.0 eq.). The reaction mixture was stirred for 4 - 12 h and then quenched with a saturated aqueous solution of NaHCO₃ and diluted with ethyl acetate. The aqueous layer was extracted with ethyl acetate (3 times) and the organic layers were combined and washed with H₂O (3 times) and then a saturated aqueous solution of NaCl before being dried over anhydrous Na₂SO₄ and filtering. Volatiles were removed by rotary evaporation and the crude product was purified by flash column chromatography (SiO₂), pTLC, or organic solvent washes (i.e., the organic solvent was added into the vial and mixed with the solid decanting).



General Procedure 2: Synthesis of amide analogues using acyl chlorides

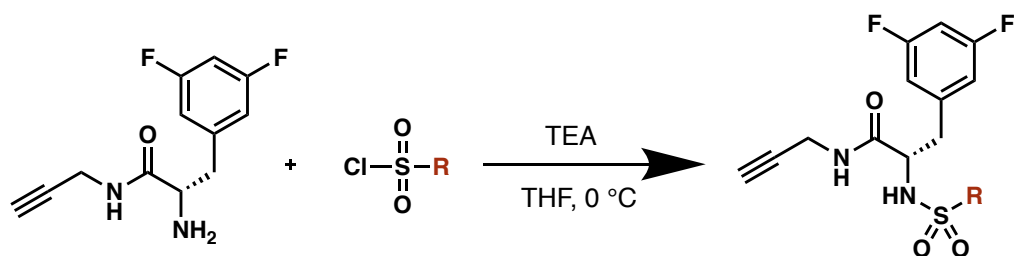
To a solution of amine (1.0 eq.) in dry THF at 0 °C was added TEA (3.0 eq.) and the reaction was stirred for 15 min before the acyl chloride (1.5 eq.) was added. The reaction mixture was stirred for 4 h – 12 h and then quenched with a saturated aqueous solution of

NaHCO₃ and diluted with ethyl acetate. The aqueous layer was extracted with ethyl acetate (3 times) and the organic layers were combined and washed with H₂O (3 times) and then with a saturated aqueous solution of NaCl before being dried over anhydrous Na₂SO₄ and filtered. Volatiles were removed by rotary evaporation and the crude product was purified by flash column chromatography (SiO₂).



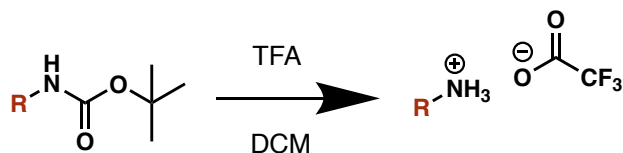
General Procedure 3: Synthesis of urea analogues from isocyanates

To a solution of amine (1.0 eq.) in dry THF at 0 °C was added TEA (3.0 eq.) and the reaction was stirred for 15 min before the isocyanate (1.0 eq.) was added. The reaction mixture was stirred for 4 – 12 h and then quenched with a saturated aqueous solution of NaHCO₃ and diluted with ethyl acetate. The aqueous layer was extracted with ethyl acetate (3 times) and the organic layers were combined and washed with H₂O (3 times) and then with a saturated aqueous solution of NaCl before being dried over anhydrous Na₂SO₄ and filtering. Volatiles were removed by rotary evaporation and the crude product was purified by flash column chromatography (SiO₂) or an organic solvent wash (the organic solvent was added into the vial and mixed with the solid before decanting).



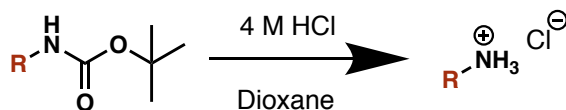
General Procedure 4: Synthesis of sulfonamide analogues from sulfonyl chlorides

To a solution of amine (1.0 eq.) in dry THF at 0 °C was added TEA (3.0 eq.) and the reaction was stirred for 15 min before the sulfonyl chloride (1.5 eq.) was added. The reaction mixture was stirred for 4 – 12 h and then quenched with a saturated aqueous solution of NaHCO₃ and diluted with ethyl acetate. The aqueous layer was extracted with ethyl acetate (3 times) and the organic layers were combined and washed with H₂O (3 times) and then with a saturated aqueous solution of NaCl before being dried over anhydrous Na₂SO₄ and filtered. Volatiles were removed by rotary evaporation and the crude product was purified by flash column chromatography (SiO₂), pTLC, or organic solvent washes (the organic solvent was added into the vial and mixed with the solid before decanting).



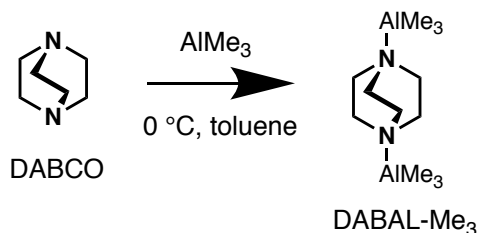
General Procedure 5: Boc deprotection with TFA

To a solution of Boc protected amine (1.0 eq.) in dry DCM was added a solution of TFA (>10.0 eq.). The reaction mixture was stirred at room temperature 3 - 12 h. The crude product was concentrated through a nitrogen flow, diluted in DCM and evaporated again. No purification was needed.



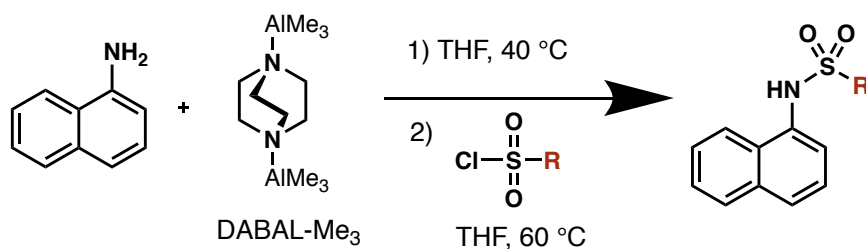
General Procedure 6: Boc deprotection using 4M HCl in Dioxane

To Boc protected amine solid (1.0 eq.) was added a solution of 4M HCl in Dioxane (>10.0 eq.). The reaction mixture was stirred at room temperature 2 - 12 h. The crude product was concentrated through a nitrogen flow, diluted in DCM and evaporated again. The resulting salt was purified with acetone washes (the organic solvent was added into the vial and mixed with the solid before decanting).



Complex Formation : DABAL-Me₃

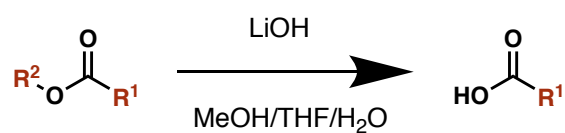
To a solution of DABCO (652.0 mg, 5.813 mmol, 1.0 eq.) in toluene (6 mL) at 0 °C was added carefully AlMe₃ (10.404 mmol, 1.79 eq.). The reaction mixture was stirred for few minutes and the resulting white precipitate was allowed to settle. The supernatant was removed and the precipitate was washed with diethyl ether (5 x 3 mL). The white solid was dried under vacuum to obtain DABAL-Me₃. The aluminium complex was stored under nitrogen and placed in a dry-box at room temperature.⁶⁶



General Procedure 7: Sulfonylation of aryl amine using DABAL-Me₃ for the synthesis of NPN-sulfonamide analogues

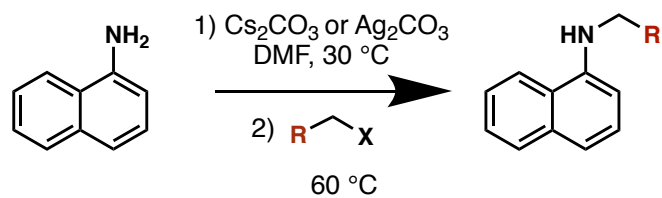
A solution of 1-naphthylamine (1.5 eq.) and DABAL-Me₃ (1.5 eq.) in dry THF was allowed to stir for 1 h at 40 °C under nitrogen. Sulfonyl chloride (1.0 eq.) was then added and the reaction mixture was stirred overnight at reflux. The solution was cooled to room temperature, quenched with aqueous 1 M HCl and diluted with ethyl acetate. The aqueous

layer was extracted with ethyl acetate (3 times) and the organic layers were combined and washed with H₂O (3 times) and then with a saturated aqueous solution of NaCl before being dried over anhydrous Na₂SO₄ and filtering. Volatiles were removed by rotary evaporation and the crude product was purified by flash column chromatography (SiO₂), pTLC, or organic solvent washes (the organic solvent was added into the vial and mixed with the solid before decanting).⁶⁴



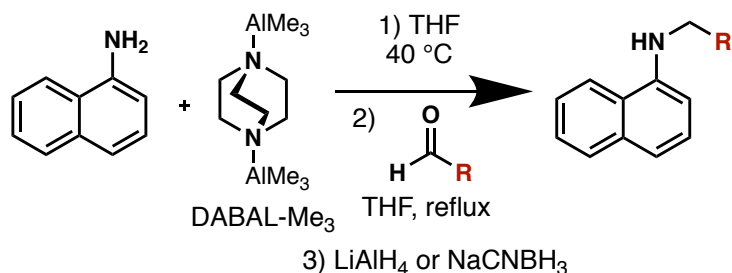
General Procedure 8: Ester hydrolysis

The ester (1.0 eq.) was dissolved in a mixture of THF/MeOH/H₂O (3:1:2) and LiOH, H₂O (7.0 eq.) was added. The reaction mixture was stirred at room temperature 3 – 12 h. The solvents were evaporated and the residue was acidified with 1 M aqueous HCl to pH 1 before being extracted with ethyl acetate, dried over anhydrous Na₂SO₄ and filtered. The organic solvent was evaporated and no purification was needed.



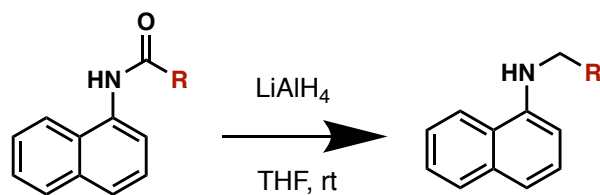
General Procedure 9: N-Alkylation using Cs_2CO_3 for the synthesis of NPN-amine analogues

A solution of 1-naphthylamine (1.2 eq.) and Cs_2CO_3 (or Ag_2CO_3) (1.2 eq.) in DMF was stirred at 30 °C for 1 h and alkyl halide (1.0 eq.) was added dropwise. The reaction mixture was stirred 5 h at 60 °C and then quenched with a saturated aqueous solution of NaHCO_3 and diluted with ethyl acetate. The aqueous layer was extracted with ethyl acetate (3 times) and the organic layers were combined and washed with H_2O (3 times) and then with a saturated aqueous solution of NaCl before being dried over anhydrous Na_2SO_4 and filtering. Volatiles were removed by rotary evaporation and the crude product was purified by flash column chromatography (SiO_2) or pTLC



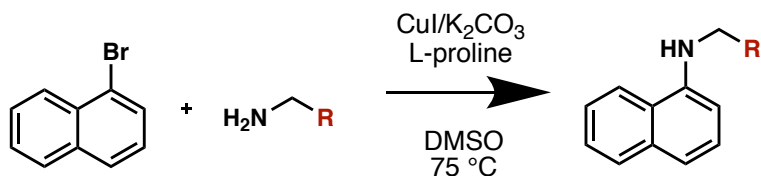
General Procedure 10: N-Alkylation using reductive amination for the synthesis of NPN-amine analogues

A solution of 1-naphthylamine (1.0 eq.) and DABAL-Me₃ (1.0 eq.) in dry THF was allowed to stir for 1 h at 40 °C under nitrogen. Aldehyde (1.0 eq.) was then added and the reaction mixture was stirred 2 – 12 h at reflux until imine formation is complete. The solution was cooled to room temperature and the reductive agent LiAlH₄ or NaCNBH₃ (1.5 eq.) was added. The solution was stirred again 2 – 12 h until the reaction is complete, then quenched dropwise with a saturated aqueous solution of NaHCO₃ and diluted with ethyl acetate. The aqueous layer was extracted with ethyl acetate (3 times) and the organic layers were combined and washed with H₂O (3 times) and then with a saturated aqueous solution of NaCl before being dried over anhydrous Na₂SO₄ and filtering. Volatiles were removed by rotary evaporation and the crude product was purified by flash column chromatography (SiO₂) or pTLC.



General Procedure 11: Amide Reduction for the synthesis of NPN-amine analogues

To a solution of amide (1.0 eq.) in THF at room temperature was added LiAlH_4 (2 eq.). The reaction mixture was stirred 3 h and then quenched carefully with a saturated aqueous solution of NaHCO_3 and diluted with ethyl acetate. The aqueous layer was extracted with ethyl acetate (3 times) and the organic layers were combined and washed with H_2O (3 times) and then with a saturated aqueous solution of NaCl before being dried over anhydrous Na_2SO_4 and filtering. Volatiles were removed by rotary evaporation and the crude product was purified by flash column chromatography (SiO_2).



General Procedure 12: N-Alkylation using Ullmann coupling conditions from 1-bromonaphthalene and alkyl amines

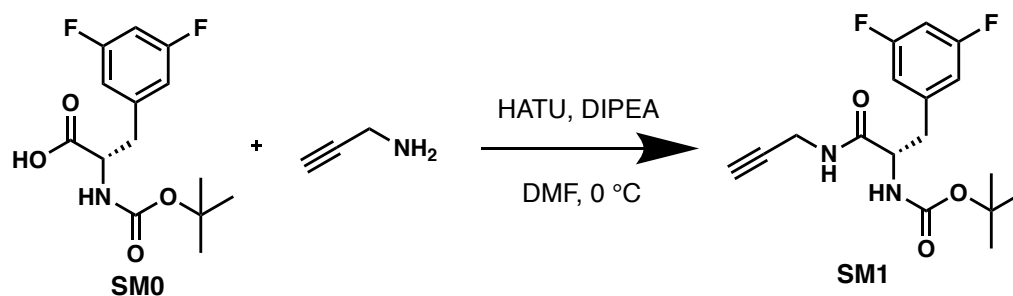
A solution of 1-bromonaphthalene (1.0 eq.), alkyl amine (1.5 eq.), CuI (0.1 eq.), K_2CO_3 (2.0 eq.) and L-proline (0.2 eq.) in DMSO was stirred 24 h at 75°C . The reaction mixture was allowed to cool at room temperature and then quenched with a saturated aqueous solution of NaHCO_3 and diluted with ethyl acetate. The aqueous layer was extracted with

ethyl acetate (3 times) and the organic layers were combined and washed with H₂O (3 times) and then with a saturated aqueous solution of NaCl before being dried over anhydrous Na₂SO₄ and filtering. Volatiles were removed by rotary evaporation and the crude product was purified by flash column chromatography (SiO₂) or pTLC.⁷⁶



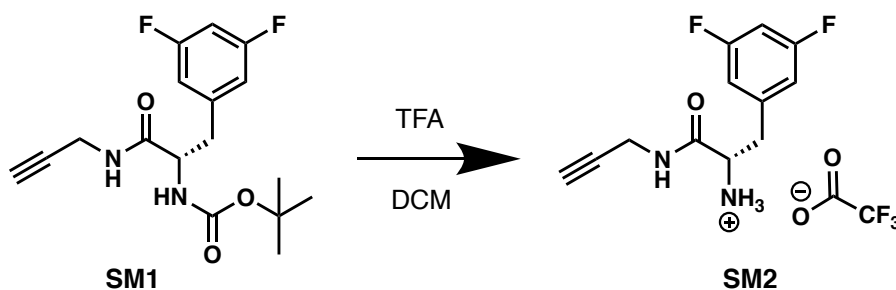
General Procedure 13: N-Alkylation using Ullmann coupling conditions from 1-naphthylamine and iodo arenes

A solution of 1-naphthylamine (1.5 eq.), iodo aryl (1.0 eq.), CuI (0.1 eq.), K₂CO₃ (2.0 eq.) and L-Proline (0.2 eq.) in DMSO was stirred 24 h at 90 °C. The reaction mixture was allowed to cool at room temperature and then quenched with a saturated aqueous solution of NaHCO₃ and diluted with ethyl acetate. The aqueous layer was extracted with ethyl acetate (3 times) and the organic layers were combined and washed with H₂O (3 times) and then with a saturated aqueous solution of NaCl before being dried over anhydrous Na₂SO₄ and filtering. Volatiles were removed by rotary evaporation and the crude product was purified by flash column chromatography (SiO₂) or pTLC.⁷⁶



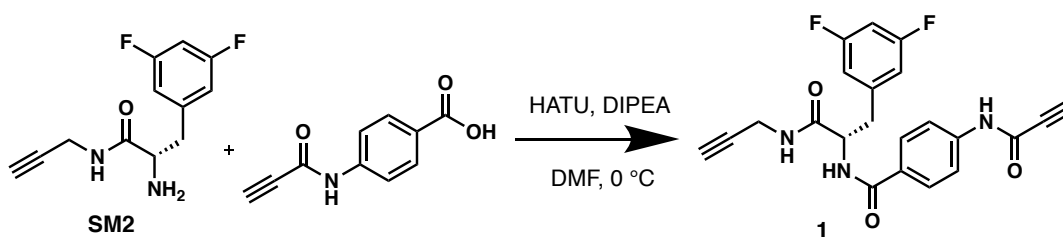
Tert-butyl (S)-3-(3,5-difluorophenyl)-1-oxo-1-(prop-2-yn-1-ylamino)propan-2-yl)carbamate (SM1)

General Procedure 1. Reaction scale: 200.0 mg (0.664 mmol) of SM0. Purified by flash chromatography (SiO₂, EtOAc/Hexane, gradient from 10 to 50% in EtOAc) to afford SM1 as a white solid (210.4 mg, 94%). ¹H NMR (300 MHz, Methanol-*d*₄) δ 6.86 (d, *J* = 6.2 Hz, 2H), 6.78 (t, *J* = 8.9 Hz, 1H), 4.30 (dd, *J* = 9.4, 5.5, 1H), 3.99 (dd, *J* = 17.8, 2.5 Hz, 1H), 3.90 (dd, *J* = 17.4, 2.6 Hz, 1H), 3.10 (dd, *J* = 13.7, 5.6 Hz, 1H), 2.82 (dd, *J* = 13.6, 9.3 Hz, 1H), 2.56 (t, 2.4 Hz, 1H), 1.36 (s, 9H) ppm. ¹³C NMR (75 MHz, Methanol-*d*₄) δ 173.3, 164.3 (dd, *J* = 245.3, 13.0 Hz, 2C), 143.0 (t, *J* = 9.5 Hz), 113.3 (dd, *J* = 18.0, 6.8 Hz, 2C), 102.8 (t, *J* = 25.3 Hz), 80.7, 80.3, 72.3, 56.7, 54.8, 39.0, 29.5, 28.6 (3C) ppm.



(S)-2-amino-3-(3,5-difluorophenyl)-N-(prop-2-yn-1-yl)propanamide (SM2)

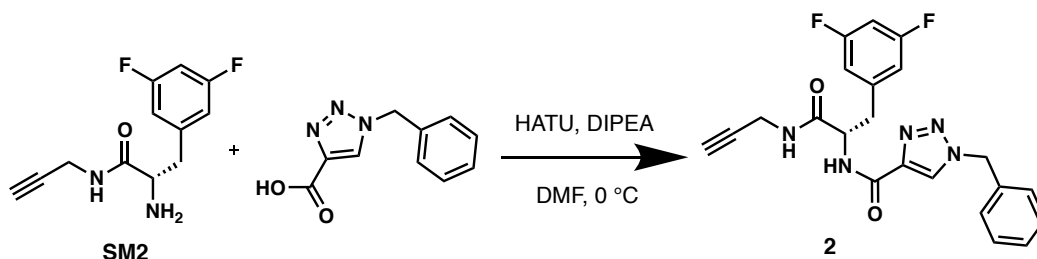
General Procedure 5. Reaction scale: 210.4 mg (0.622 mmol) of SM1. The crude product was used for the next step without purification and SM2 was afforded as a white solid that became brown with time (227.7 mg, 100%). ¹H NMR (300 MHz, Methanol-*d*₄) δ 6.90 (d, *J* = 6.0 Hz, 2H), 6.83 (td, *J* = 9.1, 2.4 Hz, 1H), 4.09 (t, *J* = 7.1, 1H), 4.04 (dd, *J* = 17.4, 2.5 Hz, 1H), 3.88 (dd, *J* = 17.5, 2.5 Hz, 1H), 3.15 (m, 2H), 2.55 (t, 2.2 Hz, 1H) ppm. ¹³C NMR (75 MHz, Methanol-*d*₄) δ 168.9, 164.6 (dd, *J* = 246.8, 13.0 Hz, 2C), 139.6 (t, *J* = 9.4 Hz), 113.7 (dd, *J* = 17.3, 7.8 Hz, 2C), 104.0 (t, *J* = 25.6 Hz), 79.6, 72.7, 55.2, 37.9, 29.5 ppm.



(*S*)-*N*-(3-(3,5-difluorophenyl)-1-oxo-1-(prop-2-yn-1-ylamino)propan-2-yl)-4-propiolamidobenzamide (1)

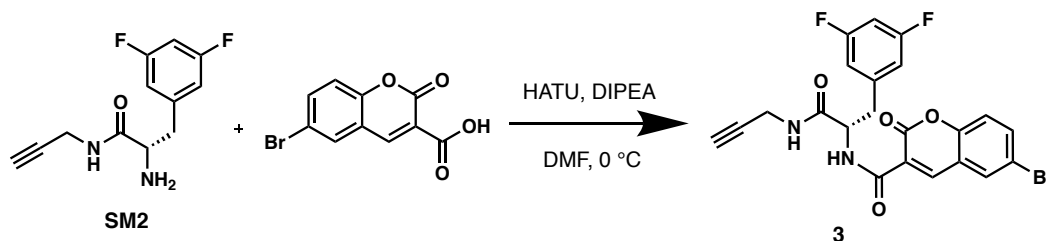
General Procedure 1. Reaction scale: 8.7 mg (0.037 mmol) of SM2. Purified by flash chromatography (SiO₂, EtOAc/hexane, gradient from 30 to 80% in EtOAc) to afford 1 as a white solid (10.6 mg, 71%). ¹H NMR (300 MHz, Methanol-*d*₄) δ 7.72 (dd, *J* = 28.3, 8.7 Hz, 4H), 6.91 (d, *J* = 6.5 Hz, 2H), 6.78 (tt, *J* = 9.2, 2.1 Hz, 1H), 4.81 (dd, *J* = 9.0, 6.1, 1H), 4.01 (dd, *J* = 17.4, 2.4 Hz, 1H), 3.91 (dd, *J* = 17.5, 2.3 Hz, 1H), 3.34 (s, 1H), 3.24 (dd, *J* = 13.7, 6.2 Hz, 1H), 3.05 (dd, *J* = 13.7, 9.1 Hz, 1H), 2.58 (t, 2.6 Hz, 1H) ppm. ¹³C NMR (101 MHz, Methanol-*d*₄) δ 172.8, 169.3, 165.7, 163.4, 148.2, 142.6, 139.2, 130.8,

129.5 (2C), 120.4 (2C), 113.3 (dd, $J = 18.2, 6.8$ Hz, 2C), 103.0, 85.8, 80.3, 72.3, 56.0, 38.5, 29.5 ppm.



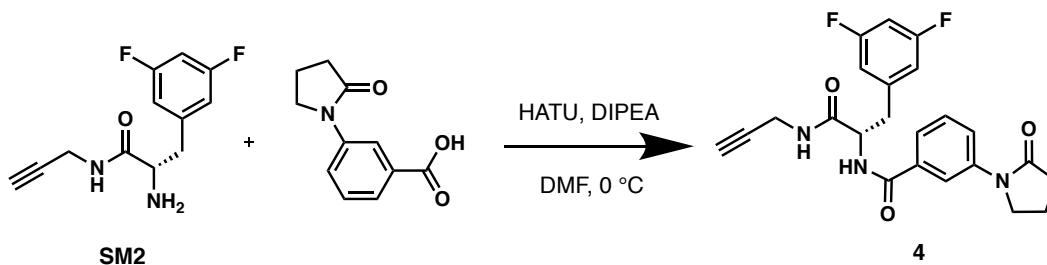
(S)-1-benzyl-N-(3-(3,5-difluorophenyl)-1-oxo-1-(prop-2-yn-1-ylamino)propan-2-yl)-1H-1,2,3-triazole-4-carboxamide (2)

General Procedure 1. Reaction scale: 8.4 mg (0.035 mmol) of SM2. Purified by flash chromatography (SiO₂, EtOAc/hexane, gradient from 50 to 70% in EtOAc) to afford 2 as a white solid (11.9 mg, 80%). ¹H NMR (300 MHz, Methanol-*d*₄) δ 8.32 (s, 1H), 7.35 (d, $J = 4.8$ Hz, 5H), 6.89 (d, $J = 6.3$ Hz, 2H), 6.76 (tt, $J = 9.2, 2.6$ Hz, 1H), 5.63 (s, 2H), 4.81 (dd, $J = 8.5, 6.0$, 1H), 4.00 (dd, $J = 17.5, 2.6$ Hz, 1H), 3.90 (dd, $J = 17.5, 2.7$ Hz, 1H), 3.23 (dd, $J = 13.7, 6.0$ Hz, 1H), 3.06 (dd, $J = 13.7, 8.6$ Hz, 1H), 2.57 (t, 2.6 Hz, 1H) ppm. ¹³C NMR (101 MHz, Methanol-*d*₄) δ 172.5, 170.9, 166.5, 165.7, 139.4, 136.6, 136.4, 130.1 (2C), 129.8 (2C), 129.2, 127.4, 113.4 (dd, $J = 18.2, 6.5$ Hz, 2C), 103.1 (t, $J = 25.5$ Hz), 80.2, 72.4, 55.2, 55.1, 38.7, 29.5 ppm.



(S)-6-bromo-N-(3-(3,5-difluorophenyl)-1-oxo-1-(prop-2-yn-1-ylamino)propan-2-yl)-2-oxo-2H-chromene-3-carboxamide (3)

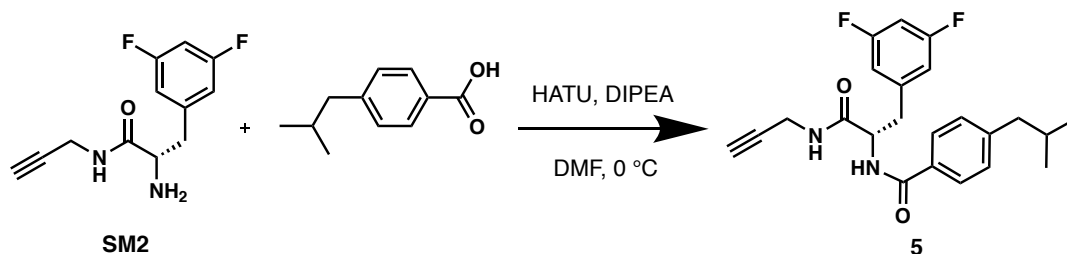
General Procedure 1. Reaction scale: 7.3 mg (0.031 mmol) of SM2. Purified by flash chromatography (SiO₂, EtOAc/hexane, gradient from 40 to 60% in EtOAc) to afford 3 as a white solid (15.8 mg, 100%). ¹H NMR (400 MHz, Chloroform-*d*) δ 8.77 (s, 1H), 7.82 (s, 1H), 7.77 (d, *J* = 8.7 Hz, 1H), 7.31 (d, *J* = 8.8 Hz, 1H), 6.82 (d, *J* = 7.0 Hz, 2H), 6.68 (t, *J* = 9.2, Hz, 1H), 5.63 (s, 2H), 4.78 (t, *J* = 6.8 Hz, 1H), 4.02 (q, *J* = 18.1 Hz, 2H), 3.26 (dd, *J* = 14.1, 6.6 Hz, 1H), 3.16 (dd, *J* = 14.1, 7.5 Hz, 1H), 2.21 (s, 1H) ppm. ¹³C NMR (101 MHz, Chloroform-*d*) δ 173.8, 168.0, 164.4, 160.7, 157.7, 150.7, 139.5, 138.6, 132.1, 128.5, 120.8, 120.0, 118.9, 118.7, 112.6, 112.3, 102.9, 89.2, 72.1, 52.8, 37.0, 34.7 ppm.



(S)-N-(3-(3,5-difluorophenyl)-1-oxo-1-(prop-2-yn-1-ylamino)propan-2-yl)-3-(2-oxopyrrolidin-1-yl)benzamide (4)

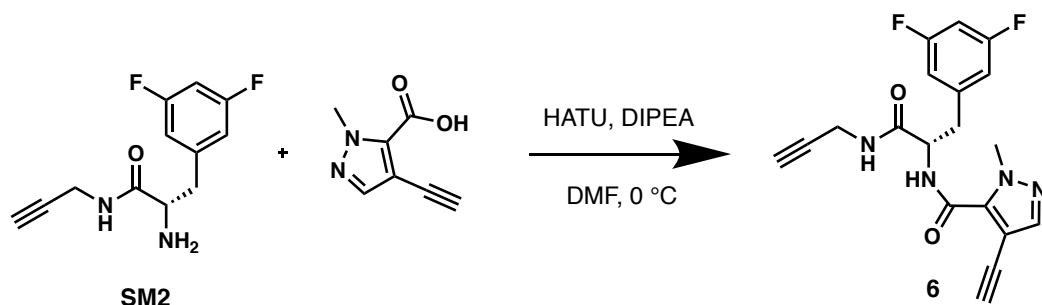
General Procedure 1. Reaction scale: 8.4 mg (0.035 mmol) of SM2. Purified by flash chromatography (SiO₂, EtOAc/hexane, gradient from 70 to 95% in EtOAc) to afford 4 as a white solid (13.6 mg, 91%). ¹H NMR (400 MHz, Chloroform-*d*) δ 7.89 (d, *J* = 10.2 Hz, 2H), 7.47 (d, *J* = 7.6 Hz, 1H), 7.40 (t, *J* = 7.7 Hz, 1H), 7.15 (d, *J* = 7.9 Hz, 1H), 6.82 (d, *J* = 6.8 Hz, 2H), 6.68 (t, *J* = 8.6 Hz, 1H), 6.62 (t, *J* = 5.4 Hz, 1H), 4.86 (q, *J* = 7.0 Hz, 1H),

4.08 (ddd, $J = 17.5, 5.9, 2.6$ Hz, 2H), 3.91 (m, 3H), 3.18 (d, $J = 6.9$ Hz, 2H), 2.62 (t, $J = 8.1$ Hz, 2H), 2.19 (m, 3H) ppm. ^{13}C NMR (101 MHz, Chloroform- d) δ 174.7, 170.2, 167.3, 164.8, 163.2, 140.5, 139.9, 134.1, 129.4, 123.7, 122.9, 118.5, 112.5 (dd, $J = 18.2, 13.0$ Hz, 2C), 102.8, 78.9, 72.0, 54.6, 48.9, 38.1, 32.8, 29.3, 18.1 ppm.



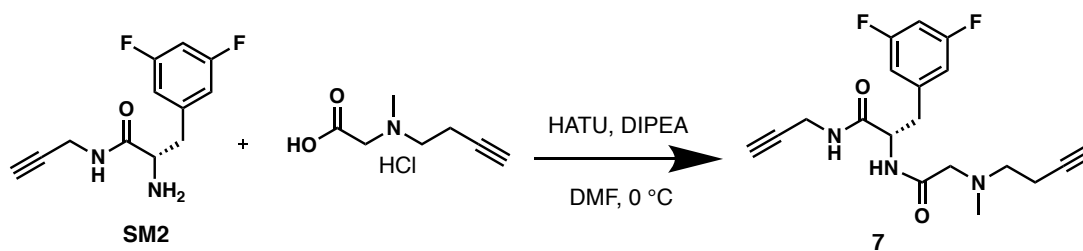
(S)-N-(3-(3,5-difluorophenyl)-1-oxo-1-(prop-2-yn-1-ylamino)propan-2-yl)-4-isobutylbenzamide (5)

General Procedure 1. Reaction scale: 9.0 mg (0.038 mmol) of SM2. Purified by flash chromatography (SiO_2 , EtOAc/hexane, gradient from 20 to 50% in EtOAc) to afford 5 as a white solid (7.3 mg, 48%). ^1H NMR (400 MHz, Chloroform- d) δ 7.66 (d, $J = 7.6$ Hz, 2H), 7.18 (d, $J = 7.7$ Hz, 2H), 6.99 (d, $J = 7.8$ Hz, 1H), 6.84 (m, 3H), 6.67 (t, $J = 9.3$ Hz, 1H), 4.97 (q, $J = 7.4$ Hz, 1H), 4.07 (dt, $J = 18.0, 3.1$ Hz, 1H), 3.88 (dt, $J = 17.3, 2.8$ Hz, 1H), 3.18 (d, $J = 6.9$ Hz, 2H), 2.51 (d, $J = 7.1$ Hz, 2H), 2.19 (s, 1H), 1.87 (p, $J = 7.0$ Hz, 1H), 0.89 (d, $J = 6.5$ Hz, 6H) ppm. ^{13}C NMR (101 MHz, Chloroform- d) δ 170.5, 167.6, 163.2 (dd, $J = 249.5, 13.1$ Hz, 2C), 146.6, 140.0, 130.7, 129.5 (2C), 127.1 (2C), 112.5 (dd, $J = 18.2, 6.7$ Hz, 2C), 102.8, 78.9, 71.9, 54.4, 45.4, 38.4, 30.3, 29.3, 22.4 (2C) ppm.



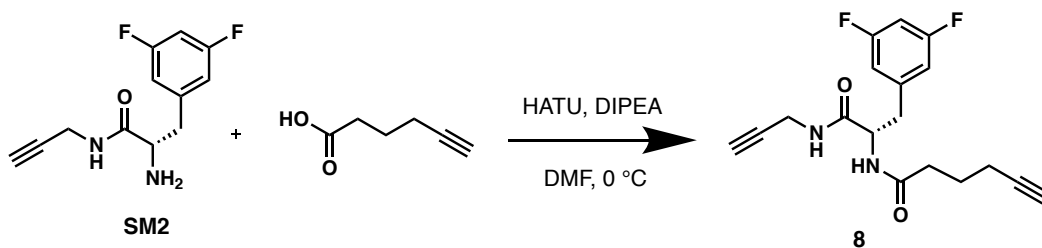
(S)-N-(3-(3,5-difluorophenyl)-1-oxo-1-(prop-2-yn-1-ylamino)propan-2-yl)-4-ethynyl-1-methyl-1H-pyrazole-5-carboxamide (6)

General Procedure 1. Reaction scale: 9.6 mg (0.041 mmol) of SM2. Purified by flash chromatography (SiO₂, EtOAc/hexane, gradient from 30 to 50% in EtOAc) to afford 6 as a white solid (9.6 mg, 64%). ¹H NMR (400 MHz, Chloroform-*d*) δ 7.83 (d, *J* = 7.8 Hz, 1H), 7.60 (s, 1H), 6.81 (dd, *J* = 8.1, 2.2 Hz, 2H), 6.72 (tt, *J* = 9.0, 2.3 Hz, 1H), 4.80 (q, *J* = 7.4 Hz, 1H), 4.18 (s, 3H), 4.07 (ddd, *J* = 17.5, 5.7, 2.6 Hz, 1H), 3.97 (ddd, *J* = 17.5, 5.2, 2.6 Hz, 1H), 3.44 (s, 1H), 3.22 (dd, *J* = 13.8, 6.0 Hz, 1H), 3.13 (dd, *J* = 13.8, 7.4 Hz, 1H), 2.24 (t, *J* = 2.6 Hz, 1H) ppm. ¹³C NMR (101 MHz, Chloroform-*d*) δ 169.4, 164.4, 159.4, 158.5, 141.4, 135.9, 133.9, 112.7, 112.5, 103.0, 103.0, 85.1, 78.7, 78.5, 72.2, 54.4, 40.8, 38.1, 29.4 ppm.



(S)-2-(2-(but-3-yn-1-yl(methyl)amino)acetamido)-3-(3,5-difluorophenyl)-N-(prop-2-yn-1-yl)propanamide (7)

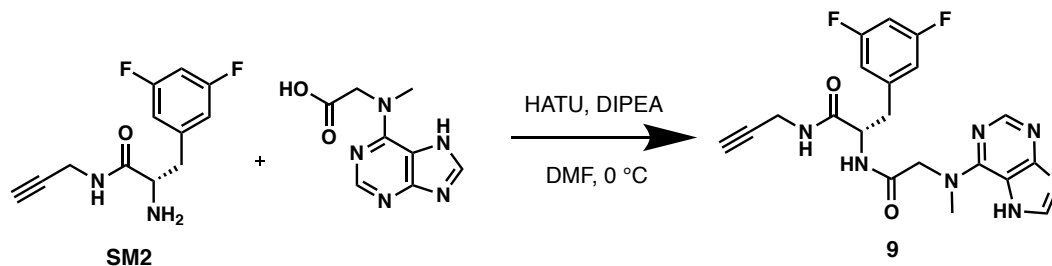
General Procedure 1. Reaction scale: 9.9 mg (0.042 mmol) of SM2. Purified by flash chromatography (SiO₂, EtOAc/hexane, gradient from 35 to 90% in EtOAc) to afford 6 as a translucent solid (9.5 mg, 63%). ¹H NMR (400 MHz, Methanol-*d*₄) δ 6.89 (dd, *J* = 8.1, 1.8 Hz, 2H), 6.72 (tt, *J* = 9.3, 2.3 Hz, 1H), 4.68 (dd, *J* = 8.6, 5.9 Hz, 1H), 3.99 (dd, *J* = 17.5, 2.3 Hz, 1H), 3.91 (dd, *J* = 17.5, 2.3 Hz, 1H), 3.14 (m, 2H), 3.00 (m, 2H), 2.60 (t, *J* = 6.8 Hz, 3H), 2.35 (m, 3H), 2.26 (s, 3H) ppm. ¹³C NMR (101 MHz, Methanol-*d*₄) δ 172.3, 169.3, 164.3 (dd, *J* = 260.6, 13.0 Hz, 2C), 142.5, 113.4 (dd, *J* = 19.2, 7.1 Hz, 2C), 103.2, 83.1, 80.2, 72.4, 71.1, 61.3, 57.2, 54.7, 42.7, 38.8, 29.5, 18.0 ppm.



(S)-N-(3-(3,5-difluorophenyl)-1-oxo-1-(prop-2-yn-1-ylamino)propan-2-yl)hex-5-ynamide (8)

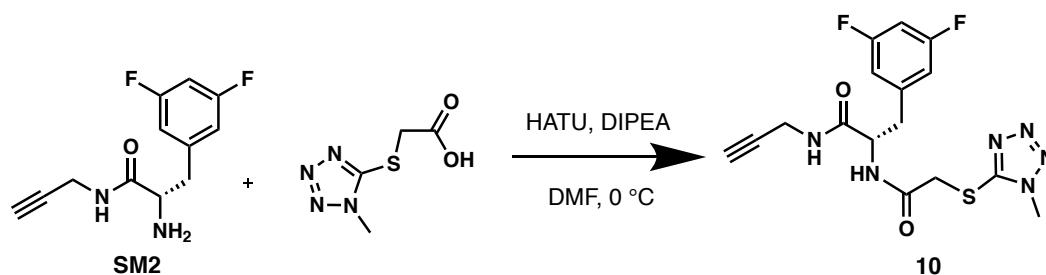
General Procedure 1. Reaction scale: 10.8 mg (0.045 mmol) of SM2. Purified by flash chromatography (SiO₂, EtOAc/hexane, gradient from 60 to 70% in EtOAc) to afford 7 as a white solid (12.9 mg, 86%). ¹H NMR (400 MHz, Acetonitrile-*d*₃) δ 7.00 (s, 1H), 6.83 (m, 3H), 6.69 (d, *J* = 7.2 Hz, 1H), 4.57 (td, *J* = 8.5, 5.9 Hz, 1H), 3.90 (dd, *J* = 5.4, 2.1 Hz, 2H), 3.12 (dd, *J* = 13.9, 5.4 Hz, 1H), 2.86 (dd, *J* = 13.9, 8.9 Hz, 1H), 2.43 (t, *J* = 2.6 Hz,

1H), 2.22 (m, 3H), 2.09 (td, $J = 7.0, 2.3$ Hz, 2H), 1.65 (p, $J = 7.0$ Hz, 2H) ppm. ^{13}C NMR (101 MHz, Chloroform- d) δ 172.6, 170.3, 164.3, 162.0, 140.3 (t, $J = 9.2$ Hz), 112.4 (dd, $J = 17.2, 6.9$ Hz, 2C), 102.8 (t, $J = 25.1$ Hz), 83.3, 78.9, 72.0, 69.7, 53.8, 38.3, 34.8, 29.2, 24.0, 17.8 ppm.



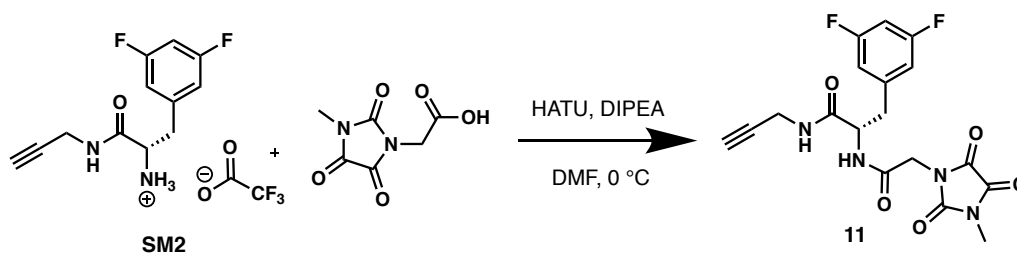
(S)-3-(3,5-difluorophenyl)-2-(2-(methyl(7H-purin-6-yl)amino)acetamido)-N-(prop-2-yn-1-yl)propanamide (9)

General Procedure 1. Reaction scale: 8.4 mg (0.035 mmol) of SM2. Purified by pTLC (MeOH/DCM, 10:90) to afford 9 as a translucent solid (3.9 mg, 26%). ^1H NMR (400 MHz, DMSO- d_3) δ 8.67 (t, $J = 5.0$ Hz, 1H), 8.49 (d, $J = 8.5$ Hz, 1H), 8.07 (s, 1H), 7.90 (s, 1H), 7.04 (t, $J = 9.4$ Hz, 1H), 6.95 (d, $J = 7.0$ Hz, 2H), 4.54 (m, 3H), 3.84 (d, $J = 4.6$ Hz, 2H), 3.19 (s, 3H), 3.11 (t, $J = 2.3$ Hz, 1H), 3.08 (dd, $J = 13.6, 4.0$ Hz, 1H), 2.82 (dd, $J = 13.2, 10.7$ Hz, 1H) ppm. ^{13}C NMR (101 MHz, DMSO- d_3) δ 172.3, 170.3, 152.7, 151.2, 143.5, 142.4, 140.8, 125.8, 112.5, 112.3, 101.3, 86.7, 73.2, 59.6, 53.2, 37.0, 36.9, 31.3 ppm.



(S)-3-(3,5-difluorophenyl)-2-(2-((1-methyl-1H-tetrazol-5-yl)thio)acetamido)-N-(prop-2-yn-1-yl)propanamide (10)

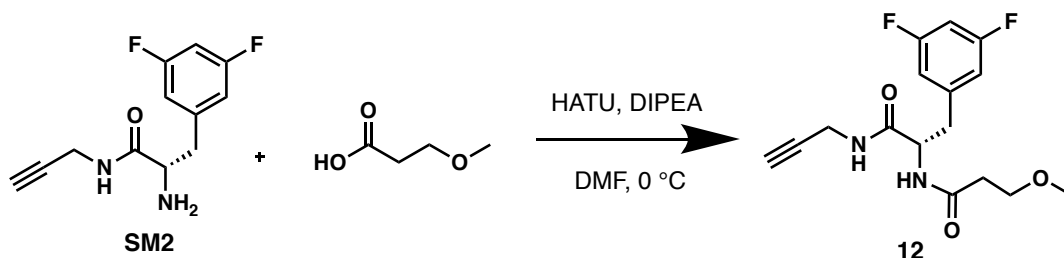
General Procedure 1. Reaction scale: 9.1 mg (0.038 mmol) of SM2. Purified by pTLC (MeOH/DCM/toluene, 5:70:25) to afford 10 as a white/translucent solid (9.0 mg, 60%). ¹H NMR (300 MHz, Acetonitrile-*d*₃) δ 7.42 (s, 1H), 7.26 (d, *J* = 7.2 Hz, 1H), 6.81 (m, 3H), 4.59 (td, *J* = 8.4, 5.3 Hz, 1H), 3.93 (dd, *J* = 5.5, 2.2 Hz, 2H), 3.88 (d, *J* = 3.7 Hz, 5H), 3.17 (dd, *J* = 14.1, 5.0 Hz, 1H), 2.94 (dd, *J* = 14.1, 8.6 Hz, 1H), 2.41 (t, *J* = 2.6 Hz, 1H) ppm. ¹³C NMR (101 MHz, Acetonitrile-*d*₃) δ 170.7, 167.7, 163.0, 162.5, 154.7, 144.6, 113.3, 113.1, 102.8, 81.0, 71.6, 55.0, 37.6, 36.8, 34.4, 29.1 ppm.



(S)-3-(3,5-difluorophenyl)-2-(2-(3-methyl-2,4,5-trioxoimidazolidin-1-yl)acetamido)-N-(prop-2-yn-1-yl)propanamide (11)

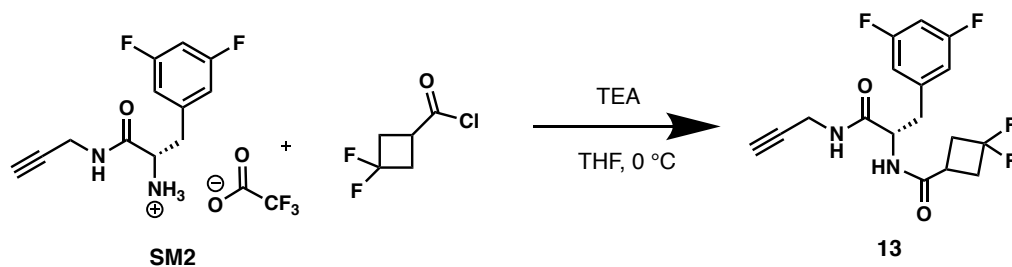
General Procedure 1. Reaction scale: 13.0 mg (0.037 mmol) of SM2. Crude solid was purified by Et₂O/MeOH wash to afford 11 as a white solid (8.4 mg, 56%). ¹H NMR (400

MHz, DMSO-*d*₃) δ 8.60 (t, *J* = 4.9 Hz, 1H), 8.54 (d, *J* = 8.4 Hz, 1H), 7.05 (t, *J* = 9.3 Hz, 1H), 6.90 (d, *J* = 6.8 Hz, 2H), 4.53 (td, *J* = 9.2, 4.8 Hz, 1H), 4.13 (d, *J* = 17.0 Hz, 1H), 4.04 (d, *J* = 17.0 Hz, 1H), 3.87 (dd, *J* = 5.3, 2.6 Hz, 2H), 3.15 (t, *J* = 2.3 Hz, 1H), 3.01 (s, 3H), 2.97 (dd, *J* = 13.6, 9.5 Hz, 1H), 2.76 (dd, *J* = 13.2, 10.1 Hz, 1H) ppm. ¹³C NMR (101 MHz, DMSO-*d*₃) δ 170.0, 165.2, 162.1 (dd, *J* = 246.4, 13.3 Hz, 2C), 157.6, 157.2, 153.8, 141.9 (t, *J* = 9.6 Hz), 112.4 (dd, *J* = 18.2, 6.8 Hz, 2C),, 102.0, 80.7, 73.4, 53.5, 40.6, 37.2, 28.0, 24.5 ppm.



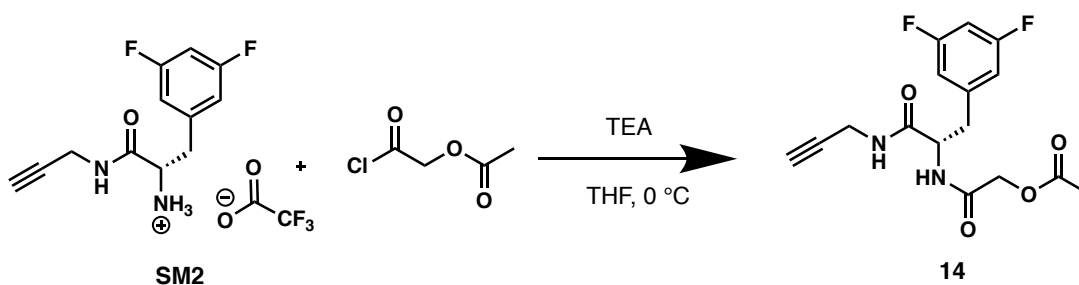
(S)-3-(3,5-difluorophenyl)-2-(3-methoxypropanamido)-N-(prop-2-yn-1-yl)propanamide (12)

General Procedure 1. Reaction scale: 11.0 mg (0.046 mmol) of SM2. Purified by flash chromatography (SiO₂, EtOAc/hexane, gradient from 60 to 90% in EtOAc) to afford 12 as a white solid (11.9 mg, 79%). ¹H NMR (300 MHz, Chloroform-*d*) δ 6.73 (m, 5H), 4.72 (q, *J* = 7.0 Hz, 1H), 3.99 (dd, *J* = 3.99 Hz, 2H), 3.57 (m, 2H), 3.34 (s, 3H), 3.08 (m, 2H), 2.45 (t, *J* = 4.5 Hz, 2H), 2.21 (t, *J* = 2.6 Hz, 1H) ppm. ¹³C NMR (101 MHz, Chloroform-*d*) δ 172.0, 170.2, 164.4, 161.9, 140.5, 112.4 (dd, *J* = 18.2, 6.7 Hz, 2C), 102.7, 79.2, 71.8, 68.6, 59.0, 53.7, 37.5, 37.1, 31.1 ppm.



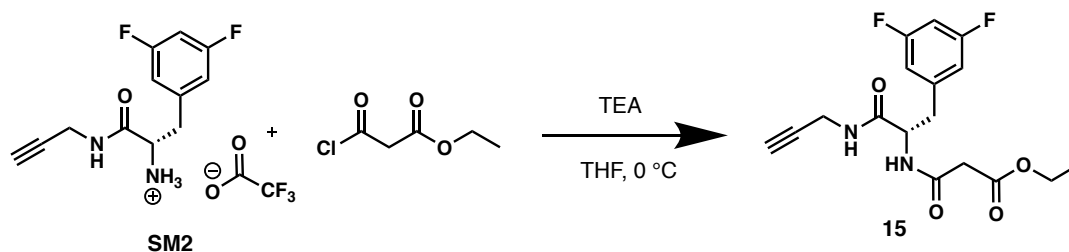
(S)-N-(3-(3,5-difluorophenyl)-1-oxo-1-(prop-2-yn-1-ylamino)propan-2-yl)-3,3-difluorocyclobutane-1-carboxamide (13)

General Procedure 2. Reaction scale: 14.8 mg (0.042 mmol) of SM2. Purified by flash chromatography (SiO₂, EtOAc/hexane, 70:30) to afford 13 as a white solid (14.5 mg, 97%). ¹H NMR (300 MHz, Methanol-*d*₄) δ 6.84 (m, 3H), 4.62 (dd, *J* = 8.9, 6.0 Hz, 1H), 3.98 (dd, *J* = 17.5, 2.2 Hz, 1H), 3.90 (dd, *J* = 17.5, 2.2 Hz, 1H), 3.14 (dd, *J* = 13.7, 5.9 Hz, 1H), 2.89 (m, 2H), 2.63 (m, 5H) ppm. ¹³C NMR (101 MHz, Methanol-*d*₄) δ 174.9, 172.5, 164.4 (dd, *J* = 247.5, 13.0 Hz, 2C), 142.8 (t, *J* = 10.1 Hz), 113.3 (dd, *J* = 18.2, 6.5 Hz, 2C), 103.0 (t, *J* = 25.8 Hz), 80.2, 72.3, 55.4, 39.5, 38.8, 29.4, 28.3 (d, *J* = 4.4 Hz), 28.1 (d, *J* = 3.7 Hz) ppm.



(S)-2-((3-(3,5-difluorophenyl)-1-oxo-1-(prop-2-yn-1-ylamino)propan-2-yl)amino)-2-oxoethyl acetate (14)

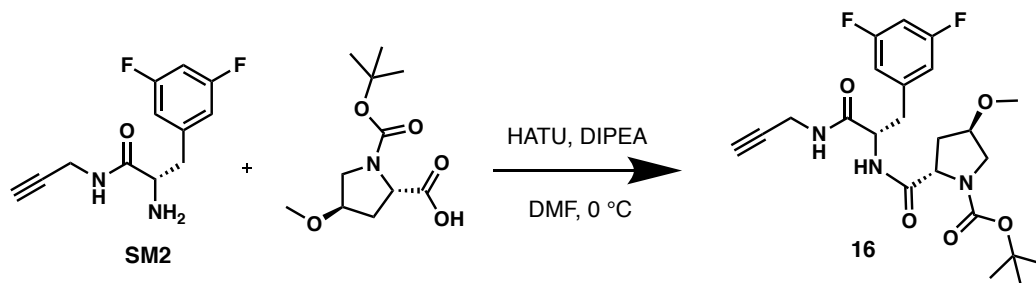
General Procedure 2. Reaction scale: 15.6 mg (0.044 mmol) of SM2. Purified by flash chromatography (SiO₂, EtOAc/hexane, gradient from 70 to 80% in EtOAc) to afford 14 as a white solid (10.6 mg, 71%). ¹H NMR (300 MHz, Methanol-*d*₄) δ 6.84 (m, 3H), 4.65 (dd, *J* = 8.5, 6.0 Hz, 1H), 4.51 (s, 2H), 3.99 (dd, *J* = 17.5, 1.9 Hz, 1H), 3.90 (dd, *J* = 17.5, 1.9 Hz, 1H), 3.15 (dd, *J* = 13.7, 5.9 Hz, 1H), 2.94 (dd, *J* = 13.6, 8.6 Hz, 1H), 2.58 (t, *J* = 2.4 Hz, 1H), 2.11 (s, 3H) ppm. ¹³C NMR (101 MHz, Methanol-*d*₄) δ 172.2, 171.8, 167.0, 164.4 (dd, *J* = 248.5, 13.1 Hz, 2C), 142.6 (t, *J* = 9.1 Hz), 113.3 (dd, *J* = 19.2, 6.7 Hz, 2C), 103.1 (t, *J* = 25.8 Hz), 80.2, 72.4, 63.4, 55.0, 38.5, 29.5, 20.4 ppm.



Ethyl (S)-3-((3-(3,5-difluorophenyl)-1-oxo-1-(prop-2-yn-1-ylamino)propan-2-yl)amino)-3-oxopropanoate (15)

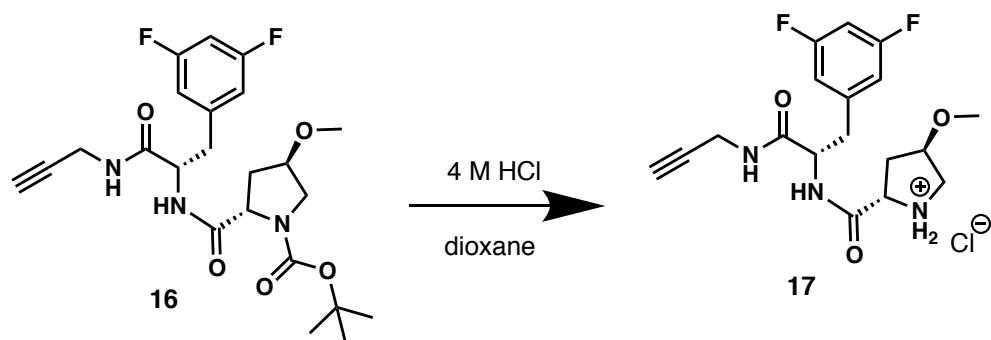
General Procedure 2. Reaction scale: 15.0 mg (0.043 mmol) of SM2. Purified by flash chromatography (SiO₂, EtOAc/hexane, gradient from 70 to 90% in EtOAc) to afford 15 as a white solid (6.8 mg, 45%). ¹H NMR (300 MHz, Methanol-*d*₄) δ 6.88 (d, *J* = 6.5 Hz, 2H), 6.81 (t, *J* = 10.4 Hz, 1H), 4.63 (dd, *J* = 7.9, 6.3 Hz, 1H), 4.16 (q, *J* = 7.1 Hz, 2H), 3.99 (dd, *J* = 17.5, 1.9 Hz, 1H), 3.90 (dd, *J* = 17.6, 2.0 Hz, 1H), 3.16 (dd, *J* = 13.8, 5.8

Hz, 1H), 2.94 (dd, $J = 13.7, 8.5$ Hz, 1H), 2.58 (t, $J = 2.6$ Hz, 1H), 1.24 (t, $J = 7.1$ Hz, 3H) ppm. ^{13}C NMR (101 MHz, Methanol- d_4) δ 172.2 (2C), 168.3, 164.4 (dd, $J = 247.5, 13.1$ Hz, 2C), 142.6 (t, $J = 9.5$ Hz), 113.4 (dd, $J = 19.2, 6.7$ Hz, 2C), 103.0 (t, $J = 27.3$ Hz), 80.2, 72.4, 62.5, 55.5, 43.0, 38.5, 29.5, 14.4 ppm.



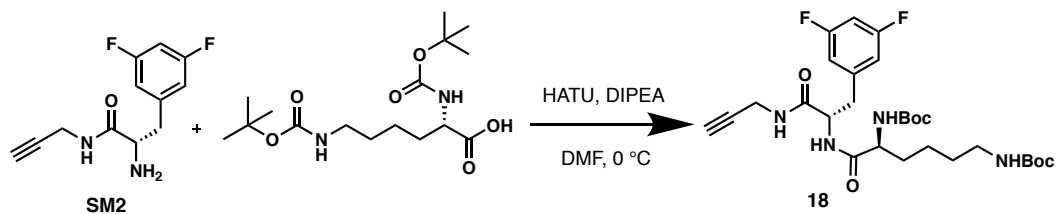
Tert-butyl (2S,4R)-2-(((S)-3-(3,5-difluorophenyl)-1-oxo-1-(prop-2-yn-1-ylamino)propan-2-yl)carbamoyl)-4-methoxypyrrolidine-1-carboxylate (16)

General Procedure 1. Reaction scale: 7.7 mg (0.032 mmol) of SM2. Purified by flash chromatography (SiO_2 , EtOAc/hexane, gradient from 50 to 90% in EtOAc) to afford 16 as a white solid (14.7 mg, 98%). ^1H NMR (500 MHz, Acetonitrile- d_3 , 60 °C) δ 7.19 (s, 1H), 6.98 (d, $J = 6.7$ Hz, 1H), 6.84 (d, $J = 7.8$ Hz, 2H), 6.79 (tt, $J = 9.3, 2.3$ Hz, 1H), 4.58 (s, 1H), 4.14 (d, $J = 9.3$ Hz, 1H), 3.94 (m, 3H), 3.47 (m, 2H), 3.23 (s, 3H), 3.20 (d, $J = 4.5$ Hz, 1H), 3.01 (dd, $J = 14.3, 8.8$ Hz, 1H), 2.41 (d, $J = 2.4$ Hz, 1H), 2.24 (m, 1H), 2.14 (d, $J = 13.9$ Hz, 1H), 1.41 (s, 9H) ppm. ^{13}C NMR (101 MHz, Acetonitrile- d_3) δ 171.4, 171.3, 164.9, 162.4, 155.9, 143.3, 113.3, 113.1, 102.7, 81.1, 80.8, 71.9, 60.7, 56.9, 55.3, 54.5, 52.7, 37.1, 35.8, 29.2, 28.5, 28.3, 28.2 ppm.



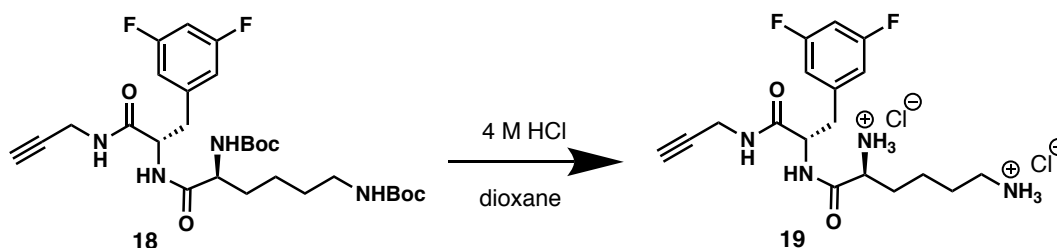
(2*S*,4*R*)-*N*-((*S*)-3-(3,5-difluorophenyl)-1-oxo-1-(prop-2-yn-1-ylamino)propan-2-yl)-4-methoxypyrrolidine-2-carboxamide (17)

General Procedure 6. Reaction scale: 14.2 mg (0.031 mmol) of SM2. Crude solid was purified by acetone washes to afford 17 as a white solid (10.9 mg, 89%). ¹H NMR (400 MHz, Methanol-*d*₄) δ 7.11 (dd, *J* = 8.5, 2.0 Hz, 2H), 7.02 (tt, *J* = 9.2, 2.2 Hz, 1H), 4.89 (dd, *J* = 9.8, 5.1 Hz, 1H), 4.56 (dd, *J* = 10.3, 4.2 Hz, 1H), 4.25 (s, 1H), 4.17 (m, 2H), 3.70 (d, *J* = 12.3 Hz, 1H), 3.51 (s, 2H), 3.46 (dd, *J* = 12.4, 4.0 Hz, 1H), 3.40 (dd, *J* = 14.0, 5.1 Hz, 1H), 3.11 (dd, *J* = 13.8, 10.1 Hz, 1H), 2.81 (t, *J* = 2.4 Hz, 1H), 2.69 (ddd, *J* = 14.8, 10.5, 4.9 Hz, 1H), 2.10 (td, *J* = 14.2, 1.8 Hz, 1H) ppm. ¹³C NMR (101 MHz, Methanol-*d*₄) δ 172.2, 169.5, 164.4 (dd, *J* = 248.5, 13.1 Hz, 2C), 142.7 (t, *J* = 9.4 Hz), 113.3 (dd, *J* = 20.2, 6.6 Hz, 2C), 103.1 (t, *J* = 25. Hz), 80.2, 79.4, 72.4, 59.8, 56.6, 55.6, 51.4, 38.6, 36.5, 29.5 ppm.



Di-*tert*-butyl ((*S*)-6-(((*S*)-3-(3,5-difluorophenyl)-1-oxo-1-(prop-2-yn-1-ylamino)propan-2-yl)amino)-6-oxohexane-1,5-diyl)dicarbamate (18)

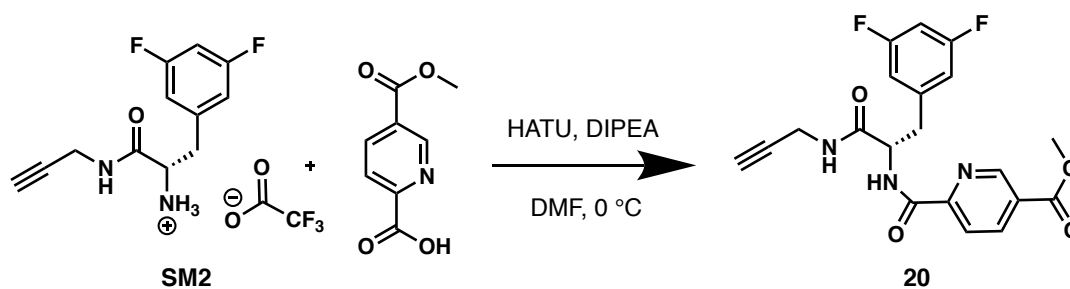
General Procedure 1. Reaction scale: 6.3 mg (0.026 mmol) of SM2. Purified by flash chromatography (SiO₂, EtOAc/hexane, gradient from 70 to 90% in EtOAc) and then by flash chromatography (Aluminum Oxide Basic, MeOH/DCM, gradient from 1 to 2% in MeOH) to afford 18 as a white solid (10.6 mg, 71%). ¹H NMR (300 MHz, Acetonitrile-*d*₃) δ 7.17 (s, 1H), 6.86 (m, 4H), 5.78 (s, 1H), 5.31 (s, 1H), 4.58 (td, *J* = 8.7, 4.5 Hz, 1H), 3.92 (m, 2H), 3.78 (m, 1H), 2.94 (m, 4H), 2.43 (t, *J* = 2.8 Hz, 1H), 1.41 (s, 26H) ppm. ¹³C NMR (101 MHz, Acetonitrile-*d*₃) δ 173.2, 171.6, 171.1, 164.9 (d, *J* = 13.5 Hz), 164.1 (d, *J* = 25.3 Hz), 162.4, 143.0, 113.2 (dd, *J* = 20.2, 6.5 Hz, 2C), 102.8 (t, *J* = 26.8 Hz), 80.4, 79.0, 79.0, 71.9, 56.6, 54.2, 40.0, 37.3, 31.6, 30.4, 29.2, 28.5 (6C), 22.9 ppm.



(*S*)-2,6-diamino-*N*-((*S*)-3-(3,5-difluorophenyl)-1-oxo-1-(prop-2-yn-1-ylamino)propan-2-yl)hexanamide (19)

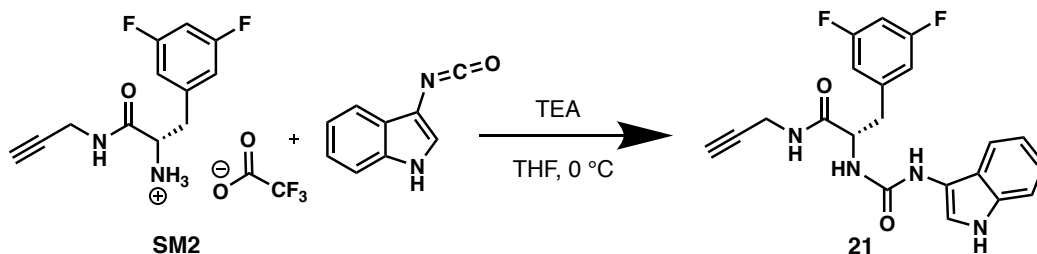
General Procedure 6. Reaction scale: 12.3 mg (0.022 mmol) of SM2. Crude solid was purified by EtOAc/acetone washes to afford 19 as a white solid (7.6 mg, 95%). ¹H NMR (400 MHz, Methanol-*d*₄) δ 6.95 (d, *J* = 6.3 Hz, 2H), 6.82 (t, *J* = 9.0 Hz, 1H), 4.61 (dd, *J*

= 8.2, 5.7 Hz, 1H), 3.93 (m, 3H), 3.11 (dd, $J = 13.8, 5.7$ Hz, 1H), 2.99 (m, 3H), 2.62 (s, 1H), 1.91 (td, $J = 11.6, 6.1$ Hz, 2H), 1.72 (dt, $J = 15.8, 7.8$ Hz, 2H), 1.50 (ddt, $J = 30.5, 14.3, 6.6$ Hz, 2H) ppm. ^{13}C NMR (101 MHz, Methanol- d_4) δ 172.5, 170.0, 165.4 (dd, $J = 247.5, 13.5$ Hz, 2C), 142.4 (t, $J = 9.2$ Hz), 113.3 (dd, $J = 18.2, 6.6$ Hz, 2C), 103.2 (t, $J = 25.9$ Hz), 80.2, 72.5, 55.9, 53.8, 40.2, 38.3, 32.0, 28.0, 24.2, 22.3 ppm.



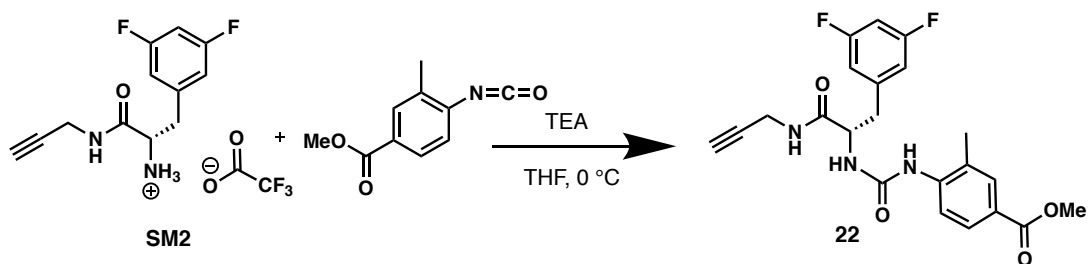
Methyl (S)-6-((3-(3,5-difluorophenyl)-1-oxo-1-(prop-2-yn-1-ylamino)propan-2-yl)carbamoyl)nicotinate (20)

General Procedure 1. Reaction scale: 13.0 mg (0.037 mmol) of SM2. Purified by flash chromatography (SiO_2 , EtOAc/hexane, gradient from 50 to 70% in EtOAc) to afford 20 as a white solid (12.3 mg, 83%). ^1H NMR (400 MHz, Methanol- d_4) δ 9.17 (dd, $J = 2.0, 0.8$ Hz, 1H), 8.48 (dd, $J = 8.1, 2.0$ Hz, 1H), 8.13 (dd, $J = 8.1, 0.6$ Hz, 1H), 6.89 (dd, $J = 8.3, 2.3$ Hz, 2H), 6.77 (tt, $J = 9.5, 2.3$ Hz, 1H), 4.85 (dd, $J = 8.0, 6.1$ Hz, 1H), 4.02 (dd, $J = 17.5, 2.5$ Hz, 1H), 3.97 (s, 3H), 3.92 (dd, $J = 17.5, 2.5$ Hz, 1H), 3.26 (dd, $J = 13.8, 6.0$ Hz, 1H), 3.13 (dd, $J = 13.7, 8.1$ Hz, 1H), 2.60 (t, $J = 2.5$ Hz, 1H) ppm. ^{13}C NMR (101 MHz, Methanol- d_4) δ 172.1, 166.3, 165.2, 164.4 (dd, $J = 248.5, 12.9$ Hz, 2C), 153.4, 150.7, 142.5 (t, $J = 9.5$ Hz), 139.8, 129.9, 123.0, 113.4 (dd, $J = 18.2, 6.7$ Hz, 2C), 103.1 (t, $J = 25.8$ Hz), 80.2, 72.4, 55.5, 53.2, 38.9, 29.5 ppm.



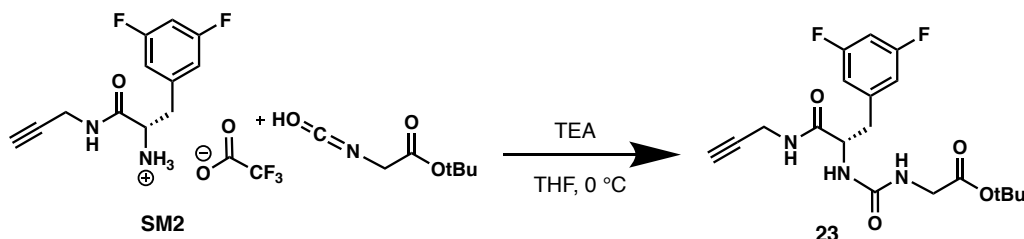
(S)-2-(3-(1*H*-indol-3-yl)ureido)-3-(3,5-difluorophenyl)-*N*-(prop-2-yn-1-yl)propanamide (21)

General Procedure 3. Reaction scale: 13.3 mg (0.038 mmol) of SM2. Purified by flash chromatography (SiO₂, EtOAc/hexane, gradient from 70 to 100% in EtOAc) to afford 21 as a green/translucent solid (8.8 mg, 51%). ¹H NMR (400 MHz, Methanol-*d*₄) δ 7.42 (d, *J* = 7.7 Hz, 1H), 7.32 (d, *J* = 8.0 Hz, 1H), 7.27 (s, 1H), 7.11 (t, *J* = 7.3 Hz, 1H), 7.00 (t, *J* = 7.3 Hz, 1H), 6.82 (m, 3H), 4.56 (t, *J* = 6.7 Hz, 1H), 4.00 (dd, *J* = 17.9, 1.9 Hz, 1H), 3.88 (dd, *J* = 17.6, 1.6 Hz, 1H), 3.08 (dd, *J* = 13.4, 5.8 Hz, 1H), 2.96 (dd, *J* = 12.6, 8.1 Hz, 1H), 2.58 (t, *J* = 2.3 Hz, 1H) ppm. ¹³C NMR (101 MHz, Methanol-*d*₄) δ 173.4, 164.4 (dd, *J* = 247.5, 13.0 Hz, 2C), 152.1, 142.6 (t, *J* = 9.1 Hz), 136.1, 123.0, 122.9, 122.9, 119.9, 118.1, 113.5 (dd, *J* = 19.2, 6.8 Hz, 2C), 112.5, 112.5, 103.0 (t, *J* = 25.6 Hz), 80.3, 72.4, 55.8, 39.5, 29.4 ppm.



Methyl (*S*)-4-(3-(3-(3,5-difluorophenyl)-1-oxo-1-(prop-2-yn-1-ylamino)propan-2-yl)ureido)-3-methylbenzoate (22)

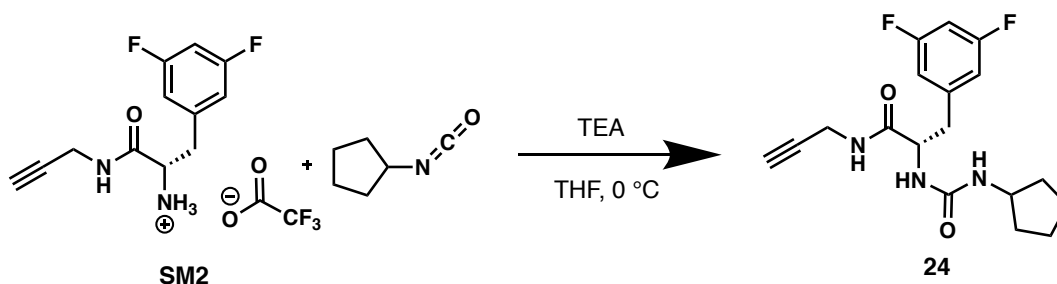
General Procedure 3. Reaction scale: 12.3 mg (0.035 mmol) of SM2. Crude solid was purified by Et₂O washes to afford 22 as a white solid (6.8 mg, 45%). ¹H NMR (300 MHz, DMSO-*d*₃) δ 8.65 (s, 1H), 8.13 (s, 1H), 8.06 (d, *J* = 8.3 Hz, 1H), 7.70 (m, 2H), 7.26 (d, *J* = 7.8 Hz, 1H), 7.06 (t, *J* = 8.6 Hz, 1H), 6.91 (d, *J* = 5.6 Hz, 2H), 4.53 (dd, *J* = 12.9, 7.7 Hz, 1H), 3.88 (s, 2H), 3.79 (s, 3H), 3.01 (dd, *J* = 13.2, 4.0 Hz, 1H), 2.85 (dd, *J* = 12.6, 7.0 Hz, 1H), 2.21 (s, 3H) ppm. ¹³C NMR (101 MHz, Methanol-*d*₄) δ 170.6, 168.5 (dd, *J* = 74.7, 3.0 Hz, 2C), 166.1, 154.1, 145.2, 142.9, 131.2, 127.8, 125.4, 122.0, 118.2, 112.7, 112.6, 102.6, 80.8, 73.3, 53.5, 51.7, 38.5, 28.0, 17.9 ppm.



(*S*)-2-(3-cyclopentylureido)-3-(3,5-difluorophenyl)-*N*-(prop-2-yn-1-yl)propanamide (23)

General Procedure 3. Reaction scale: 6.0 mg (0.038 mmol) of isocyanate. Purified by flash chromatography (SiO₂, EtOAc/hexane, gradient from 60 to 90% in EtOAc) to afford 23 as a white solid (10.0 mg, 88%). ¹H NMR (400 MHz, Chloroform-*d*) δ 7.43 (t, *J* = 5.3 Hz, 1H), 6.75 (d, *J* = 6.1 Hz, 2H), 6.63 (t, *J* = 8.3 Hz, 1H), 6.42 (d, *J* = 8.3 Hz, 1H), 5.94 (t, *J*

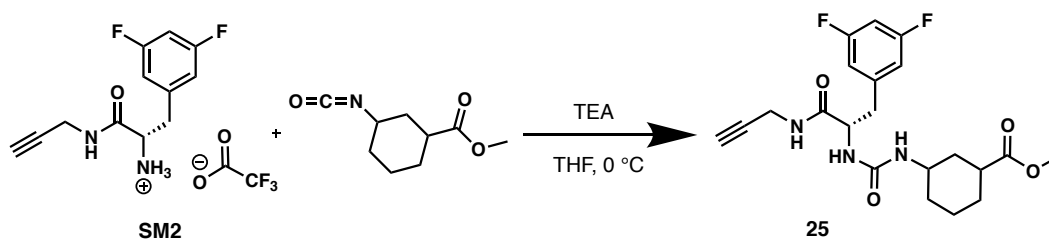
= 5.3 Hz, 1H), 4.71 (q, $J = 7.0$ Hz, 1H), 4.06 (ddd, $J = 17.4, 5.3, 2.1$ Hz, 1H), 3.85 (m, 3H), 2.97 (m, 2H), 2.18 (t, $J = 2.5$ Hz, 1H), 1.44 (s, 9H) ppm. ^{13}C NMR (101 MHz, Chloroform- d) δ 172.1, 170.3, 163.0 (dd, $J = 249.5, 13.0$ Hz, 2C), 157.7, 140.9 (t, $J = 8.6$ Hz), 112.6 (dd, $J = 17.8, 6.7$ Hz, 2C), 102.4 (t, $J = 26.2$ Hz), 82.1, 79.2, 71.7, 54.8, 43.0, 39.3, 29.2, 28.2 (3C) ppm.



Tert-butyl (S)-((3-(3,5-difluorophenyl)-1-oxo-1-(prop-2-yn-1-ylamino)propan-2-yl)carbamoyl)glycinate (24)

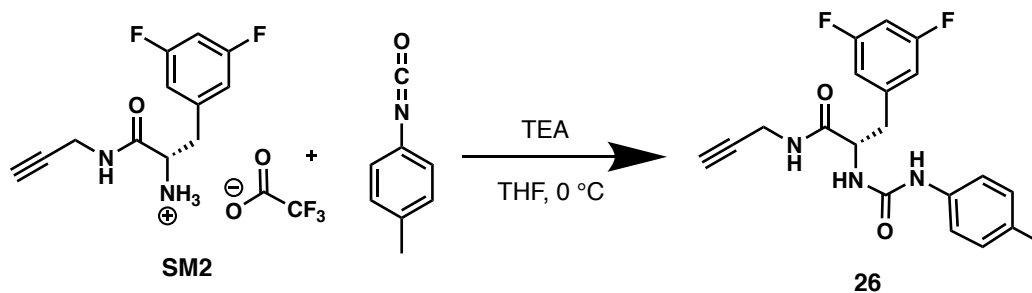
General Procedure 3. Reaction scale: 4.8 mg (0.043 mmol) of isocyanate. Purified by flash chromatography (SiO_2 , MeOH/DCM, 5:95) to afford 24 as a white solid (20.4 mg, 100%).

^1H NMR (500 MHz, Methanol- d_4) δ 6.83 (d, $J = 6.6$ Hz, 2H), 6.78 (t, $J = 9.2$ Hz, 1H), 4.46 (q, $J = 6.7$ Hz, 1H), 3.98 (dd, $J = 17.5, 2.4$ Hz, 1H), 3.89 (m, 2H), 3.05 (dd, $J = 13.7, 6.1$ Hz, 1H), 2.88 (dd, $J = 13.7, 7.9$ Hz, 1H), 2.56 (t, $J = 2.4$ Hz, 1H) 1.85 (m, 2H), 1.67 (m, 2H), 1.58 (m, 2H), 1.35 (ddt, $J = 19.9, 13.9, 6.9$ Hz, 2H) ppm. ^{13}C NMR (125 MHz, Methanol- d_4) δ 173.7, 164.3 (dd, $J = 245.0, 13.3$ Hz, 2C), 159.6, 142.8 (t, $J = 9.4$ Hz), 113.4 (dd, $J = 20.0, 5.8$ Hz, 2C), 102.9 (t, $J = 25.8$ Hz), 80.3, 72.3, 55.7, 52.9, 39.7, 34.2, 34.1, 29.4, 24.5, 24.4 ppm.



Methyl 3-(3-((S)-3-(3,5-difluorophenyl)-1-oxo-1-(prop-2-yn-1-ylamino)propan-2-yl)ureido)cyclohexane-1-carboxylate (25)

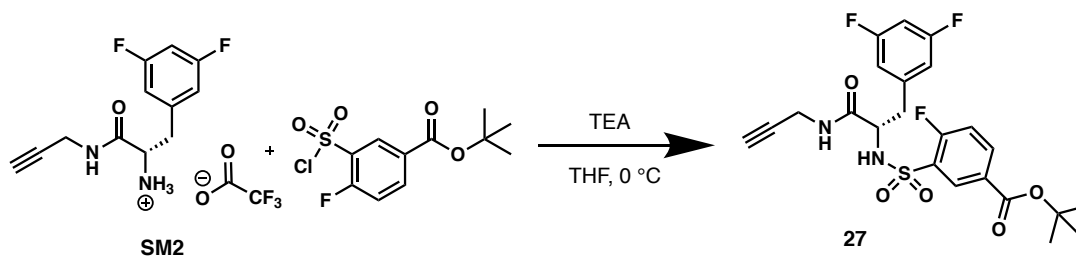
General Procedure 3. Reaction scale: 6.8 mg (0.037 mmol) of isocyanate. Purified by flash chromatography (SiO₂, EtOAc/hexane, gradient from 70 to 80% in EtOAc) to afford 25 as a white solid (10.6 mg, 65%). ¹H NMR (500 MHz, Methanol-*d*₄) δ 6.84 (d, *J* = 6.7 Hz, 2H), 6.78 (t, *J* = 9.1 Hz, 1H), 4.45 (m, 1H), 3.98 (d, *J* = 17.5 Hz, 1H), 3.88 (d, *J* = 17.5 Hz, 1H), 3.66 (t, *J* = 5.2 Hz, 3H), 3.42 (td, *J* = 11.4, 3.8 Hz, 1H), 3.06 (dd, *J* = 13.5, 5.5 Hz, 1H), 2.88 (dd, *J* = 13.2, 8.5 Hz, 1H), 2.57 (s, 1H), 2.4 (td, *J* = 12.1, 2.7 Hz, 1H), 2.08 (t, *J* = 14.0 Hz, 1H), 1.85 (m, 3H), 1.59 (m, 1H), 1.38 (q, *J* = 13.3 Hz, 1H), 1.19 (m, 1H), 1.05 (m, 1H) ppm. ¹³C NMR (101 MHz, Methanol-*d*₄) δ 177.4, 173.7, 164.3 (dd, *J* = 247.5, 13.2 Hz, 2C), 159.2, 142.8, 113.4 (dd, *J* = 18.2, 5.5 Hz, 2C), 102.9 (t, *J* = 26.3 Hz), 80.3, 72.3, 55.8, 52.3, 43.5, 39.6, 36.8, 34.5, 33.8, 29.4, 29.3, 25.3 ppm.



(S)-3-(3,5-difluorophenyl)-N-(prop-2-yn-1-yl)-2-(3-(p-tolyl)ureido)propanamide

(26)

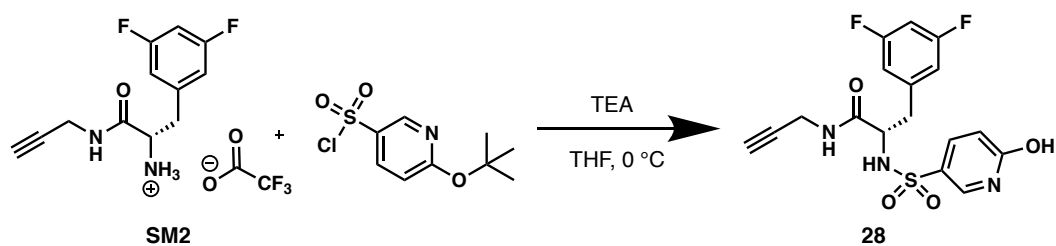
General Procedure 3. Reaction scale: 4.5 mg (0.034 mmol) of isocyanate. Crude solid was purified by DCM/Et₂O washes to afford 26 as a light brown solid (10.7 mg, 94%). ¹H NMR (400 MHz, Methanol-*d*₄) δ 7.17 (d, *J* = 8.1 Hz, 2H), 7.05 (d, *J* = 8.0 Hz, 2H), 6.87 (dd, *J* = 8.8, 2.3 Hz, 2H), 6.80 (tt, *J* = 9.4, 2.3 Hz, 1H), 4.52 (t, *J* = 6.8 Hz, 1H), 4.00 (dd, *J* = 17.5, 2.6 Hz, 1H), 3.89 (dd, *J* = 17.5, 2.6 Hz, 1H), 3.09 (dd, *J* = 13.6, 6.2 Hz, 1H), 2.97 (dd, *J* = 13.6, 7.5 Hz, 1H), 2.58 (t, *J* = 2.5 Hz, 1H), 2.26 (s, 3H) ppm. ¹³C NMR (101 MHz, Methanol-*d*₄) δ 173.4, 164.4 (dd, *J* = 247.5, 12.7 Hz, 2C), 157.4, 142.6 (t, *J* = 9.1 Hz), 137.8, 133.4, 130.3 (2C), 120.5 (2C), 113.5 (dd, *J* = 19.2, 6.6 Hz, 2C), 103.0 (t, *J* = 25.9 Hz), 80.3, 72.3, 55.7, 39.6, 29.4, 20.8 ppm.



Tert-butyl (S)-3-(N-(3-(3,5-difluorophenyl)-1-oxo-1-(prop-2-yn-1-ylamino)propan-2-yl)sulfamoyl)-4-fluorobenzoate (27)

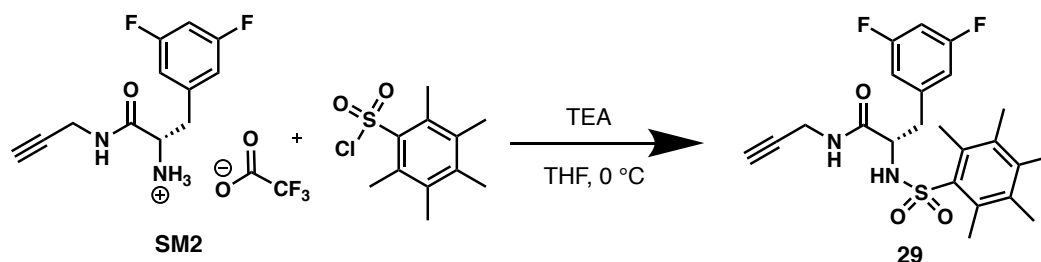
General Procedure 4. Reaction scale: 10.6 mg (0.030 mmol) of SM2. Purified by flash chromatography (SiO₂, MeOH/DCM, gradient from 1 to 4% in MeOH) to afford 27 as a translucent solid (14.8 mg, 99%). ¹H NMR (300 MHz, Methanol-*d*₄) δ 8.22 (dd, *J* = 6.8, 2.0 Hz, 1H), 8.11 (ddd, *J* = 8.1, 4.5, 2.1 Hz, 1H), 7.20 (t, *J* = 9.2 Hz, 1H), 6.73 (dd, *J* =

8.5, 2.1 Hz, 2H), 6.63 (tt, $J = 9.1, 2.3$ Hz, 1H), 4.06 (dd, $J = 9.8, 5.1$ Hz, 1H), 3.80 (dd, $J = 17.5, 2.3$ Hz, 1H), 3.69 (dd, $J = 17.5, 2.4$ Hz, 1H), 2.97 (dd, $J = 13.7, 4.9$ Hz, 1H), 2.76 (dd, $J = 13.6, 10.0$ Hz, 1H), 2.53 (t, $J = 2.3$ Hz, 1H), 1.59 (s, 9H) ppm. ^{13}C NMR (101 MHz, Methanol- d_4) δ 172.2, 164.9, 164.1 (dd, $J = 248.5, 12.9$ Hz, 2C), 163.8, 161.2, 142.4 (t, $J = 9.6$ Hz), 137.1 (d, $J = 10.3$ Hz), 132.0 (2C), 129.5, 118.5 (d, $J = 22.6$ Hz), 113.3 (dd, $J = 19.2, 6.8$ Hz, 2C), 103.2 (t, $J = 25.7$ Hz), 83.3, 79.9, 72.5, 59.5, 39.3, 29.5, 28.3 (3C) ppm.



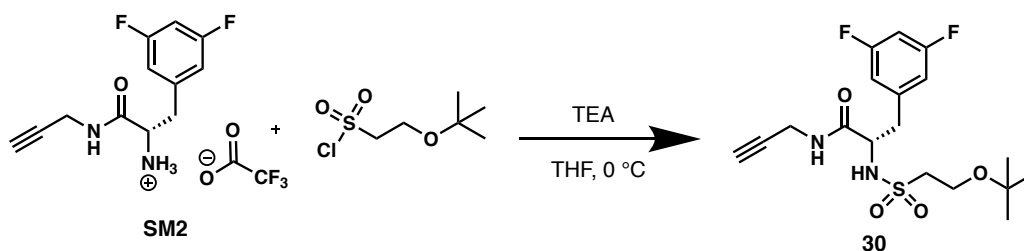
(S)-3-(3,5-difluorophenyl)-2-((6-hydroxypyridine)-3-sulfonylamido)-N-(prop-2-yn-1-yl)propanamide (28)

General Procedure 4. Reaction scale: 11.7 mg (0.033 mmol) of SM2. Purified by pTLC (MeOH/DCM, 5:95) to afford 28 as a white/green solid (6.7 mg, 49%). ^1H NMR (300 MHz, Methanol- d_4) δ 7.83 (d, $J = 2.0$ Hz, 1H), 7.52 (dd, $J = 9.5, 2.4$ Hz, 1H), 6.80 (d, $J = 6.4$ Hz, 2H), 6.75 (m, 1H), 6.38 (d, $J = 9.6$ Hz, 1H), 3.95 (dd, $J = 9.2, 5.6$ Hz, 1H), 3.83 (t, $J = 2.4$ Hz, 2H), 3.00 (dd, $J = 13.7, 5.5$ Hz, 1H), 2.79 (dd, $J = 13.6, 9.4$ Hz, 1H), 2.56 (t, $J = 2.6$ Hz, 1H) ppm. ^{13}C NMR (101 MHz, Methanol- d_4) δ 172.3, 165.8, 164.3 (dd, $J = 248.5, 13.1$ Hz, 2C), 142.4 (t, $J = 9.4$ Hz), 139.7, 139.1, 121.6, 120.7, 113.5 (dd, $J = 19.2, 6.5$ Hz, 2C), 103.1 (t, $J = 25.8$ Hz), 80.0, 72.5, 59.0, 39.5, 29.4 ppm.



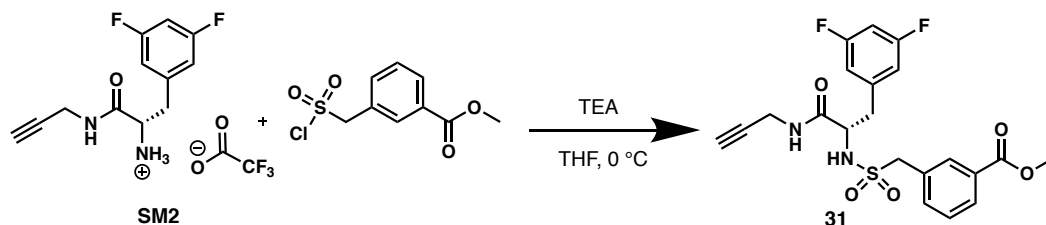
(S)-3-(3,5-difluorophenyl)-2-((2,3,4,5,6-pentamethylphenyl)sulfonamido)-N-(prop-2-yn-1-yl)propanamide (29)

General Procedure 4. Reaction scale: 11.8 mg (0.033 mmol) of SM2. Purified by flash chromatography (SiO₂, EtOAc/hexane, gradient from 10 to 50% in EtOAc) and Et₂O wash to afford 29 as a white solid (4.1 mg, 27%). ¹H NMR (400 MHz, Methanol-*d*₄) δ 6.62 (d, *J* = 6.5 Hz, 2H), 6.59 (d, *J* = 9.1 Hz, 1H), 3.94 (dd, *J* = 10.0, 4.9 Hz, 1H), 3.88 (dd, *J* = 17.5, 2.3 Hz, 1H), 3.75 (dd, *J* = 17.5, 2.3 Hz, 1H), 2.98 (dd, *J* = 13.8, 4.7 Hz, 1H), 2.71 (dd, *J* = 13.7, 10.2 Hz, 1H), 2.60 (t, *J* = 2.6 Hz, 1H), 2.42 (s, 6H), 2.27 (s, 3H), 2.19 (s, 6H) ppm. ¹³C NMR (101 MHz, Methanol-*d*₄) δ 172.7, 164.0 (dd, *J* = 247.5, 13.0 Hz, 2C), 142.5 (t, *J* = 9.4 Hz), 140.6, 137.2, 135.8 (2C), 135.2 (2C), 113.0 (dd, *J* = 18.2, 6.5 Hz, 2C), 102.7 (t, *J* = 25.9 Hz), 80.0, 72.6, 58.9, 39.3, 29.6, 19.2 (2C), 17.9, 17.1 (2C) ppm.



(S)-2-((2-(tert-butoxy)ethyl)sulfonamido)-3-(3,5-difluorophenyl)-N-(prop-2-yn-1-yl)propenamide (30)

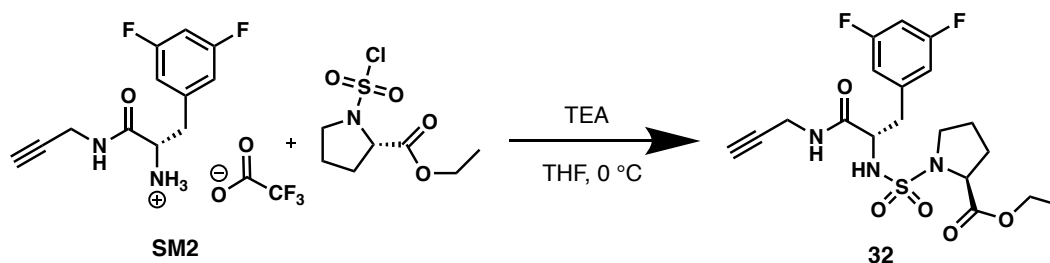
General Procedure 4. Reaction scale: 13.1 mg (0.037 mmol) of SM2. Purified by pTLC (MeOH/DCM, 5:95) to afford 30 as a yellow oil (7.9 mg, 53%). ¹H NMR (300 MHz, Methanol-*d*₄) δ 6.90 (dd, *J* = 8.5, 2.2 Hz, 2H), 6.81 (tt, *J* = 9.4, 2.2 Hz, 1H), 4.14 (dd, *J* = 8.1, 6.3 Hz, 1H), 3.99 (dd, *J* = 17.3, 2.3 Hz, 1H), 3.91 (dd, *J* = 17.4, 1.8 Hz, 1H), 3.66 (m, 2H), 3.06 (m, 3H), 2.91 (dd, *J* = 13.6, 8.2 Hz, 1H), 2.59 (t, *J* = 2.5 Hz, 1H), 1.19 (s, 9H) ppm. ¹³C NMR (125 MHz, Methanol-*d*₄) δ 172.8, 165.4, 165.3, 142.6, 113.6 (dd, *J* = 18.8, 5.8 Hz, 2C), 103.1 (t, *J* = 25.0 Hz), 82.5, 79.7, 75.1, 59.0, 57.5, 54.8, 40.1, 29.4, 27.7 (3C) ppm.



Methyl (S)-3-((N-(3-(3,5-difluorophenyl)-1-oxo-1-(prop-2-yn-1-ylamino)propan-2-yl)sulfamoyl)methyl)benzoate (31)

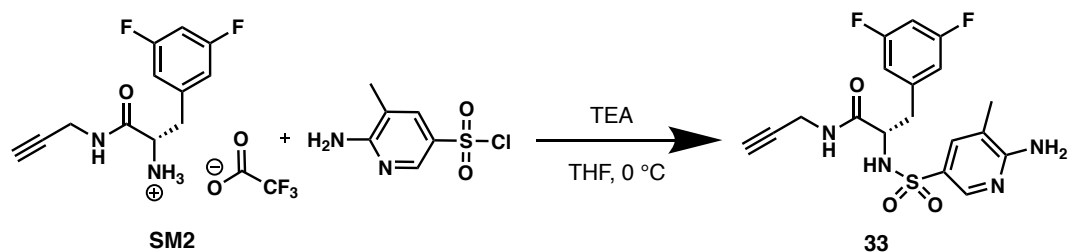
General Procedure 4. Reaction scale: 11.7 mg (0.033 mmol) of SM2. Purified by flash chromatography (SiO₂, MeOH/DCM, 5:95) to afford 31 as a white solid (10.8 mg, 72%). ¹H NMR (500 MHz, Acetonitrile-*d*₃) δ 7.99 (d, *J* = 5.4 Hz, 2H), 7.56 (d, *J* = 7.6 Hz, 1H), 7.49 (t, *J* = 7.9 Hz, 1H), 6.82 (m, 3H), 4.24 (s, 2H), 3.97 (t, *J* = 6.9 Hz, 1H), 3.93 (dd, *J* =

17.7, 1.9 Hz, 1H), 3.87 (m, 4H), 2.97 (dd, $J = 13.7, 6.5$ Hz, 1H), 2.89 (dd, $J = 13.7, 7.4$ Hz, 1H), 2.44 (t, $J = 2.6$ Hz, 1H) ppm. ^{13}C NMR (125 MHz, Acetonitrile- d_3) δ 170.7, 167.2, 163.7 (dd, $J = 245.0, 12.9$ Hz, 2C), 141.8 (t, $J = 8.9$ Hz), 136.3, 132.5, 131.5, 131.3, 130.2, 129.8, 113.6 (dd, $J = 18.8, 5.9$ Hz, 2C), 103.1 (t, $J = 25.7$ Hz), 80.6, 72.1, 59.4, 58.5, 52.5, 39.7, 29.1 ppm.



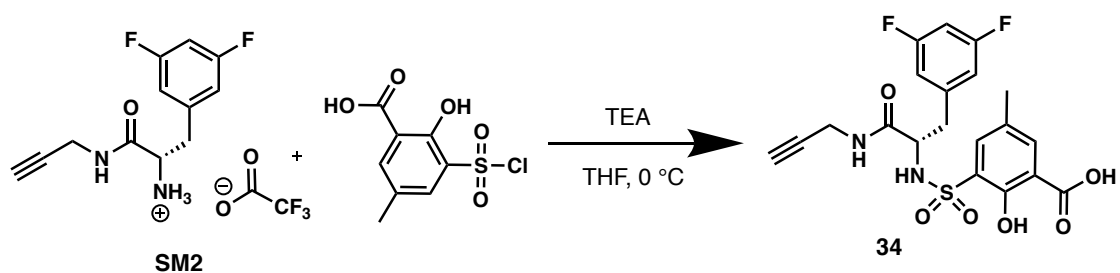
Ethyl (*N*-((*S*)-3-(3,5-difluorophenyl)-1-oxo-1-(prop-2-yn-1-ylamino)propan-2-yl)sulfamoyl)-*L*-prolinate (32)

General Procedure 4. Reaction scale: 11.9 mg (0.034 mmol) of SM2. Purified by pTLC (MeOH/DCM, 1:99) to afford 32 as a yellow oil (7.6 mg, 51%). ^1H NMR (500 MHz, Chloroform- d) δ 6.84 (d, $J = 6.2$ Hz, 2H), 6.76 (s, 1H), 6.70 (t, $J = 8.2$ Hz, 1H), 4.46 (t, $J = 4.9$ Hz, 1H), 4.38 (dd, $J = 7.9, 4.3$ Hz, 1H), 4.22 (q, $J = 6.8$ Hz, 2H), 4.06 (dd, $J = 17.6, 2.6$ Hz, 1H), 3.98 (dd, $J = 17.5, 2.3$ Hz, 1H), 3.34 (q, $J = 7.2$ Hz, 1H), 3.11 (m, 2H), 2.93 (q, $J = 7.8$ Hz, 1H), 2.28 (dq, $J = 16.0, 8.1$ Hz, 1H), 2.21 (m, 1H), 2.00 (m, 1H), 1.88 (m, 2H) ppm. ^{13}C NMR (125 MHz, Chloroform- d) δ 173.7, 170.7, 164.1, 162.1, 141.6, 112.9 (dd, $J = 20.0, 6.1$ Hz, 2C), 102.7, 79.1, 71.8, 62.0, 61.4, 57.2, 48.1, 38.3, 31.0, 29.5, 25.1, 14.2 ppm.



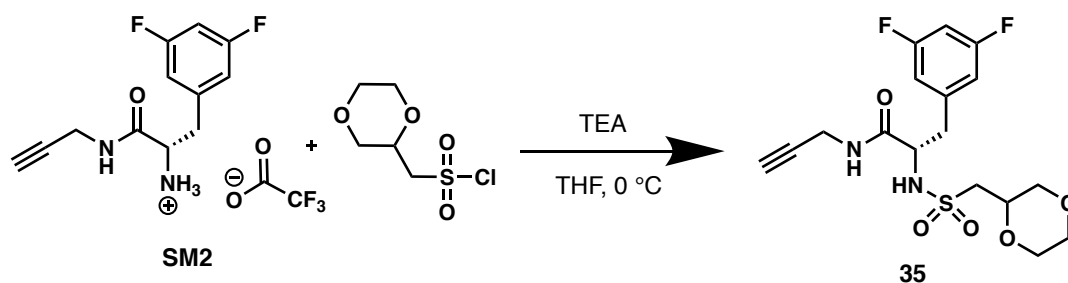
(S)-2-(((6-amino-5-methylpyridin-3-yl)sulfonyl)amino)-3-(3,5-difluorophenyl)-N-(prop-2-yn-1-yl)propanamide (33)

General Procedure 4. Reaction scale: 12.9 mg (0.037 mmol) of SM2. Crude solid was purified by DCM washes to afford 33 as a white solid (7.4 mg, 49%). ¹H NMR (400 MHz, Methanol-*d*₄) δ 8.05 (s, 1H), 7.37 (s, 1H), 6.72 (s, 3H), 3.88 (m, 2H), 3.74 (d, *J* = 17.6 Hz, 1H), 2.97 (d, *J* = 13.3 Hz, 1H), 2.72 (t, *J* = 11.2 Hz, 1H), 2.57 (s, 1H), 2.07 (s, 3H) ppm. ¹³C NMR (101 MHz, Methanol-*d*₄) δ 172.5, 165.4, 162.9, 161.9, 146.2, 142.4 (t, *J* = 7.1 Hz), 136.3, 125.7, 118.2, 113.3 (dd, *J* = 19.2, 6.1 Hz, 2C), 102.9 (t, *J* = 27.3 Hz), 80.0, 72.5, 59.0, 39.3, 29.5, 17.2 ppm.



(S)-3-(N-((3,5-difluorophenyl)amino)-1-oxo-1-(prop-2-yn-1-yl)amino)propan-2-ylsulfamoyl-2-hydroxy-5-methylbenzoic acid (34)

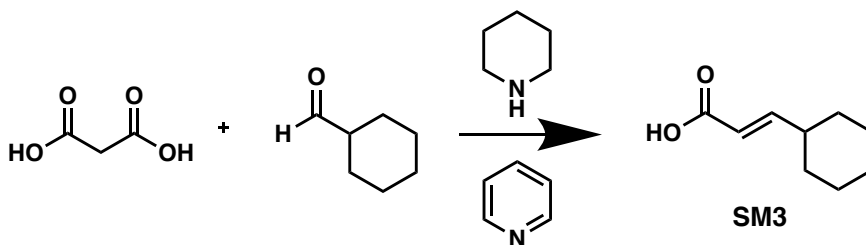
General Procedure 4. Reaction scale: 11.7 mg (0.033 mmol) of SM2. No purification was needed and 34 was afforded as a pink solid (13.4 mg, 89%). ¹H NMR (400 MHz, Methanol-*d*₄) δ 7.85 (s, 1H), 7.64 (s, 1H), 6.71 (d, *J* = 6.5 Hz, 2H), 6.62 (t, *J* = 9.0 Hz, 1H), 4.06 (dd, *J* = 9.1, 5.1 Hz, 1H), 3.85 (dd, *J* = 17.5, 1.7 Hz, 1H), 3.74 (dd, *J* = 17.4, 1.4 Hz, 1H), 3.02 (dd, *J* = 13.8, 4.9 Hz, 1H), 2.80 (dd, *J* = 13.7, 9.5 Hz, 1H), 2.56 (t, *J* = 2.4 Hz, 1H), 2.30 (s, 3H) ppm. ¹³C NMR (101 MHz, Methanol-*d*₄) δ 172.5, 164.1 (dd, *J* = 248.5, 13.0 Hz, 2C), 158.2, 142.2 (t, *J* = 9.4 Hz), 136.7, 136.7, 135.4, 128.6, 127.6, 113.2 (dd, *J* = 19.2, 6.7 Hz, 2C), 103.1 (t, *J* = 25.9 Hz), 79.9, 72.5, 59.5, 39.3, 29.5, 20.3 ppm.



(2*S*)-2-(((1,4-dioxan-2-yl)methyl)sulfonamido)-3-(3,5-difluorophenyl)-*N*-(prop-2-yn-1-yl)propanamide (35)

General Procedure 4. Reaction scale: 13.1 mg (0.037 mmol) of SM2. Purified by flash chromatography (SiO₂, MeOH/DCM, 5:95) and DCM wash to afford 35 as a white solid (5.3 mg, 35%). ¹H NMR (400 MHz, Acetonitrile-*d*₃) δ 6.89 (m, 2H), 6.83 (m, 1H), 4.12 (q, *J* = 7.4 Hz, 1H), 3.94 (m, 3H), 3.78 (m, 1H), 3.66 (m, 3H), 3.52 (m, 1H), 3.22 (m, 1H), 3.08 (m, 2H), 2.94 (m, 2H), 2.47 (m, 1H) ppm. ¹³C NMR (101 MHz, Acetonitrile-*d*₃) δ 170.6, 163.7 (dd, *J* = 247.5, 12.6 Hz, 2C), 142.2 (t, *J* = 10.1 Hz), 113.7 (dd, *J* = 16.2, 6.4

Hz, 2C), 102.9 (t, $J = 26.3$ Hz), 80.8, 72.2, 69.9, 67.3, 66.8, 58.6, 55.0, 54.7, 39.4, 29.2 ppm.

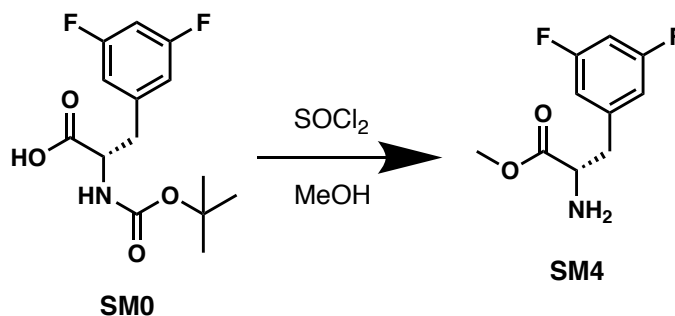


(E)-3-cyclohexylacrylic acid (SM3)

To a solution of cyclohexanecarboxaldehyde (600 mg, 5.35 mmol, 1.0 eq.) in pyridine (10 ml) was added malonic acid (556.6 mg, 5.35 mmol, 1.0 eq.) and piperidine (42.3 μ L, 0.428 mmol, 0.08 eq.). The reaction mixture was first stirred at room temperature for 1 h and then at 80 °C for 5 h. The reaction mixture was then allowed to warm to room temperature and poured into ice-cooled 12 M aqueous hydrochloric acid (10 mL).⁵⁷ The resulting solution was then extracted with ethyl acetate (3 x 10 mL) and the organic layers were combined and washed with a solution of Cu(OAc)₂ (2 x 10 mL), a solution of EDTA (1 x 10 mL) and a NaCl saturated aqueous solution (1 x 10 mL). The resulting organic layers were dried over Na₂SO₄ and volatiles were removed by rotary evaporation. The crude product was purified by flash chromatography (SiO₂, EtOAc/hexane, gradient from 60 to 70% in EtOAc) to afford SM3 as a white solid (619.2 mg, 75%). ¹H NMR (400 MHz, Chloroform-*d*) δ 7.03 (dd, $J = 15.7, 6.6$ Hz, 1H), 5.77 (d, $J = 15.7$ Hz, 1H), 2.16 (dd, $J = 16.3, 10.4$ Hz, 1H), 1.76 (m, 4H), 1.68 (d, $J = 12.0$ Hz, 1H), 1.30 (p, $J = 12.4$ Hz,

2H), 1.16 (p, $J = 12.1$ Hz, 3H) ppm. ^{13}C NMR (101 MHz, Chloroform- d) δ 172.8, 157.4, 118.4, 40.7, 31.6 (2C), 26.0, 25.9 (2C) ppm.

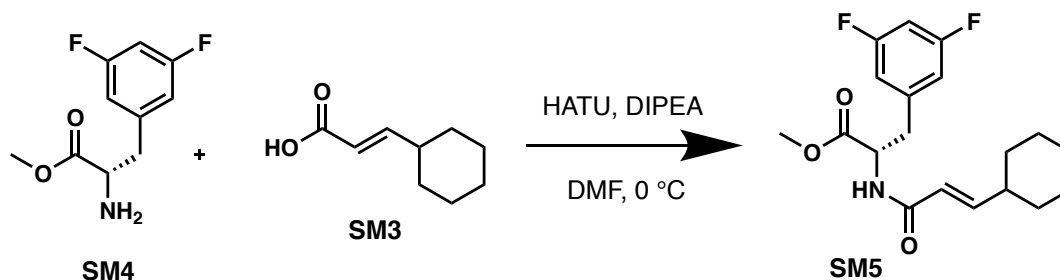
From *Bioorganic & Medicinal Chemistry*, 19(13), 4028-4042; 2011



**Methyl (*S*)-2-((*tert*-butoxycarbonyl)amino)-3-(3,5-difluorophenyl)propanoate
(SM4)**

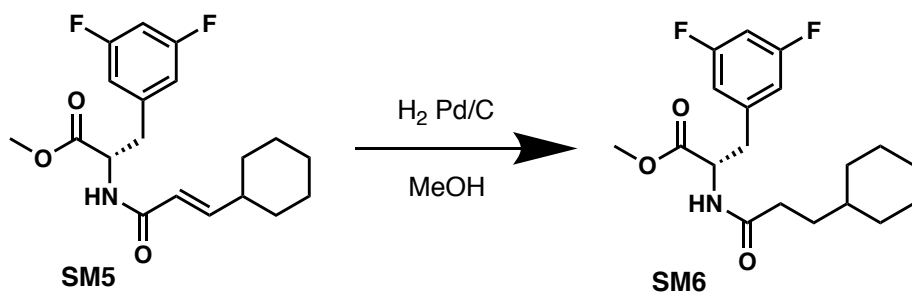
In a 50 mL round-bottomed flask was dissolved SM0 (532.7 mg, 1.768 mmol, 1.0 eq.) in MeOH (15 mL). SOCl_2 (5 mL, 68.925 mmol, 39.0 eq.) was carefully added dropwise. The reaction mixture was heated at reflux for 3 h and allowed after reaction to cool down to room temperature. The pH of the reaction mixture was carefully basified with aqueous NaOH (2 M) until a pH of ~ 11 was achieved. The resulting solution was extracted with ethyl acetate (3 x 10 mL) and the organic layers were combined and washed with H_2O (3 x 10 mL) and then with saturated aqueous NaCl (1 x 10 mL) before being dried over Na_2SO_4 and filtering. The volatiles were removed by rotary evaporation. The crude product was purified by flash chromatography (SiO_2 , EtOAc/hexane, 70:30) to afford SM4 as a yellow oil (268.4 mg, 71%). ^1H NMR (400 MHz, Chloroform- d) δ 6.72 (d, $J = 6.1$ Hz, 2H), 6.67 (t, $J = 8.8$ Hz, 1H), 3.71 (s, 4H), 3.04 (dd, $J = 13.5, 4.8$ Hz, 1H), 2.82

(dd, $J = 13.4, 7.9$ Hz, 1H) ppm. ^{13}C NMR (101 MHz, Chloroform- d) δ 175.1, 163.1 (dd, $J = 249.5, 12.8$ Hz, 2C), 141.3 (t, $J = 9.1$ Hz), 112.2 (dd, $J = 18.2, 6.6$ Hz, 2C), 102.5 (t, $J = 25.3$ Hz), 55.5, 52.3, 40.7 ppm.



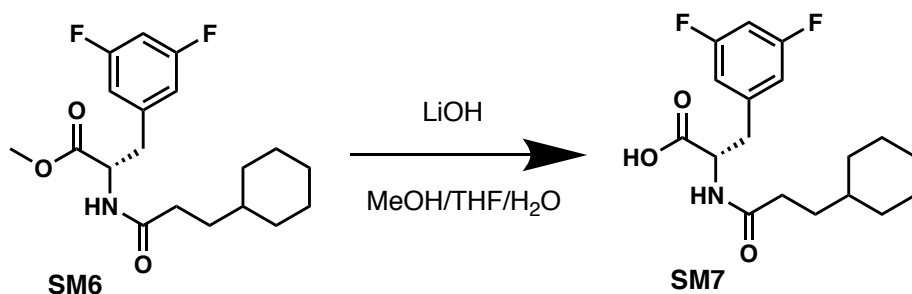
Methyl (*S,E*)-2-(3-cyclohexylacrylamido)-3-(3,5-difluorophenyl)propanoate (SM5)

General Procedure 1. Purified by flash chromatography (SiO_2 , EtOAc/hexane, gradient from 20 to 40% in EtOAc) to afford SM5 as a white solid (349.5 mg, 80%). ^1H NMR (400 MHz, Methanol- d_4) δ 6.84 (d, $J = 6.7$ Hz, 2H), 6.79 (d, $J = 9.4$ Hz, 2H), 6.71 (dd, $J = 15.5, 6.8$ Hz, 1H), 5.88 (d, $J = 15.5$ Hz, 1H), 4.74 (dd, $J = 8.9, 5.5$ Hz, 1H), 3.71 (s, 3H), 3.21 (dd, $J = 13.9, 5.3$ Hz, 1H), 2.99 (dd, $J = 13.8, 9.3$ Hz, 1H), 2.12 (dd, $J = 18.7, 11.8$ Hz, 1H), 1.76 (d, $J = 10.7$ Hz, 4H), 1.69 (d, $J = 12.1$ Hz, 1H), 1.32 (q, $J = 11.9$ Hz, 2H), 1.17 (m, 3H) ppm. ^{13}C NMR (101 MHz, Methanol- d_4) δ 173.0, 168.8, 164.4 (dd, $J = 248.5, 13.0$ Hz, 2C), 151.9, 142.9 (t, $J = 9.2$ Hz), 121.5, 113.2 (dd, $J = 19.2, 6.5$ Hz, 2C), 103.0 (t, $J = 25.7$ Hz), 54.7, 52.8, 41.6, 37.8, 33.1 (2C), 27.1, 26.9 (2C) ppm.



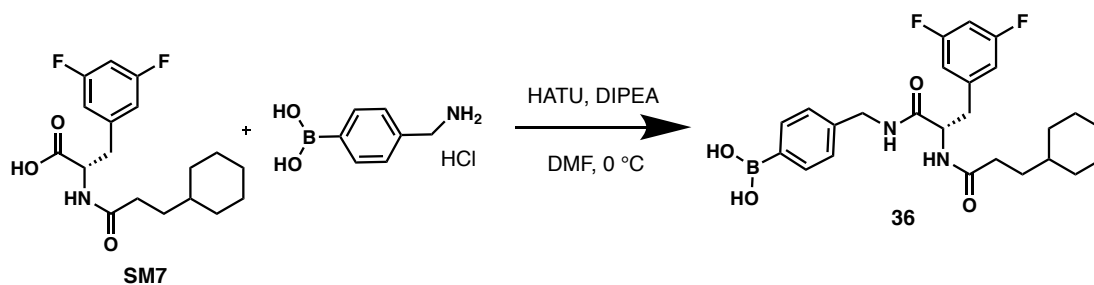
Methyl (*S*)-2-(3-cyclohexylpropanamido)-3-(3,5-difluorophenyl)propanoate (SM6)

To a solution of SM5 (349.0 mg, 0.993 mmol, 1.0 eq.) in MeOH (10 mL) was added Pd/C (21.4 mg, 0.199 mmol, 0.2 eq.). A nitrogen flow was added into the sealed vial for few minutes before adding a balloon of H₂. The reaction mixture was stirred overnight at room temperature. After the reaction is complete, the methanol was evaporated, the residue was dissolved in ethyl acetate (5 mL) and the mixture was filtered on cellite. The volatiles were removed by rotary evaporation. Purification was not needed, and the crude product was used for next step. SM6 was afforded as a white solid (266.6 mg, 76%). ¹H NMR (400 MHz, Methanol-*d*₄) δ 6.85 (d, *J* = 7.0 Hz, 2H), 6.80 (tt, *J* = 9.1, 2.2 Hz, 1H), 4.70 (dd, *J* = 9.8, 5.0 Hz, 1H), 3.72 (s, 3H), 3.22 (dd, *J* = 14.0, 4.9 Hz, 1H), 2.94 (dd, *J* = 13.9, 10.1 Hz, 1H), 2.17 (t, *J* = 7.7 Hz, 2H), 1.67 (m, 5H), 1.39 (q, *J* = 7.2 Hz, 2H), 1.18 (m, 4H), 0.86 (m, 2H) ppm. ¹³C NMR (101 MHz, Methanol-*d*₄) δ 176.5, 173.1, 167.3 (dd, *J* = 371.7, 12.4 Hz, 2C), 143.0, 113.2 (dd, *J* = 18.2, 6.8 Hz, 2C), 103.0 (t, *J* = 25.6 Hz), 54.3, 52.8, 38.4, 37.8, 34.4, 34.2, 34.2, 34.1, 27.7, 27.3, 27.3 ppm.



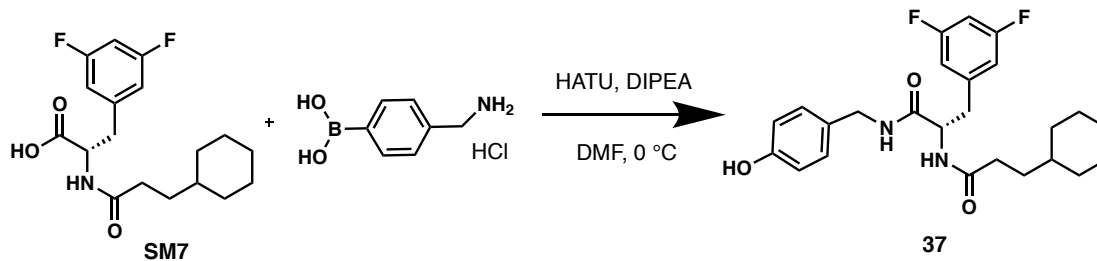
(S)-2-(3-cyclohexylpropanamido)-3-(3,5-difluorophenyl)propanoic acid (SM7)

General Procedure 8. Purification was not needed, and the crude product was used for next step. SM7 was afforded as a white solid (236.6 mg, 93%). ¹H NMR (400 MHz, Methanol-*d*₄) δ 6.85 (d, *J* = 6.8 Hz, 2H), 6.80 (tt, *J* = 9.2, 2.3 Hz, 1H), 4.69 (dd, *J* = 9.7, 4.7 Hz, 1H), 3.25 (dd, *J* = 14.1, 4.7 Hz, 1H), 2.95 (dd, *J* = 14.0, 9.9 Hz, 1H), 2.18 (t, *J* = 7.7 Hz, 2H), 1.67 (m, 5H), 1.39 (q, *J* = 7.2 Hz, 2H), 1.18 (m, 4H), 0.85 (m, 2H) ppm. ¹³C NMR (101 MHz, Methanol-*d*₄) δ 176.5, 174.2, 164.4 (dd, *J* = 247.5, 12.9 Hz, 2C), 143.2 (t, *J* = 9.4 Hz), 113.2 (dd, *J* = 20.2, 6.6 Hz, 2C), 102.9 (d, *J* = 25.6 Hz), 54.2, 38.4, 38.0, 34.4, 34.3, 34.2, 34.1, 27.7, 27.3, 27.3 ppm.



(S)-4-((2-(3-cyclohexylpropanamido)-3-(3,5-difluorophenyl)propanamido)methyl)phenylboronic acid (36)

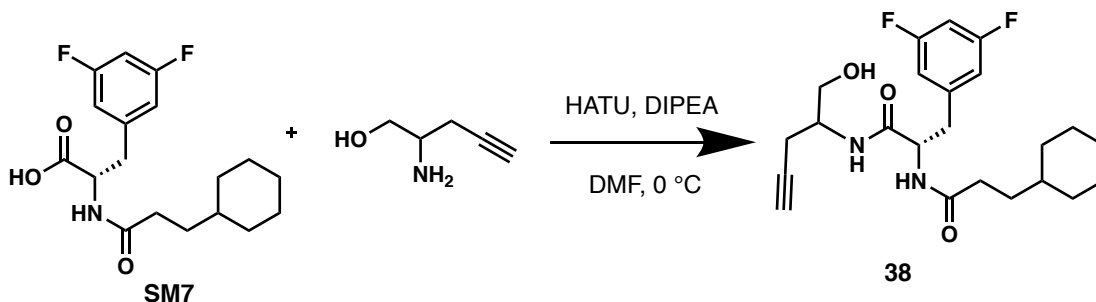
General Procedure 1. Reaction scale: 10.8 mg (0.032 mmol) of SM2. Crude solid was purified by DCM washes to afford 36 as a white solid (6.9 mg, 46%). ¹H NMR (400 MHz, Methanol-*d*₄) δ 7.61 (dd, *J* = 55.8, 7.4 Hz, 2H), 7.17 (m, 2H), 6.87 (dd, *J* = 8.2, 1.7 Hz, 2H), 6.80 (tt, *J* = 9.2, 2.0 Hz, 1H), 4.67 (dd, *J* = 8.9, 6.3 Hz, 1H), 4.35 (dd, *J* = 20.8, 15.4 Hz, 2H), 3.14 (dd, *J* = 13.8, 6.2 Hz, 1H), 2.90 (dd, *J* = 13.6, 9.2 Hz, 1H), 2.19 (t, *J* = 7.7 Hz, 2H), 1.66 (m, 5H), 1.38 (q, *J* = 7.1 Hz, 2H), 1.16 (m, 4H), 0.85 (m, 2H) ppm. ¹³C NMR (101 MHz, Methanol-*d*₄) δ 176.5, 173.1, 164.4 (dd, *J* = 247.5, 12.8 Hz, 2C), 145.9, 143.1 (t, *J* = 9.1 Hz), 135.2, 134.8 (2C), 127.6 (2C), 113.3 (dd, *J* = 18.2, 6.7 Hz, 2C), 103.0 (t, *J* = 25.7 Hz), 55.5, 44.0, 38.6, 38.5, 34.5, 34.4, 34.2, 34.1, 27.6, 27.3 (2C) ppm.



(S)-2-(3-cyclohexylpropanamido)-3-(3,5-difluorophenyl)-N-(4-hydroxybenzyl)propenamide (37)

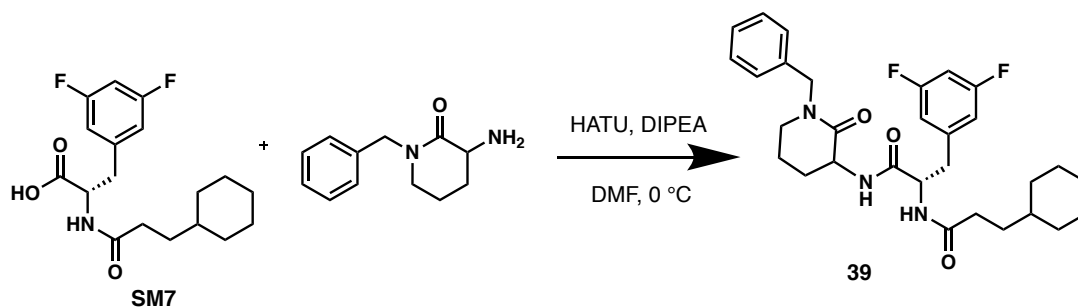
General Procedure 1. Reaction scale: 10.8 mg (0.032 mmol) of SM2. Purified by flash chromatography (SiO₂, EtOAc/hexane, gradient from 60 to 90% in EtOAc, then MeOH/DCM, 5:95) to afford 37 as a white solid (4.8 mg, 34%). ¹H NMR (400 MHz, Methanol-*d*₄) δ 7.01 (d, *J* = 8.0 Hz, 2H), 6.86 (d, *J* = 7.0 Hz, 2H), 6.79 (t, *J* = 9.0 Hz, 1H), 6.70 (d, *J* = 8.0 Hz, 2H), 4.63 (dd, *J* = 8.8, 6.5 Hz, 1H), 4.23 (q, *J* = 14.6 Hz, 2H), 3.11 (dd, *J* = 13.7, 6.1 Hz, 1H), 2.88 (dd, *J* = 13.5, 9.3 Hz, 1H), 2.18 (t, *J* = 7.7 Hz, 2H), 1.67

(m, 5H), 1.37 (q, $J = 7.2$ Hz, 2H), 1.15 (m, 4H), 0.86 (m, 2H) ppm. ^{13}C NMR (101 MHz, Methanol- d_4) δ 176.5, 172.8, 157.9, 143.1, 130.2, 129.9 (2C) 116.2 (2C), 113.3 (dd, $J = 18.2, 5.5$ Hz, 2C), 102.9, 55.5, 43.7, 38.6, 38.5, 34.4, 34.4, 34.2, 34.10, 3.64, 27.3, 27.3 ppm.



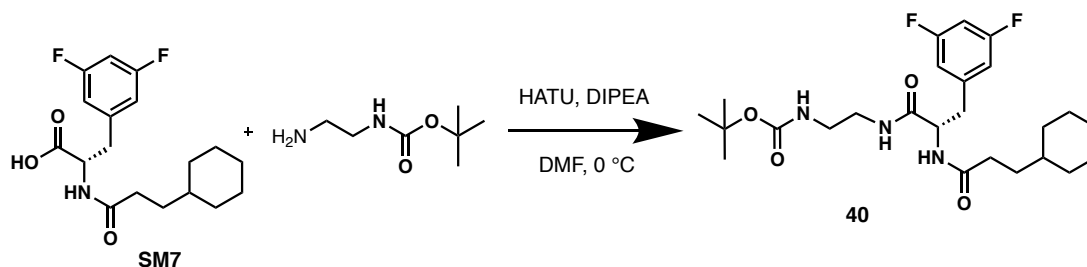
(2S)-2-(3-cyclohexylpropanamido)-3-(3,5-difluorophenyl)-N-(1-hydroxy-4-yn-2-yl)propanamide (38)

General Procedure 1. Reaction scale: 12.1 mg (0.036 mmol) of SM2. Purified by flash chromatography (SiO_2 , EtOAc/hexane, gradient from 70 to 100% in EtOAc) to afford 38 as a white solid (6.0 mg, 40%). ^1H NMR (400 MHz, Methanol- d_4) δ 6.89 (d, $J = 6.5$ Hz, 2H), 6.79 (t, $J = 9.0$ Hz, 1H), 4.66 (dd, $J = 9.5, 5.3$ Hz, 1H), 3.95 (p, $J = 5.6$ Hz, 1H), 3.60 (dd, $J = 10.8, 5.3$ Hz, 1H), 3.54 (dd, $J = 11.0, 5.6$ Hz, 1H), 3.15 (dd, $J = 13.9, 4.9$ Hz, 1H), 2.87 (dd, $J = 13.8, 10.0$ Hz, 1H), 2.45 (m, 2H), 2.30 (s, 1H), 2.18 (t, $J = 7.6$ Hz, 2H), 1.67 (m, 5H), 1.37 (q, $J = 7.2$ Hz, 2H), 1.15 (m, 4H), 0.87 (m, 2H) ppm. ^{13}C NMR (101 MHz, Methanol- d_4) δ 176.5, 173.1, 165.5, 165.4, 143.1 (t, $J = 6.2$ Hz), 113.3 (dd, $J = 19.2, 6.5$ Hz, 2C), 102.8 (d, $J = 26.6$ Hz), 81.1, 71.6, 63.0, 55.2, 51.7, 38.6, 38.5, 34.5, 34.4, 34.2, 34.1, 27.6, 27.3, 27.3, 21.2 ppm.



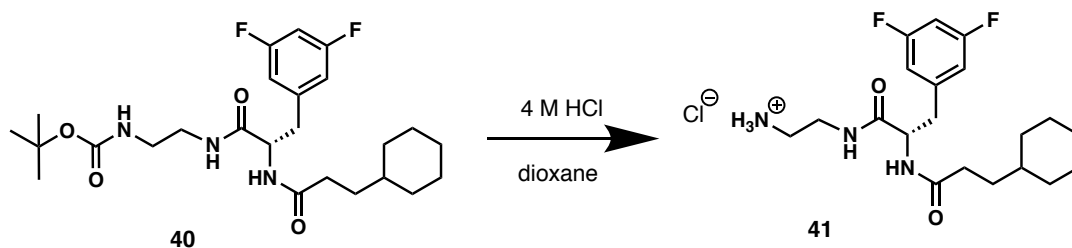
(2*S*)-*N*-(1-benzyl-2-oxopiperidin-3-yl)-2-(3-cyclohexylpropanamido)-3-(3,5-difluorophenyl)propanamide (39)

General Procedure 1. Reaction scale: 9.7 mg (0.029 mmol) of SM2. Purified by flash chromatography (SiO₂, EtOAc/hexane, gradient from 70 to 100% in EtOAc) to afford 39 as a white solid (14.5 mg, 97%). ¹H NMR (400 MHz, Methanol-*d*₄) δ 7.31 (m, 5H), 6.91 (dd, *J* = 12.3, 7.2 Hz, 2H), 6.79 (t, *J* = 9.0 Hz, 1H), 4.72 (dt, *J* = 10.0, 4.7 Hz, 1H), 4.60 (dd, *J* = 14.1, 9.8 Hz, 2H), 3.38 (m, 1H), 3.28 (m, 1H), 3.21 (m, 1H), 2.91 (m, 2H), 2.19 (q, *J* = 8.2 Hz, 2H), 2.07 (m, 1H), 1.87 (m, 3H), 1.66 (m, 5H), 1.36 (dt, *J* = 12.4, 6.9 Hz, 2H), 1.15 (m, 4H), 0.86 (m, 2H) ppm. ¹³C NMR (101 MHz, Methanol-*d*₄) δ 176.4 (d, *J* = 3.5 Hz), 172.9 (d, *J* = 34.3 Hz), 170.8 (d, *J* = 10.9 Hz), 164.3 (dd, *J* = 247.5, 13.3 Hz, 2C), 143.3 (t, *J* = 9.2 Hz), 138.1, 129.7 (2C), 129.0 (2C), 128.5, 113.3 (dd, *J* = 25.3, 4.0 Hz, 2C), 102.8 (d, *J* = 25.7 Hz), 55.1, 51.7, 51.7, 51.5, 38.7 (t, *J* = 14.9 Hz), 38.4, 34.5, 34.4, 34.2, 34.1, 28.7, 27.6, 27.3, 27.3, 22.1 (d, *J* = 5.1 Hz) ppm.



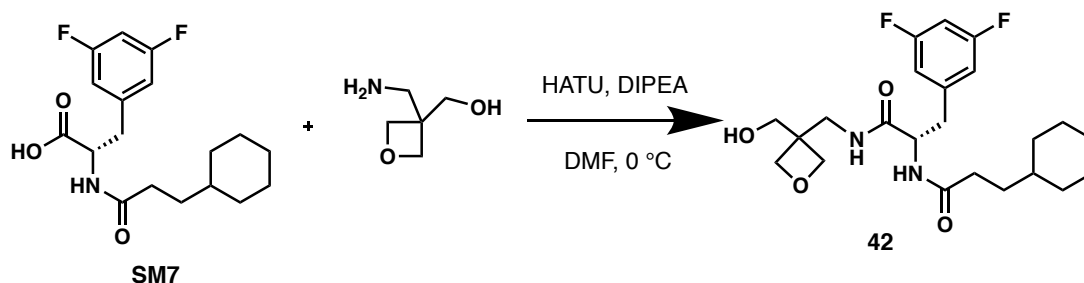
Tert-butyl (S)-2-(2-(3-cyclohexylpropanamido)-3-(3,5-difluorophenyl)propanamido)ethyl)carbamate (40)

General Procedure 1. Reaction scale: 21.2 mg (0.062 mmol) of SM2. Purified by flash chromatography (SiO_2 , EtOAc/Hexane, gradient from 70 to 90% in EtOAc) to afford 40 as a white solid (16.8 mg, 56%). ^1H NMR (400 MHz, Methanol- d_4) δ 6.87 (d, $J = 6.5$ Hz, 2H), 6.80 (t, $J = 9.0$ Hz, 1H), 4.59 (dd, $J = 9.7, 5.3$ Hz, 1H), 3.23 (m, 2H), 3.12 (m, 3H), 2.86 (dd, $J = 13.5, 10.3$ Hz, 1H), 2.19 (t, $J = 7.6$ Hz, 2H), 1.66 (m, 5H), 1.43 (s, 9H), 1.36 (q, $J = 7.2$ Hz, 2H), 1.15 (m, 4H), 0.86 (m, 2H) ppm. ^{13}C NMR (101 MHz, Methanol- d_4) δ 176.5, 173.5, 164.4 (dd, $J = 247.5, 13.0$ Hz, 2C), 158.6, 143.3, 113.2 (dd, $J = 18.2, 6.8$ Hz, 2C), 102.9 (t, $J = 25.6$ Hz), 80.2, 55.4, 40.8, 40.8, 38.6 (t, $J = 2.0$ Hz), 38.5, 34.5, 34.4, 34.2, 34.1, 28.8 (3C), 27.6, 27.3, 27.3 ppm.



(S)-N-(2-aminoethyl)-2-(3-cyclohexylpropanamido)-3-(3,5-difluorophenyl)propanamide (41)

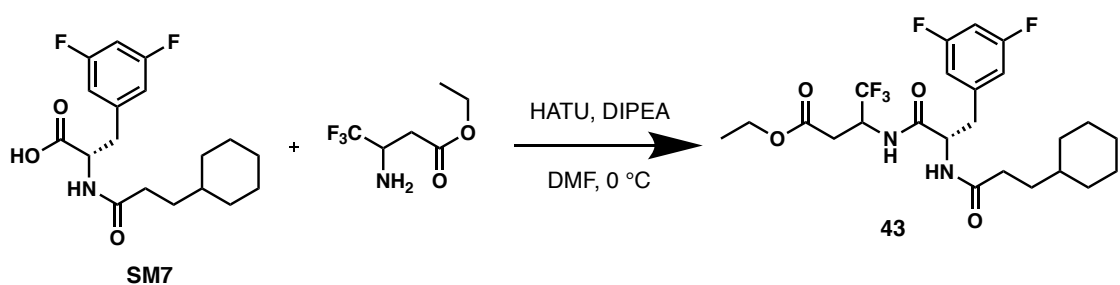
General Procedure 6. Reaction scale: 10.0 mg (0.021 mmol) of compound 40. Crude solid was purified by acetone washes to afford 41 as a white solid (4.6 mg, 53%). ¹H NMR (400 MHz, Methanol-*d*₄) δ 6.89 (dd, *J* = 8.7, 2.2 Hz, 2H), 6.82 (t, *J* = 9.0, 2.0 Hz, 1H), 4.51 (dd, *J* = 9.7, 5.5 Hz, 1H), 3.53 (m, 1H), 3.37 (m, 1H), 3.18 (dd, *J* = 13.9, 5.4 Hz, 1H), 3.03 (m, 2H), 2.92 (dd, *J* = 13.8, 9.9 Hz, 1H), 2.21 (td, *J* = 7.3, 2.1 Hz, 2H), 1.67 (m, 5H), 1.37 (q, *J* = 7.3 Hz, 2H), 1.16 (m, 4H), 0.86 (m, 2H) ppm. ¹³C NMR (101 MHz, Methanol-*d*₄) δ 177.0, 174.6, 164.4 (dd, *J* = 250.5, 13.2 Hz, 2C), 143.1 (t, *J* = 9.4 Hz), 113.2 (dd, *J* = 19.2, 6.8 Hz, 2C), 103.1 (t, *J* = 25.9 Hz), 55.9, 40.7, 40.7, 38.5, 38.0 (t, *J* = 24.8 Hz), 34.4, 34.3, 34.2, 34.1, 27.6, 27.3, 27.3 ppm.



(S)-2-(3-cyclohexylpropanamido)-3-(3,5-difluorophenyl)-N-((3-(hydroxymethyl)oxetan-3-yl)methyl)propanamide (42)

General Procedure 1. Reaction scale: 11.6 mg (0.034 mmol) of SM2. Purified by pTLC (MeOH/DCM, 10:90) to afford 42 as a yellow oil (13.2 mg, 88%). ¹H NMR (400 MHz, Methanol-*d*₄) δ 6.89 (d, *J* = 6.4 Hz, 2H), 6.81 (t, *J* = 9.1 Hz, 1H), 4.63 (dd, *J* = 9.1, 6.1

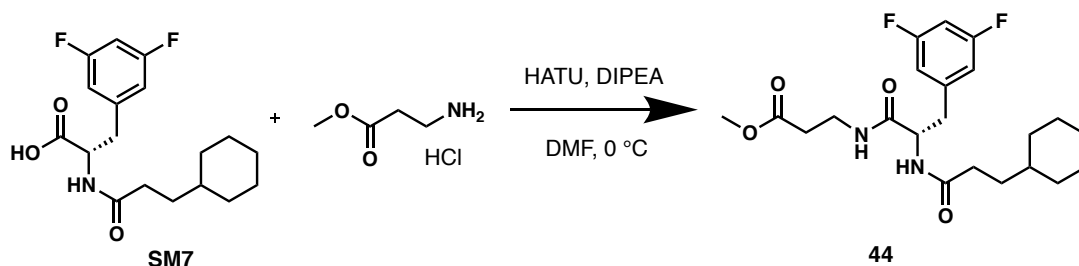
Hz, 1H), 4.39 (p, $J = 6.2$ Hz, 4H), 3.65 (dd, $J = 13.0, 11.7$ Hz, 2H), 3.48 (s, 2H), 3.13 (dd, $J = 13.8, 5.9$ Hz, 1H), 2.90 (dd, $J = 13.7, 9.5$ Hz, 1H), 2.19 (t, $J = 7.7$ Hz, 2H), 1.67 (m, 5H), 1.38 (q, $J = 7.1$ Hz, 2H), 1.14 (m, 4H), 0.86 (m, 2H) ppm. ^{13}C NMR (101 MHz, Methanol- d_4) δ 176.5, 174.1, 164.4 (dd, $J = 248.5, 13.4$ Hz, 2C), 143.1 (t, $J = 9.5$ Hz), 113.2 (dd, $J = 20.2, 6.6$ Hz, 2C), 103.0 (t, $J = 25.6$ Hz), 77.5, 65.1, 55.5, 46.0, 42.9, 38.5, 34.4, 34.3, 34.2, 34.1, 27.6, 27.31, 27.3 ppm.



Ethyl 3-((S)-2-(3-cyclohexylpropanamido)-3-(3,5-difluorophenyl)propanamido)-4,4,4-trifluorobutanoate (43)

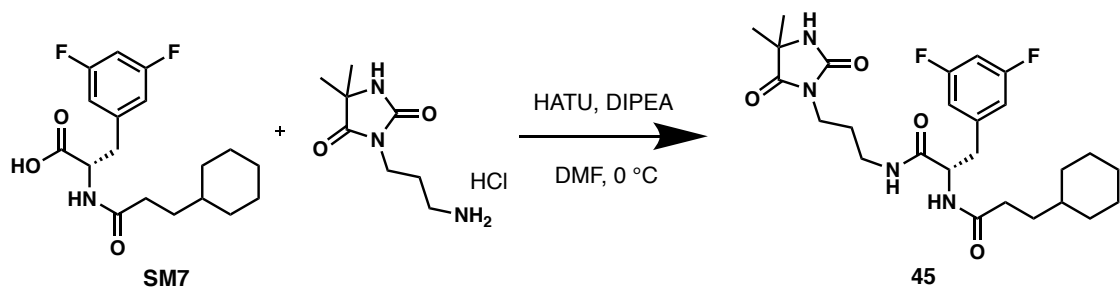
General Procedure 1. Reaction scale: 10.1 mg (0.030 mmol) of SM2. Purified by flash chromatography (SiO_2 , EtOAc/hexane, gradient from 20 to 60% in EtOAc) to afford 43 as a white solid (9.1 mg, 60%). ^1H NMR (300 MHz, Methanol- d_4) δ 6.87 (m, 2H), 6.80 (t, $J = 9.4$ Hz, 1H), 4.99 (m, 1H), 4.66 (m, 1H), 4.14 (m, 2H), 3.07 (m, 1H), 2.90 (m, 1H), 2.82 (m, 1H), 2.64 (ddd, $J = 15.8, 9.9, 4.9$ Hz, 1H), 2.17 (t, $J = 7.7$ Hz, 2H), 1.67 (m, 5H), 1.35 (m, 2H), 1.21 (m, 7H), 0.88 (m, 2H) ppm. ^{13}C NMR (101 MHz, Methanol- d_4) δ 176.4 (d, $J = 17.9$ Hz), 173.3 (d, $J = 19.1$ Hz), 170.3 (d, $J = 20.7$ Hz), 164.4 (dd, $J = 248.5, 13.1$ Hz, 2C), 142.8, 124.71, 113.3 (ddd, $J = 18.2, 8.1, 2.0$ Hz, 2C), 103.0 (t, $J = 25.9$ Hz), 62.4,

55.0 (d, $J = 13.9$ Hz), 38.8 (t, $J = 4.2$ Hz), 38.5 38.4 (d, $J = 8.0$ Hz), 34.4, 34.3, 34.1 (dd, $J = 9.1, 3.2$ Hz, 2C), 27.7, 27.3, 14.4 ppm.



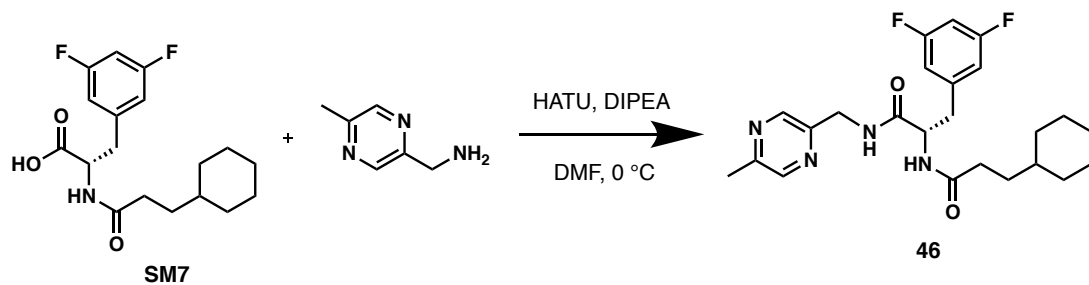
Methyl (*S*)-3-(2-(3-cyclohexylpropanamido)-3-(3,5-difluorophenyl)propanamido)-propanoate (44)

General Procedure 1. Reaction scale: 12.0 mg (0.035 mmol) of SM2. Purified by flash chromatography (SiO₂, EtOAc/hexane, gradient from 70 to 90% in EtOAc) to afford 44 as a white solid (13.6 mg, 90%). ¹H NMR (300 MHz, Methanol-*d*₄) δ 6.86 (d, $J = 6.9$ Hz, 2H), 6.80 (t, $J = 9.2$ Hz, 1H), 4.58 (dd, $J = 9.1, 5.9$ Hz, 1H), 3.67 (s, 3H), 3.41 (m, 2H), 3.10 (dd, $J = 13.7, 5.7$ Hz, 1H), 2.86 (t, $J = 13.6, 9.6$ Hz, 1H), 2.48 (t, $J = 6.3$ Hz, 2H), 2.18 (t, $J = 7.7$ Hz, 2H), 1.67 (m, 5H), 1.37 (q, $J = 7.0$ Hz, 2H), 1.16 (m, 4H), 0.87 (m, 2H) ppm. ¹³C NMR (101 MHz, Methanol-*d*₄) δ 176.4, 173.7, 173.2, 165.2, 163.6, 143.1, 113.2 (dd, $J = 14.1, 4.7$ Hz, 2C), 102.9 (t, $J = 17.1$ Hz), 55.3, 52.2, 38.6, 38.5 36.4, 36.3, 34.5, 34.4, 34.2, 34.1, 27.6, 27.3, 27.3 ppm.



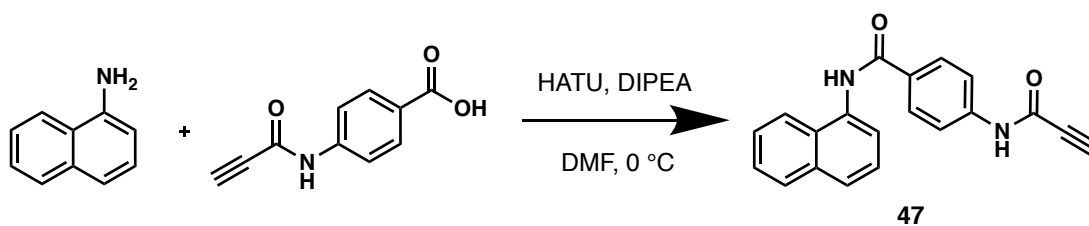
(S)-2-(3-cyclohexylpropanamido)-3-(3,5-difluorophenyl)-N-(3-(4,4-dimethyl-2,5-dioxoimidazolidin-1-yl)propyl)propanamide (45)

General Procedure 1. Reaction scale: 10.0 mg (0.030 mmol) of SM2. Purified by flash chromatography (SiO₂, EtOAc/hexane, 70:30, then MeOH/DCM gradient from 3 to 5% in MeOH) to afford 45 as a white solid (12.7 mg, 85%). ¹H NMR (500 MHz, Methanol-*d*₄) δ 6.88 (dd, *J* = 8.3, 1.7 Hz, 2H), 6.79 (tt, *J* = 9.0, 2.3 Hz, 1H), 4.59 (dd, *J* = 9.7, 5.5 Hz, 1H), 3.45 (ddq, *J* = 20.8, 13.9, 6.7 Hz, 2H), 3.19 (m, 2H), 3.12 (m, 1H), 2.87 (dd, *J* = 13.9, 9.8 Hz, 1H), 2.21 (t, *J* = 7.6 Hz, 2H), 1.73 (q, *J* = 6.7 Hz, 2H), 1.66 (m, 5H), 1.38 (m, 8H), 1.16 (m, 4H), 0.85 (m, 2H) ppm. ¹³C NMR (125 MHz, Methanol-*d*₄) δ 180.0, 176.6, 173.1, 164.4 (dd, *J* = 246.3, 13.7 Hz, 2C), 157.9, 143.4 (t, *J* = 9.5 Hz), 113.2 (dd, *J* = 20.0, 5.8 Hz, 2C), 102.9 (t, *J* = 25.8 Hz), 55.7, 55.5, 38.5, 38.4, 37.4, 36.5, 34.4, 34.3, 34.2, 34.1, 28.8, 27.6, 27.3, 27.3, 24.9 (2C) ppm.



(S)-2-(3-cyclohexylpropanamido)-3-(3,5-difluorophenyl)-N-((5-methylpyrazin-2-yl)methyl)propanamide (46)

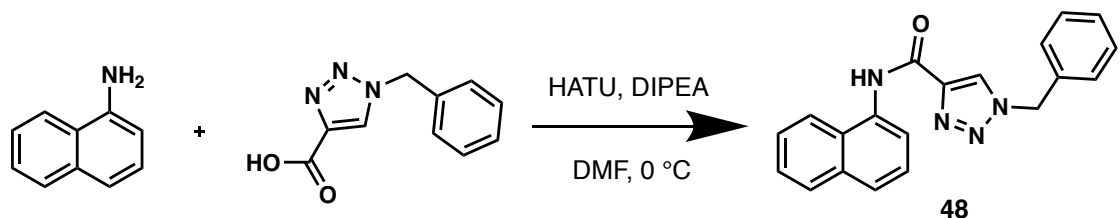
General Procedure 1. Reaction scale: 11.5 mg (0.034 mmol) of SM2. Purified by flash chromatography (SiO₂, MeOH/DCM gradient from 1 to 10% in MeOH) to afford 46 as a white solid (10.4 mg, 69%). ¹H NMR (400 MHz, Methanol-*d*₄) δ 8.44 (s, 1H), 8.38 (s, 1H), 6.84 (dd, *J* = 8.2, 1.9 Hz, 2H), 6.78 (tt, *J* = 9.2, 2.4 Hz, 1H), 4.68 (dd, *J* = 9.0, 6.1 Hz, 1H), 4.49 (d, *J* = 15.7 Hz, 1H), 4.43 (d, *J* = 15.7 Hz, 1H), 3.15 (dd, *J* = 13.8, 5.9 Hz, 1H), 2.90 (dd, *J* = 13.7, 9.3 Hz, 1H), 2.53 (s, 3H), 2.20 (t, *J* = 7.7 Hz, 2H), 1.67 (m, 5H), 1.38 (q, *J* = 7.1 Hz, 2H), 1.15 (m, 4H), 0.85 (m, 2H) ppm. ¹³C NMR (101 MHz, Methanol-*d*₄) δ 176.5, 173.5, 164.3 (dd, *J* = 247.5, 12.8 Hz, 2C), 153.8, 151.7, 145.0, 143.2, 143.0, 113.2 (dd, *J* = 18.2, 6.7 Hz, 2C), 103.0 (t, *J* = 25.8 Hz), 55.4, 43.4, 38.5, 38.4, 34.4, 34.4, 34.2, 34.1, 27.6, 27.3, 27.28, 20.9 ppm.



N-(naphthalen-1-yl)-4-propiolamidobenzamide (47)

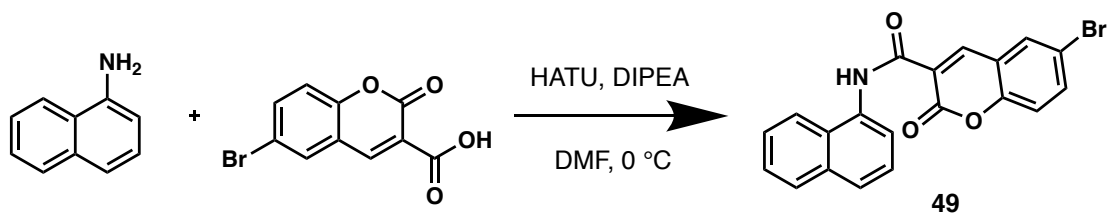
General Procedure 1. Reaction scale: 6.8 mg (0.048 mmol) of 1-naphthylamine. Purified by flash chromatography (SiO₂, EtOAc/hexane, gradient from 20 to 90% in EtOAc) and hexane wash to afford 47 as a white/yellow solid (7.8 mg, 52%). ¹H NMR (400 MHz,

Methanol-*d*₄) δ 8.06 (d, *J* = 8.4 Hz, 2H), 7.98 (m, 1H), 7.92 (m, 1H), 7.85 (d, *J* = 8.1 Hz, 1H), 7.79 (d, *J* = 8.5 Hz, 2H), 7.58 (d, *J* = 7.1 Hz, 1H), 7.53 (m, 3H), 2.81 (s, 1H) ppm. ¹³C NMR (101 MHz, Methanol-*d*₄) δ 170.5, 152.4, 142.8, 135.8, 134.5, 131.3, 131.0, 129.9 (2C), 129.4, 128.3, 127.4, 127.2, 126.5, 125.3, 123.9, 120.7 (2C), 78.0, 38.9 ppm.



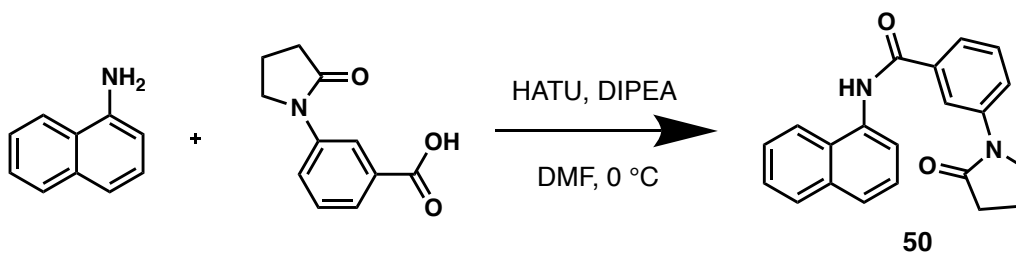
1-benzyl-*N*-(naphthalen-1-yl)-1*H*-1,2,3-triazole-4-carboxamide (48)

General Procedure 1. Reaction scale: 6.5 mg (0.046 mmol) of 1-naphthylamine. Crude solid was purified by methanol washes to afford 48 as a white solid (11.8 mg, 79%). ¹H NMR (400 MHz, DMSO-*d*₃) δ 10.58 (s, 1H), 8.87 (s, 1H), 7.96 (m, 2H), 7.86 (d, *J* = 8.2 Hz, 1H), 7.62 (d, *J* = 7.3 Hz, 1H), 7.55 (m, 3H), 7.42 (m, 4H), 7.37 (m, 1H), 5.73 (s, 2H), 2.81 (s, 1H) ppm. ¹³C NMR (101 MHz, DMSO-*d*₃) δ 159.2, 142.9, 135.7, 133.8, 133.1, 129.4, 128.9 (2C), 128.6, 128.5, 128.2 (2C), 128.0, 127.7, 126.4, 126.2, 125.78, 123.2, 123.0, 53.3 ppm.



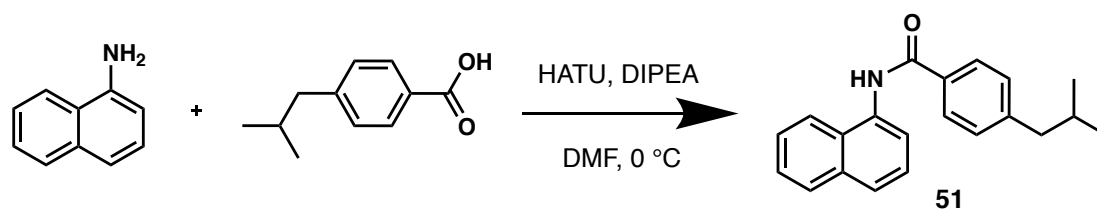
6-bromo-*N*-(naphthalen-1-yl)-2-oxo-2*H*-chromene-3-carboxamide (49)

General Procedure 1. Reaction scale: 5.4 mg (0.038 mmol) of 1-naphthylamine. Crude solid was purified by methanol washes to afford 49 as a yellow solid (14.4 mg, 97%). ¹H NMR (400 MHz, DMSO-*d*₃) δ 11.21 (s, 1H), 9.01 (s, 1H), 8.34 (s, 1H), 8.27 (d, *J* = 7.5 Hz, 1H), 8.10 (d, *J* = 8.4 Hz, 1H), 8.01 (d, *J* = 8.1 Hz, 1H), 7.95 (dd, *J* = 8.9, 2.5 Hz, 1H), 7.81 (d, *J* = 8.2 Hz, 1H), 7.68 (t, *J* = 7.6 Hz, 1H), 7.59 (m, 3H) ppm. ¹³C NMR (101 MHz, DMSO-*d*₃) δ 161.0, 159.8, 153.0, 146.8, 136.7, 133.7, 132.6, 132.3, 128.8, 126.7, 126.4, 126.4, 125.9, 125.9, 125.3, 120.7, 120.5, 118.9, 118.6, 117.0 ppm.



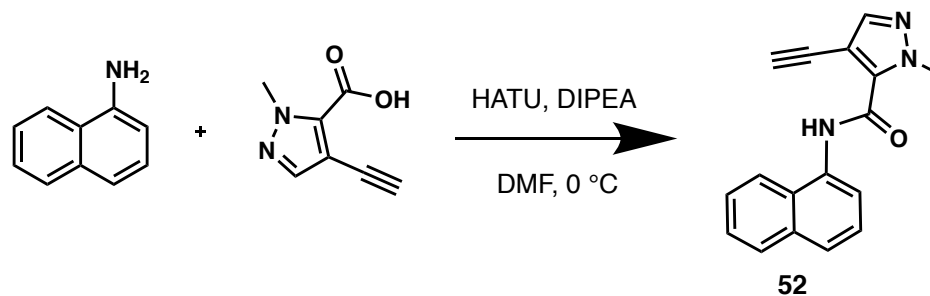
N-(naphthalen-1-yl)-3-(2-oxopyrrolidin-1-yl)benzamide (50)

General Procedure 1. Reaction scale: 6.5 mg (0.045 mmol) of 1-naphthylamine. Crude solid was purified by methanol washes to afford 50 as a white solid (5.0 mg, 33%). ¹H NMR (400 MHz, DMSO-*d*₃) δ 10.48 (s, 1H), 8.22 (s, 1H), 7.99 (m, 3H), 7.87 (m, 2H), 7.57 (m, 5H), 3.94 (t, *J* = 7.0 Hz, 2H), 2.54 (t, *J* = 8.0 Hz, 2H), 2.10 (p, *J* = 7.6 Hz, 2H) ppm. ¹³C NMR (101 MHz, DMSO-*d*₃) δ 174.2, 166.0, 139.8, 135.0, 133.8 (2C), 129.2, 128.8, 128.1, 126.4, 126.1, 126.1, 125.6, 124.0, 123.4, 123.1, 122.6, 118.7, 48.2, 32.4, 17.5 ppm.



4-isobutyl-N-(naphthalen-1-yl)benzamide (51)

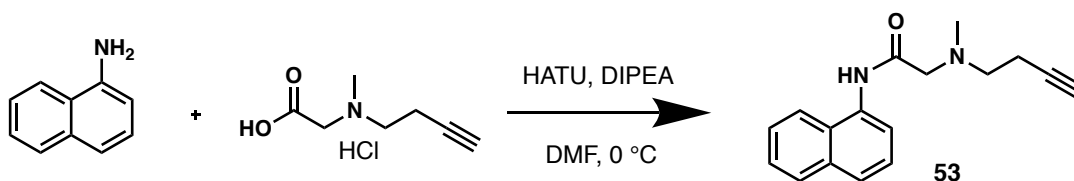
General Procedure 1. Reaction scale: 7.1 mg (0.049 mmol) of 1-naphthylamine. Purified by flash chromatography (SiO₂, EtOAc/hexane, gradient from 20 to 50% in EtOAc) to afford 51 as a white solid (11.4 mg, 76%). ¹H NMR (400 MHz, Acetone-*d*₆) δ 9.60 (s, 1H), 8.13 (m, 1H), 8.08 (d, *J* = 8.2 Hz, 2H), 7.95 (m, 1H), 7.82 (d, *J* = 7.9 Hz, 2H), 7.53 (m, 3H), 7.36 (d, *J* = 8.2 Hz, 2H), 2.60 (d, *J* = 7.2 Hz, 2H), 1.94 (m, 1H), 0.94 (d, *J* = 6.6 Hz, 6H) ppm. ¹³C NMR (101 MHz, Acetone-*d*₆) δ 166.8, 146.5, 135.2, 135.0, 133.5, 130.0 (2C), 129.9, 129.1, 128.5 (2C), 126.8 (2C), 126.7, 126.4, 123.7, 123.7, 45.7, 30.9, 22.6 (2C) ppm.



4-ethynyl-1-methyl-N-(naphthalen-1-yl)-1H-pyrazole-5-carboxamide (52)

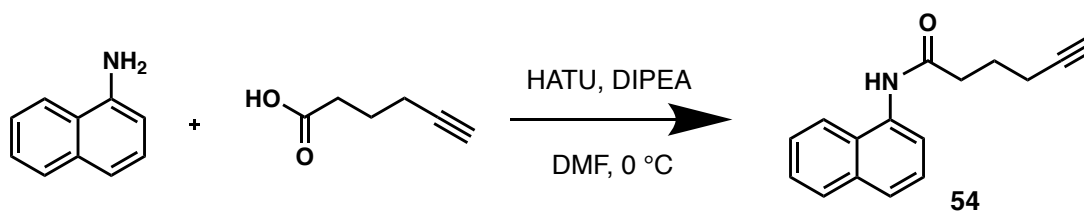
General Procedure 1. Reaction scale: 7.8 mg (0.054 mmol) of 1-naphthylamine. Purified by flash chromatography (SiO₂, EtOAc/hexane, gradient from 20 to 50% in EtOAc) to

afford 52 as a white solid (12.2 mg, 81%). ^1H NMR (400 MHz, Acetone- d_6) δ 9.56 (s, 1H), 8.30 (d, $J = 8.2$ Hz, 1H), 8.16 (d, $J = 7.5$ Hz, 1H), 7.99 (d, $J = 7.9$ Hz, 1H), 7.84 (d, $J = 8.2$ Hz, 1H), 7.77 (s, 1H), 7.59 (m, 3H), 4.35 (s, 1H), 4.20 (s, 3H) ppm. ^{13}C NMR (101 MHz, Acetone- d_6) δ 158.2, 141.8, 138.5, 135.1, 133.4, 129.5, 128.3, 127.8, 127.0, 126.8, 126.4, 122.4, 121.8, 103.0, 86.4, 76.1, 40.5 ppm.



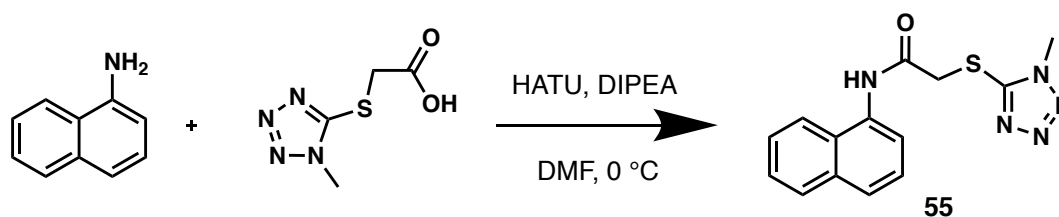
2-(but-3-yn-1-yl(methyl)amino)-*N*-(naphthalen-1-yl)acetamide (53)

General Procedure 1. Reaction scale: 8.1 mg (0.056 mmol) of 1-naphthylamine. Purified by pTLC (EtOAc/hexane, 20:80) to afford 53 as a white/yellow solid (8.1 mg, 54%). ^1H NMR (400 MHz, Acetone- d_6) δ 8.26 (dd, $J = 7.1, 5.1$ Hz, 1H), 8.07 (d, $J = 8.2$ Hz, 1H), 7.94 (d, $J = 7.8$ Hz, 1H), 7.70 (d, $J = 8.2$ Hz, 1H), 7.56 (m, 2H), 7.49 (t, $J = 7.9$ Hz, 1H), 3.32 (s, 2H), 2.86 (t, $J = 6.8$ Hz, 1H), 2.58 (td, $J = 6.8, 2.5$ Hz, 2H), 2.54 (s, 3H), 2.39 (t, $J = 2.5$ Hz, 1H) ppm. ^{13}C NMR (101 MHz, Acetone- d_6) δ 169.5, 135.0, 134.1, 129.4, 126.9, 126.8, 126.6, 125.0, 121.7, 118.6, 118.5, 83.5, 71.0, 62.6, 57.1, 43.1, 18.2 ppm.



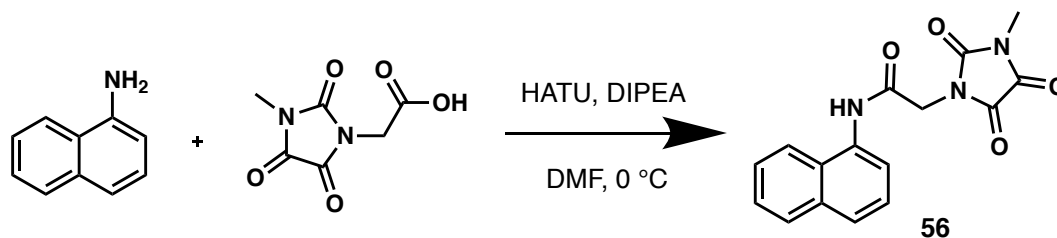
***N*-(naphthalen-1-yl)hex-5-ynamide (54)**

General Procedure 1. Reaction scale: 9.1 mg (0.063 mmol) of 1-naphthylamine. Purified by flash chromatography (SiO₂, EtOAc/hexane, gradient from 20 to 50% in EtOAc) to afford 54 as a white solid (14.5 mg, 96%). ¹H NMR (400 MHz, Acetone-*d*₆) δ 9.22 (s, 1H), 8.14 (m, 1H), 7.92 (m, 2H), 7.73 (d, *J* = 8.2 Hz, 1H), 7.49 (m, 3H), 2.71 (t, *J* = 7.3 Hz, 2H), 2.42 (s, 1H), 2.34 (td, *J* = 7.2, 2.6 Hz, 2H), 1.95 (p, *J* = 7.2 Hz, 2H) ppm. ¹³C NMR (101 MHz, Acetone-*d*₆) δ 171.8, 135.1, 134.7, 129.1, 128.5, 126.7, 126.6, 126.4, 125.8, 122.9, 121.8, 84.4, 70.4, 35.9, 25.3, 18.4 ppm.



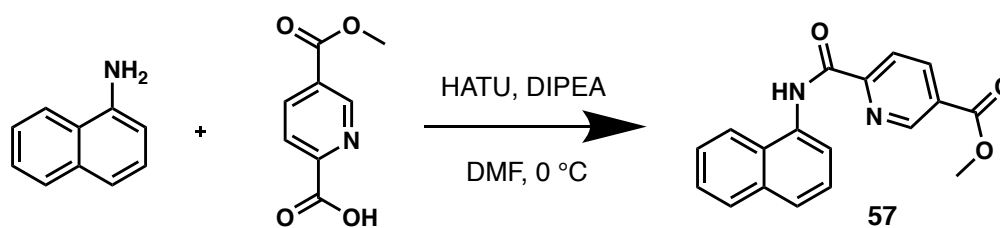
2-((1-methyl-1H-tetrazol-5-yl)thio)-*N*-(naphthalen-1-yl)acetamide (55)

General Procedure 1. Reaction scale: 7.2 mg (0.050 mmol) of 1-naphthylamine. Purified by flash chromatography (SiO₂, EtOAc/hexane, gradient from 40 to 80% in EtOAc) to afford 55 as a white solid (10.3 mg, 68%). ¹H NMR (400 MHz, Acetone-*d*₆) δ 9.73 (s, 1H), 8.18 (m, 1H), 7.91 (m, 2H), 7.76 (d, *J* = 8.2 Hz, 1H), 7.53 (m, 2H), 7.49 (t, *J* = 7.9 Hz, 1H), 4.47 (s, 2H), 4.05 (s, 3H), 1.95 (p, *J* = 7.2 Hz, 2H) ppm. ¹³C NMR (101 MHz, Acetone-*d*₆) δ 166.7, 154.6, 135.1, 134.2, 129.2, 128.4, 126.9 (2C), 126.4, 126.4, 122.9, 121.6, 38.3, 34.1 ppm.



2-(3-methyl-2,4,5-trioximidazolidin-1-yl)-N-(naphthalen-1-yl)acetamide (56)

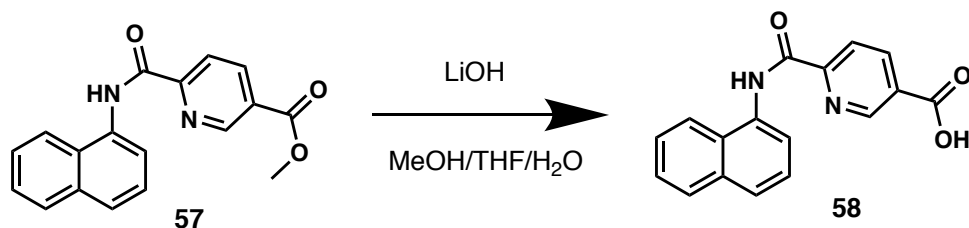
General Procedure 1. Reaction scale: 6.9 mg (0.048 mmol) of 1-naphthylamine. Purified by flash chromatography (SiO₂, EtOAc/hexane, gradient from 40 to 90% in EtOAc) and hexane wash to afford 56 as a white/yellow solid (5.6 mg, 37%). ¹H NMR (400 MHz, Acetone-*d*₆) δ 9.58 (s, 1H), 8.13 (m, 1H), 7.94 (m, 1H), 7.80 (m, 2H), 7.55 (t, *J* = 3.9 Hz, 2H), 7.50 (t, *J* = 7.9 Hz, 1H), 4.72 (s, 2H), 3.17 (s, 3H) ppm. ¹³C NMR (101 MHz, Acetone-*d*₆) δ 165.4, 158.2, 158.1, 155.1, 135.1, 133.7, 129.2, 128.9, 127.0, 126.9 (2C), 126.4, 123.0, 122.6, 42.3, 25.0 ppm.



Methyl 6-(naphthalen-1-ylcarbamoyl)nicotinate (57)

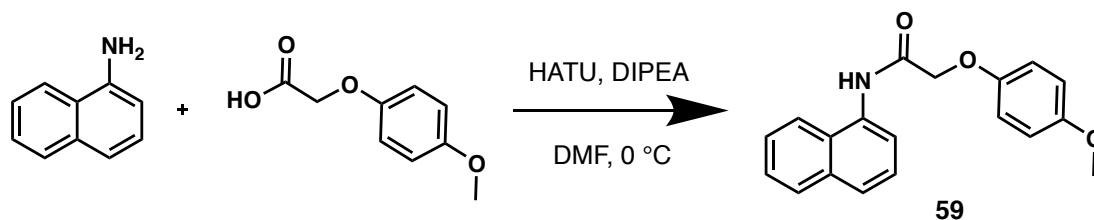
General Procedure 1. Reaction scale: 7.0 mg (0.049 mmol) of 1-naphthylamine. Purified by flash chromatography (SiO₂, EtOAc/hexane, gradient from 40 to 70% in EtOAc) to afford 57 as a yellow solid (11.5 mg, 65%). ¹H NMR (400 MHz, DMSO-*d*₃) δ 11.03 (s, 1H), 9.25 (s, 1H), 8.57 (dd, *J* = 8.2, 2.1 Hz, 1H), 8.32 (d, *J* = 8.1 Hz, 1H), 7.98 (dt, *J* =

9.8, 5.4 Hz, 2H), 7.86 (dd, $J = 11.4, 7.7$ Hz, 2H), 7.58 (m, 3H), 3.96 (s, 3H) ppm. ^{13}C NMR (101 MHz, $\text{DMSO-}d_3$) δ 164.7, 162.3, 153.0, 149.1, 139.0, 133.7, 133.0, 128.3, 128.1, 128.1, 126.3, 126.2, 126.1, 125.7, 122.6, 122.4, 122.1, 52.8 ppm.



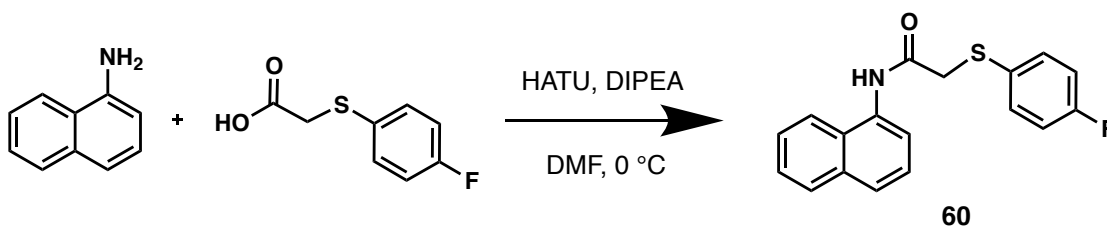
6-(naphthalen-1-ylcarbamoyl)nicotinic acid (58)

General Procedure 8. Reaction scale: 7.0 mg (0.023 mmol) of compound 57. No purification was needed and 58 was afforded as a white/yellow solid (2.7 mg, 40%). ^1H NMR (400 MHz, Methanol- d_4) δ 9.33 (s, 1H), 8.60 (d, $J = 6.9$ Hz, 1H), 8.35 (d, $J = 8.0$ Hz, 1H), 8.04 (dd, $J = 15.2, 7.7$ Hz, 2H), 7.95 (d, $J = 7.7$ Hz, 1H), 7.82 (d, $J = 8.2$ Hz, 1H), 7.58 (m, 3H) ppm. ^{13}C NMR (101 MHz, Methanol- d_4) δ 166.8, 164.3, 154.8, 151.0, 140.3, 135.7, 133.6, 129.7, 129.6, 129.1, 127.6, 127.4, 127.3, 126.6, 123.2, 122.5, 122.2 ppm.



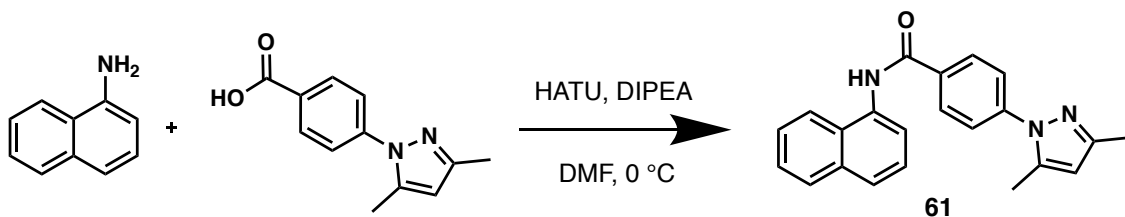
2-(4-methoxyphenoxy)-N-(naphthalen-1-yl)acetamide (59)

General Procedure 1. Reaction scale: 28.6 mg (0.200 mmol) of 1-naphthylamine. Purified by flash chromatography (SiO₂, EtOAc/hexane, gradient from 30 to 60% in EtOAc) to afford 59 as a white solid (61.5 mg, 100%). ¹H NMR (300 MHz, Acetone-*d*₆) δ 9.41 (s, 1H), 7.93 (m, 3H), 7.79 (d, *J* = 8.1 Hz, 1H), 7.52 (m, 3H), 7.11 (d, *J* = 8.6 Hz, 2H), 6.94 (d, *J* = 8.7 Hz, 2H), 4.75 (s, 2H), 3.77 (s, 3H) ppm. ¹³C NMR (75 MHz, Acetone-*d*₆) δ 168.0, 155.7, 152.8, 135.1, 133.6, 129.2, 128.8, 126.9, 126.9, 126.6, 126.4, 122.7, 122.3, 116.7 (2C), 115.5 (2C), 69.2, 55.8 ppm.



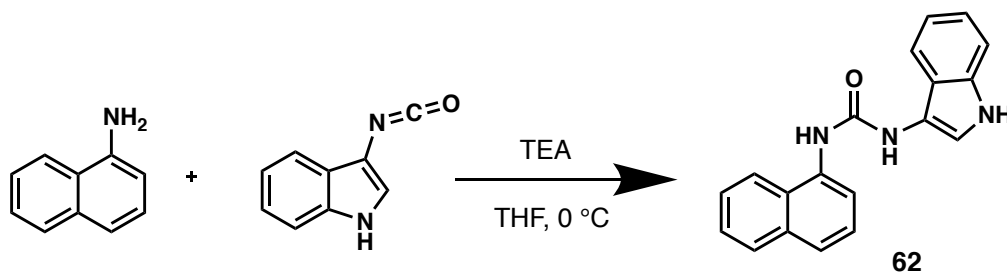
2-((4-fluorophenyl)thio)-*N*-(naphthalen-1-yl)acetamide (60)

General Procedure 1. Reaction scale: 28.6 mg (0.200 mmol) of 1-naphthylamine. Purified by flash chromatography (SiO₂, EtOAc/hexane, gradient from 30 to 70% in EtOAc) to afford 60 as a white/orange solid (50.9 mg, 82%). ¹H NMR (400 MHz, Acetone-*d*₆) δ 9.42 (s, 1H), 7.90 (t, *J* = 6.5 Hz, 2H), 7.83 (d, *J* = 7.4 Hz, 1H), 7.74 (d, *J* = 8.2 Hz, 1H), 7.61 (dd, *J* = 8.3, 5.4 Hz, 2H), 7.48 (m, 3H), 7.14 (t, *J* = 8.7 Hz, 2H), 3.99 (s, 2H) ppm. ¹³C NMR (101 MHz, Acetone-*d*₆) δ 168.1, 162.7, 135.0, 134.1, 133.3, 133.2, 131.8 (d, *J* = 3.0 Hz), 129.2, 128.6, 126.8, 126.8, 126.3 (2C), 122.6, 121.9, 117.0, 116.8, 39.9 ppm.



4-(3,5-dimethyl-1H-pyrazol-1-yl)-N-(naphthalen-1-yl)benzamide (61)

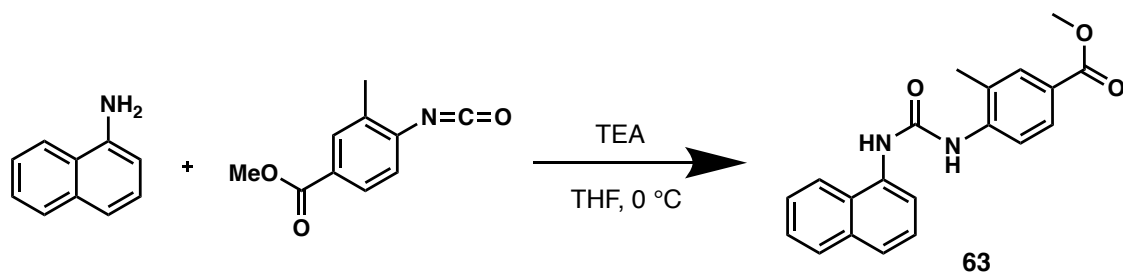
General Procedure 1. Reaction scale: 28.6 mg (0.200 mmol) of 1-naphthylamine. Purified by flash chromatography (SiO₂, EtOAc/hexane, gradient from 20 to 60% in EtOAc) to afford 61 as a white/brown solid (48.6 mg, 72%). ¹H NMR (500 MHz, Acetone-*d*₆) δ 9.74 (s, 1H), 8.26 (d, *J* = 8.5 Hz, 2H), 8.16 (dd, *J* = 6.3, 3.3 Hz, 1H), 7.96 (dd, *J* = 6.2, 3.2 Hz, 1H), 7.84 (d, *J* = 7.8 Hz, 2H), 7.72 (d, *J* = 8.5 Hz, 2H), 7.54 (m, 3H), 6.10 (s, 1H), 2.44 (s, 3H), 2.23 (s, 3H) ppm. ¹³C NMR (125 MHz, Acetone-*d*₆) δ 166.2, 149.9, 143.8, 140.4, 135.2, 134.8, 133.8, 130.0, 129.5 (2C), 129.1, 127.0, 126.8, 126.8, 126.4, 124.2 (2C), 123.8, 123.7, 108.8, 13.6, 12.9 ppm.



1-(1H-indol-3-yl)-3-(naphthalen-1-yl)urea (62)

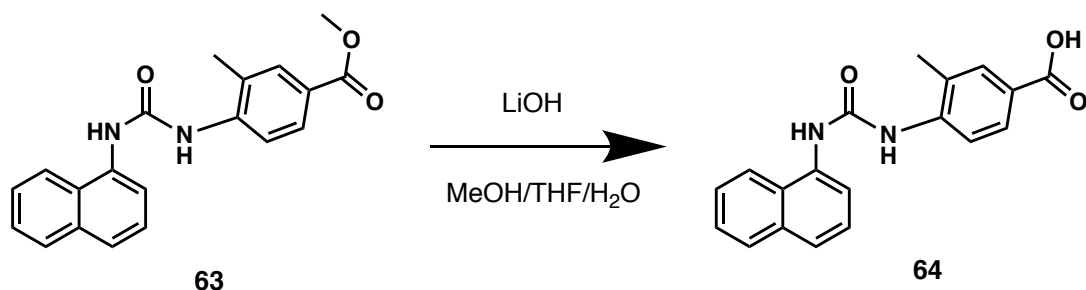
General Procedure 3. Reaction scale: 7.9 mg (0.050 mmol) of isocyanate. Crude solid was purified by DCM/EtOAc washes to afford 62 as a white solid (6.0 mg, 40%). ¹H NMR

(400 MHz, Acetone- d_6) δ 8.41 (d, J = 16.2 Hz, 1H), 8.21 (d, J = 6.7 Hz, 1H), 8.12 (s, 1H), 7.91 (m, 1H), 7.73 (s, 1H), 7.61 (m, 2H), 7.48 (m, 2H), 7.39 (t, J = 9.5 Hz, 1H), 7.12 (q, J = 8.0 Hz, 1H), 7.01 (m, 1H) ppm. ^{13}C NMR (101 MHz, Acetone- d_6) δ 154.2, 135.9, 135.3, 135.2, 129.4, 126.7, 126.5, 126.4, 125.1, 123.7, 122.6, 122.4, 121.9, 119.3, 118.3, 118.2, 117.8, 112.3, 112.2 ppm.



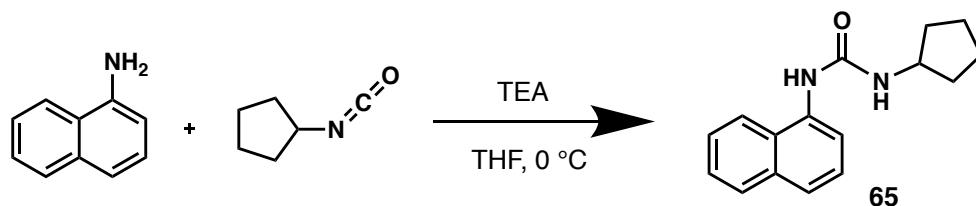
Methyl 3-methyl-4-(3-(naphthalen-1-yl)ureido)benzoate (63)

General Procedure 3. Reaction scale: 8.6 mg (0.045 mmol) of isocyanate. Crude solid was purified by acetone/MeOH washes to afford 63 as a white solid (10.4 mg, 70%). ^1H NMR (400 MHz, DMSO- d_3) δ 9.35 (s, 1H), 8.59 (s, 1H), 8.25 (d, J = 8.6 Hz, 1H), 8.18 (d, J = 8.5 Hz, 1H), 7.99 (d, J = 7.5 Hz, 1H), 7.95 (d, J = 8.0 Hz, 1H), 7.82 (s, 1H), 7.79 (d, J = 8.6 Hz, 1H), 7.68 (d, J = 8.2 Hz, 1H), 7.62 (t, J = 7.4 Hz, 1H), 7.56 (t, J = 7.4 Hz, 1H), 7.50 (t, J = 7.9 Hz, 1H), 3.82 (s, 3H), 2.39 (s, 3H) ppm. ^{13}C NMR (101 MHz, DMSO- d_3) δ 166.1, 152.7, 142.6, 134.0, 133.8, 131.3, 128.5, 127.9, 126.2, 126.1, 126.0, 125.9, 125.8, 123.4, 122.6, 121.6, 118.7, 118.2, 51.8, 18.1 ppm.



3-methyl-4-(3-(naphthalen-1-yl)ureido)benzoic acid (64)

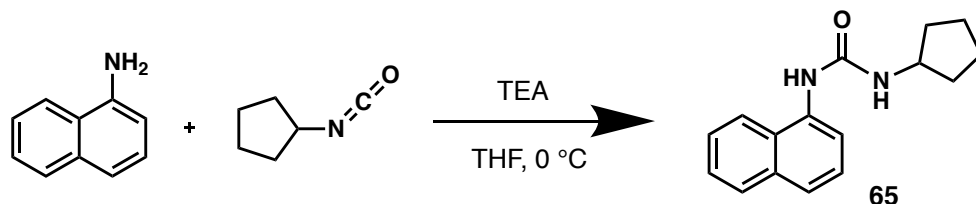
General Procedure 8. Reaction scale: 6.4 mg (0.019 mmol) of compound 63. No purification was needed and 64 was afforded as a white solid (3.2 mg, 52%). ¹H NMR (300 MHz, Methanol-*d*₄) δ 8.09 (t, *J* = 9.4 Hz, 2H), 7.88 (m, 4H), 7.71 (d, *J* = 8.1 Hz, 1H), 7.52 (m, 3H), 2.40 (s, 3H) ppm. ¹³C NMR (75 MHz, Methanol-*d*₄) δ 167.1, 161.6, 137.8, 135.8, 133.2, 132.8, 131.3, 129.3, 128.7, 128.6, 127.4, 127.3, 126.4, 125.3, 125.1, 123.5, 118.6, 118.4, 28.2 ppm.



1-cyclopentyl-3-(naphthalen-1-yl)urea (65)

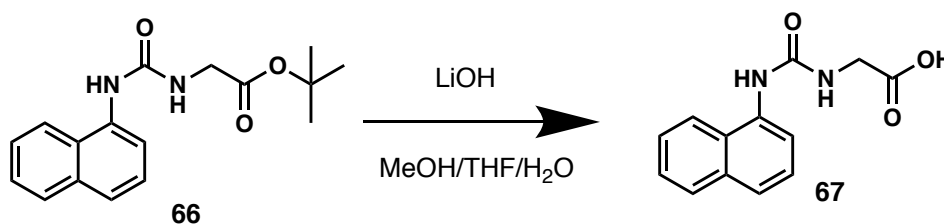
General Procedure 3. Reaction scale: 6.6 mg (0.059 mmol) of isocyanate. Crude solid was purified by MeOH washes to afford 65 as a white solid (4.9 mg, 33%). ¹H NMR (400 MHz, DMSO-*d*₃) δ 8.38 (s, 1H), 8.05 (t, *J* = 8.4 Hz, 2H), 7.88 (d, *J* = 8.0 Hz, 1H), 7.52 (m, 3H), 7.40 (t, *J* = 7.9 Hz, 1H), 6.64 (d, *J* = 7.1 Hz, 1H), 3.99 (h, *J* = 6.6 Hz, 1H), 1.88

(dq $J = 12.2, 6.4$ Hz, 2H), 1.67 (m, 2H), 1.57 (m, 2H), 1.41 (dq, $J = 11.7, 6.0$ Hz, 2H) ppm. ^{13}C NMR (101 MHz, DMSO- d_3) δ 155.0, 135.2, 133.7, 128.4, 126.0, 125.7, 125.4, 125.1, 121.7, 121.1, 115.7, 51.0, 33.0 (2C), 23.2 (2C) ppm.



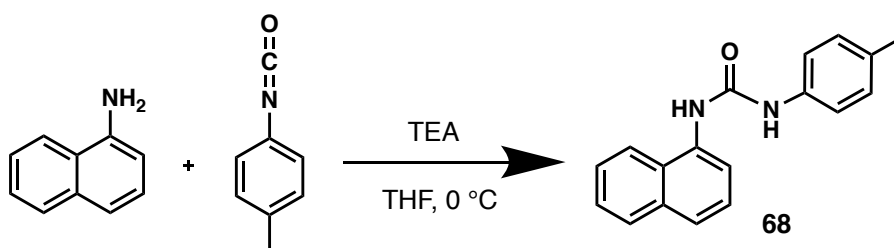
***Tert*-butyl (naphthalen-1-ylcarbamoyl)glycinate (66)**

General Procedure 3. Reaction scale: 7.8 mg (0.050 mmol) of isocyanate. Purified by flash chromatography (SiO₂, EtOAc/Hexane, gradient from 50 to 70% in EtOAc) to afford 66 as a white/brown solid (13.7 mg, 59%). ^1H NMR (400 MHz, Methanol- d_4) δ 8.06 (m, 1H), 7.86 (m, 1H), 7.67 (d, $J = 7.7$ Hz, 2H), 7.50 (m, 2H), 7.44 (t, $J = 7.9$ Hz, 1H), 3.88 (s, 2H), 1.49 (s, 9H) ppm. ^{13}C NMR (101 MHz, Methanol- d_4) δ 171.7, 159.3, 135.8, 134.1, 129.8, 129.4, 127.0, 127.0, 126.7, 126.1, 123.0, 122.2, 82.7, 43.6, 28.3 (3C) ppm.



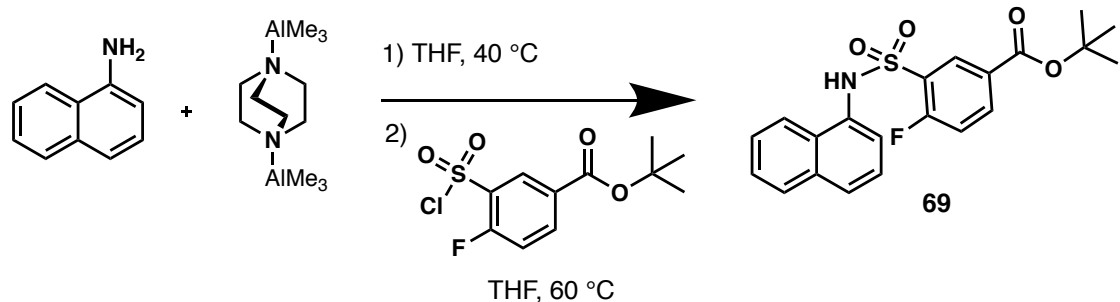
(naphthalen-1-ylcarbamoyl)glycine (67)

General Procedure 8. Reaction scale: 9.5 mg (0.032 mmol) of compound 66. No purification was needed and 67 was afforded as a white solid (8.1 mg, 100%). ¹H NMR (400 MHz, Methanol-*d*₄) δ 8.06 (m, 1H), 7.86 (m, 1H), 7.68 (t, *J* = 7.5 Hz, 2H), 7.50 (m, 2H), 7.44 (t, *J* = 7.8 Hz, 1H), 3.98 (s, 2H) ppm. ¹³C NMR (101 MHz, Methanol-*d*₄) δ 174.1, 159.3, 135.8, 135.1, 129.7, 129.4, 127.0, 127.0, 126.7, 126.0, 122.9, 122.0, 42.6 ppm.



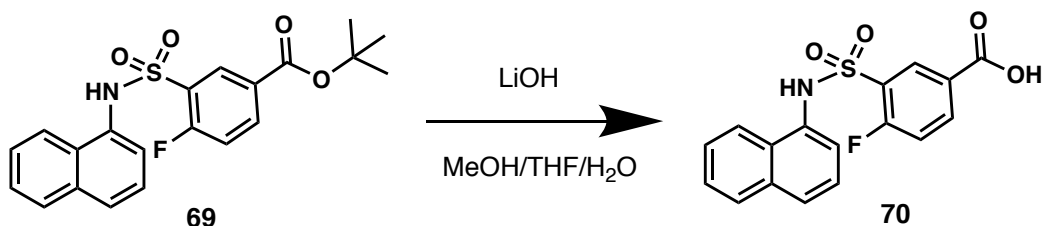
1-(naphthalen-1-yl)-3-(*p*-tolyl)urea (68)

General Procedure 3. Reaction scale: 7.8 mg (0.054 mmol) of isocyanate. Crude solid was purified by MeOH washes to afford 68 as a white solid (11.1 mg, 74%). ¹H NMR (400 MHz, DMSO-*d*₃) δ 8.96 (s, 1H), 8.74 (s, 1H), 8.13 (d, *J* = 8.3 Hz, 1H), 8.03 (d, *J* = 7.5 Hz, 1H), 7.93 (d, *J* = 7.9 Hz, 1H), 7.58 (m, 3H), 7.47 (t, *J* = 7.9 Hz, 1H), 7.40 (d, *J* = 8.2 Hz, 2H), 7.12 (d, *J* = 8.1 Hz, 2H), 2.26 (s, 3H), ppm. ¹³C NMR (101 MHz, DMSO-*d*₃) δ 153.4, 137.7, 134.9, 134.2, 131.1, 129.7 (2C), 128.9, 126.3 (2C), 126.2, 126.1, 123.2, 121.7, 118.6 (2C), 117.6, 20.8 ppm.



***Tert*-butyl 4-fluoro-3-(*N*-(naphthalen-1-yl)sulfamoyl)benzoate (**69**)**

General Procedure 7. Reaction scale: 22.0 mg (0.075 mmol) of sulfonyl chloride. Purified by PTLC (EtOAc/hexane, 40:60) to afford **69** as a brown oil (23.1 mg, 77%). ¹H NMR (400 MHz, Acetone-*d*₆) δ 8.29 (m, 2H), 8.16 (ddd, *J* = 8.2, 4.6, 2.1 Hz, 1H), 7.86 (m, 1H), 7.72 (d, *J* = 7.6 Hz, 1H), 7.47 (m, 2H), 7.39 (m, 3H), 1.52 (s, 9H) ppm. ¹³C NMR (101 MHz, Acetone-*d*₆) δ 163.6 (d, *J* = 22.5 Hz), 160.9, 137.2 (d, *J* = 9.9 Hz), 135.3, 134.3, 132.5, 132.3, 130.9, 129.5, 129.4 (t, *J* = 3.0 Hz), 129.1, 128.5, 127.3, 127.2, 126.3, 124.9, 123.5, 118.4 (d, *J* = 22.3 Hz), 28.1 (3C) ppm.

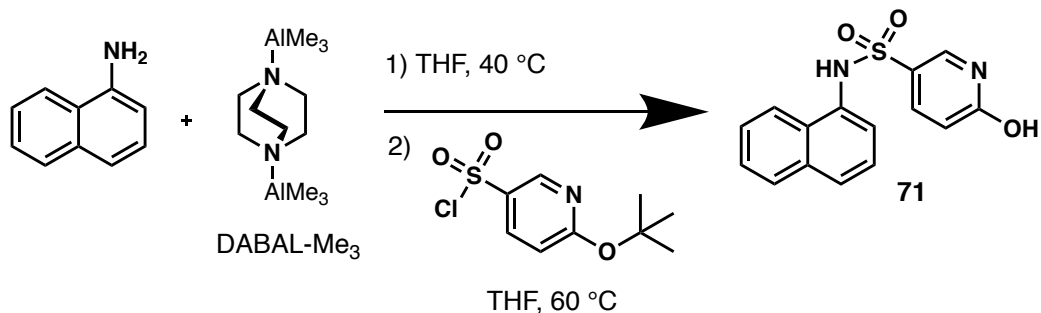


4-fluoro-3-(*N*-(naphthalen-1-yl)sulfamoyl)benzoic acid (70**)**

General Procedure 8. Reaction scale: 16.9 mg (0.042 mmol) of compound **69**. No purification was needed and **70** was afforded as a white/translucent solid (12.0 mg, 83%).

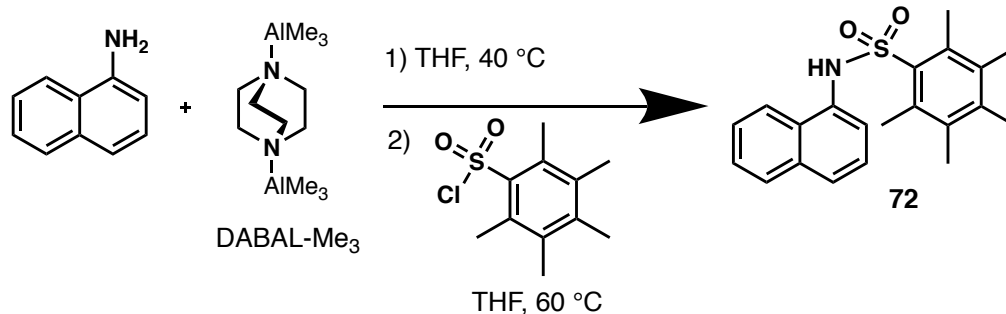
¹H NMR (400 MHz, Methanol-*d*₄) δ 8.29 (d, *J* = 6.5 Hz, 1H), 8.18 (m, 1H), 8.06 (m, 1H),

7.82 (m, 1H), 7.74 (m, 1H), 7.43 (m, 2H), 7.33 (m, 3H) ppm. ^{13}C NMR (101 MHz, Methanol- d_4) δ 166.9, 162.9, 137.5 (d, $J = 9.9$ Hz), 135.6, 133.0, 132.6 (d, $J = 9.0$ Hz), 131.1, 129.0, 128.5, 128.4, 127.2, 127.1, 126.2, 125.1, 124.9, 123.3, 118.3 (d, $J = 22.4$ Hz) ppm.



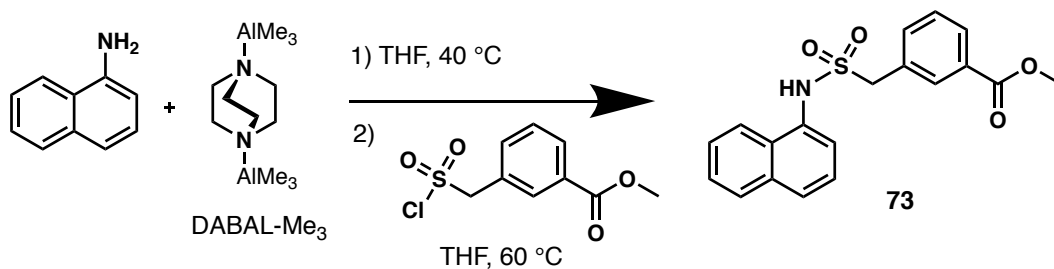
6-hydroxy-*N*-(naphthalen-1-yl)pyridine-3-sulfonamide (71)

General Procedure 7. Reaction scale: 21.0 mg (0.084 mmol) of sulfonyl chloride. Crude solid was purified by DCM washes to afford 71 as a white solid (19.4 mg, 77%). ^1H NMR (400 MHz, Methanol- d_4) δ 8.01 (d, $J = 7.1$ Hz, 1H), 7.86 (d, $J = 6.1$ Hz, 1H), 7.80 (d, $J = 7.9$ Hz, 1H), 7.71 (d, $J = 9.2$ Hz, 1H), 7.59 (s, 1H), 7.46 (m, 2H), 7.42 (d, $J = 8.0$ Hz, 1H), 7.37 (d, $J = 6.9$ Hz, 1H), 6.46 (d, $J = 9.6$ Hz, 1H) ppm. ^{13}C NMR (101 MHz, Methanol- d_4) δ 164.7, 139.7, 139.1, 135.9, 133.3, 131.3, 129.3, 128.7, 127.5, 127.4, 126.5, 125.8, 123.9, 121.3, 121.0 ppm.



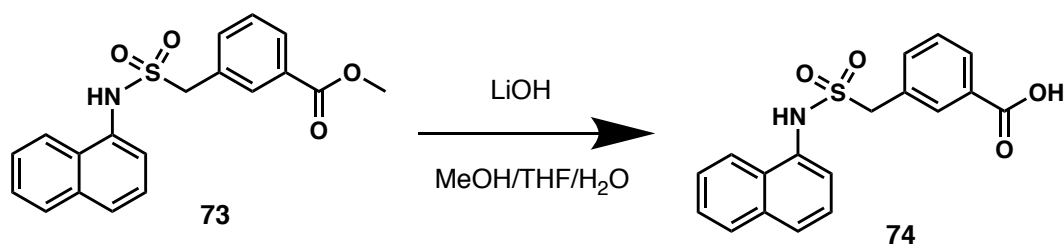
2,3,4,5,6-pentamethyl-*N*-(naphthalen-1-yl)benzenesulfonamide (72)

General Procedure 7. Reaction scale: 10.4 mg (0.042 mmol) of sulfonyl chloride. Purified by flash chromatography (SiO₂, EtOAc/hexane, gradient from 10 to 50% in EtOAc) and Et₂O wash to afford 72 as a white/pink solid (12.8 mg, 86%). ¹H NMR (400 MHz, Acetone-*d*₆) δ 8.87 (s, 1H), 8.30 (dd, *J* = 6.0, 3.5 Hz, 1H), 7.89 (m, 1H), 7.77 (d, *J* = 8.2 Hz, 1H), 7.51 (dd, *J* = 6.3, 3.3 Hz, 2H), 7.34 (t, *J* = 7.8 Hz, 1H), 7.18 (d, *J* = 7.4 Hz, 1H), 2.44 (s, 6H), 2.25 (s, 3H), 2.19 (s, 6H) ppm. ¹³C NMR (101 MHz, Acetone-*d*₆) δ 140.2, 135.5 (2C), 135.4, 135.3, 133.7, 131.1, 128.9 (2C), 127.6, 127.1, 126.9, 126.2, 124.1 (2C), 123.9, 19.5 (2C), 17.8, 17.1 (2C) ppm.



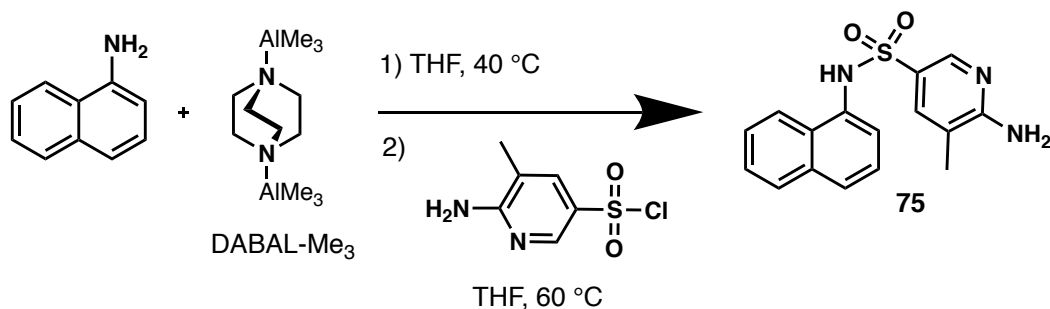
Methyl 3-((*N*-(naphthalen-1-yl)sulfamoyl)methyl)benzoate (73)

General Procedure 7. Reaction scale: 20.9 mg (0.084 mmol) of sulfonyl chloride. Purified by flash chromatography (SiO₂, EtOAc/hexane, gradient from 20 to 70% in EtOAc) to afford 73 as a pink oil (19.4 mg, 65%). ¹H NMR (400 MHz, Acetone-*d*₆) δ 8.84 (s, 1H), 8.33 (m, 1H), 8.04 (d, *J* = 6.8 Hz, 3H), 7.92 (d, *J* = 8.2 Hz, 1H), 7.78 (d, *J* = 7.3 Hz, 1H), 7.71 (d, *J* = 7.7 Hz, 1H), 7.63 (m, 3H), 7.54 (t, *J* = 8.0 Hz, 1H), 4.72 (s, 2H), 3.91 (s, 3H) ppm. ¹³C NMR (101 MHz, Acetone-*d*₆) δ 166.7, 136.4, 135.4, 133.8, 132.8, 131.4, 131.3, 130.0, 129.8, 129.5, 129.1, 127.3, 127.1 (2C), 126.5, 123.6, 122.5, 58.4, 52.4 ppm.



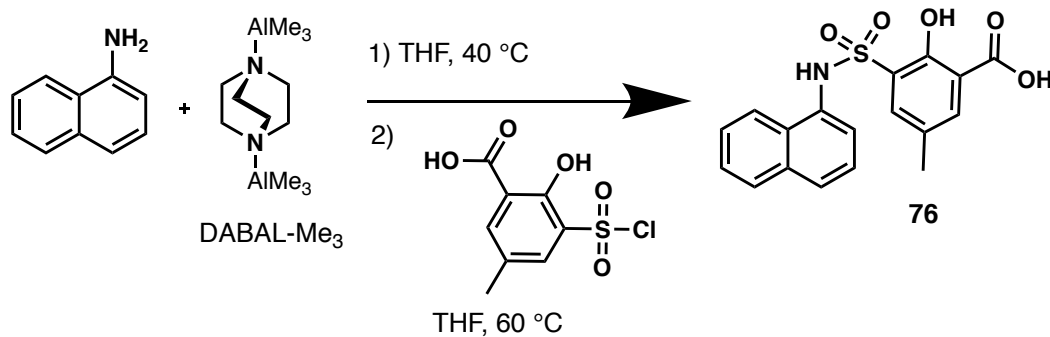
3-((*N*-(naphthalen-1-yl)sulfamoyl)methyl)benzoic acid (74)

General Procedure 8. Reaction scale: 10.8 mg (0.030 mmol) of compound 73. No purification was needed and 74 was afforded as a pink solid (6.1 mg, 59%). ¹H NMR (400 MHz, Methanol-*d*₄) δ 8.07 (m, 1H), 7.97 (m, 2H), 7.88 (m, 1H), 7.77 (d, *J* = 8.1 Hz, 1H), 7.54 (m, 4H), 7.45 (t, *J* = 7.9 Hz, 1H), 7.38 (t, *J* = 7.8 Hz, 1H), 4.51 (s, 2H) ppm. ¹³C NMR (101 MHz, Methanol-*d*₄) δ 169.4, 136.5, 136.2, 135.9, 134.0, 133.4, 131.4, 130.7, 130.5, 129.6, 129.3, 127.8, 127.5, 127.4, 126.6, 123.8, 123.1, 58.8 ppm.



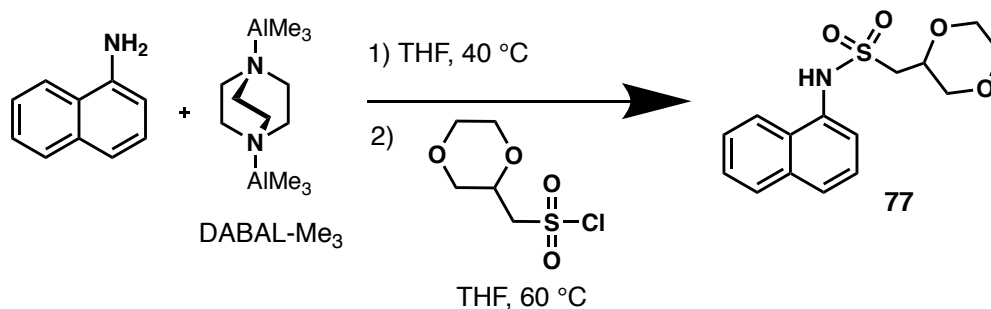
6-amino-5-methyl-N-(naphthalen-1-yl)pyridine-3-sulfonamide (75)

General Procedure 7. Reaction scale: 9.9 mg (0.048 mmol) of sulfonyl chloride. Purified by flash chromatography (SiO₂, EtOAc/hexane, gradient from 50 to 100% in EtOAc) to afford 75 as an orange oil (13.7 mg, 91%). ¹H NMR (400 MHz, Acetone-*d*₆) δ 8.85 (s, 1H), 8.21 (m, 1H), 8.10 (s, 1H), 7.88 (m, 1H), 7.78 (d, *J* = 7.9 Hz, 1H), 7.50 (s, 1H), 7.46 (m, 2H), 7.39 (m, 2H), 6.05 (s, 2H), 2.07 (s, 3H) ppm. ¹³C NMR (101 MHz, Acetone-*d*₆) δ 161.7, 146.9, 136.1, 135.3, 133.8, 130.4, 129.0, 127.5, 127.0, 126.9, 126.3, 125.3, 123.9, 123.7, 116.5, 17.1 ppm.



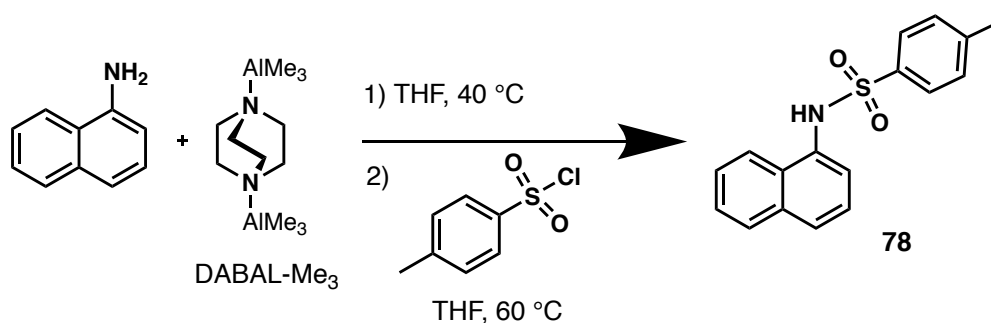
2-hydroxy-5-methyl-3-(N-(naphthalen-1-yl)sulfamoyl)benzoic acid (76)

General Procedure 7. Reaction scale: 10.5 mg (0.042 mmol) of sulfonyl chloride. Crude solid was purified by Et₂O washes to afford 76 as a brown/pink solid (6.6 mg, 44%). ¹H NMR (400 MHz, Acetone-*d*₆) δ 8.45 (m, 1H), 7.90 (s, 1H), 7.86 (m, 1H), 7.74 (d, *J* = 7.6 Hz, 1H), 7.63 (s, 1H), 7.50 (m, 2H), 7.37 (m, 2H), 2.23 (s, 3H) ppm. ¹³C NMR (101 MHz, Acetone-*d*₆) δ 172.2, 158.2, 136.8, 136.1, 135.3, 133.5, 130.8, 128.8, 128.8, 127.9, 127.7, 127.1, 126.9, 126.3, 124.2, 123.3, 115.0, 20.0 ppm.



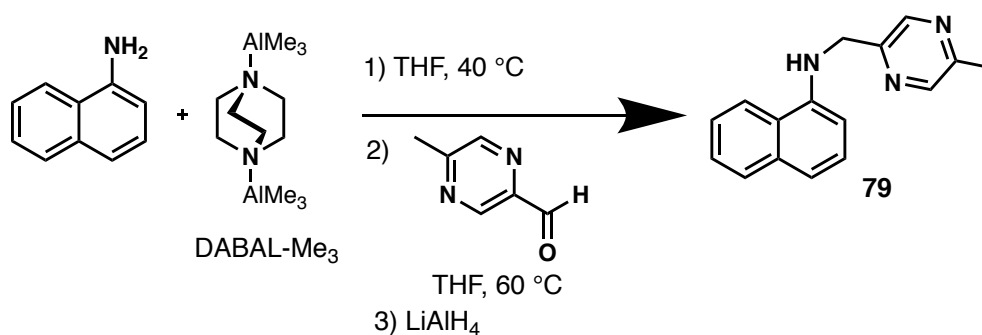
1-(1,4-dioxan-2-yl)-*N*-(naphthalen-1-yl)methanesulfonamide (77)

General Procedure 7. Reaction scale: 10.5 mg (0.042 mmol) of sulfonyl chloride. Purified by flash chromatography (SiO₂, EtOAc/hexane, gradient from 20 to 100% in EtOAc) to afford 77 as an orange oil (13.8 mg, 92%). ¹H NMR (400 MHz, Acetone-*d*₆) δ 8.61 (s, 1H), 8.42 (d, *J* = 8.2 Hz, 1H), 7.95 (d, *J* = 7.4 Hz, 1H), 7.85 (d, *J* = 8.2 Hz, 1H), 7.72 (d, *J* = 7.2 Hz, 1H), 7.55 (m, 3H), 4.13 (m, 1H), 3.83 (dd, *J* = 11.5, 2.3 Hz, 1H), 3.75 (dd, *J* = 11.3, 2.2 Hz, 1H), 3.65 (m, 2H), 3.50 (td, *J* = 11.8, 2.8 Hz, 1H), 3.32 (m, 2H), 3.22 (dd, *J* = 14.7, 4.9 Hz, 1H) ppm. ¹³C NMR (101 MHz, Acetone-*d*₆) δ 135.4, 134.0, 130.5, 129.0, 127.6, 127.1, 127.0, 126.4, 124.2, 123.3, 72.0, 70.4, 67.3, 66.8, 53.4 ppm.



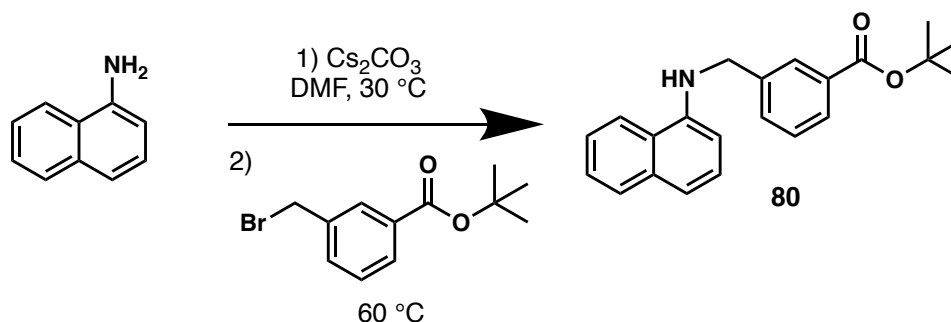
4-methyl-*N*-(naphthalen-1-yl)benzenesulfonamide (**78**)

General Procedure 7. Reaction scale: 12.8 mg (0.067 mmol) of sulfonyl chloride. Purified by flash chromatography (SiO₂, EtOAc/hexane, gradient from 40 to 50% in EtOAc) to afford **78** as a brown solid (16.5 mg, 82%). ¹H NMR (400 MHz, Acetone-*d*₆) δ 8.94 (s, 1H), 8.15 (d, *J* = 8.2 Hz, 1H), 7.88 (d, *J* = 7.7 Hz, 1H), 7.78 (d, *J* = 8.1 Hz, 1H), 7.62 (d, *J* = 8.2 Hz, 2H), 7.44 (m, 3H), 7.32 (d, *J* = 6.9 Hz, 1H), 7.27 (d, *J* = 8.0 Hz, 2H), 2.34 (s, 3H) ppm. ¹³C NMR (101 MHz, Acetone-*d*₆) δ 144.2, 138.5, 135.3, 133.6, 130.5, 130.3 (2C), 128.9, 128.1 (2C), 127.7, 127.0, 126.9, 126.2, 123.9, 123.8, 21.3 ppm.



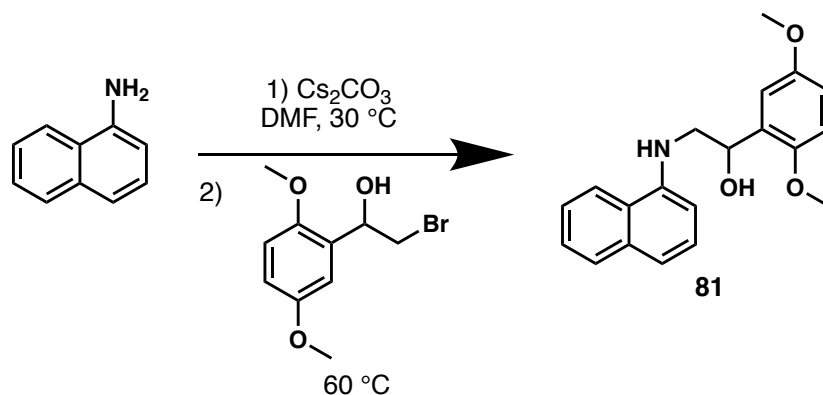
N-((5-methylpyrazin-2-yl)methyl)naphthalen-1-amine (**79**)

General Procedure 10. Reaction scale: 21.5 mg (0.150 mmol) of 1-naphthylamine. Purified by flash chromatography (SiO₂, EtOAc/hexane, gradient from 50 to 80% in EtOAc) to afford 79 as a yellow oil (8.9 mg, 24%). ¹H NMR (300 MHz, Acetone-*d*₆) δ 8.59 (s, 1H), 8.48 (s, 1H), 8.17 (m, 1H), 7.79 (m, 1H), 7.46 (m, 2H), 7.22 (m, 2H), 6.56 (d, *J* = 7.2 Hz, 1H), 6.41 (s, 1H), 4.68 (d, *J* = 5.3 Hz, 2H), 2.49 (s, 3H) ppm. ¹³C NMR (75 MHz, Methanol-*d*₄) δ 153.0, 152.4, 144.3, 144.2, 143.4, 135.5, 129.2, 127.4, 126.5, 125.3, 124.5, 121.6, 117.7, 105.1, 47.7, 21.1 ppm.



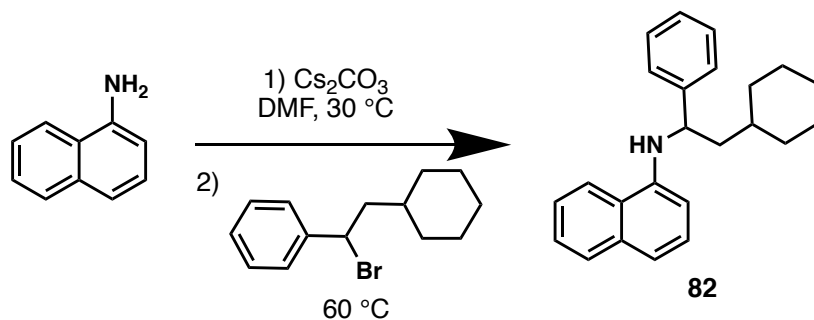
tert-butyl 3-((naphthalen-1-ylamino)methyl)benzoate (80)

General Procedure 9. Reaction scale: 12.2 mg (0.045 mmol) of alkyl halide. Purified by flash chromatography (SiO₂, EtOAc/hexane, gradient from 20 to 40% in EtOAc) to afford 80 as a white solid (12.2 mg, 81%). ¹H NMR (400 MHz, Acetone-*d*₆) δ 8.21 (m, 1H), 8.09 (s, 1H), 7.84 (d, *J* = 7.7 Hz, 1H), 7.78 (m, 1H), 7.68 (d, *J* = 7.4 Hz, 1H), 7.43 (m, 3H), 7.21 (t, *J* = 7.8 Hz, 1H), 7.16 (d, *J* = 8.0 Hz, 1H), 6.50 (d, *J* = 7.3 Hz, 1H), 6.36 (s, 1H), 4.65 (d, *J* = 5.5 Hz, 2H), 1.55 (s, 3H) ppm. ¹³C NMR (101 MHz, Acetone-*d*₆) δ 166.0, 144.5, 141.5, 135.5, 133.1, 132.2, 129.3, 129.1, 128.9, 128.6, 127.4, 126.4, 125.2, 124.5, 121.8, 117.4, 105.1, 81.2, 47.9, 28.3 (3C) ppm.



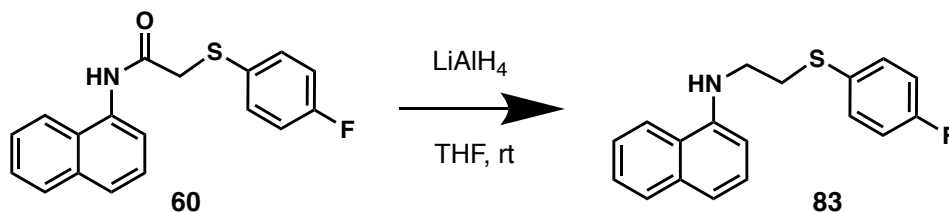
1-(2,5-dimethoxyphenyl)-2-(naphthalen-1-ylamino)ethan-1-ol (81)

General Procedure 9. Reaction scale: 12.0 mg (0.046 mmol) of alkyl halide. Purified by flash chromatography (SiO_2 , EtOAc/hexane, gradient from 20 to 60% in EtOAc) to afford 81 as a yellow oil (3.8 mg, 26%). ^1H NMR (400 MHz, Acetone- d_6) δ 8.22 (m, 1H), 7.77 (m, 1H), 7.46 (m, 2H), 7.13 (d, $J = 4.4$ Hz, 2H), 7.02 (d, $J = 3.1$ Hz, 1H), 6.97 (d, $J = 8.9$ Hz, 1H), 6.76 (dd, $J = 8.9, 3.2$ Hz, 1H), 6.32 (p, $J = 4.4$ Hz, 1H), 5.88 (d, $J = 3.5$ Hz, 1H), 5.05 (p, $J = 4.3$ Hz, 1H), 4.28 (s, 1H), 3.92 (s, 3H), 3.78 (m, 2H), 3.58 (s, 3H) ppm. ^{13}C NMR (101 MHz, Acetone- d_6) δ 154.8, 152.2, 144.0, 135.4, 130.7, 129.2, 127.4, 126.4, 125.2, 124.7, 121.6, 117.5, 114.6, 112.4, 112.3, 106.1, 65.8, 56.4, 55.5, 55.4 ppm



***N*-(2-cyclohexyl-1-phenylethyl)naphthalen-1-amine (82)**

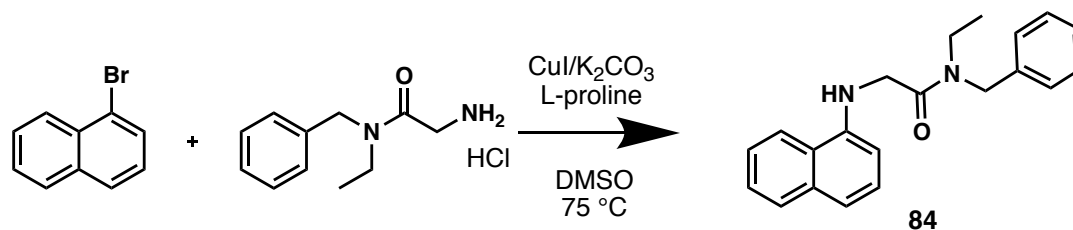
General Procedure 9. Reaction scale: 12.3 mg (0.046 mmol) of alkyl halide. Purified by flash chromatography (SiO₂, EtOAc/hexane, 10:90) to afford 82 as a brown oil (12.2 mg, 81%). ¹H NMR (400 MHz, Methanol-*d*₄) δ 8.18 (d, *J* = 7.6 Hz, 1H), 7.70 (dd, *J* = 6.8, 1.7 Hz, 1H), 7.40 (m, 4H), 7.27 (t, *J* = 7.5 Hz, 2H), 7.16 (t, *J* = 7.2 Hz, 2H), 7.06 (m, 2H), 6.34 (d, *J* = 7.2 Hz, 1H), 4.60 (dd, *J* = 8.2, 6.1 Hz, 1H), 1.96 (m, 3H), 1.67 (m, 10H) ppm. ¹³C NMR (101 MHz, Methanol-*d*₄) δ 143.6, 140.8, 132.7, 129.4 (2C), 129.3, 128.8, 127.7, 127.5 (2C), 127.4, 126.4, 125.2, 121.9, 117.3, 106.4, 56.6, 47.9, 36.0, 35.0, 34.1, 27.7, 27.5, 27.4 ppm.



***N*-(2-((4-fluorophenyl)thio)ethyl)naphthalen-1-amine (83)**

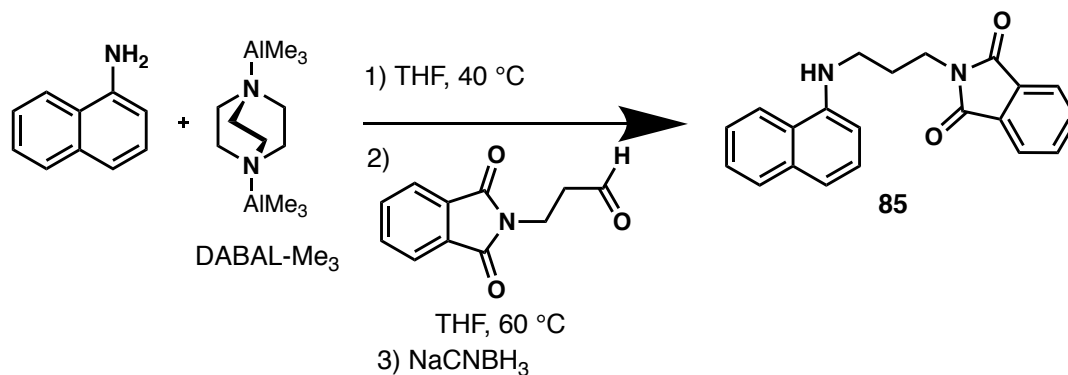
General Procedure 11. Reaction scale: 20.0 mg (0.064 mmol) of compound 60. Purified by flash chromatography (SiO₂, EtOAc/hexane, gradient from 10 to 60% in EtOAc) to afford 83 as a white oil (7.4 mg, 39%). ¹H NMR (400 MHz, Acetone-*d*₆) δ 8.00 (d, *J* = 8.2 Hz, 1H), 7.77 (d, *J* = 7.7 Hz, 1H), 7.53 (dd, *J* = 8.7, 5.3 Hz, 2H), 7.41 (p, *J* = 6.7 Hz, 2H), 7.27 (t, *J* = 7.9 Hz, 1H), 7.14 (m, 3H), 6.53 (d, *J* = 7.5 Hz, 1H), 5.73 (s, 1H), 3.55 (q, *J* = 6.5 Hz, 2H), 3.32 (t, *J* = 7.0 Hz, 2H) ppm. ¹³C NMR (101 MHz, Acetone-*d*₆) δ 163.9,

144.3, 135.5, 133.5, 133.4, 133.0, 129.1, 127.5, 126.5, 125.1, 124.5, 121.6, 117.5, 117.0, 116.7, 104.4, 43.8, 34.1 ppm.



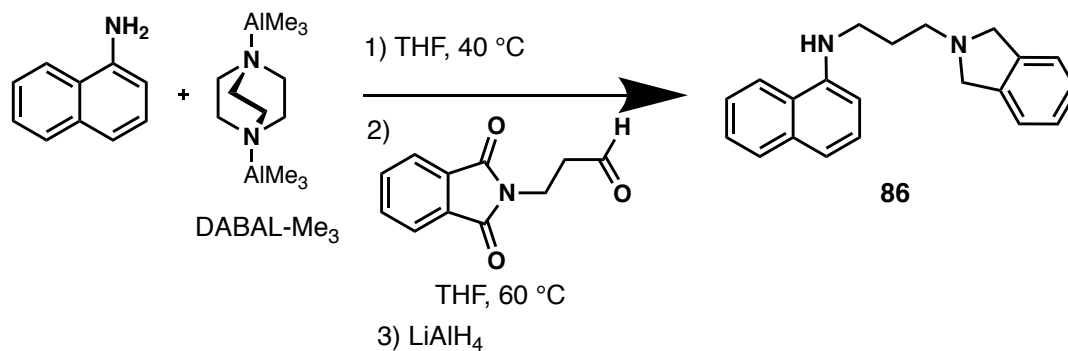
***N*-benzyl-*N*-ethyl-2-(naphthalen-1-ylamino)acetamide (84)**

General Procedure 12. Reaction scale: 13.0 mg (0.063 mmol) of 1-bromonaphthalene. Purified by flash chromatography (SiO₂, EtOAc/hexane, gradient from 20 to 40% in EtOAc) to afford 84 as a yellow oil (3.1 mg, 16%). ¹H NMR (400 MHz, Acetone-*d*₆) δ 8.00 (t, *J* = 7.7 Hz, 1H), 7.80 (t, *J* = 6.8 Hz, 1H), 7.48 (m, 2H), 7.29 (m, 7H), 6.58 (dd, *J* = 46.1, 7.4 Hz, 1H), 6.00 (s, 1H), 4.77 (d, *J* = 18.8 Hz, 2H), 4.20 (dd, *J* = 34.0, 3.7 Hz, 2H), 3.51 (p, *J* = 6.8 Hz, 2H), 1.26 (t, *J* = 7.1 Hz, 3H) ppm. ¹³C NMR (101 MHz, Acetone-*d*₆) δ 169.7 (d, *J* = 8.6 Hz), 143.8 (d, *J* = 8.4 Hz), 138.7 (d, *J* = 71.2 Hz), 135.3 (d, *J* = 3.0 Hz), 129.7, 129.3 (d, *J* = 4.9 Hz), 128.7, 128.3, 128.0, 127.7, 127.6 (d, *J* = 3.7 Hz), 126.6, 125.5, 124.2 (d, *J* = 4.2 Hz), 121.1 (d, *J* = 3.6 Hz), 117.4, 105.0 (d, *J* = 5.1 Hz), 49.4, 45.9, 41.5, 13.4 ppm



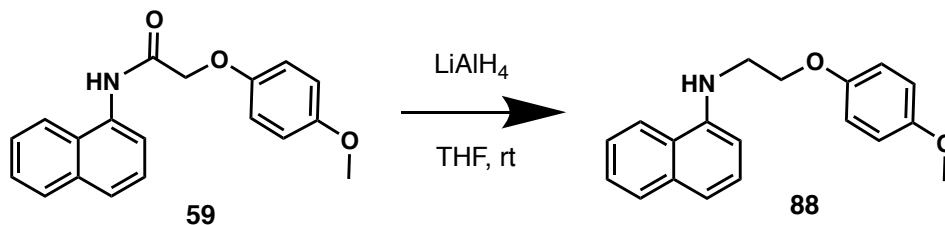
2-(3-(naphthalen-1-ylamino)propyl)isoindoline-1,3-dione (85)

General Procedure 10. Reaction scale: 12.5 mg (0.088 mmol) of 1-naphthylamine. Purified by pTLC (EtOAc/toluene, 25:75) to afford 85 as a yellow oil (16.3 mg, 57%). ¹H NMR (500 MHz, Acetone-*d*₆) δ 8.08 (d, *J* = 8.1 Hz, 1H), 7.84 (m, 4H), 7.75 (d, *J* = 7.8 Hz, 1H), 7.40 (p, *J* = 6.5 Hz, 2H), 7.28 (t, *J* = 7.9 Hz, 1H), 7.14 (d, *J* = 8.1 Hz, 1H), 6.60 (d, *J* = 7.6 Hz, 1H), 5.59 (s, 1H), 3.86 (t, *J* = 6.7 Hz, 2H), 3.41 (q, *J* = 6.4 Hz, 2H), 2.14 (p, *J* = 6.7 Hz, 2H) ppm. ¹³C NMR (125 MHz, Acetone-*d*₆) δ 169.1 (2C), 144.8, 135.5, 135.0 (2C), 133.2 (2C), 129.1, 127.6, 126.3, 125.0, 124.6, 123.7 (2C), 121.6, 117.1, 104.4, 41.8, 36.5, 28.3 ppm



***N*-(3-(isoindolin-2-yl)propyl)naphthalen-1-amine (86)**

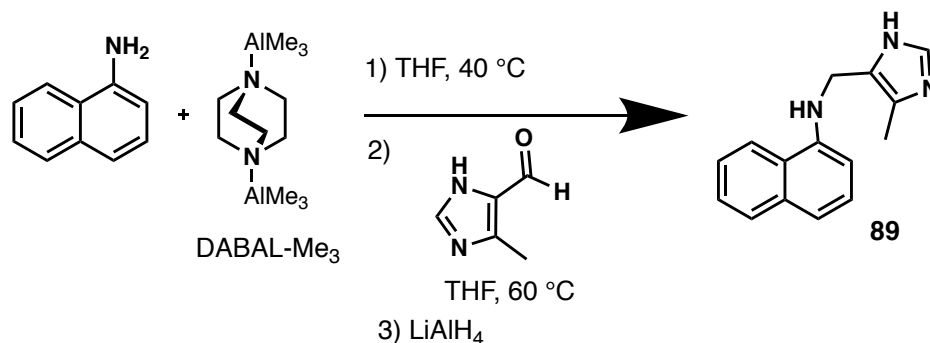
General Procedure 10. Reaction scale: 12.5 mg (0.088 mmol) of 1-naphthylamine. Purified by flash chromatography (SiO₂, EtOAc/hexane, gradient from 10 to 60% in EtOAc) to afford 86 as a brown oil (5.2 mg, 20%). ¹H NMR (500 MHz, Acetone-*d*₆) δ 7.69 (dd, *J* = 14.3, 8.4 Hz, 2H), 7.32 (t, *J* = 7.6 Hz, 1H), 7.26 (m, 5H), 7.09 (d, *J* = 8.1 Hz, 1H), 6.99 (t, *J* = 7.6 Hz, 1H), 6.68 (s, 1H), 6.53 (d, *J* = 7.6 Hz, 1H), 4.01 (s, 4H), 3.42 (t, *J* = 6.3 Hz, 2H), 3.02 (t, *J* = 6.2 Hz, 2H), 2.08 (m, 2H) ppm. ¹³C NMR (125 MHz, Acetone-*d*₆) δ 145.8, 141.3 (2C), 135.4, 129.0, 127.7, 127.5 (2C), 126.2, 124.7, 124.5, 123.1 (2C), 121.8, 116.5, 103.7, 59.6 (2C), 55.5, 44.5, 27.7 ppm



***N*-(2-(4-methoxyphenoxy)ethyl)naphthalen-1-amine (88)**

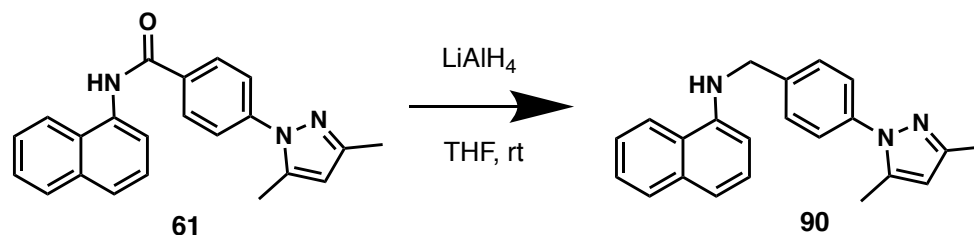
General Procedure 11. Reaction scale: 21.5 mg (0.070 mmol) of compound 59. Purified by flash chromatography (SiO₂, EtOAc/hexane, gradient from 10 to 20% in EtOAc) to afford 88 as a yellow oil (3.2 mg, 16%). ¹H NMR (500 MHz, Acetone-*d*₆) δ 8.10 (d, *J* = 8.2 Hz, 1H), 7.78 (d, *J* = 7.9 Hz, 1H), 7.42 (m, 2H), 7.33 (t, *J* = 7.9 Hz, 1H), 7.19 (d, *J* = 8.1 Hz, 1H), 6.93 (d, *J* = 9.1 Hz, 1H), 6.86 (d, *J* = 9.1 Hz, 1H), 6.70 (d, *J* = 7.6 Hz, 1H), 5.68 (s, 1H), 4.29 (t, *J* = 5.6 Hz, 2H), 3.73 (s, 3H), 3.70 (q, *J* = 5.6 Hz, 2H) ppm. ¹³C NMR

(125 MHz, Acetone-*d*₆) δ 154.1, 153.0, 143.9, 134.6, 128.3, 126.7, 125.6, 124.3, 123.7, 120.8, 116.6, 115.5 (2C), 114.5 (2C), 103.6, 66.7, 54.9, 43.3 ppm



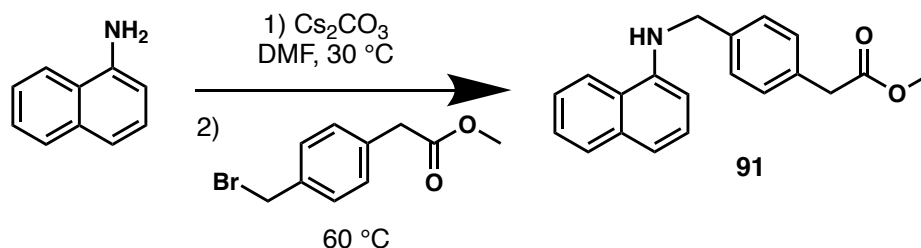
***N*-((4-methyl-1*H*-imidazol-5-yl)methyl)naphthalen-1-amine (89)**

General Procedure 10. Reaction scale: 21.5 mg (0.150 mmol) of 1-naphthylamine. Crude solid was purified by acetone washes to afford 89 as a white/brown solid (18.6 mg, 52%).
¹H NMR (300 MHz, Methanol-*d*₄) δ 7.98 (m, 1H), 7.72 (m, 1H), 7.52 (s, 1H), 7.38 (m, 2H), 7.26 (t, *J* = 7.8 Hz, 1H), 7.16 (d, *J* = 8.1 Hz, 1H), 6.63 (d, *J* = 7.4 Hz, 1H), 4.36 (s, 2H), 2.24 (s, 3H) ppm. ¹³C NMR (75 MHz, Methanol-*d*₄) δ 145.0, 135.8, 134.6, 129.3, 127.5, 126.5, 126.5, 125.4, 125.3, 125.7, 121.8, 118.2, 105.5, 40.9, 10.2 ppm.



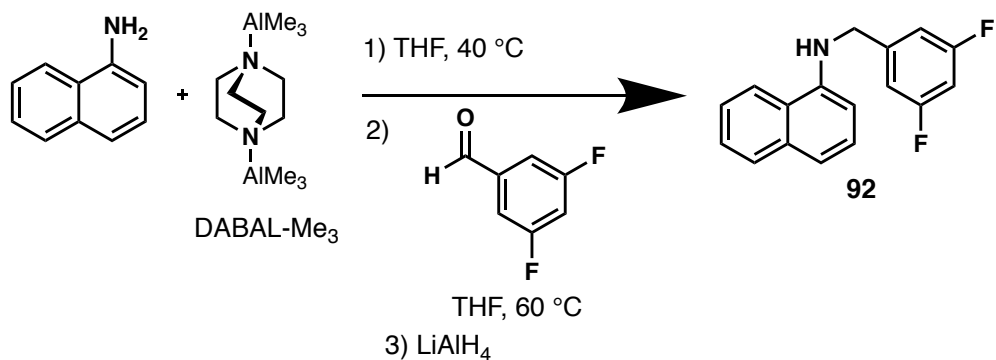
***N*-(4-(3,5-dimethyl-1*H*-pyrazol-1-yl)benzyl)naphthalen-1-amine (90)**

General Procedure 11. Reaction scale: 20.0 mg (0.059 mmol) of compound 61. Purified by flash chromatography (SiO₂, EtOAc/hexane, gradient from 20 to 60% in EtOAc) to afford 90 as a white/yellow solid (4.5 mg, 23%). ¹H NMR (500 MHz, Acetone-*d*₆) δ 8.22 (d, *J* = 7.7 Hz, 1H), 7.79 (d, *J* = 7.7 Hz, 1H), 7.57 (d, *J* = 8.0 Hz, 2H), 7.45 (d, *J* = 7.6 Hz, 4H), 7.23 (t, *J* = 7.8 Hz, 1H), 7.17 (d, *J* = 8.1 Hz, 1H), 6.54 (d, *J* = 7.5 Hz, 1H), 6.30 (s, 1H), 6.00 (s, 1H), 4.65 (d, *J* = 5.4 Hz, 2H), 2.30 (s, 3H), 2.18 (s, 3H) ppm. ¹³C NMR (125 MHz, Acetone-*d*₆) δ 148.9, 144.6, 139.8, 139.7 (2C), 135.5, 129.2, 128.5 (2C), 127.5, 126.4, 125.2, 125.1 (2C), 124.6, 121.8, 117.4, 107.7, 105.1, 47.8, 13.6, 12.6 ppm.



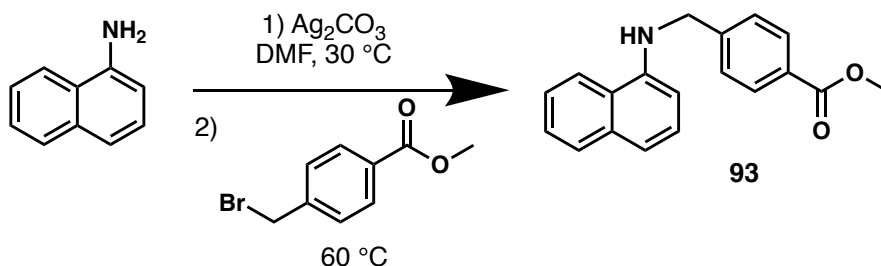
Methyl 2-(4-((naphthalen-1-ylamino)methyl)phenyl)acetate (91)

General Procedure 9. Reaction scale: 11.9 mg (0.049 mmol) of alkyl halide. Purified by flash chromatography (SiO₂, EtOAc/hexane, gradient from 20 to 50% in EtOAc) to afford 91 as a yellow oil (6.2 mg, 42%). ¹H NMR (400 MHz, Methanol-*d*₄) δ 8.07 (m, 1H), 7.73 (m, 1H), 7.41 (dd, *J* = 6.4, 3.3 Hz, 2H), 7.38 (d, *J* = 8.0 Hz, 2H), 7.22 (d, *J* = 8.0 Hz, 2H), 7.17 (t, *J* = 7.8 Hz, 1H), 7.11 (d, *J* = 8.1 Hz, 1H), 6.44 (d, *J* = 7.4 Hz, 1H), 4.52 (s, 2H), 3.66 (s, 3H), 3.62 (s, 2H) ppm. ¹³C NMR (101 MHz, Methanol-*d*₄) δ 159.7, 145.0, 141.8, 134.4, 134.1, 130.4 (2C), 129.3, 128.3 (2C), 127.5, 126.5, 125.3, 125.0, 121.9, 117.6, 105.6, 52.0, 48.3, 41.4 ppm.



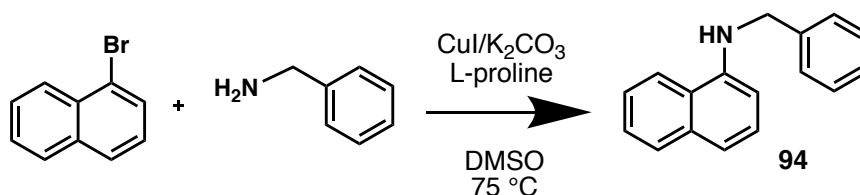
N-(3,5-difluorobenzyl)naphthalen-1-amine (**92**)

General Procedure 10. Reaction scale: 15.9 mg (0.111 mmol) of 1-naphthylamine. Purified by flash chromatography (SiO₂, EtOAc/hexane, gradient from 10 to 40% in EtOAc) to afford **92** as a yellow oil (22.9 mg, 77%). ¹H NMR (400 MHz, Acetone-*d*₆) δ 8.20 (m, 1H), 7.79 (m, 1H), 7.46 (m, 2H), 7.21 (m, 2H), 7.12 (d, *J* = 7.3 Hz, 2H), 6.87 (t, *J* = 9.4 Hz, 1H), 6.43 (m, 2H), 4.65 (d, *J* = 5.8 Hz, 2H) ppm. ¹³C NMR (101 MHz, Acetone-*d*₆) δ 164.1 (dd, *J* = 247.5, 13.1 Hz, 2C), 146.5 (t, *J* = 8.1 Hz), 144.1, 141.8, 135.5, 129.2, 130.4, 127.4, 126.5, 125.3, 124.5, 121.7, 117.7, 110.6 (dd, *J* = 19.2, 7.1 Hz, 2C), 105.2, 102.6 (t, *J* = 26.3 Hz), 47.4 (t, *J* = 2.0 Hz) ppm.



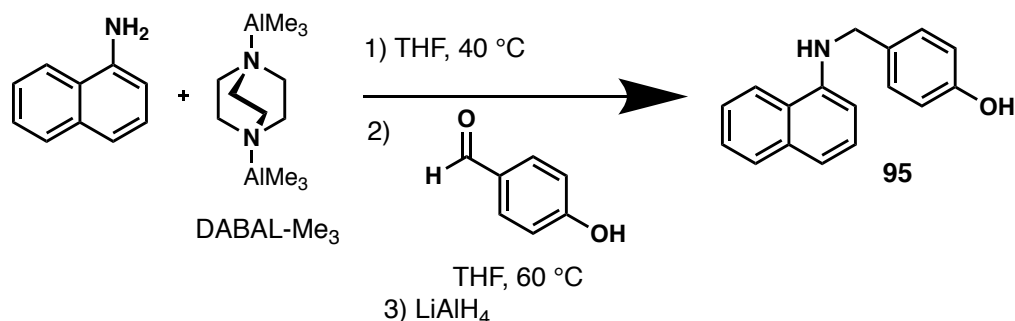
Methyl 4-((naphthalen-1-ylamino)methyl)benzoate (93)

General Procedure 9. Reaction scale: 23.6 mg (0.103 mmol) of alkyl halide. Purified by flash chromatography (SiO₂, EtOAc/hexane, 20:80) to afford 93 as a pink/orange oil (17.9 mg, 60%). ¹H NMR (300 MHz, Acetone-*d*₆) δ 8.21 (m, 1H), 7.97 (d, *J* = 8.1 Hz, 2H), 7.79 (m, 1H), 7.58 (d, *J* = 8.0 Hz, 2H), 7.45 (m, 2H), 7.17 (m, 2H), 6.41 (m, 2H), 4.68 (d, *J* = 5.6 Hz, 2H), 3.86 (s, 3H) ppm. ¹³C NMR (75 MHz, Acetone-*d*₆) δ 167.1, 146.8, 144.4, 135.5, 130.3 (2C), 129.7, 129.2, 128.0 (2C), 127.4, 126.5, 125.2, 124.5, 121.8, 117.5, 105.1, 52.2, 47.9 ppm.



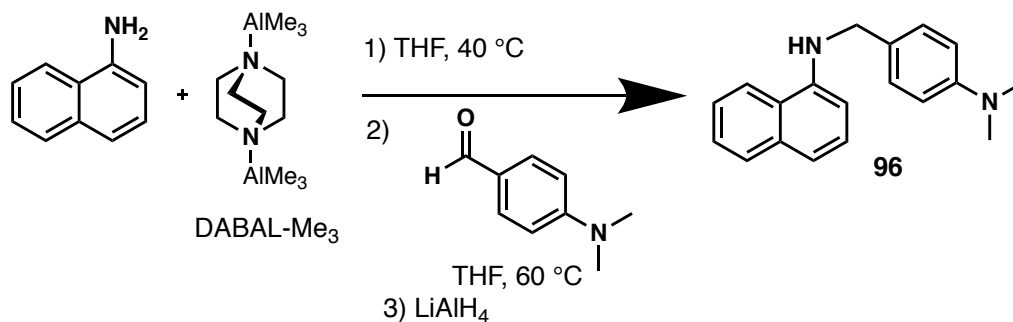
N-benzyl-1-naphthylamine (94)

General Procedure 12. Reaction scale: 26.6 mg (0.129 mmol) of 1-bromonaphthalene. Purified by pTLC (EtOAc/hexane, 20:80) to afford 94 as a white solid (6.7 mg, 22%). ¹H NMR (400 MHz, Acetone-*d*₆) δ 8.20 (d, *J* = 7.6 Hz, 1H), 7.78 (m, 1H), 7.45 (m, 4H), 7.32 (t, *J* = 7.5 Hz, 2H), 7.22 (q, *J* = 7.4 Hz, 2H), 7.15 (d, *J* = 8.1 Hz, 1H), 6.50 (d, *J* = 7.4 Hz, 1H), 6.24 (s, 1H), 4.58 (d, *J* = 5.3 Hz, 2H) ppm. ¹³C NMR (101 MHz, Acetone-*d*₆) δ 143.8, 140.1, 134.6, 128.3 (2C), 128.2, 127.1 (2C), 126.7, 126.6, 125.5, 124.2, 123.6, 120.9, 116.3, 104.2, 47.3 ppm.



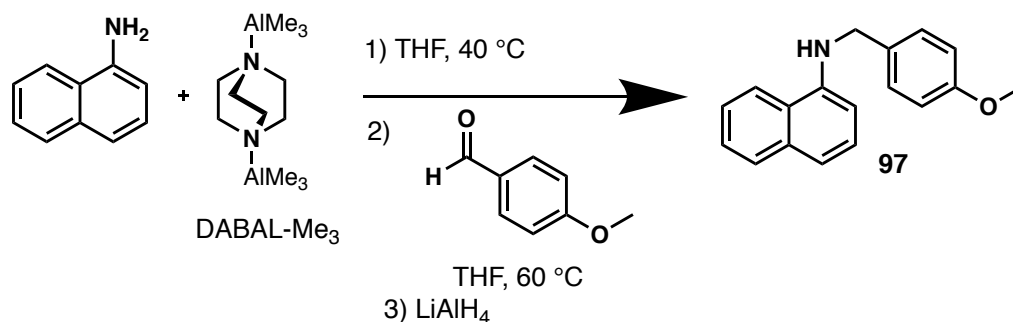
4-((naphthalen-1-ylamino)methyl)phenol (**95**)

General Procedure 10. Reaction scale: 21.5 mg (0.150 mmol) of 1-naphthylamine. Purified by flash chromatography (SiO₂, EtOAc/hexane, gradient from 30 to 70% in EtOAc) to afford **95** as a brown oil (28.7 mg, 77%). ¹H NMR (500 MHz, Acetone-*d*₆) δ 8.26 (s, 1H), 8.12 (d, *J* = 7.1 Hz, 1H), 7.73 (d, *J* = 7.6 Hz, 1H), 7.38 (p, *J* = 6.6 Hz, 2H), 7.26 (d, *J* = 8.3 Hz, 2H), 7.20 (t, *J* = 7.9 Hz, 1H), 7.11 (d, *J* = 8.1 Hz, 1H), 6.78 (d, *J* = 8.4 Hz, 2H), 6.51 (d, *J* = 7.6 Hz, 1H), 5.96 (s, 1H), 4.41 (d, *J* = 3.7 Hz, 2H) ppm. ¹³C NMR (125 MHz, Acetone-*d*₆) δ 157.2, 144.8, 135.4, 131.3, 129.4 (2C), 129.1, 127.5, 126.3, 125.0, 124.5, 121.8, 117.1, 116.0 (2C), 105.0, 47.9 ppm.



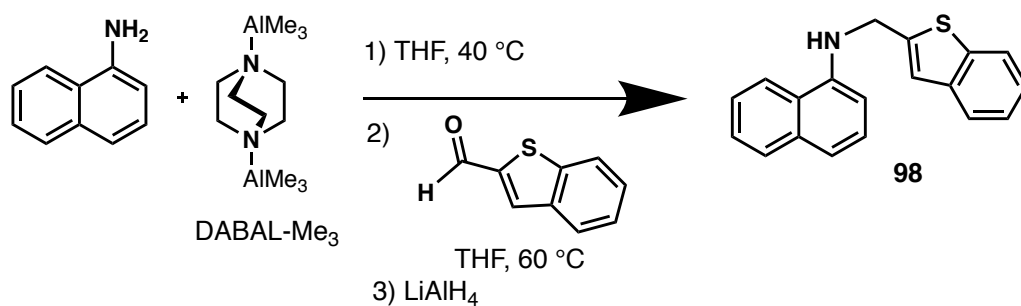
N-(4-(dimethylamino)benzyl)naphthalen-1-amine (**96**)

General Procedure 10. Reaction scale: 21.5 mg (0.150 mmol) of 1-naphthylamine. Purified by pTLC (EtOAc/hexane, 20:80) to afford 96 as a yellow oil (22.3 mg, 54%). ¹H NMR (500 MHz, Acetone-*d*₆) δ 8.15 (d, *J* = 8.2 Hz, 1H), 7.77 (d, *J* = 7.7 Hz, 1H), 7.41 (m, 2H), 7.29 (d, *J* = 8.5 Hz, 2H), 7.24 (t, *J* = 7.9 Hz, 1H), 7.14 (d, *J* = 8.1 Hz, 1H), 6.72 (d, *J* = 8.6 Hz, 2H), 6.57 (d, *J* = 7.6 Hz, 1H), 5.92 (s, 1H), 4.42 (d, *J* = 5.4 Hz, 2H), 2.89 (s, 6H) ppm. ¹³C NMR (125 MHz, Acetone-*d*₆) δ 150.9, 144.9, 135.4, 129.1, 129.1 (2C), 128.1, 127.5, 126.3, 125.0, 124.5, 121.8, 117.0, 113.5 (2C), 105.0, 48.0, 40.8 (2C) ppm.



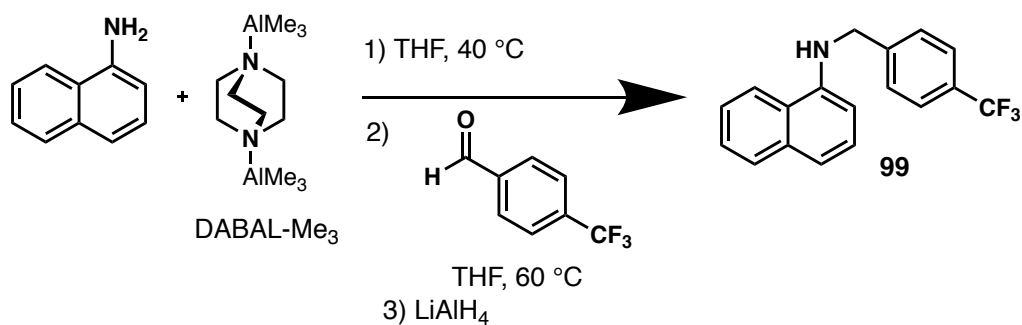
N-(4-methoxybenzyl)naphthalen-1-amine (97)

General Procedure 10. Reaction scale: 21.5 mg (0.150 mmol) of 1-naphthylamine. Purified by flash chromatography (SiO₂, EtOAc/hexane, gradient from 5 to 10% in EtOAc) to afford 97 as a yellow oil (24.7 mg, 62%). ¹H NMR (300 MHz, Acetone-*d*₆) δ 8.16 (m, 1H), 7.77 (m, 1H), 7.41 (m, 2H), 7.39 (m, 4H), 7.23 (t, *J* = 7.8 Hz, 1H), 7.15 (d, *J* = 8.0 Hz, 1H), 6.88 (d, *J* = 8.4 Hz, 2H), 6.53 (d, *J* = 7.4 Hz, 1H), 6.07 (s, 1H), 4.49 (d, *J* = 5.3 Hz, 2H), 3.76 (s, 3H) ppm. ¹³C NMR (75 MHz, Acetone-*d*₆) δ 159.7, 144.7, 135.4, 132.6, 129.3 (2C), 129.1, 127.5, 126.3, 125.0, 124.5, 121.8, 117.1, 114.6 (2C), 105.1, 55.4, 47.7 ppm.



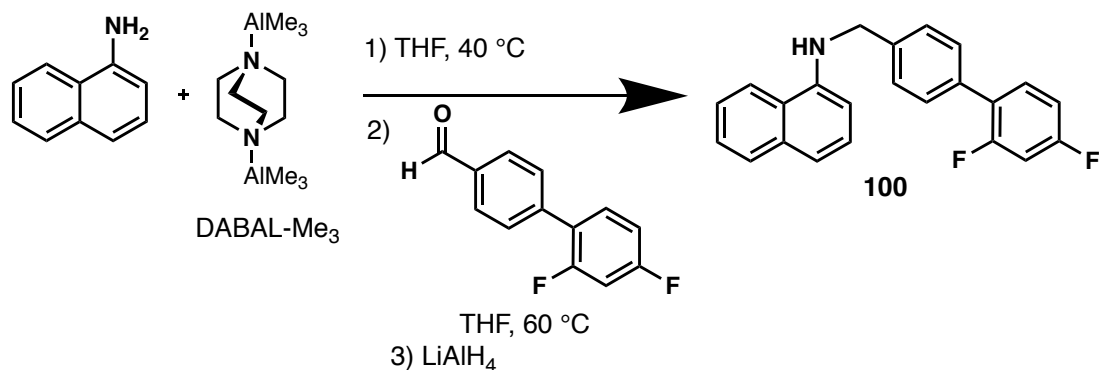
***N*-(benzo[*b*]thiophen-2-ylmethyl)naphthalen-1-amine (98)**

General Procedure 10. Reaction scale: 21.5 mg (0.150 mmol) of 1-naphthylamine. Purified by flash chromatography (SiO₂, EtOAc/hexane, gradient from 5 to 10% in EtOAc) to afford 98 as a yellow/white solid (28.4 mg, 65%). ¹H NMR (300 MHz, Acetone-*d*₆) δ 8.19 (d, *J* = 7.8 Hz, 1H), 8.04 (m, 1H), 7.96 (m, 1H), 7.79 (d, *J* = 7.4 Hz, 1H), 7.56 (s, 1H), 7.42 (m, 4H), 7.27 (t, *J* = 7.8 Hz, 1H), 7.19 (d, *J* = 8.0 Hz, 1H), 6.69 (d, *J* = 7.4 Hz, 1H), 6.13 (s, 1H), 4.82 (d, *J* = 5.1 Hz, 2H) ppm. ¹³C NMR (75 MHz, Acetone-*d*₆) δ 144.7, 141.7, 139.3, 135.5, 135.1, 129.1, 127.5, 126.4, 125.3, 125.1, 124.9, 124.6, 124.2, 123.7, 122.9, 121.9, 117.5, 105.1, 43.1 ppm.



***N*-(4-(trifluoromethyl)benzyl)naphthalen-1-amine (99)**

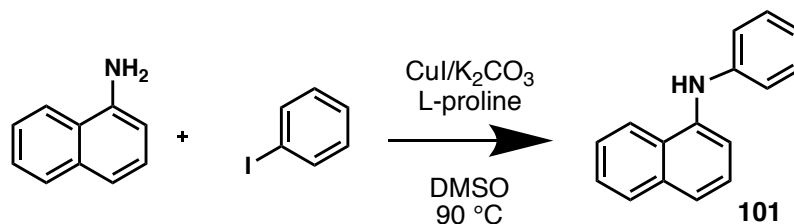
General Procedure 10. Reaction scale: 21.5 mg (0.150 mmol) of 1-naphthylamine. Purified by flash chromatography (SiO₂, EtOAc/hexane, gradient from 5 to 10% in EtOAc) to afford 99 as a yellow oil (34.8 mg, 77%). ¹H NMR (300 MHz, Acetone-*d*₆) δ 8.18 (m, 1H), 7.76 (m, 1H), 7.63 (s, 4H), 7.43 (t, *J* = 4.4 Hz, 2H), 7.16 (m, 2H), 6.40 (m, 2H), 4.67 (d, *J* = 5.5 Hz, 2H) ppm. ¹³C NMR (75 MHz, Acetone-*d*₆) δ 146.0, 144.3, 135.5, 129.2, 129.1, 128.5 (2C), 127.4, 127.3, 126.5, 126.1 (q, *J* = 5.1 Hz), 125.2, 124.5, 121.8 (2C), 117.6, 105.1, 47.7 ppm.



***N*-((2',4'-difluoro-[1,1'-biphenyl]-4-yl)methyl)naphthalen-1-amine (100)**

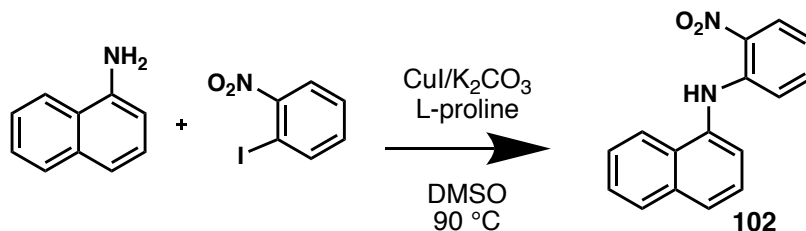
General Procedure 10. Reaction scale: 21.5 mg (0.150 mmol) of 1-naphthylamine. Purified by flash chromatography (SiO₂, EtOAc/hexane, gradient from 5 to 10% in EtOAc) to afford 100 as a yellow oil (34.5 mg, 66%). ¹H NMR (300 MHz, Acetone-*d*₆) δ 8.19 (m, 1H), 7.75 (m, 1H), 7.48 (m, 7H), 7.11 (m, 4H), 6.51 (d, *J* = 7.2 Hz, 1H), 6.27 (s, 1H), 4.61 (d, *J* = 5.5 Hz, 2H) ppm. ¹³C NMR (75 MHz, Acetone-*d*₆) δ 163.0 (dd, *J* = 245.3, 12.0 Hz, 2C), 144.6, 140.8, 135.5, 134.2, 132.8 (d, *J* = 5.3 Hz), 132.6 (d, *J* = 5.3

Hz), 129.8 (2C), 129.2, 128.3 (2C), 127.5, 126.4, 125.1, 124.5, 121.8, 117.3, 112.6 (dd, $J = 21.0, 3.0$ Hz), 105.2 (t, $J = 27.0$ Hz), 105.1, 47.9 ppm.



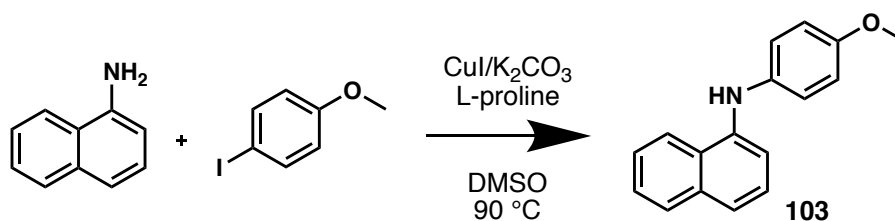
N-phenylnaphthalen-1-amine (NPN) (101)

General Procedure 13. Reaction scale: 43.0 mg (0.300 mmol) of aryl halide. Purified by flash chromatography (SiO₂, EtOAc/Hexane, 10:90) to afford **101** as a brown oil (4.0 mg, 9%). ¹H NMR (400 MHz, Acetone-*d*₆) δ 8.18 (d, $J = 8.1$ Hz, 1H), 7.89 (d, $J = 7.8$ Hz, 1H), 7.56 (d, $J = 7.4$ Hz, 1H), 7.48 (m, 3H), 7.40 (d, $J = 8.2$ Hz, 2H), 7.23 (t, $J = 7.5$ Hz, 2H), 7.08 (d, $J = 7.8$ Hz, 2H), 6.85 (t, $J = 7.2$ Hz, 1H) ppm. ¹³C NMR (101 MHz, Acetone-*d*₆) δ 146.3, 140.5, 136.9, 129.9 (2C), 129.2, 128.6, 126.9, 126.9, 126.0, 123.3, 122.9, 120.7, 118.2 (2C), 115.7 ppm.



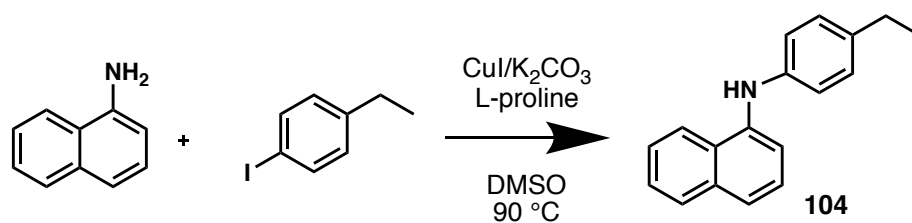
N-(2-nitrophenyl)naphthalen-1-amine (102)

General Procedure 13. Reaction scale: 49.8 mg (0.200 mmol) of aryl halide. Purified by flash chromatography (SiO₂, EtOAc/Hexane, gradient from 10 to 20% in EtOAc) to afford 102 as a red/orange solid (4.9 mg, 9%). ¹H NMR (300 MHz, Acetone-*d*₆) δ 9.76 (s, 1H), 8.24 (d, *J* = 8.4 Hz, 1H), 8.03 (t, *J* = 5.3 Hz, 2H), 7.94 (t, *J* = 4.3 Hz, 1H), 7.59 (m, 4H), 7.39 (t, *J* = 7.6 Hz, 1H), 6.84 (t, *J* = 7.7 Hz, 1H), 6.75 (d, *J* = 8.6 Hz, 1H) ppm. ¹³C NMR (75 MHz, Acetone-*d*₆) δ 145.5, 145.4, 136.8, 135.8, 135.8, 131.1, 129.4, 128.1, 127.7, 127.5, 127.1, 127.0, 125.1, 123.4, 118.0, 117.3 ppm.



***N*-(4-methoxyphenyl)naphthalen-1-amine (103)**

General Procedure 13. Reaction scale: 46.8 mg (0.200 mmol) of aryl halide. Purified by pTLC (EtOAc/Hexane, 20:80) to afford 103 as a pink solid (5.1 mg, 10%). ¹H NMR (500 MHz, Acetone-*d*₆) δ 8.22 (d, *J* = 8.2 Hz, 1H), 7.85 (d, *J* = 7.8 Hz, 1H), 7.46 (m, 2H), 7.40 (d, *J* = 8.1 Hz, 1H), 7.31 (m, 2H), 7.13 (d, *J* = 8.8 Hz, 2H), 7.10 (d, *J* = 7.5 Hz, 1H), 6.90 (d, *J* = 8.8 Hz, 2H), 3.78 (s, 3H) ppm. ¹³C NMR (125 MHz, Acetone-*d*₆) δ 155.9, 142.6, 138.2, 135.8, 129.1, 127.1, 126.9, 126.7, 125.6, 122.8, 122.6 (2C), 120.7, 115.4 (2C), 111.2, 55.7 ppm.



***N*-(4-ethylphenyl)naphthalen-1-amine (104)**

General Procedure 13. Reaction scale: 46.4 mg (0.200 mmol) of aryl halide. Purified by pTLC (EtOAc/Hexane, 20:80) to afford 104 as a brown oil (5.1 mg, 10%). ¹H NMR (500 MHz, Acetone-*d*₆) δ 8.19 (d, *J* = 8.3 Hz, 1H), 7.87 (d, *J* = 7.9 Hz, 1H), 7.47 (m, 3H), 7.38 (m, 2H), 7.31 (d, *J* = 7.4 Hz, 1H), 7.11 (d, *J* = 8.3 Hz, 2H), 7.05 (d, *J* = 8.3 Hz, 2H), 2.58 (q, *J* = 7.6 Hz, 2H), 1.20 (t, *J* = 7.6 Hz, 3H) ppm. ¹³C NMR (125 MHz, Acetone-*d*₆) δ 143.5, 141.3, 137.0, 135.8, 129.3 (2C), 129.1, 128.0, 127.0, 126.8, 125.8, 123.2, 122.0, 119.2 (2C), 114.0, 28.7, 16.4 ppm.

References

1. Organization, W. H. WHO report on global surveillance of epidemic-prone infectious diseases
2. Belongia, E. A.; Naleway, A. L., Smallpox vaccine: the good, the bad, and the ugly. *Clin Med Res* 2003, *1* (2), 87-92.
3. Organization, W. H. Frequently asked questions and answers on smallpox. <https://www.who.int/csr/disease/smallpox/faq/en/>.
4. Harris, J. B.; LaRocque, R. C.; Qadri, F.; Ryan, E. T.; Calderwood, S. B., Cholera. *The Lancet* 2012, *379* (9835), 2466-2476.
5. Jutla, A.; Whitcombe, E.; Hasan, N.; Haley, B.; Akanda, A.; Huq, A.; Alam, M.; Sack, R. B.; Colwell, R., Environmental factors influencing epidemic cholera. *Am J Trop Med Hyg* 2013, *89* (3), 597-607.
6. Taubenberger, J. K., The origin and virulence of the 1918 "Spanish" influenza virus. *Proc Am Philos Soc* 2006, *150* (1), 86-112.
7. Richter, M. F.; Hergenrother, P. J., The challenge of converting Gram-positive-only compounds into broad-spectrum antibiotics. *Ann N Y Acad Sci* 2019, *1435* (1), 18-38.
8. Pages, J. M., [Antibiotic transport and membrane permeability: new insights to fight bacterial resistance]. *Biol Aujourdhui* 2017, *211* (2), 149-154.
9. Rice, L. B., Federal funding for the study of antimicrobial resistance in nosocomial pathogens: no ESKAPE. *J Infect Dis* 2008, *197* (8), 1079-81.

10. Richter, M. F.; Drown, B. S.; Riley, A. P.; Garcia, A.; Shirai, T.; Svec, R. L.; Hergenrother, P. J., Predictive compound accumulation rules yield a broad-spectrum antibiotic. *Nature* 2017, *545* (7654), 299-304.
11. Acosta-Gutierrez, S.; Ferrara, L.; Pathania, M.; Masi, M.; Wang, J.; Bodrenko, I.; Zahn, M.; Winterhalter, M.; Stavenger, R. A.; Pages, J. M.; Naismith, J. H.; van den Berg, B.; Page, M. G. P.; Ceccarelli, M., Getting drugs into Gram-negative bacteria: rational rules for permeation through general porins. *ACS Infect Dis* 2018, *4* (10), 1487-1498.
12. Silhavy, T. J.; Kahne, D.; Walker, S., The bacterial cell envelope. *Cold Spring Harb Perspect Biol* 2010, *2* (5), a000414.
13. Vergalli, J.; Bodrenko, I. V.; Masi, M.; Moynie, L.; Acosta-Gutierrez, S.; Naismith, J. H.; Davin-Regli, A.; Ceccarelli, M.; van den Berg, B.; Winterhalter, M.; Pages, J. M., Porins and small-molecule translocation across the outer membrane of Gram-negative bacteria. *Nat Rev Microbiol* 2020, *18* (3), 164-176.
14. Ceccarelli, M.; Ruggerone, P., Physical insights into permeation of and resistance to antibiotics in bacteria. *Curr Drug Targets* 2008, *9* (9), 779-88.
15. Zgurskaya, H. I.; Lopez, C. A.; Gnanakaran, S., Permeability barrier of Gram-negative cell envelopes and approaches to bypass it. *ACS Infect Dis* 2015, *1* (11), 512-522.
16. Krishnamoorthy, G.; Leus, I. V.; Weeks, J. W.; Wolloscheck, D.; Rybenkov, V. V.; Zgurskaya, H. I., Synergy between active efflux and outer membrane diffusion defines rules of antibiotic permeation into Gram-negative bacteria. *mBio* 2017, *8* (5).
17. Opperman, T. J.; Nguyen, S. T., Recent advances toward a molecular mechanism of efflux pump inhibition. *Front Microbiol* 2015, *6*, 421.

18. Firth, N. C.; Brown, N.; Blagg, J., Plane of best fit: a novel method to characterize the three-dimensionality of molecules. *J Chem Inf Model* 2012, *52* (10), 2516-25.
19. Parker, E. N.; Drown, B. S.; Geddes, E. J.; Lee, H. Y.; Ismail, N.; Lau, G. W.; Hergenrother, P. J., Implementation of permeation rules leads to a FabI inhibitor with activity against Gram-negative pathogens. *Nat Microbiol* 2020, *5* (1), 67-75.
20. Baym, M.; Stone, L. K.; Kishony, R., Multidrug evolutionary strategies to reverse antibiotic resistance. *Science* 2016, *351* (6268), aad3292.
21. Raju, R. M.; Goldberg, A. L.; Rubin, E. J., Bacterial proteolytic complexes as therapeutic targets. *Nat Rev Drug Discov* 2012, *11* (10), 777-89.
22. Yu, A. Y.; Houry, W. A., ClpP: a distinctive family of cylindrical energy-dependent serine proteases. *FEBS Lett* 2007, *581* (19), 3749-57.
23. Leung, E.; Datti, A.; Cossette, M.; Goodreid, J.; McCaw, S. E.; Mah, M.; Nakhamchik, A.; Ogata, K.; El Bakkouri, M.; Cheng, Y. Q.; Wodak, S. J.; Eger, B. T.; Pai, E. F.; Liu, J.; Gray-Owen, S.; Batey, R. A.; Houry, W. A., Activators of cylindrical proteases as antimicrobials: identification and development of small molecule activators of ClpP protease. *Chem Biol* 2011, *18* (9), 1167-78.
24. Alexopoulos, J. A.; Guarne, A.; Ortega, J., ClpP: a structurally dynamic protease regulated by AAA+ proteins. *J Struct Biol* 2012, *179* (2), 202-10.
25. Brotz-Oesterhelt, H.; Beyer, D.; Kroll, H. P.; Endermann, R.; Ladel, C.; Schroeder, W.; Hinzen, B.; Raddatz, S.; Paulsen, H.; Henninger, K.; Bandow, J. E.; Sahl, H. G.; Labischinski, H., Dysregulation of bacterial proteolytic machinery by a new class of antibiotics. *Nat Med* 2005, *11* (10), 1082-7.

26. Goodreid, J. D.; Wong, K.; Leung, E.; McCaw, S. E.; Gray-Owen, S. D.; Lough, A.; Houry, W. A.; Batey, R. A., Total synthesis and antibacterial testing of the A54556 cyclic acyldepsipeptides isolated from *Streptomyces hawaiiensis*. *J Nat Prod* 2014, 77 (10), 2170-81.
27. Goodreid, J. D.; Janetzko, J.; Santa Maria, J. P., Jr.; Wong, K. S.; Leung, E.; Eger, B. T.; Bryson, S.; Pai, E. F.; Gray-Owen, S. D.; Walker, S.; Houry, W. A.; Batey, R. A., Development and characterization of potent cyclic acyldepsipeptide analogues with increased antimicrobial activity. *J Med Chem* 2016, 59 (2), 624-46.
28. Compton, C. L.; Carney, D. W.; Grooms, P. V.; Sello, J. K., fragment-based strategy for investigating and suppressing the efflux of bioactive small molecules. *ACS Infect Dis* 2015, 1 (1), 53-8.
29. Vahidi, S.; Ripstein, Z. A.; Bonomi, M.; Yuwen, T.; Mabanglo, M. F.; Juravsky, J. B.; Rizzolo, K.; Velyvis, A.; Houry, W. A.; Vendruscolo, M.; Rubinstein, J. L.; Kay, L. E., Reversible inhibition of the ClpP protease via an N-terminal conformational switch. *Proc Natl Acad Sci U S A* 2018, 115 (28), E6447-E6456.
30. Kirstein, J.; Hoffmann, A.; Lilie, H.; Schmidt, R.; Rubsamen-Waigmann, H.; Brotz-Oesterhelt, H.; Mogk, A.; Turgay, K., The antibiotic ADEP reprogrammes ClpP, switching it from a regulated to an uncontrolled protease. *EMBO Mol Med* 2009, 1 (1), 37-49.
31. Ye, F.; Li, J.; Yang, C. G., The development of small-molecule modulators for ClpP protease activity. *Mol Biosyst* 2016, 13 (1), 23-31.

32. Carney, D. W.; Compton, C. L.; Schmitz, K. R.; Stevens, J. P.; Sauer, R. T.; Sello, J. K., A simple fragment of cyclic acyldepsipeptides is necessary and sufficient for ClpP activation and antibacterial activity. *Chembiochem* 2014, 15 (15), 2216-20.
33. Hermanson, G. T., Fluorescent probes. *Bioconjugate Techniques* 2013, 395–463.
34. Haberstock, D. S. How to develop an optimal fluorescence assay. <https://www.tecan.com/blog/how-to-develop-an-optimal-fluorescence-assay>.
35. Trevors, J. T., Fluorescent probes for bacterial cytoplasmic membrane research. *Journal of Biochemical and Biophysical Methods* 2003, 57 (2), 87-103.
36. Gallo, E., Fluorogen-activating proteins: next-generation fluorescence probes for biological research. *Bioconjug Chem* 2020, 31 (1), 16-27.
37. Baptista, M. d. S.; Bastos, E. L., Fluorescence in pharmaceuticals and cosmetics. *Springer Series on Fluorescence* 2019, 18, 39-102.
38. Klymchenko, A. S.; Kreder, R., Fluorescent probes for lipid rafts: from model membranes to living cells. *Chem Biol* 2014, 21 (1), 97-113.
39. Stone, M. R. L.; Masi, M.; Phetsang, W.; Pages, J. M.; Cooper, M. A.; Blaskovich, M. A. T., Fluoroquinolone-derived fluorescent probes for studies of bacterial penetration and efflux. *Medchemcomm* 2019, 10 (6), 901-906.
40. Helander, I. M.; Mattila-Sandholm, T., Fluorometric assessment of gram-negative bacterial permeabilization. *J Appl Microbiol* 2000, 88 (2), 213-9.
41. Information, N. C. f. B. N-Phenyl-1-naphthylamine. <https://pubchem.ncbi.nlm.nih.gov/compound/1-%28N-phenylamino%29naphthalene> (accessed Mar. 10, 2020).

42. Cao-Hoang, L.; Marechal, P. A.; Le-Thanh, M.; Gervais, P., Synergistic action of rapid chilling and nisin on the inactivation of *Escherichia coli*. *Appl Microbiol Biotechnol* 2008, 79 (1), 105-9.
43. Boziaris, I. S.; Adams, M. R., Temperature shock, injury and transient sensitivity to nisin in Gram negatives. *J Appl Microbiol* 2001, 91 (4), 715-24.
44. Tang, H.; Zhang, P.; Kieft, T. L.; Ryan, S. J.; Baker, S. M.; Wiesmann, W. P.; Rogelj, S., Antibacterial action of a novel functionalized chitosan-arginine against Gram-negative bacteria. *Acta Biomater* 2010, 6 (7), 2562-71.
45. Liu, X.; Xia, W.; Jiang, Q.; Xu, Y.; Yu, P., Effect of kojic acid-grafted-chitosan oligosaccharides as a novel antibacterial agent on cell membrane of gram-positive and gram-negative bacteria. *J Biosci Bioeng* 2015, 120 (3), 335-9.
46. Siriyong, T.; Chusri, S.; Srimanote, P.; Tipmanee, V.; Voravuthikunchai, S. P., *Holarrhena antidysenterica* extract and its steroidal alkaloid, conessine, as resistance-modifying agents against extensively drug-resistant *acinetobacter baumannii*. *Microb Drug Resist* 2016, 22 (4), 273-82.
47. Sun, Z.; Zhang, X.; Wu, H.; Wang, H.; Bian, H.; Zhu, Y.; Xu, W.; Liu, F.; Wang, D.; Fu, L., Antibacterial activity and action mode of chlorogenic acid against *Salmonella* Enteritidis, a foodborne pathogen in chilled fresh chicken. *World J Microbiol Biotechnol* 2020, 36 (2), 24.
48. Muheim, C.; Gotzke, H.; Eriksson, A. U.; Lindberg, S.; Lauritsen, I.; Norholm, M. H. H.; Daley, D. O., Increasing the permeability of *Escherichia coli* using MAC13243. *Sci Rep* 2017, 7 (1), 17629.

49. Loh, B.; Grant, C.; Hancock, R. E., Use of the fluorescent probe 1-N-phenylnaphthylamine to study the interactions of aminoglycoside antibiotics with the outer membrane of *Pseudomonas aeruginosa*. *Antimicrob Agents Chemother* 1984, 26 (4), 546-51.
50. Famulla, K.; Sass, P.; Malik, I.; Akopian, T.; Kandror, O.; Alber, M.; Hinzen, B.; Ruebsamen-Schaeff, H.; Kalscheuer, R.; Goldberg, A. L.; Brotz-Oesterhelt, H., Acyldepsipeptide antibiotics kill mycobacteria by preventing the physiological functions of the ClpP1P2 protease. *Mol Microbiol* 2016, 101 (2), 194-209.
51. Conlon, B. P.; Nakayasu, E. S.; Fleck, L. E.; LaFleur, M. D.; Isabella, V. M.; Coleman, K.; Leonard, S. N.; Smith, R. D.; Adkins, J. N.; Lewis, K., Activated ClpP kills persisters and eradicates a chronic biofilm infection. *Nature* 2013, 503 (7476), 365-70.
52. Socha, A. M.; Tan, N. Y.; LaPlante, K. L.; Sello, J. K., Diversity-oriented synthesis of cyclic acyldepsipeptides leads to the discovery of a potent antibacterial agent. *Bioorg Med Chem* 2010, 18 (20), 7193-202.
53. Carney, D. W.; Schmitz, K. R.; Truong, J. V.; Sauer, R. T.; Sello, J. K., Restriction of the conformational dynamics of the cyclic acyldepsipeptide antibiotics improves their antibacterial activity. *J Am Chem Soc* 2014, 136 (5), 1922-9.
54. Ouyang, L.; Zhang, L.; Zhang, S.; Yao, D.; Zhao, Y.; Wang, G.; Fu, L.; Lei, P.; Liu, B., Small-molecule activator of UNC-51-Like Kinase 1 (ULK1) that induces cytoprotective autophagy for parkinson's disease treatment. *J Med Chem* 2018, 61 (7), 2776-2792.

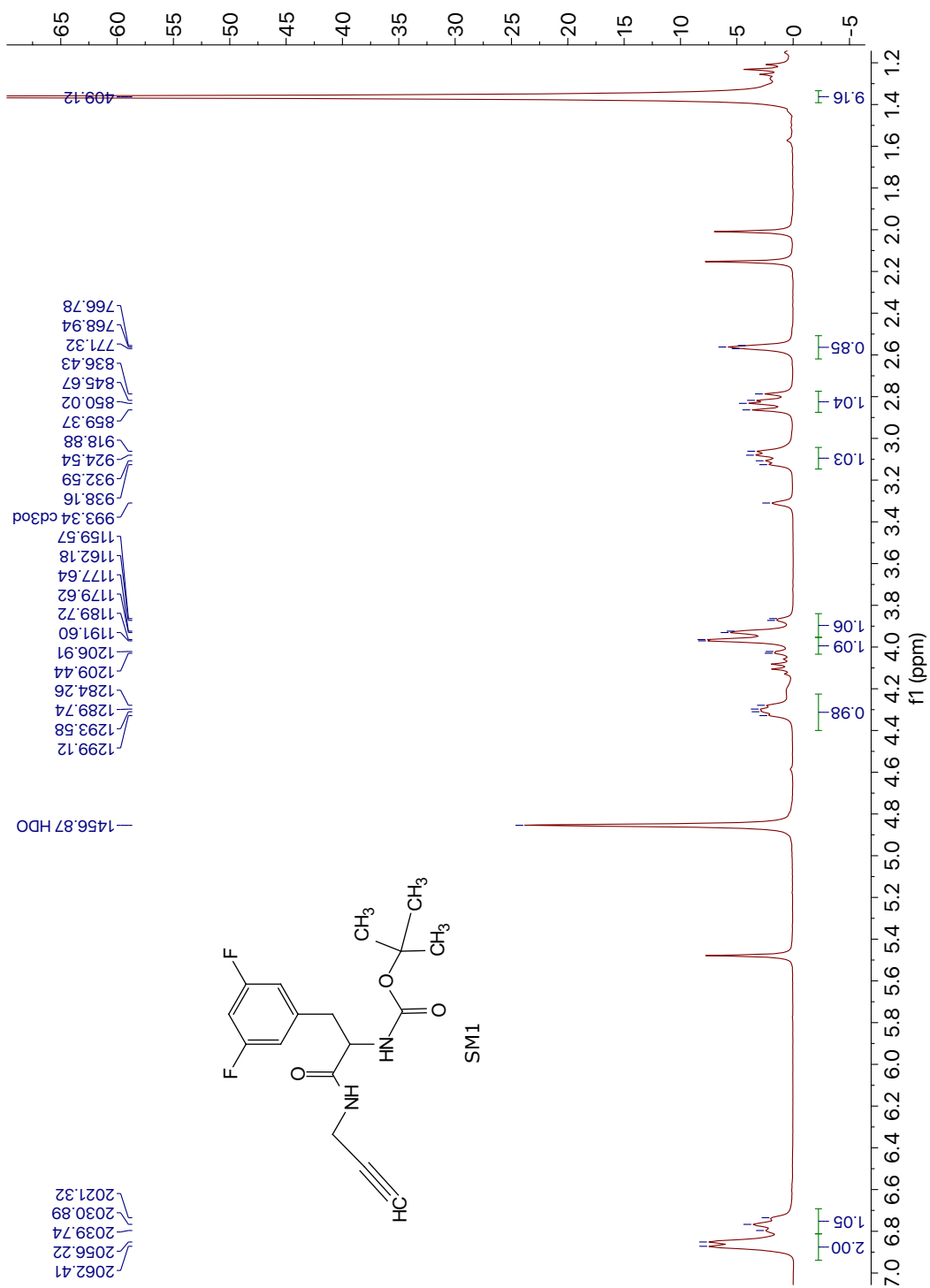
55. Ashenhurst, J. The Hofmann and Curtius rearrangements. <https://www.masterorganicchemistry.com/2017/09/19/hofmann-and-curtius-rearrangements/>.
56. Forlani, L.; Giampiero, C.; Boga, C.; Todesco, P. E.; Del Vecchio, E.; Selva, S.; Monari, M., Reinvestigation of the tautomerism of some substituted 2-hydroxypyridines. *Arkivoc* 2002, 2002 (11).
57. Nishizawa, R.; Nishiyama, T.; Hisaichi, K.; Minamoto, C.; Murota, M.; Takaoka, Y.; Nakai, H.; Tada, H.; Sagawa, K.; Shibayama, S.; Fukushima, D.; Maeda, K.; Mitsuya, H., Discovery of 4-[4-((3R)-1-butyl-3-[(R)-cyclohexyl(hydroxy)methyl]-2,5-dioxo-1,4,9-triazaspiro [5.5]undec-9-yl)methyl)phenoxy]benzoic acid hydrochloride: a highly potent orally available CCR5 selective antagonist. *Bioorg Med Chem* 2011, 19 (13), 4028-42.
58. Li, Y.; Gardner, J. J.; Fortney, K. R.; Leus, I. V.; Bonifay, V.; Zgurskaya, H. I.; Pletnev, A. A.; Zhang, S.; Zhang, Z. Y.; Gribble, G. W.; Spinola, S. M.; Duerfeldt, A. S., First-generation structure-activity relationship studies of 2,3,4,9-tetrahydro-1H-carbazol-1-amines as CpxA phosphatase inhibitors. *Bioorg Med Chem Lett* 2019, 29 (14), 1836-1841.
59. Institute, C. a. L. S., M100 performance standards for antimicrobial susceptibility testing, 30th edition. Thirtieth ed.; 2020; p 332.
60. Schwarz, F. P.; Wasik, S. P., Fluorescence measurements of benzene, naphthalene, anthracene, pyrene, fluoranthene, and benzo(e)pyrene in water. *Anal Chem* 1976, 48 (3), 524-8.

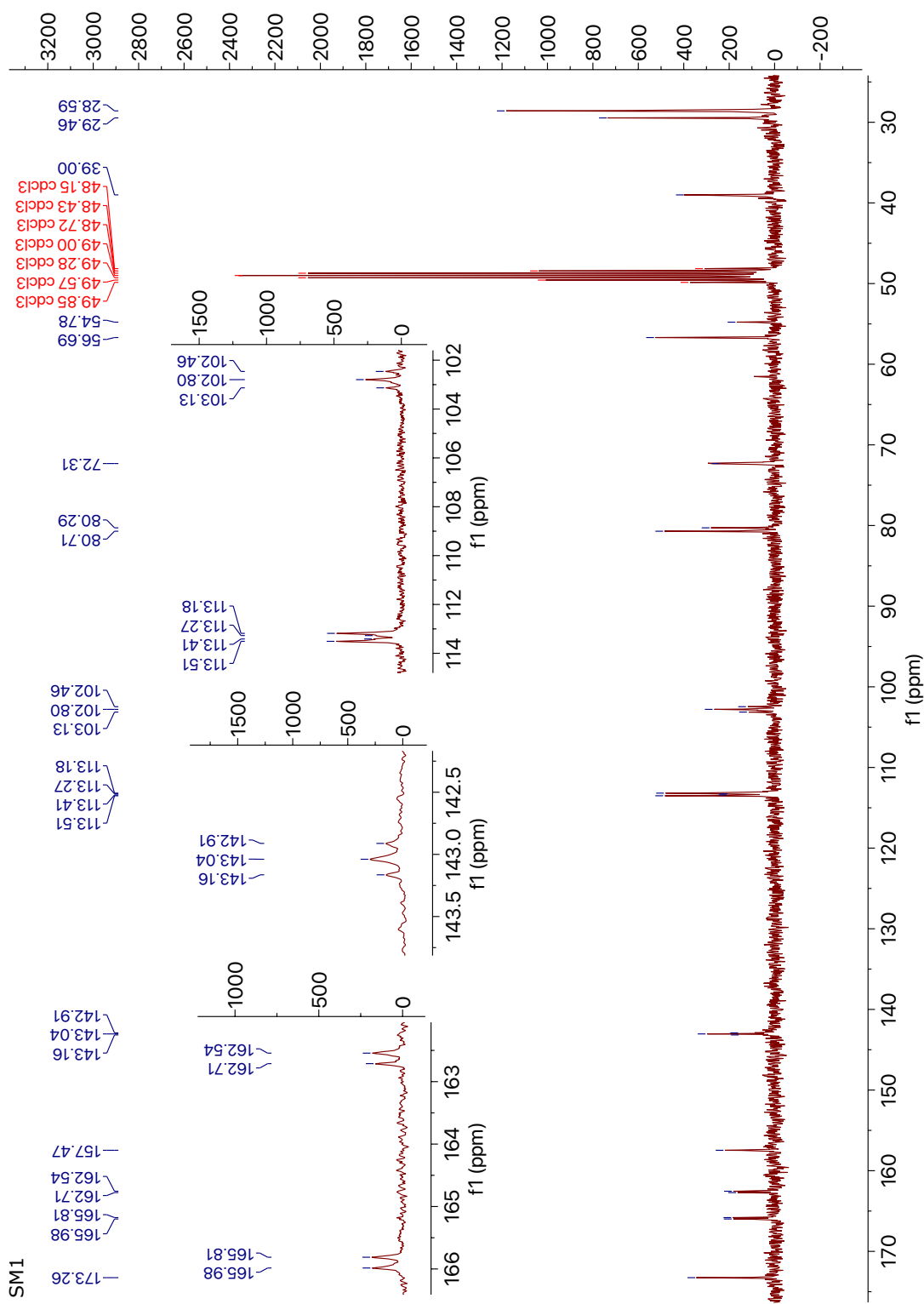
61. Massah, A.; Kazemi, F.; Azadi, D.; Farzaneh, S.; Aliyan, H.; Naghash, H.; Momeni, A., A mild and chemoselective solvent-free method for the synthesis of N-aryl and N-alkylsulfonamides. *Letters in Organic Chemistry* 2006, 3 (3), 235-241.
62. Reddy, M. B. M.; Pasha, M. A., Cs₂CO₃ catalyzed rapid and efficient conversion of amines into sulfonamides; alcohols and phenols into sulfonic esters. *Phosphorus, Sulfur, and Silicon and the Related Elements* 2011, 186 (9), 1867-1875.
63. Meshram, G. A.; Patil, V. D., A simple and efficient method for sulfonylation of amines, alcohols and phenols with cupric oxide under mild conditions. *Tetrahedron Letters* 2009, 50 (10), 1117-1121.
64. Novak, A.; Humphreys, L. D.; Walker, M. D.; Woodward, S., Amide bond formation using an air-stable source of AlMe₃. *Tetrahedron Letters* 2006, 47 (32), 5767-5769.
65. Naoum, J. N.; Chandra, K.; Shemesh, D.; Gerber, R. B.; Gilon, C.; Hurevich, M., DMAP-assisted sulfonylation as an efficient step for the methylation of primary amine motifs on solid support. *Beilstein J Org Chem* 2017, 13, 806-816.
66. Biswas, K.; Prieto, O.; Goldsmith, P. J.; Woodward, S., Remarkably stable (Me₃Al)₂-DABCO and stereoselective nickel-catalyzed AlR₃ (R=Me, Et) additions to aldehydes. *Angewandte Chemie* 2005, 117 (15), 2272-2274.
67. Norseeda, K.; Gasser, V.; Sarpong, R., A late-stage functionalization approach to derivatives of the pyrano[3,2- a]carbazole natural products. *J Org Chem* 2019, 84 (9), 5965-5973.

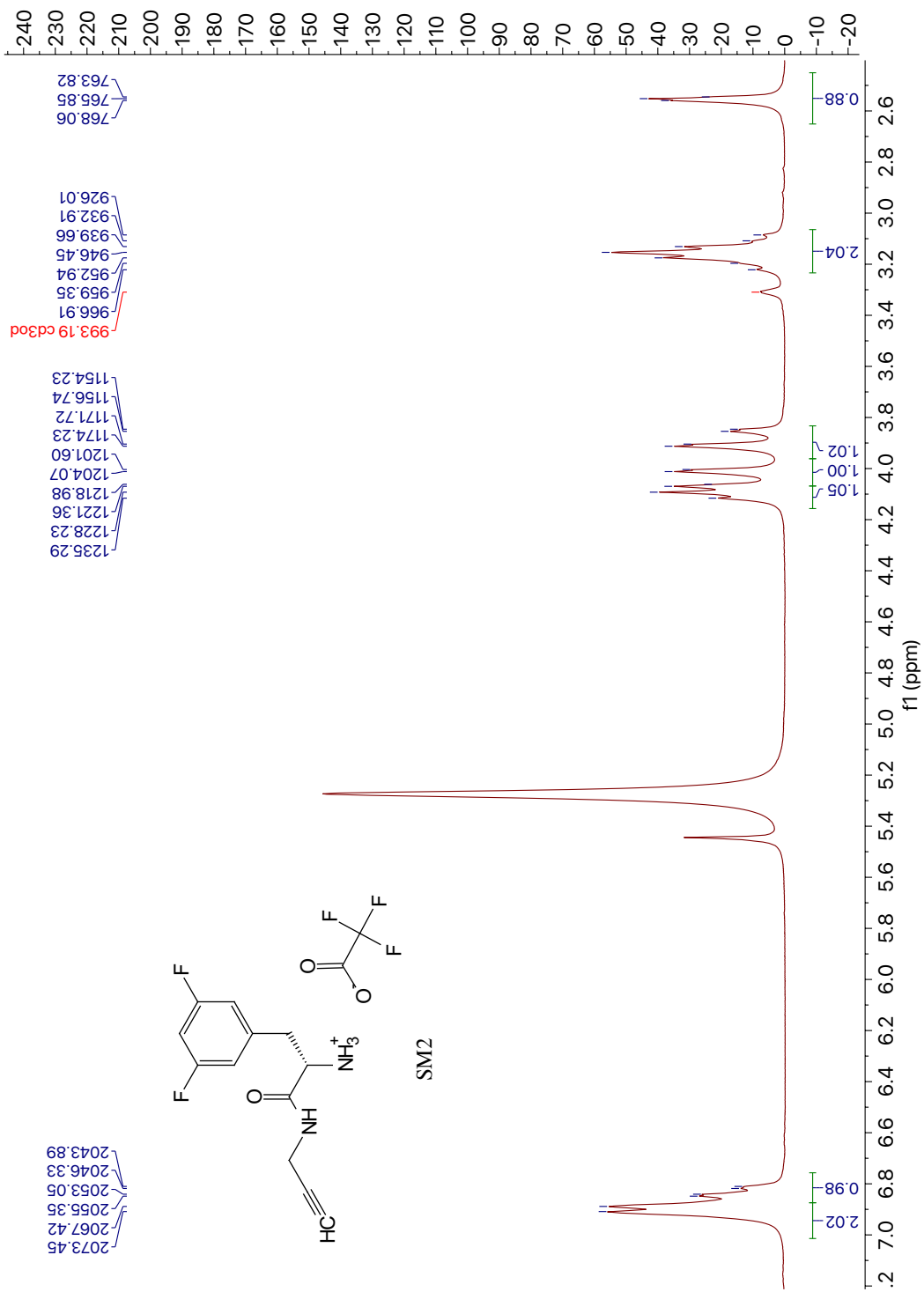
68. Conte, V.; Fiorani, G.; Floris, B.; Galloni, P.; Woodward, S., Palladium-catalysed methylation of aryl halides in ionic liquids with stabilized AlMe₃. *Applied Catalysis A: General* 2010, *381* (1-2), 161-168.
69. Cooper, T.; Novak, A.; Humphreys, L. D.; Walker, M. D.; Woodward, S., User-friendly methylation of aryl and vinyl halides and pseudohalides with DABAL-Me₃. *Advanced Synthesis & Catalysis* 2006, *348* (6), 686-690.
70. Lee, D. S.; Amara, Z.; Poliakoff, M.; Harman, T.; Reid, G.; Rhodes, B.; Brough, S.; McNally, T.; Woodward, S., Investigating scale-up and further applications of DABAL-Me₃ promoted amide synthesis. *Organic Process Research & Development* 2015, *19* (7), 831-840.
71. Kang, S.; Kim, H.-K., Facile direct synthesis of unsymmetrical ureas from N -Alloc-, N -Cbz-, and N -Boc-protected amines using DABAL-Me₃. *Tetrahedron* 2018, *74* (30), 4036-4046.
72. Pujari, V. K.; Vinnakota, S.; Kakarla, R. K.; Marojua, S., Microwave assisted synthesis and antimicrobial activity of 1-(2-chloropyridin-3-yl)-3-substituted urea derivatives. *Asian Journal of Chemistry* 2019, *31* (1), 41-44.
73. Jeong, B.-H.; Kim, H.-K.; Thompson, D. H., A facile and efficient method for the formation of unsymmetrical ureas using DABAL-Me₃. *Australian Journal of Chemistry* 2016, *69* (7).
74. Johnson, C. R.; Ansari, M. I.; Coop, A., Tetrabutylammonium bromide-promoted metal-free, efficient, rapid, and scalable synthesis of N-aryl amines. *ACS Omega* 2018, *3* (9), 10886-10890.

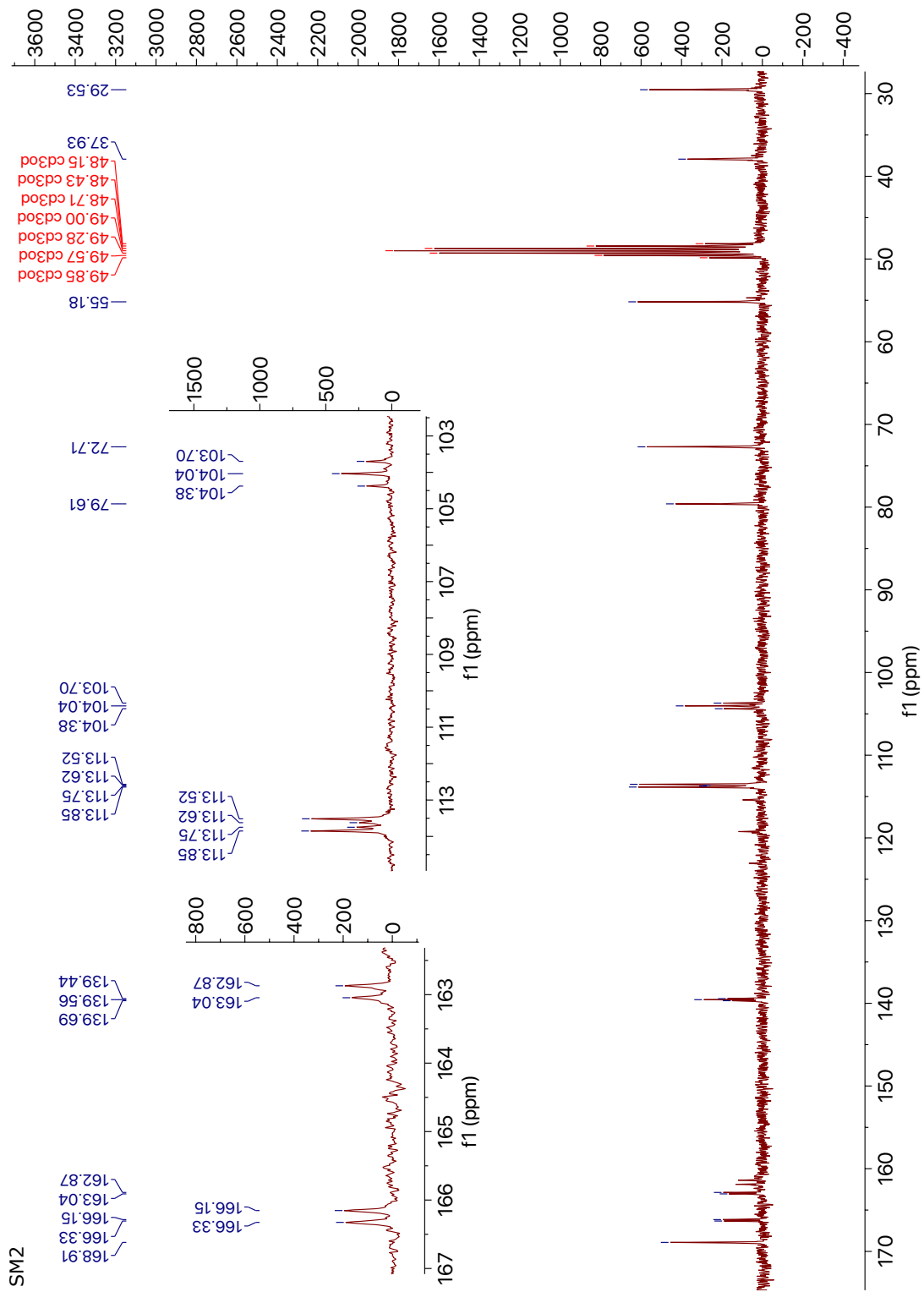
75. Nadri, S.; Rafiee, E.; Jamali, S.; Joshaghani, M., 2,6-Bis(diphenylphosphino)pyridine: a simple ligand showing high performance in palladium-catalyzed CN coupling reactions. *Tetrahedron Letters* 2014, 55 (30), 4098-4101.
76. Ma, D.; Cai, Q.; Zhang, H., Mild method for Ullmann coupling reaction of amines and aryl halides. *Org Lett* 2003, 5 (14), 2453-5.
77. Portal, O. C. Buchwald-Hartwig cross coupling reaction. <https://www.organic-chemistry.org/namedreactions/buchwald-hartwig-reaction.shtm>.
78. Guram, A. S.; Rennels, R. A.; Buchwald, S. L., A simple catalytic method for the conversion of aryl bromides to arylamines. *Angew. Chem. Int. Ed. Engl* 1995, 34 (12), 1348-1350.
79. Portal, O. C. Ullmann reaction. <https://www.organic-chemistry.org/namedreactions/ullmann-reaction.shtm>.
80. TECAN Tweaking fluorescence scans. <http://neotec.co.il/wp-content/uploads/2014/03/TN-Tweaking-Fluorescence-Intensity-scans.pdf>.
81. Westfall, D. A.; Krishnamoorthy, G.; Wolloscheck, D.; Sarkar, R.; Zgurskaya, H. I.; Rybenkov, V. V., Bifurcation kinetics of drug uptake by Gram-negative bacteria. *PLoS One* 2017, 12 (9), e0184671.

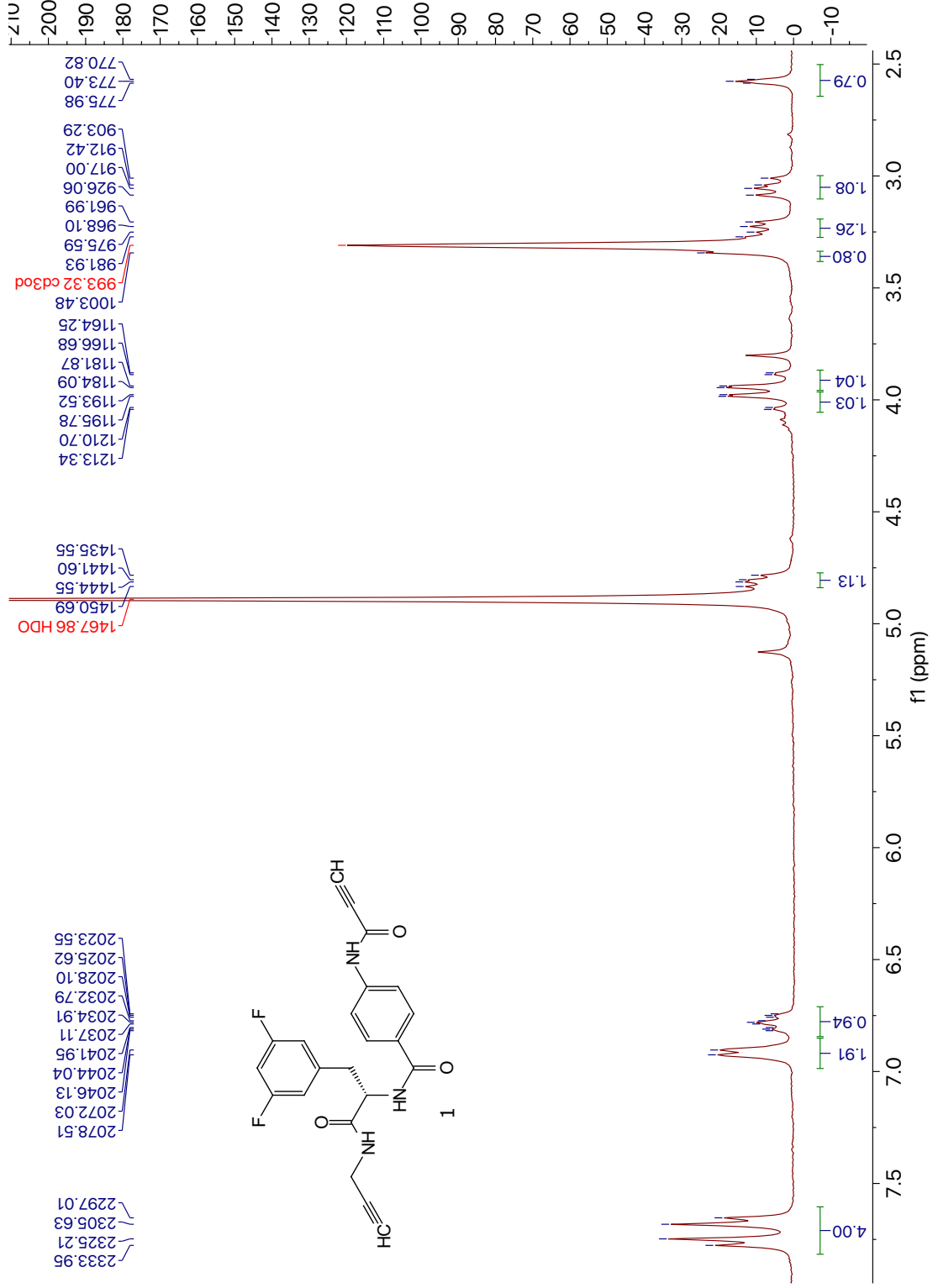
Spectral Data for All Identified Compounds and Starting Materials

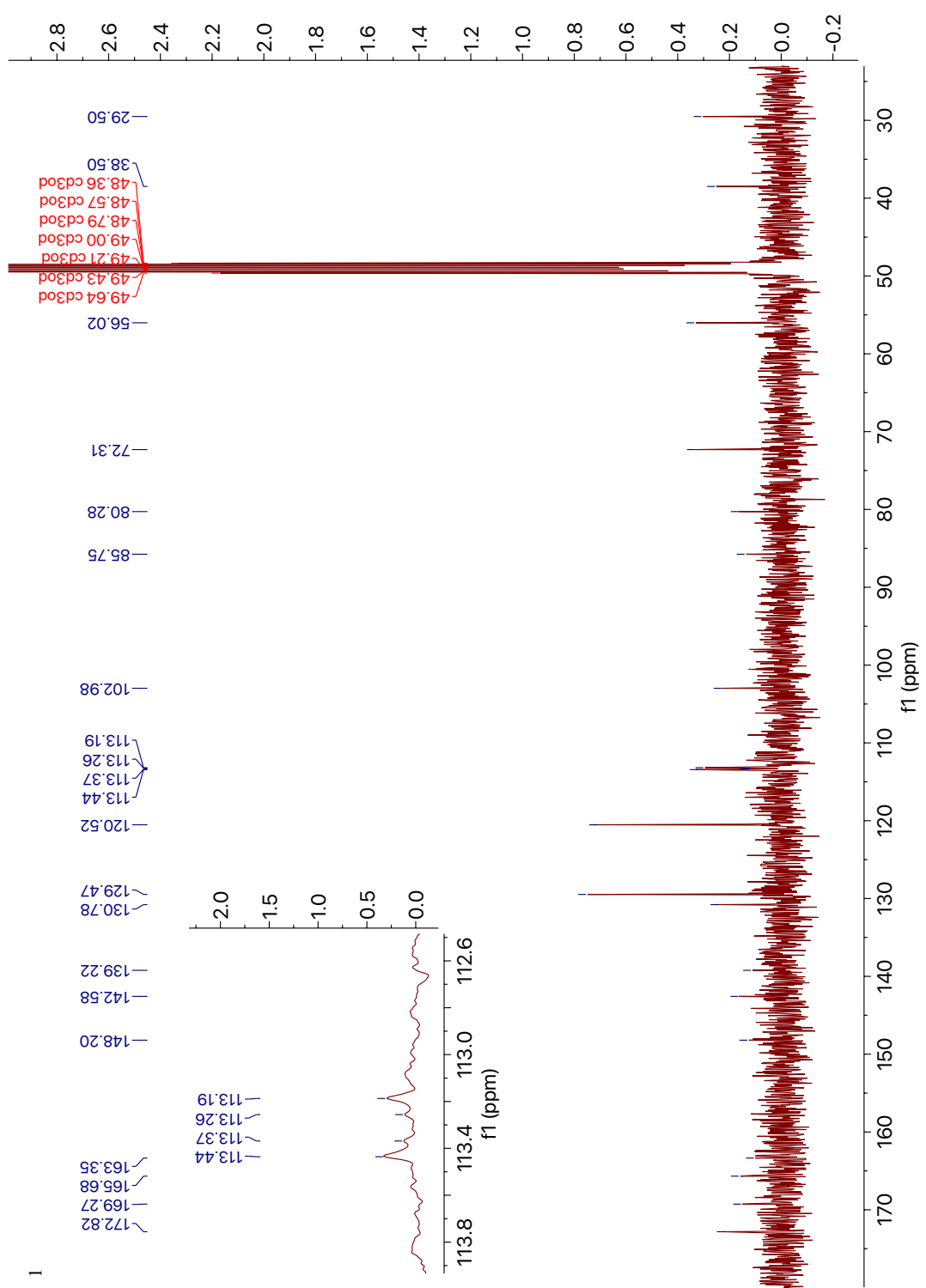


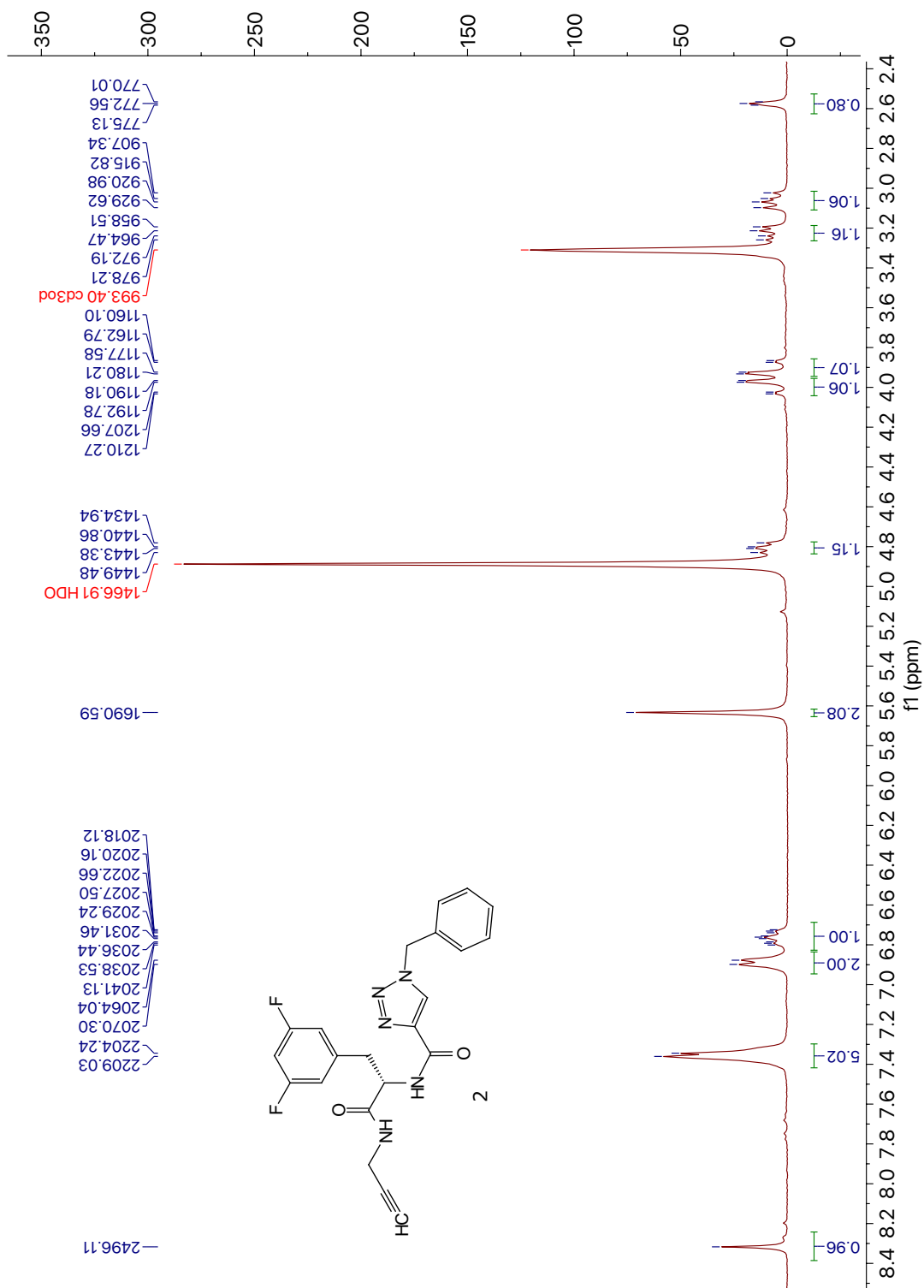


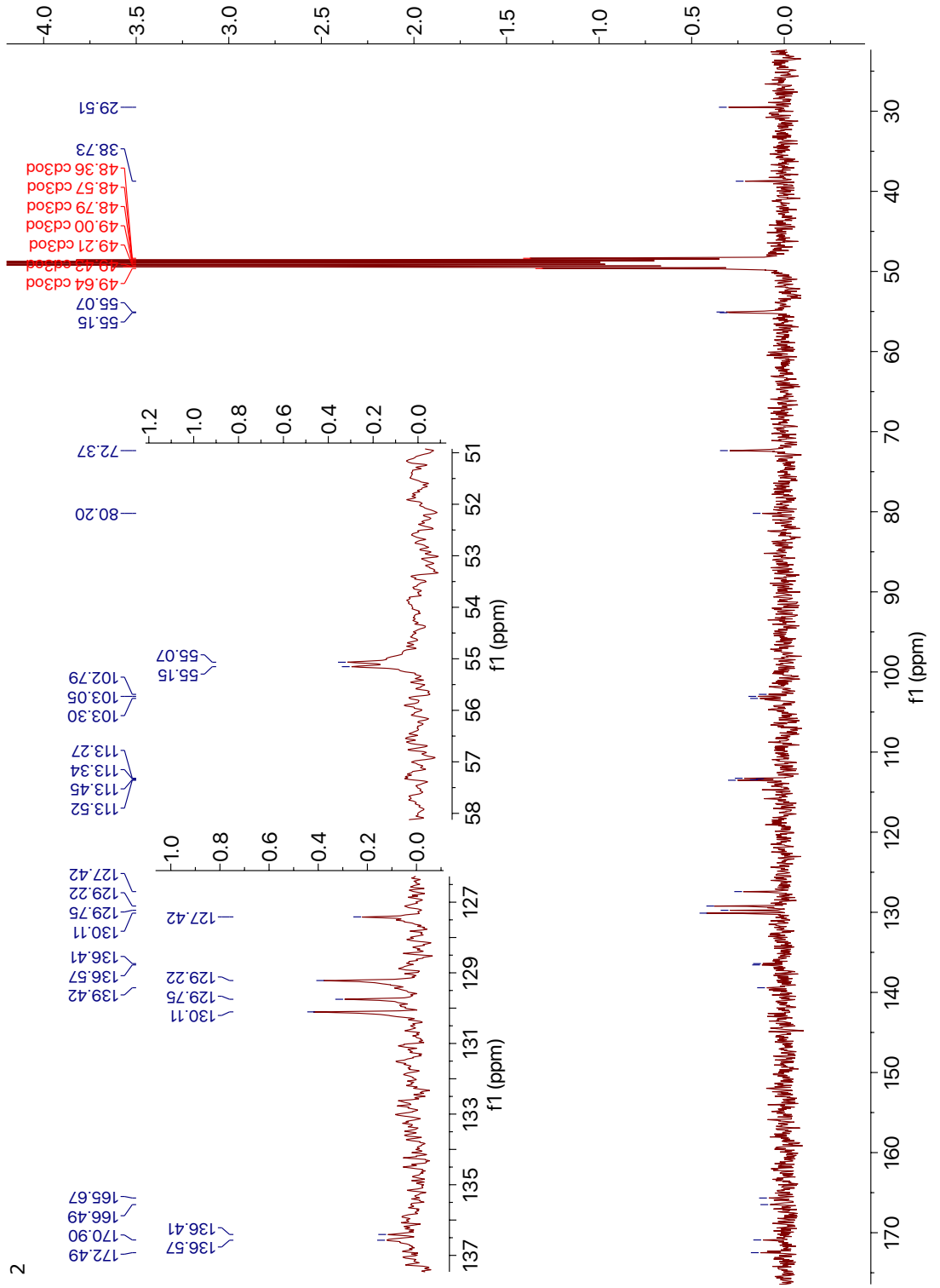




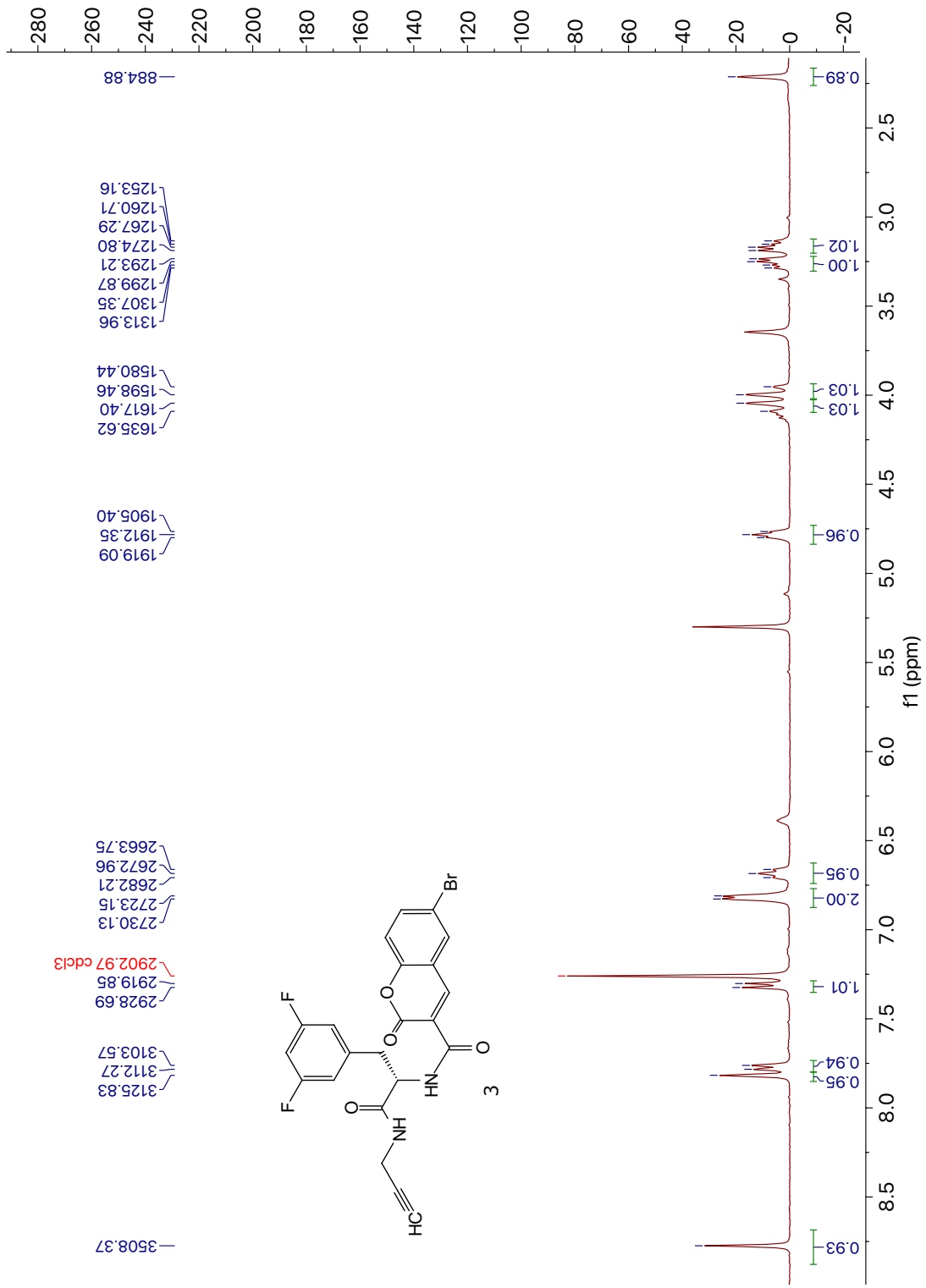


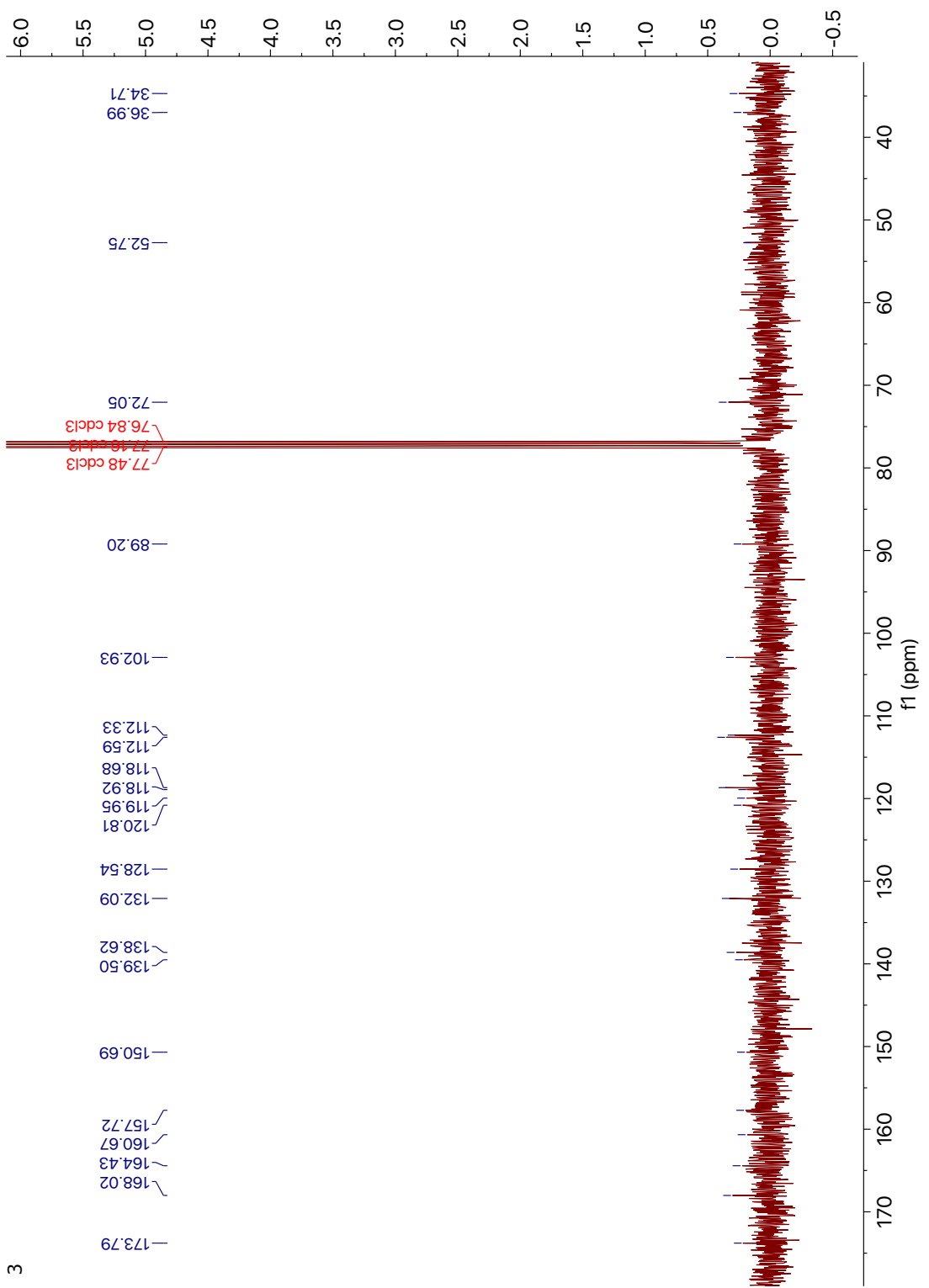




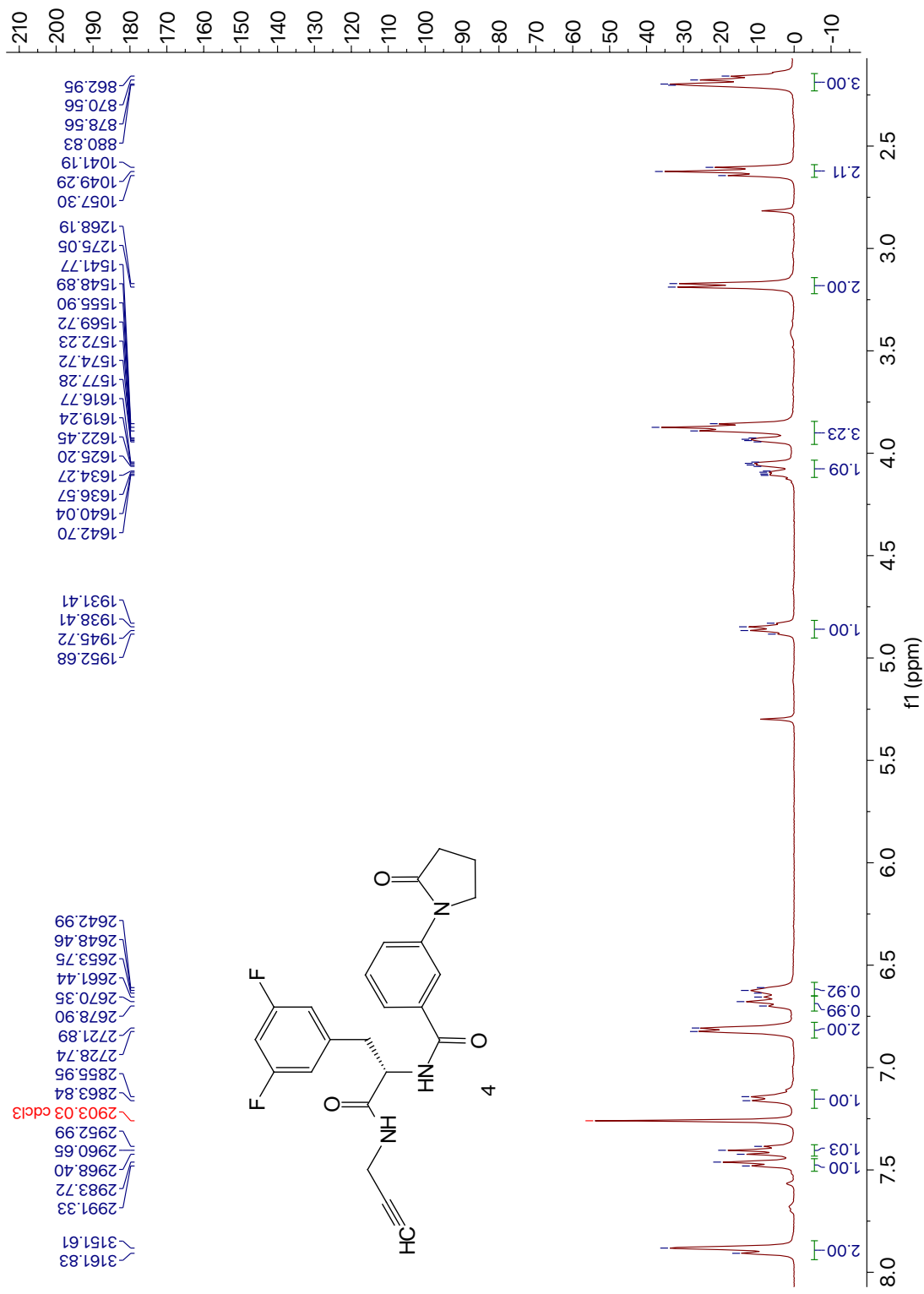


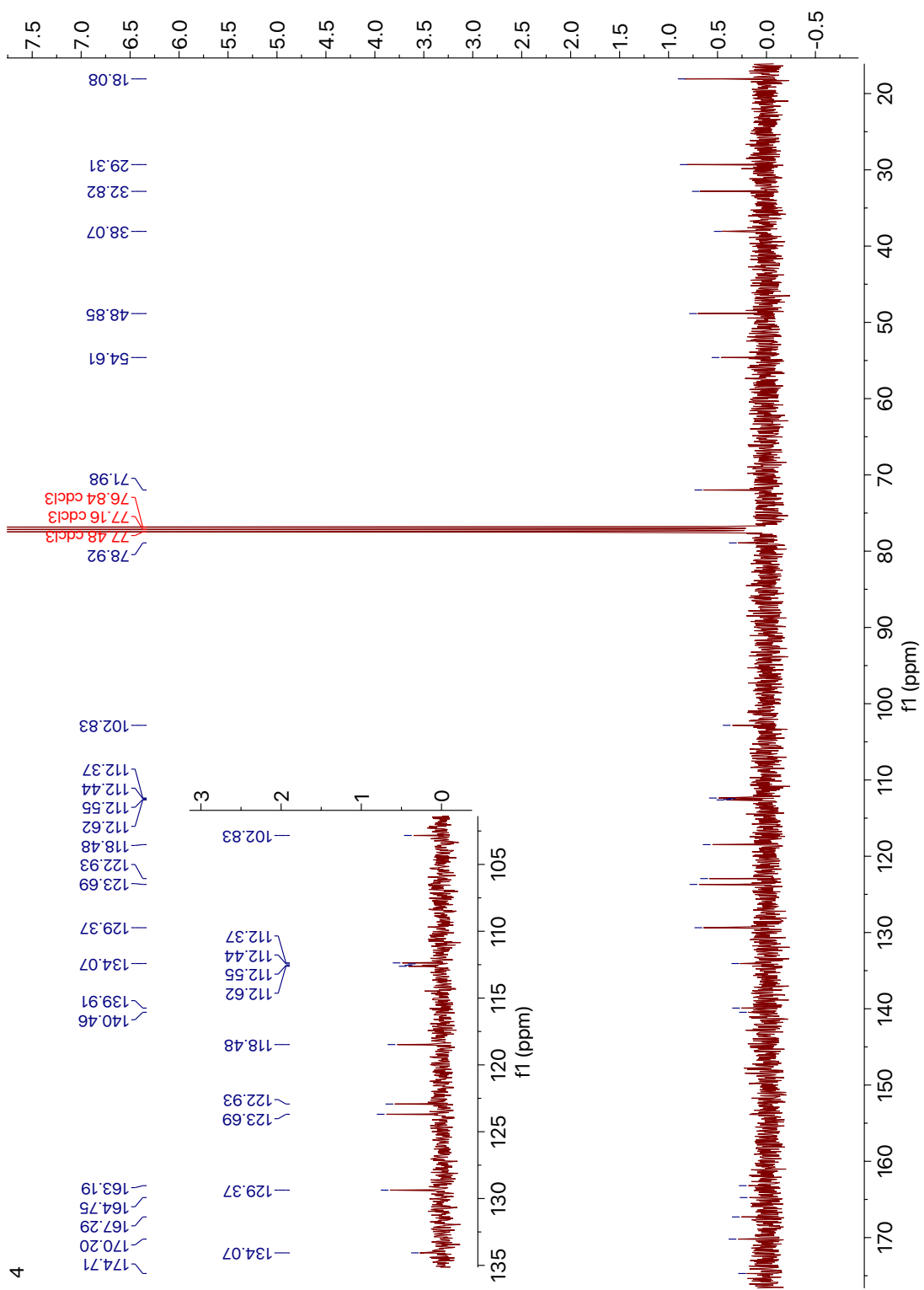
2



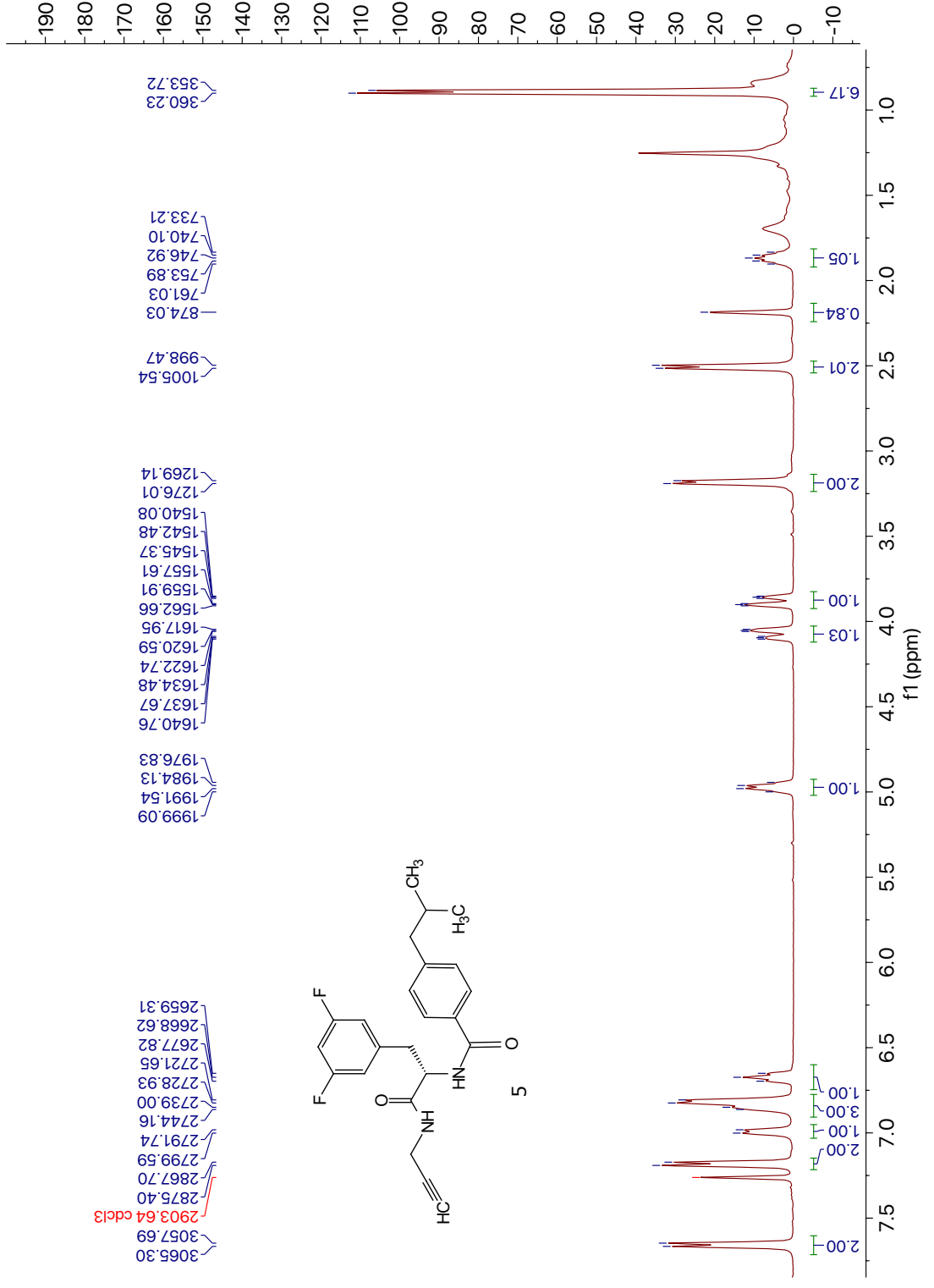


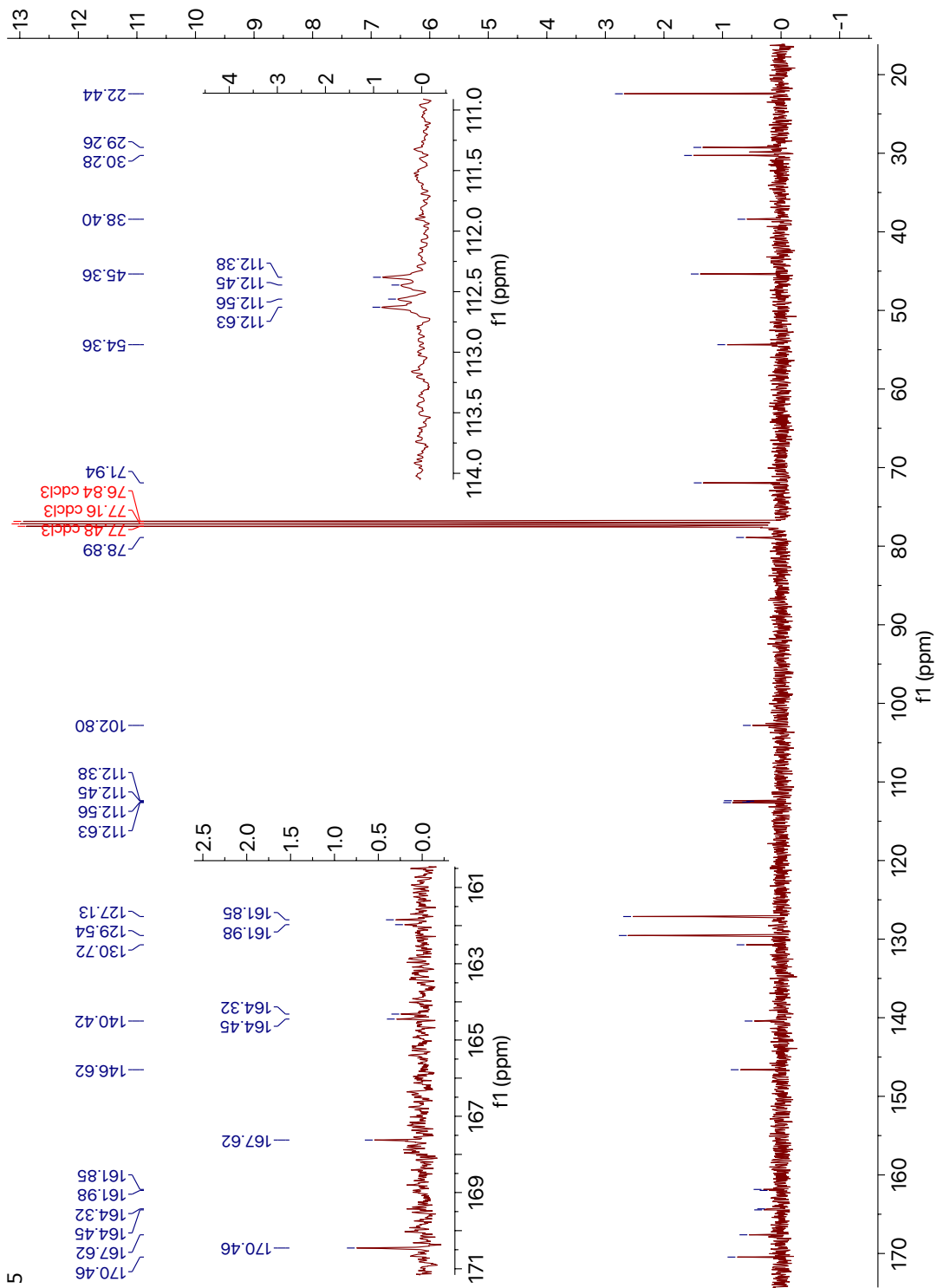
3



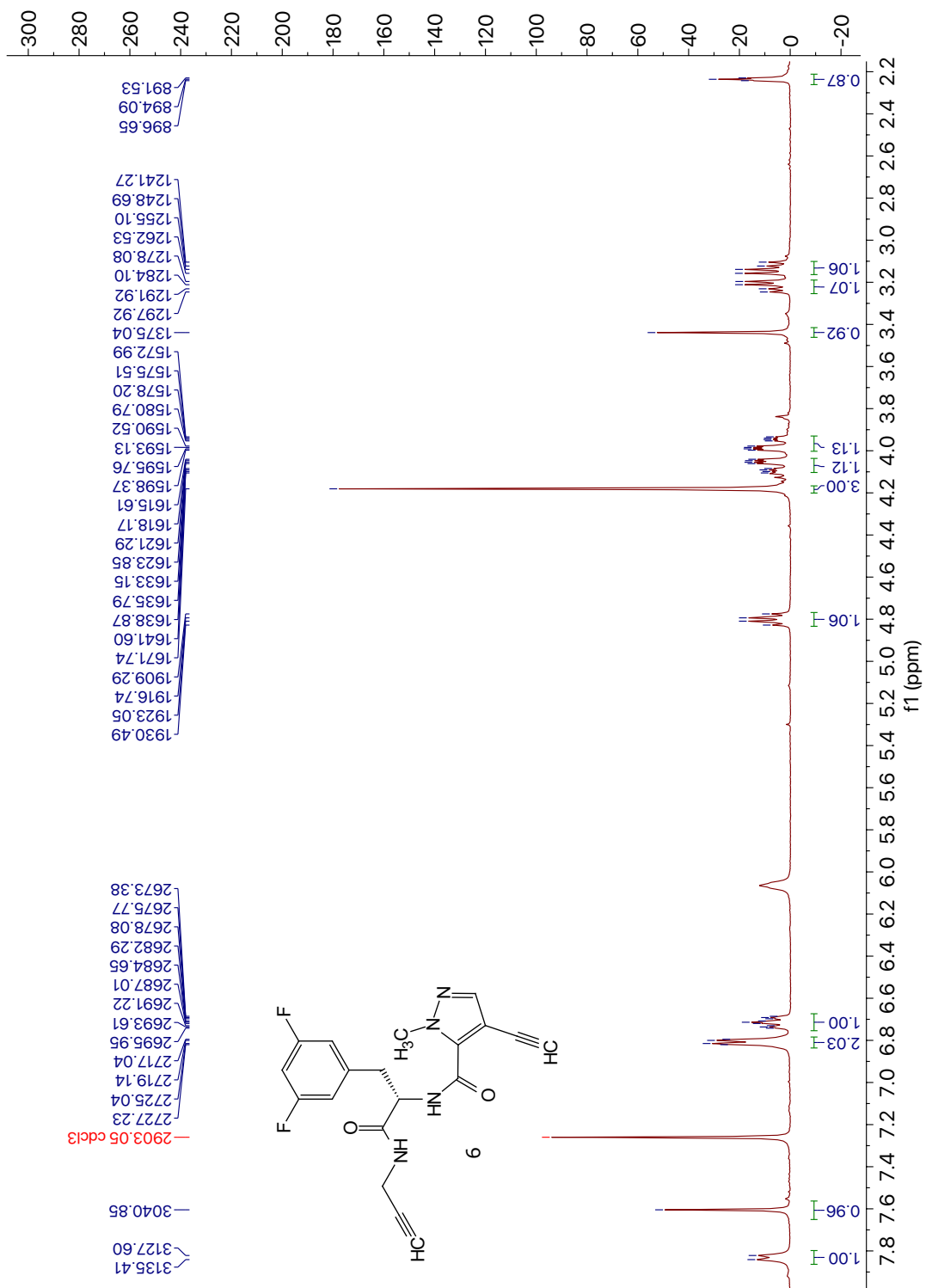


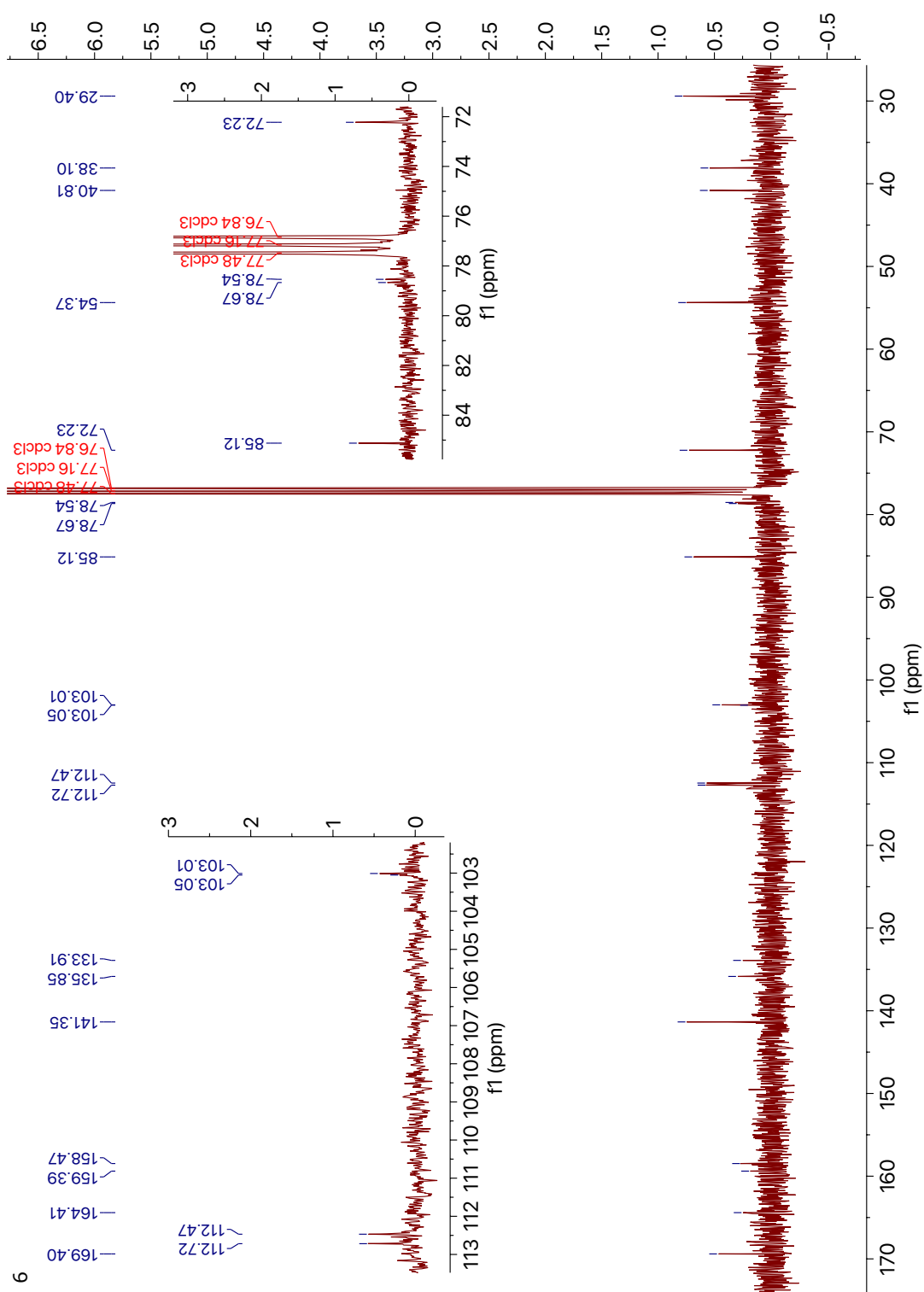
4



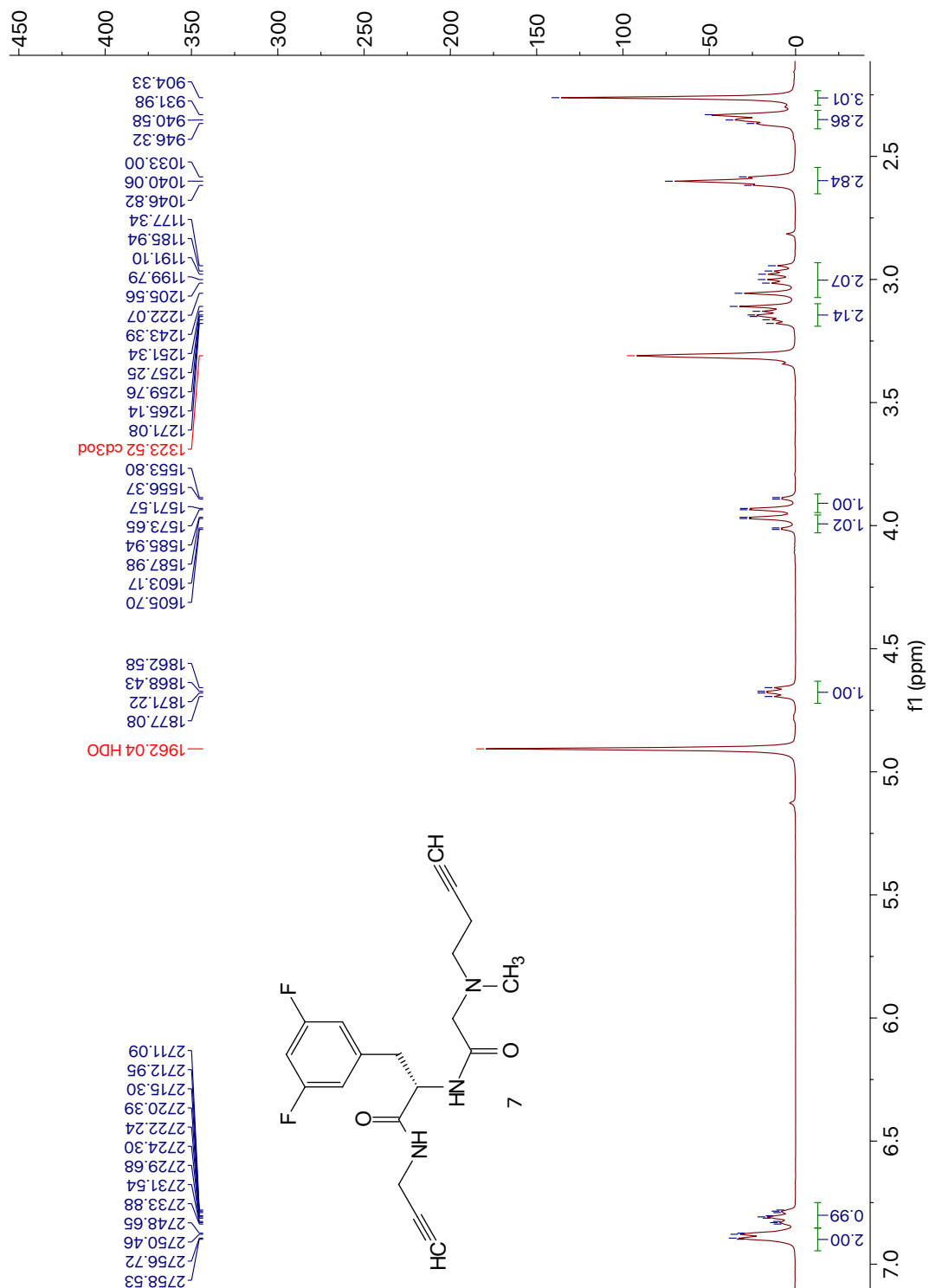


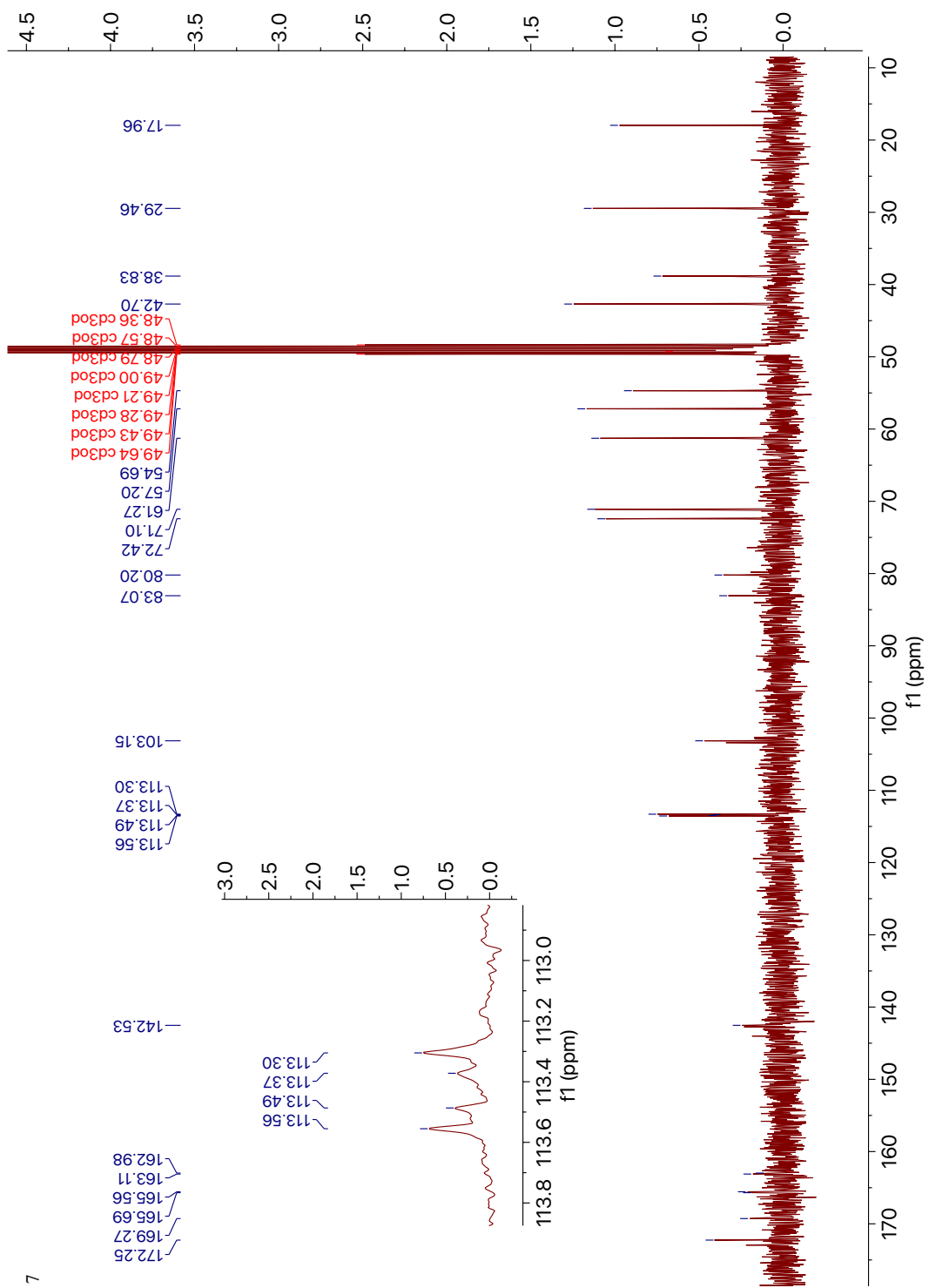
5



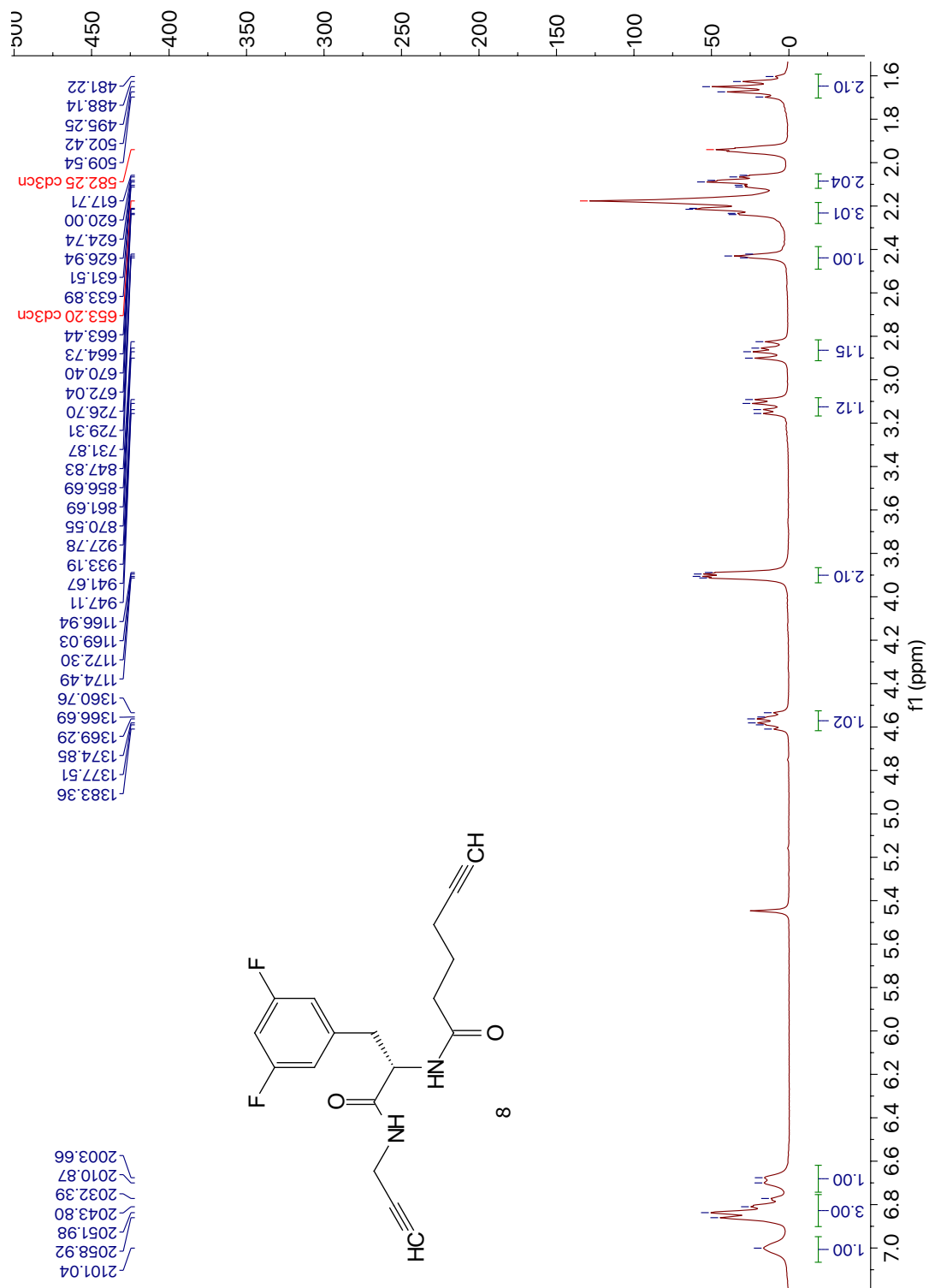


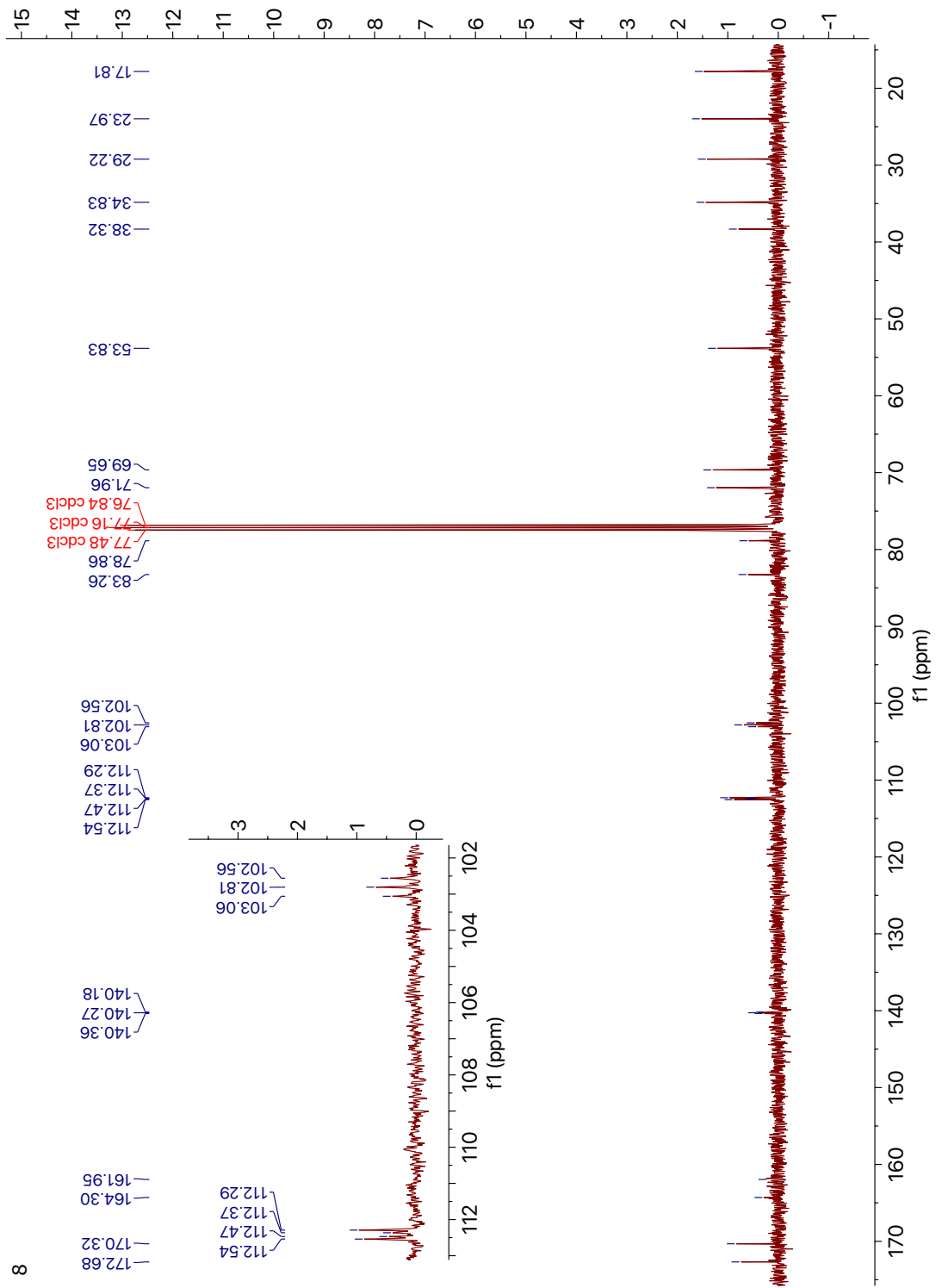
9



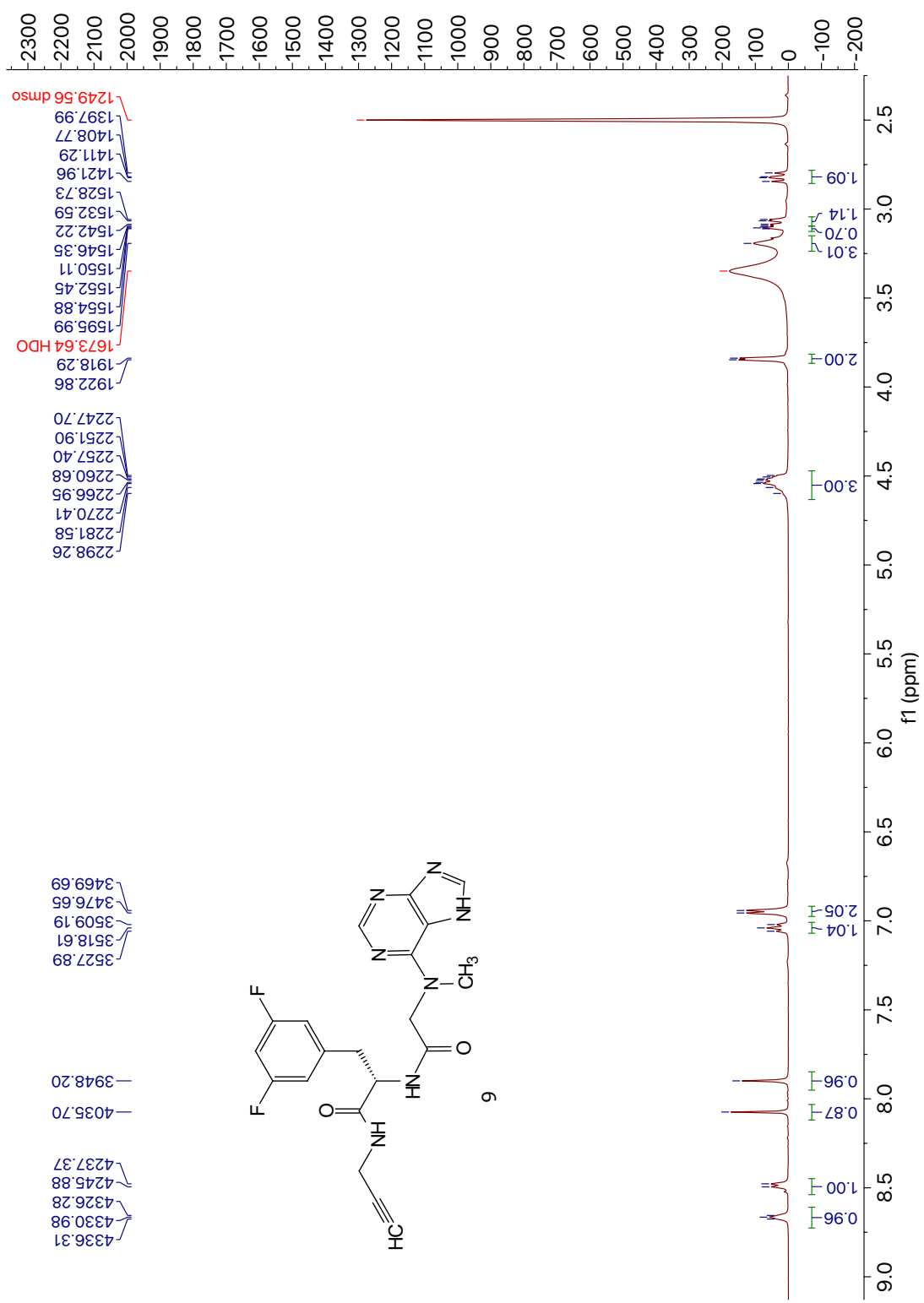


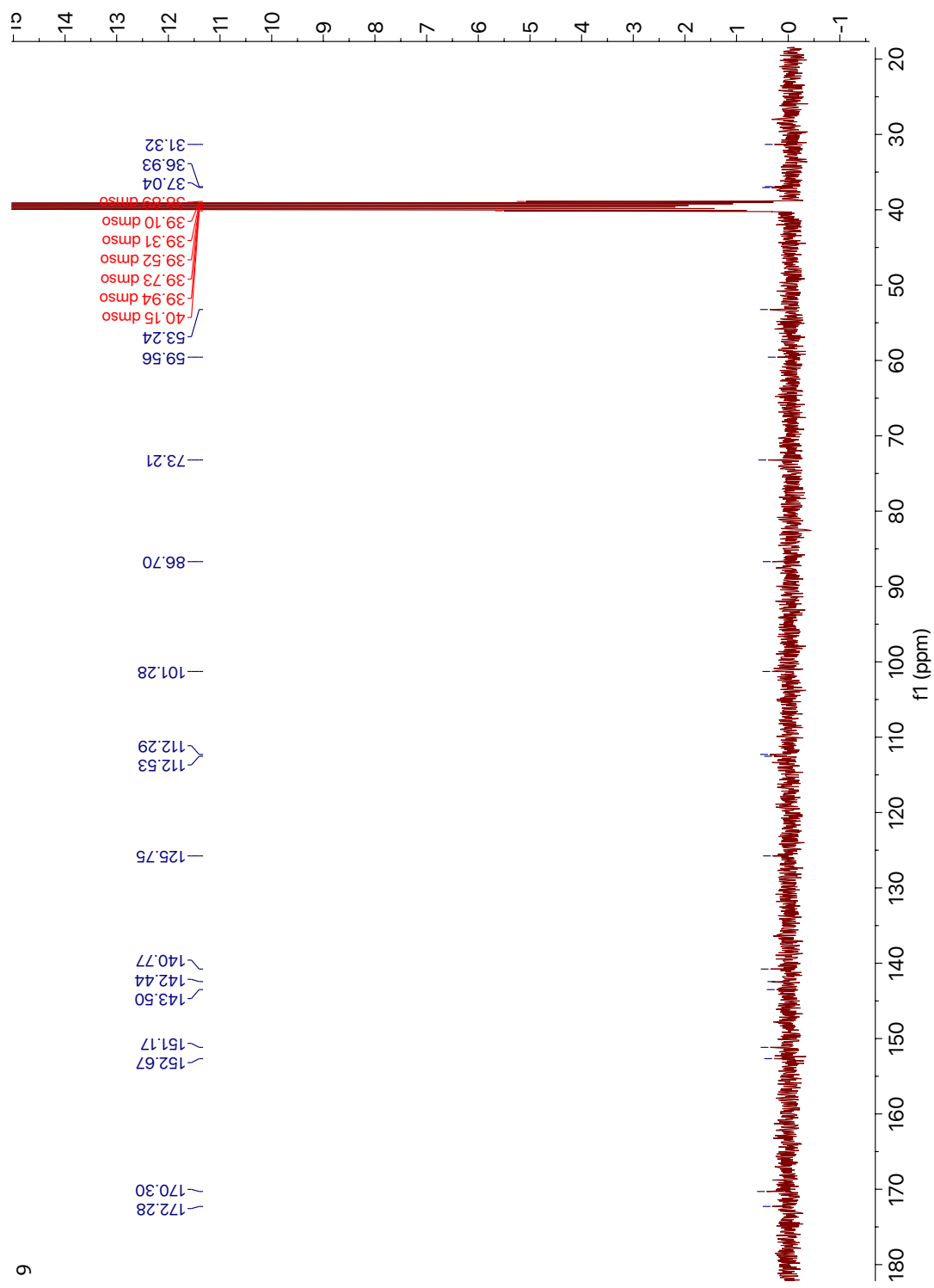
7

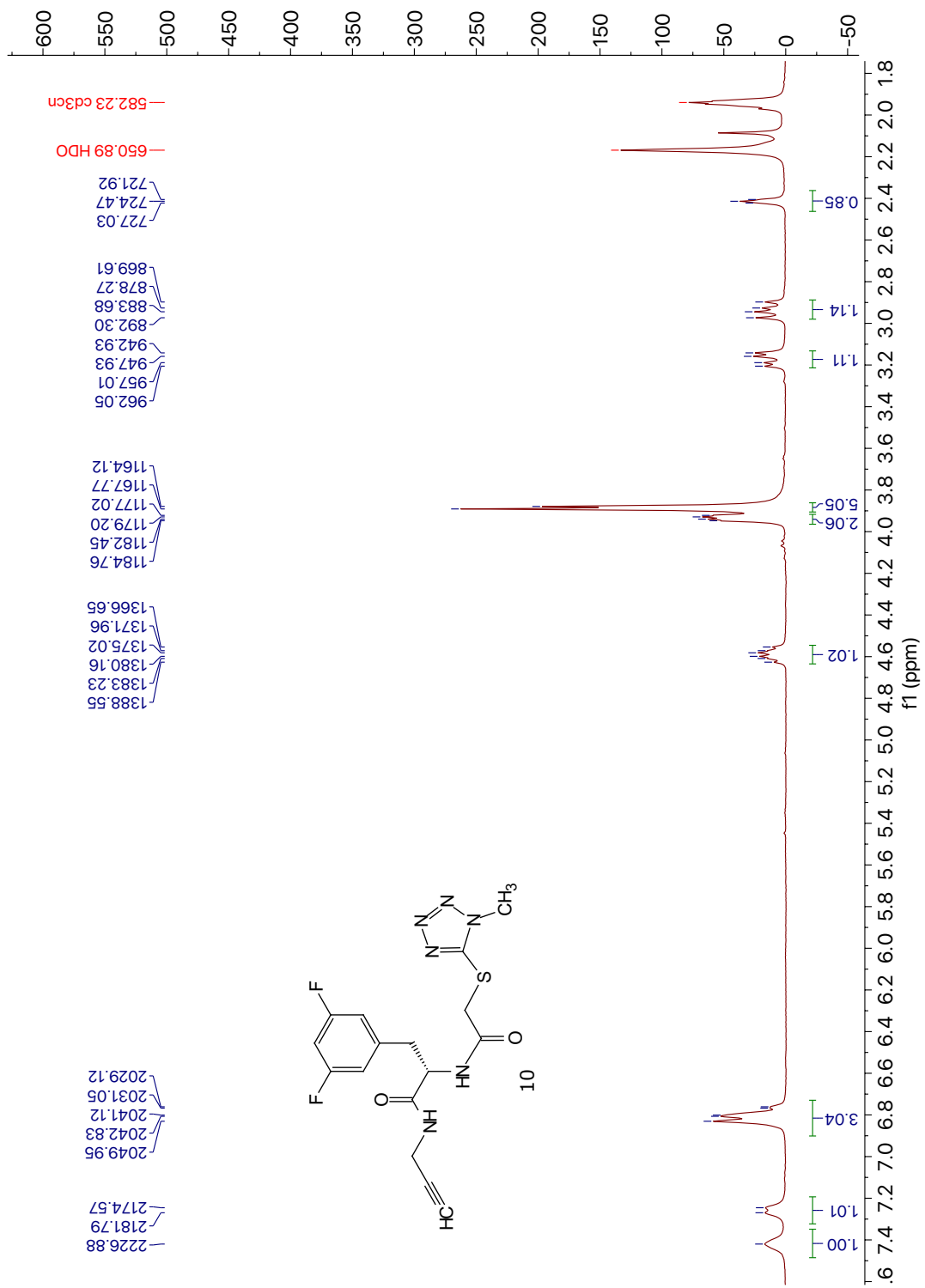


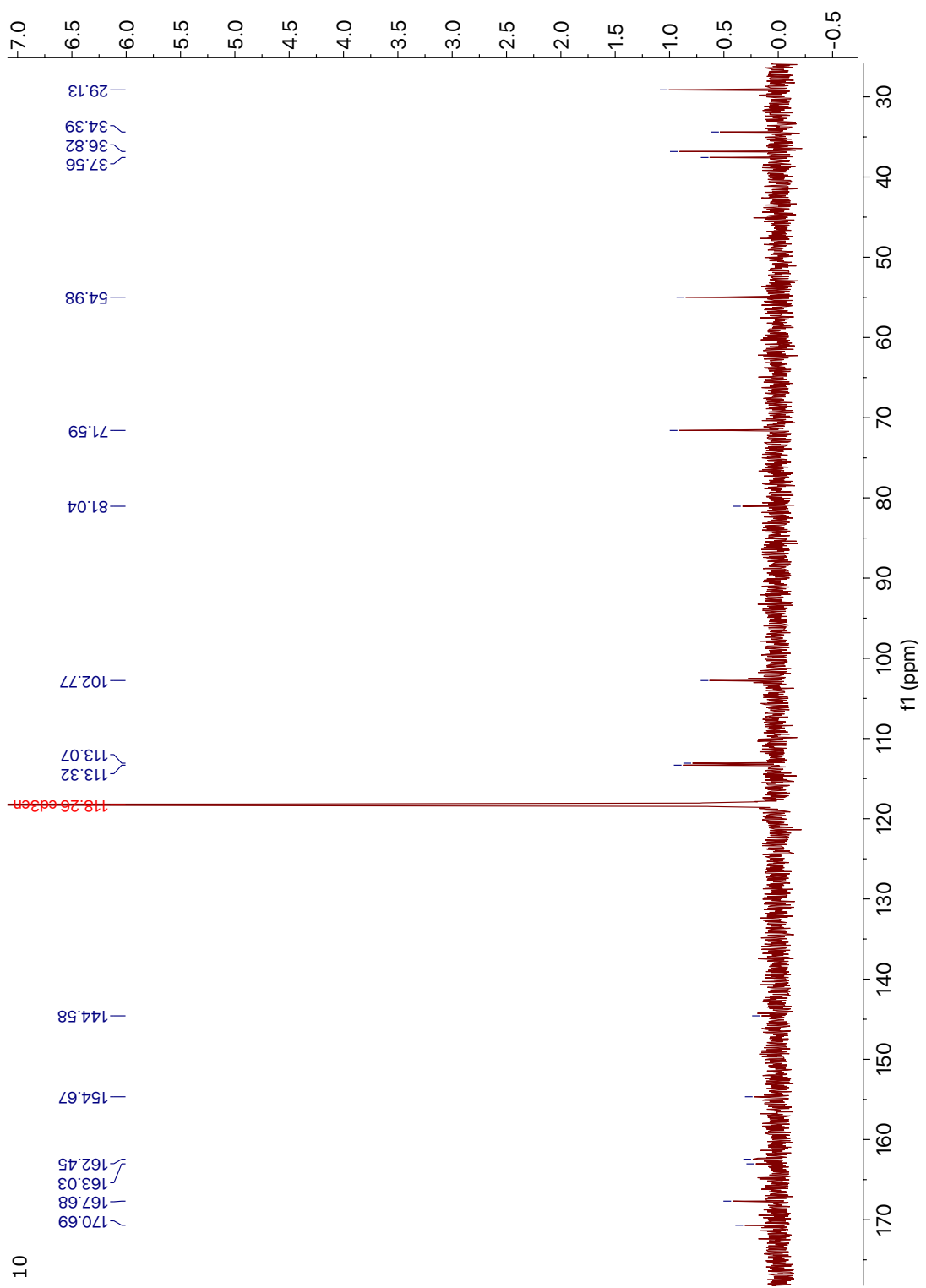


8

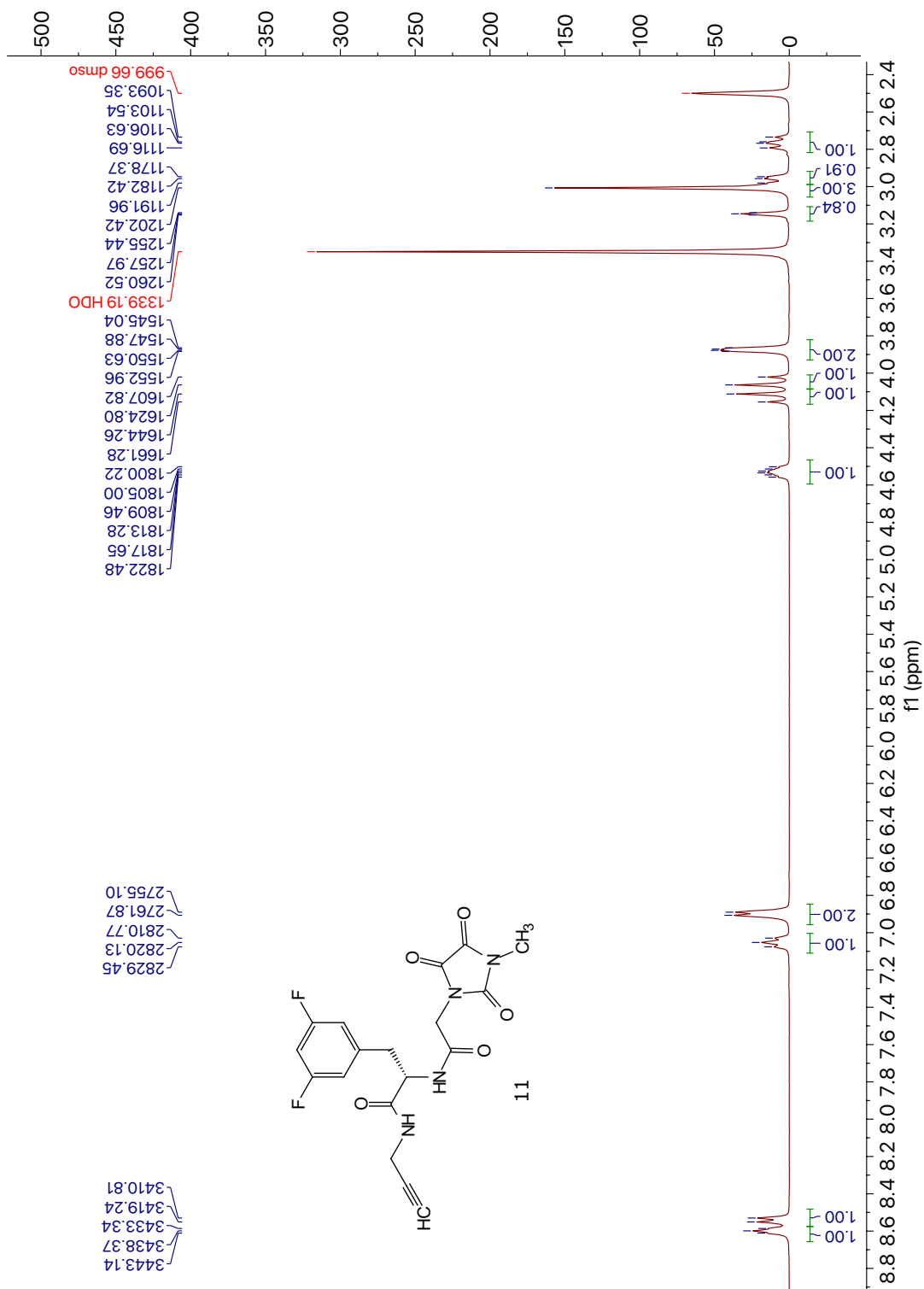


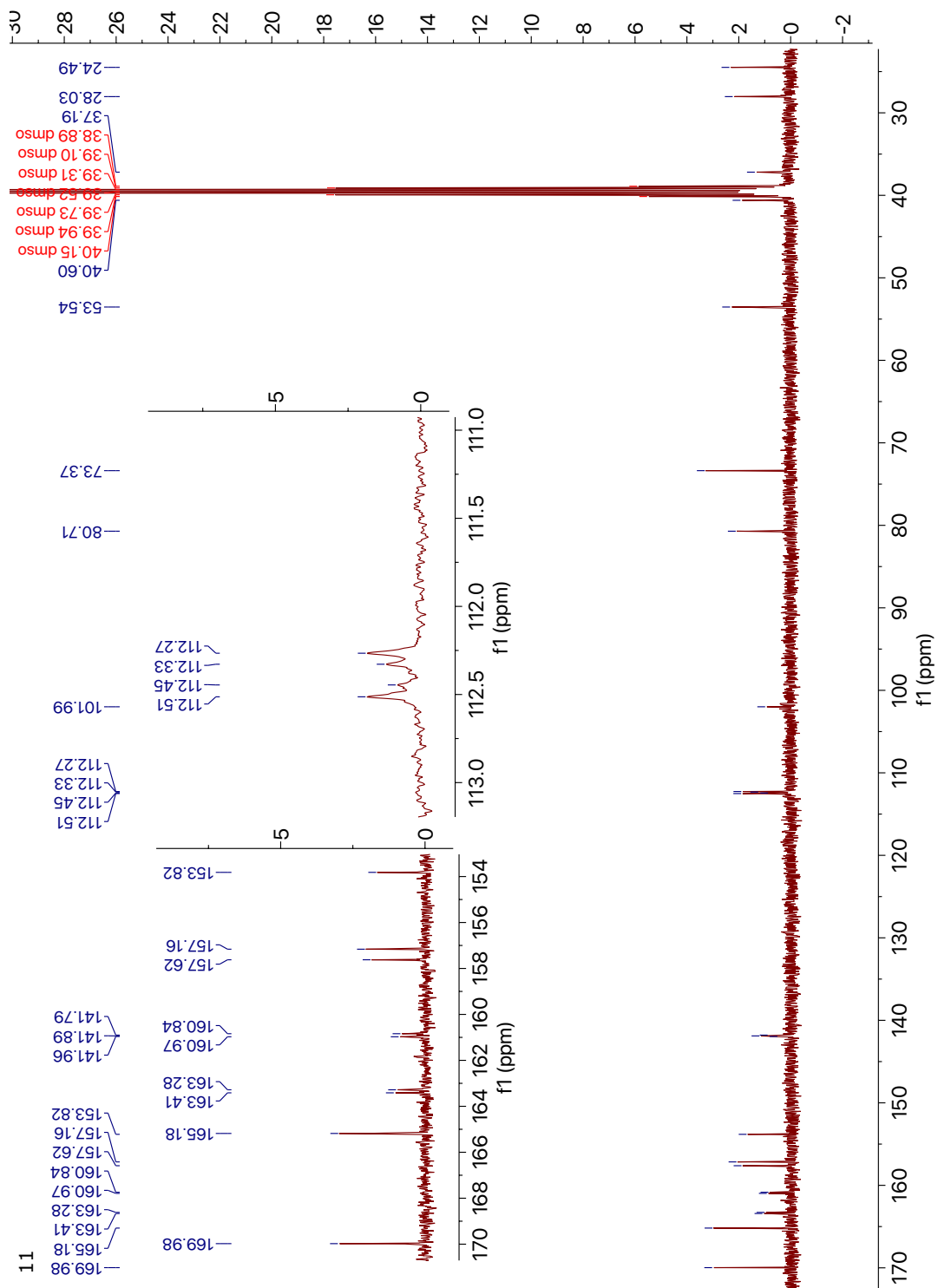


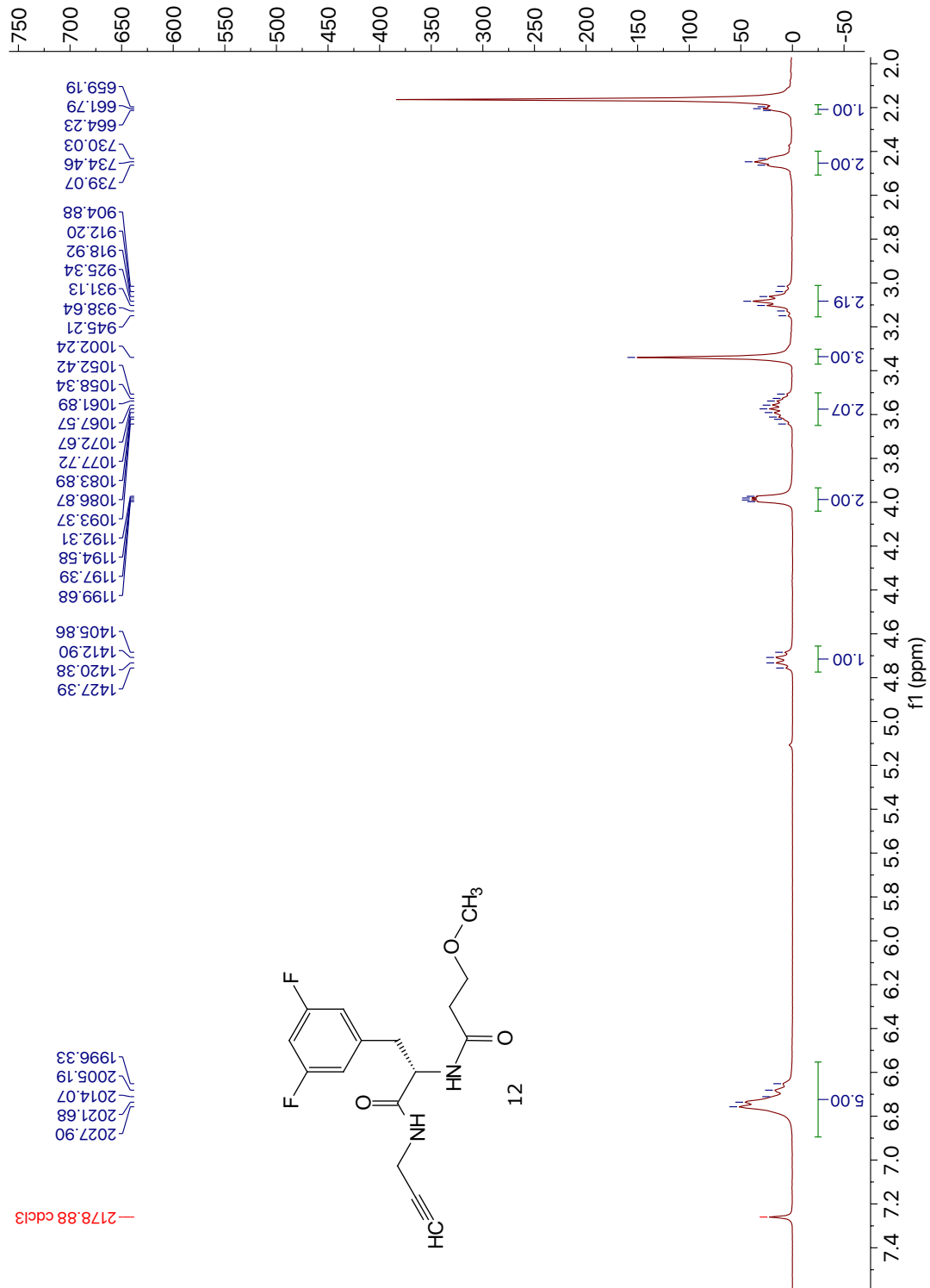


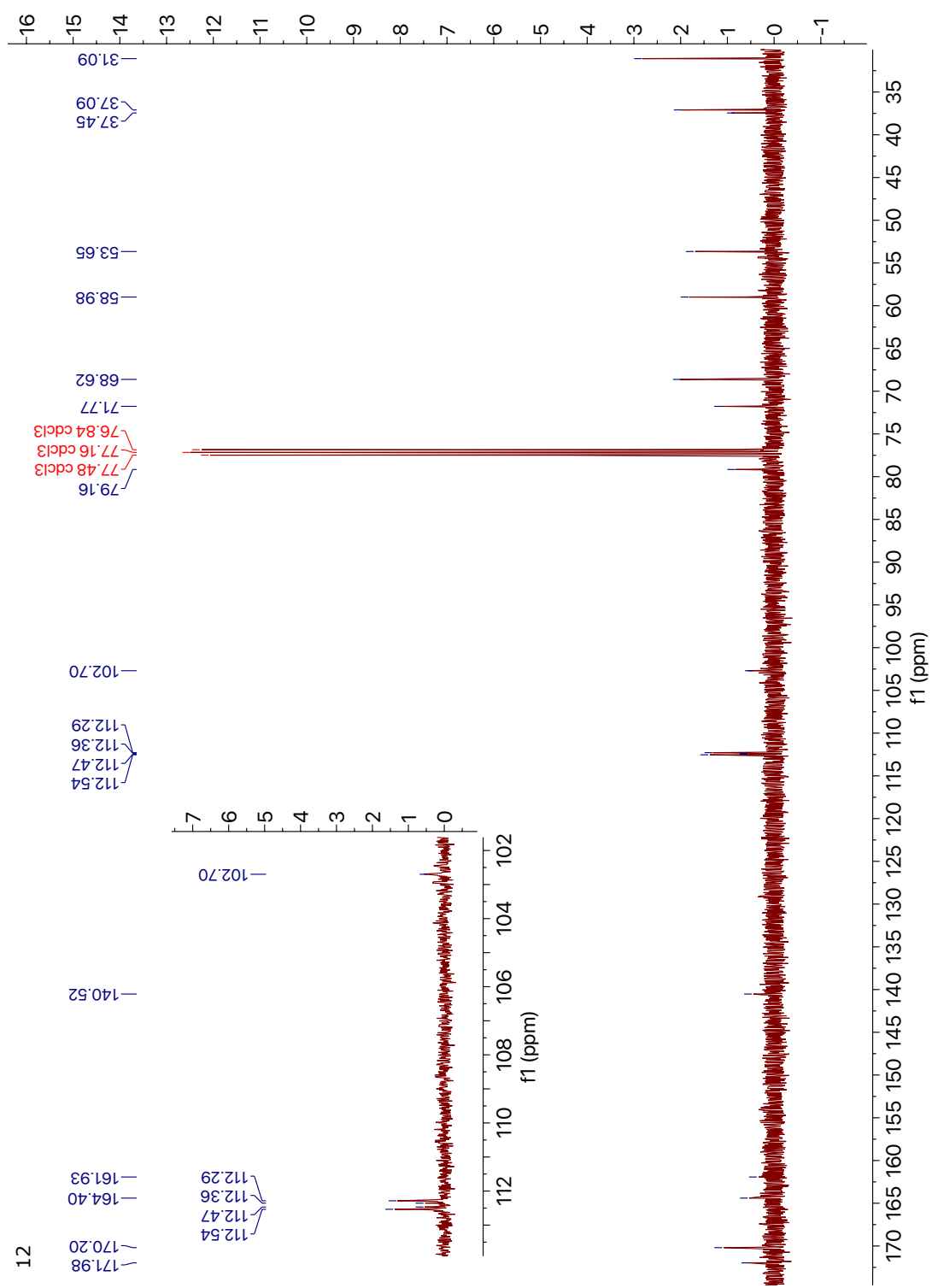


10

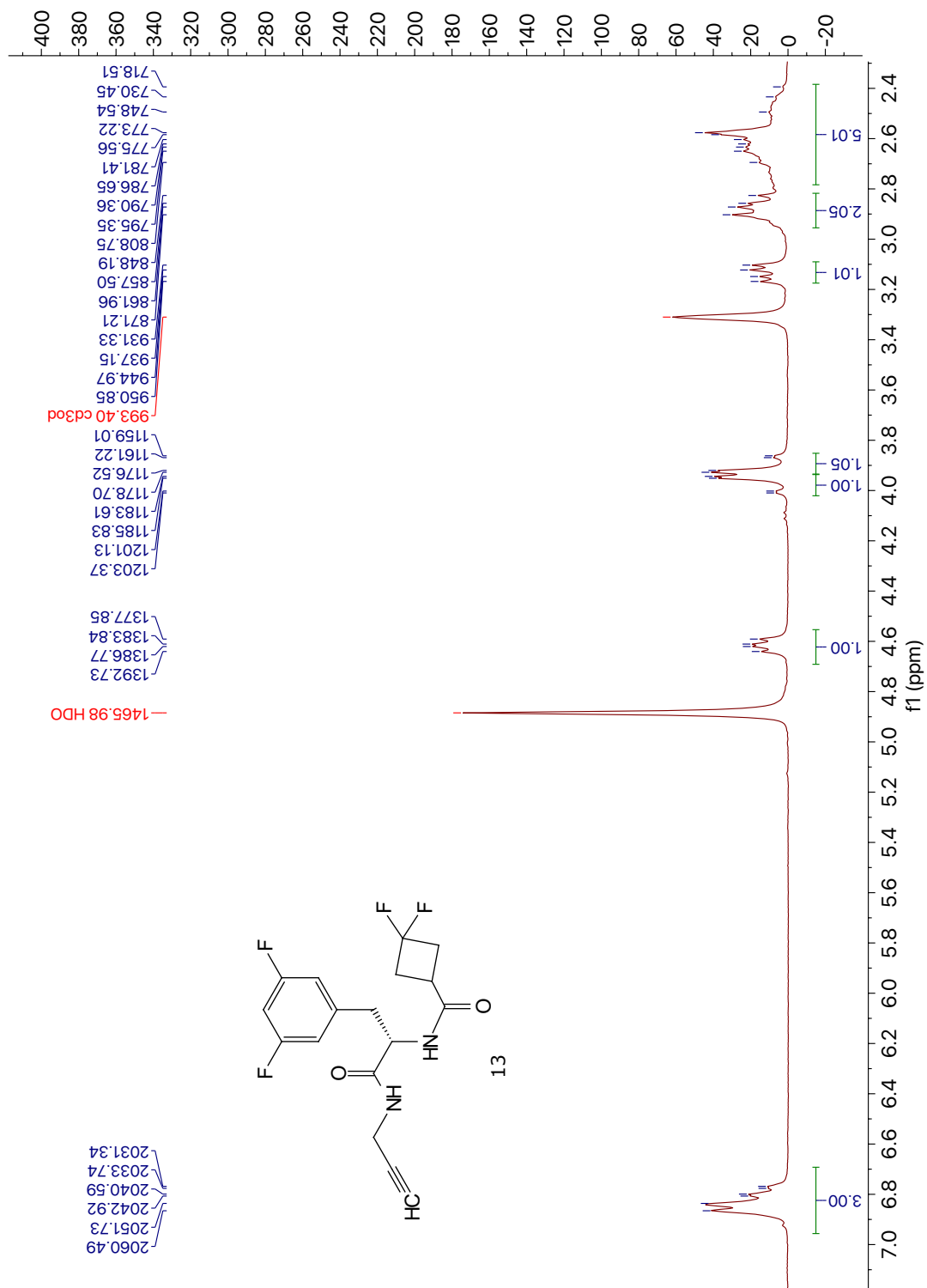


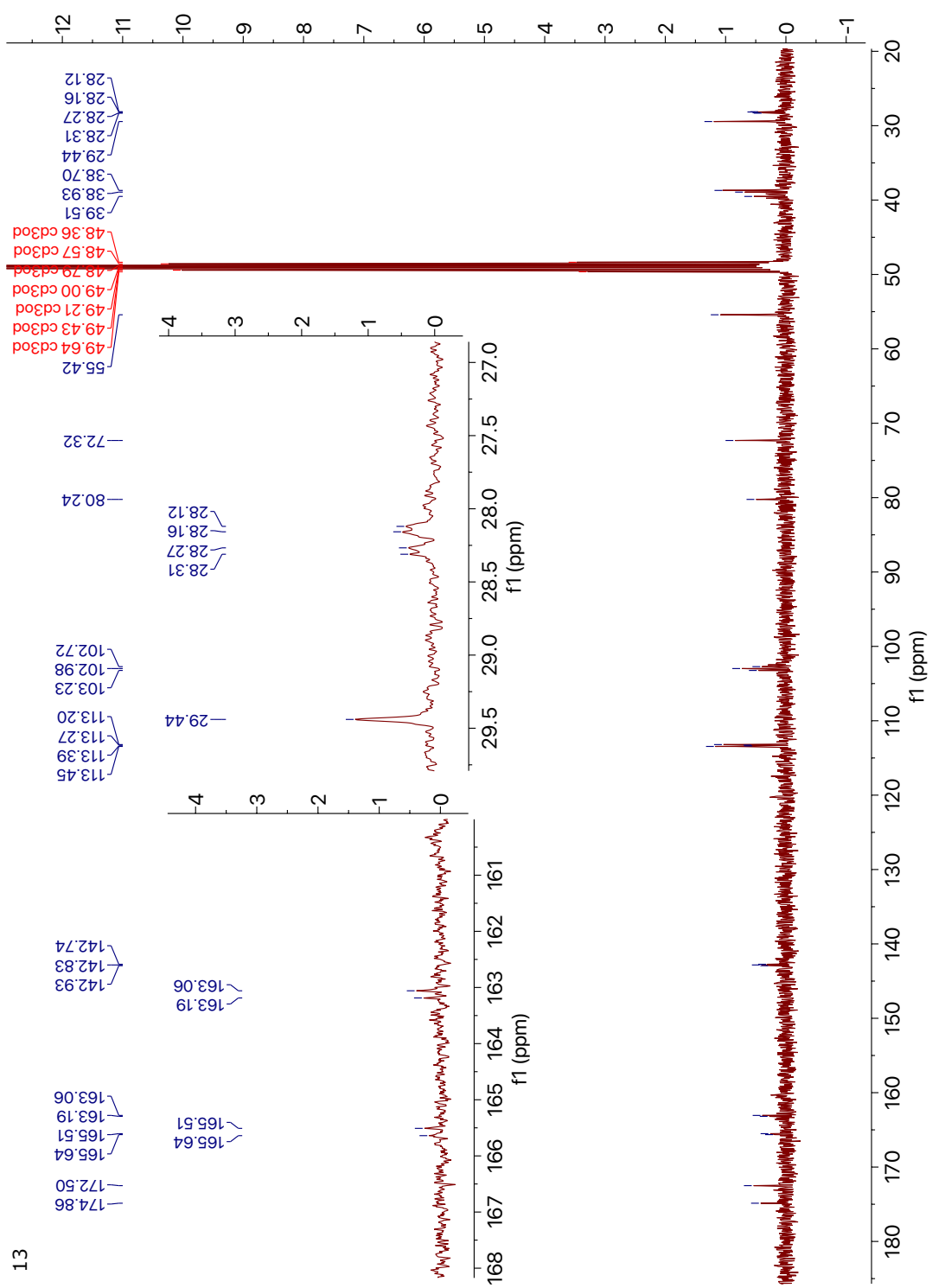




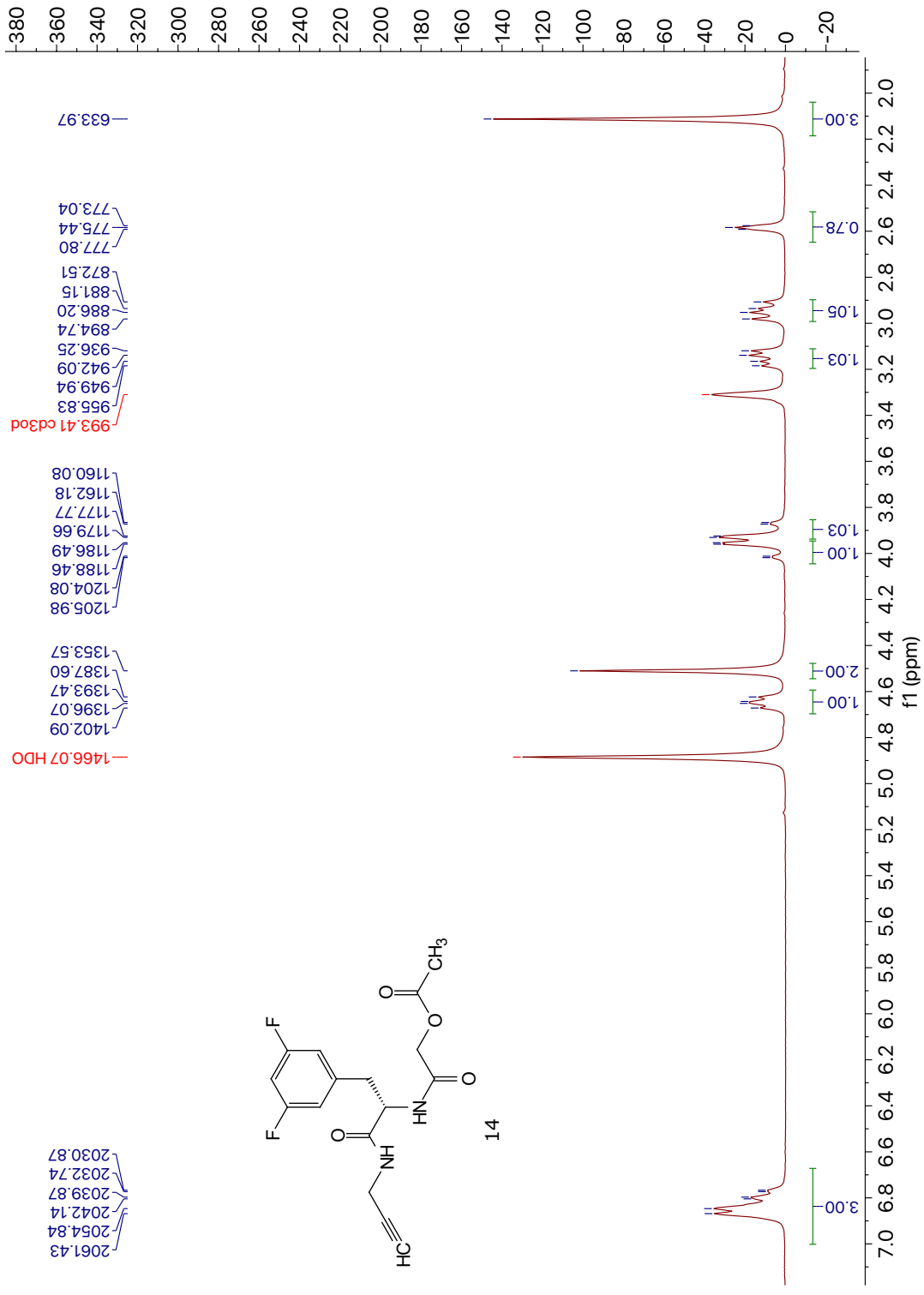


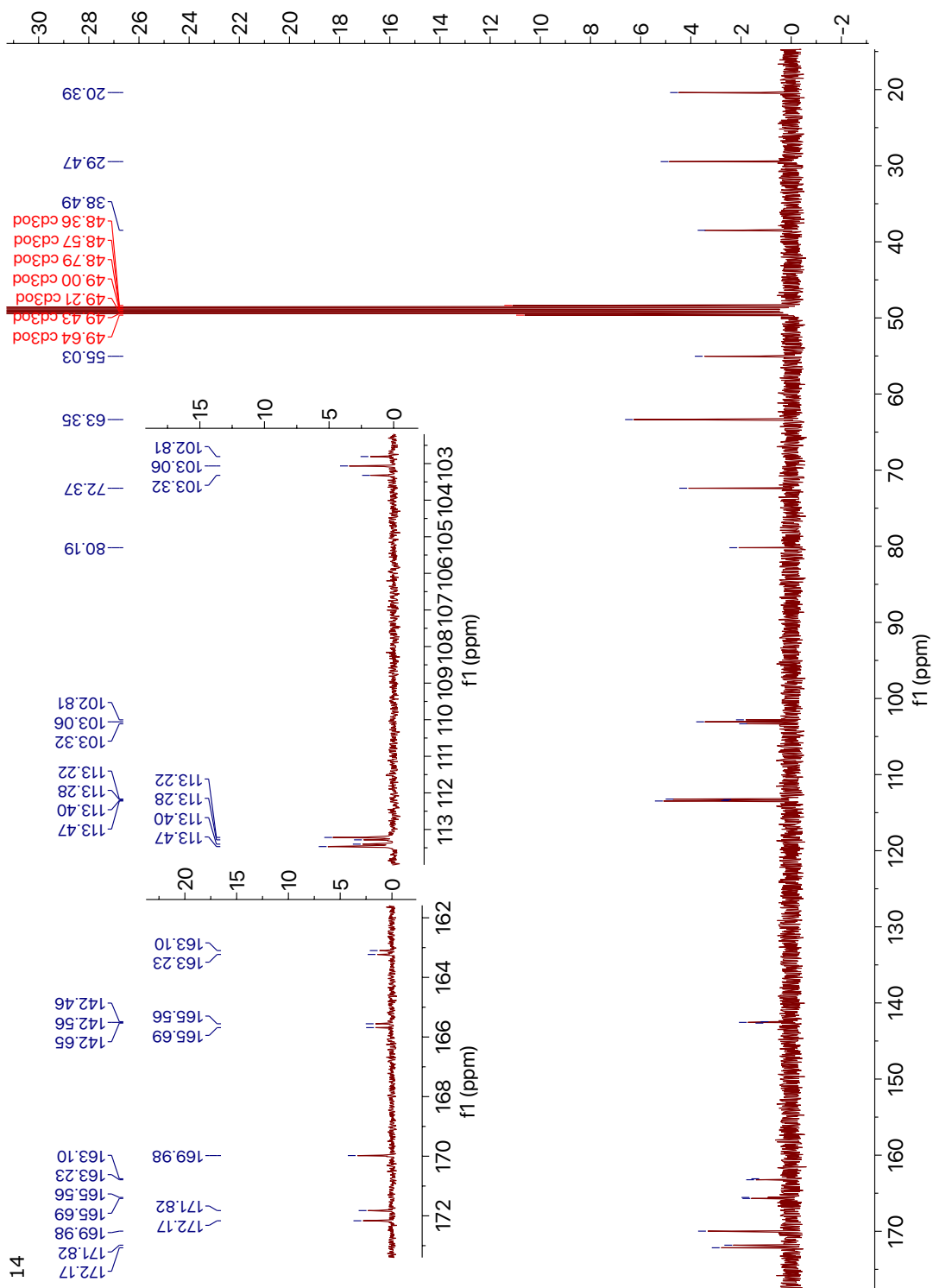
12



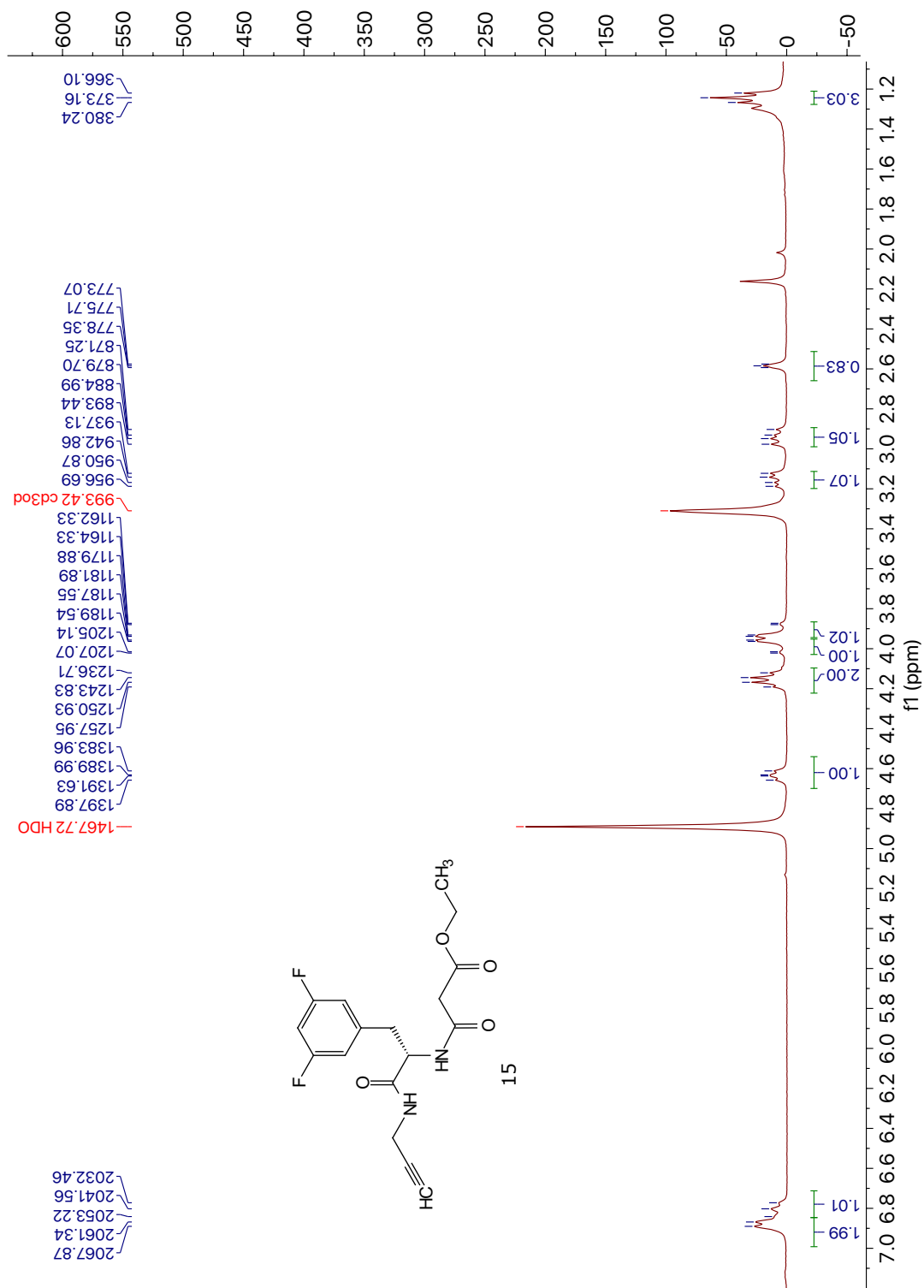


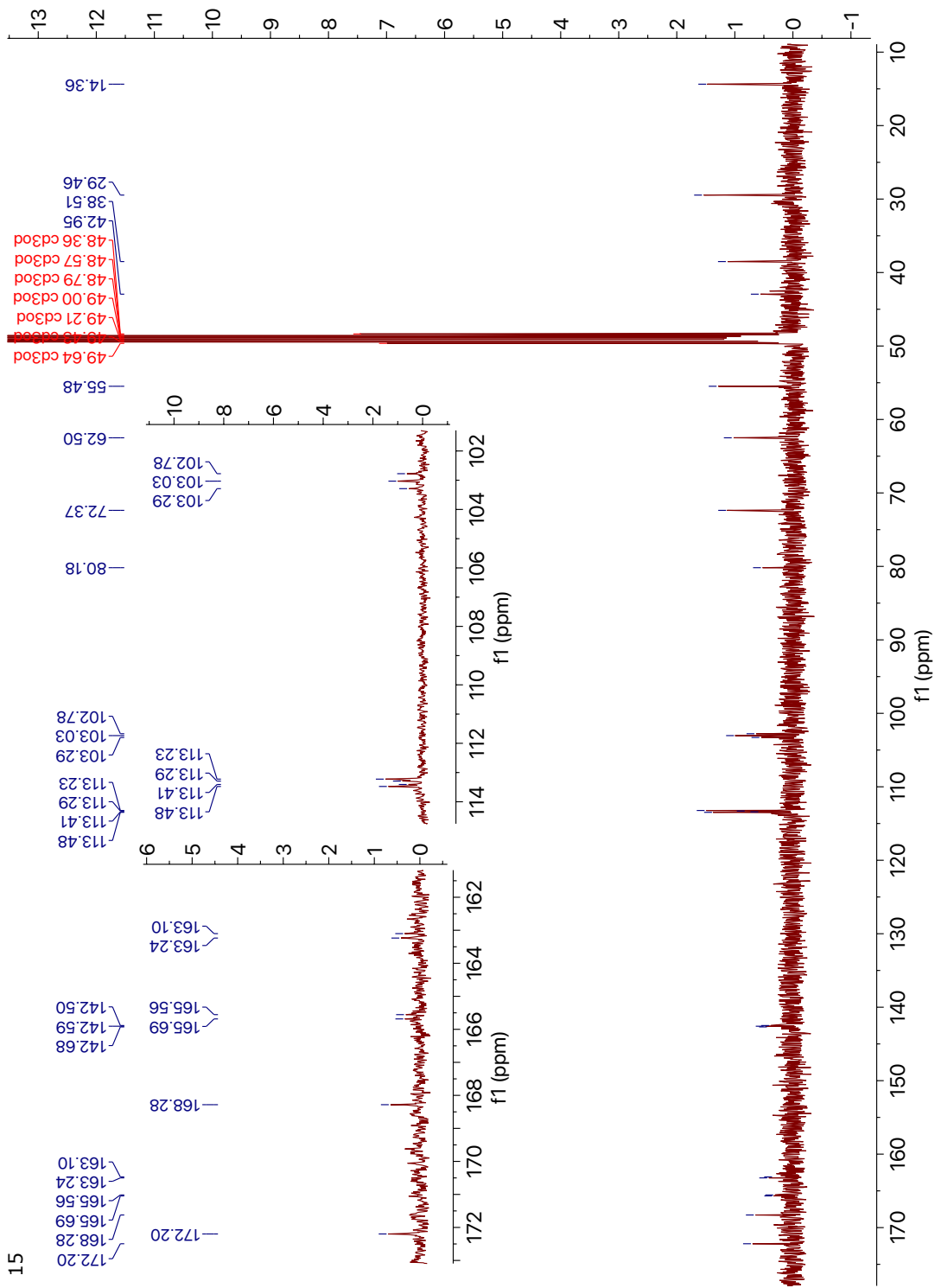
13



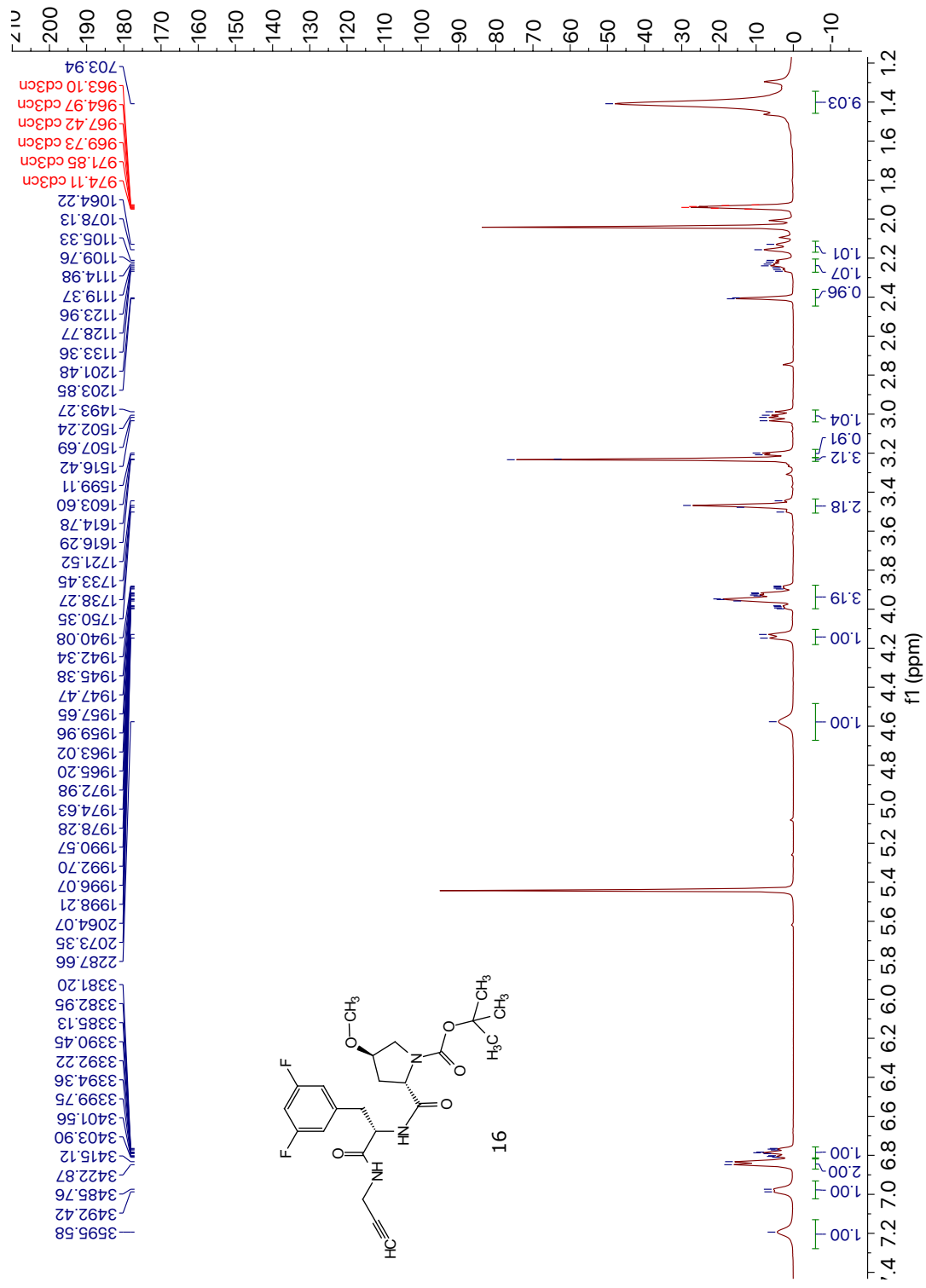


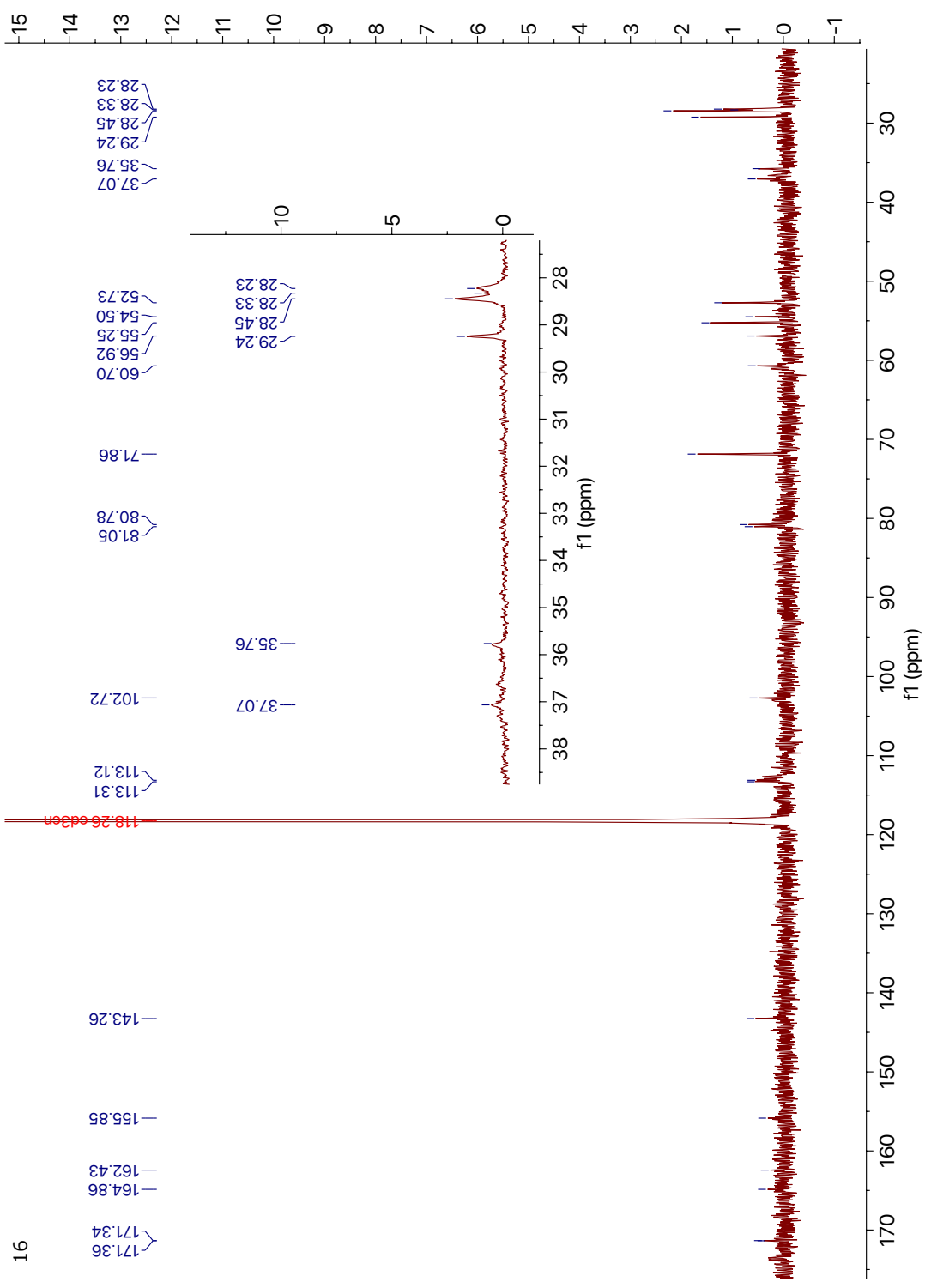
14



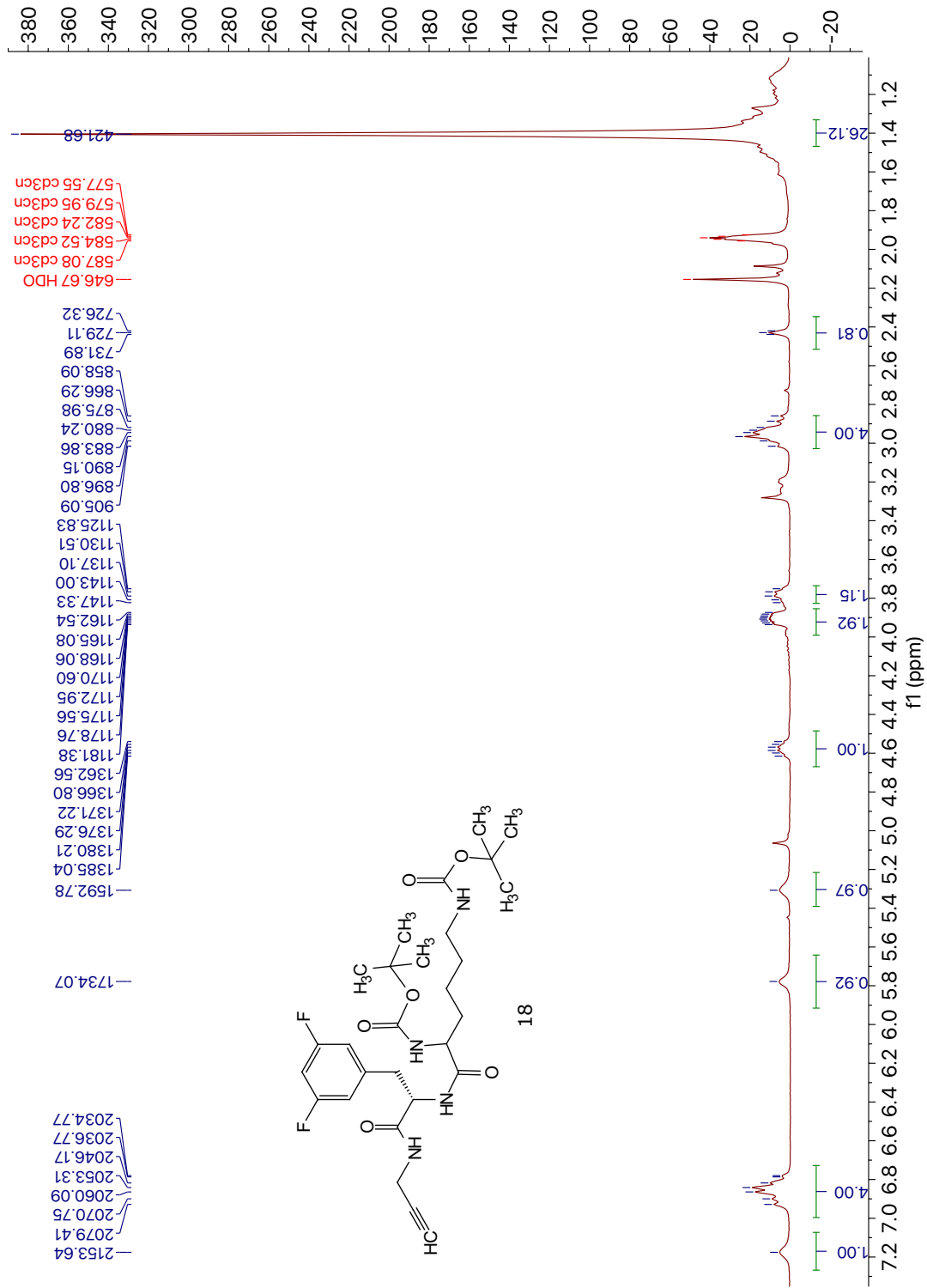


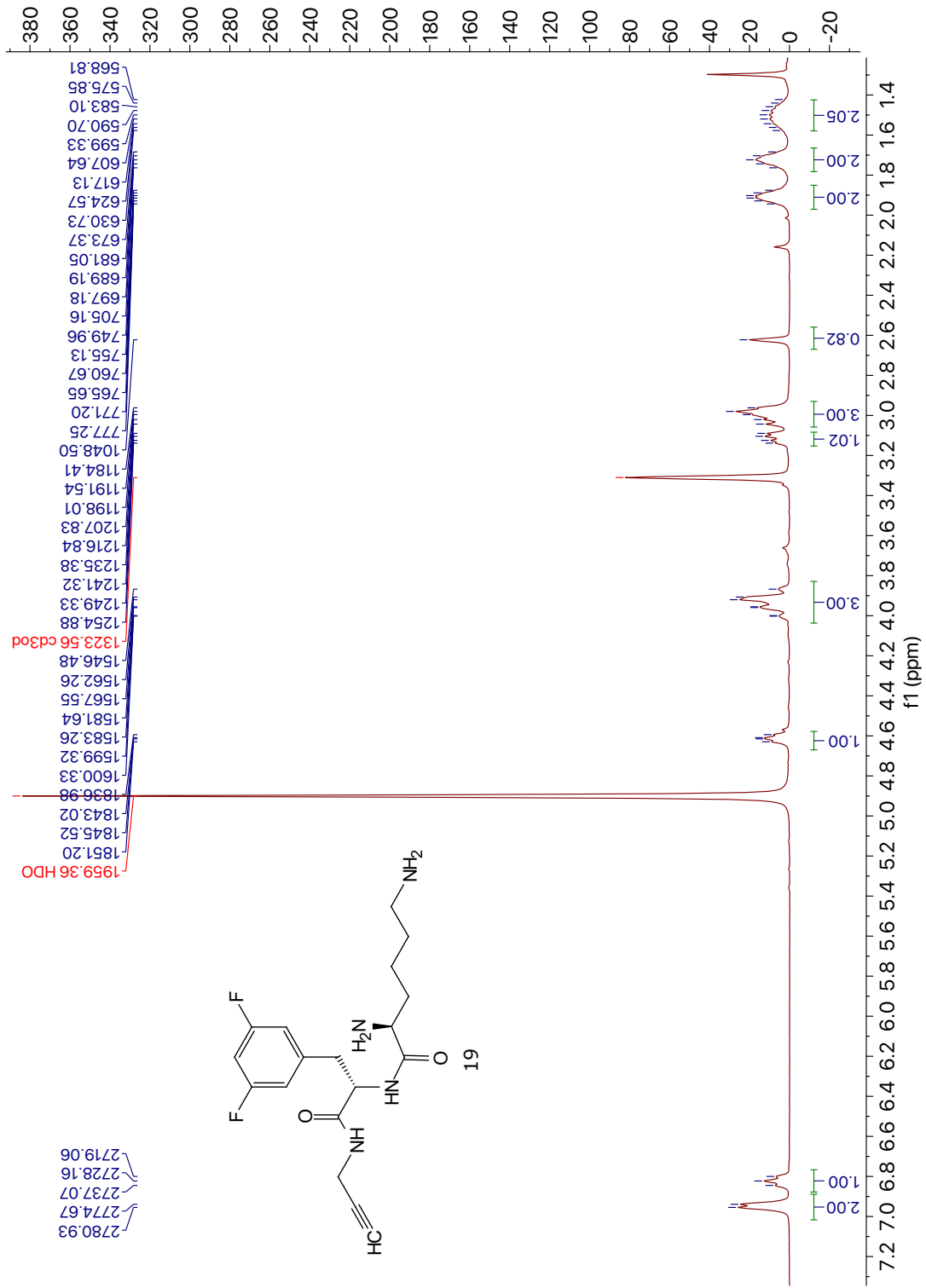
15

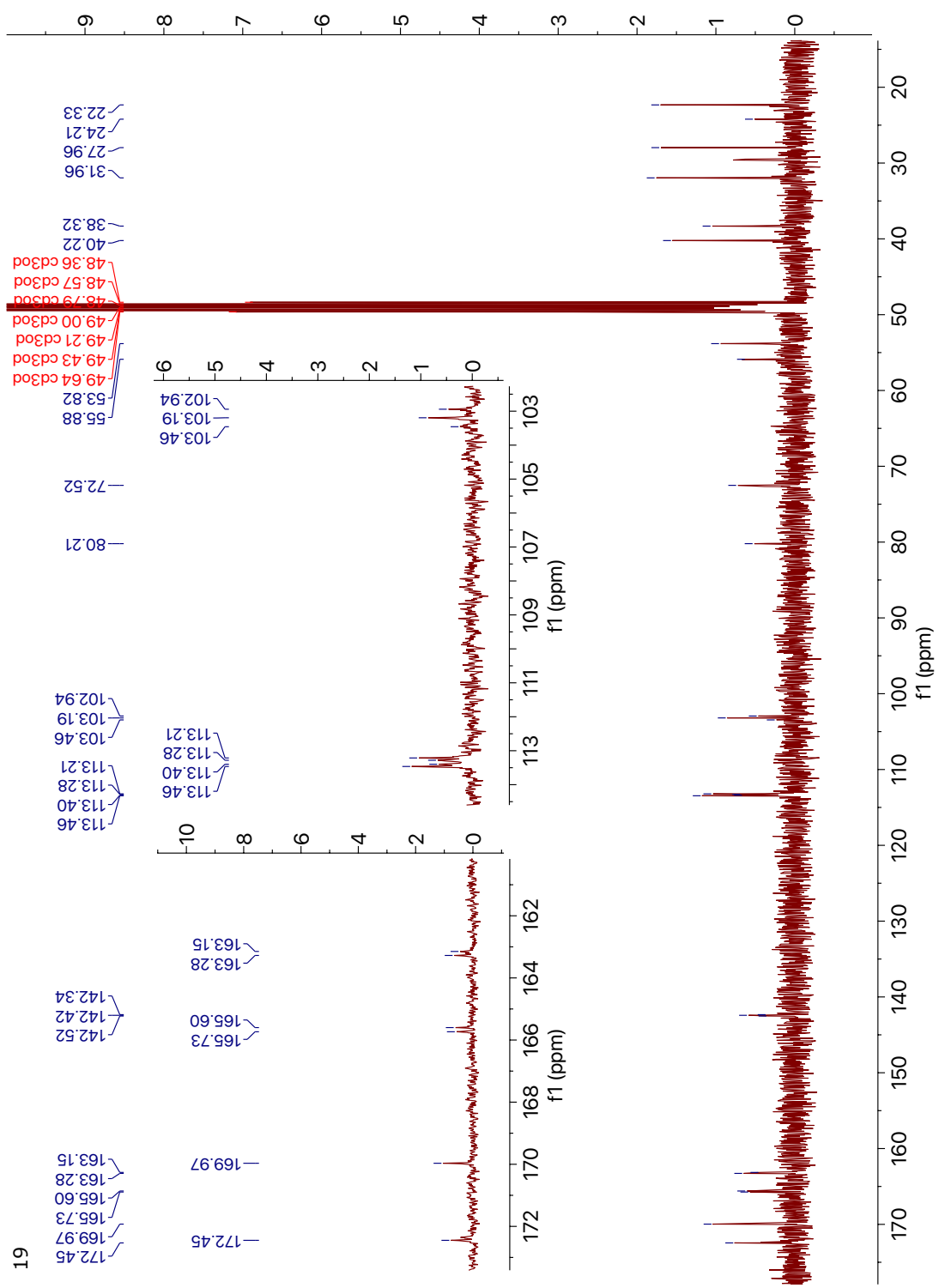




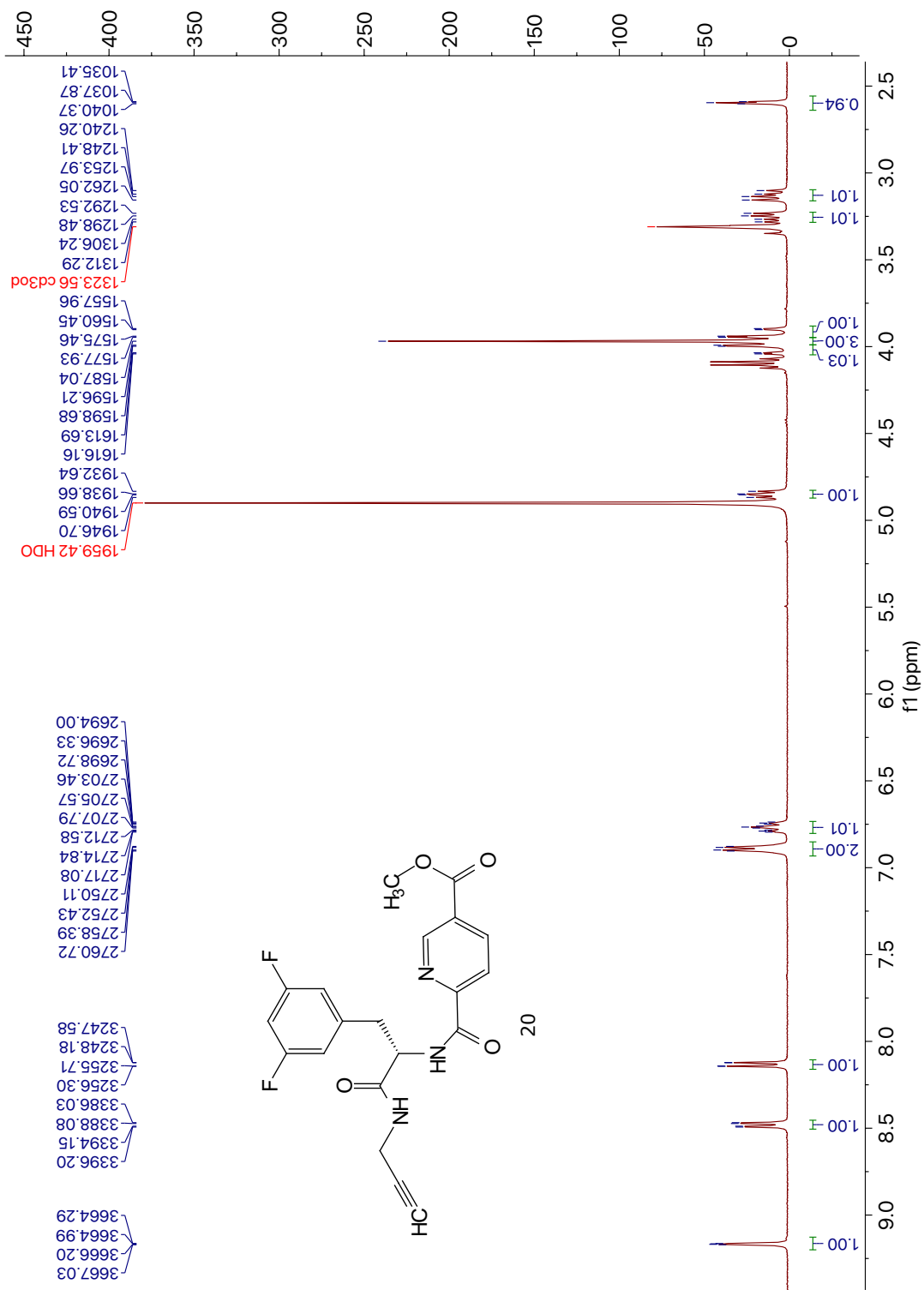
16

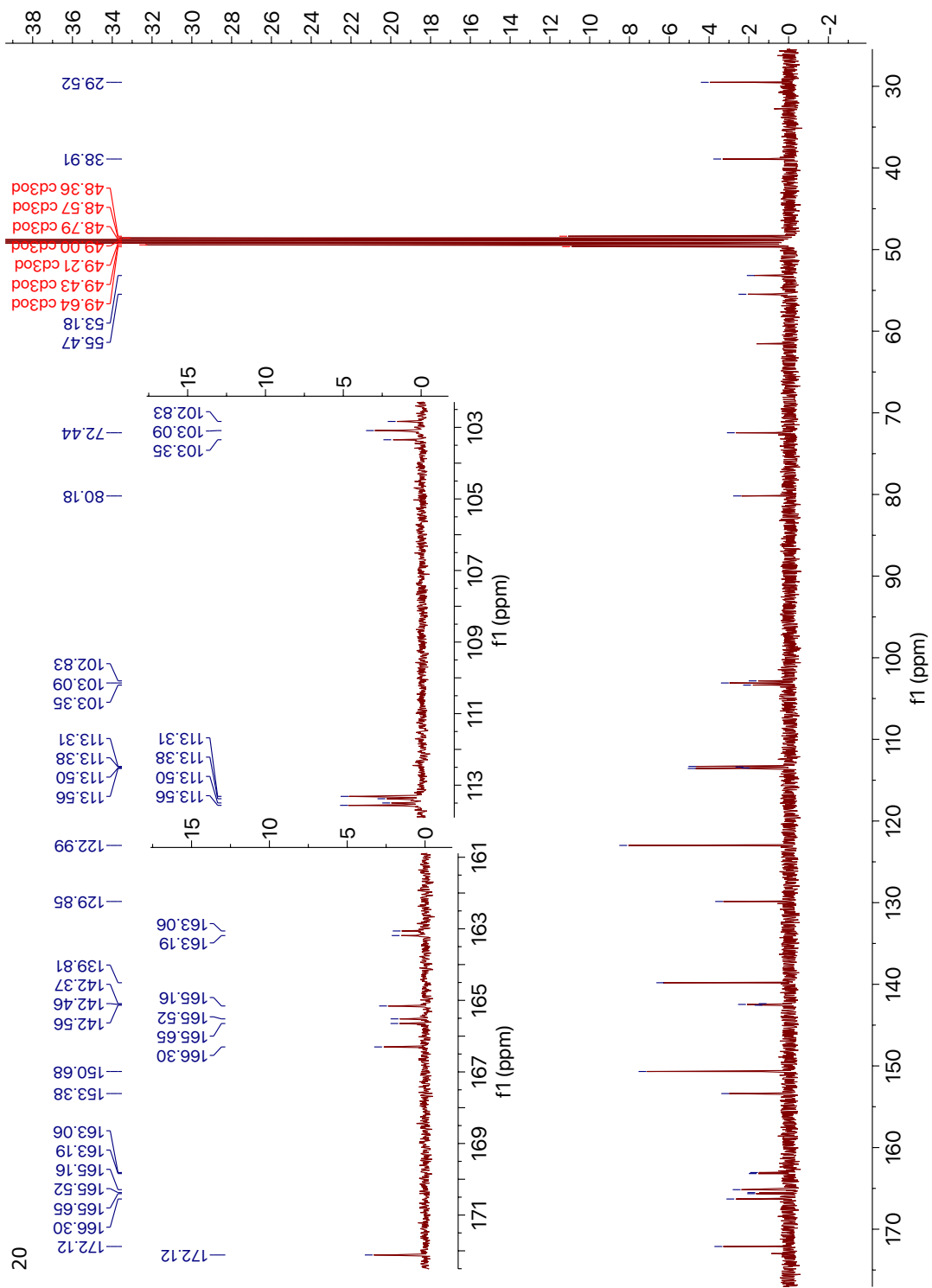




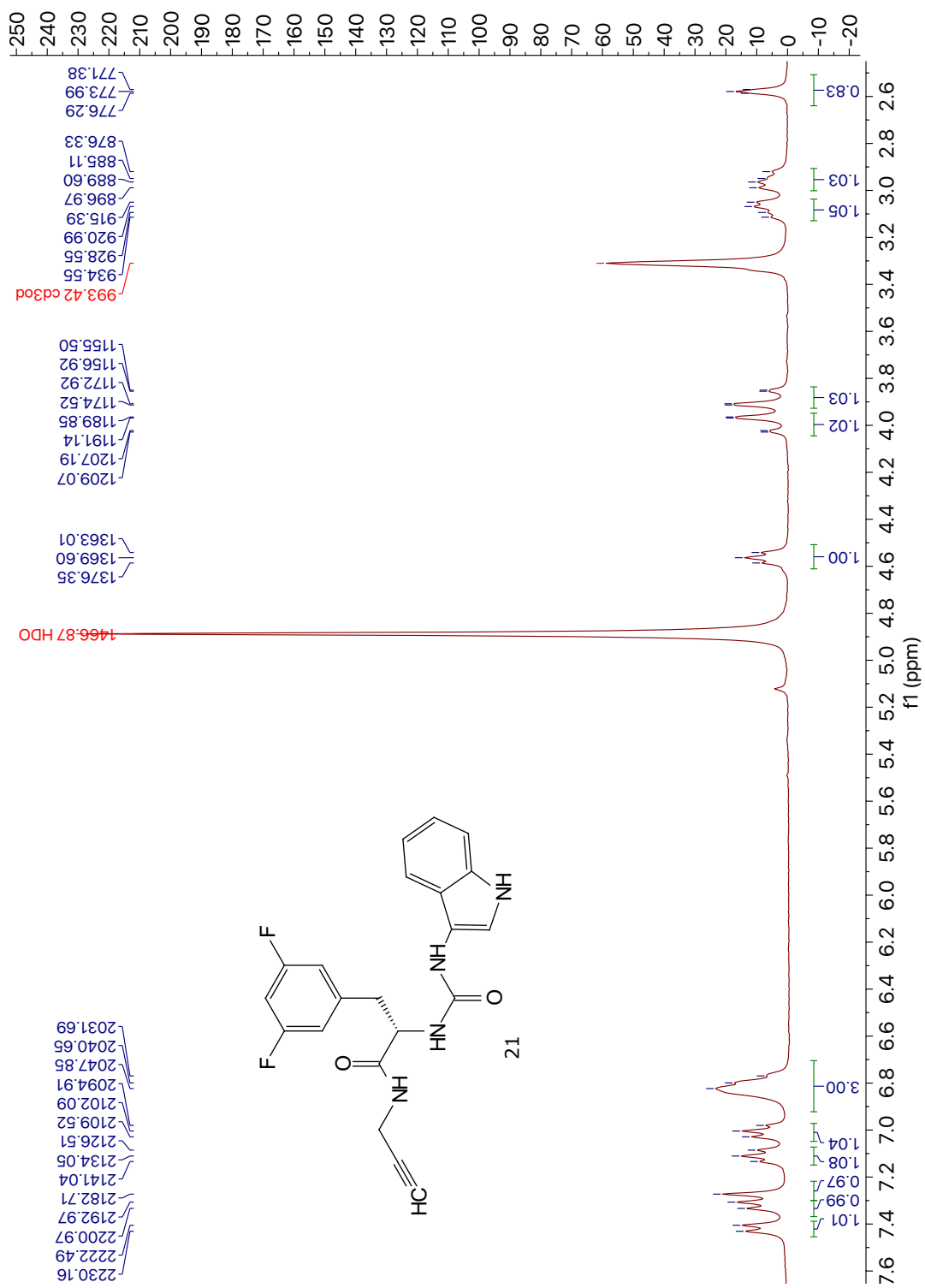


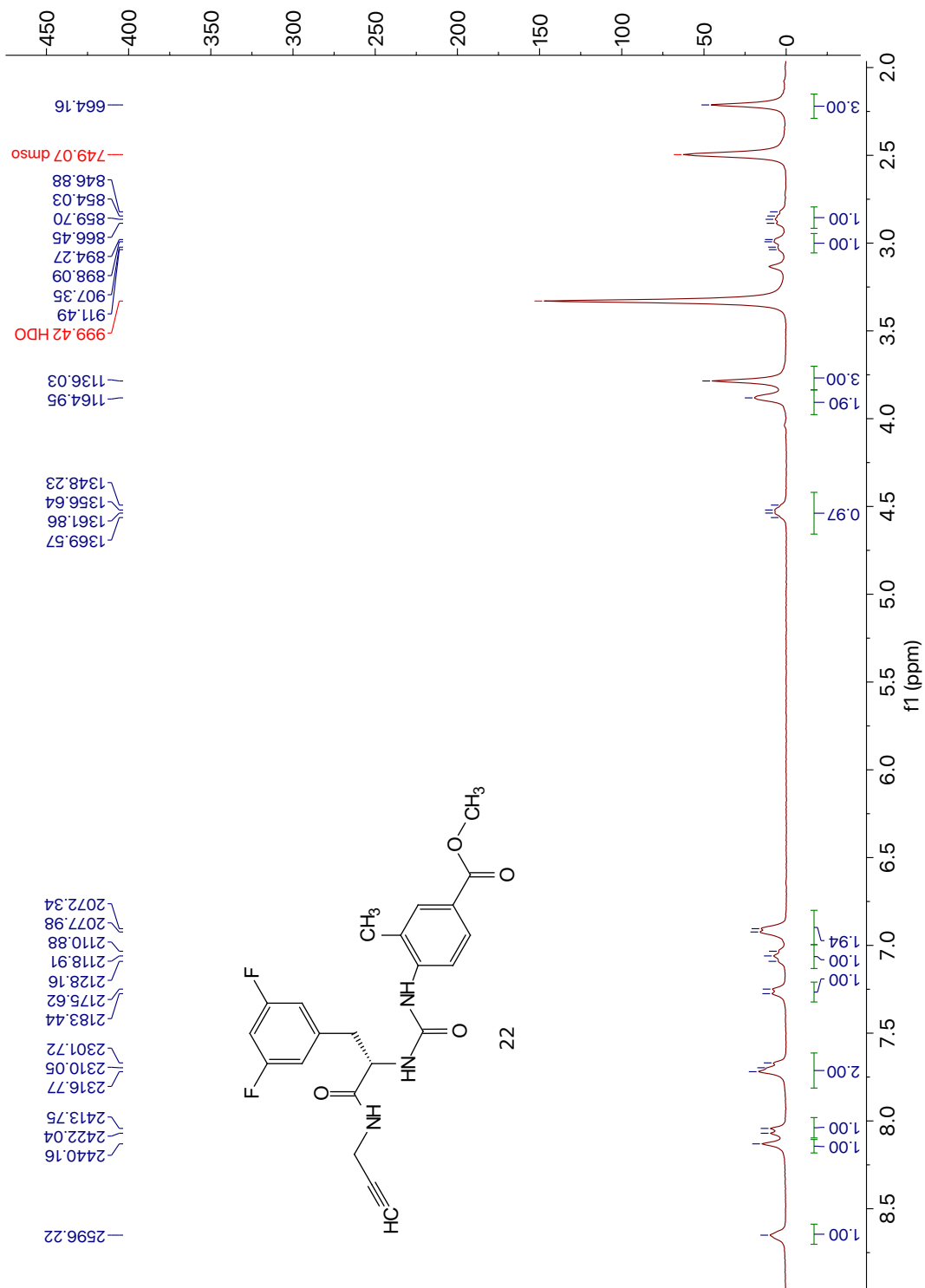
19

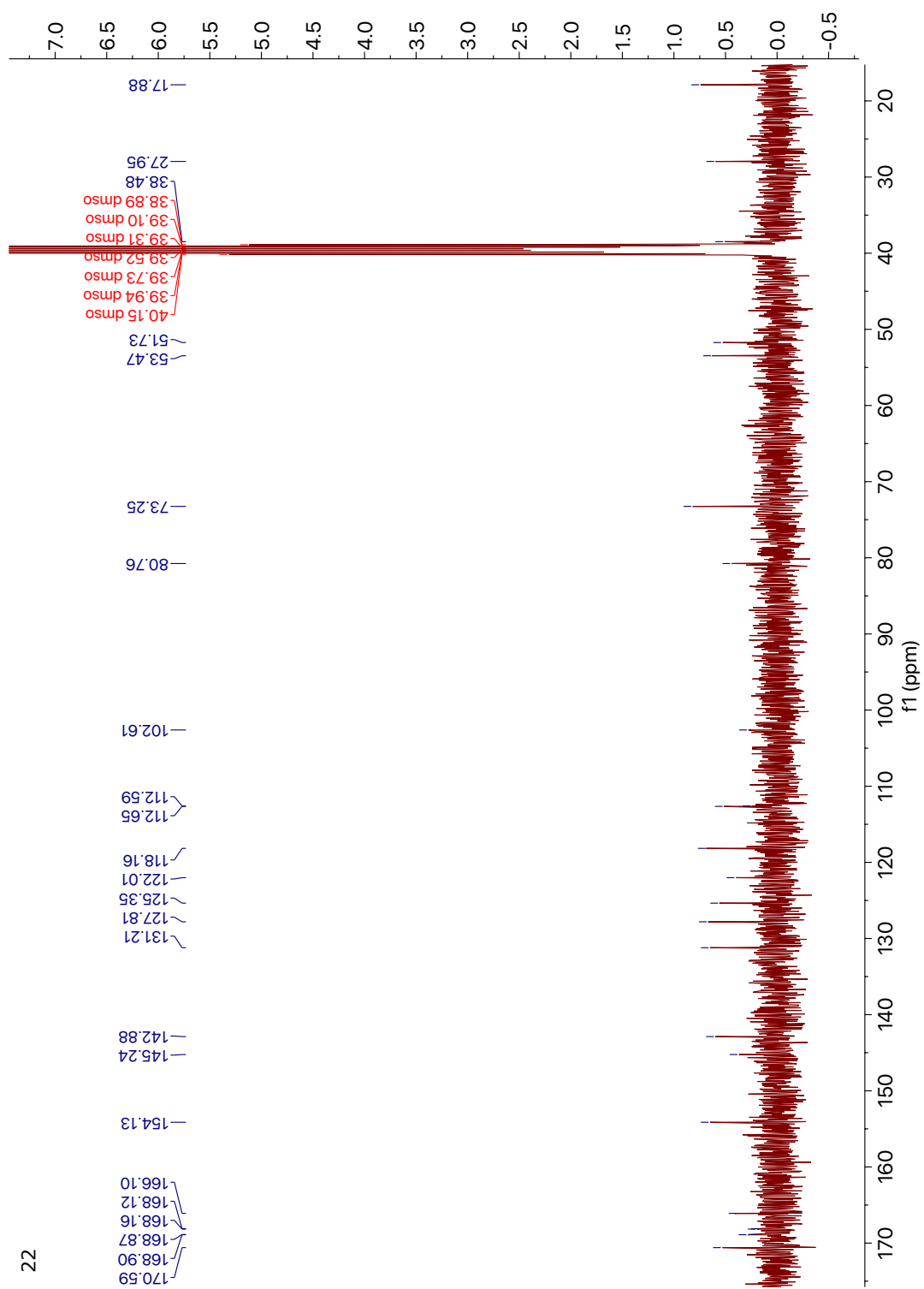


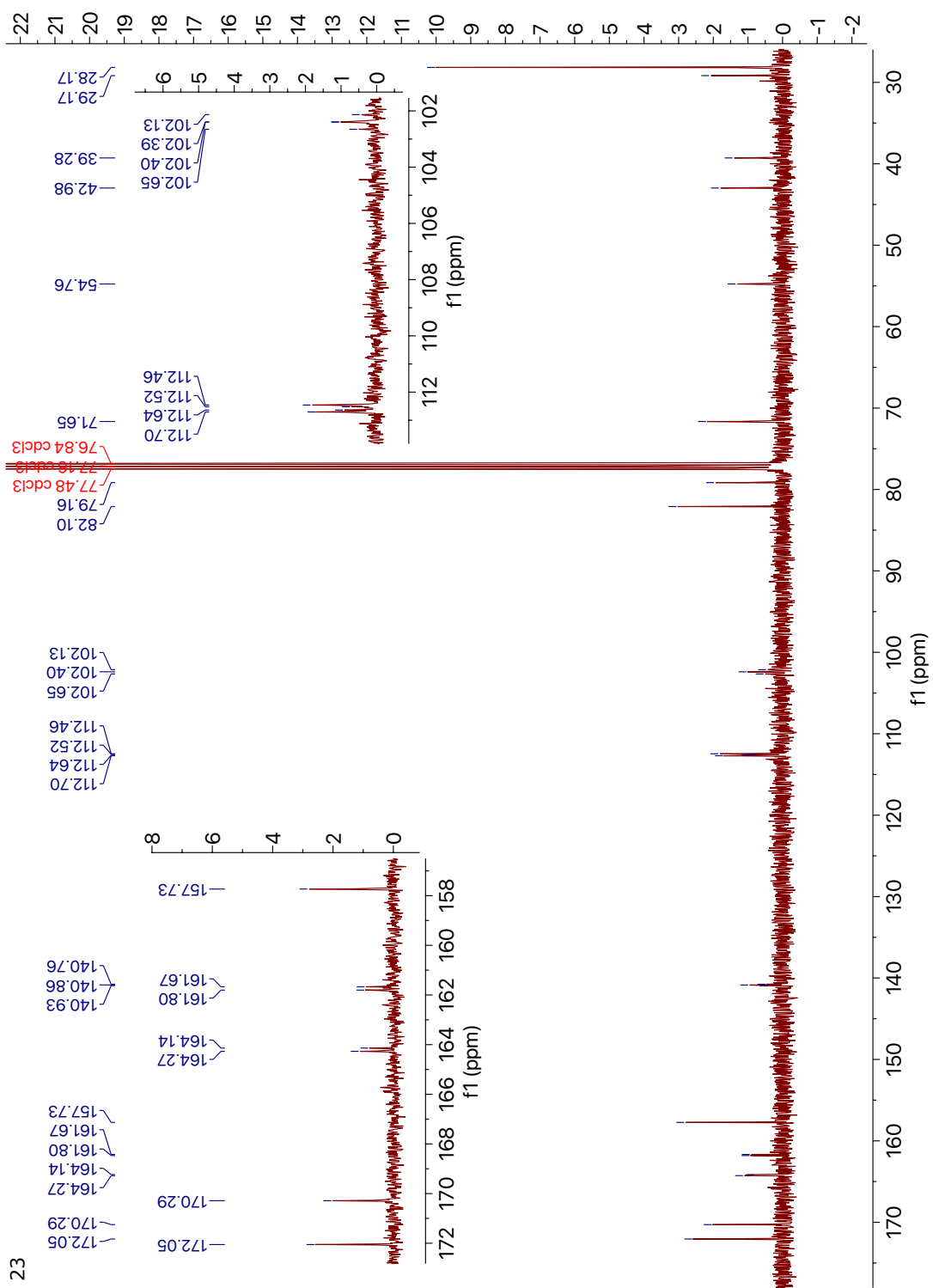


20

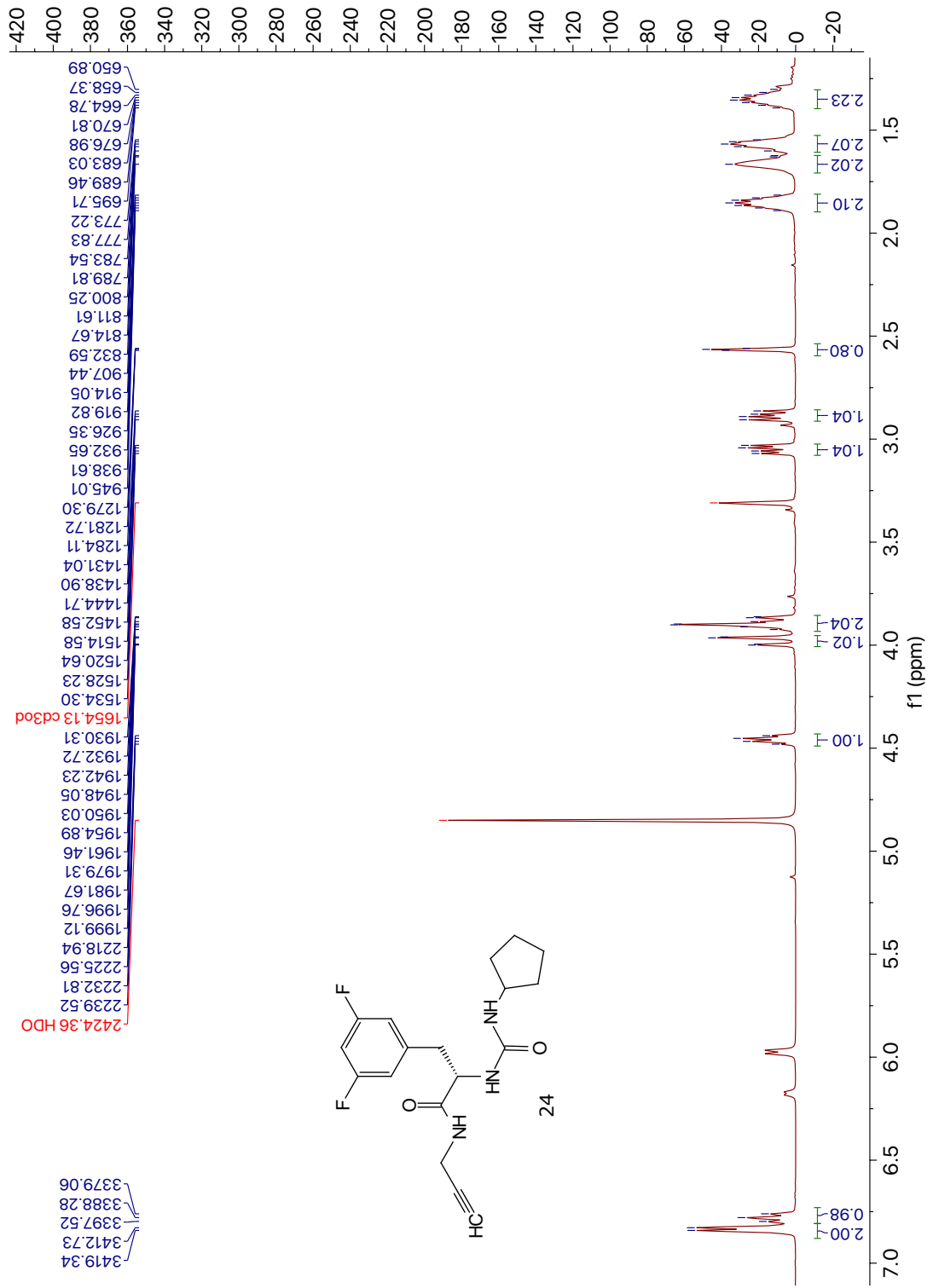


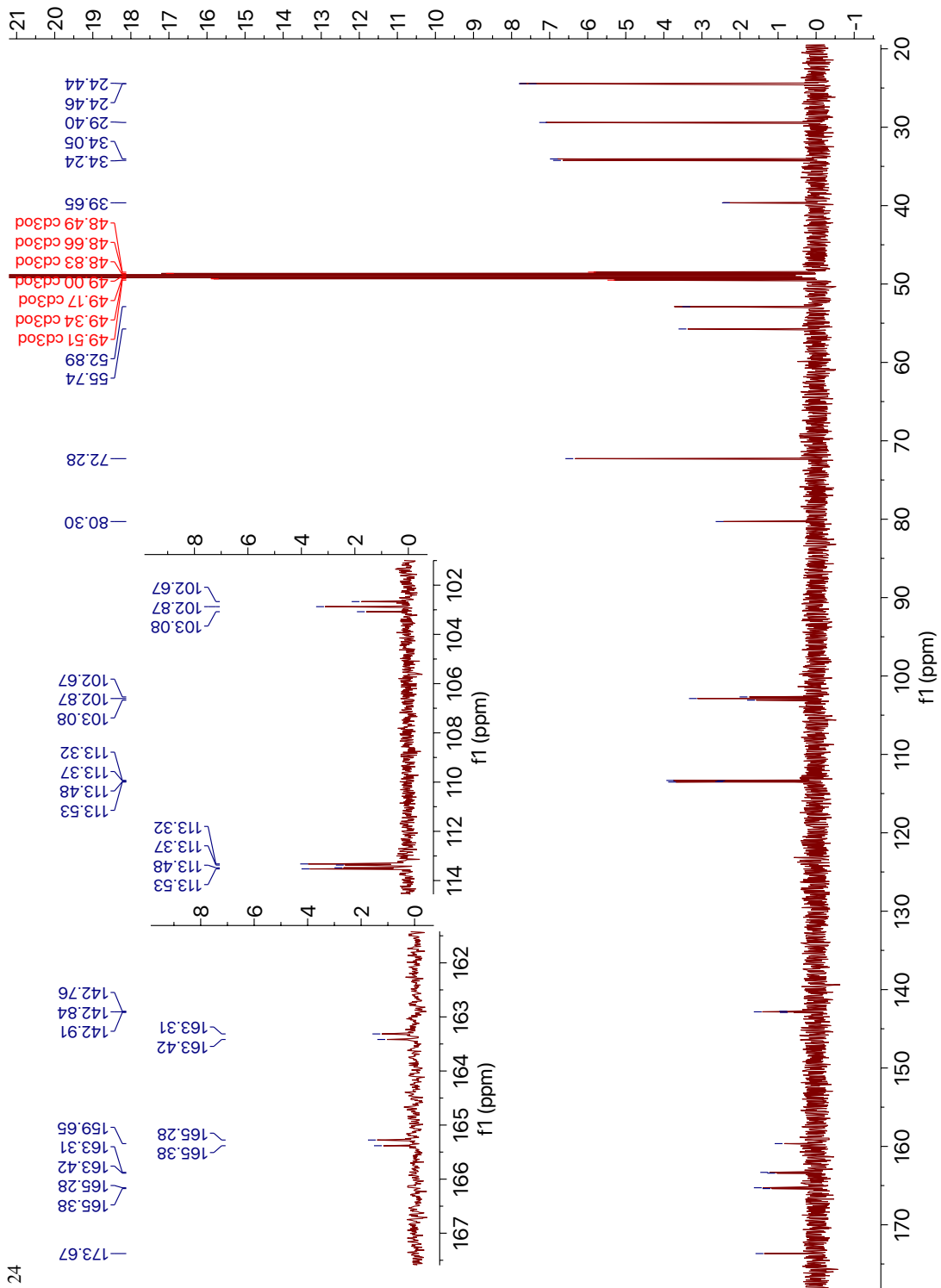


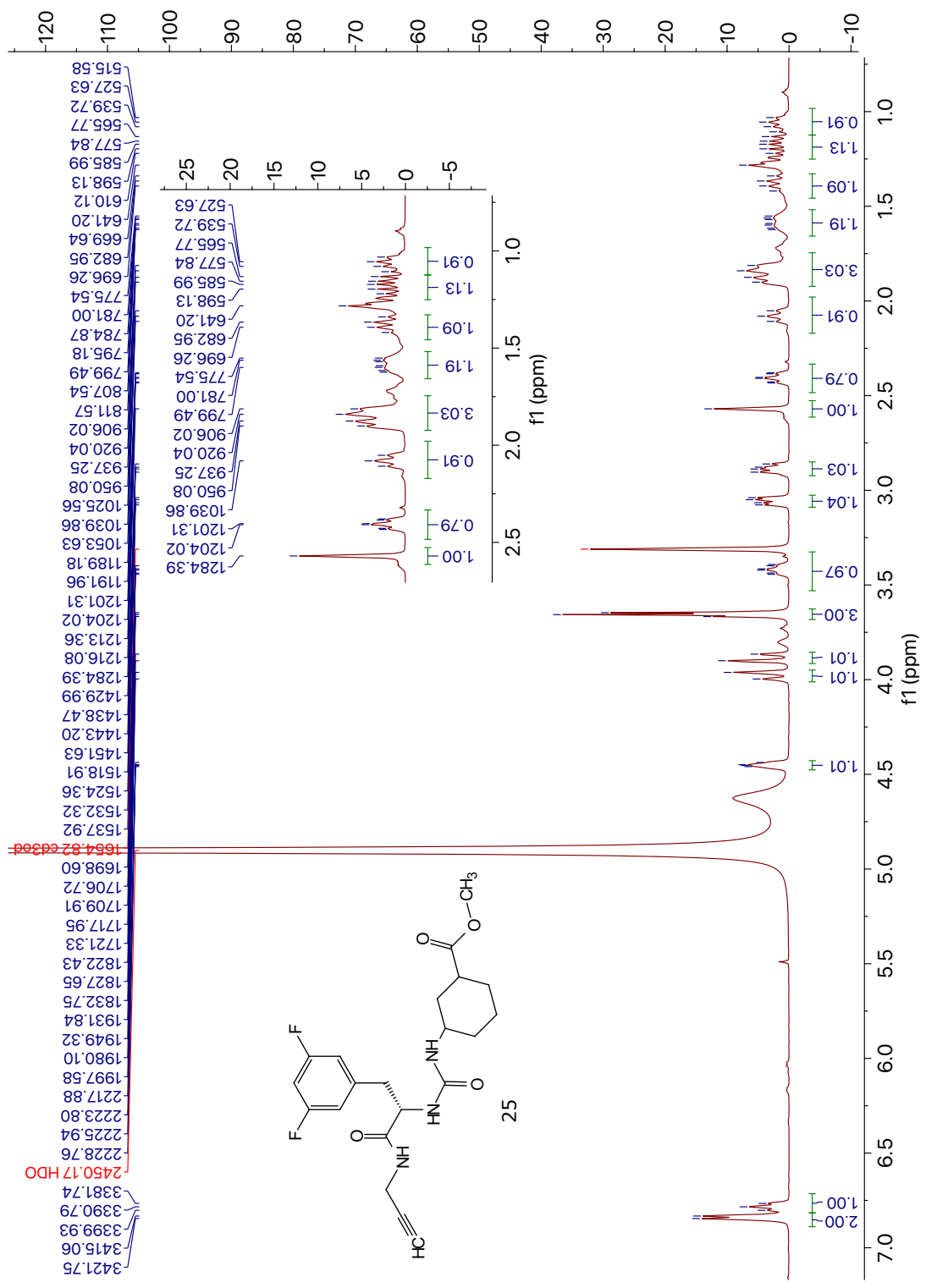


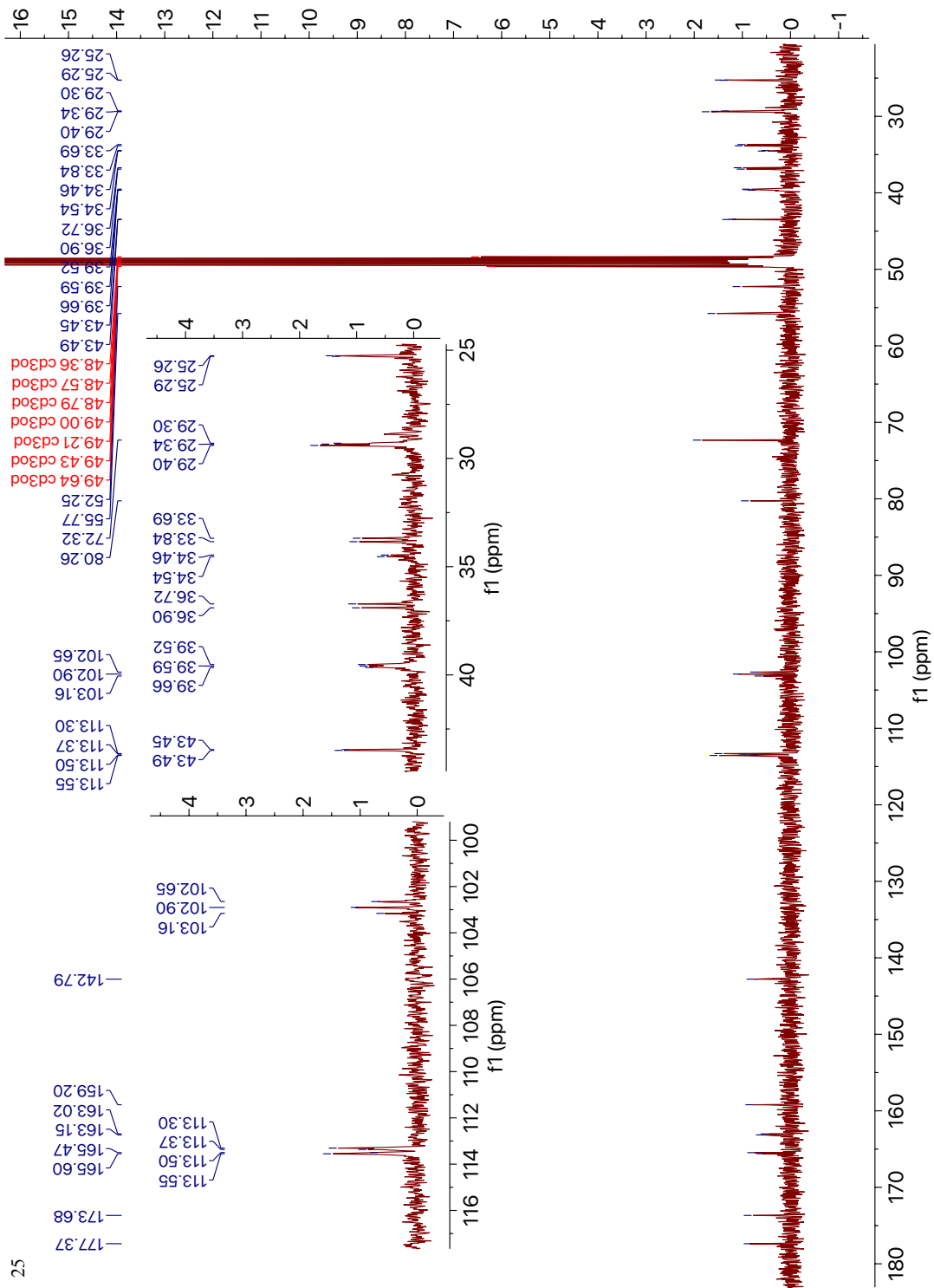


23

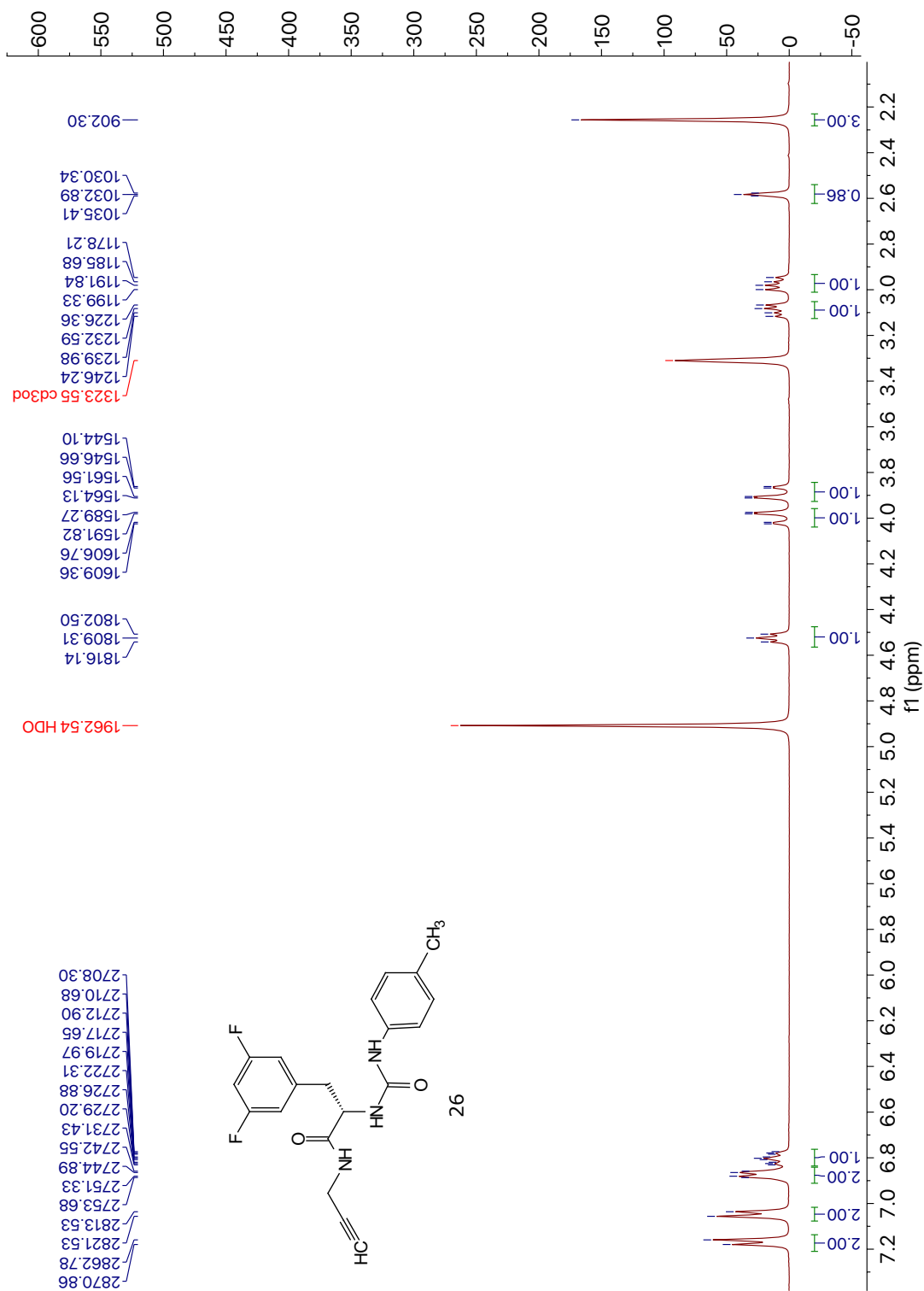


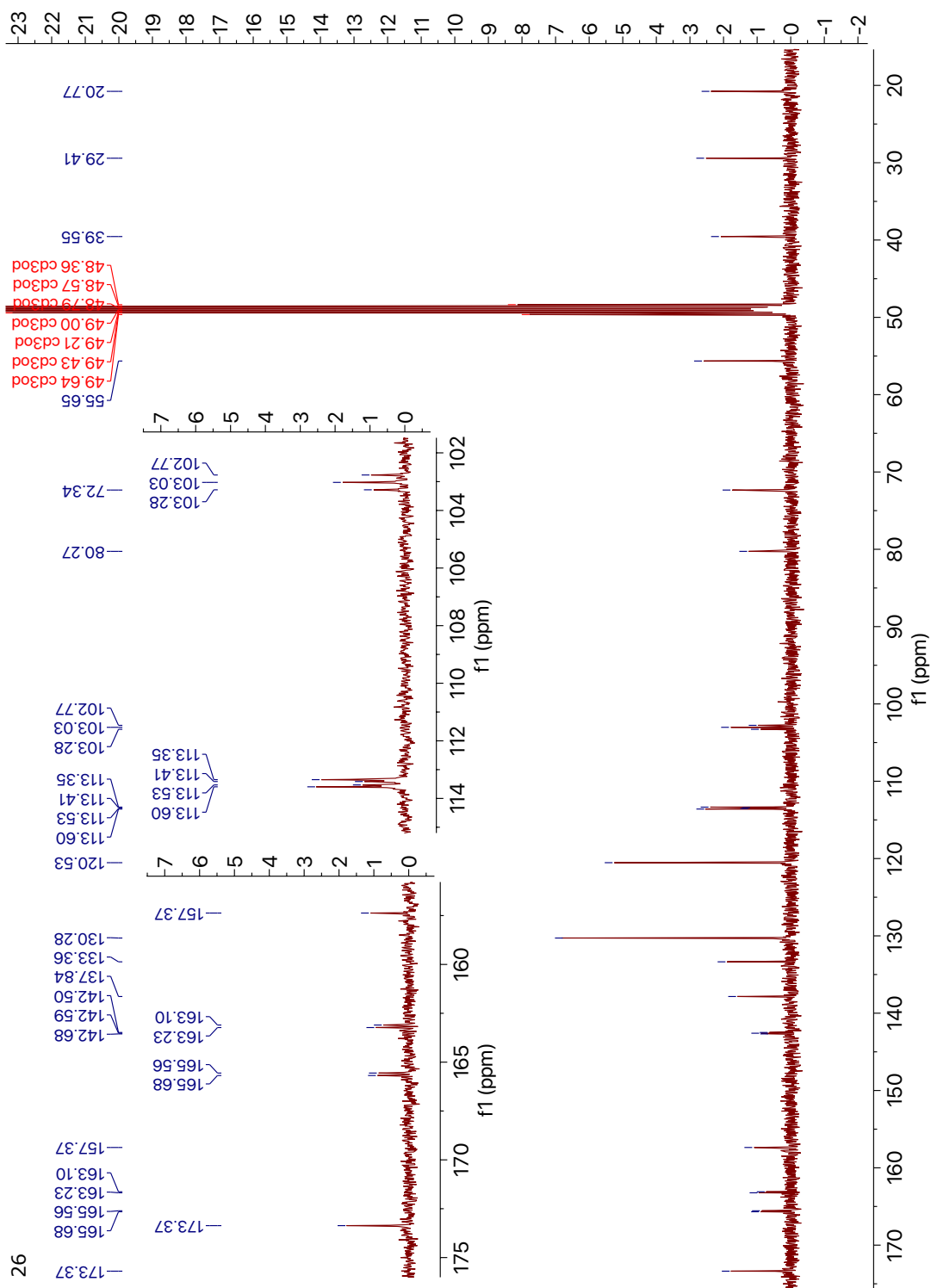




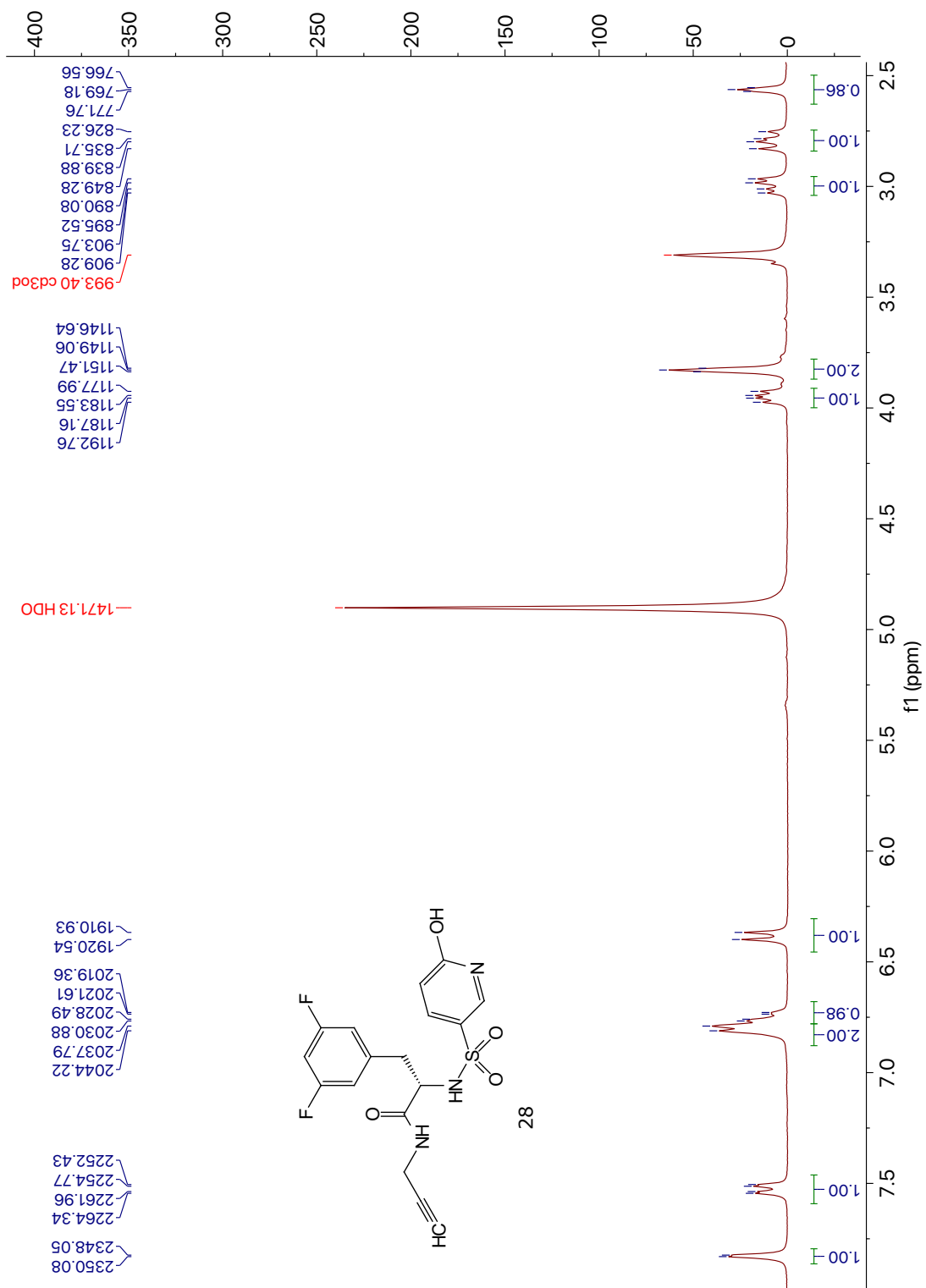


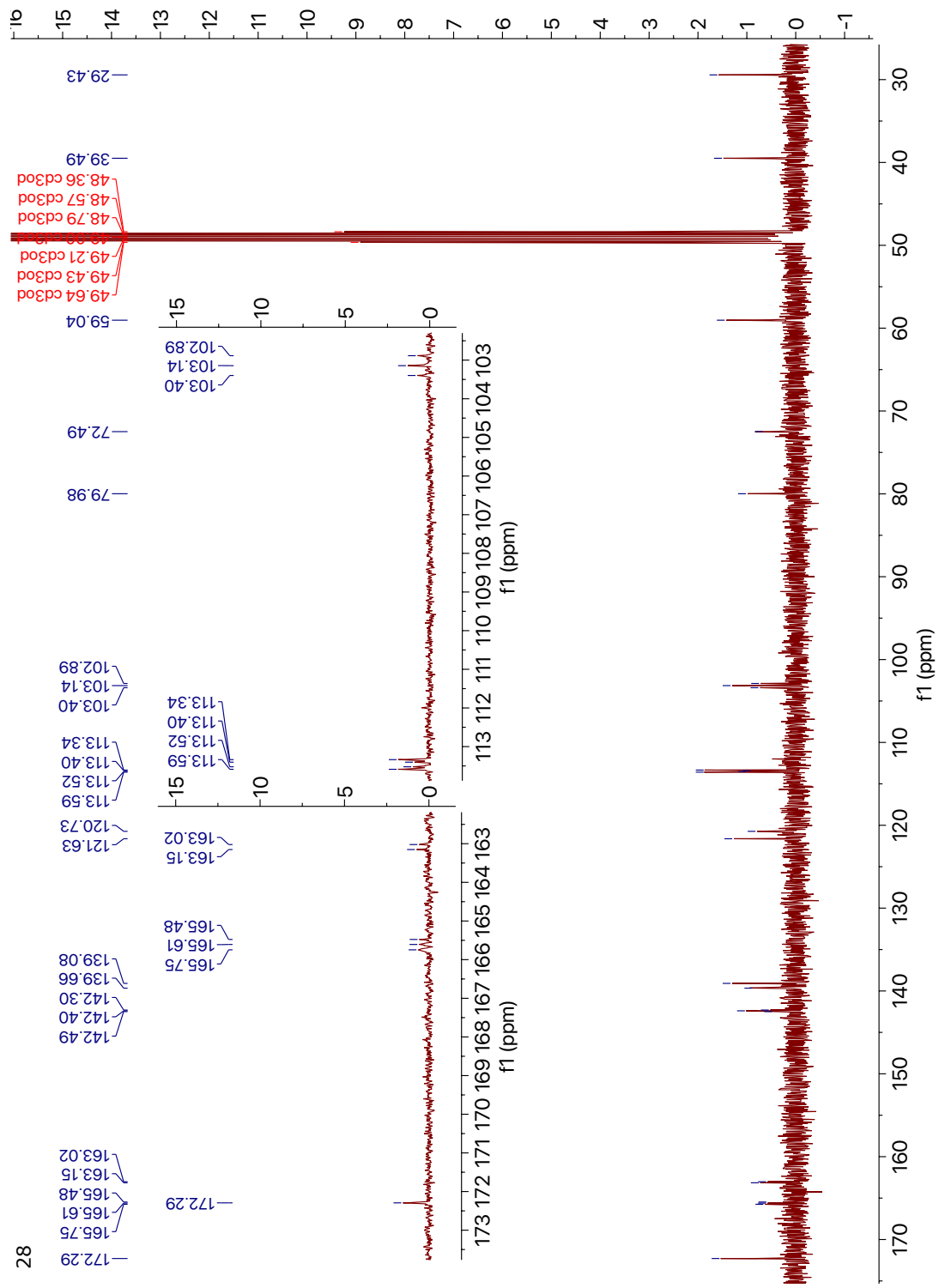
25



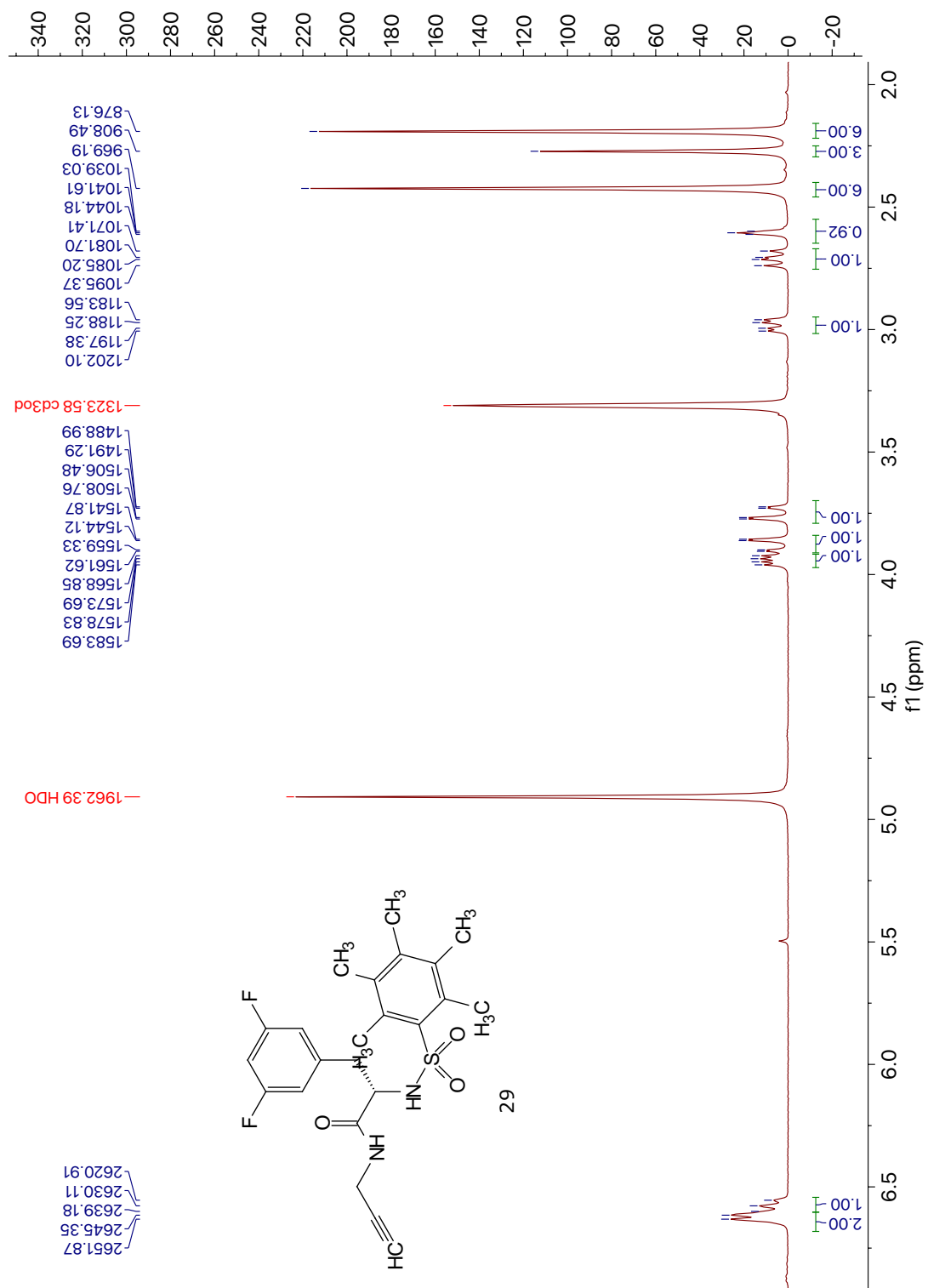


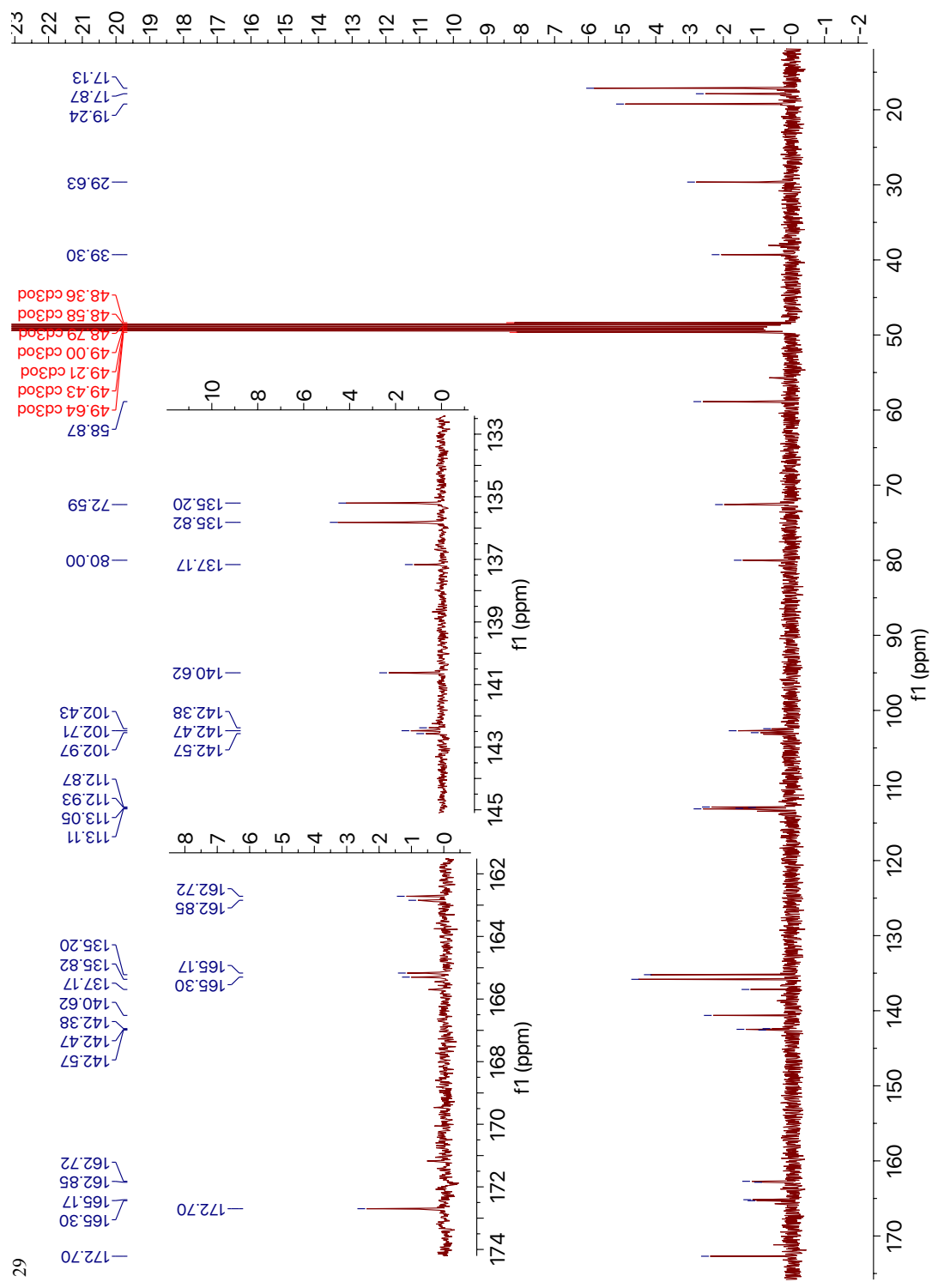
26



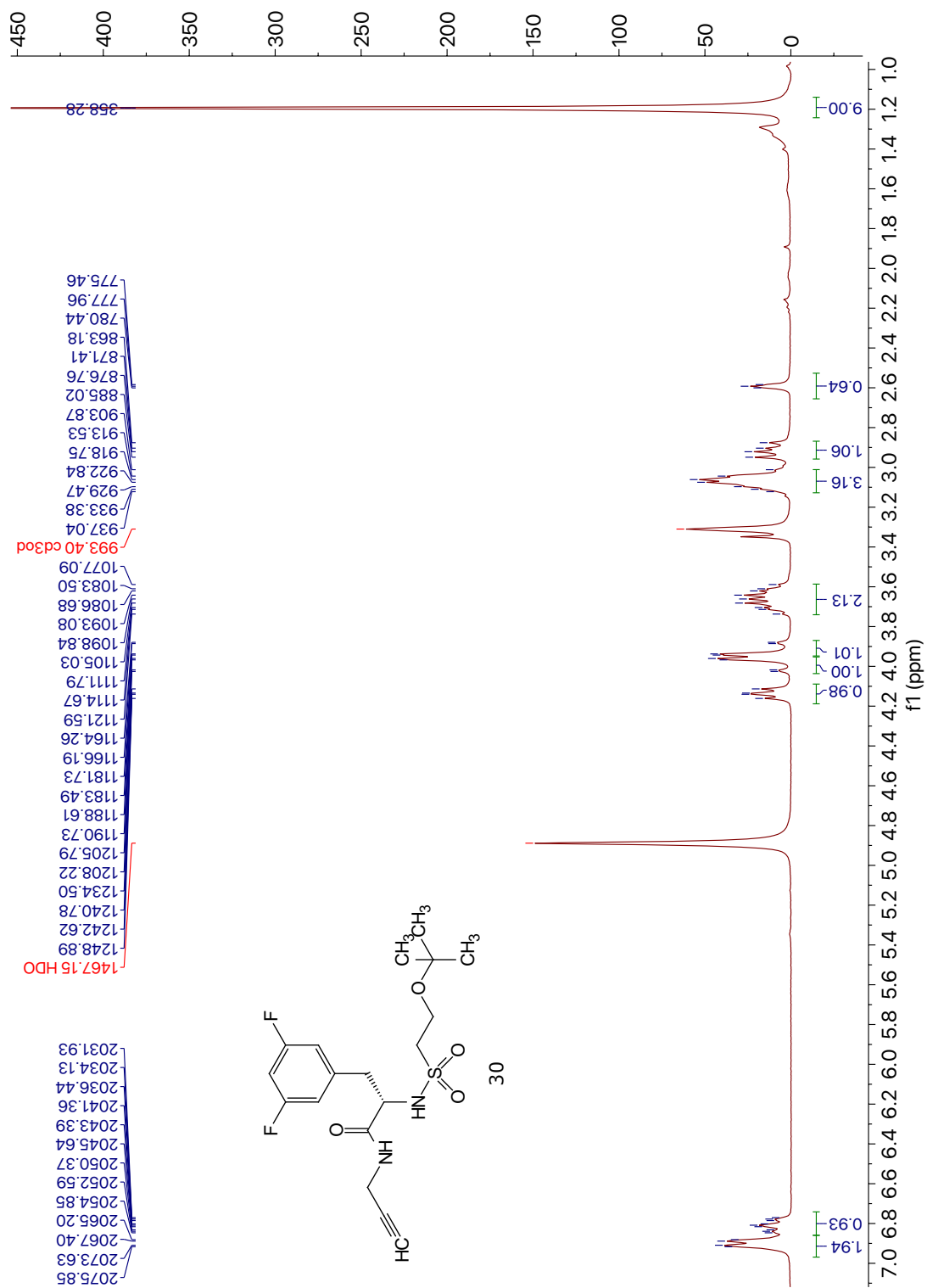


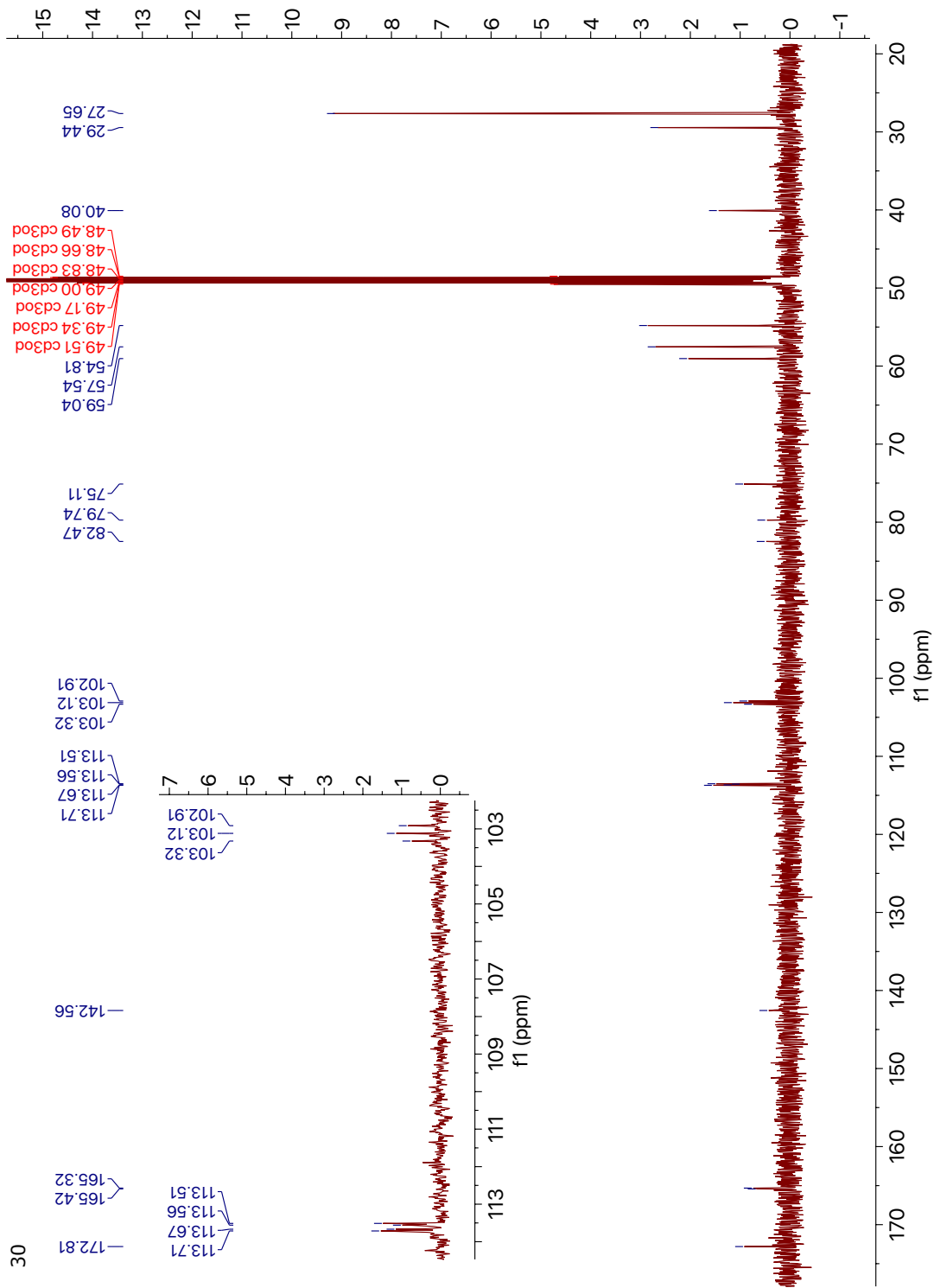
28

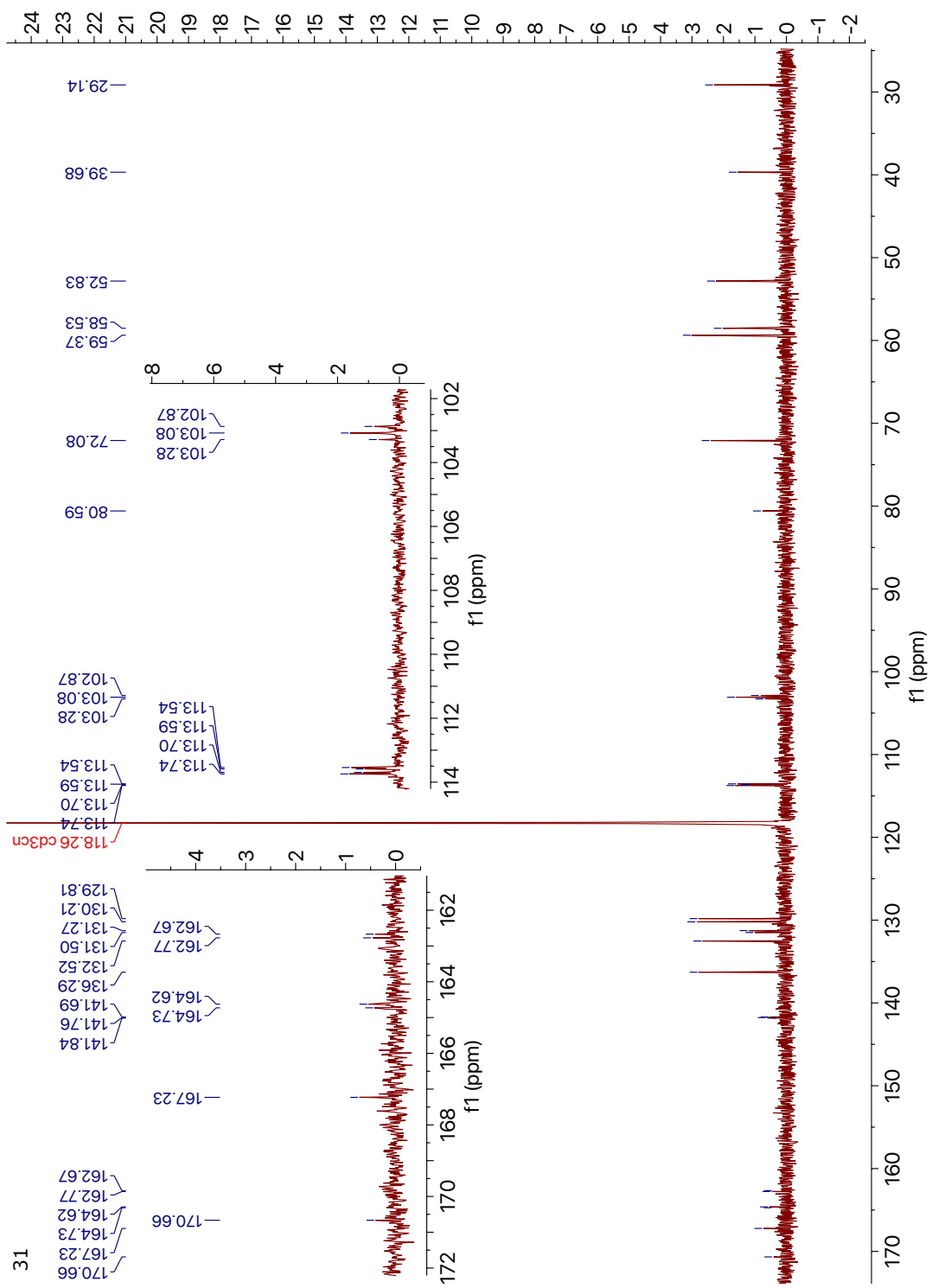




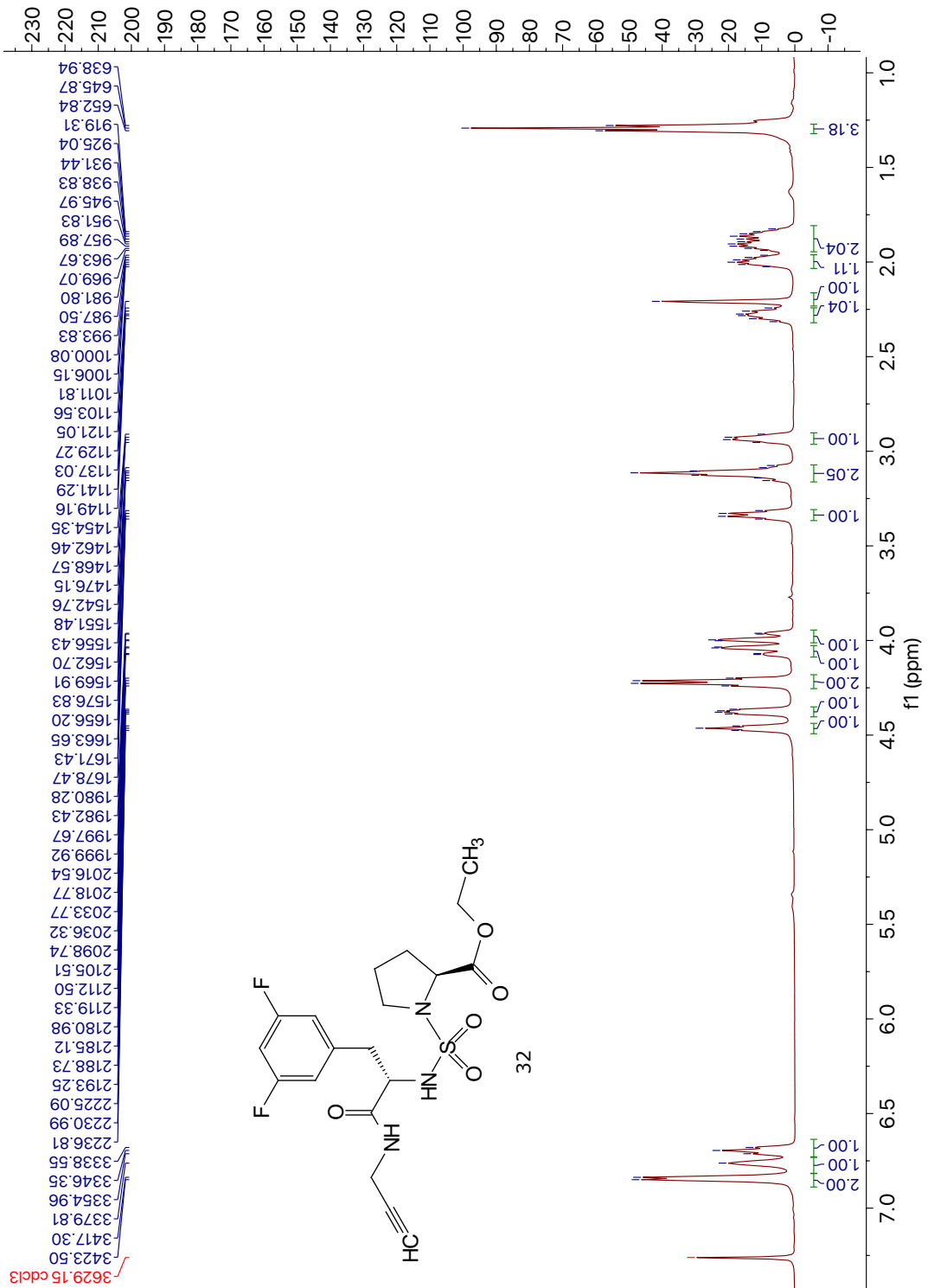
29

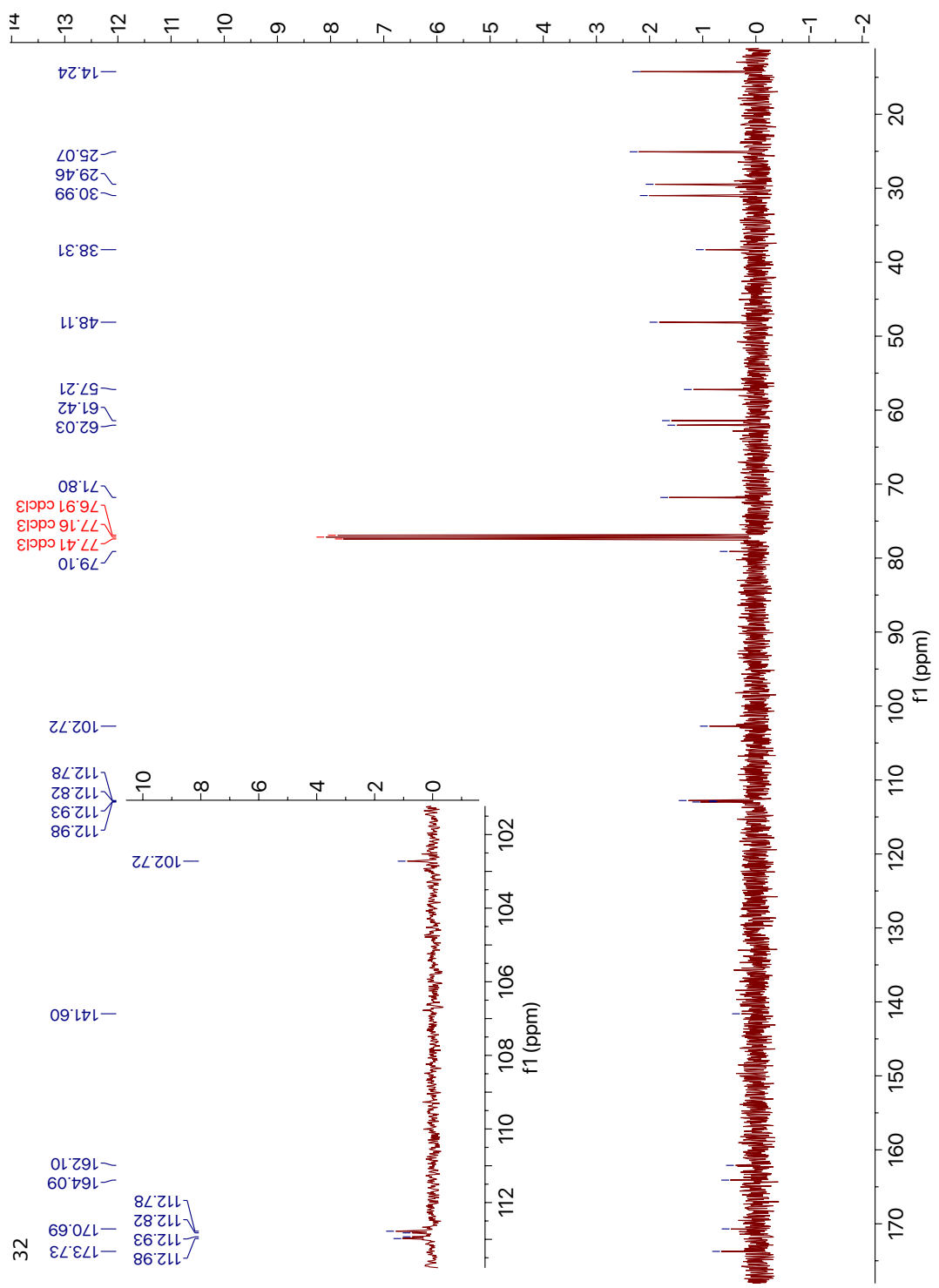




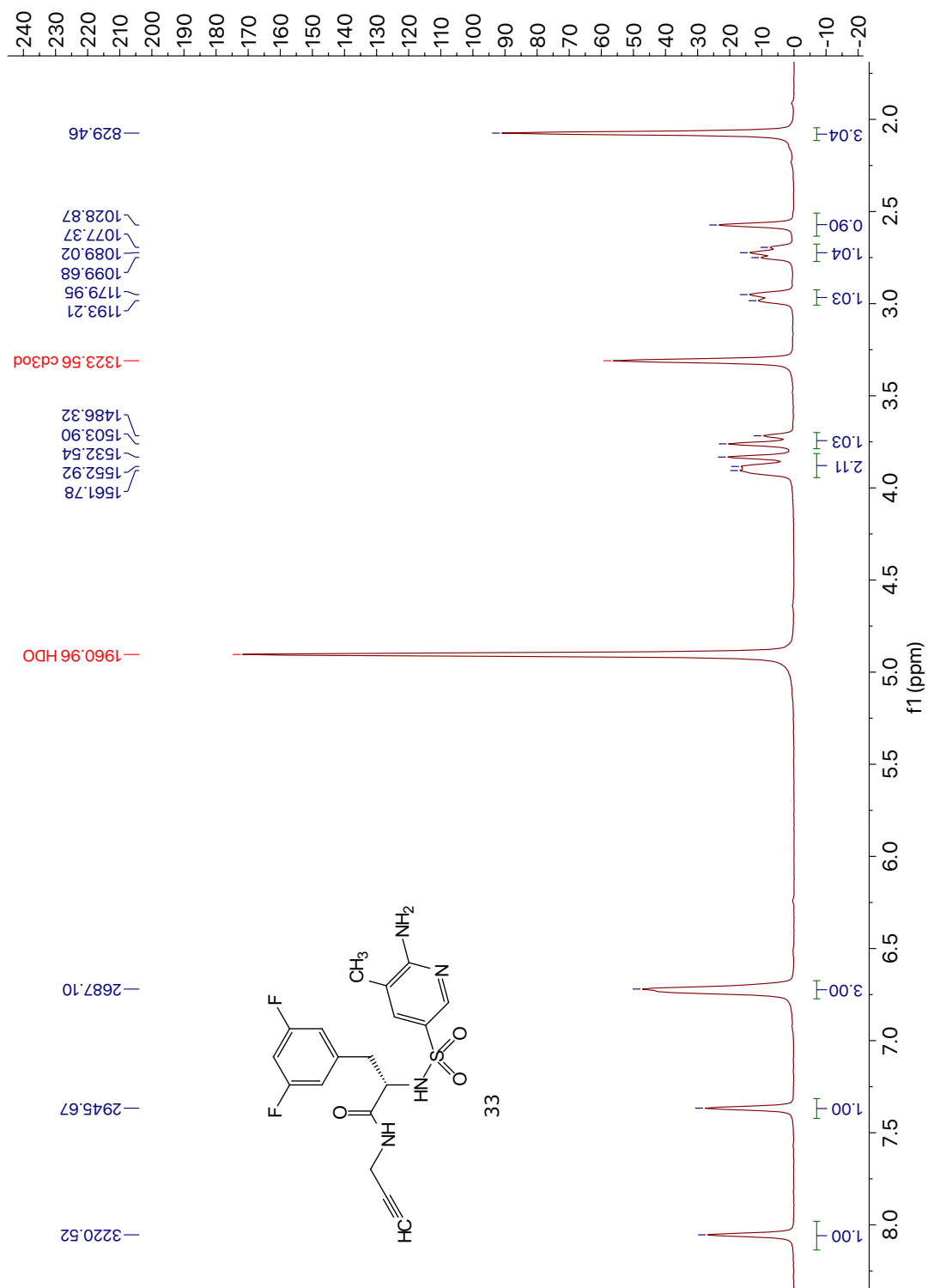


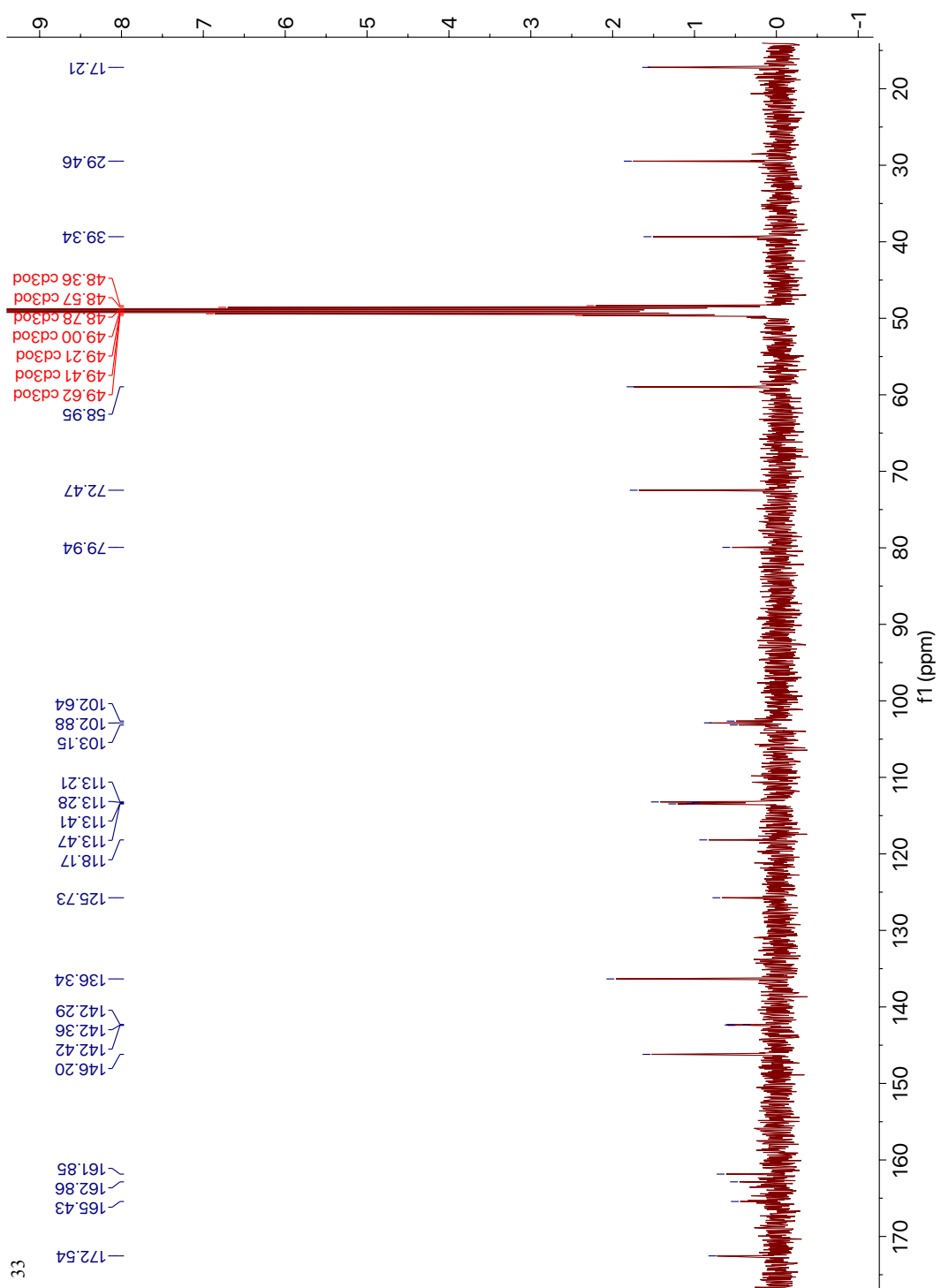
31



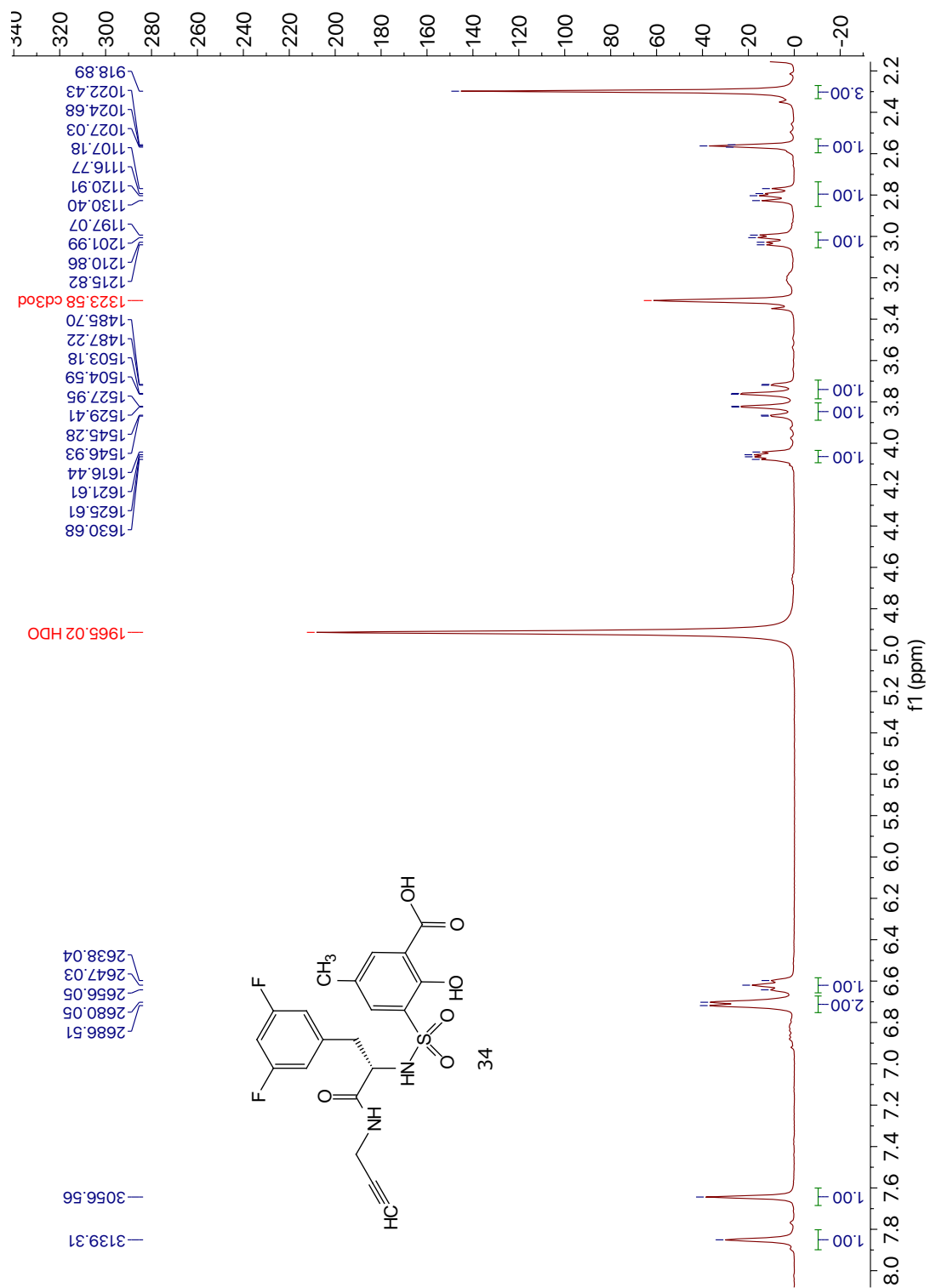


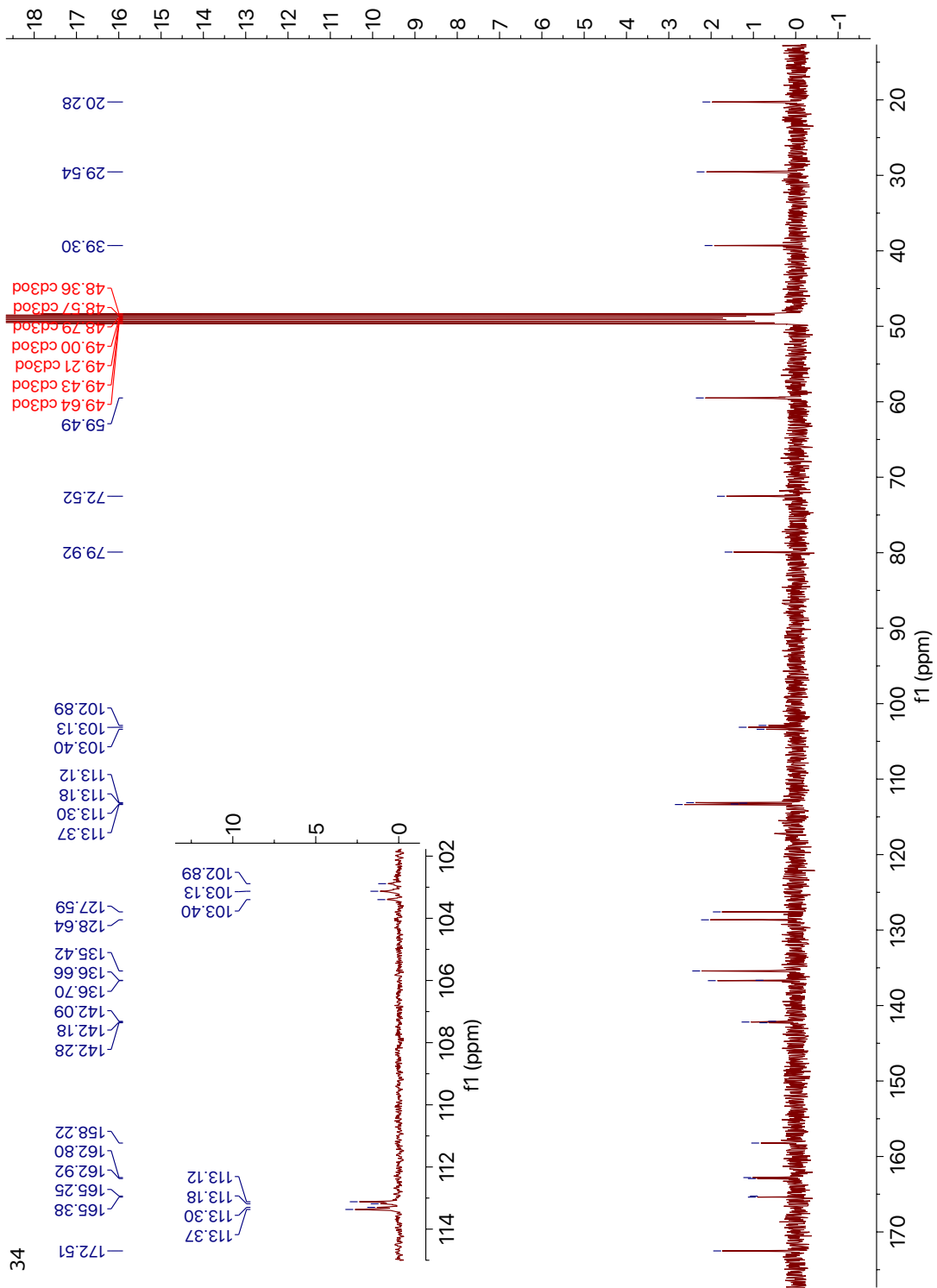
32



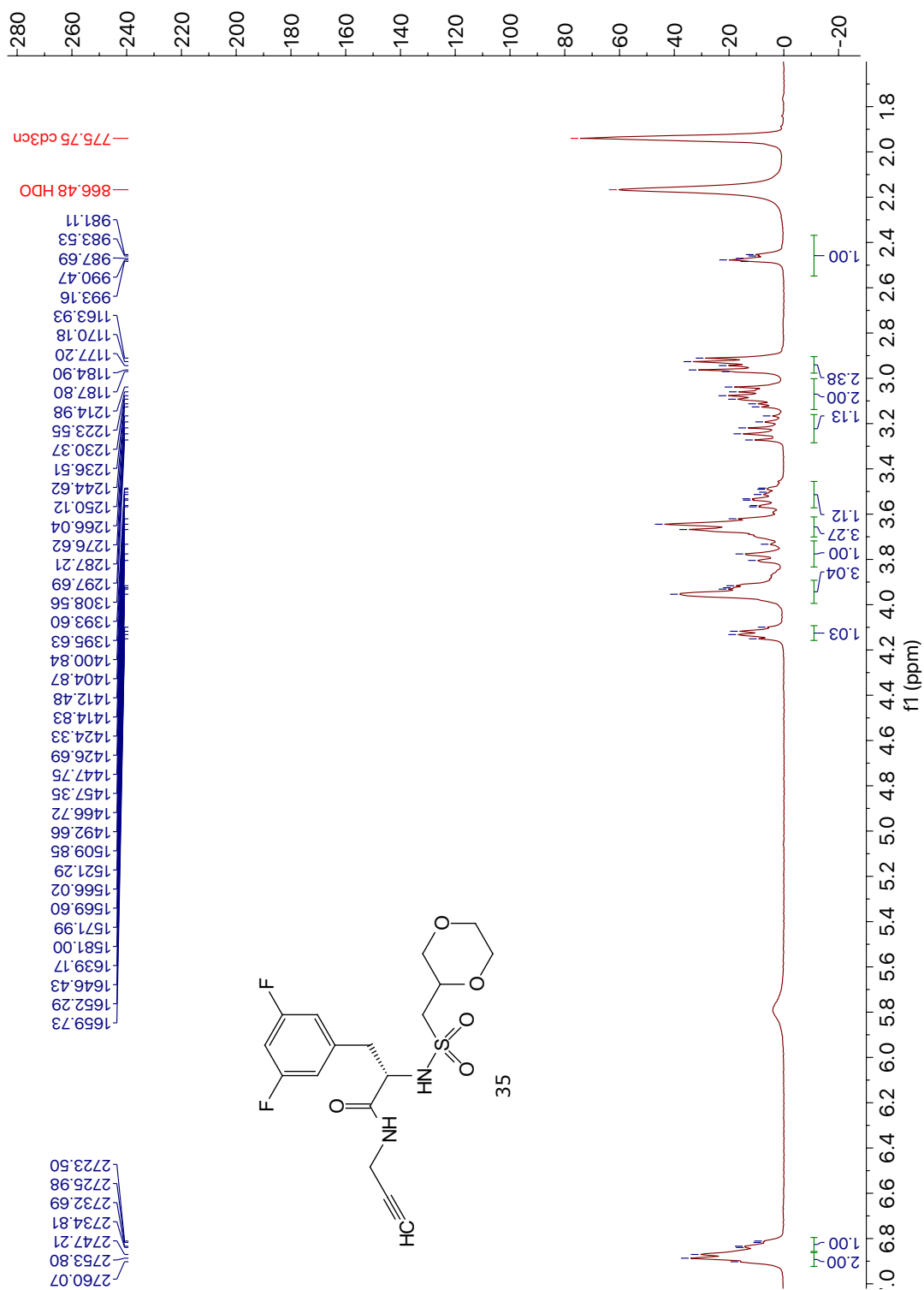


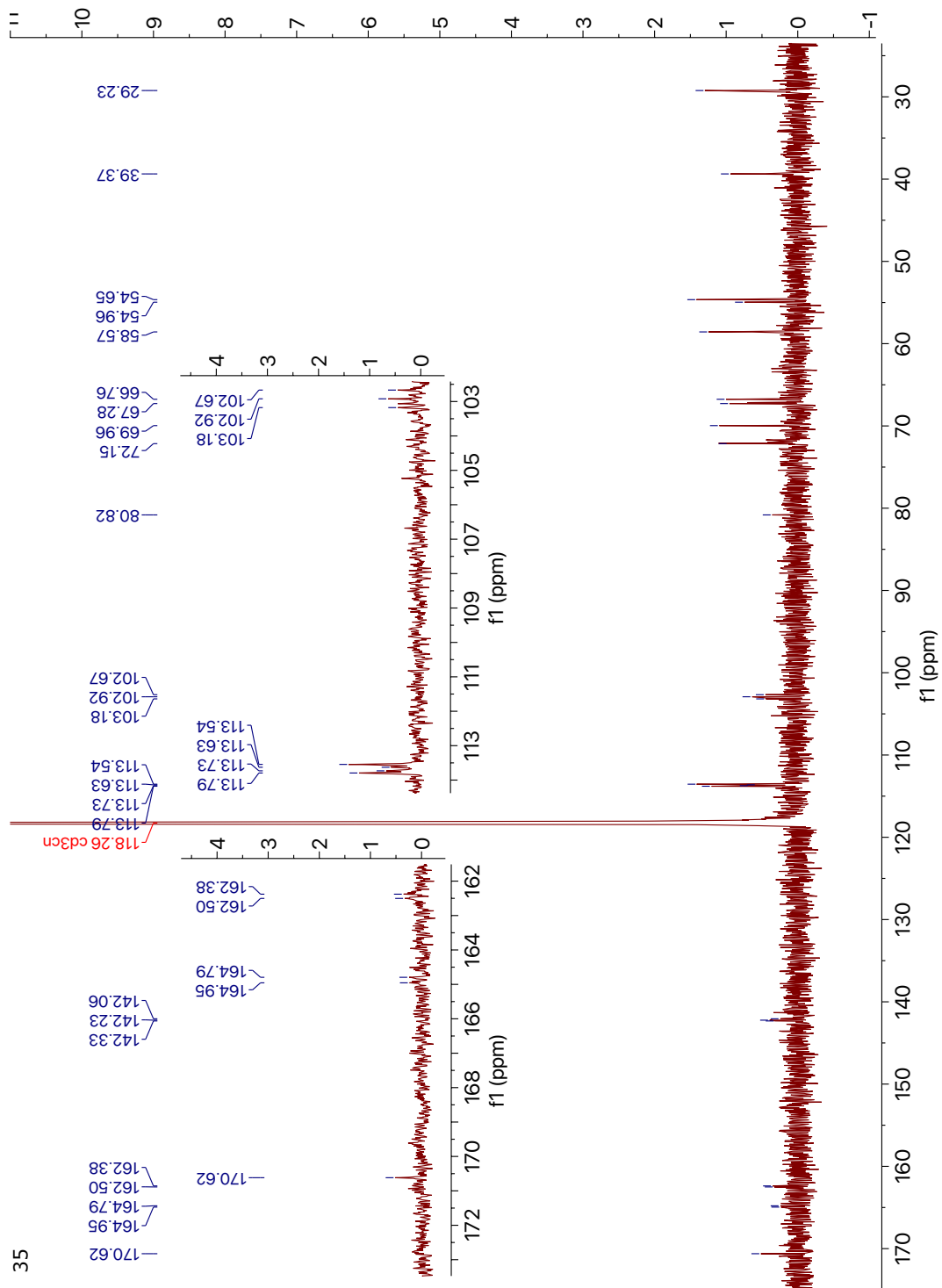
33



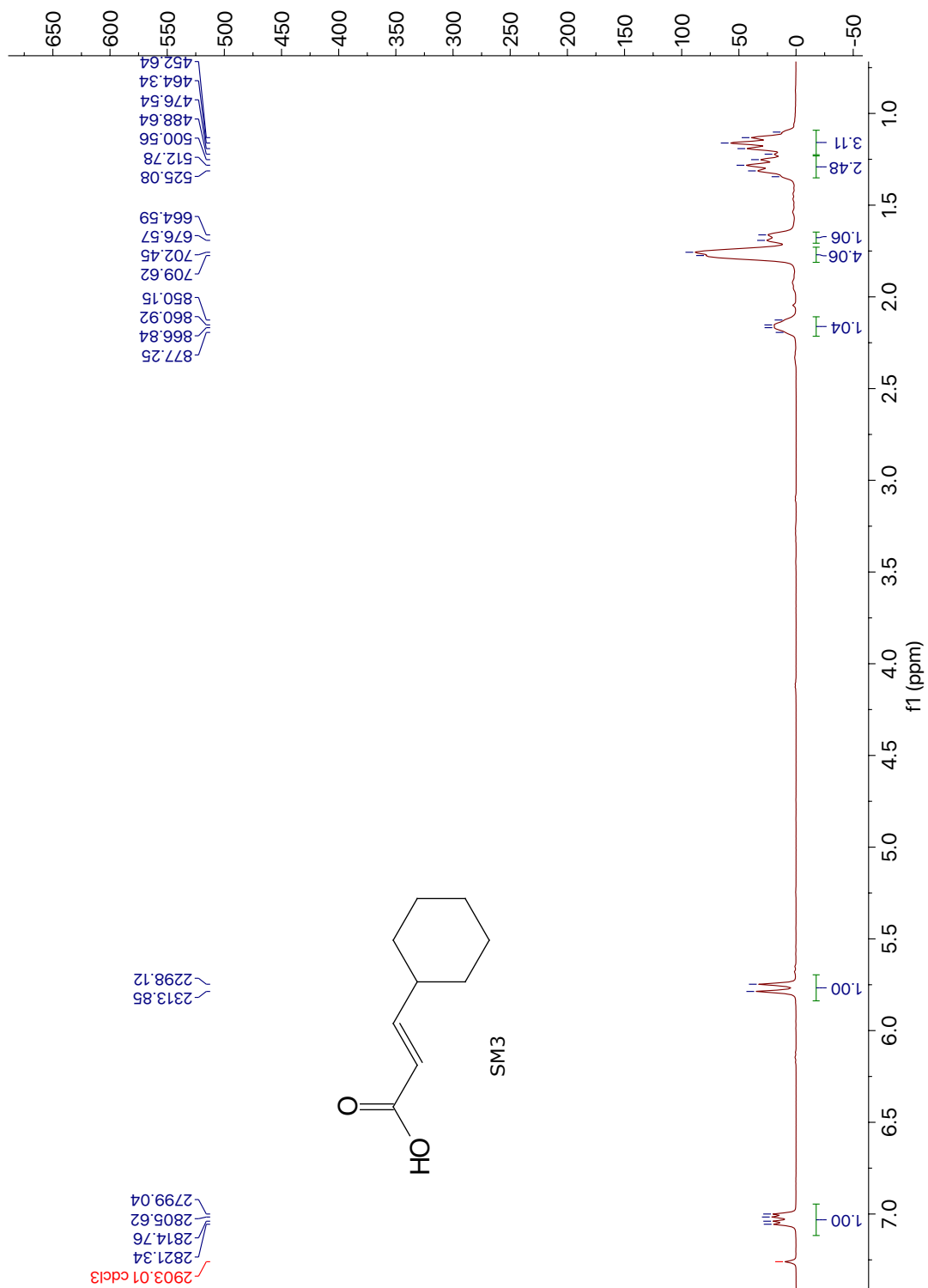


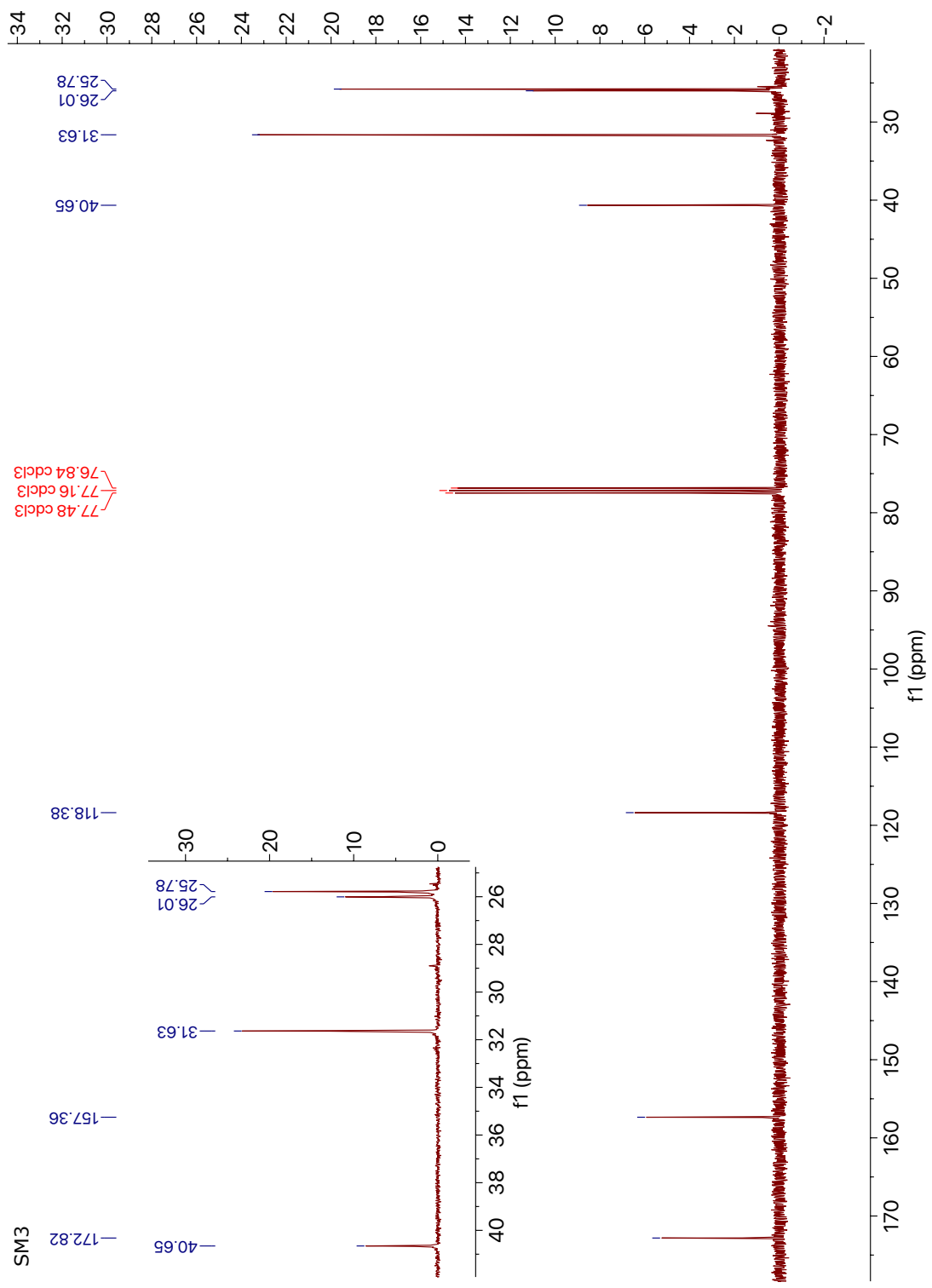
34

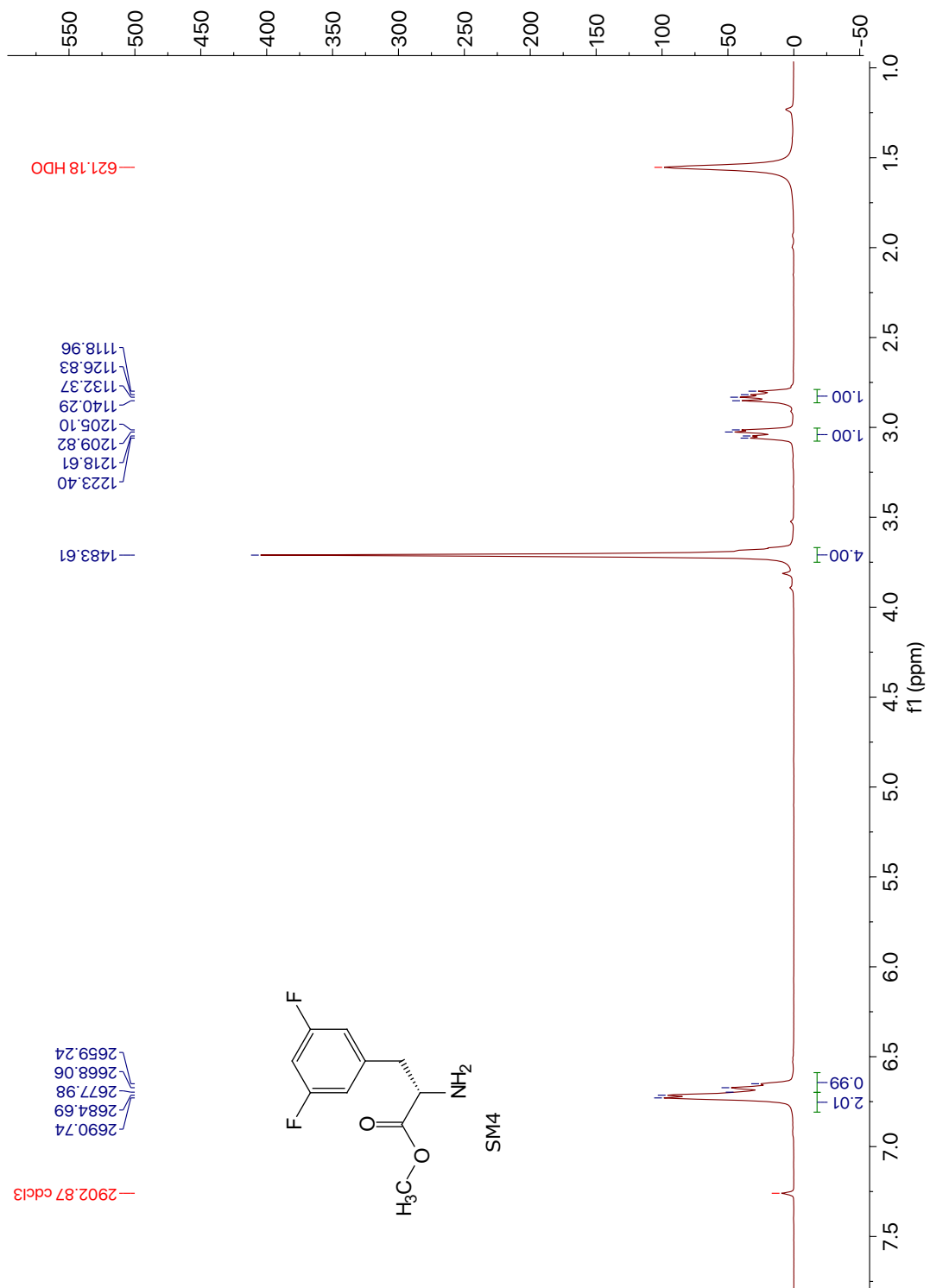


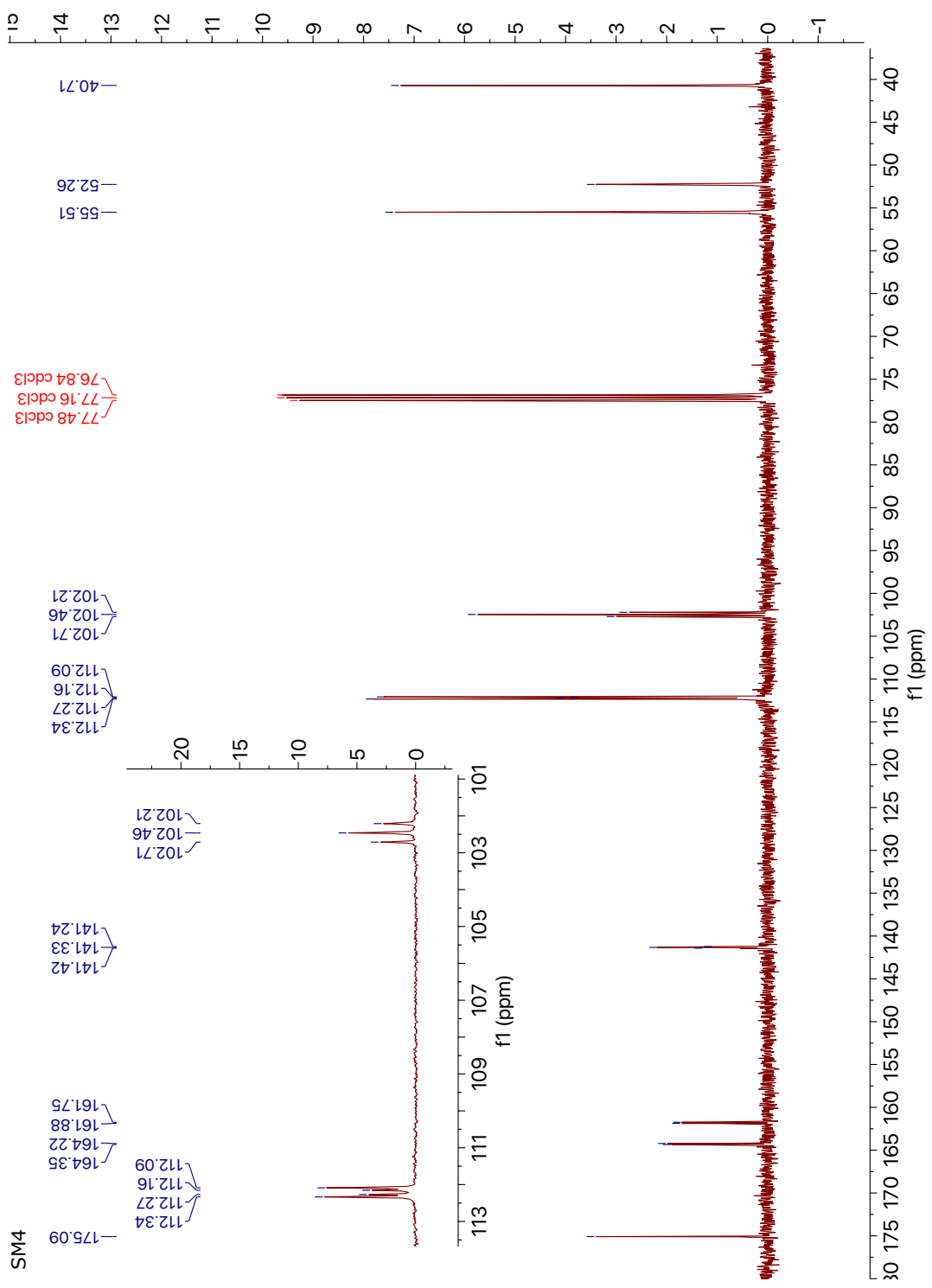


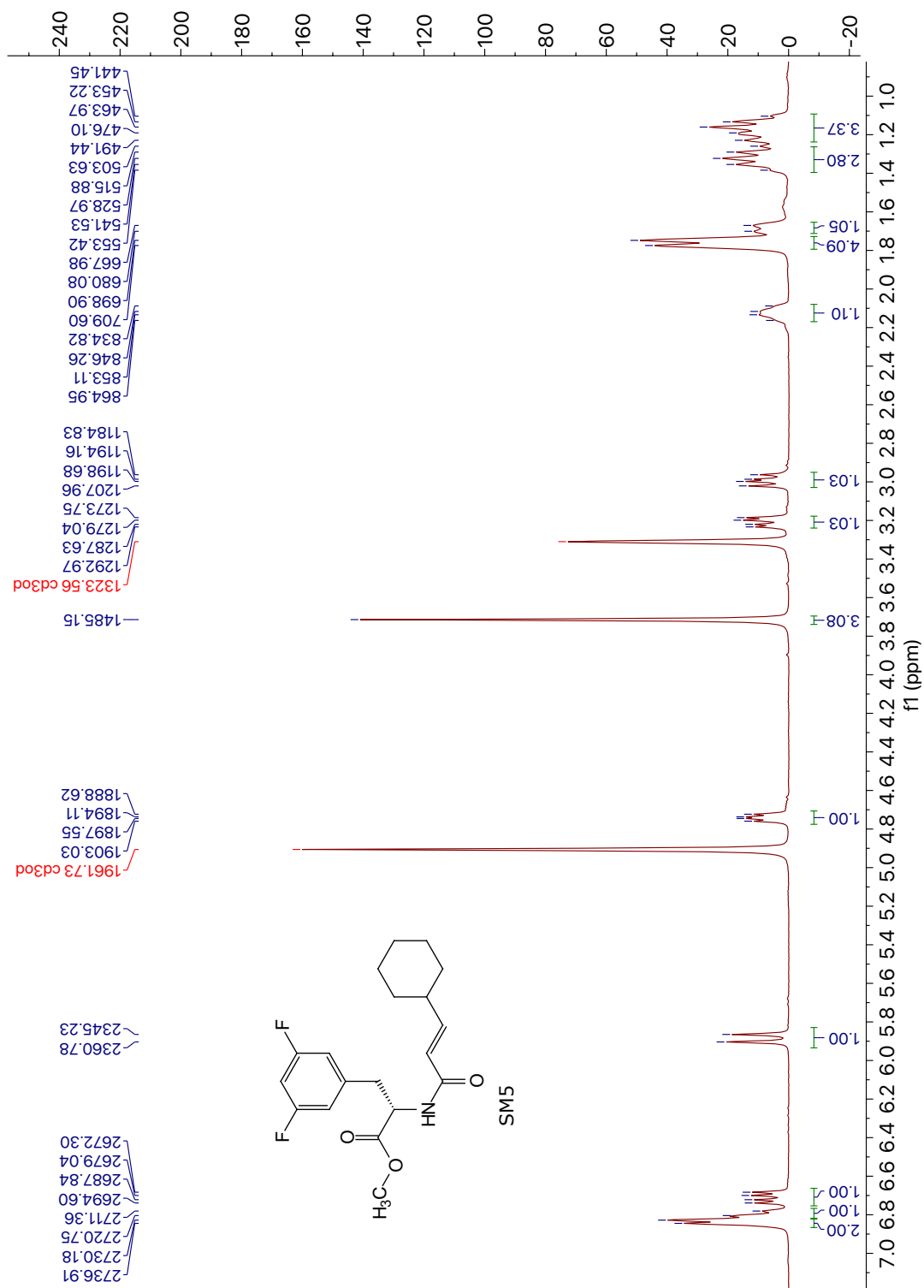
35

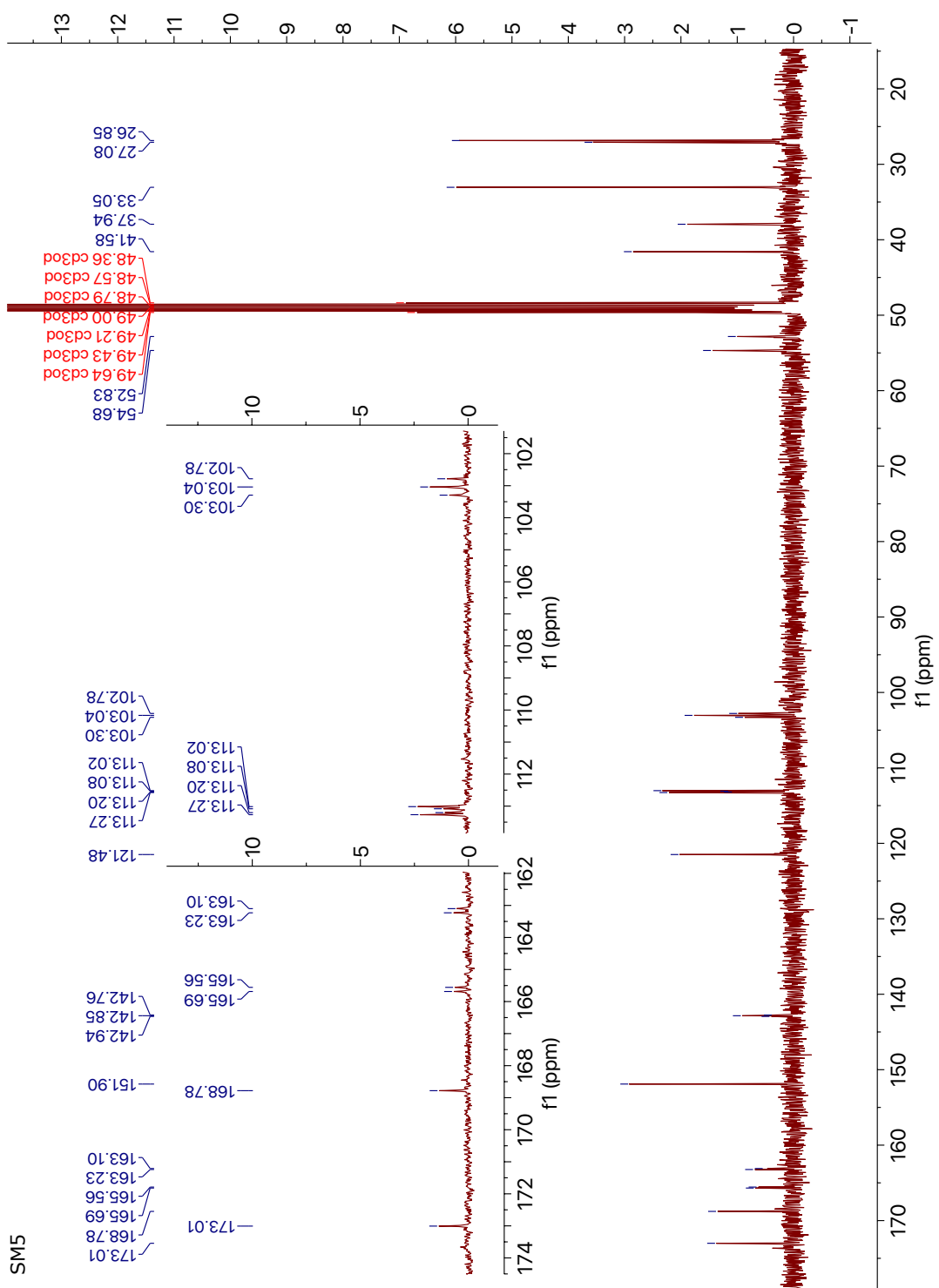


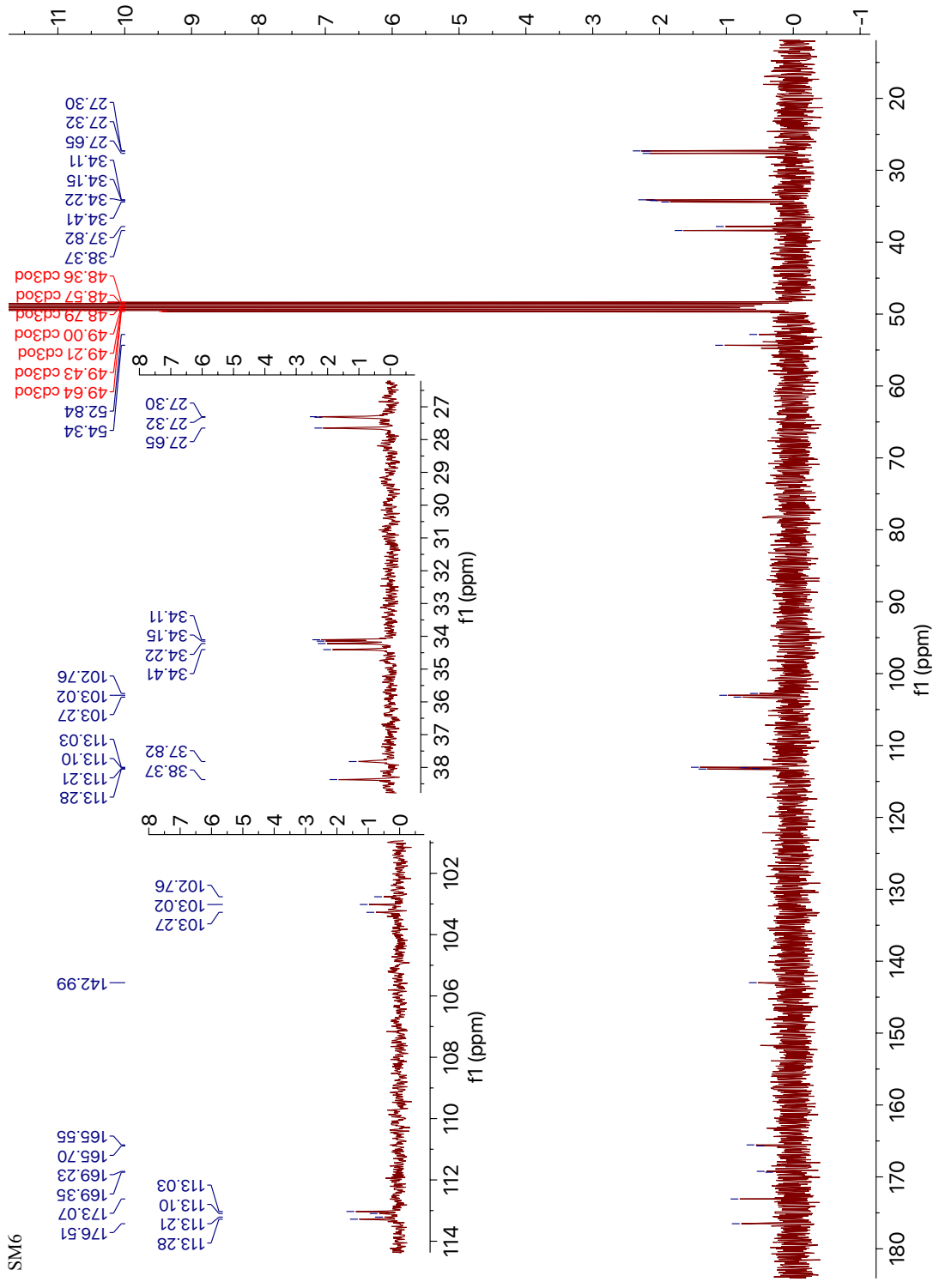




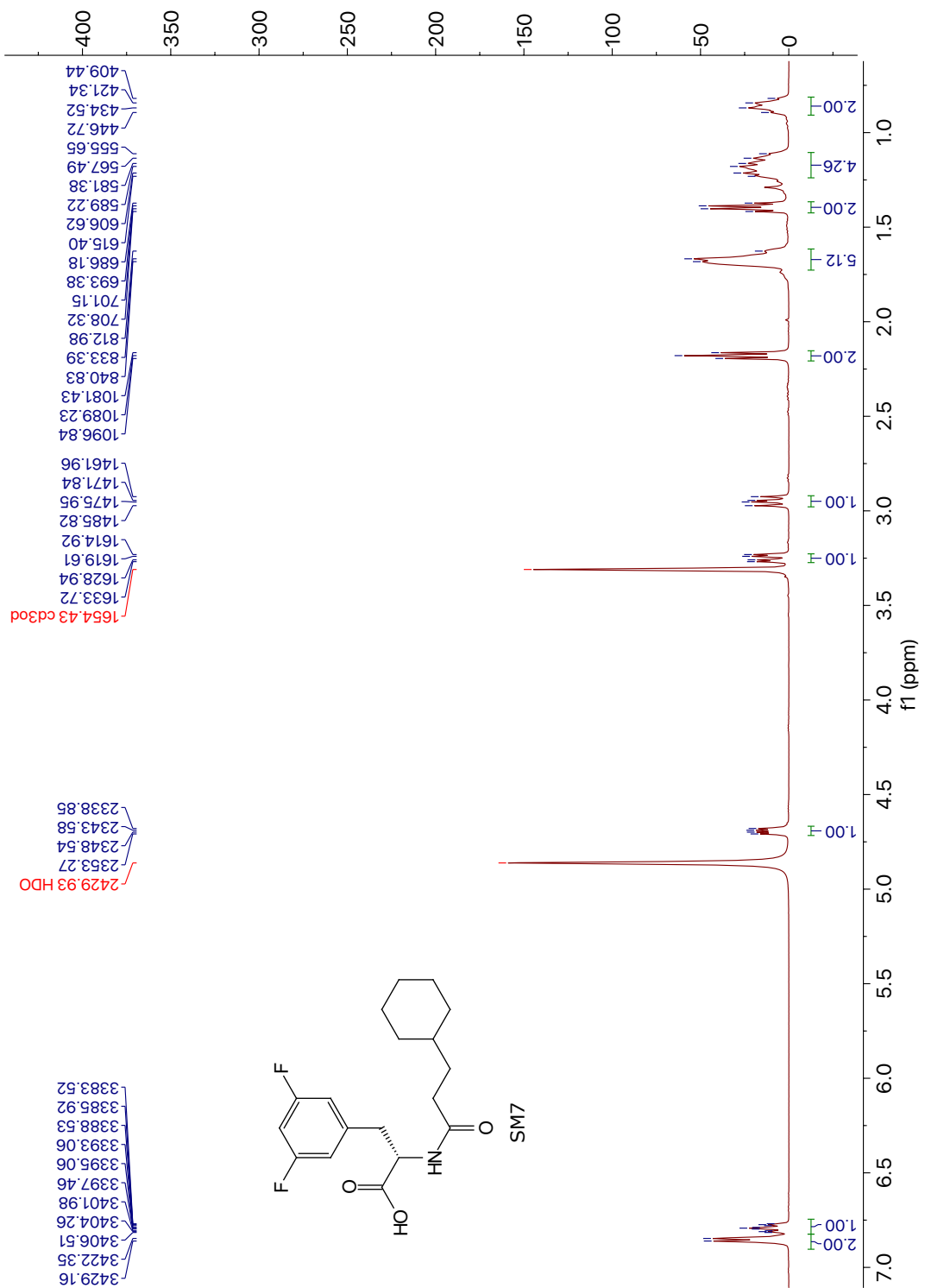


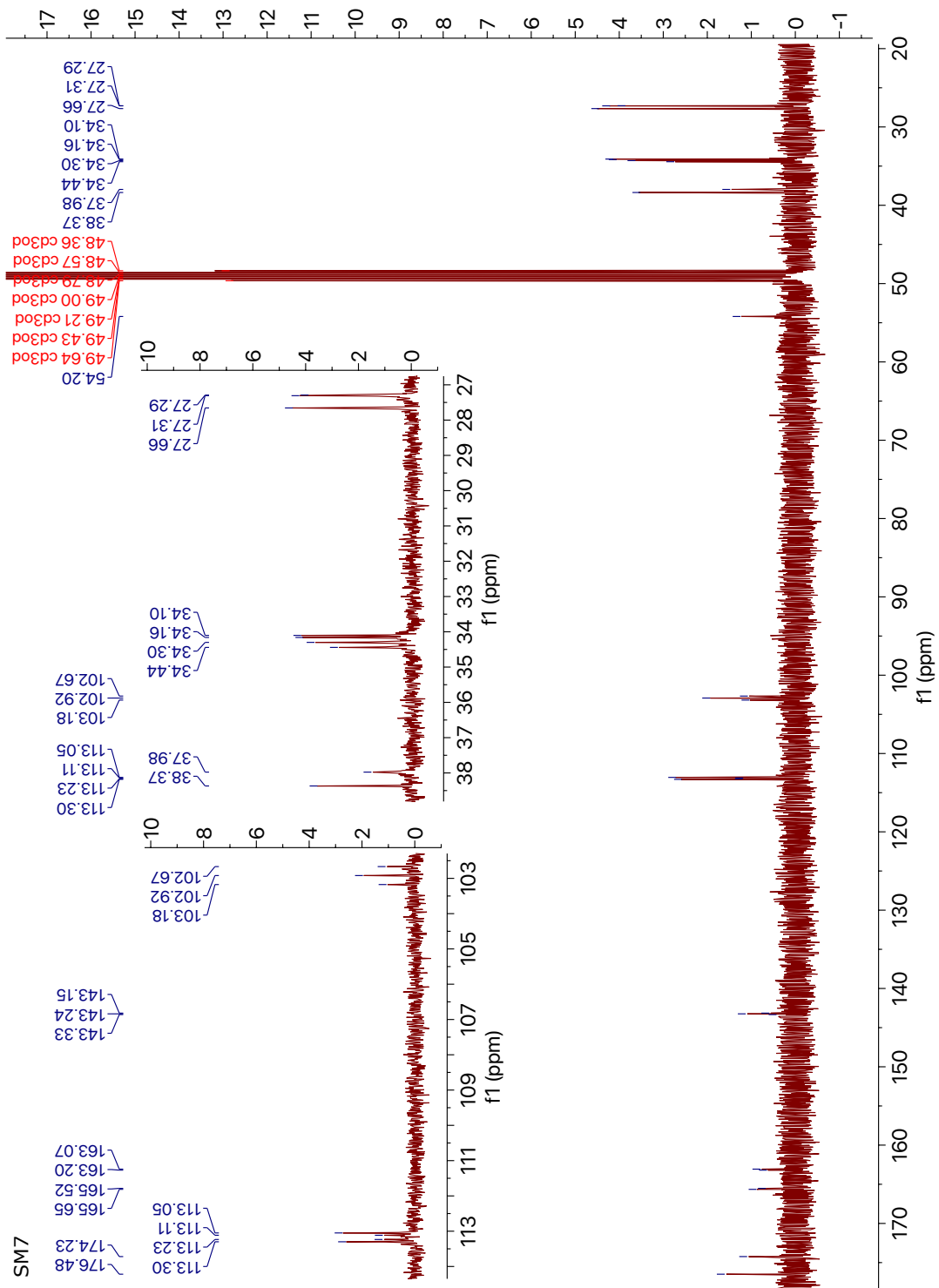


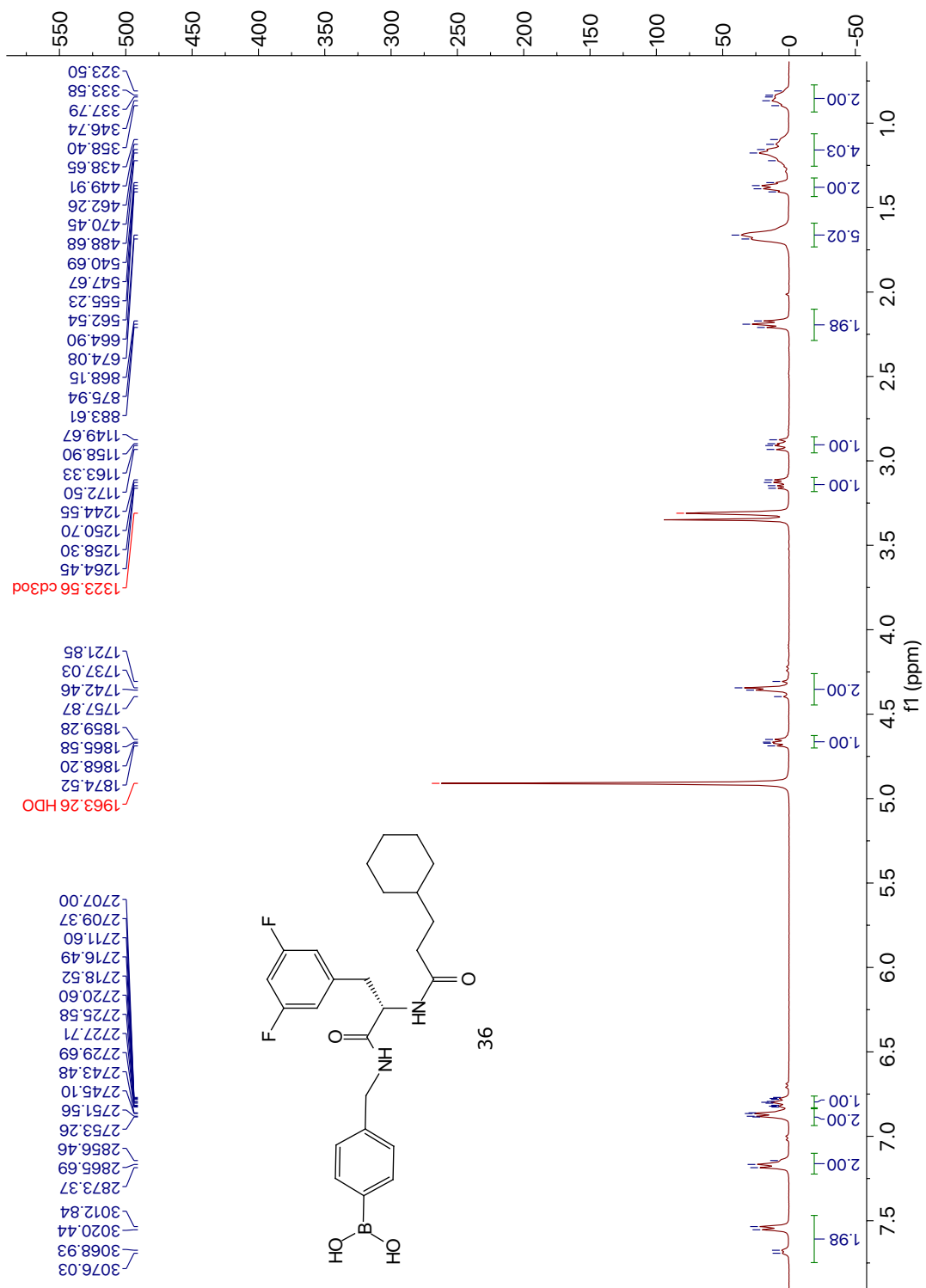


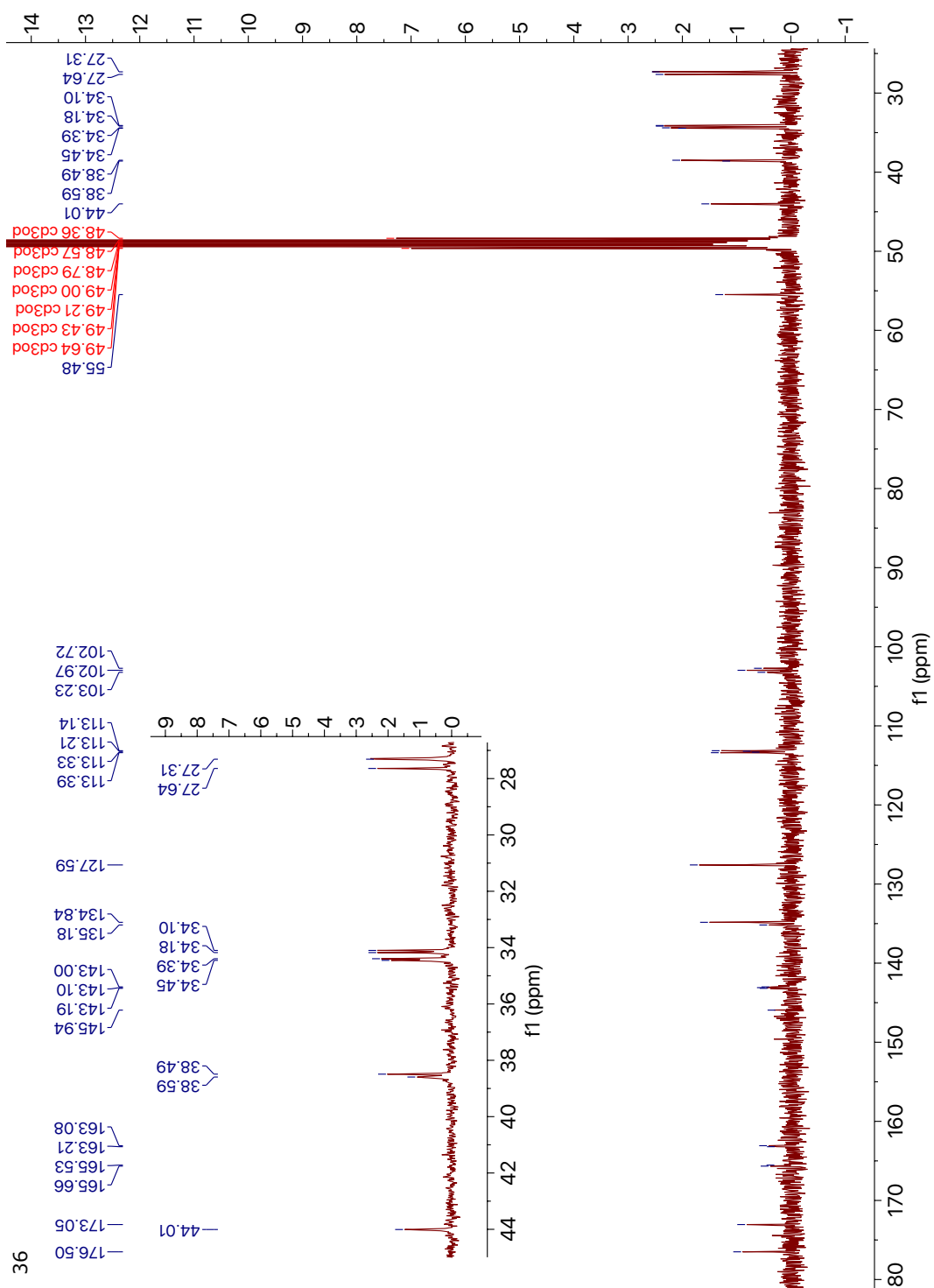


SM6

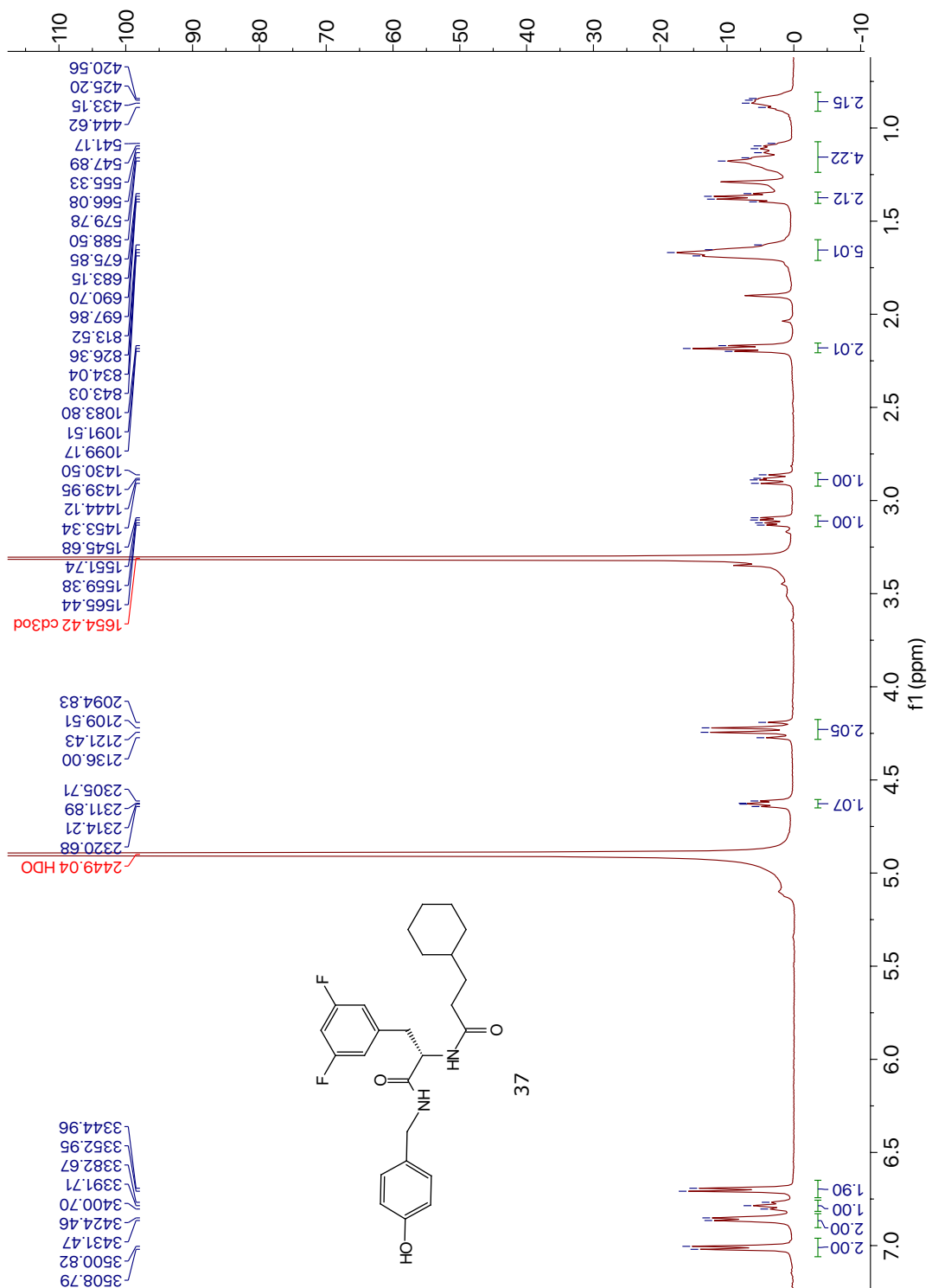


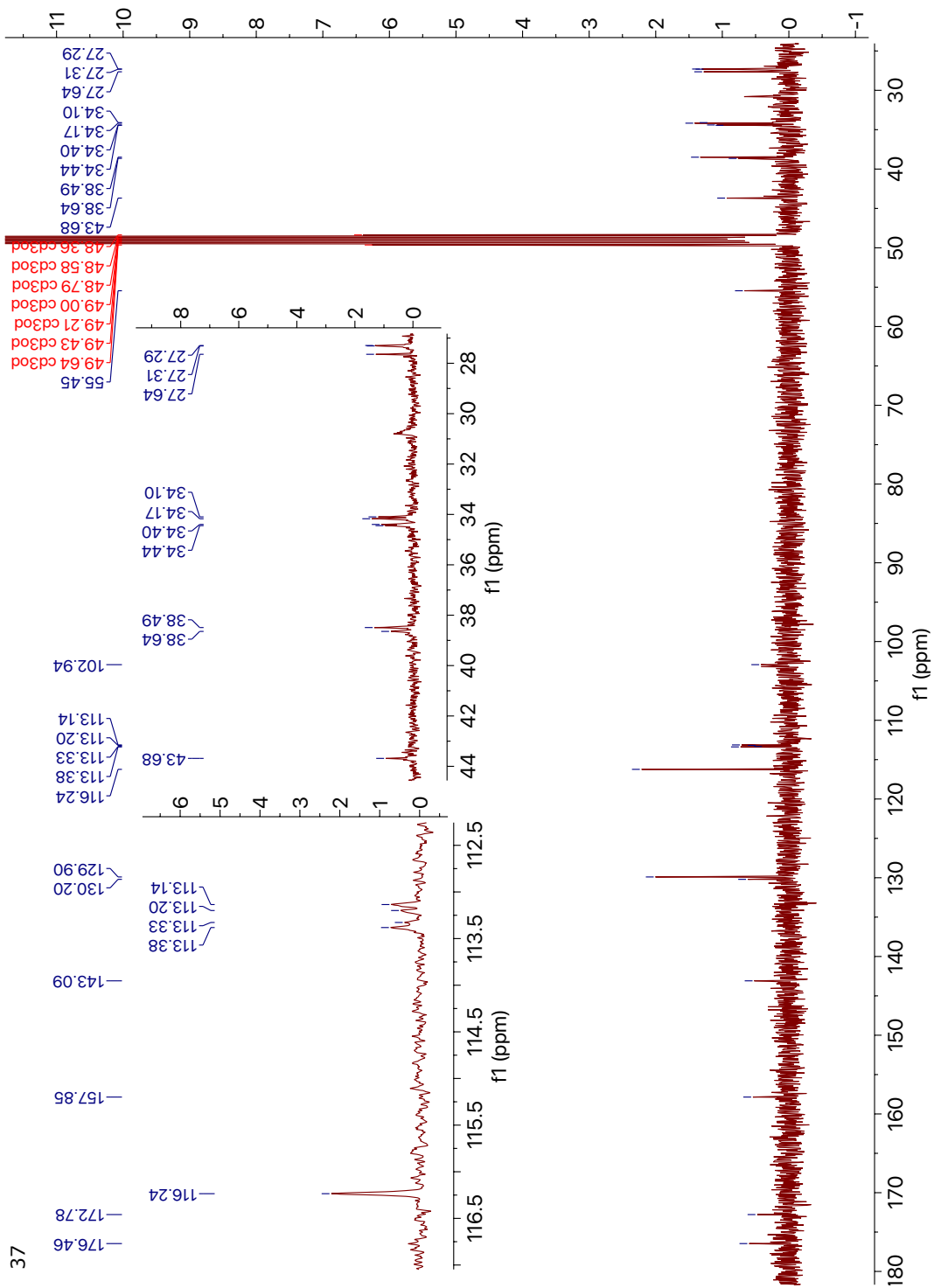




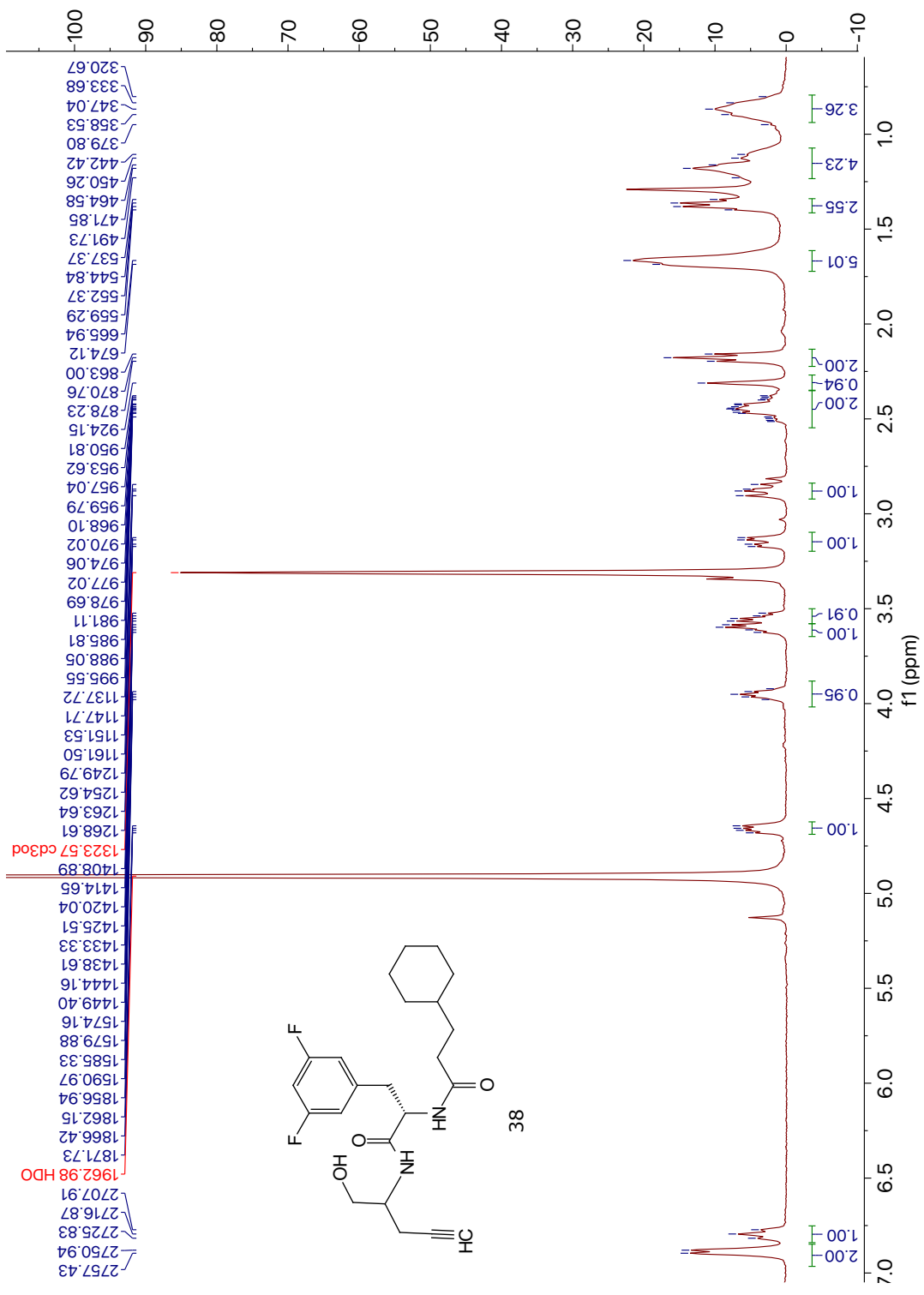


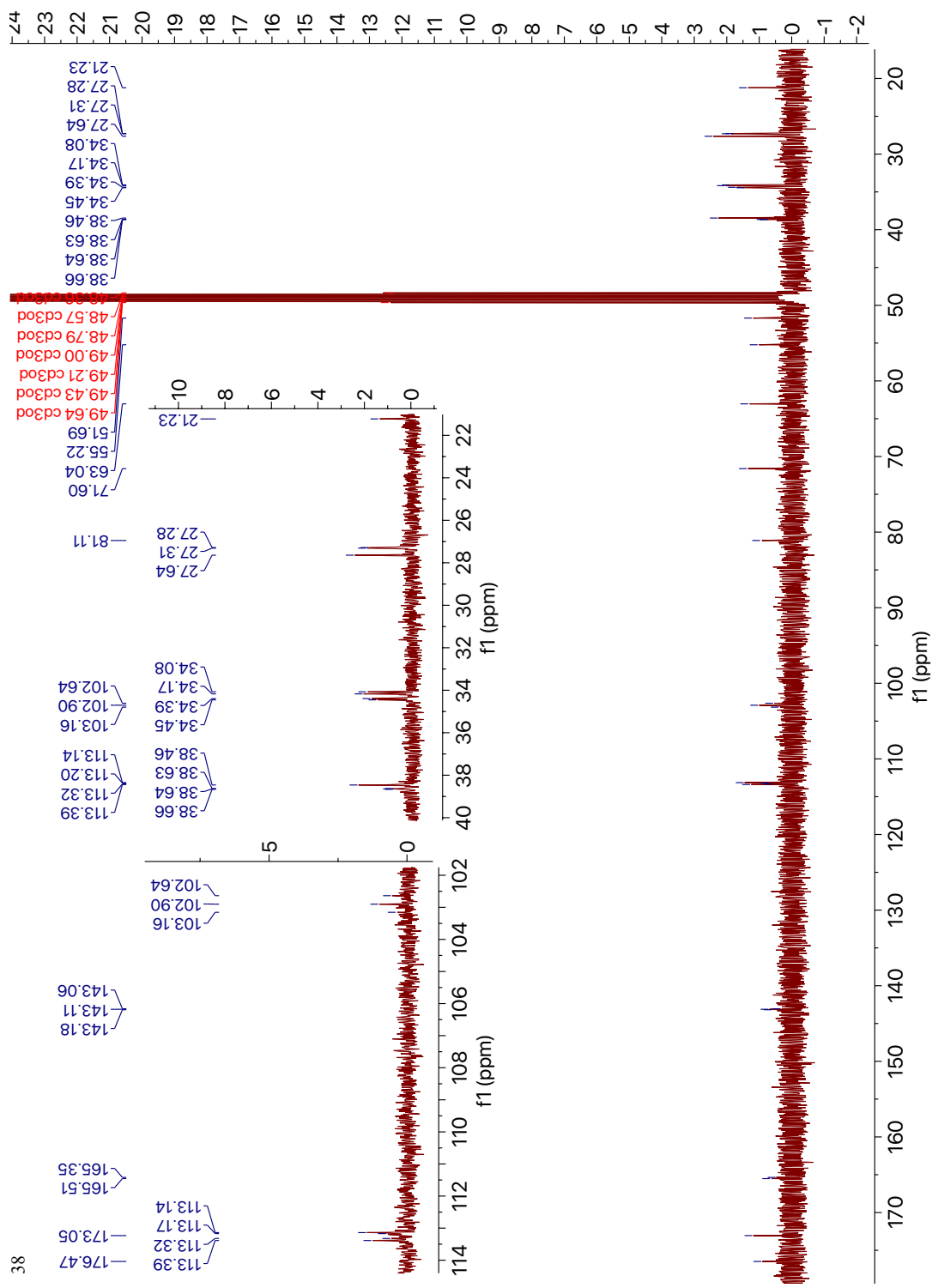
36



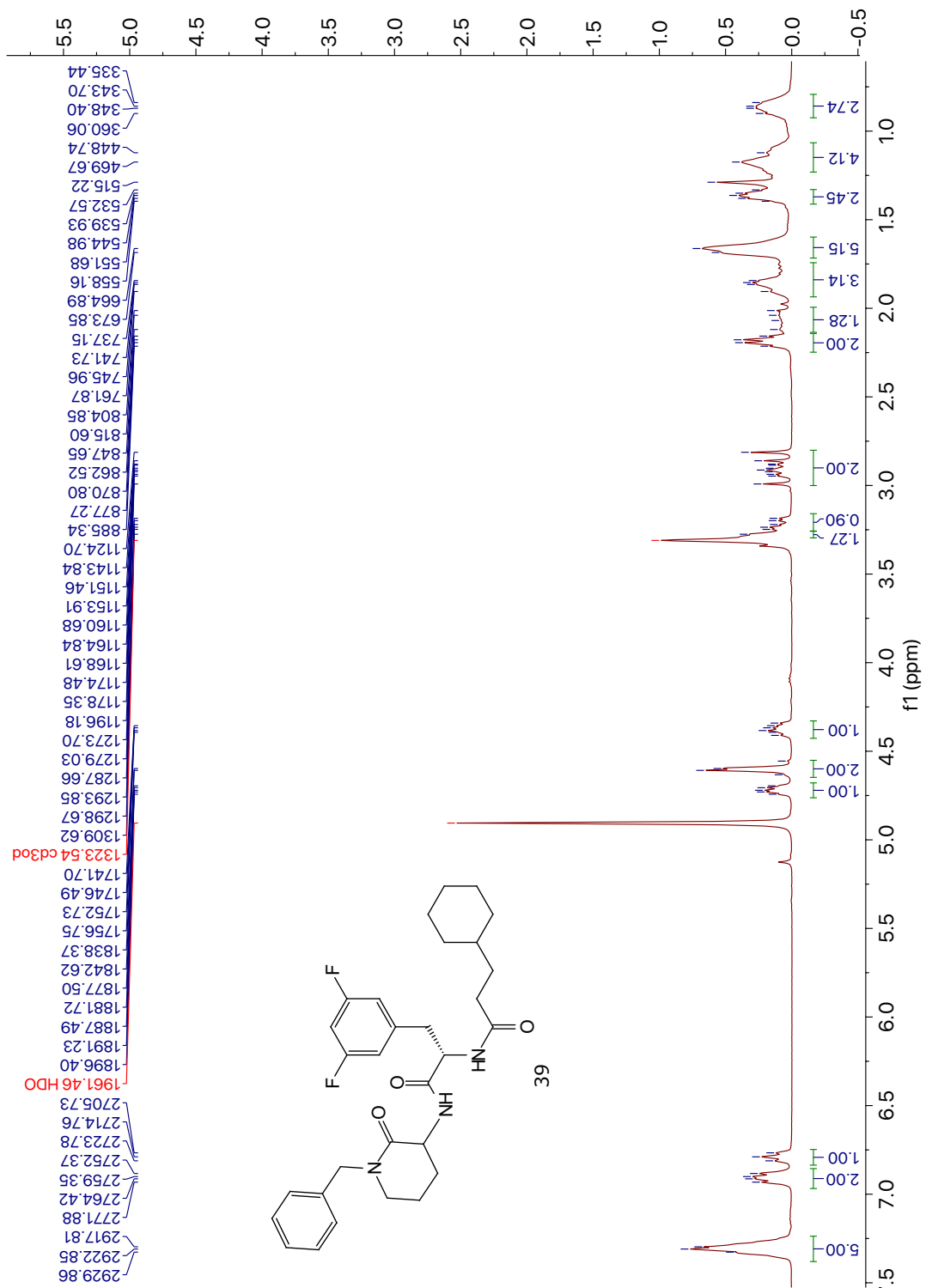


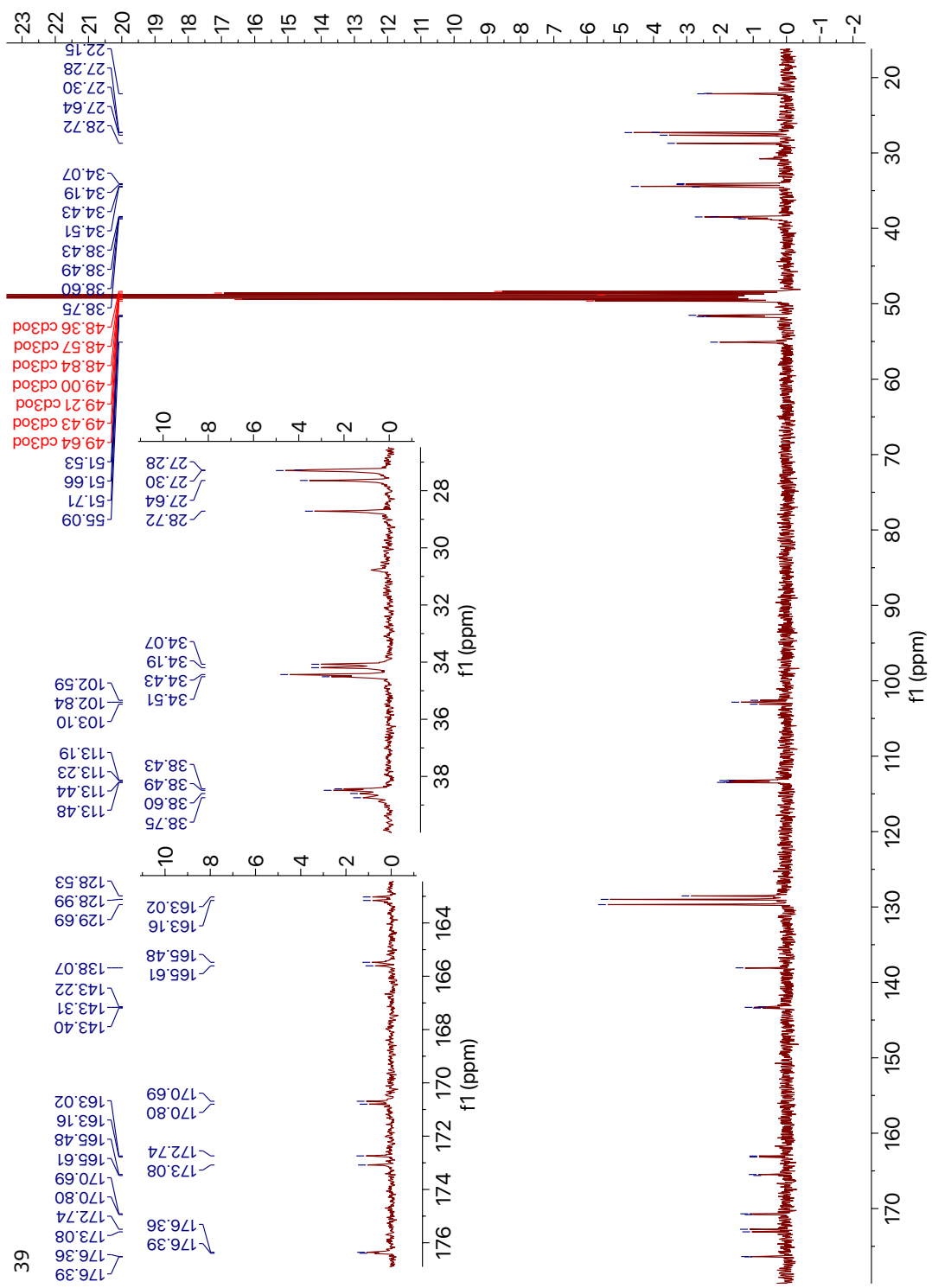
37

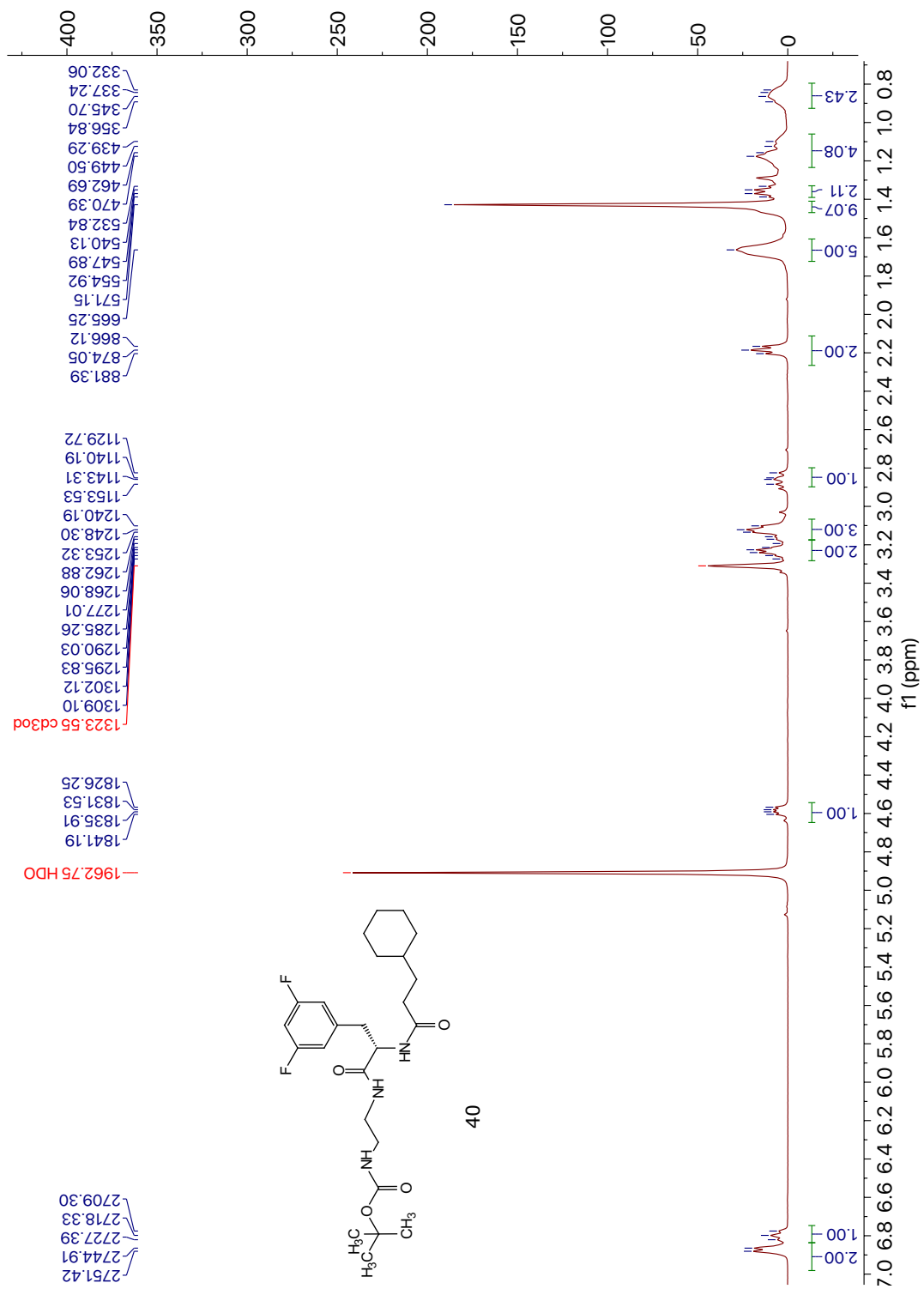


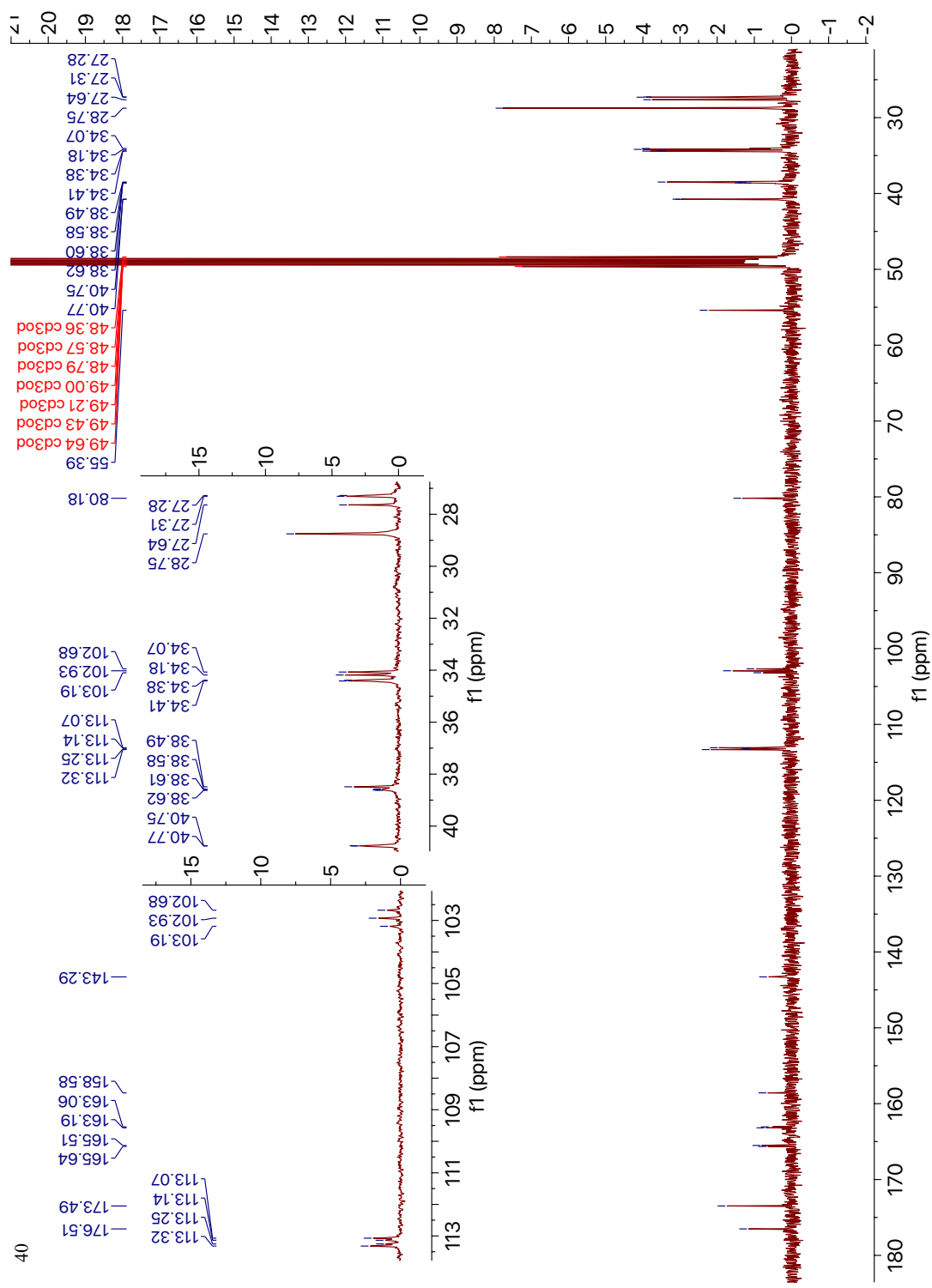


38

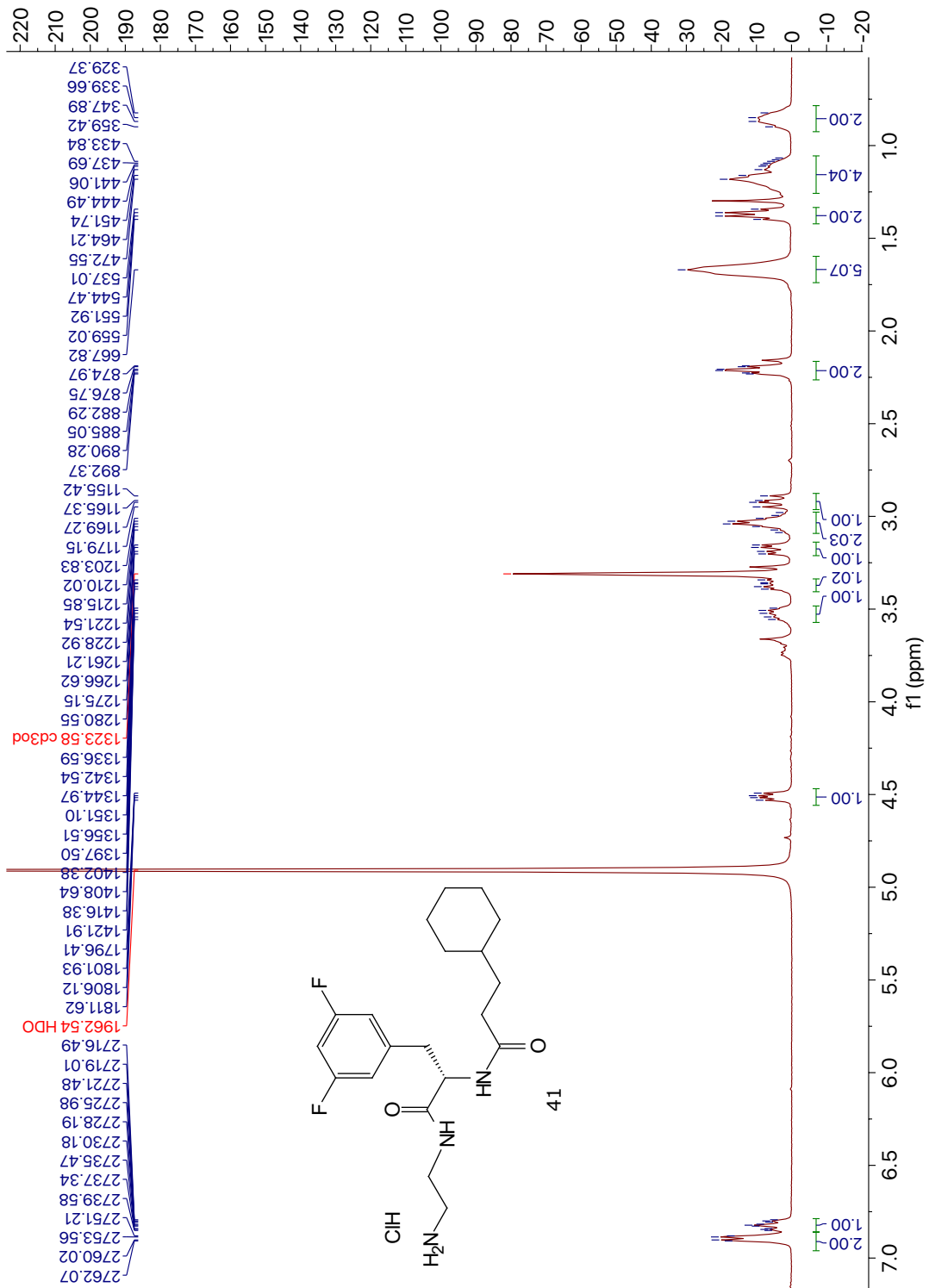


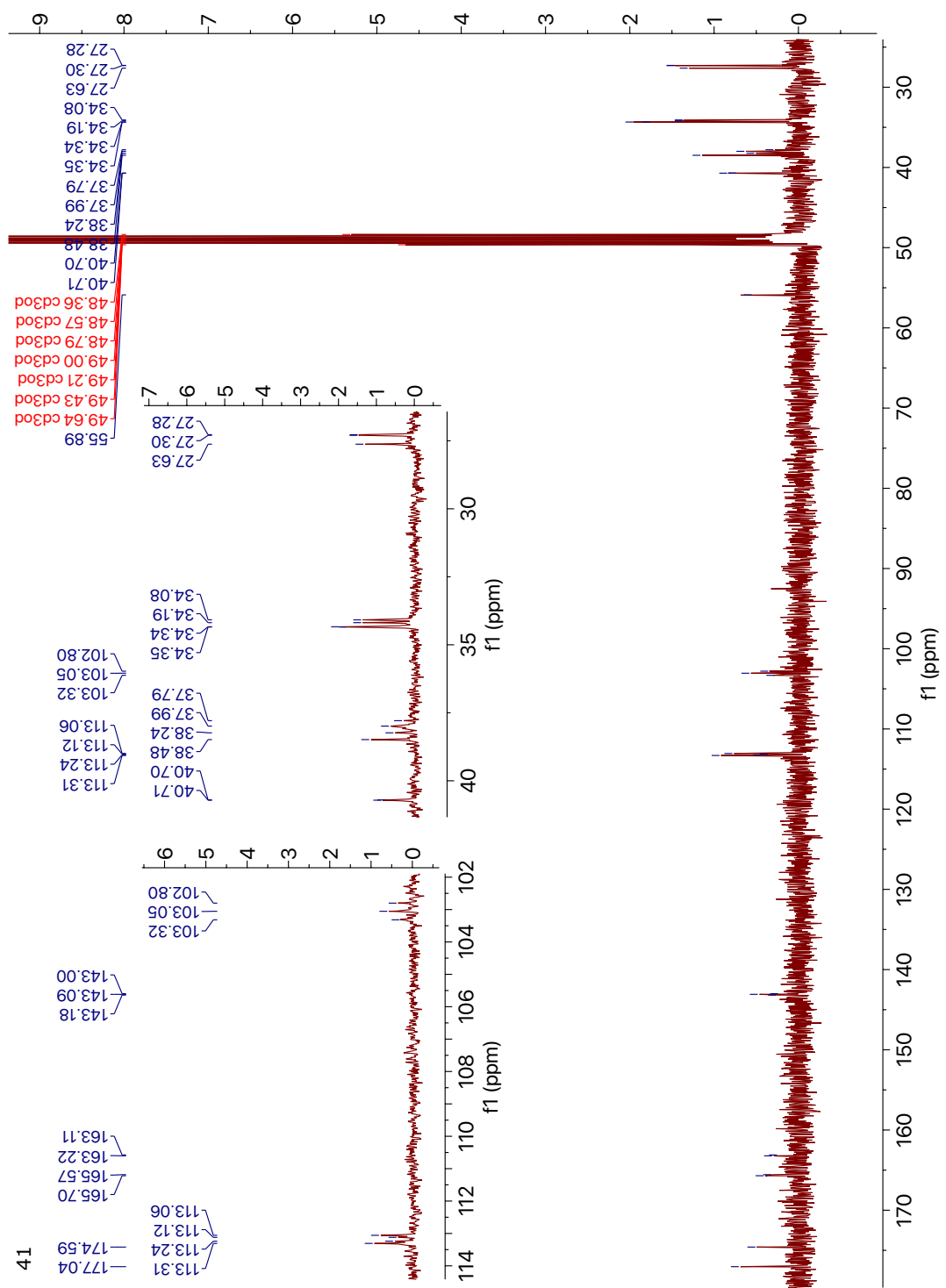




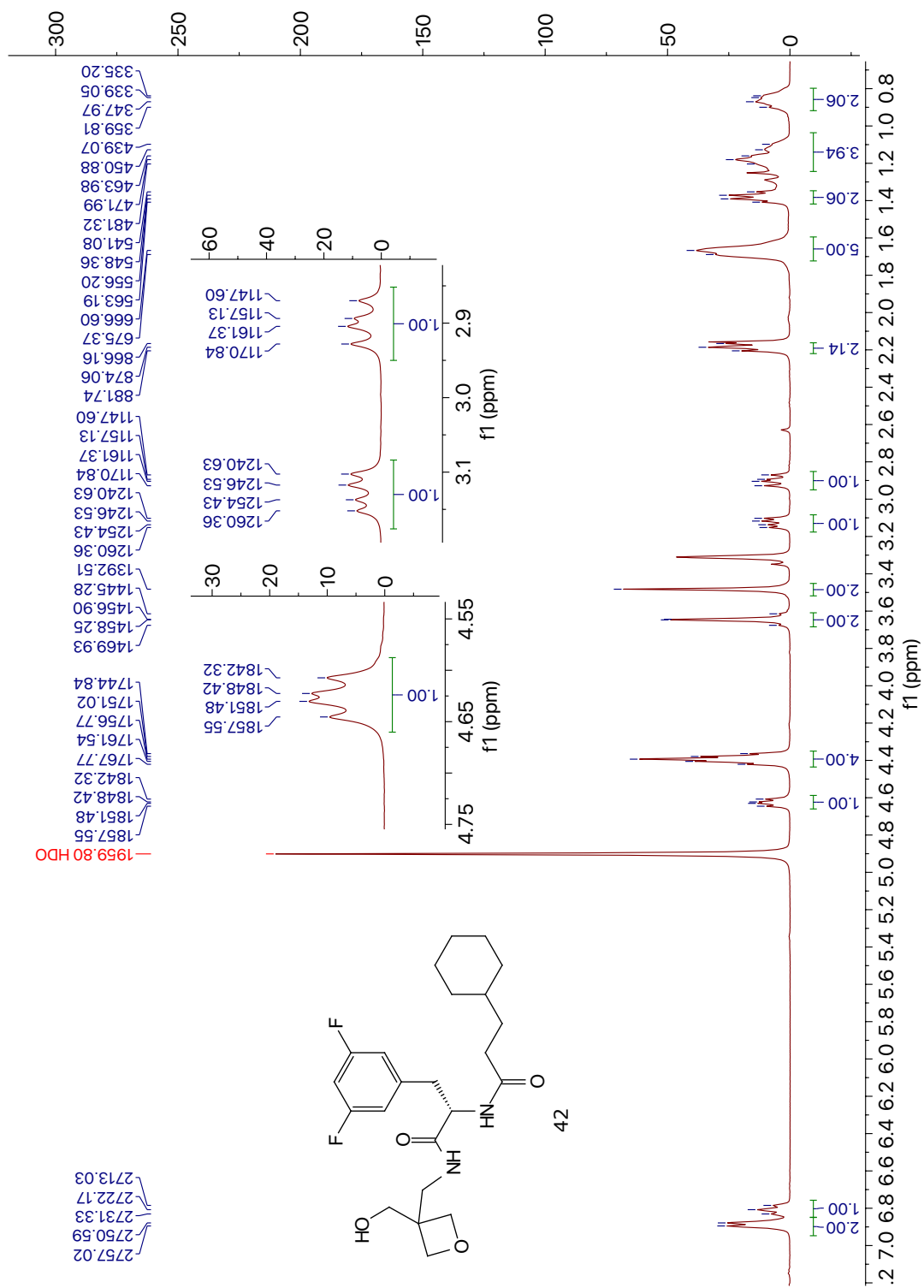


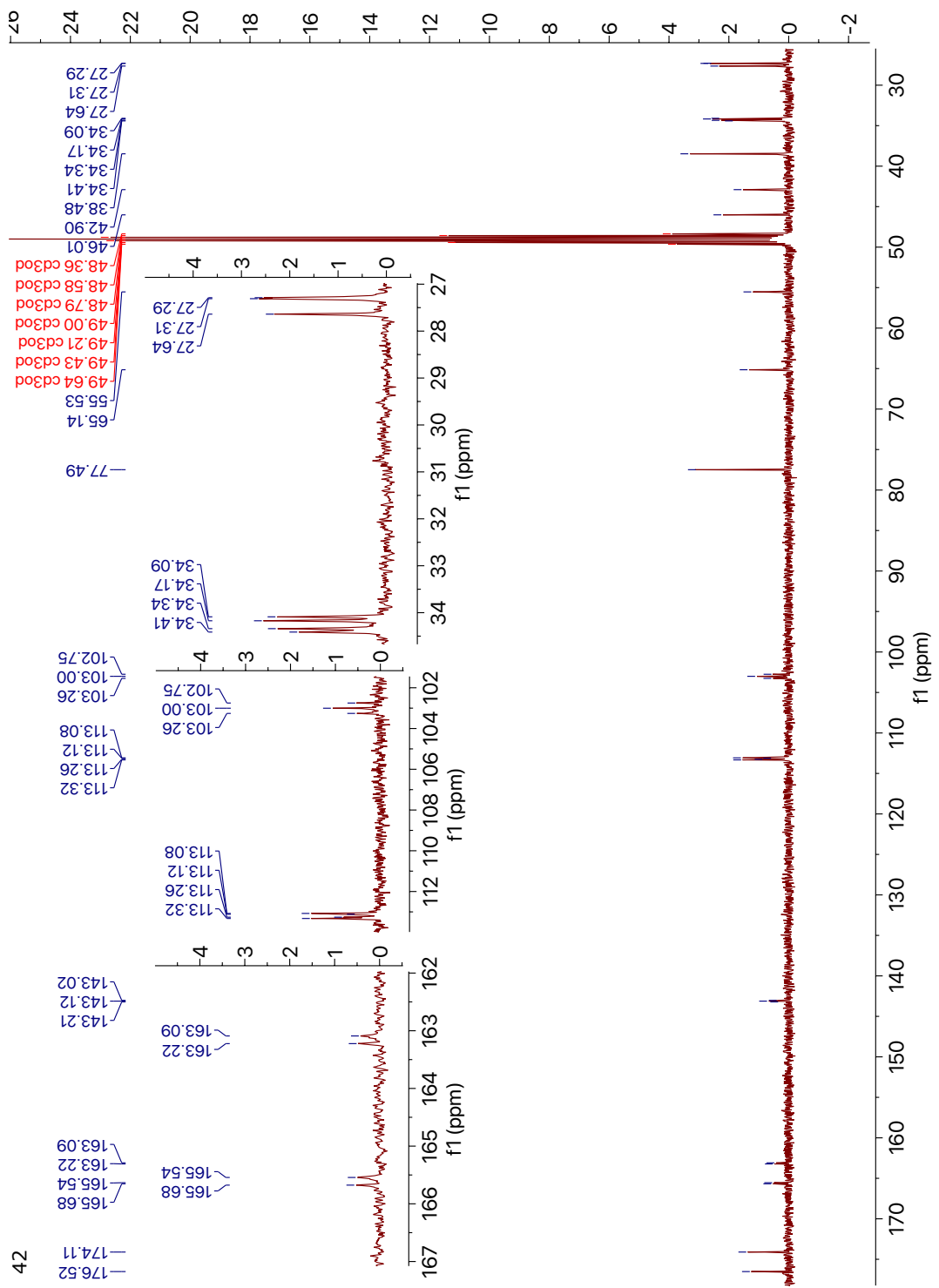
40



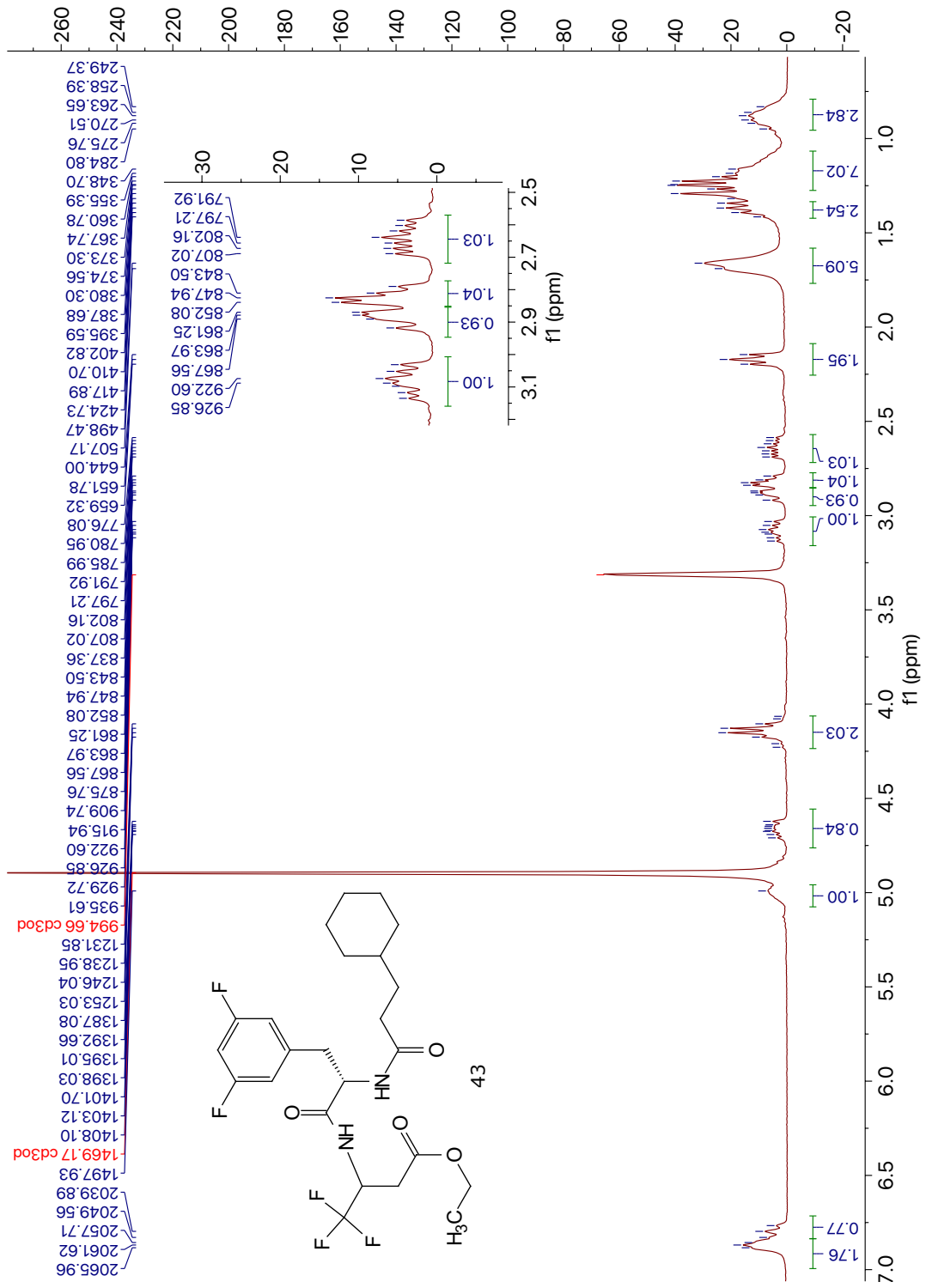


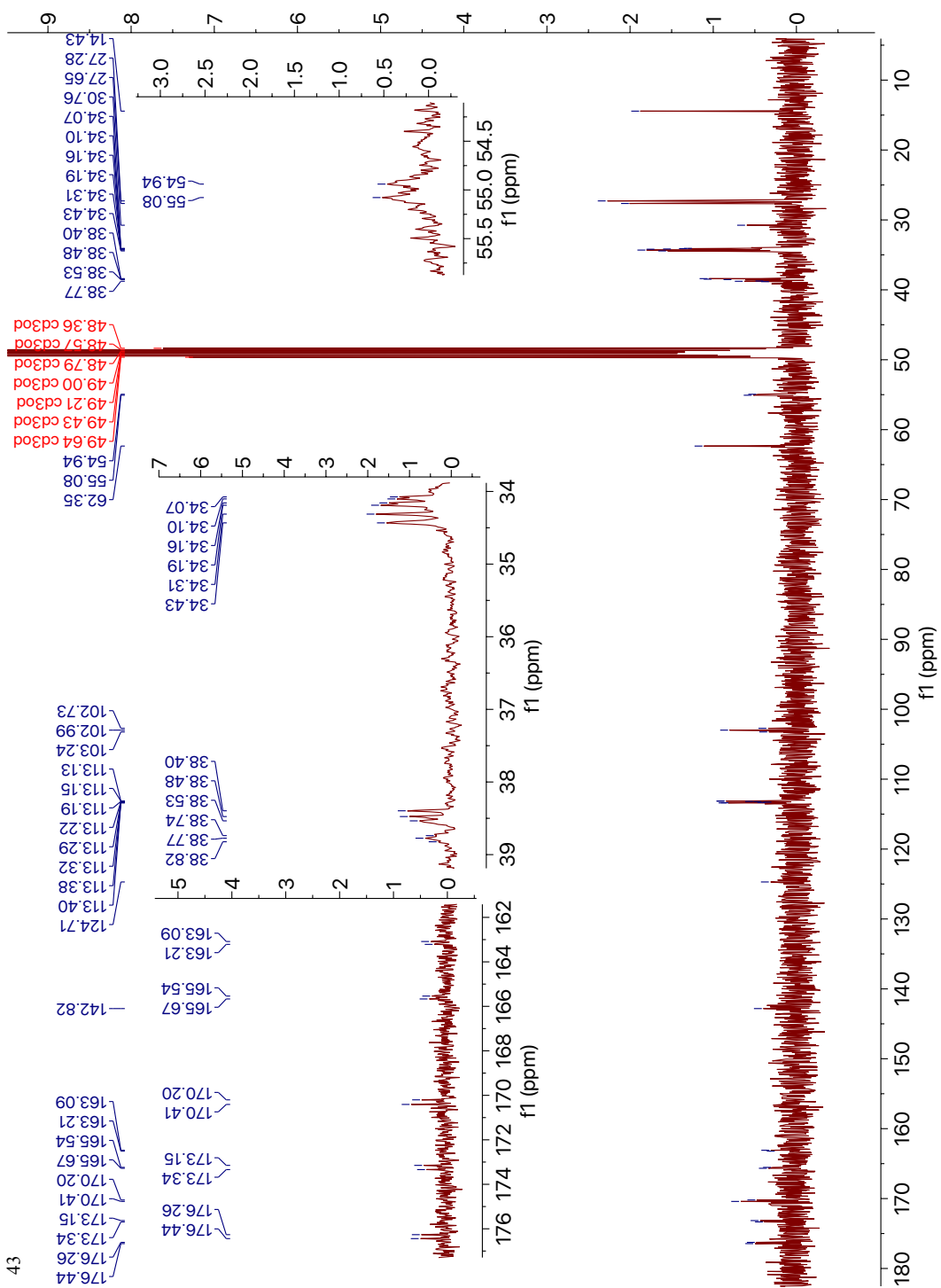
41

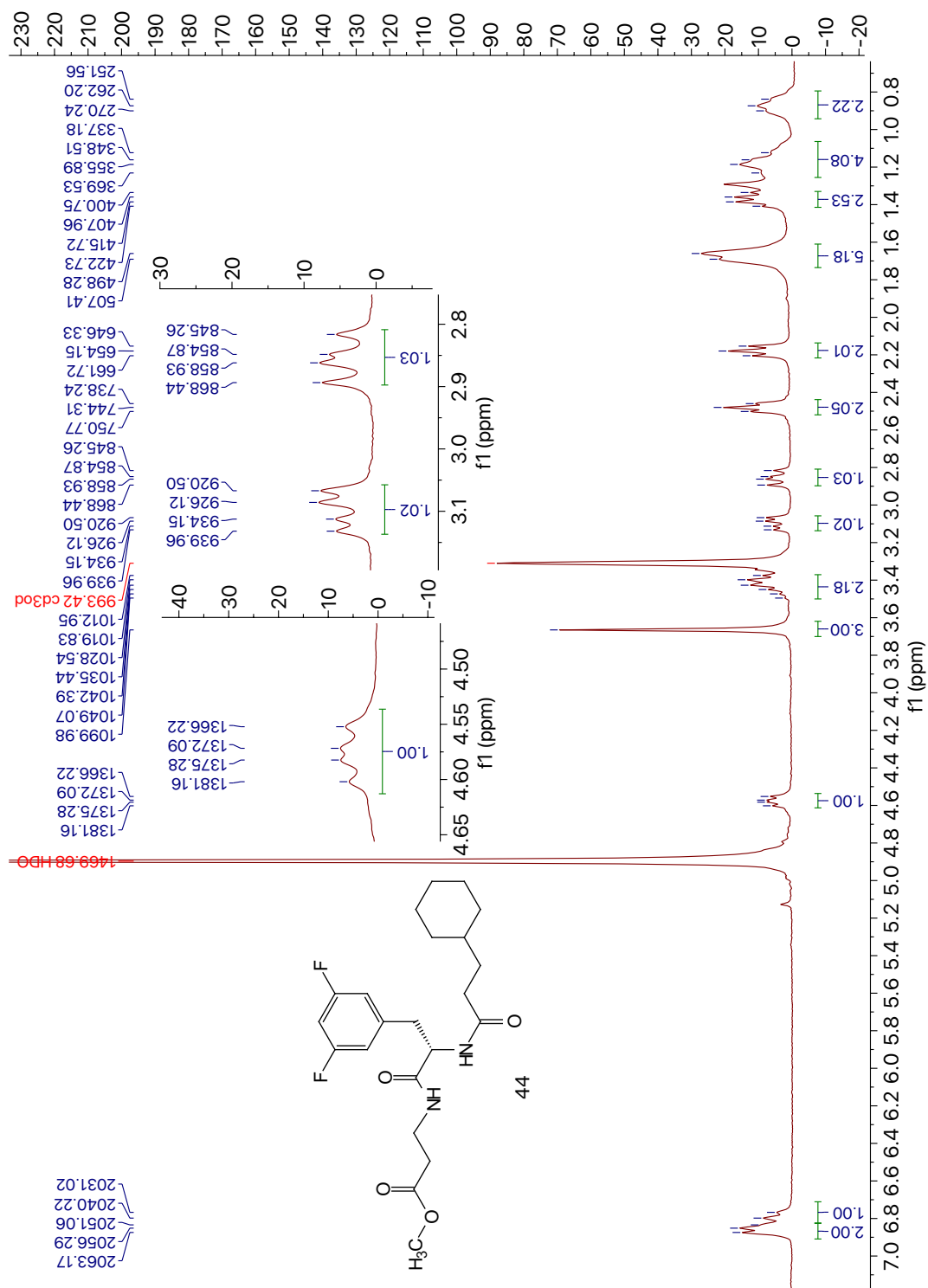


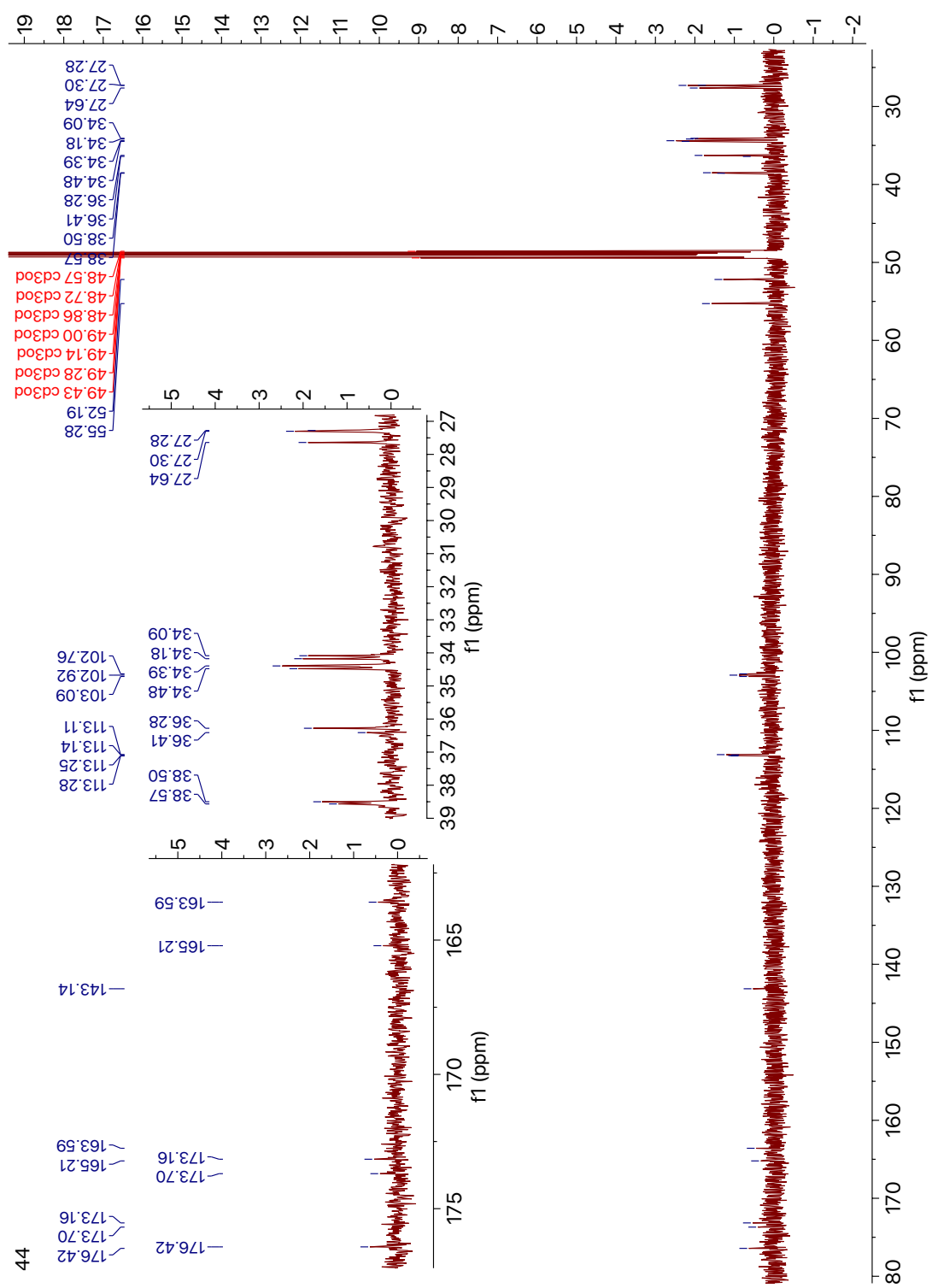


42

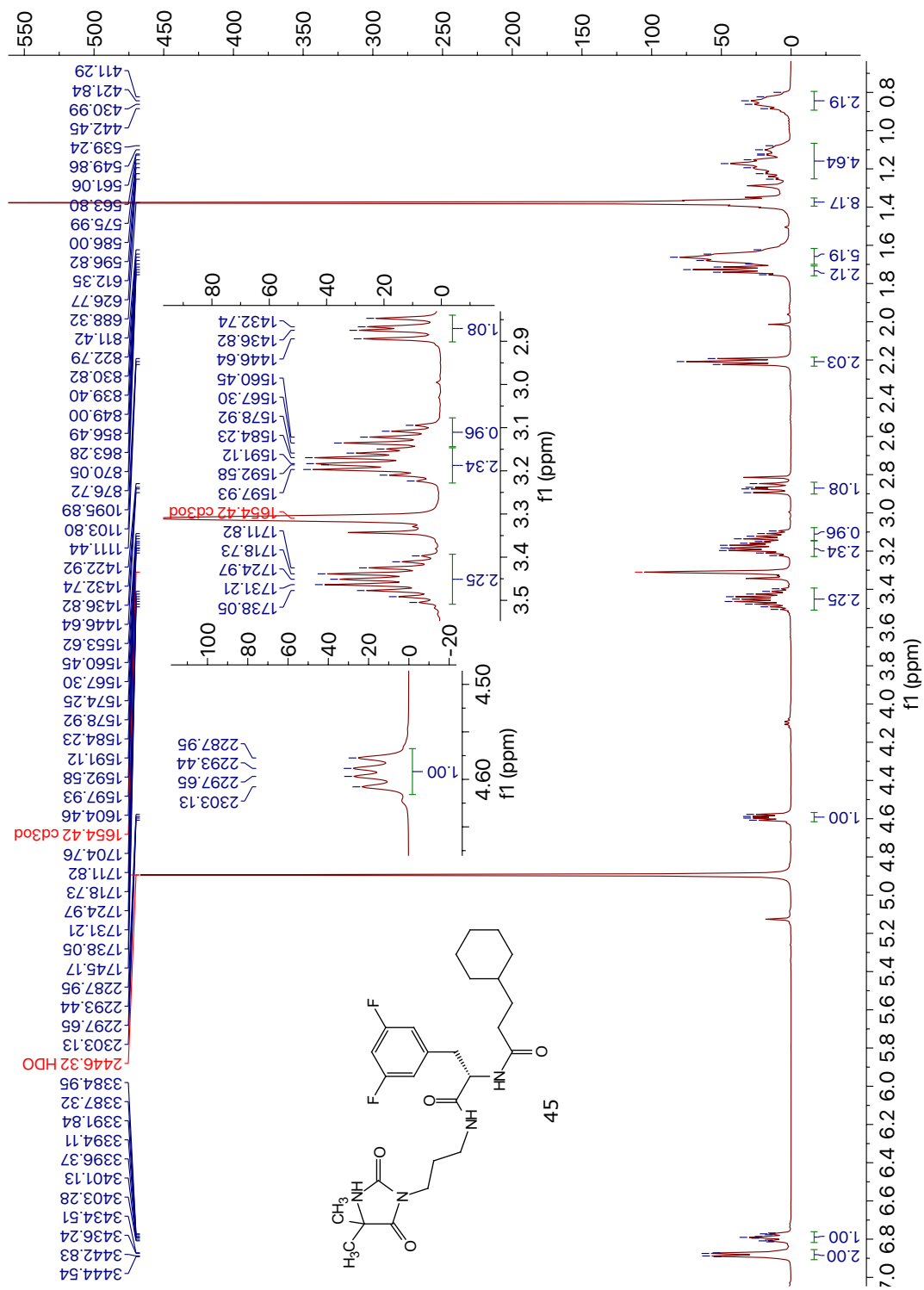


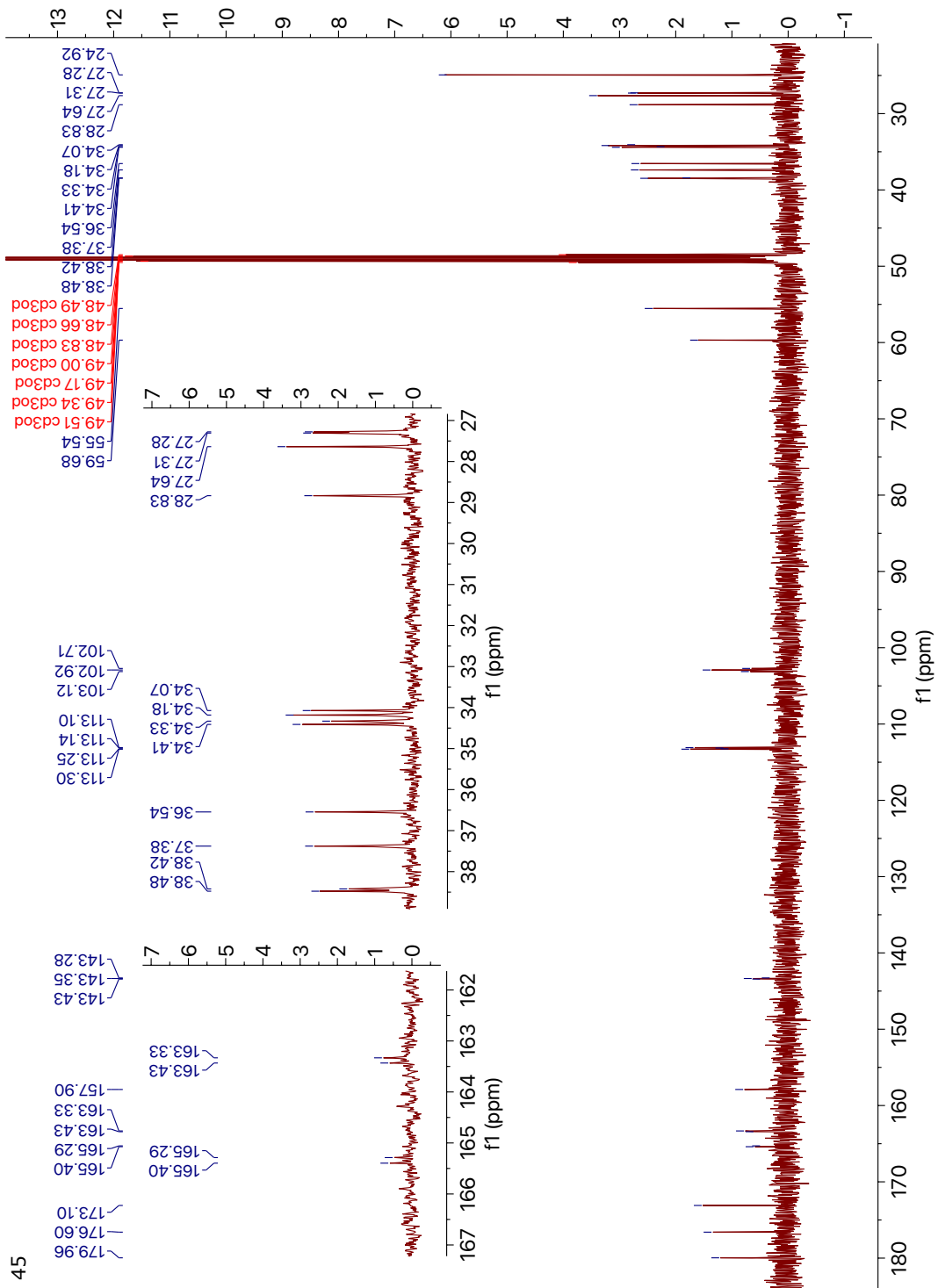




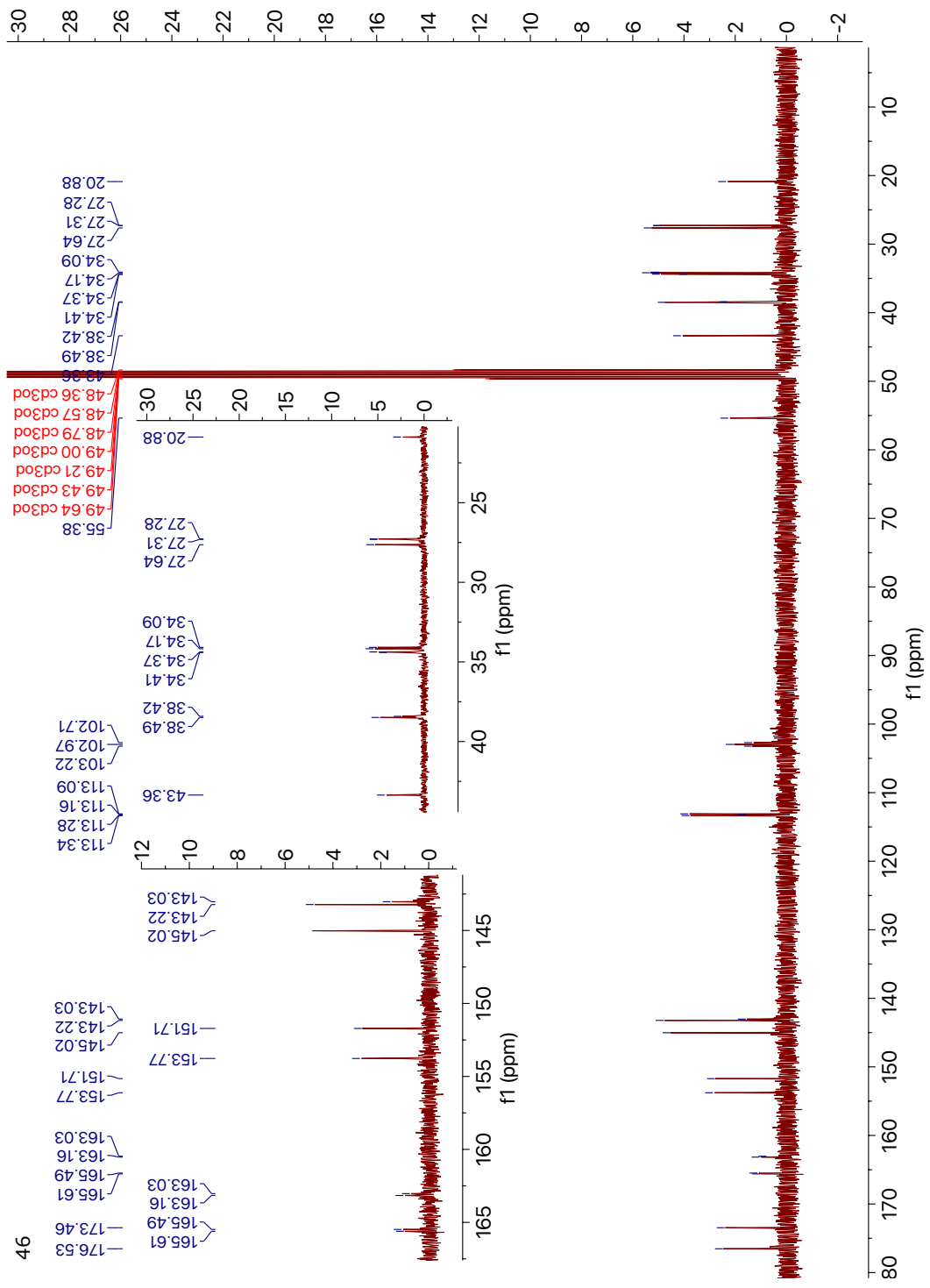


44

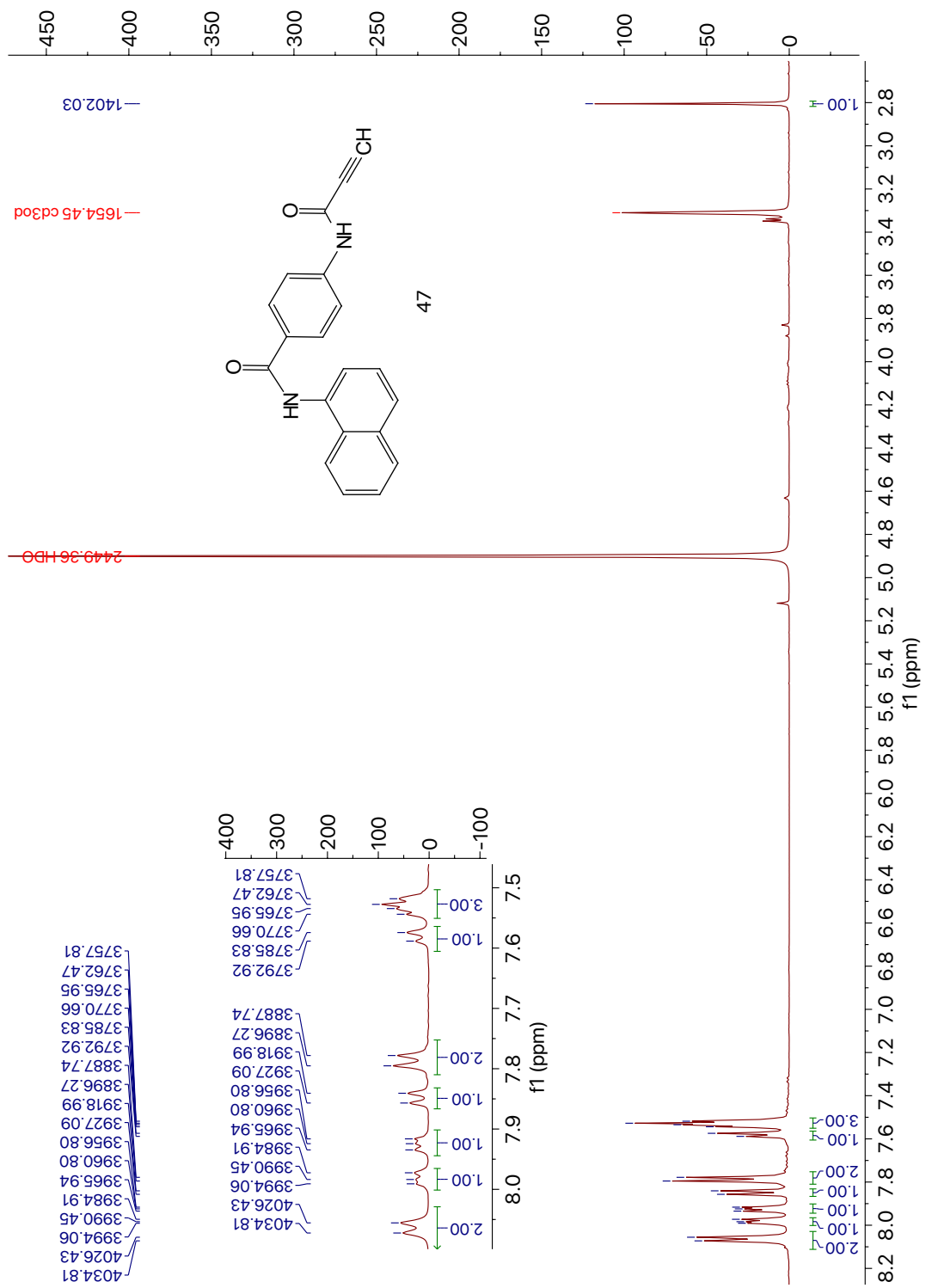


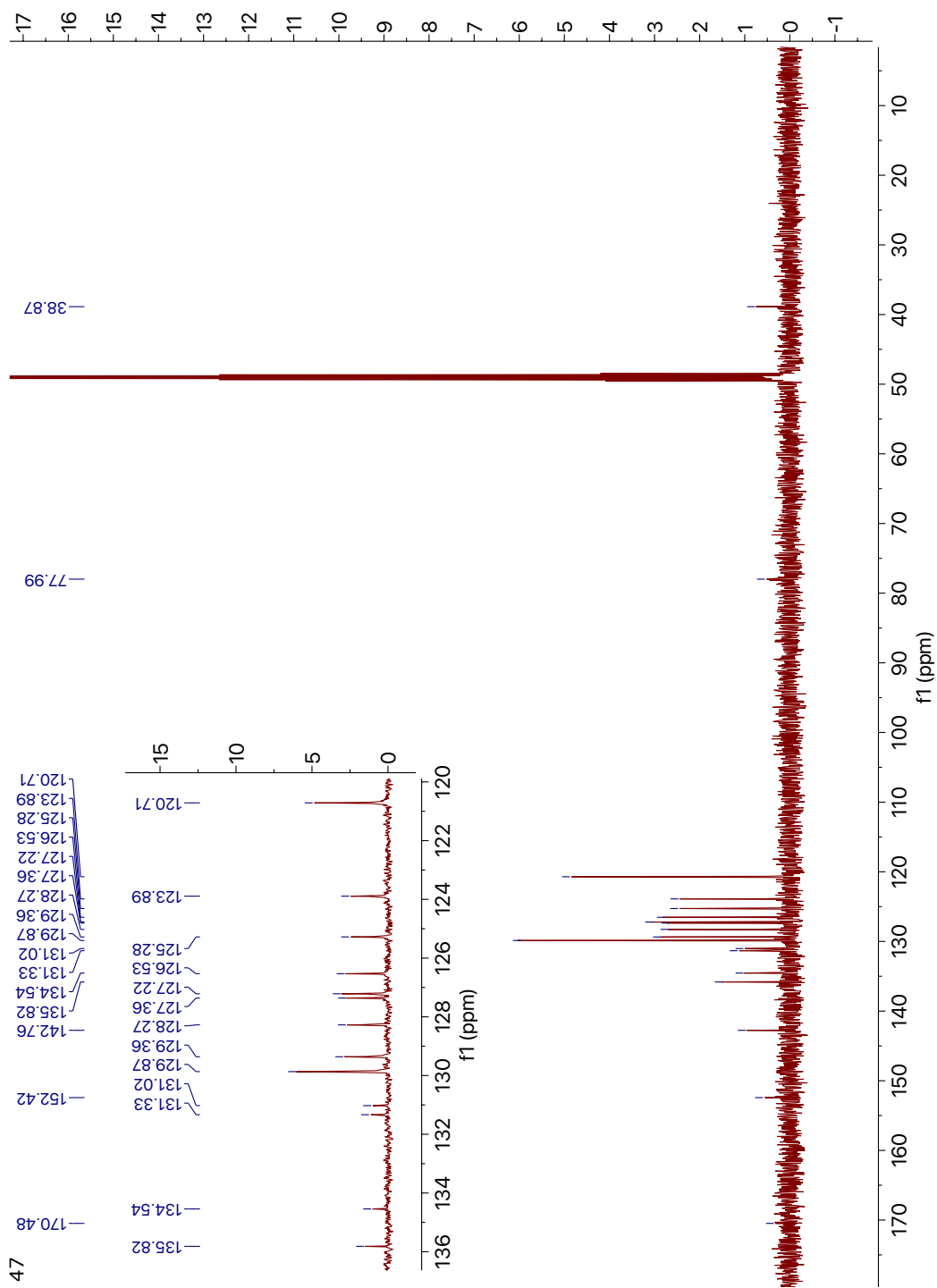


45

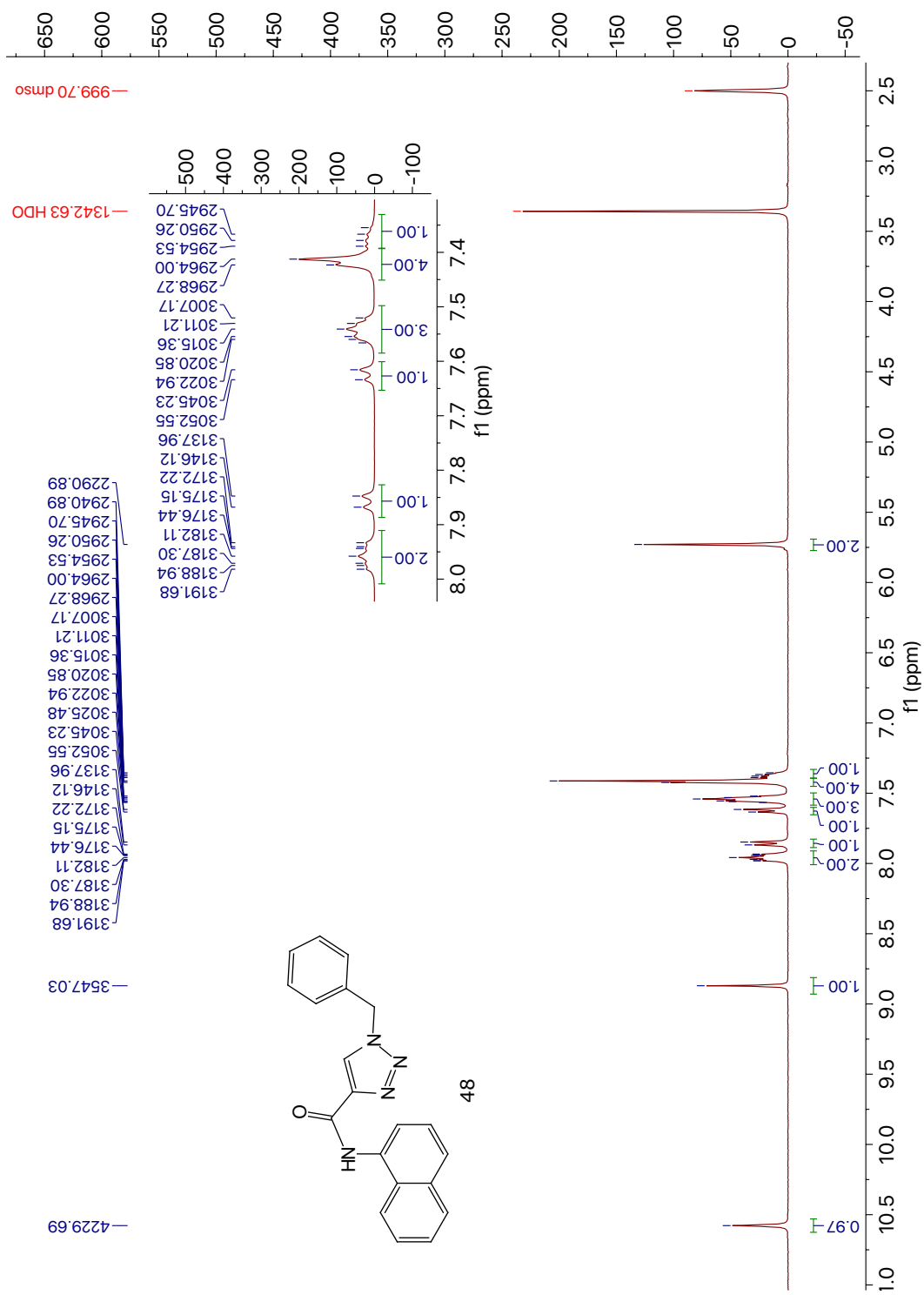


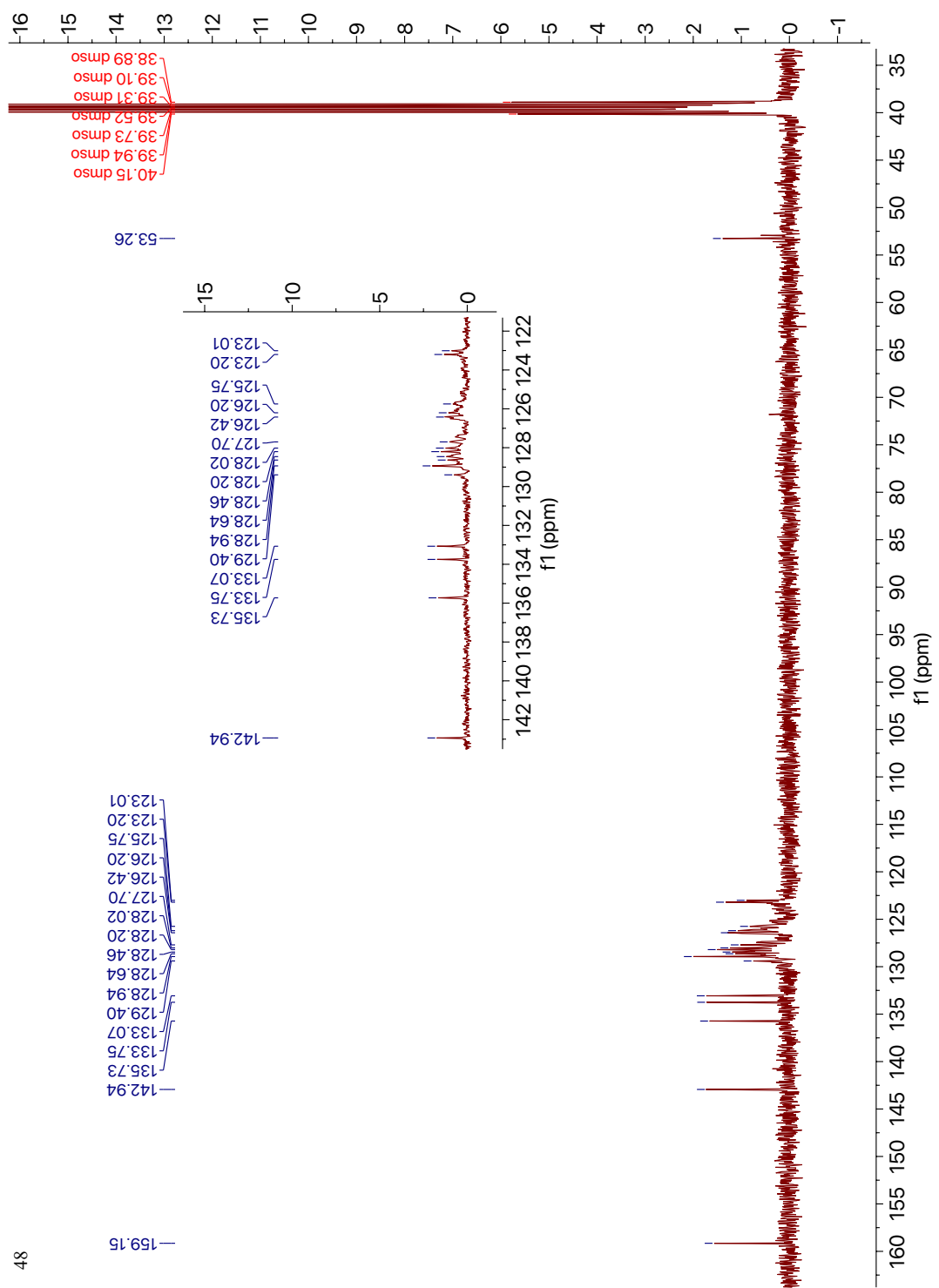
46

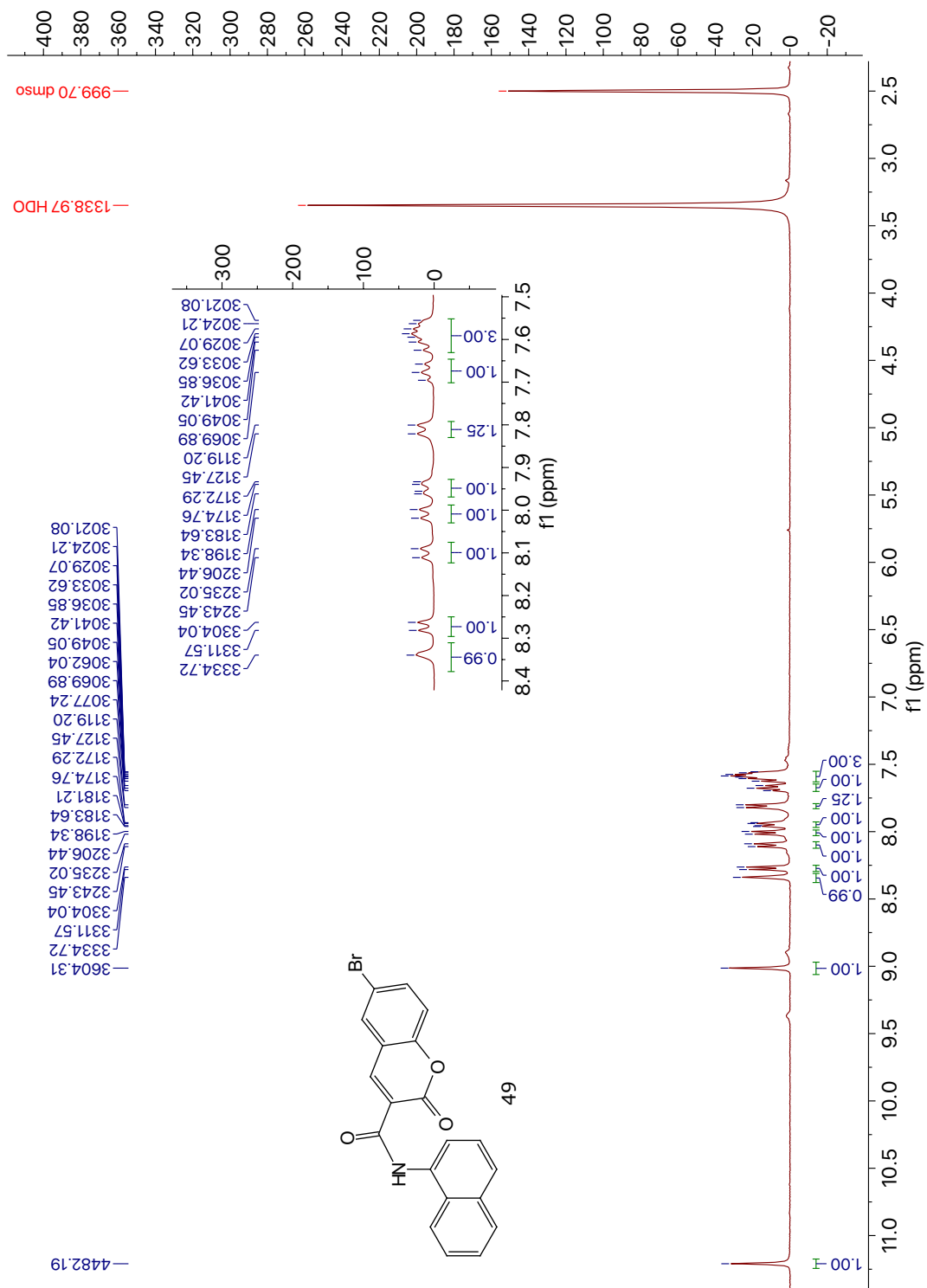


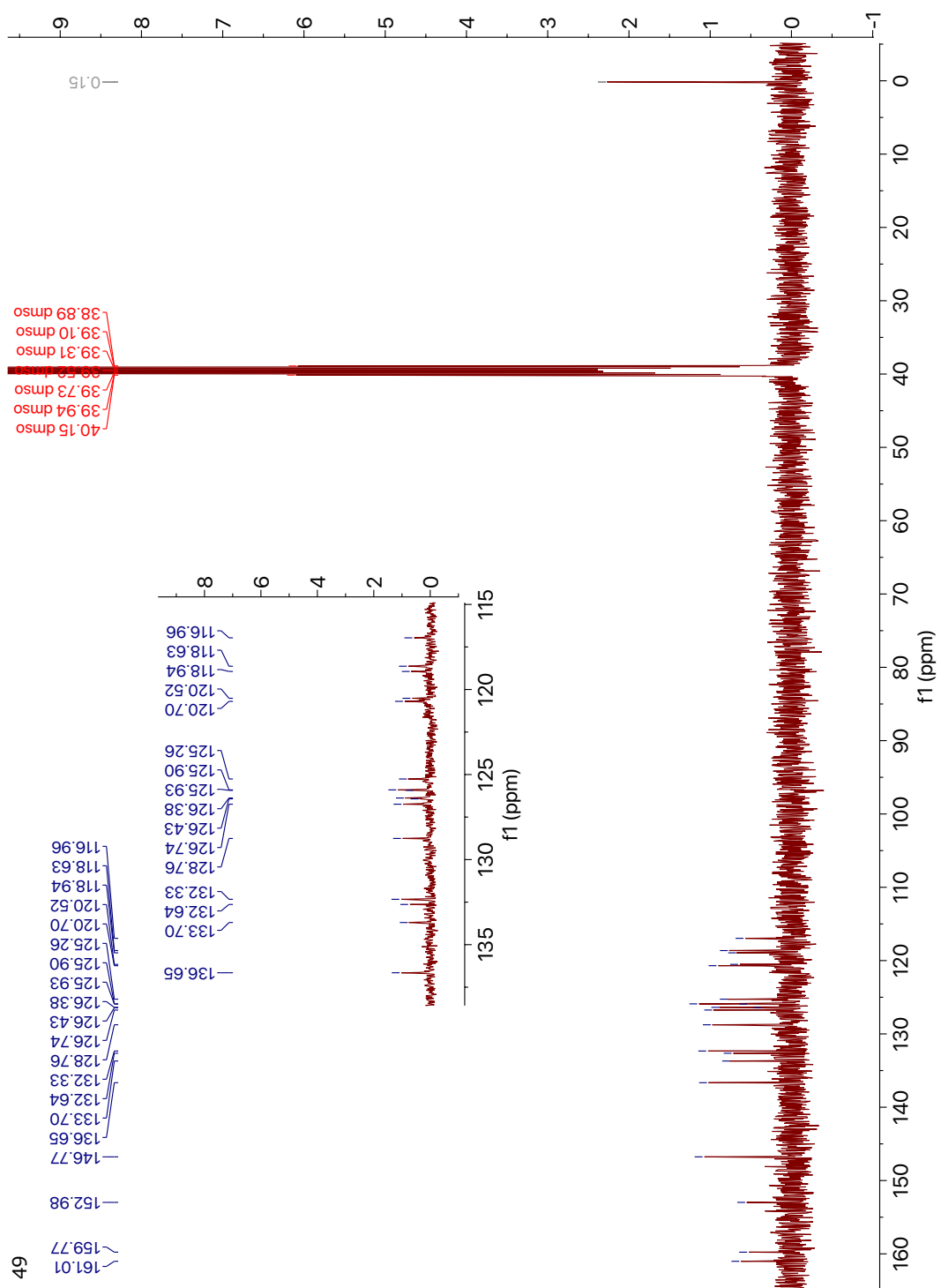


47

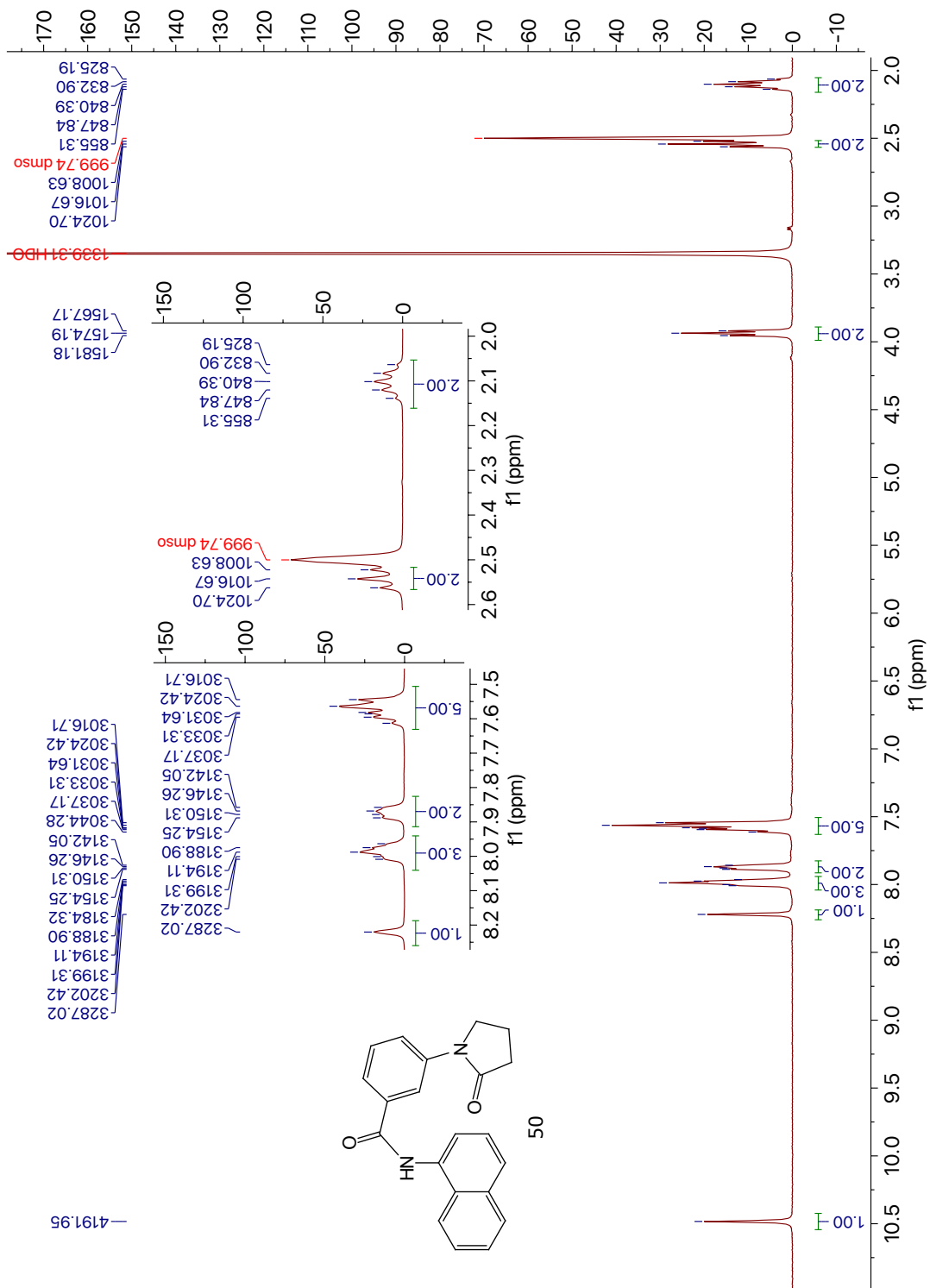


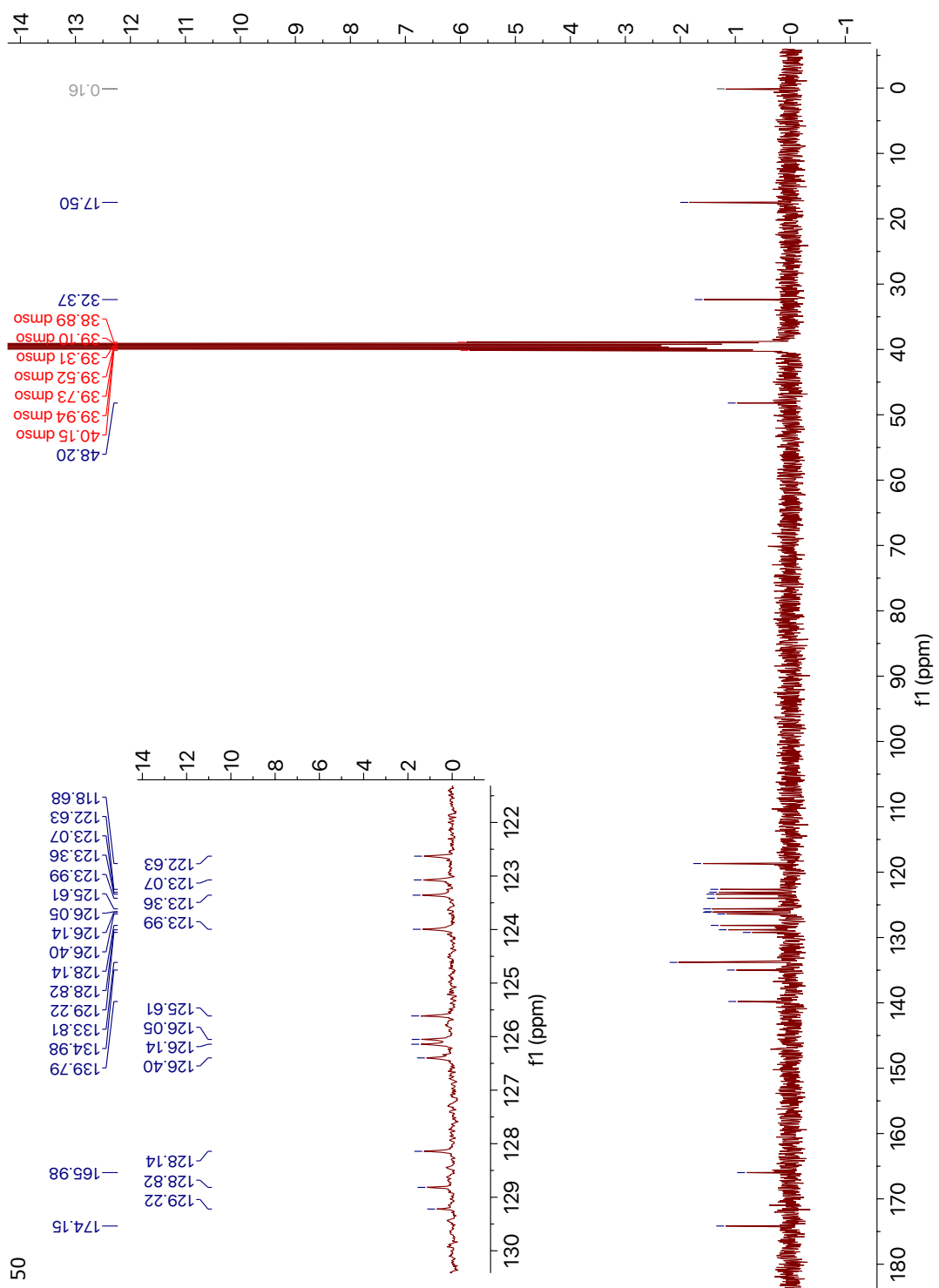




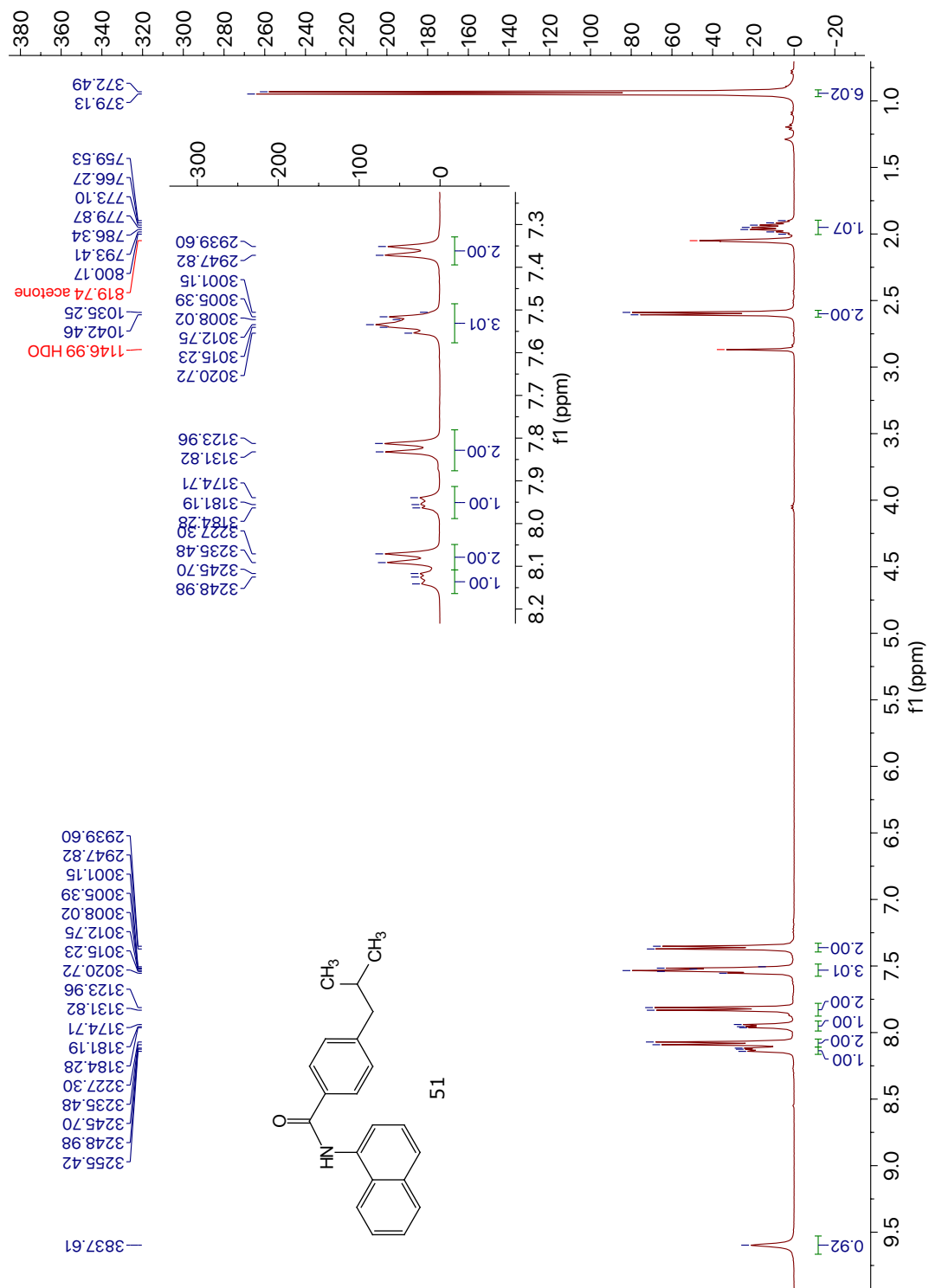


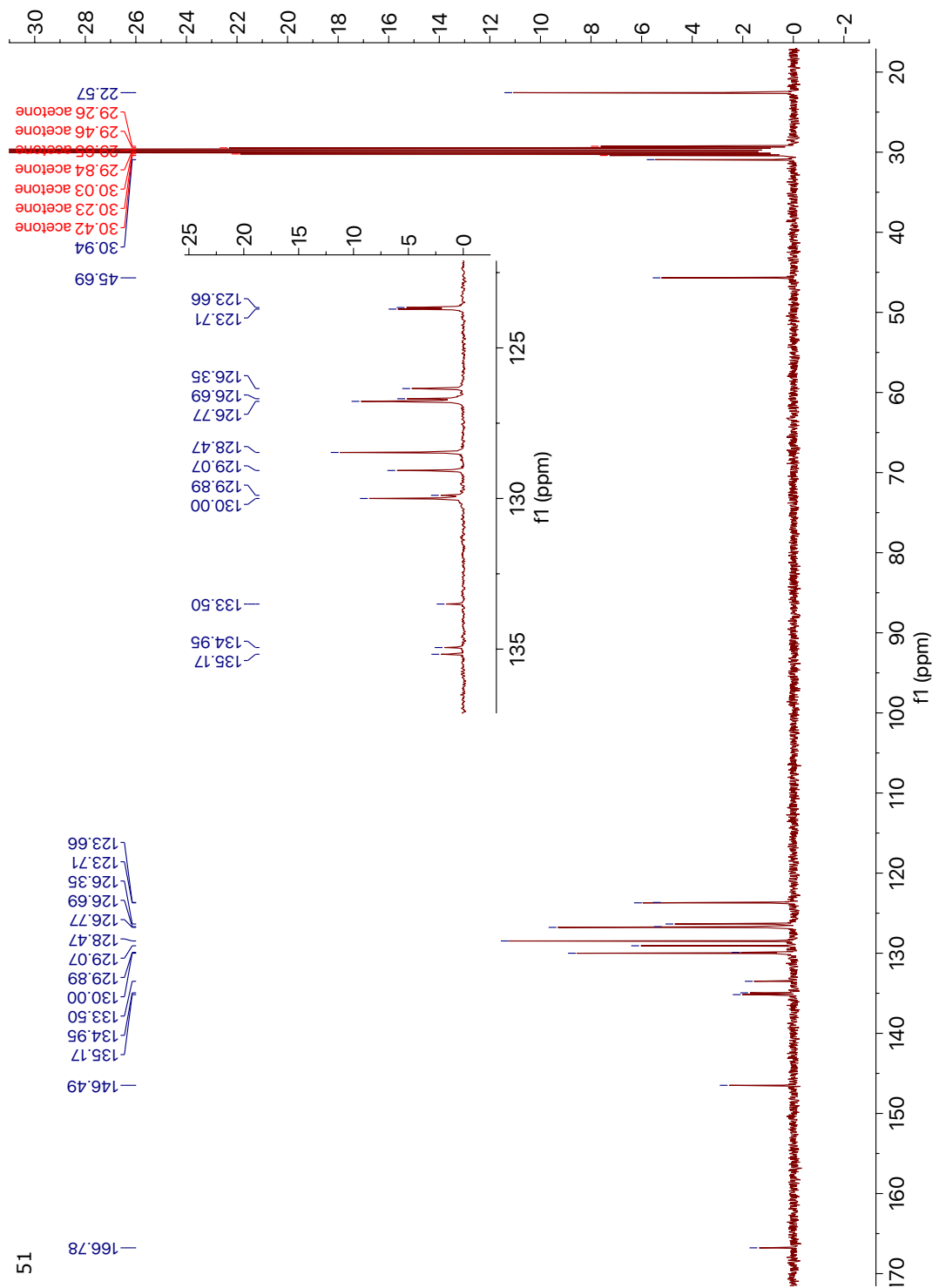
49



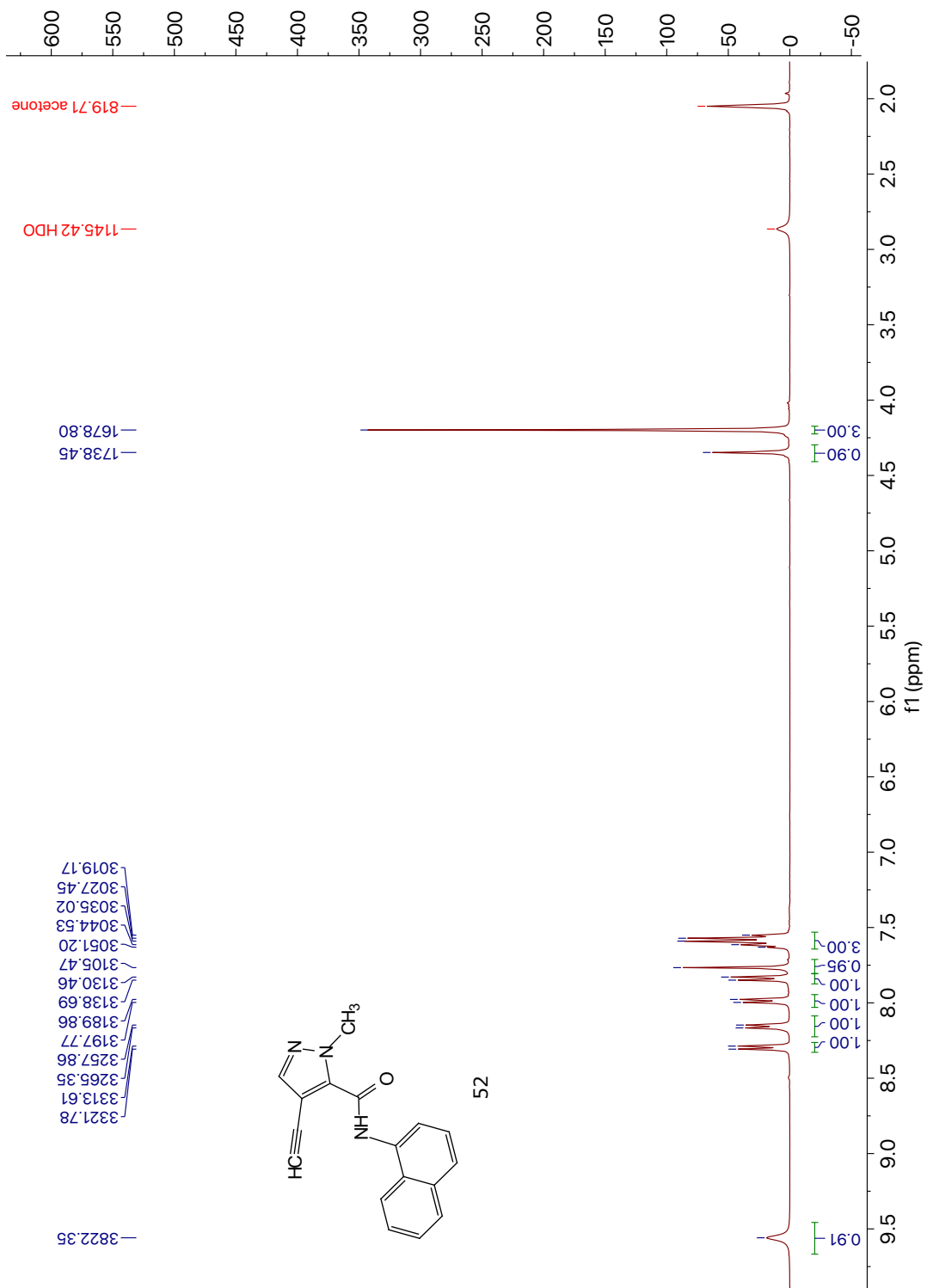


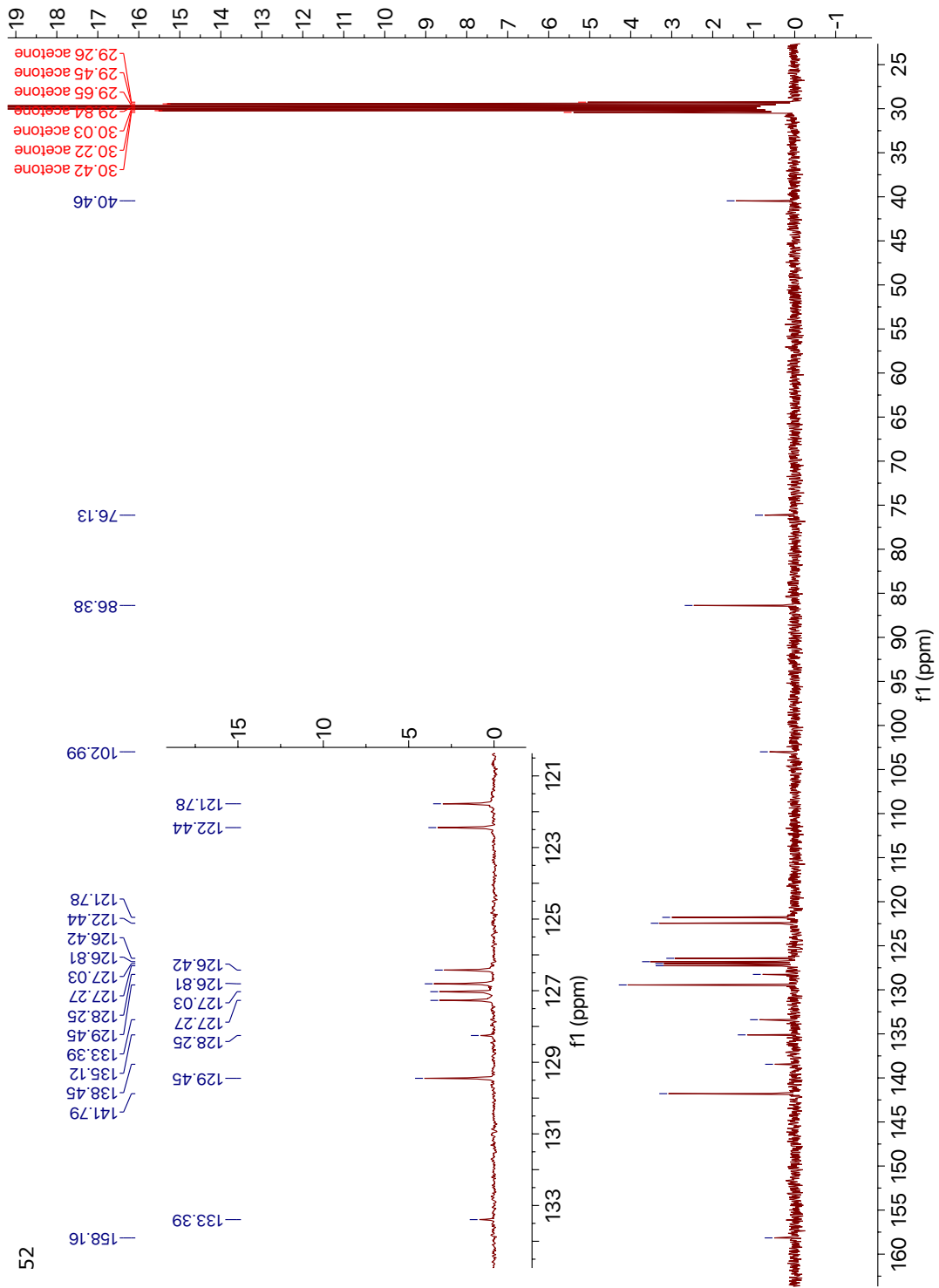
50



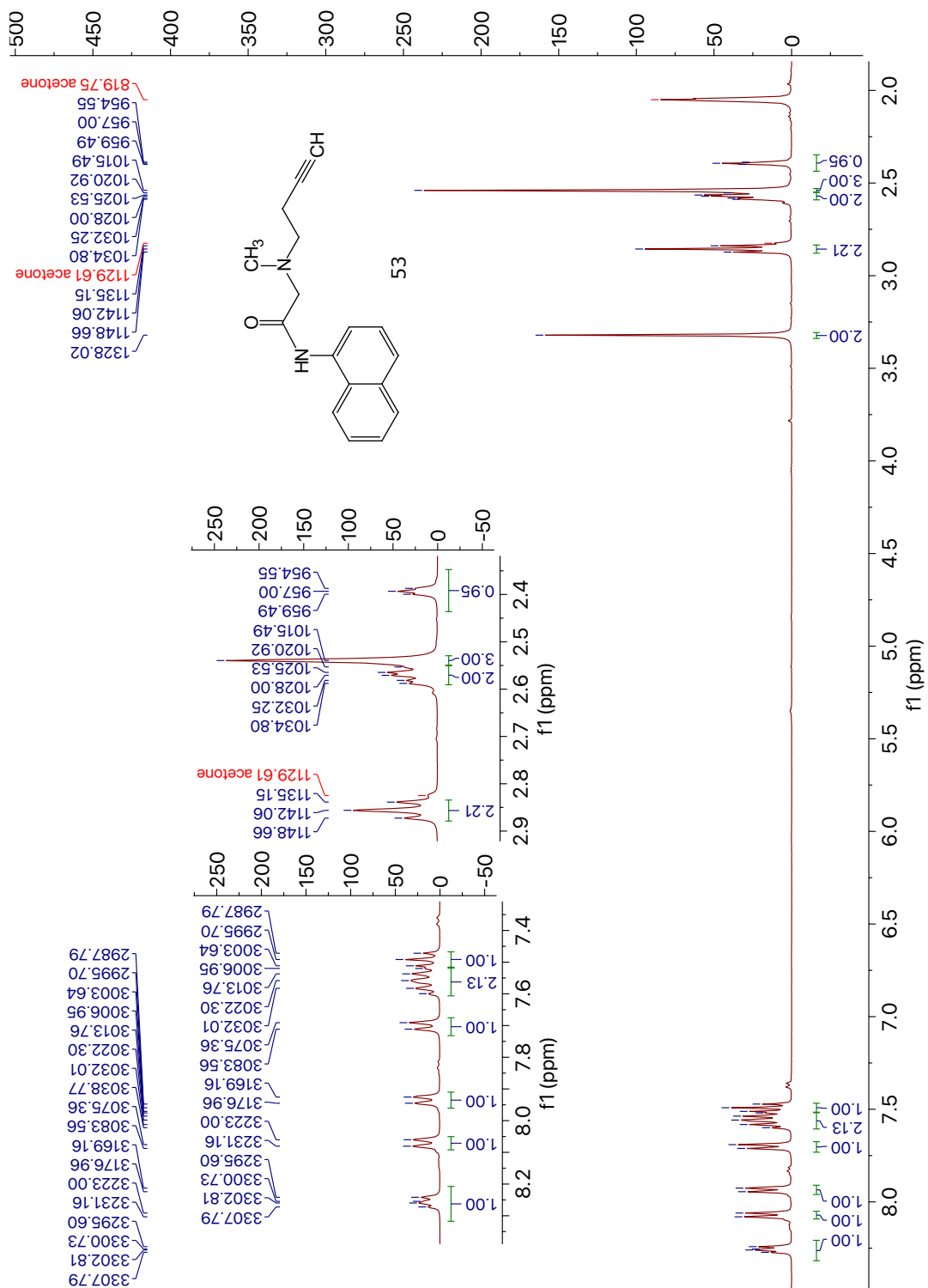


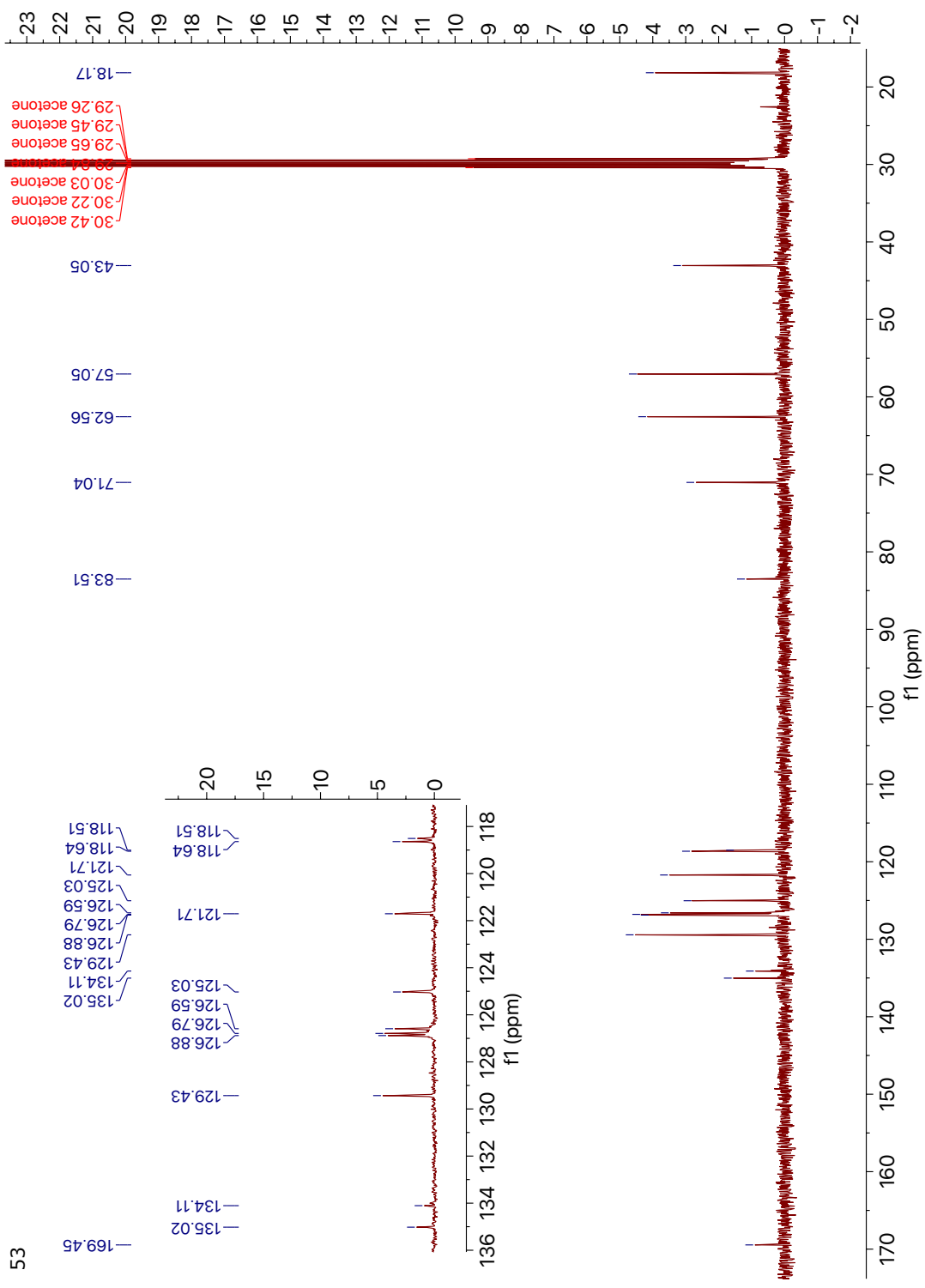
51



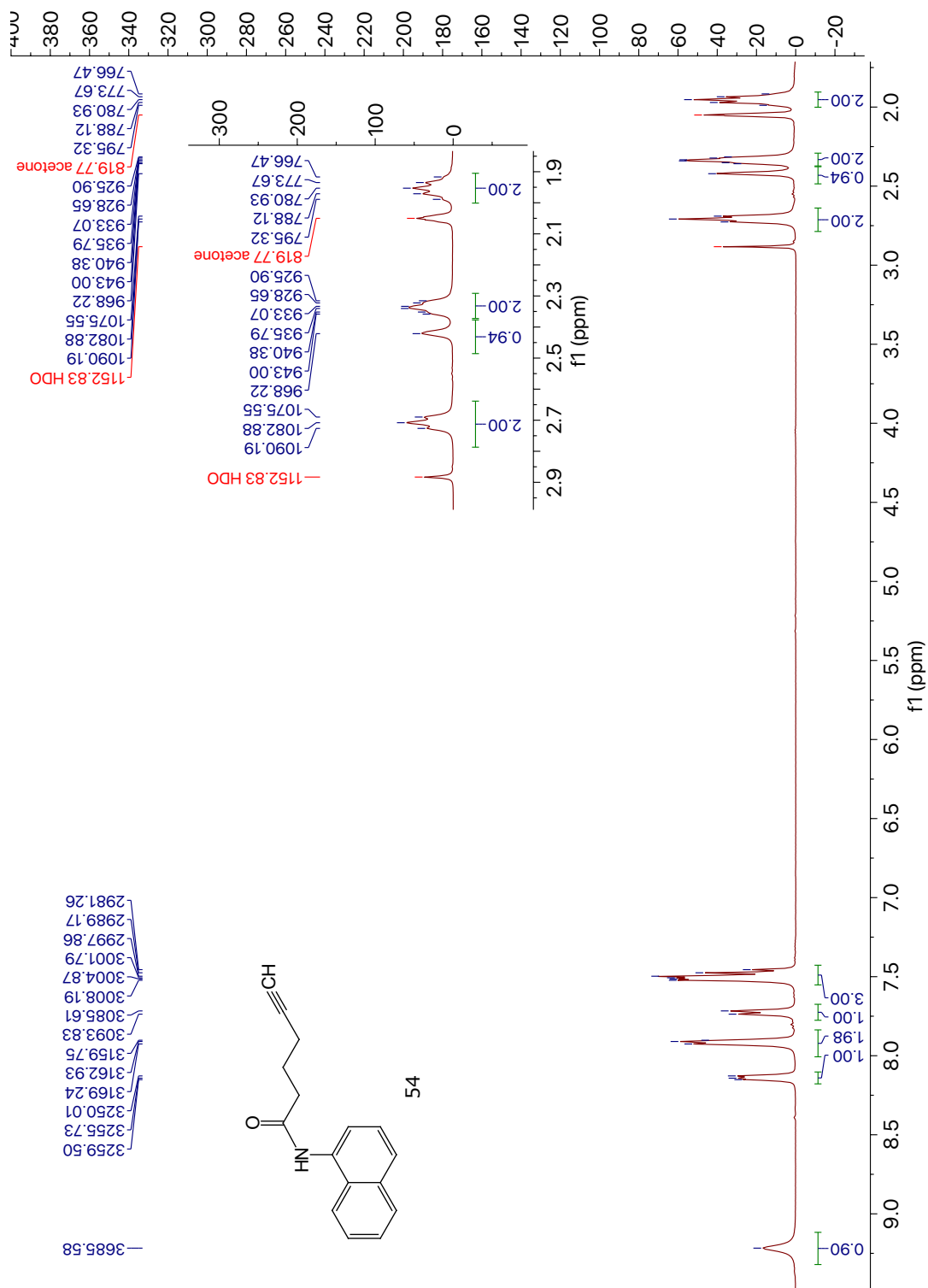


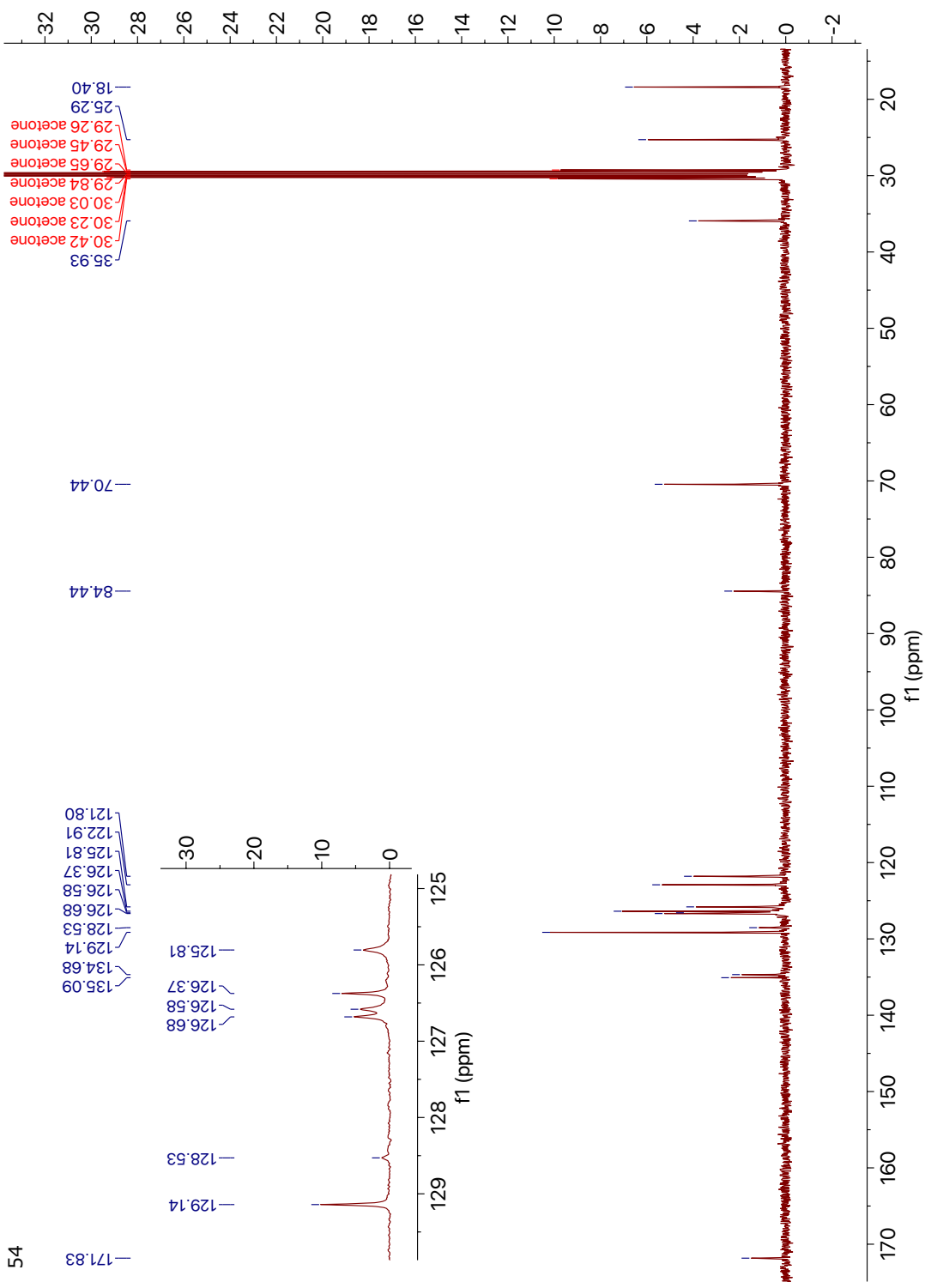
52



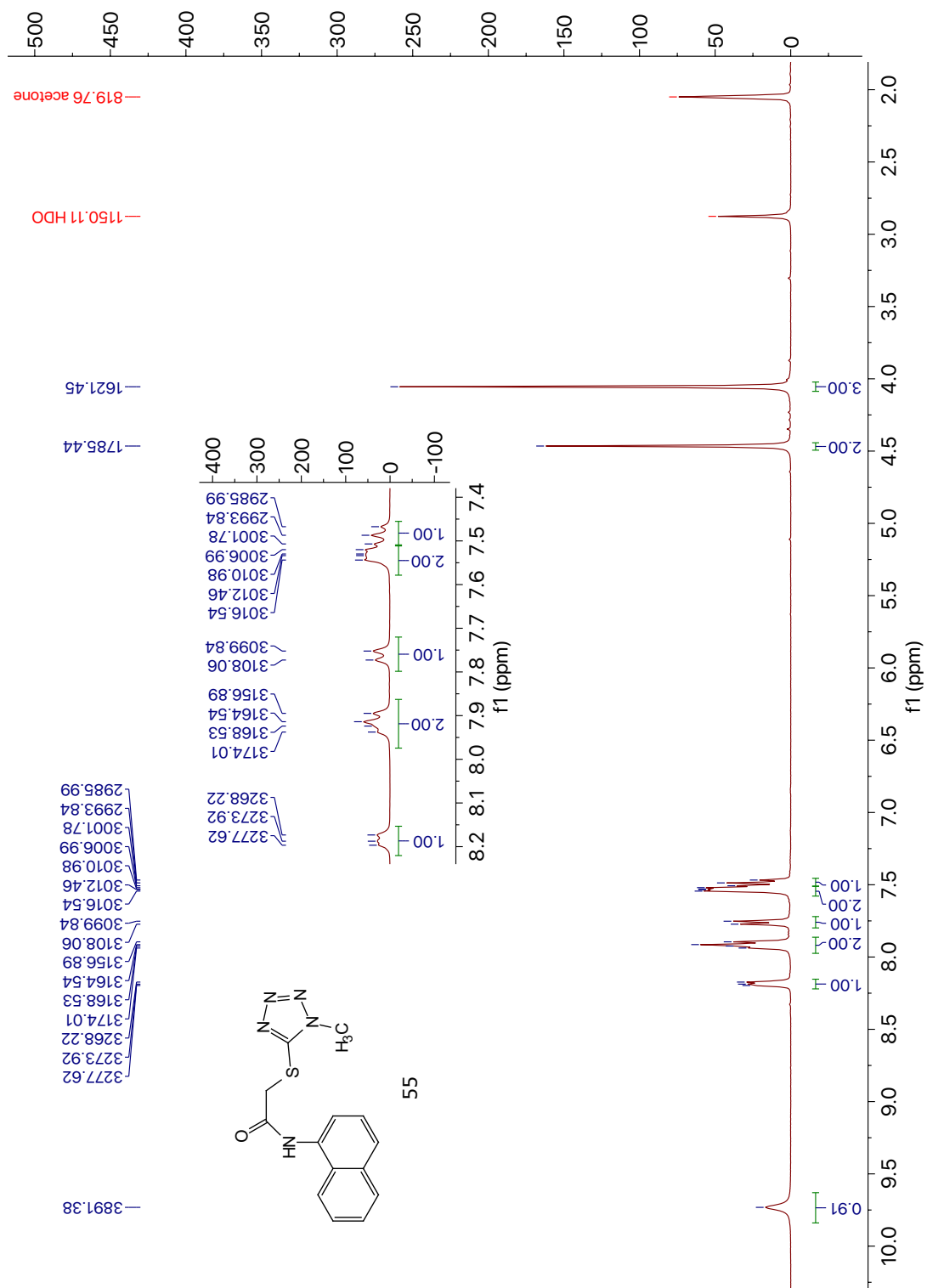


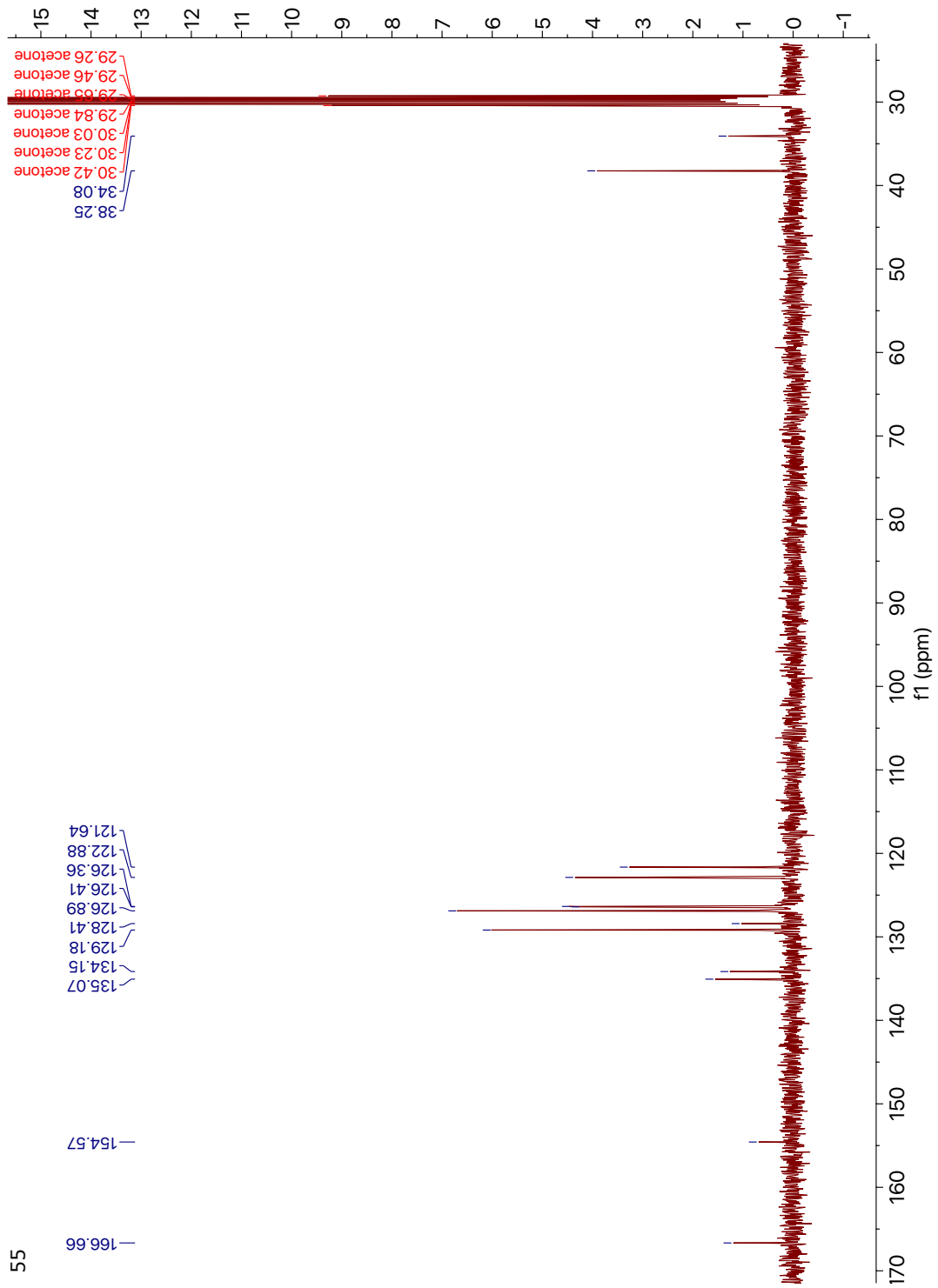
53

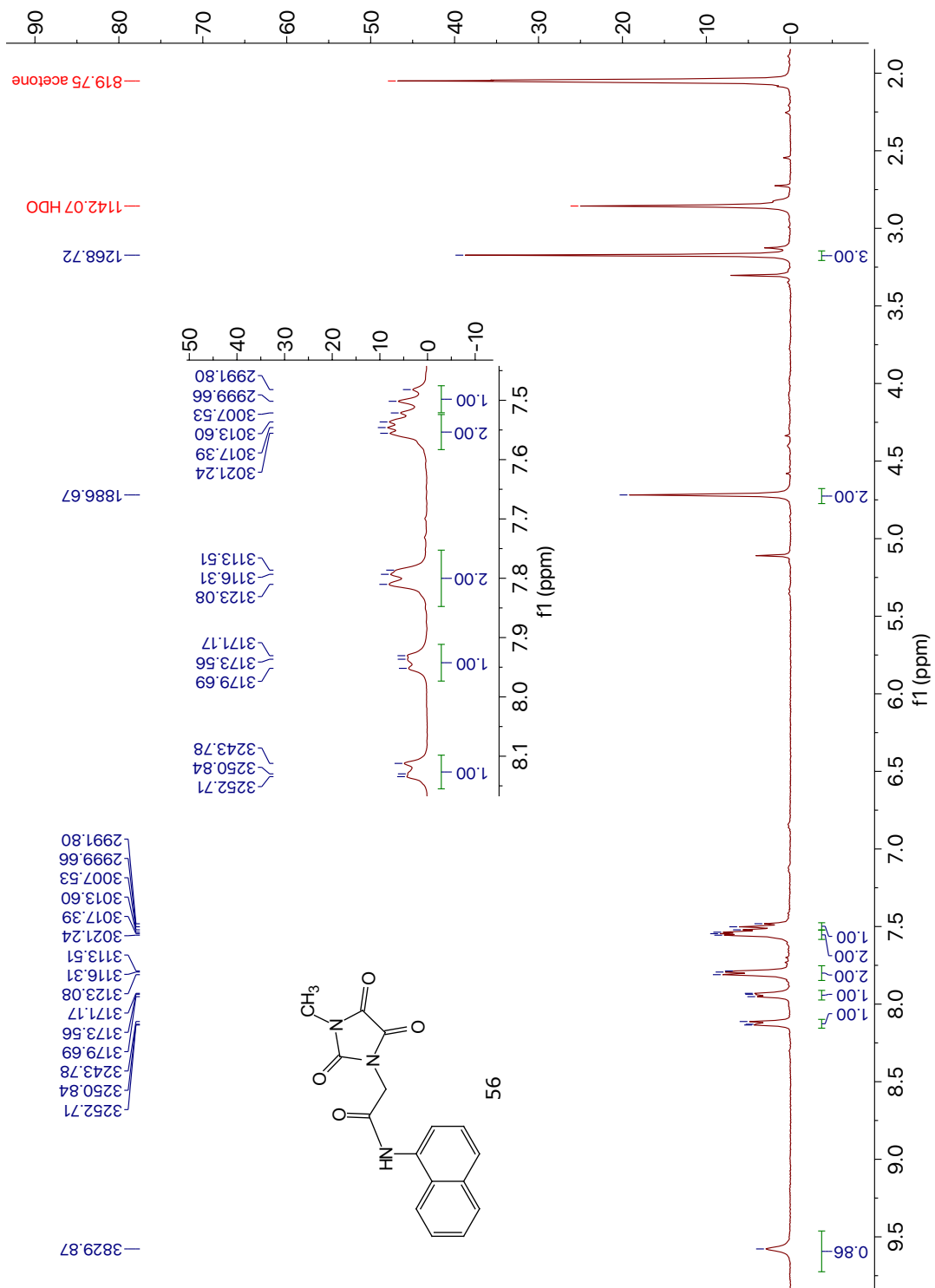


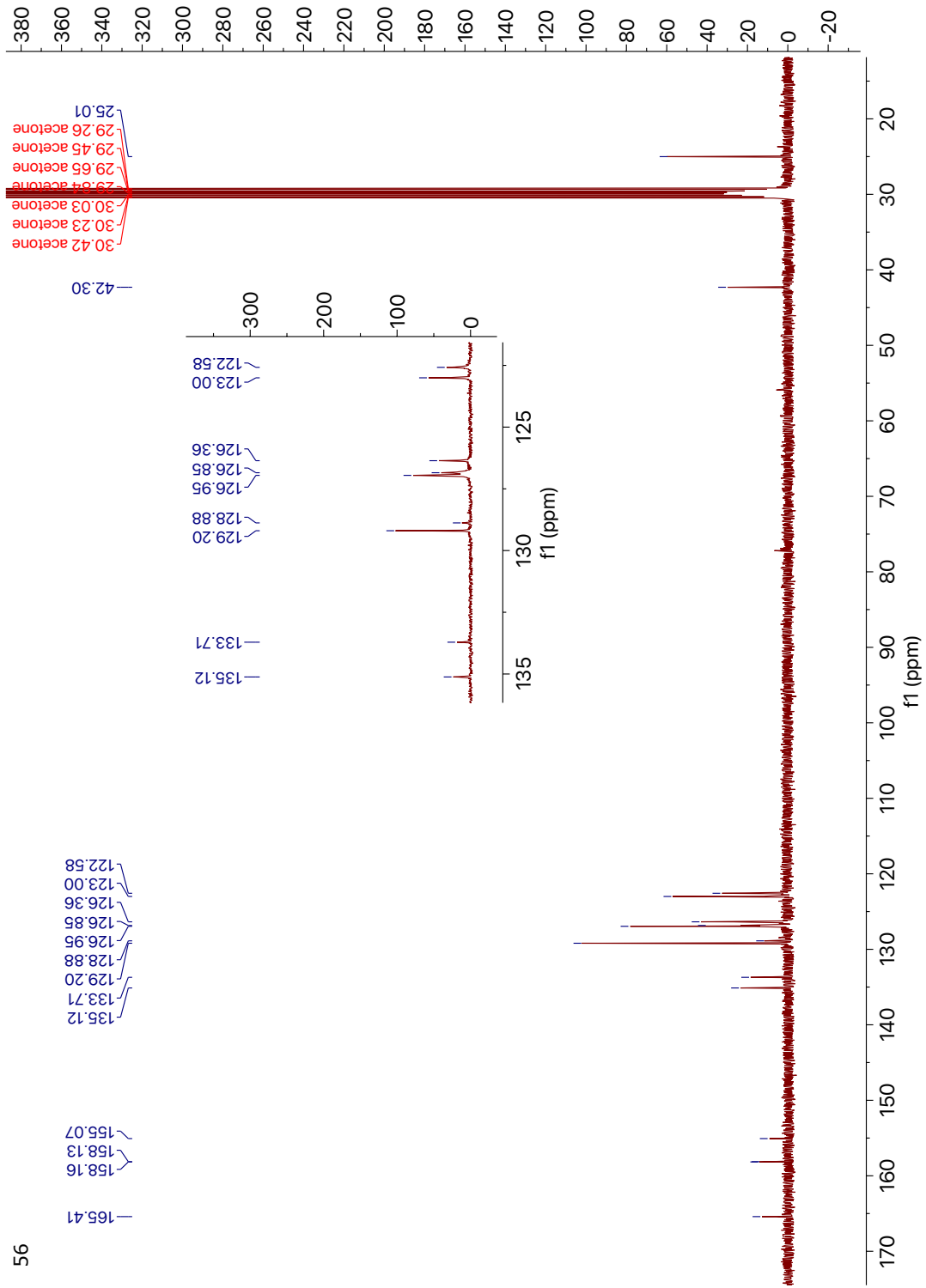


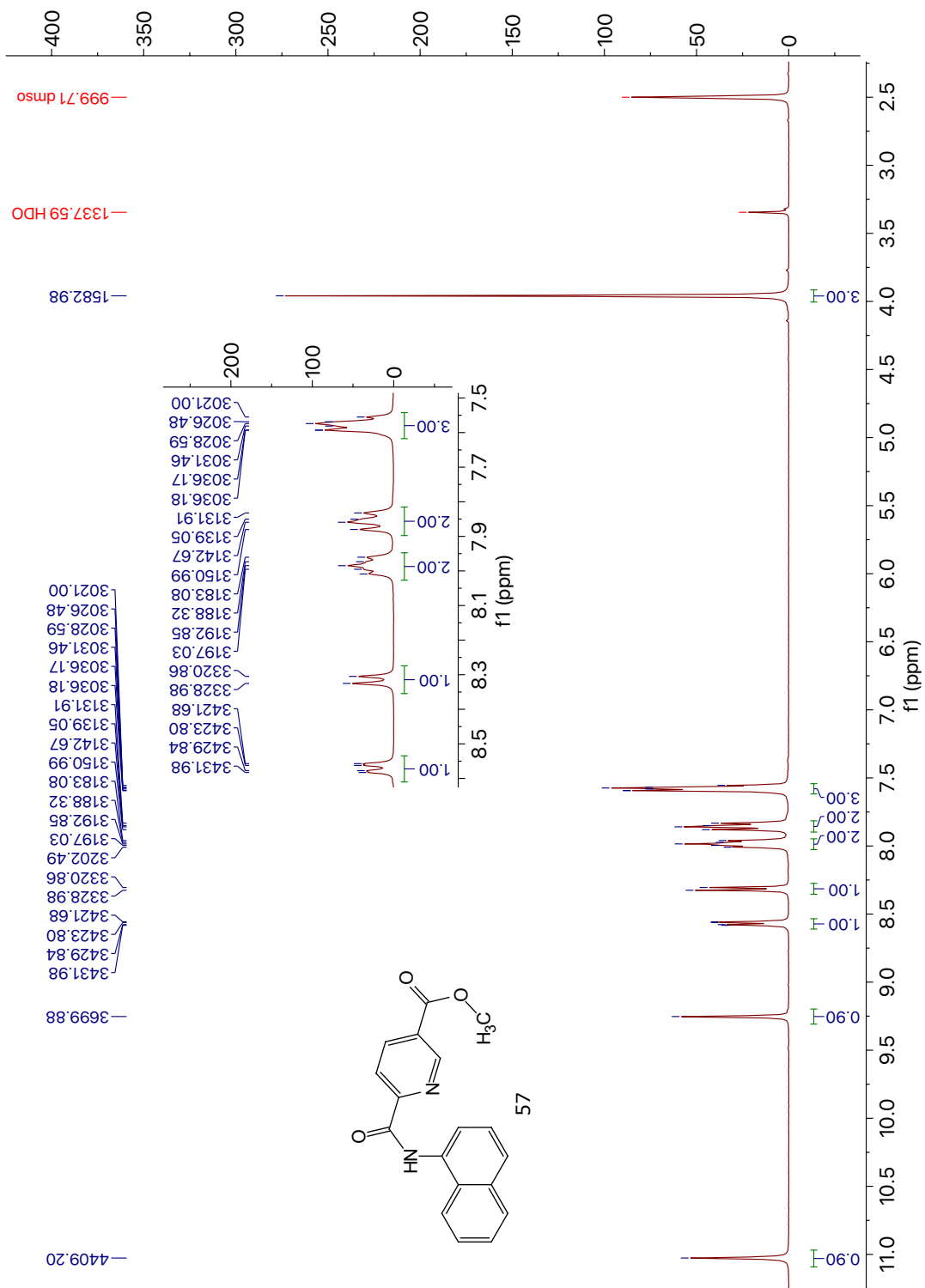
54

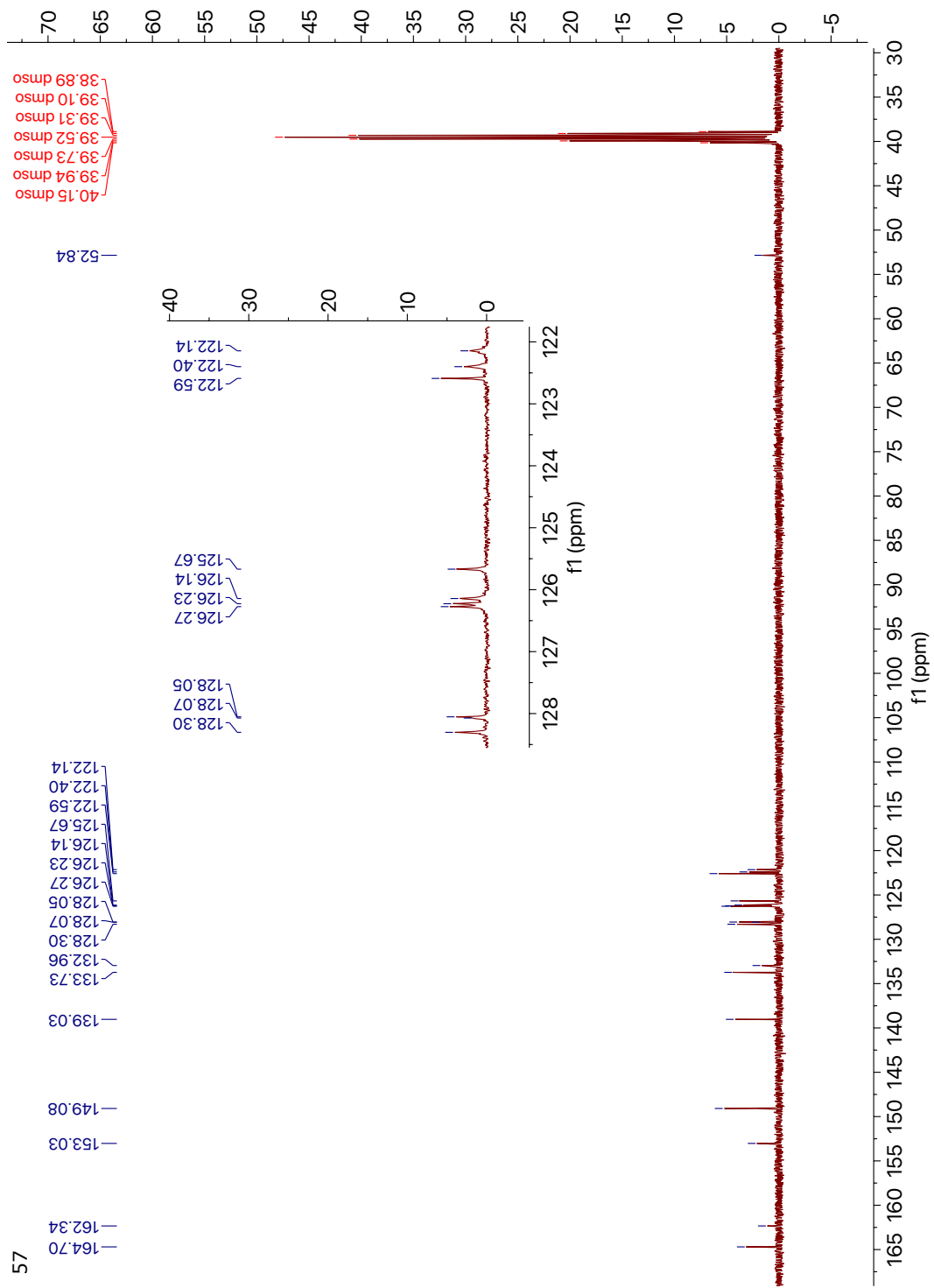


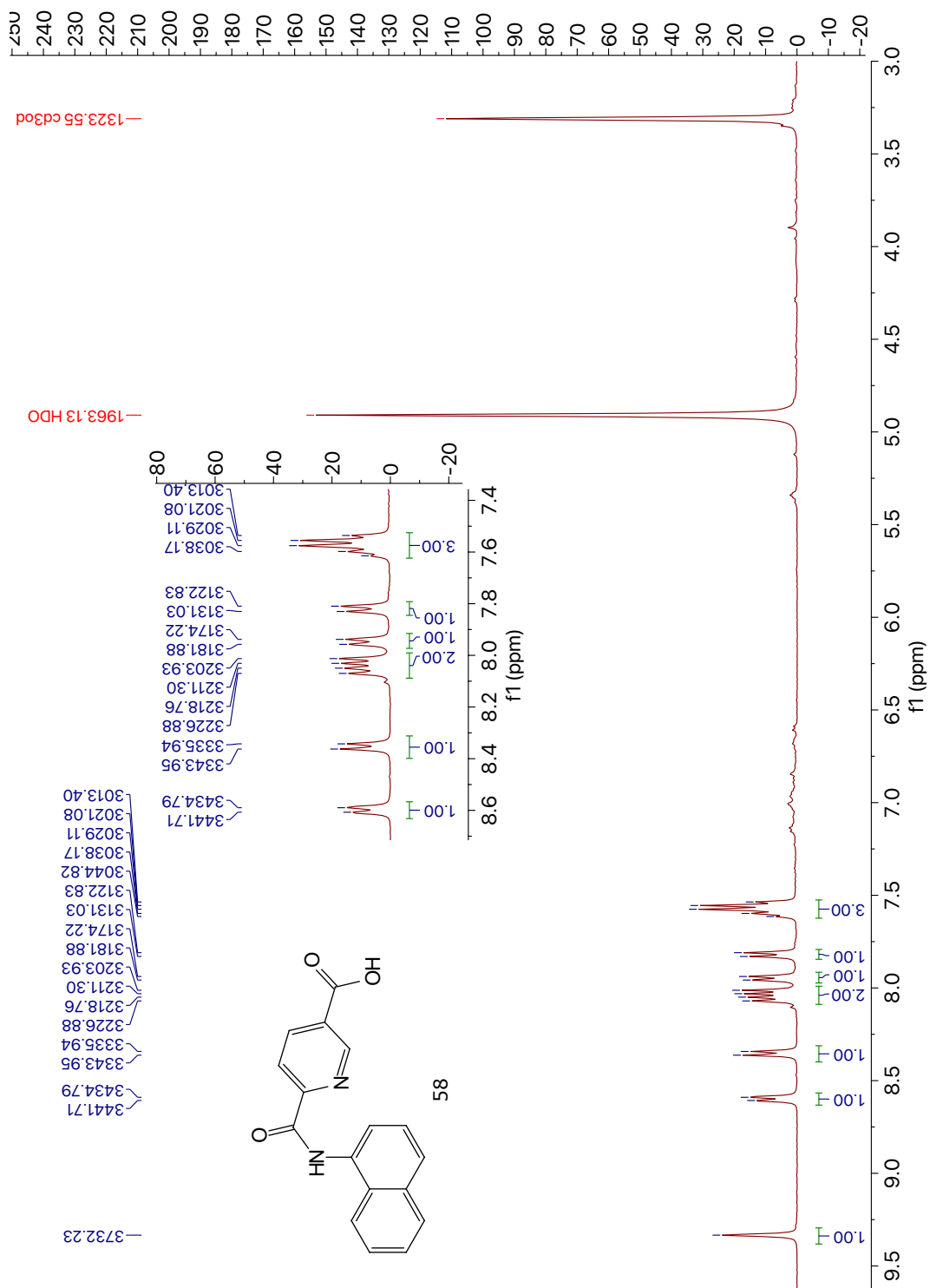


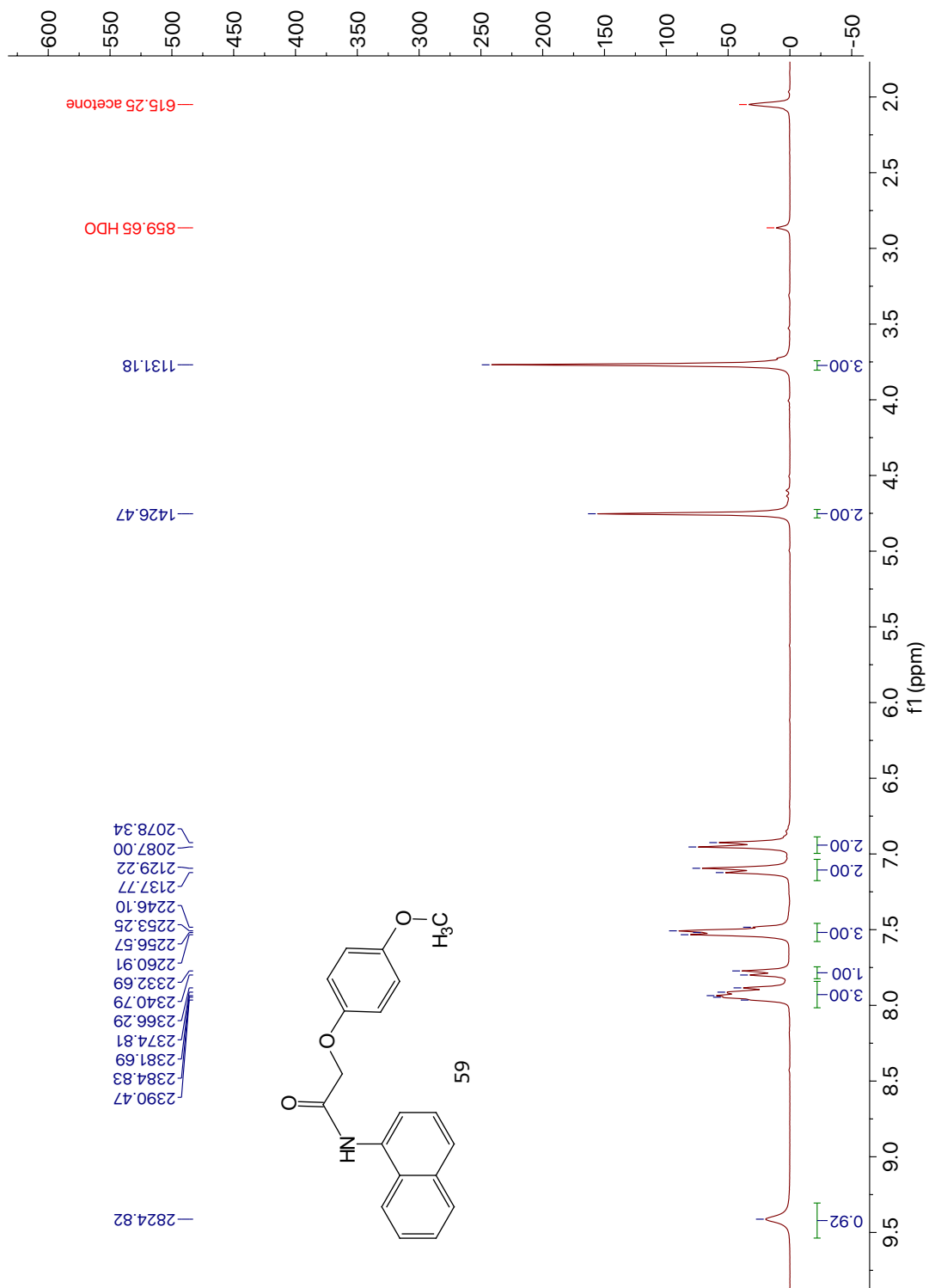


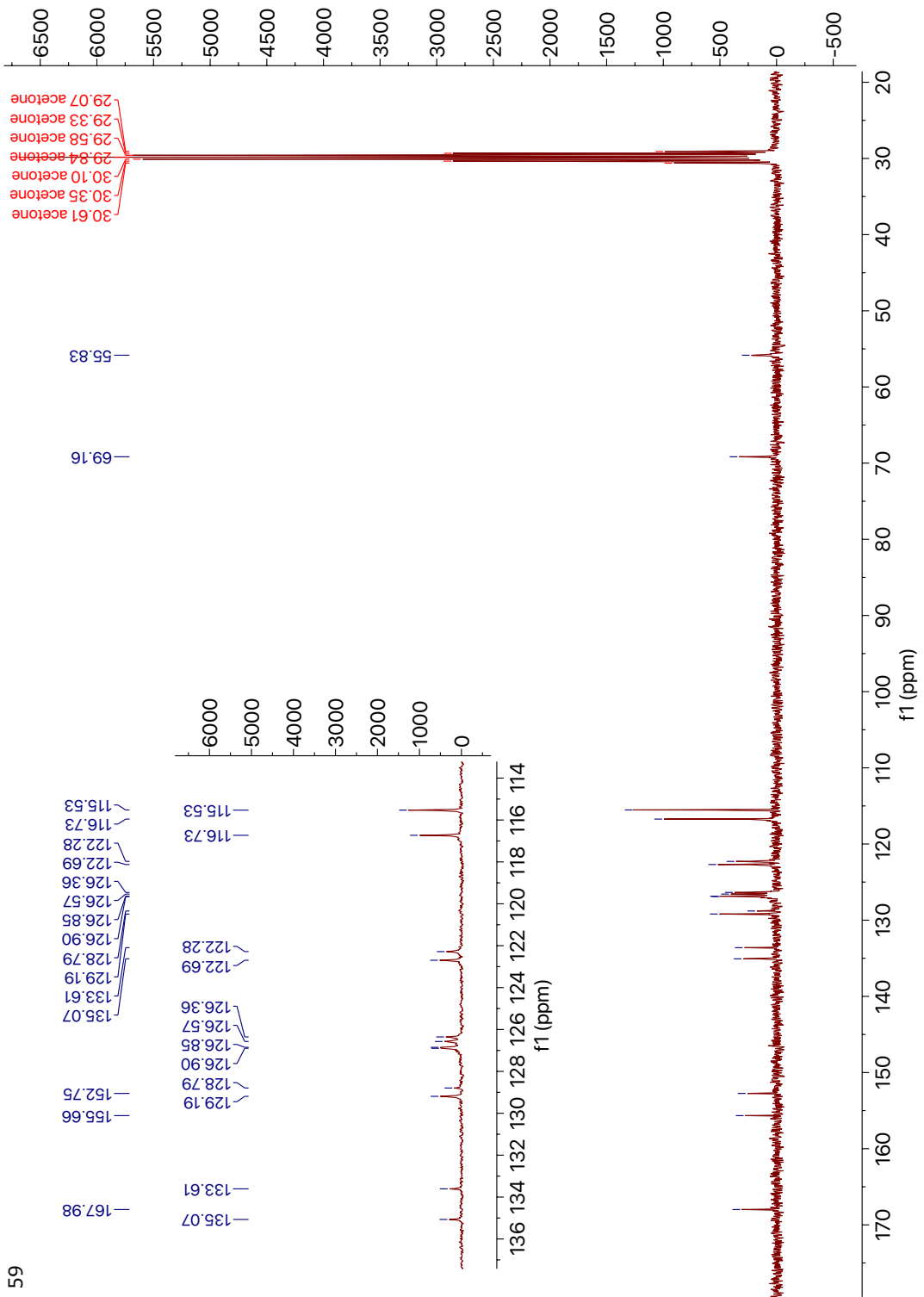




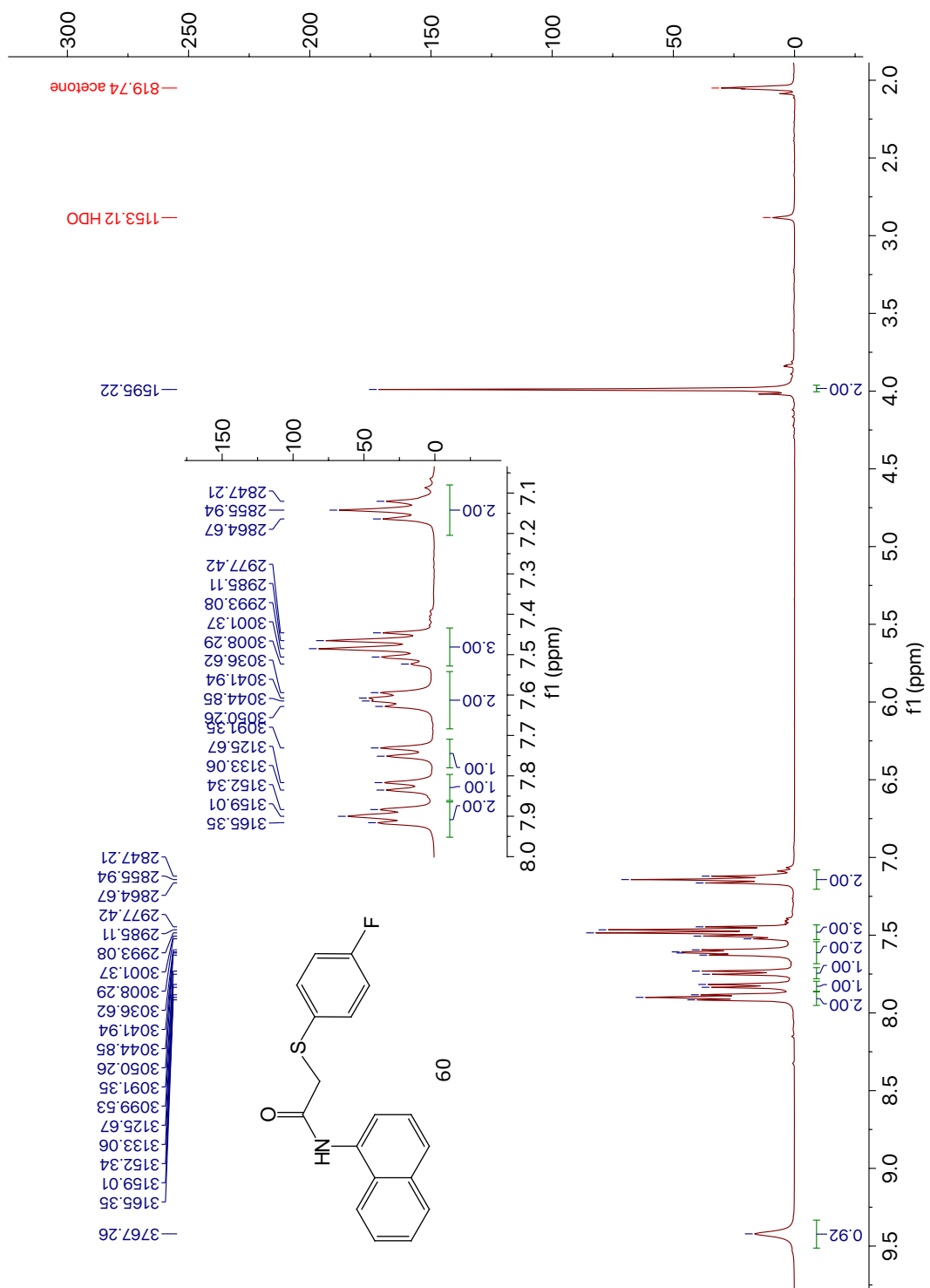


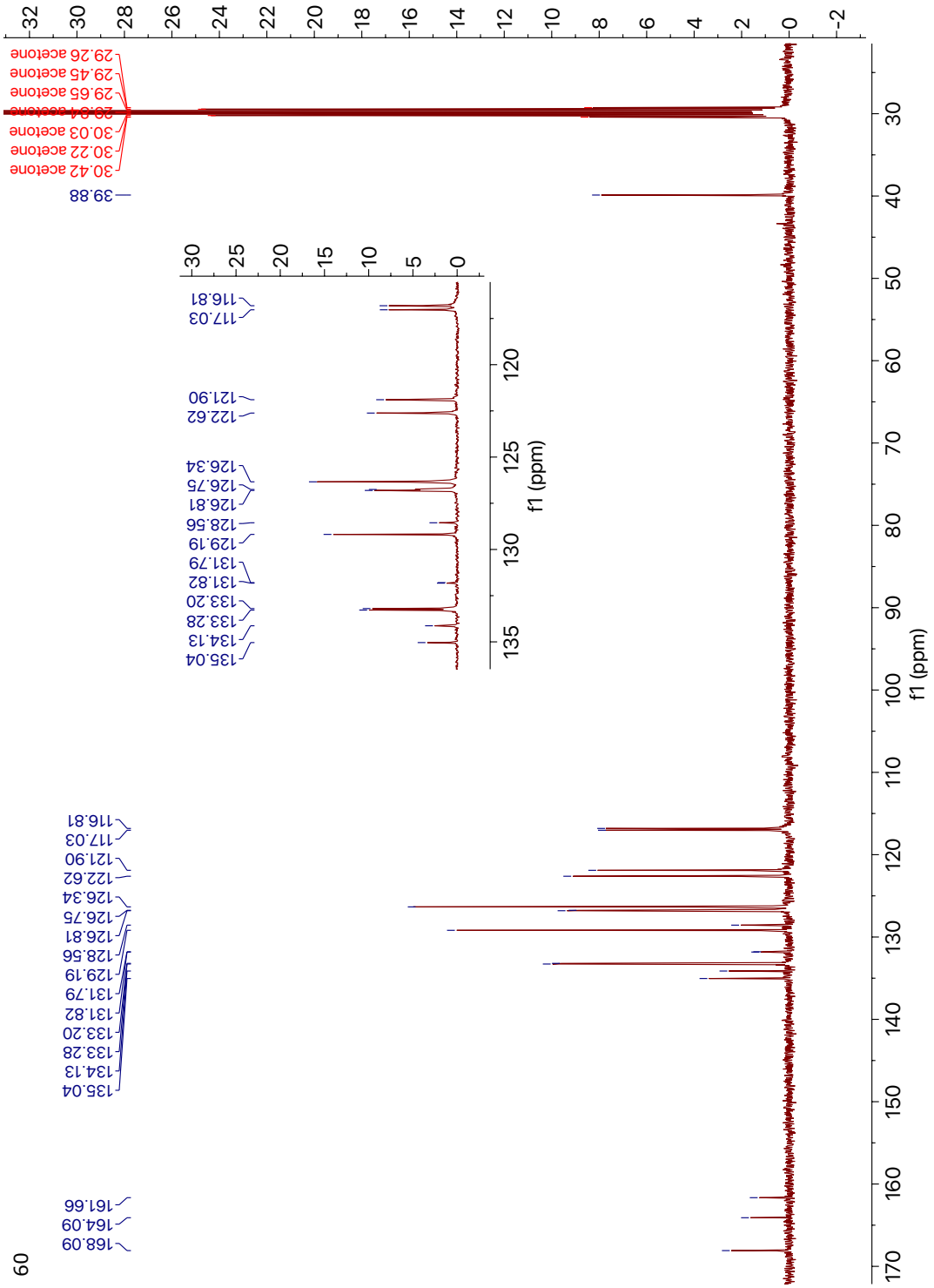




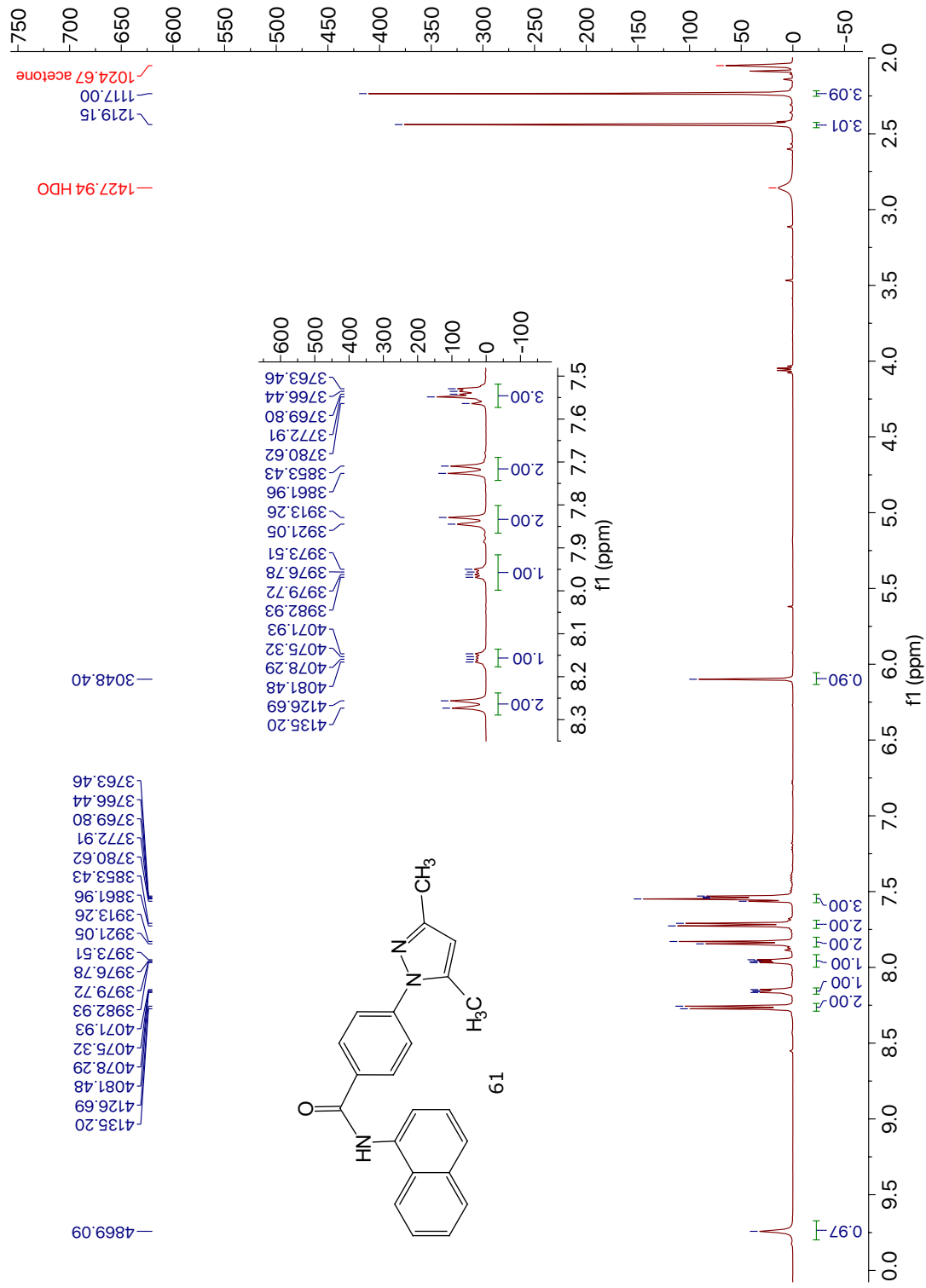


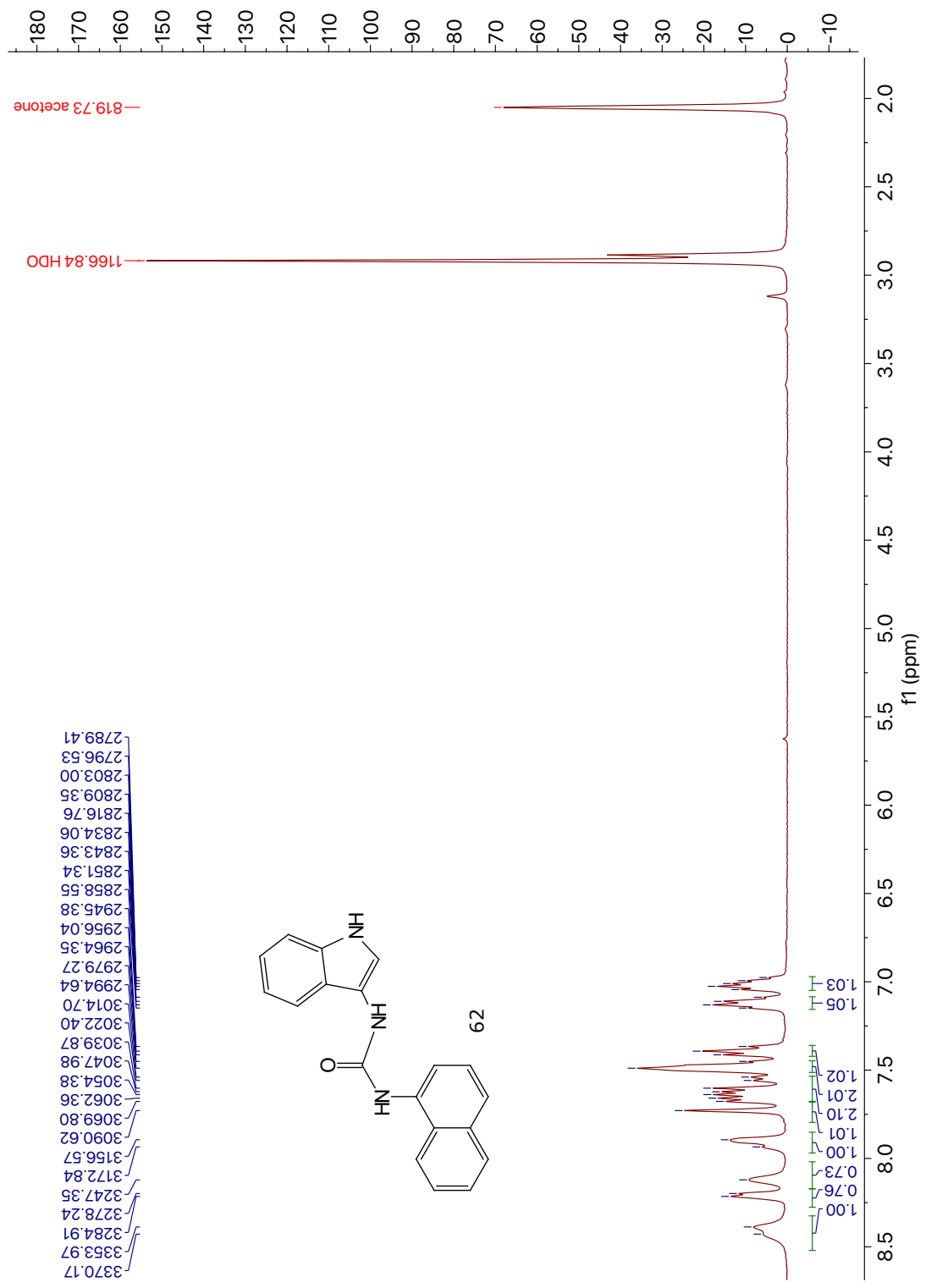
59

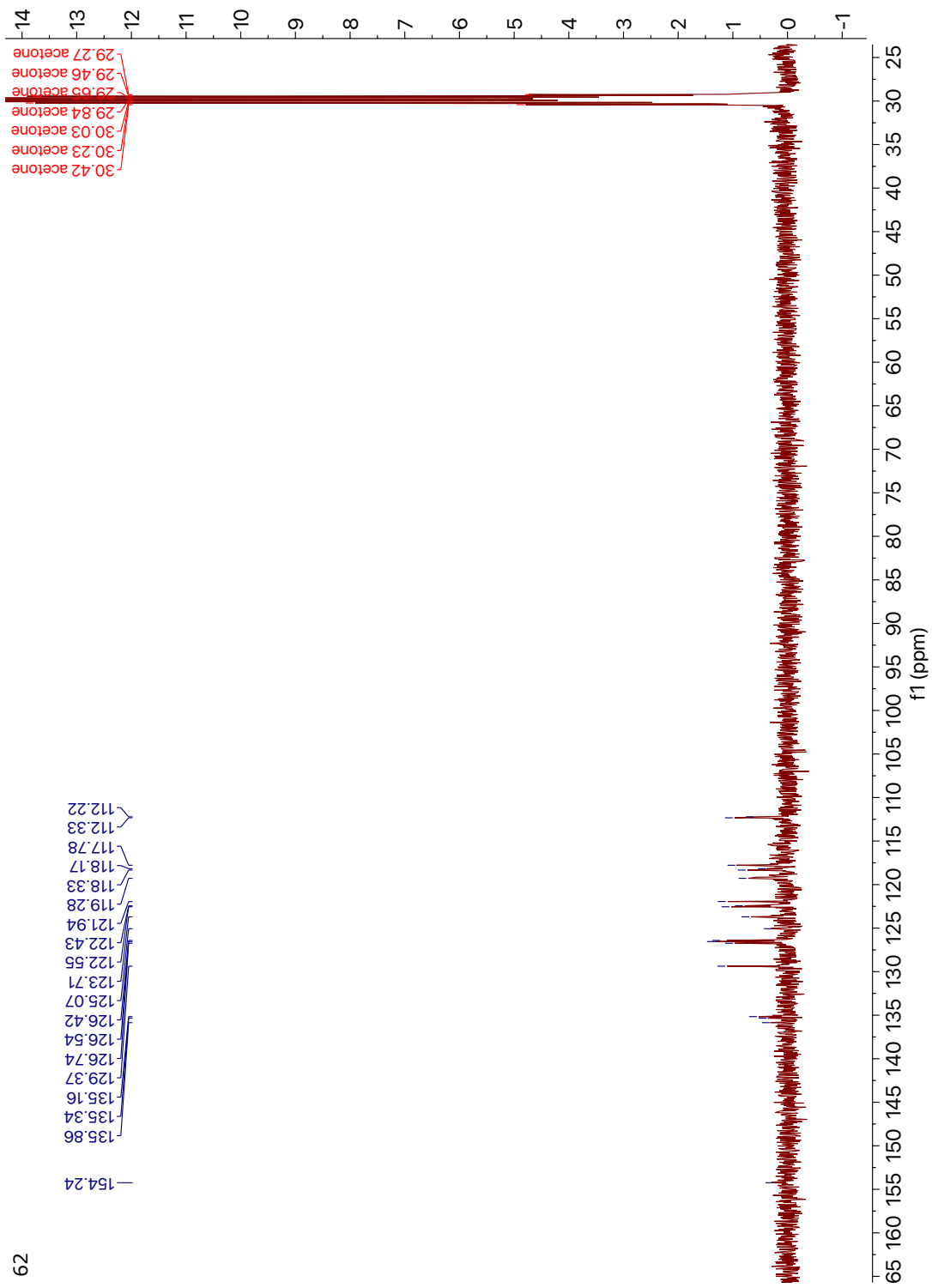




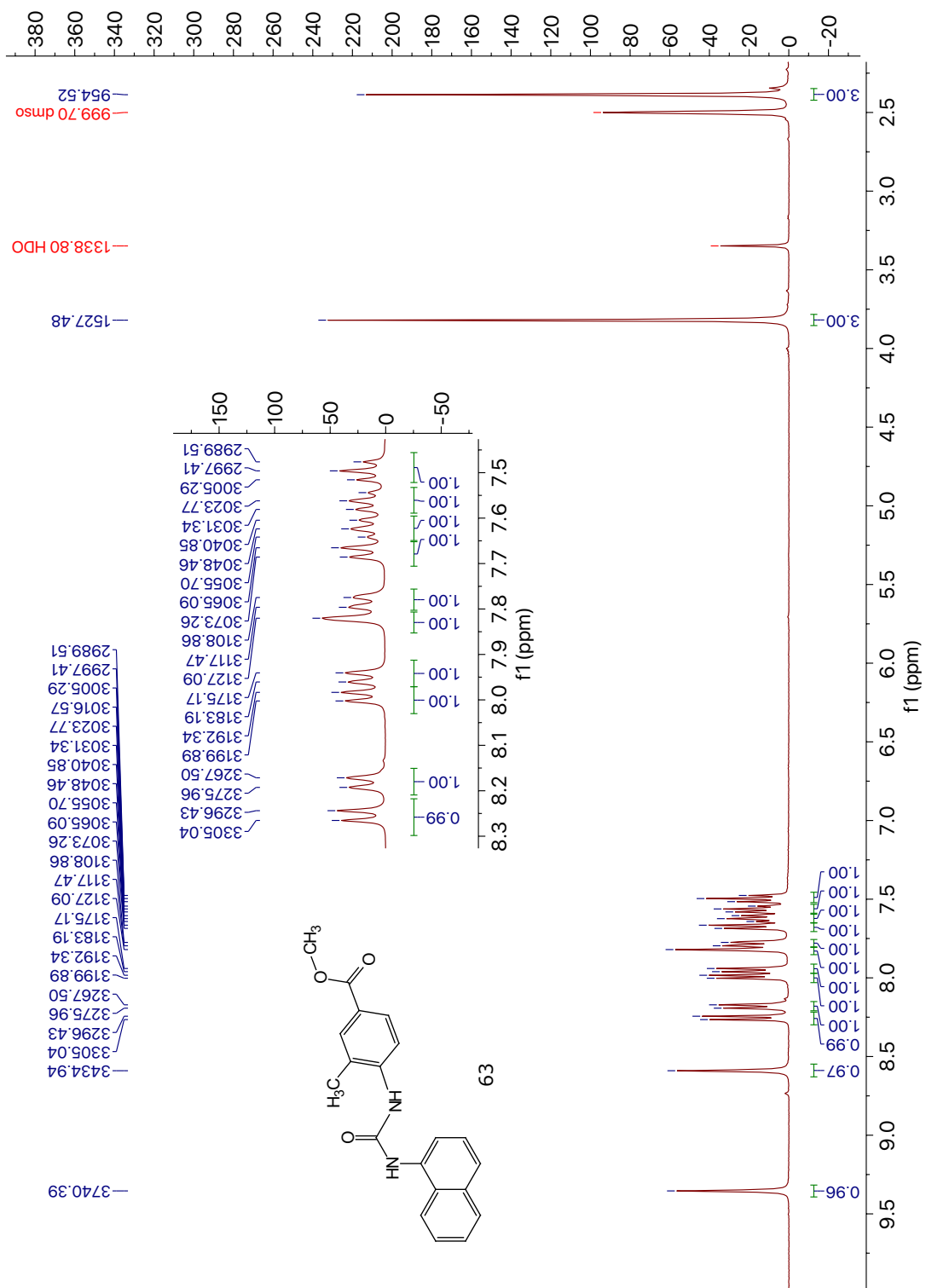
60

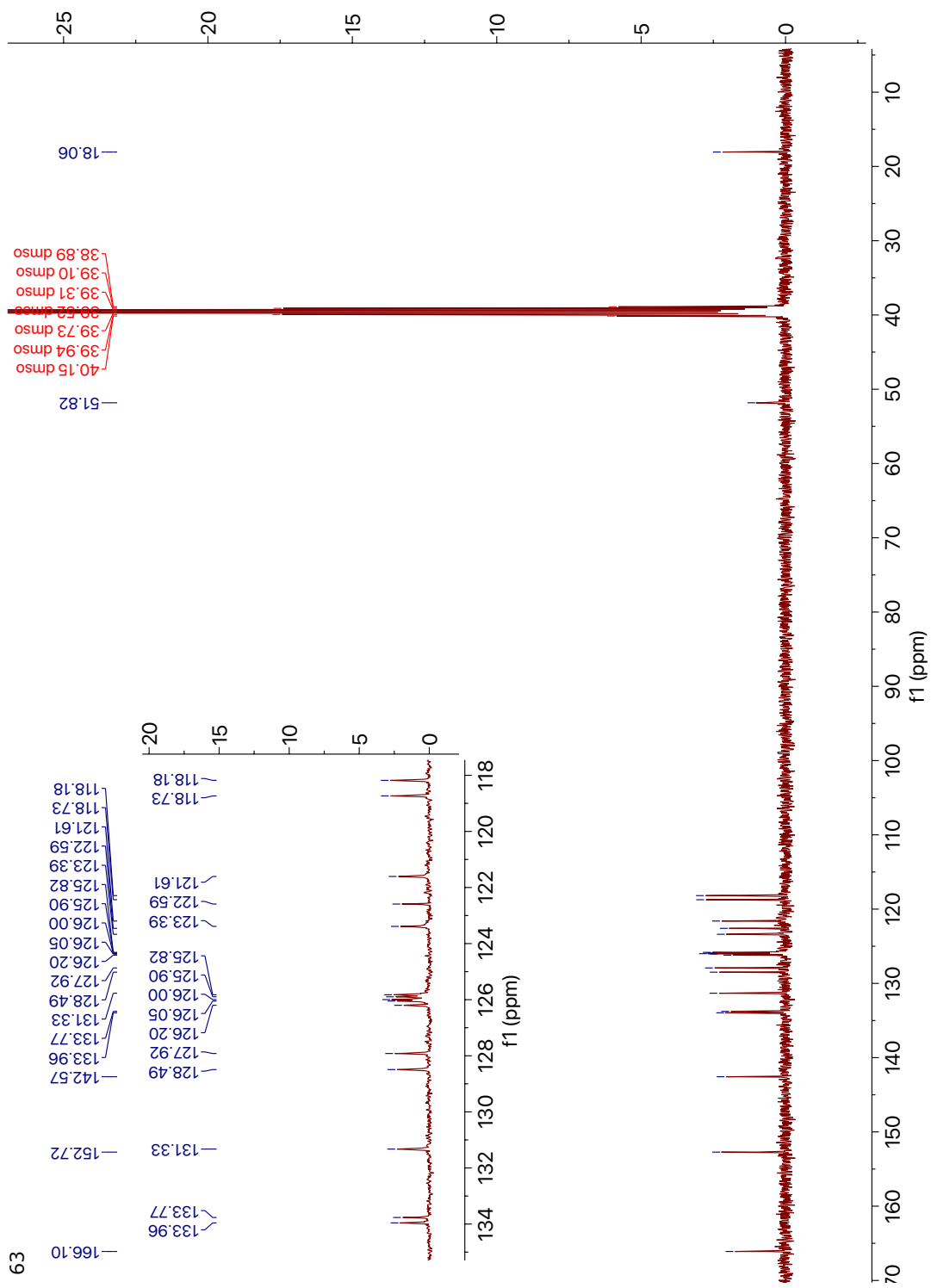




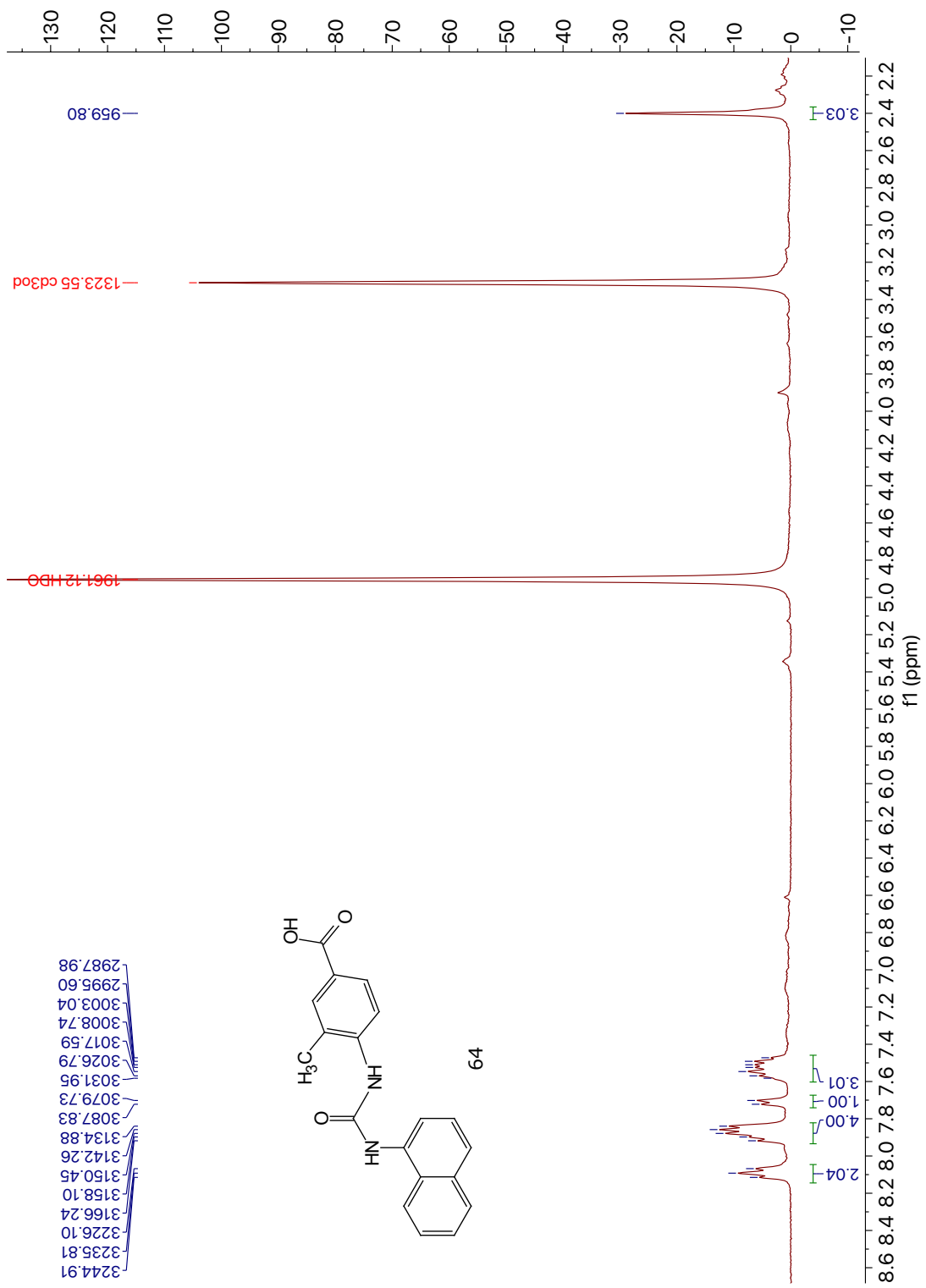


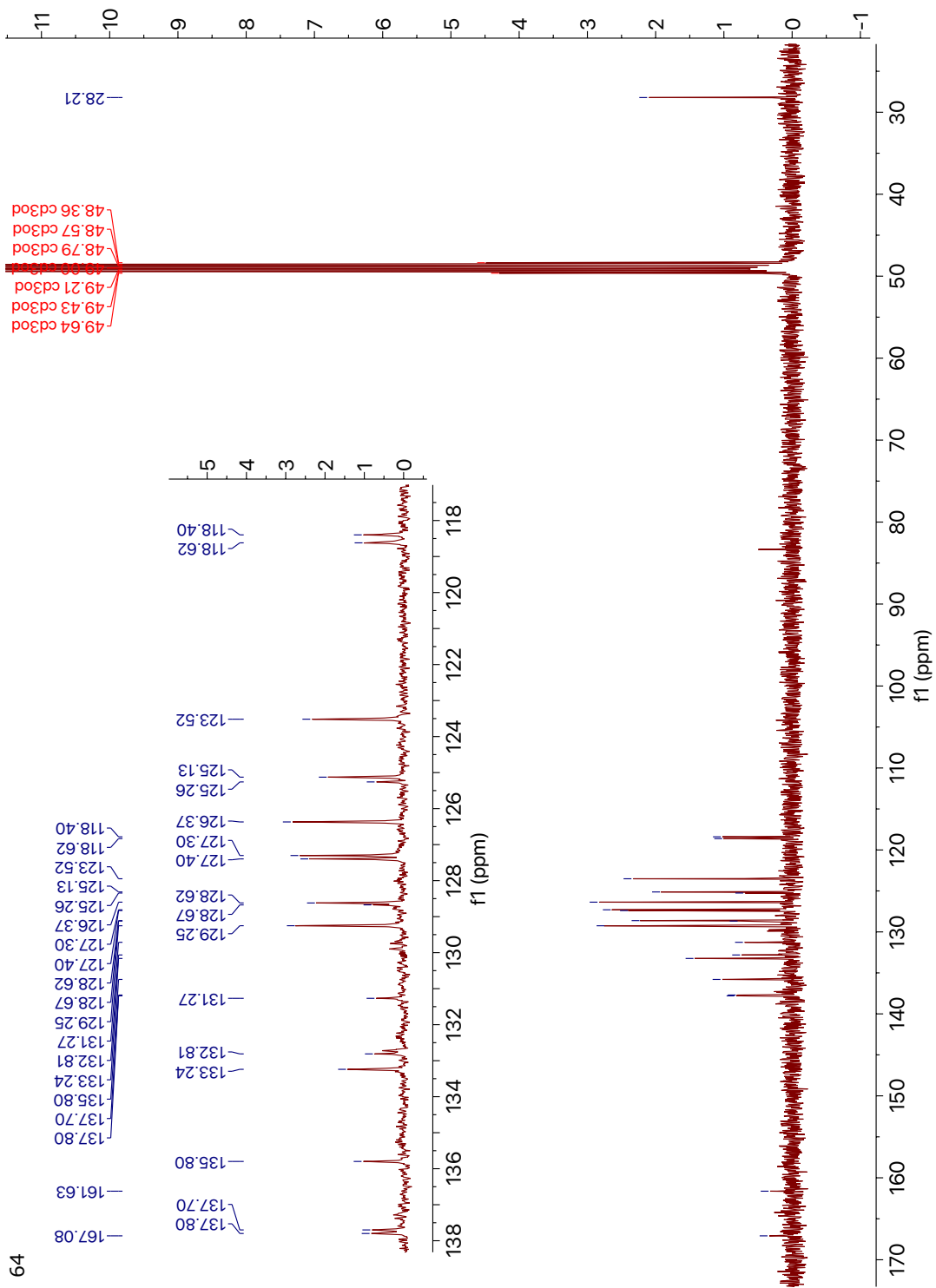
62



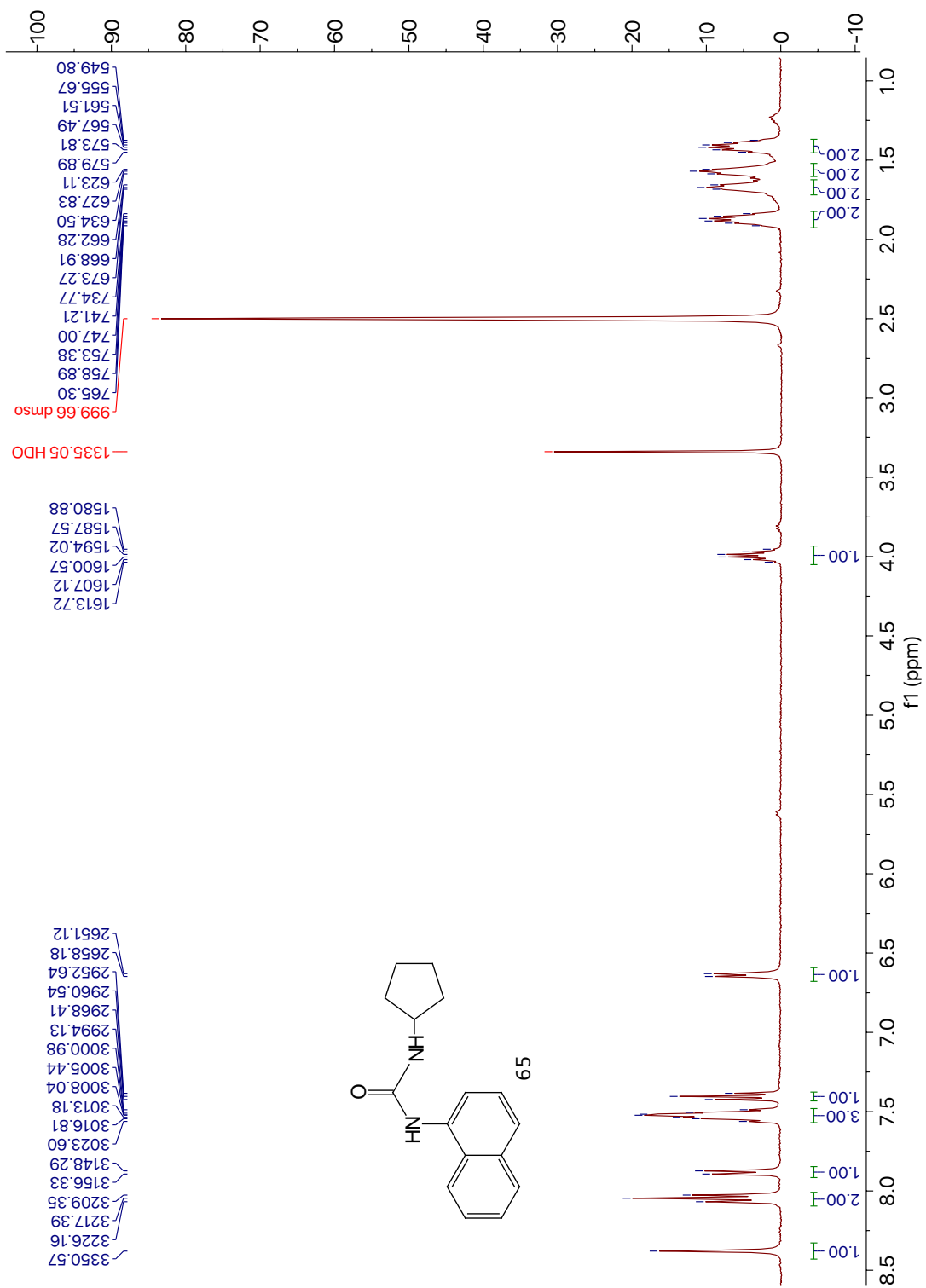


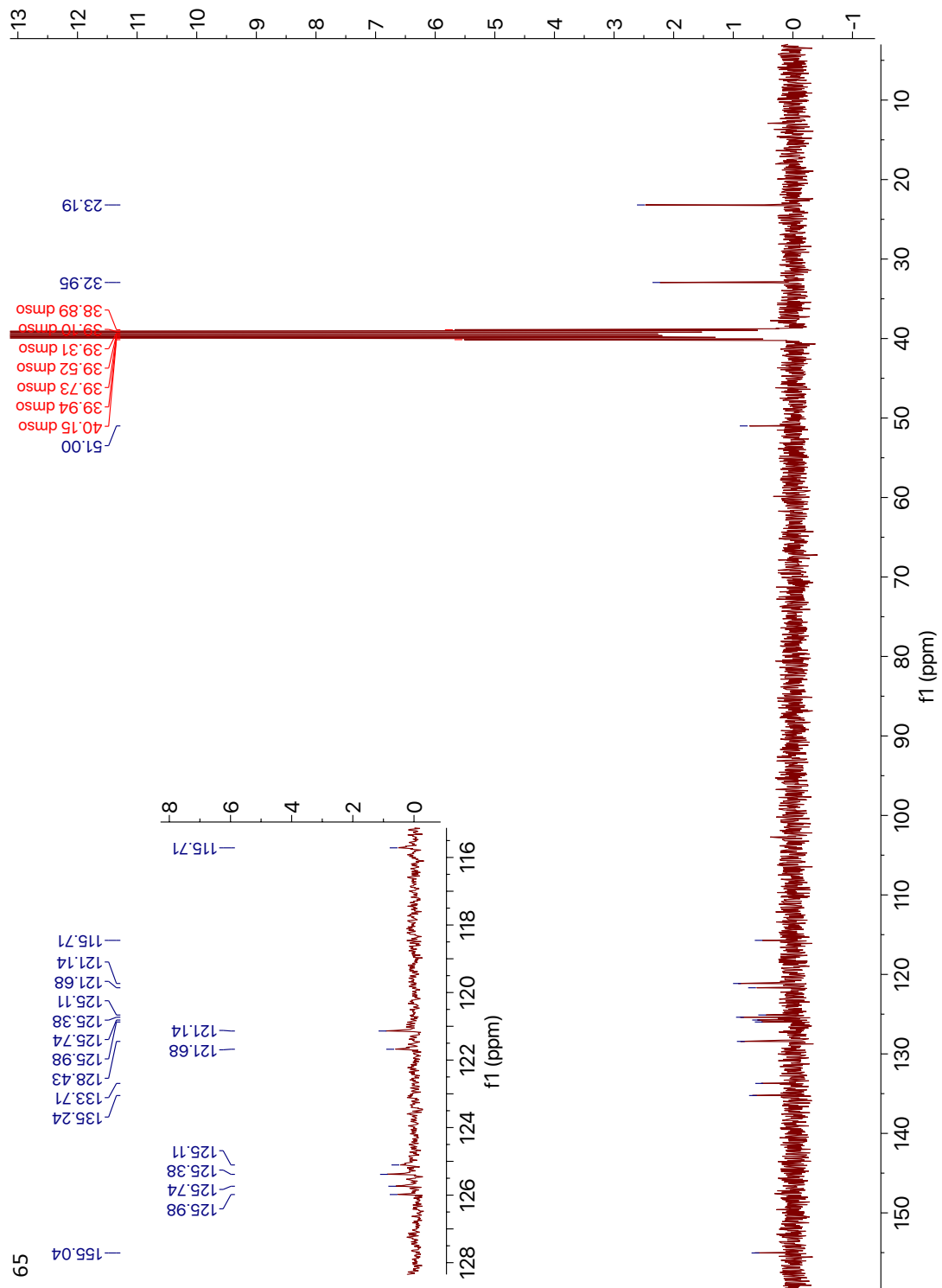
63

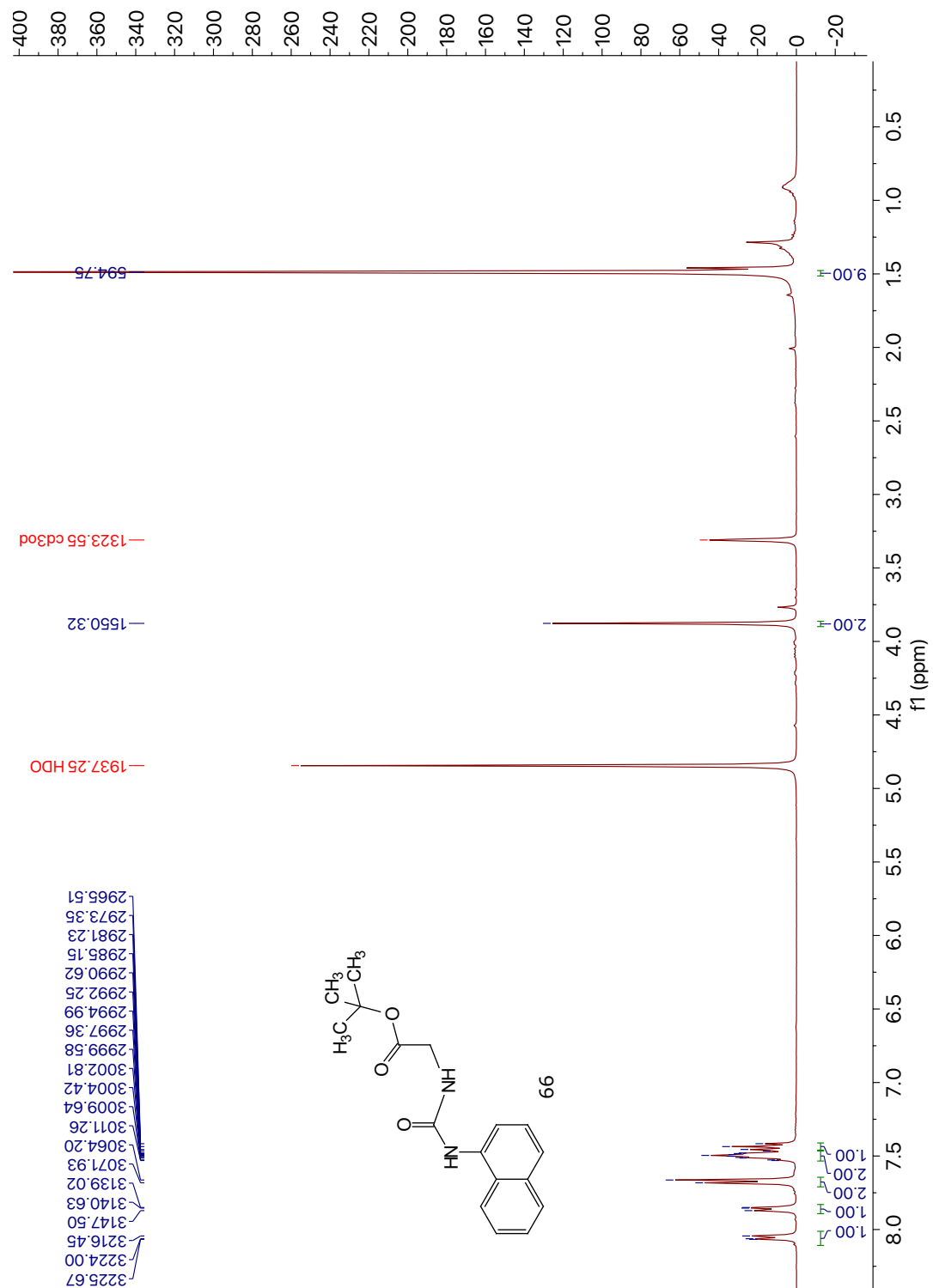


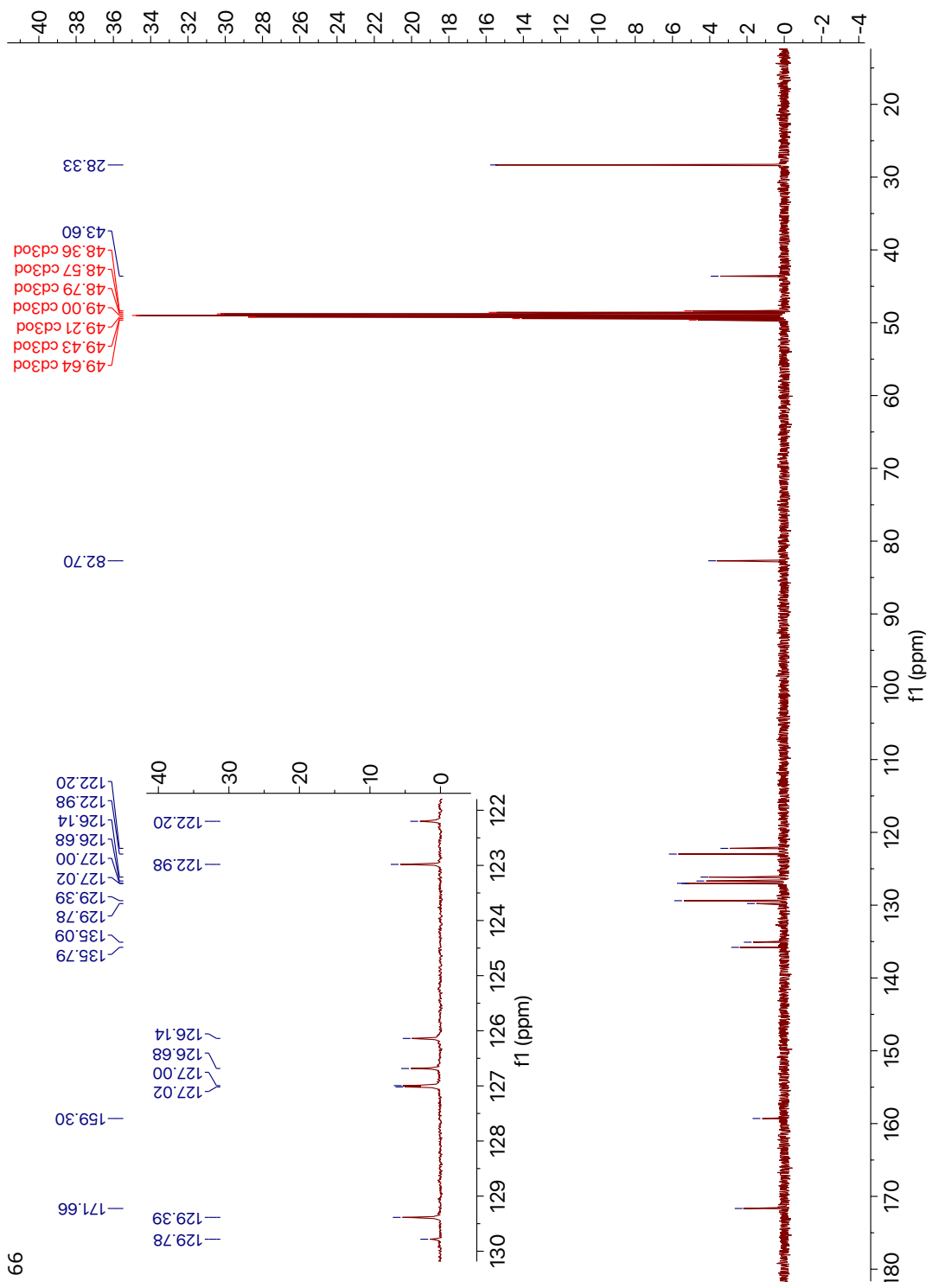


64

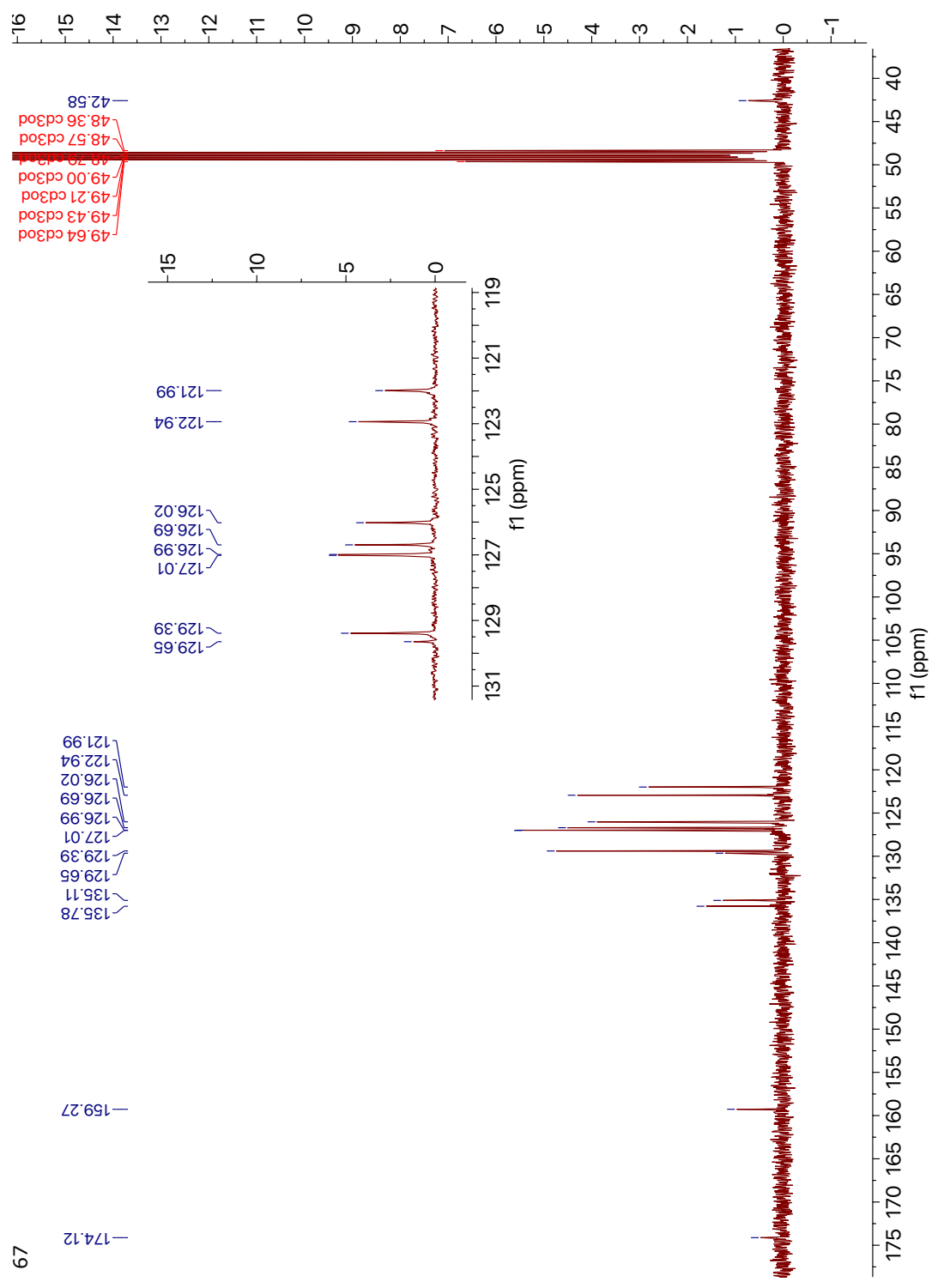




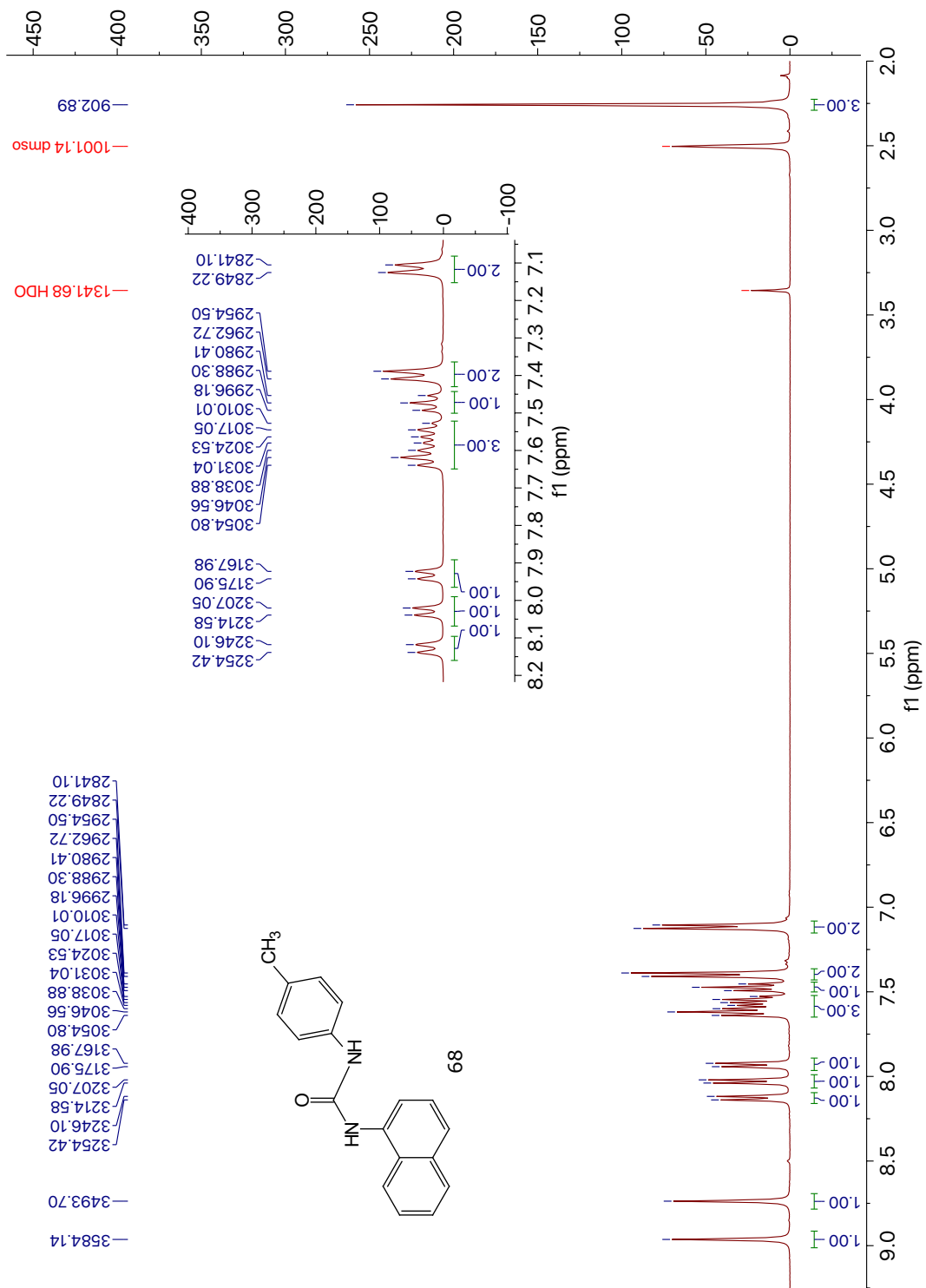


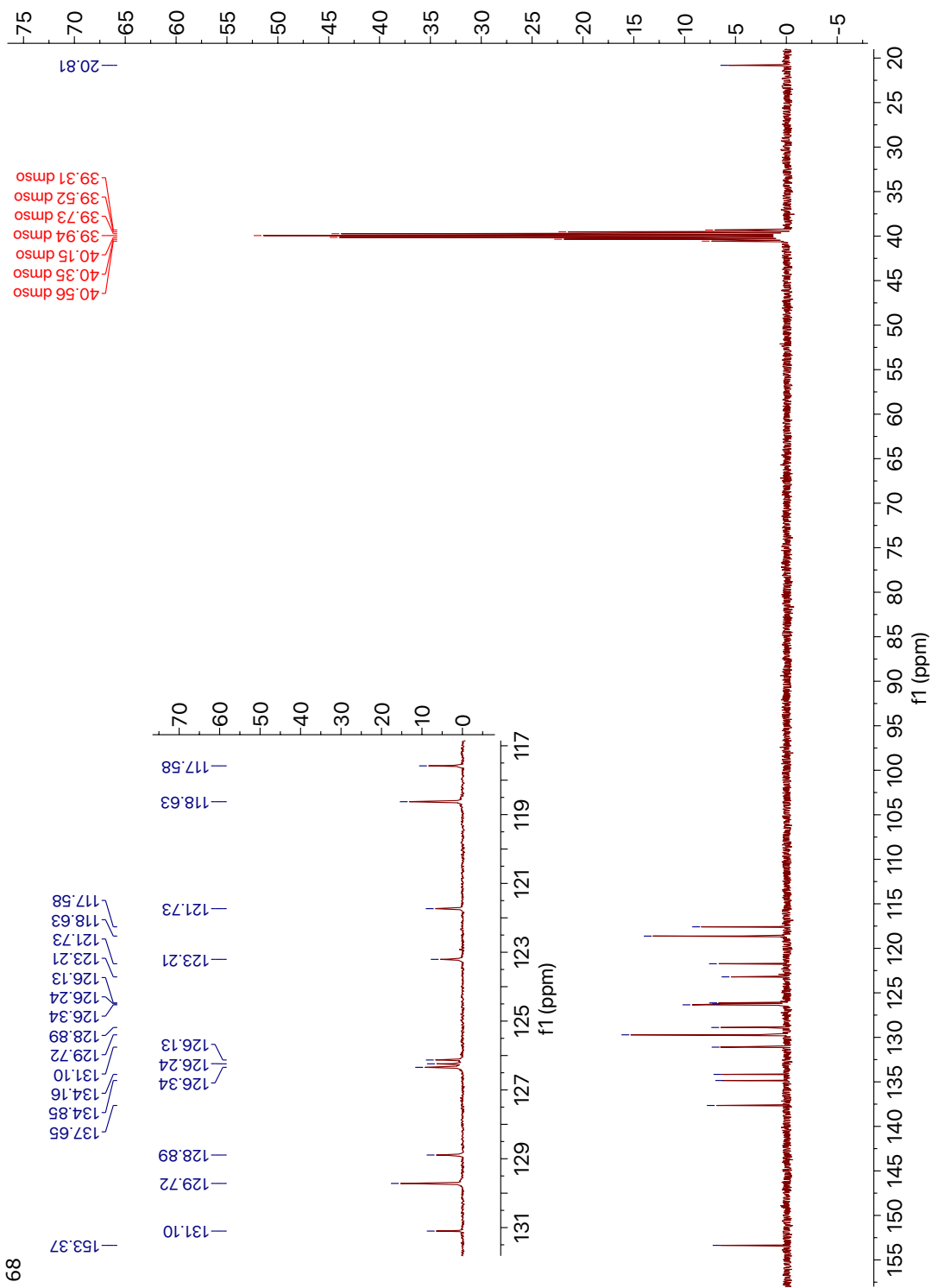


66

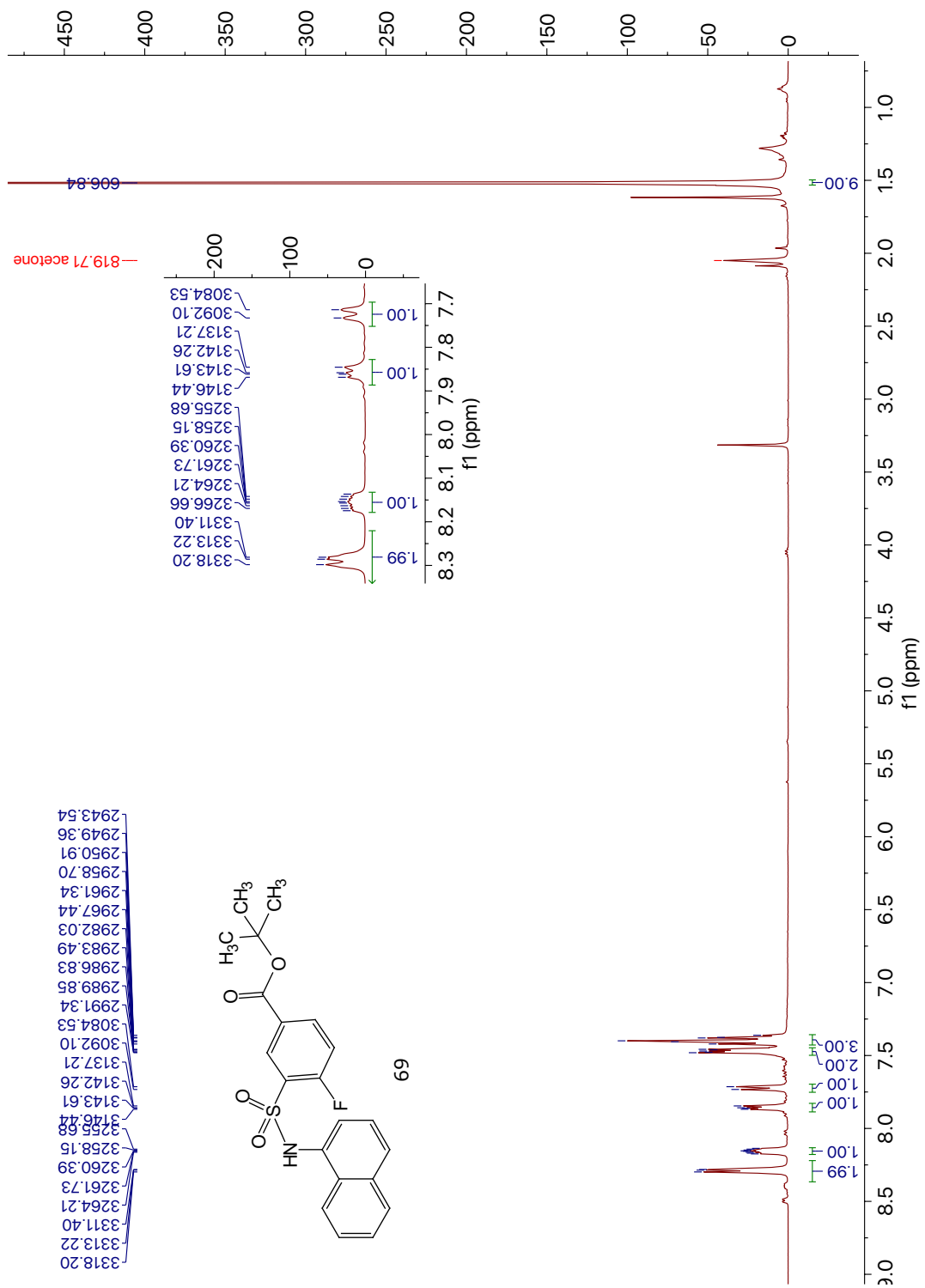


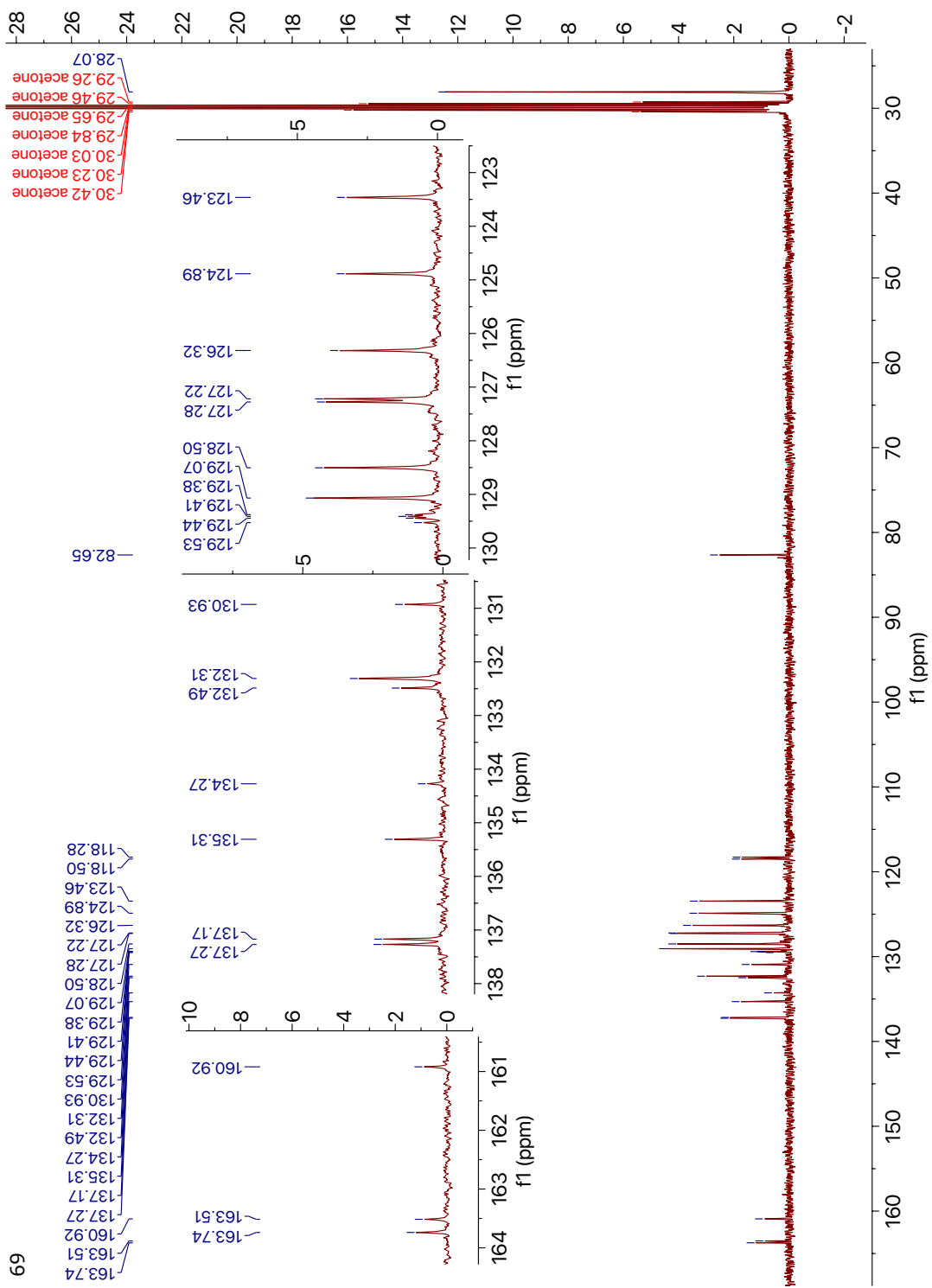
67



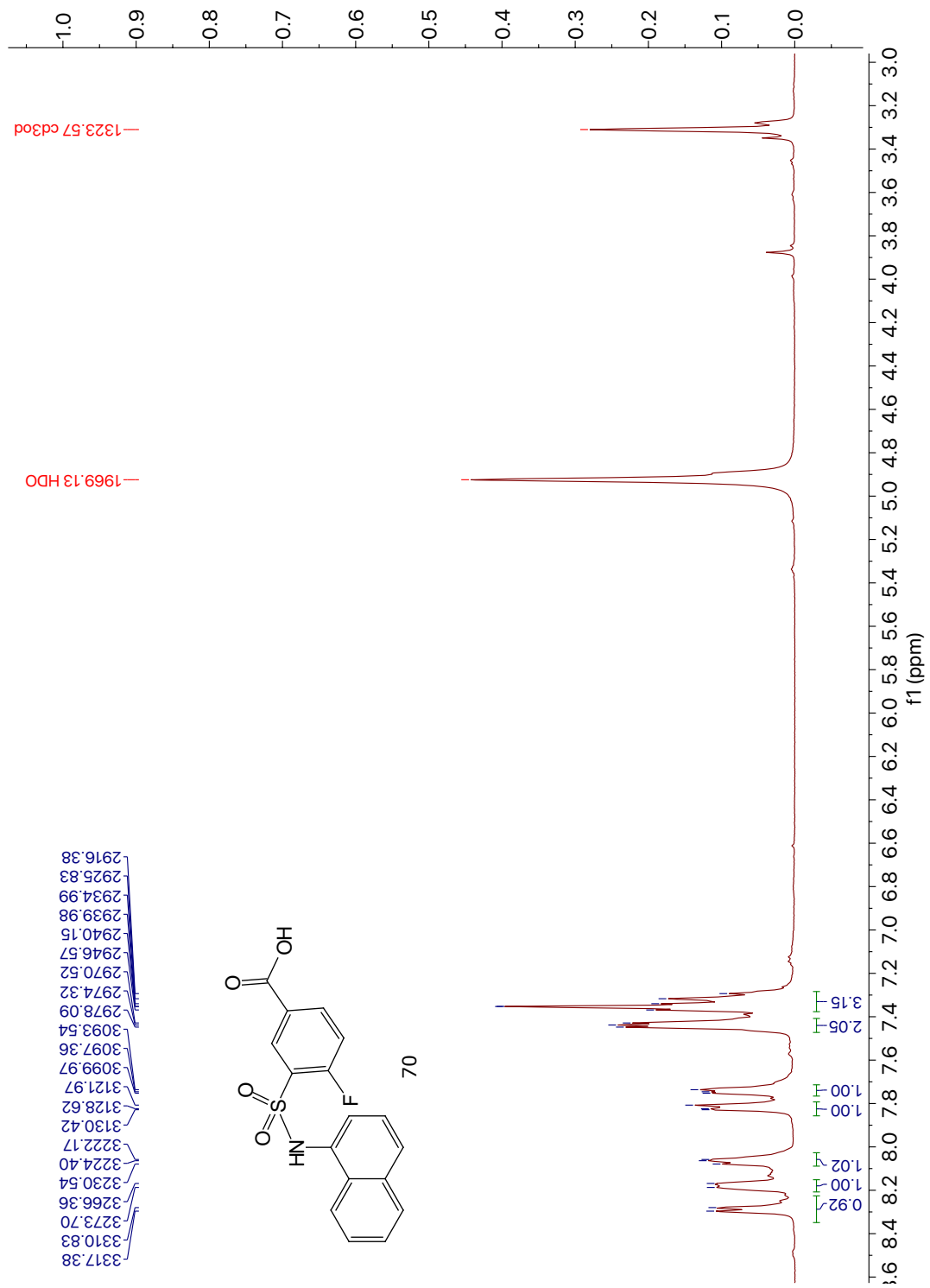


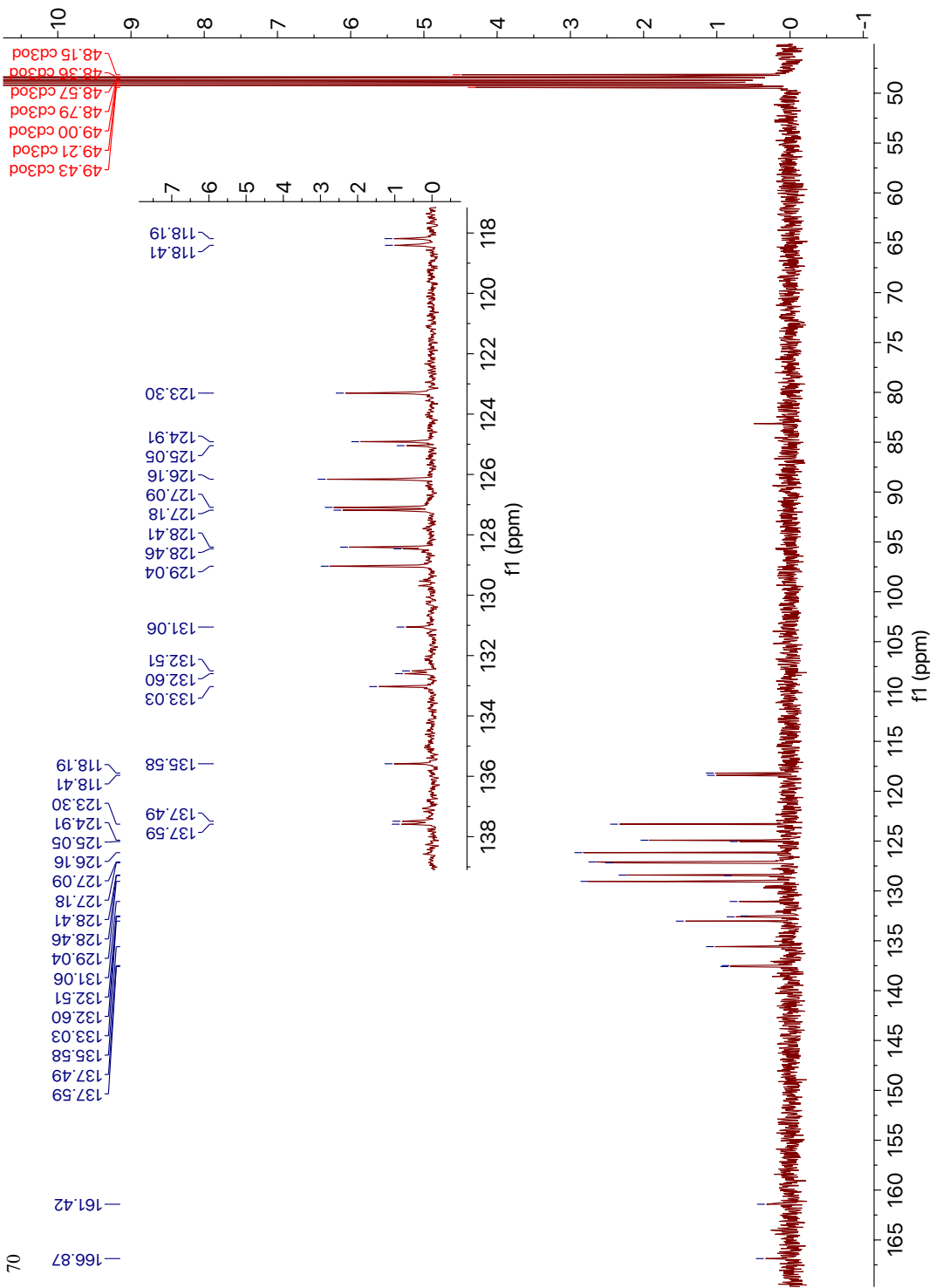
68

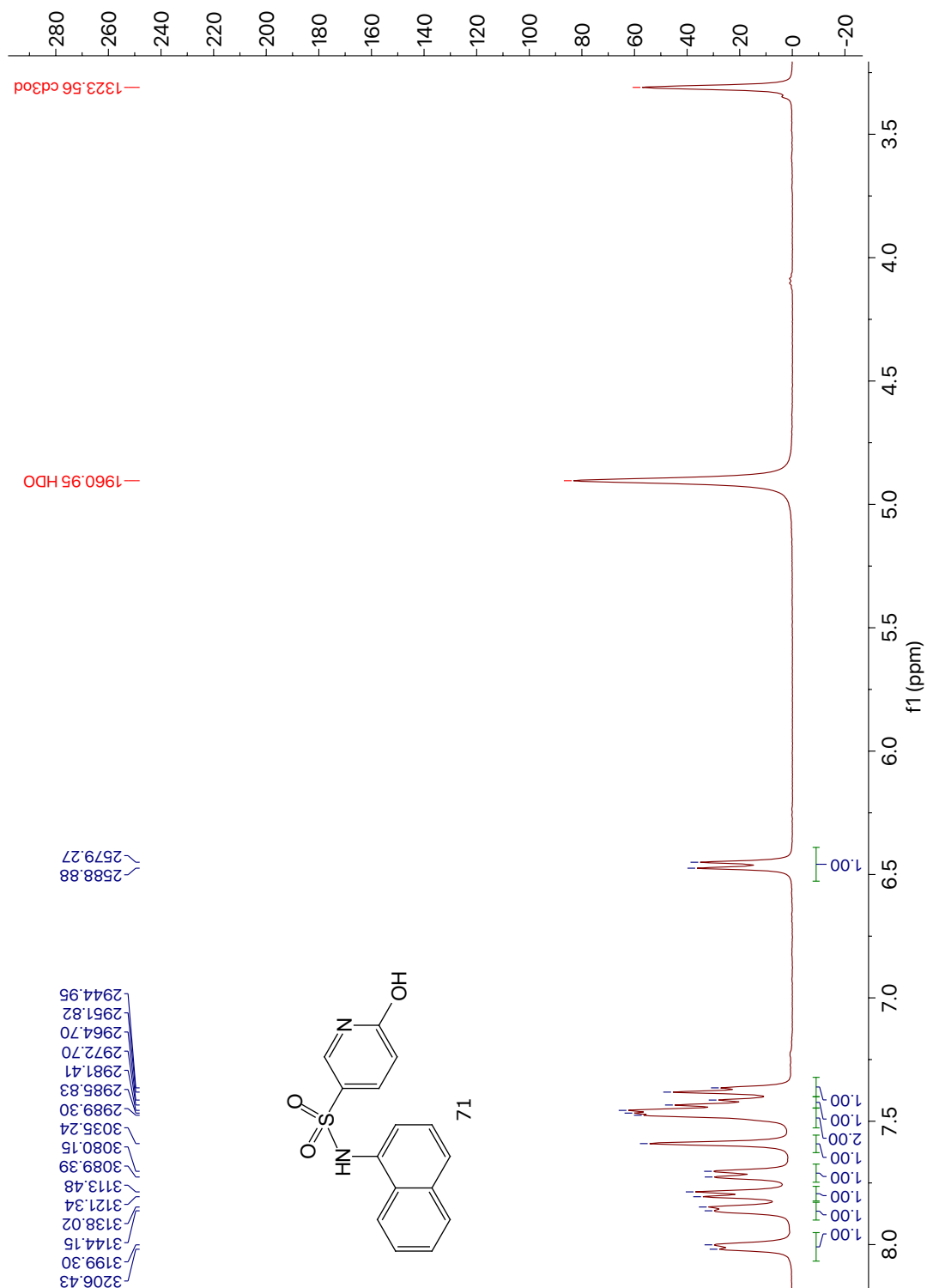


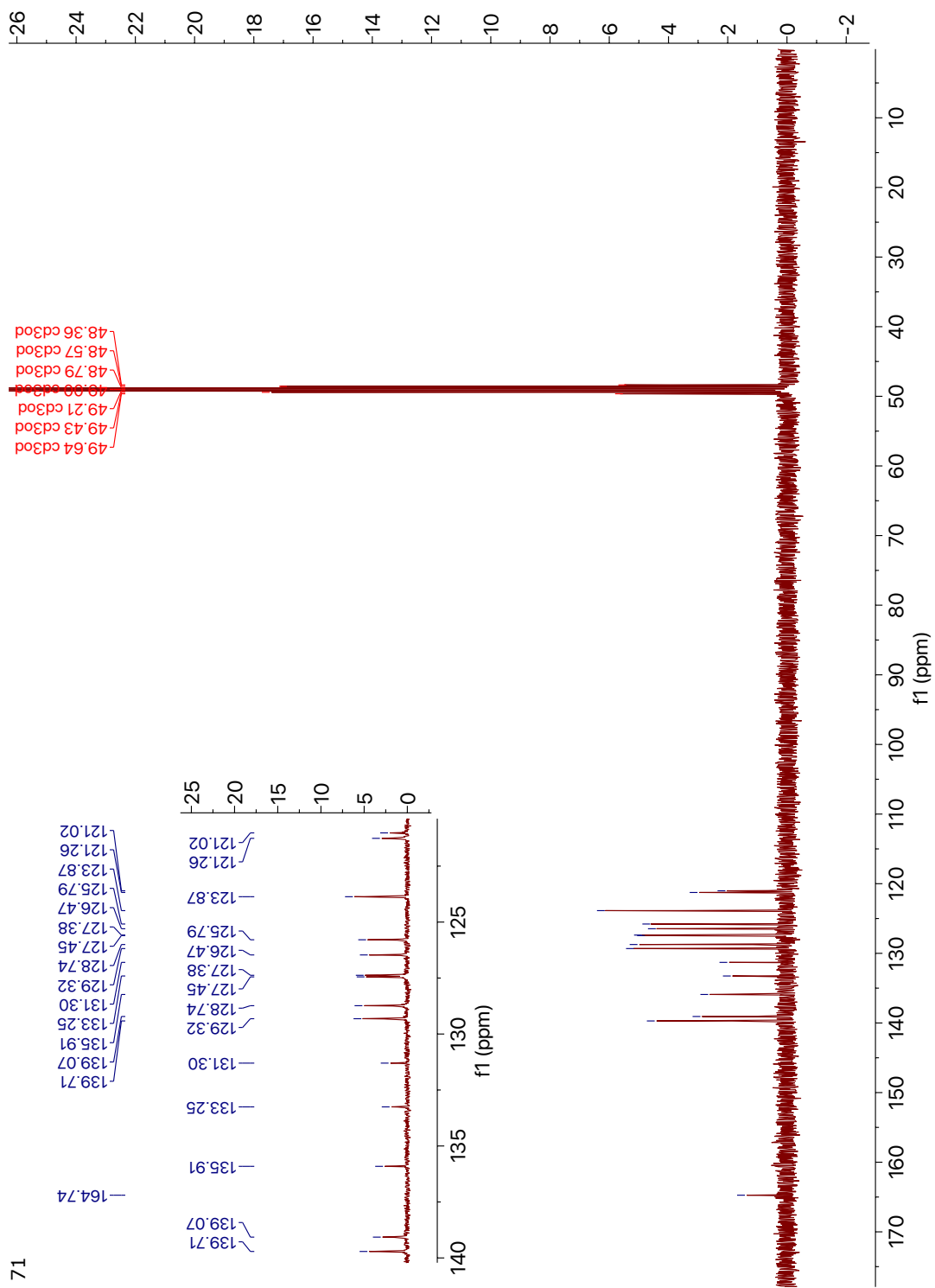


69

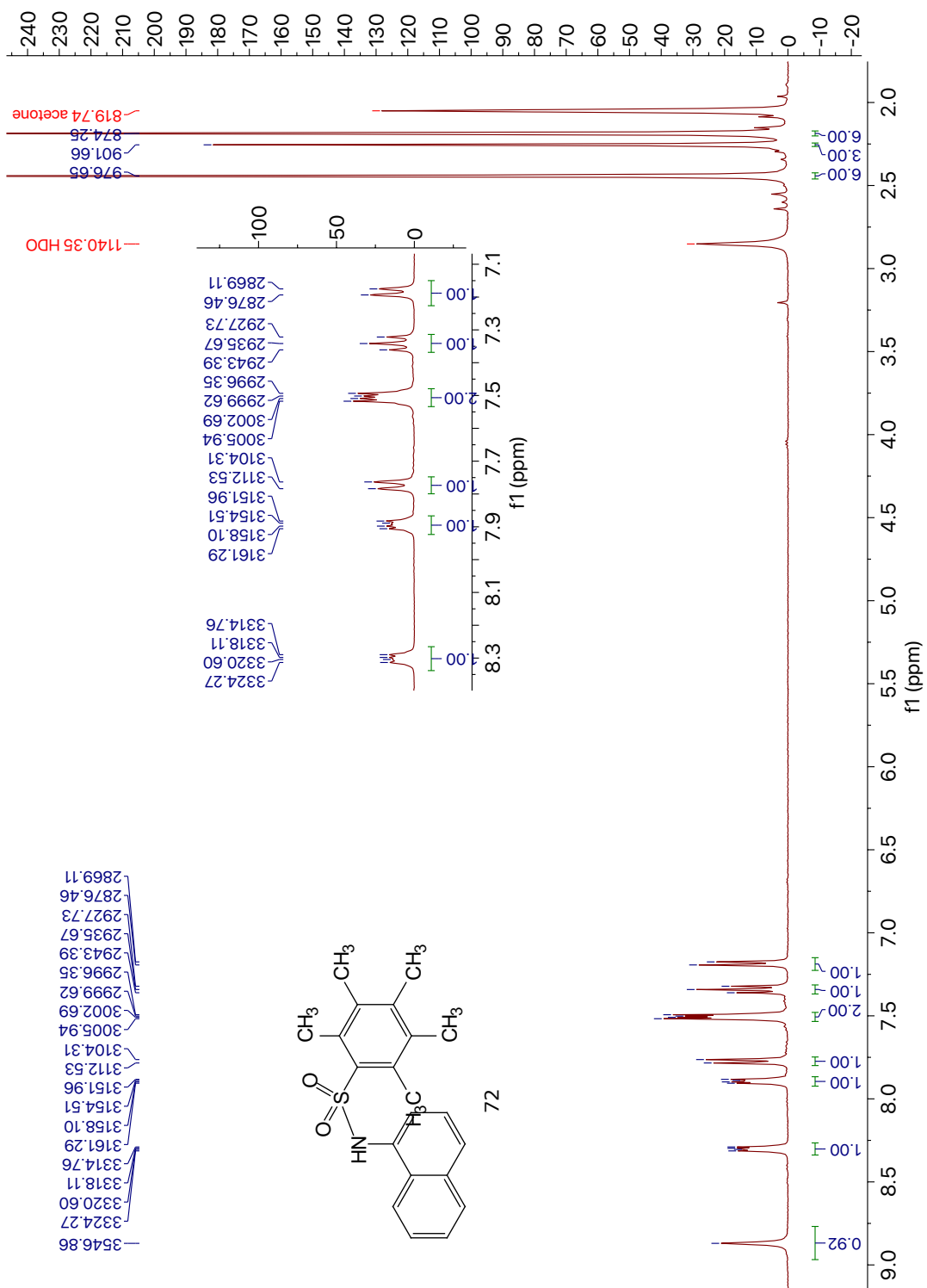


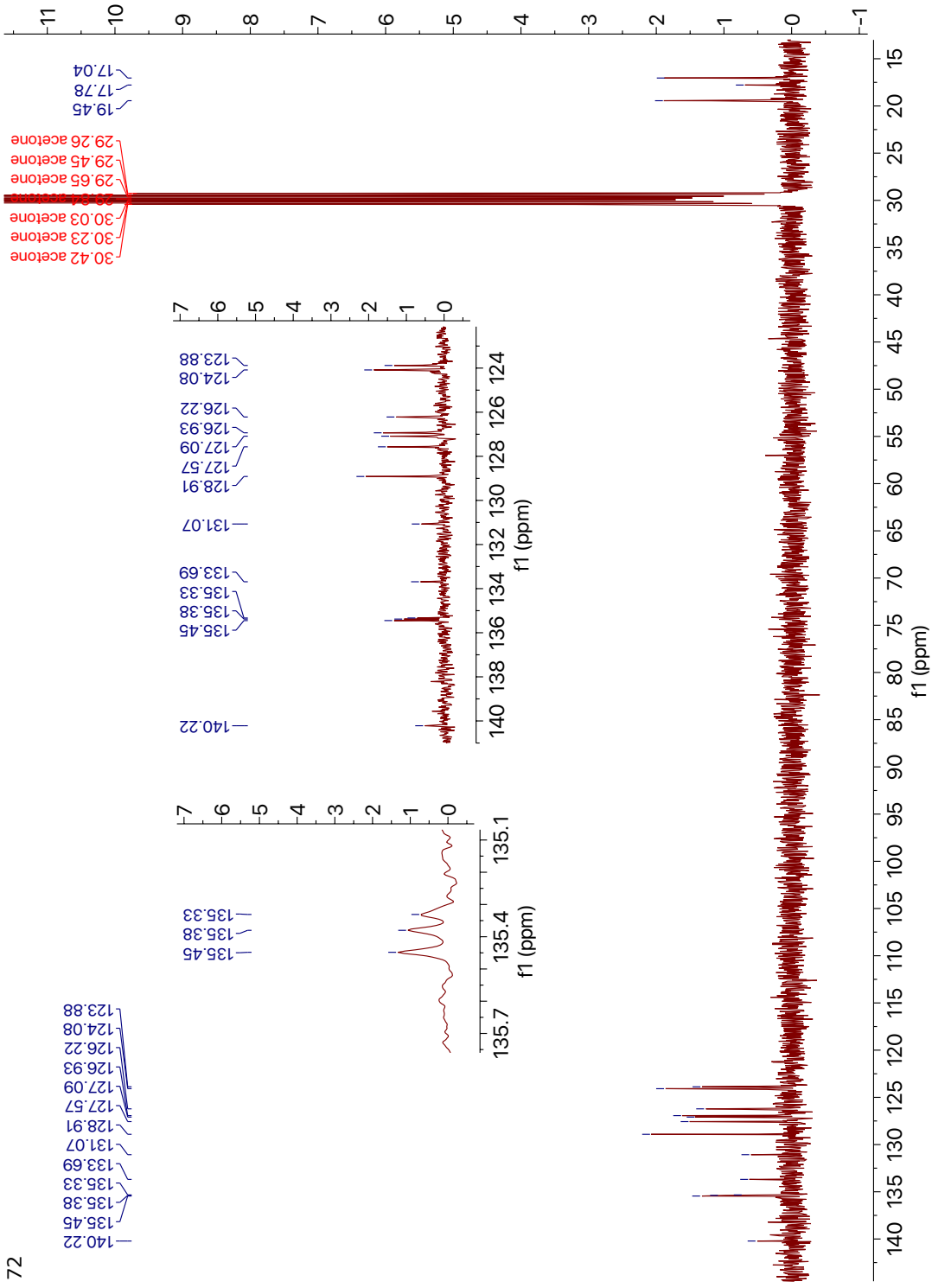


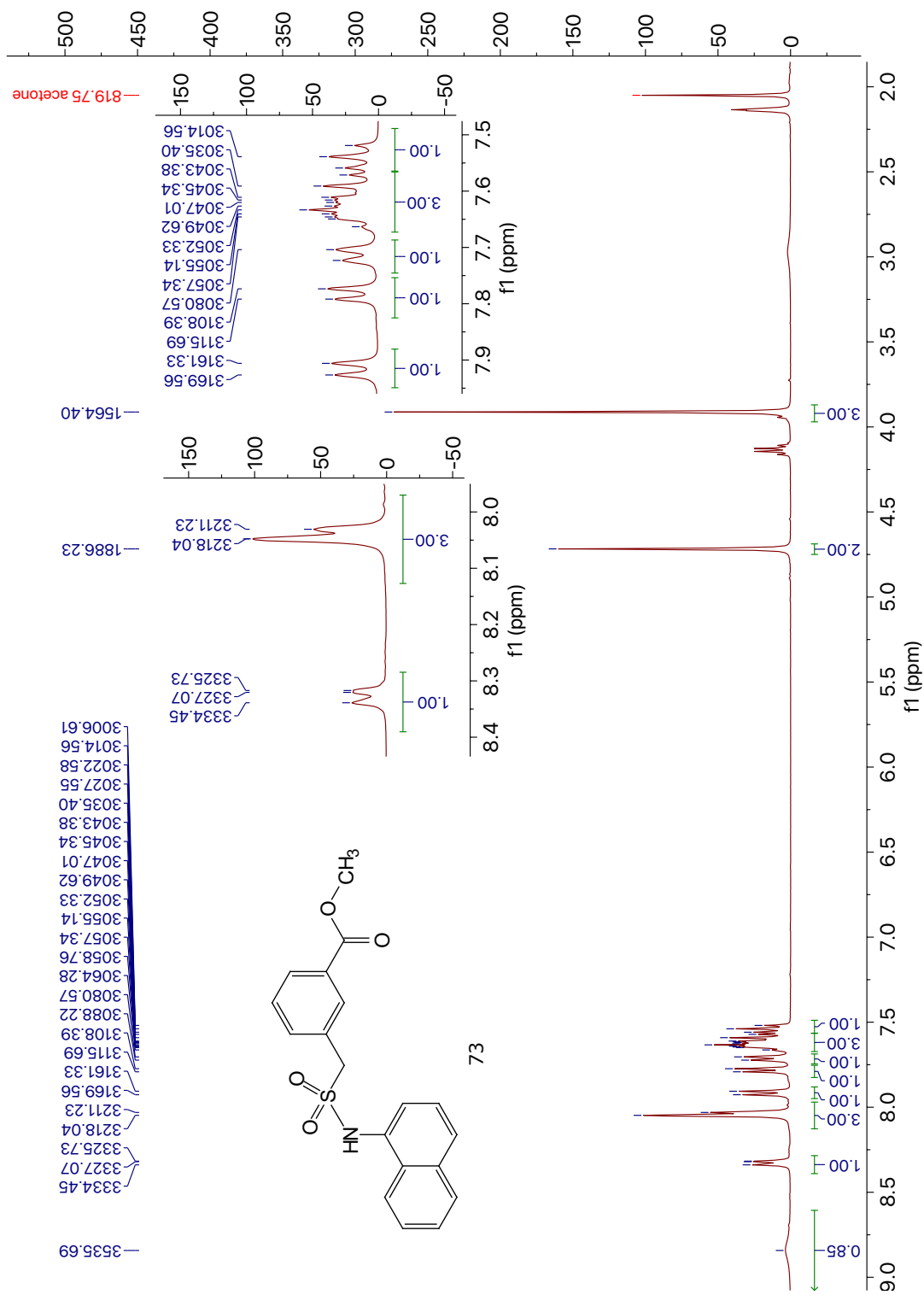


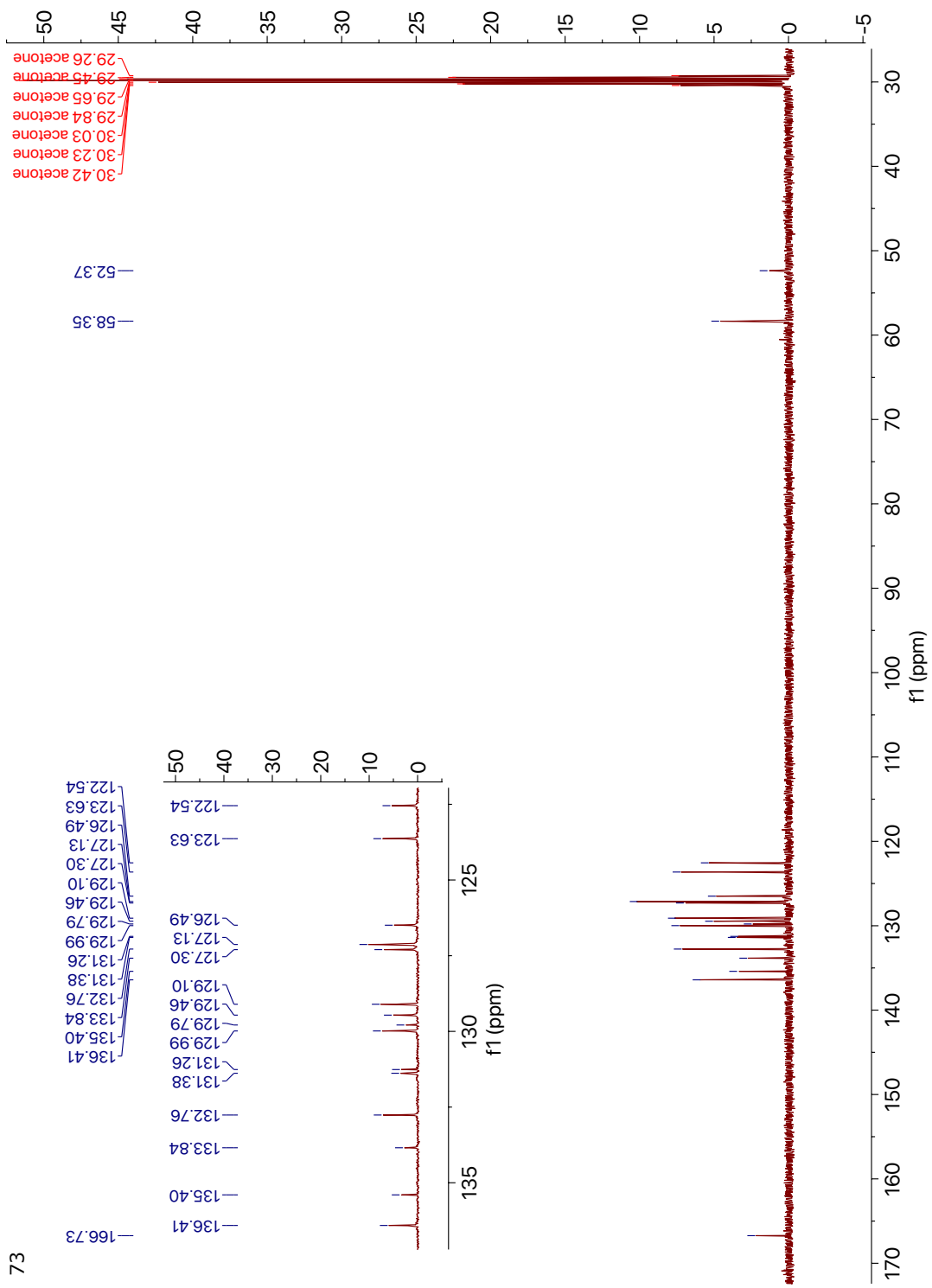


71

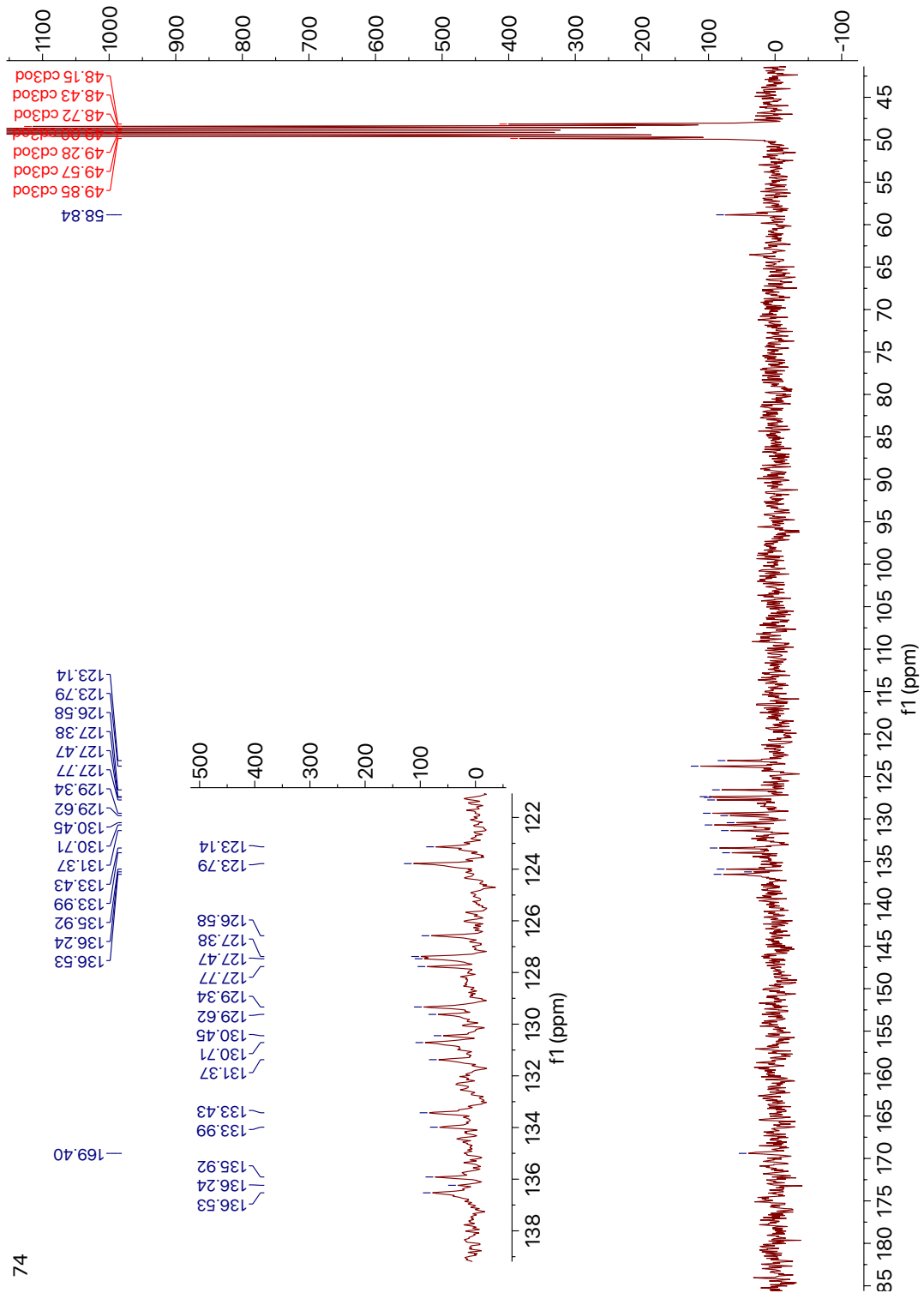




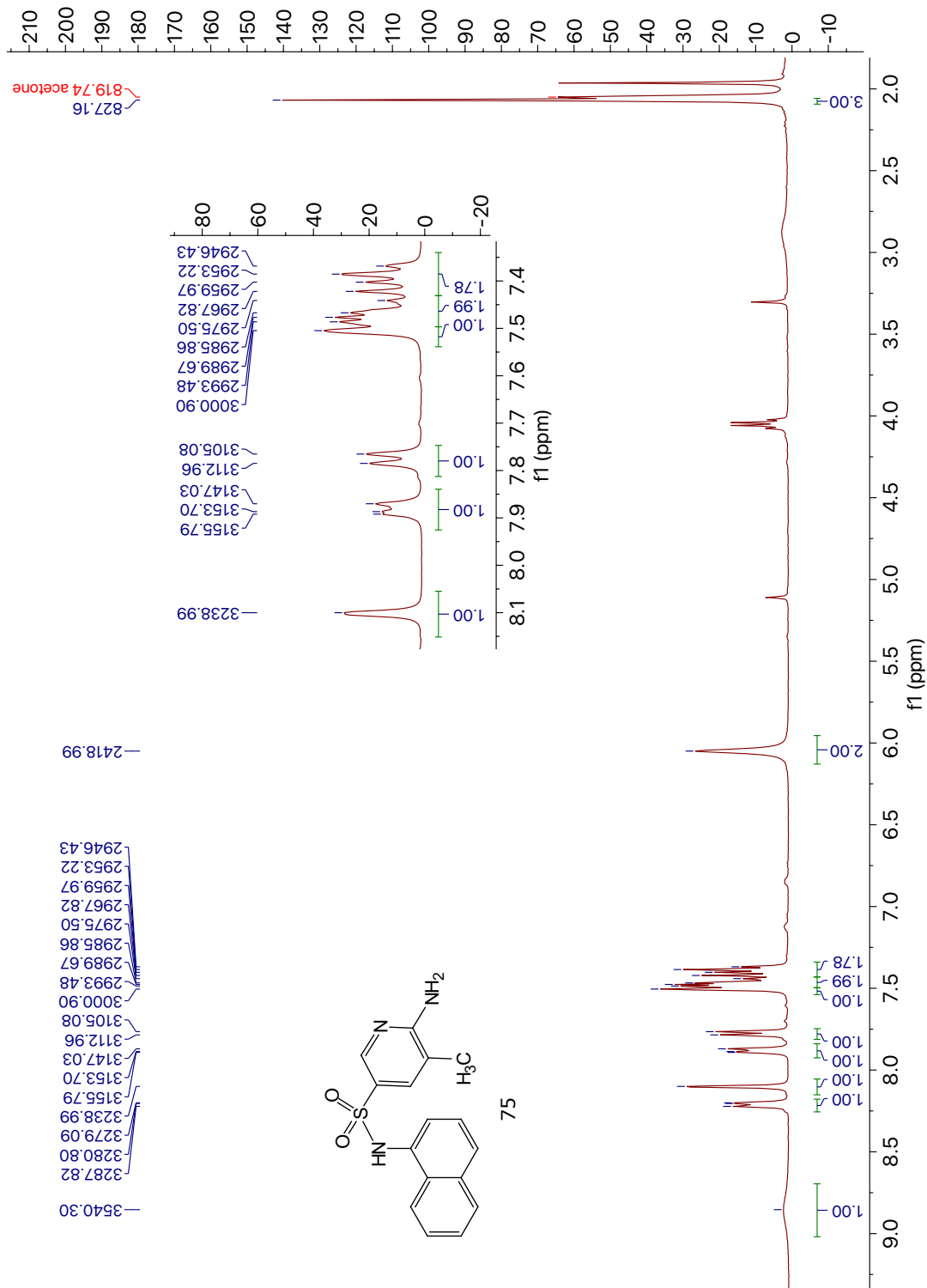


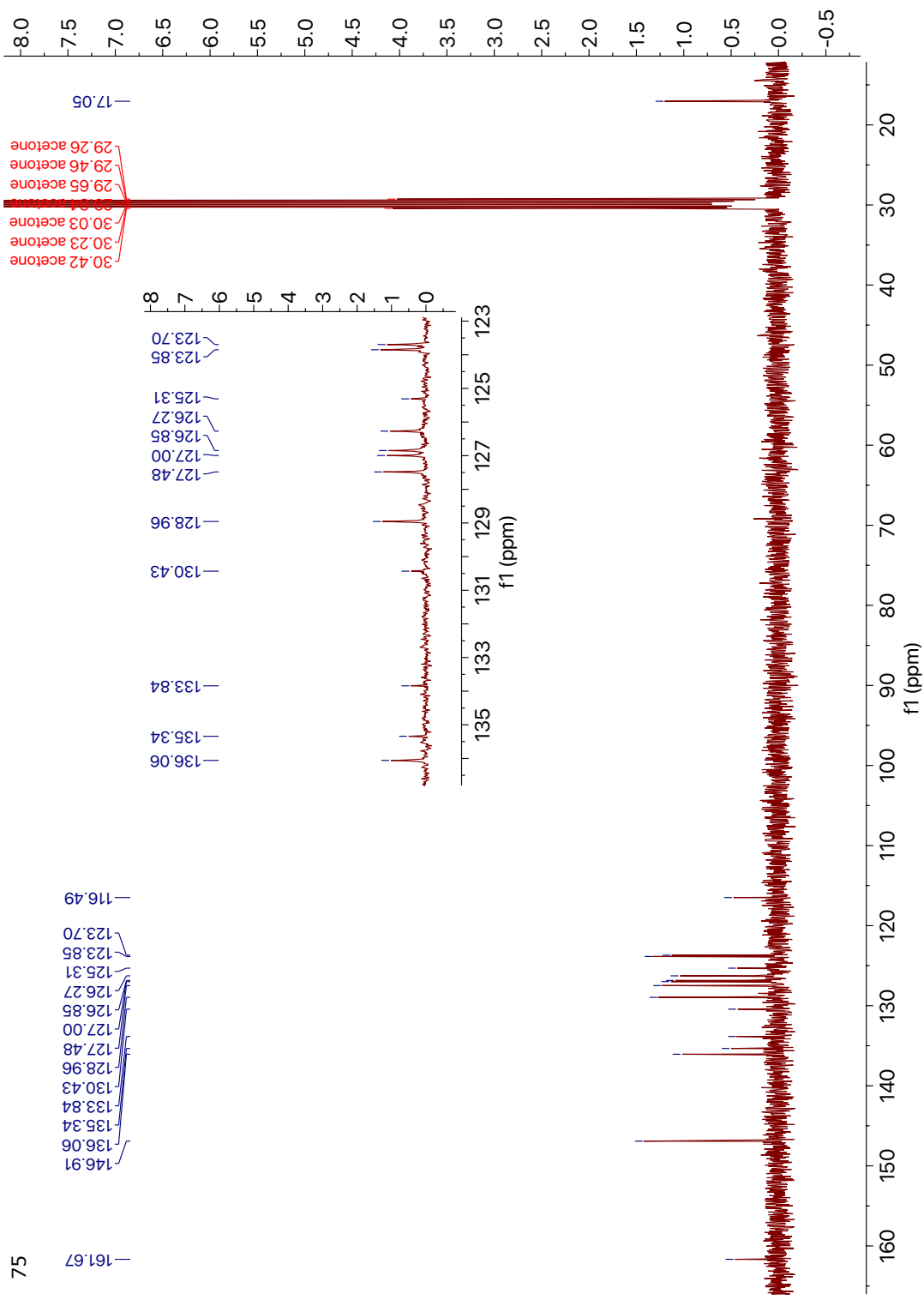


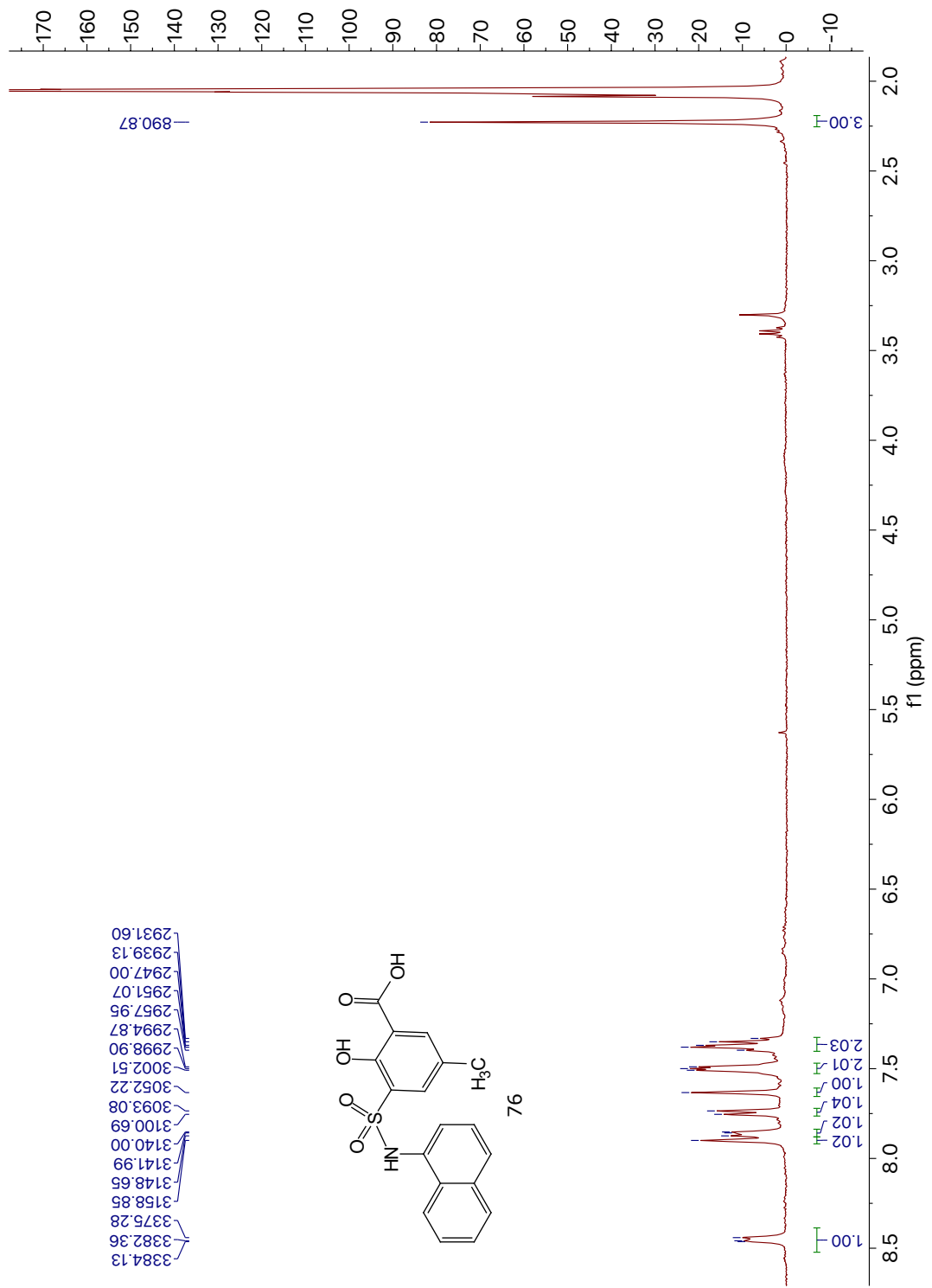
73

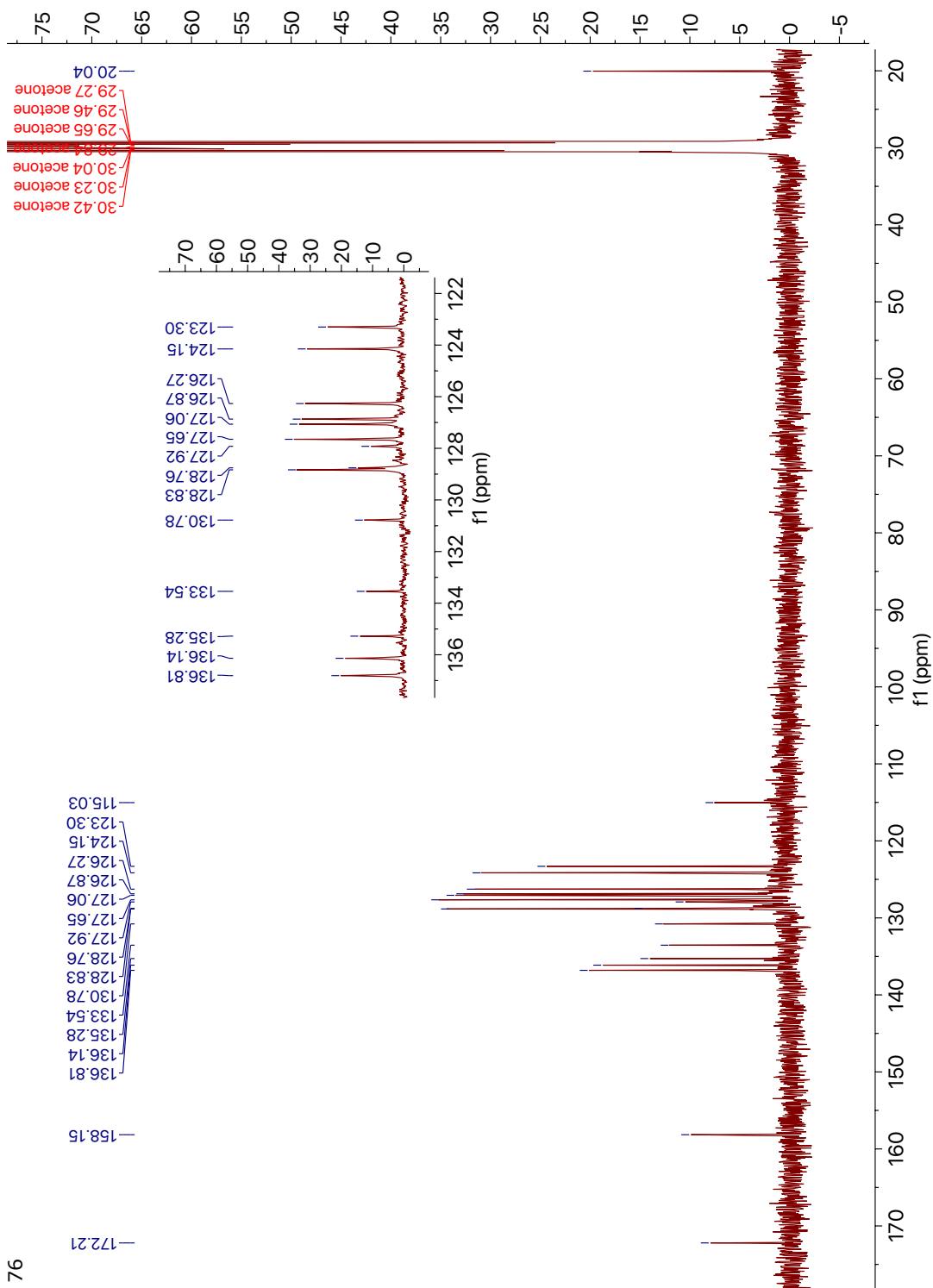


74

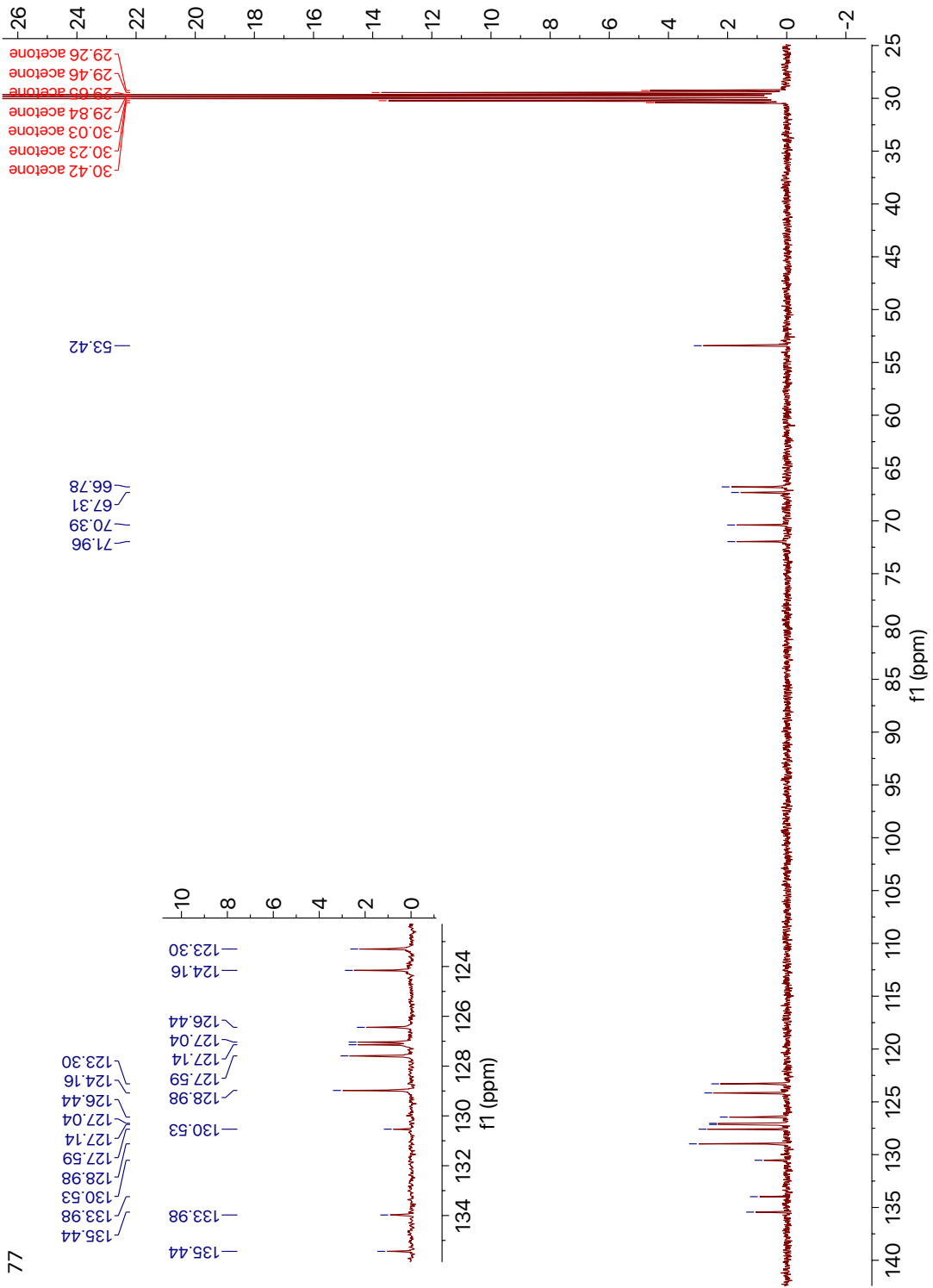




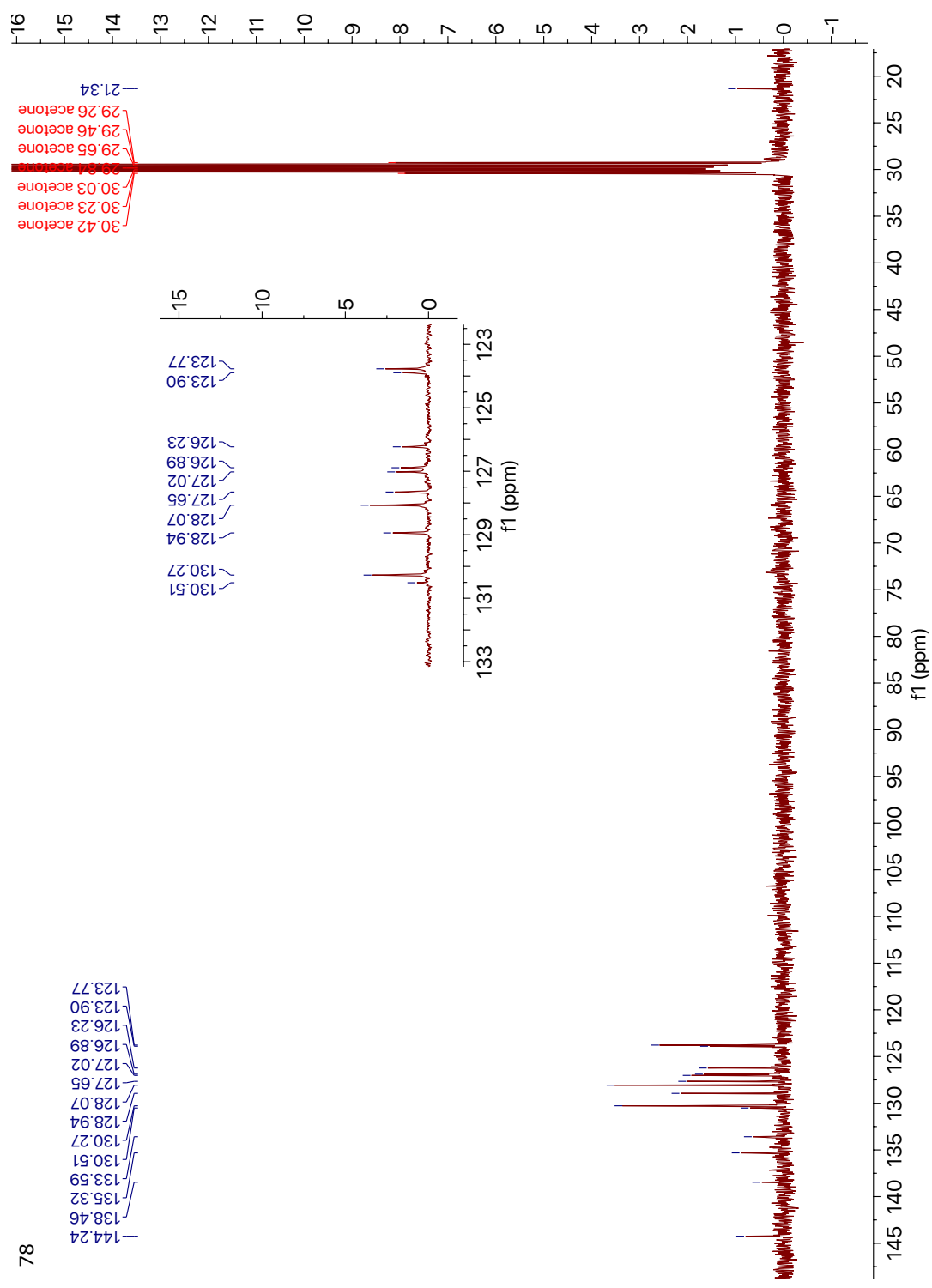




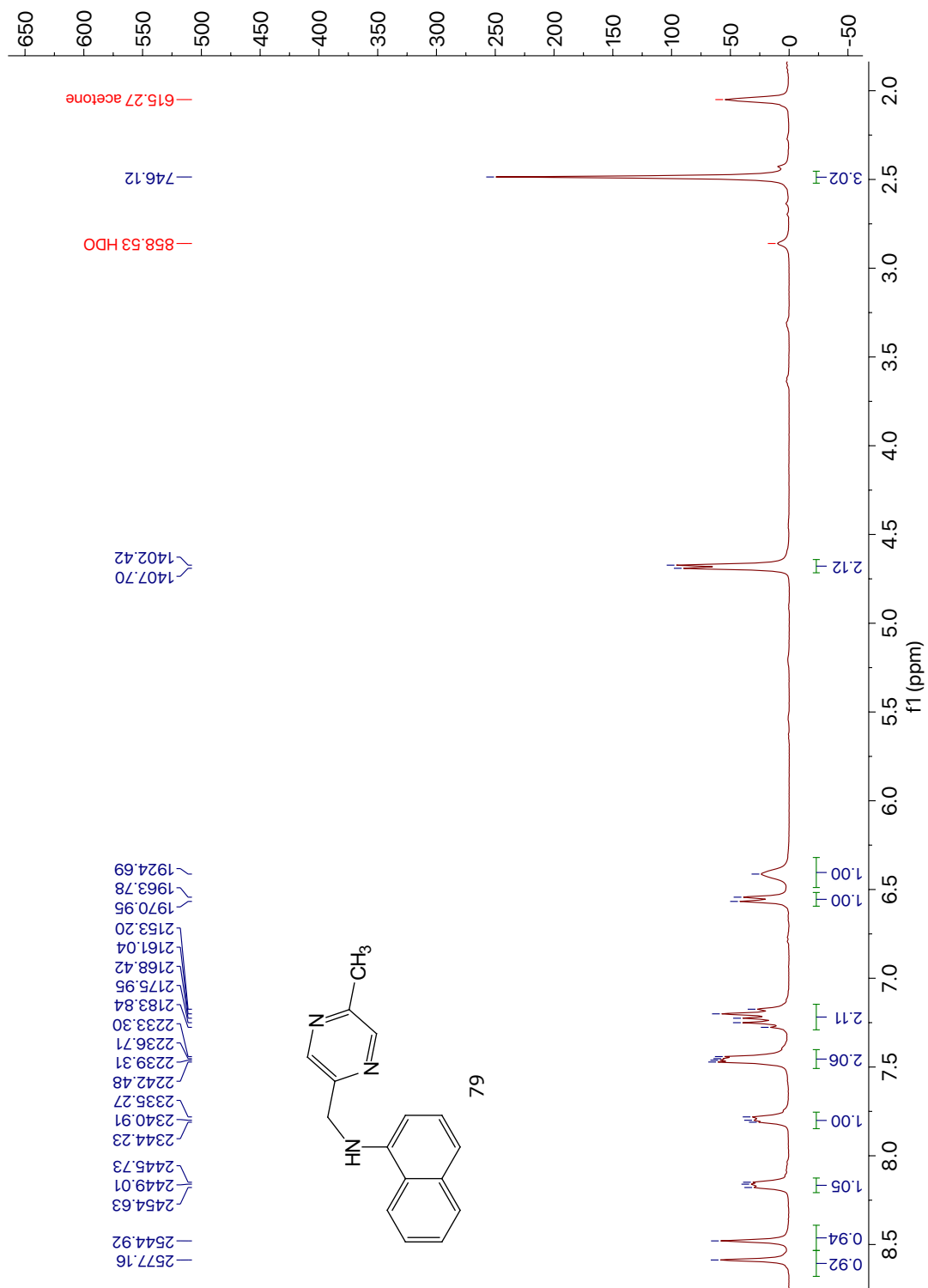
76

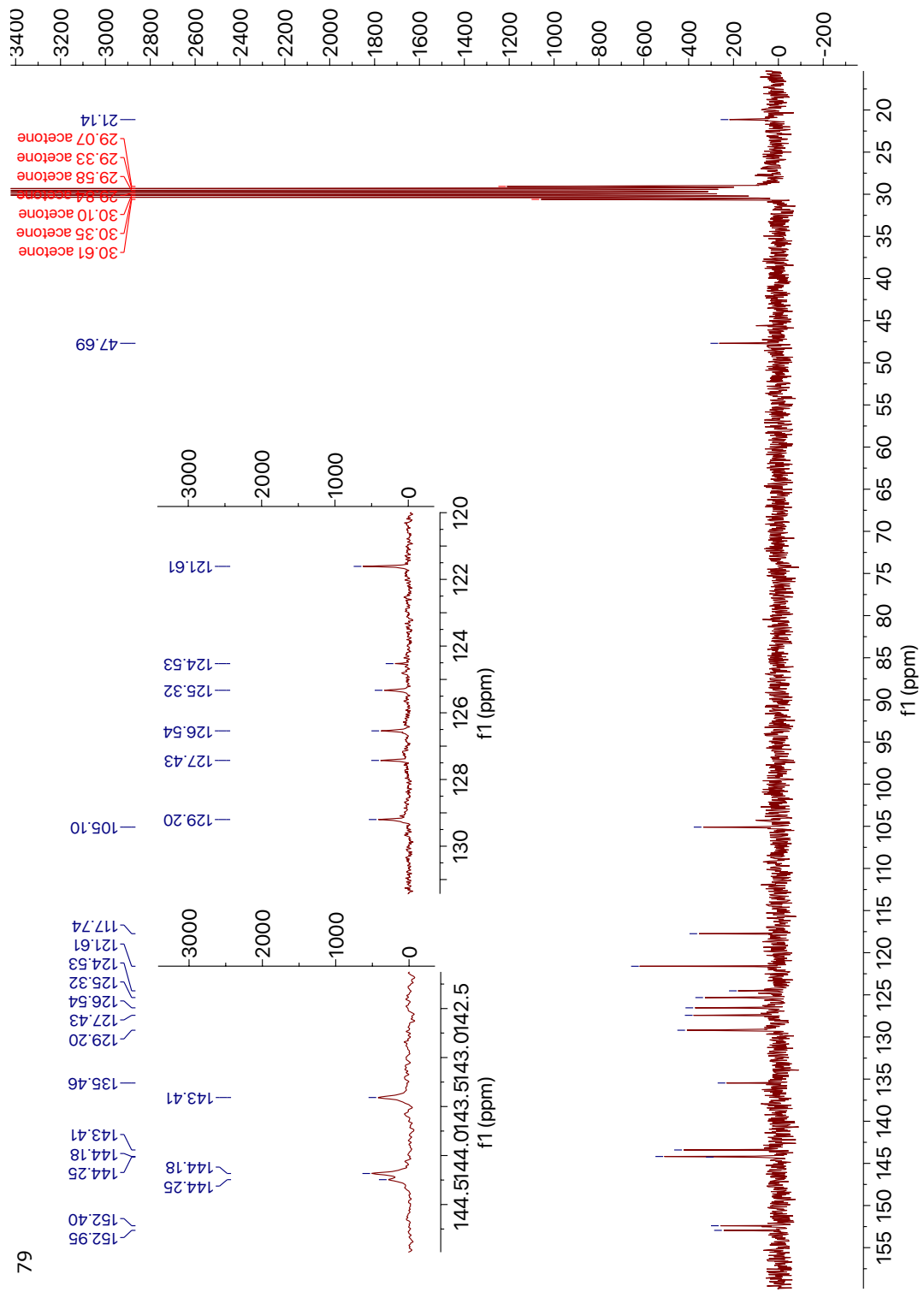


77

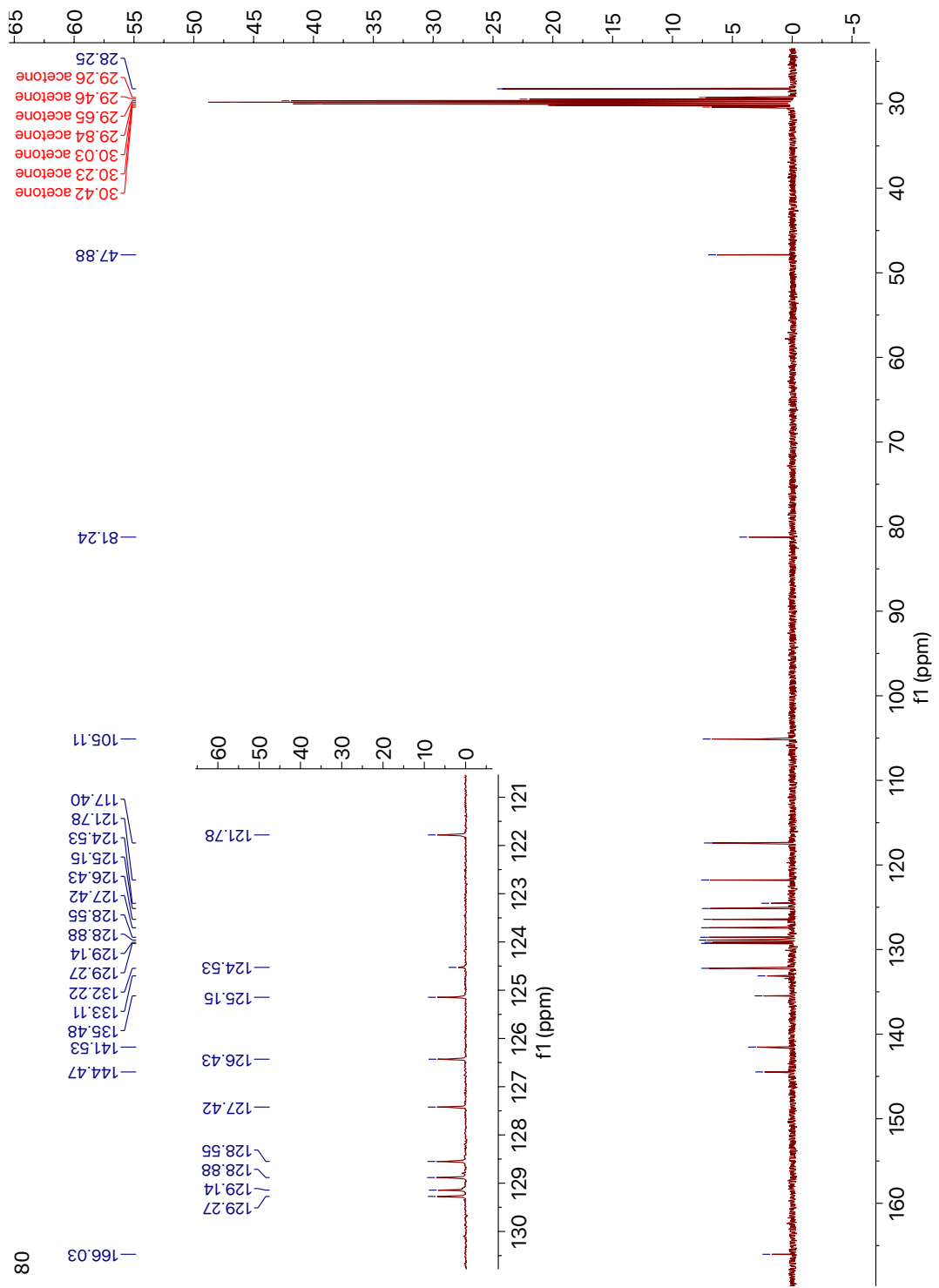


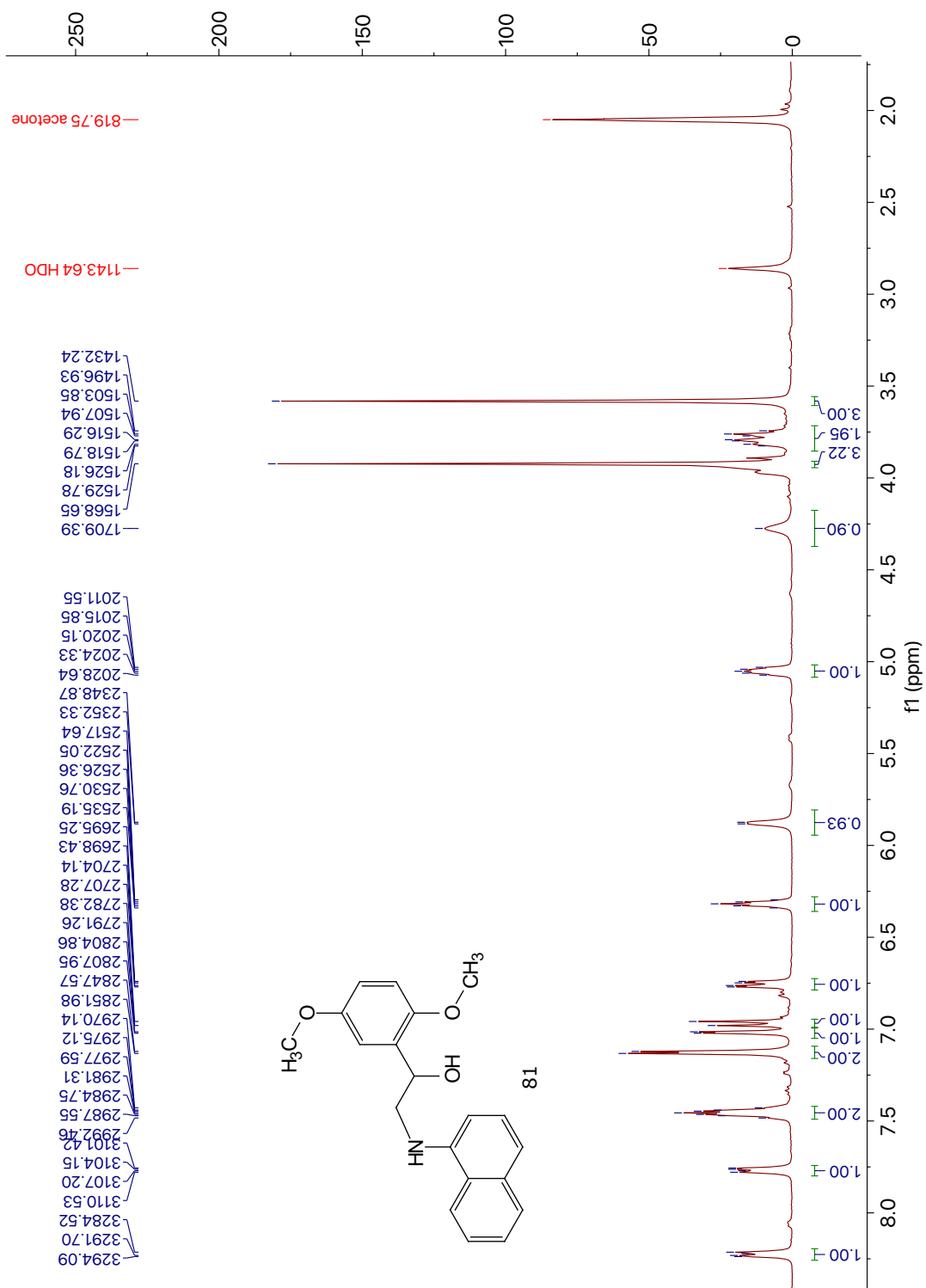
78

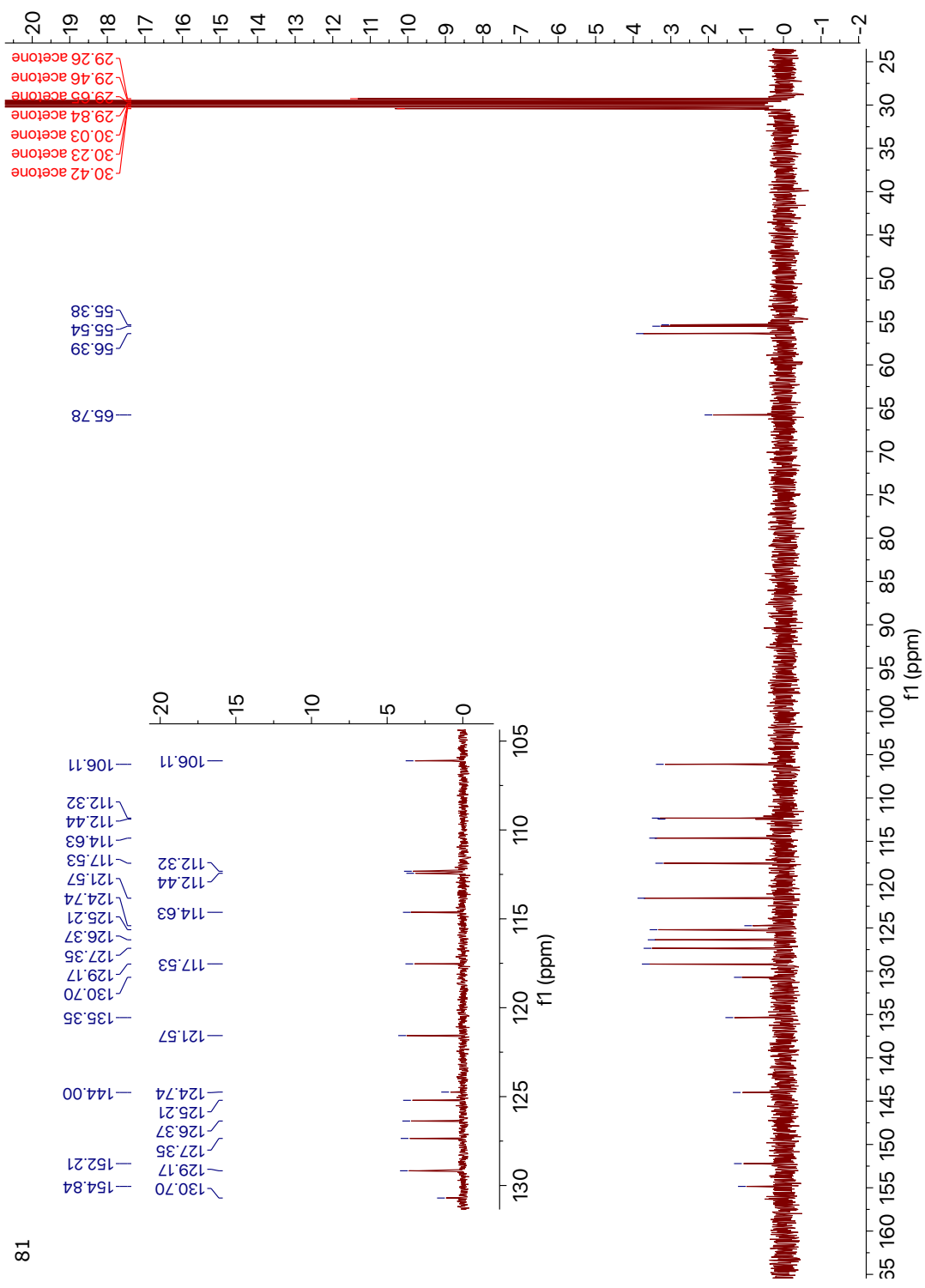




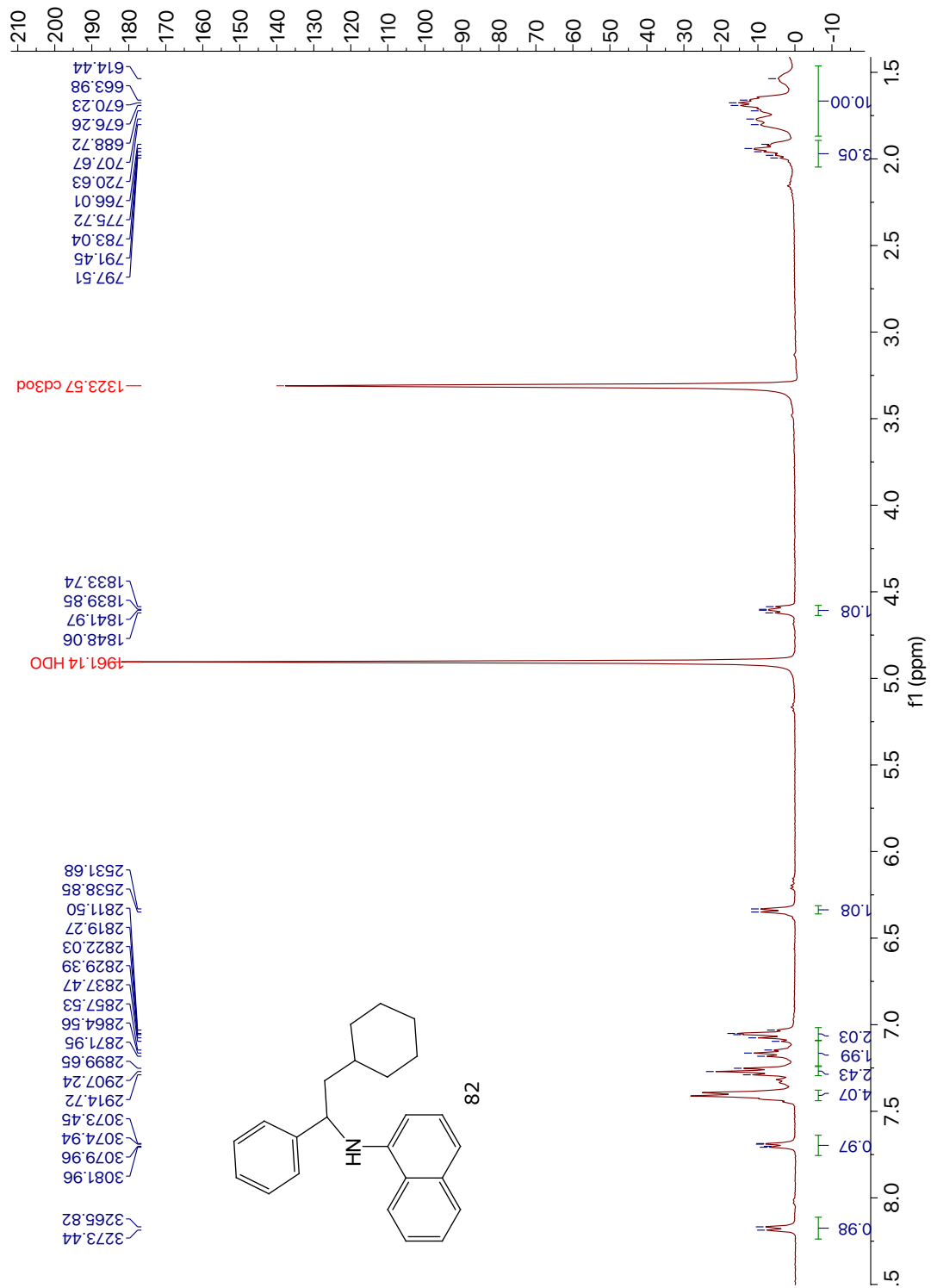
79

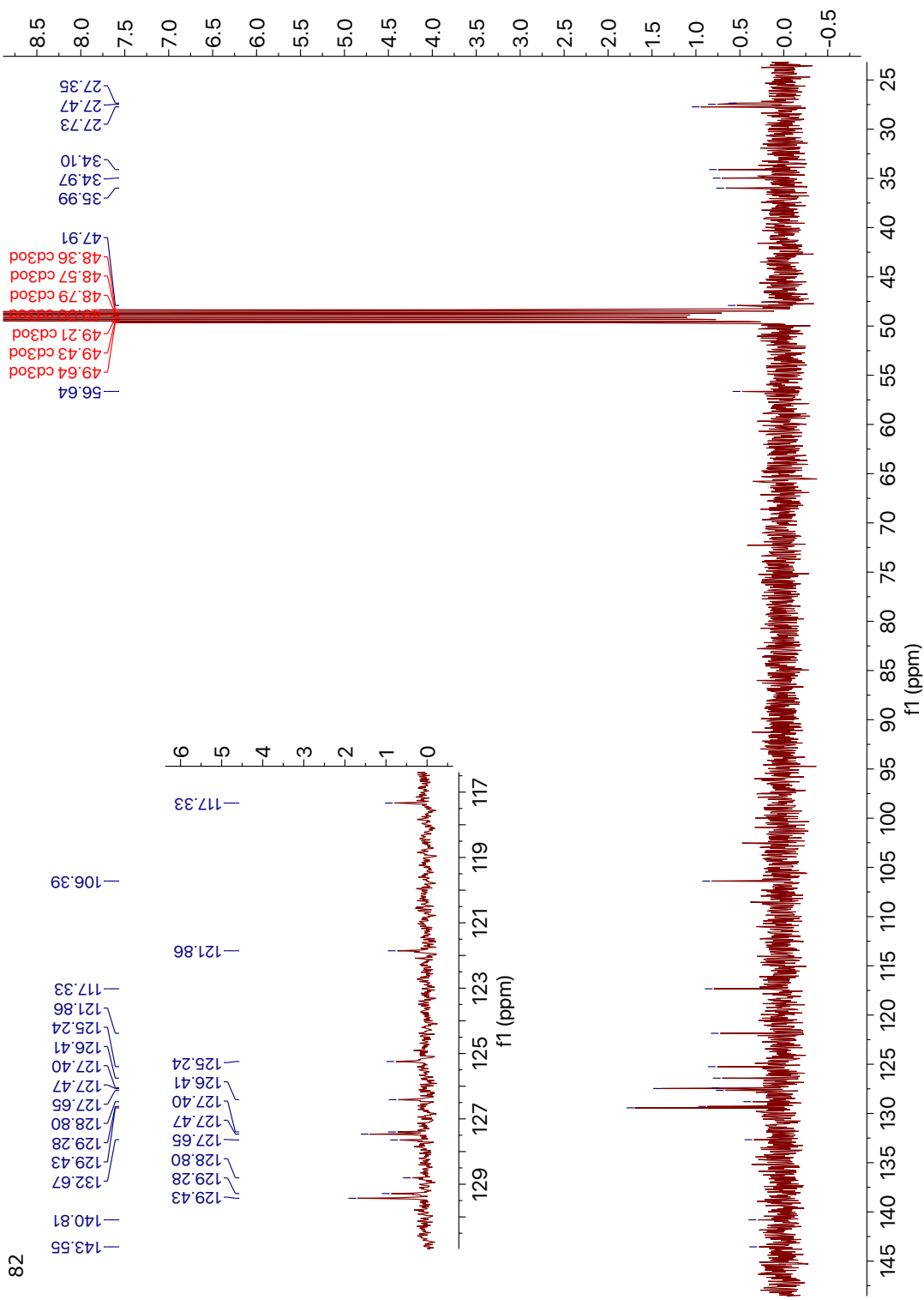




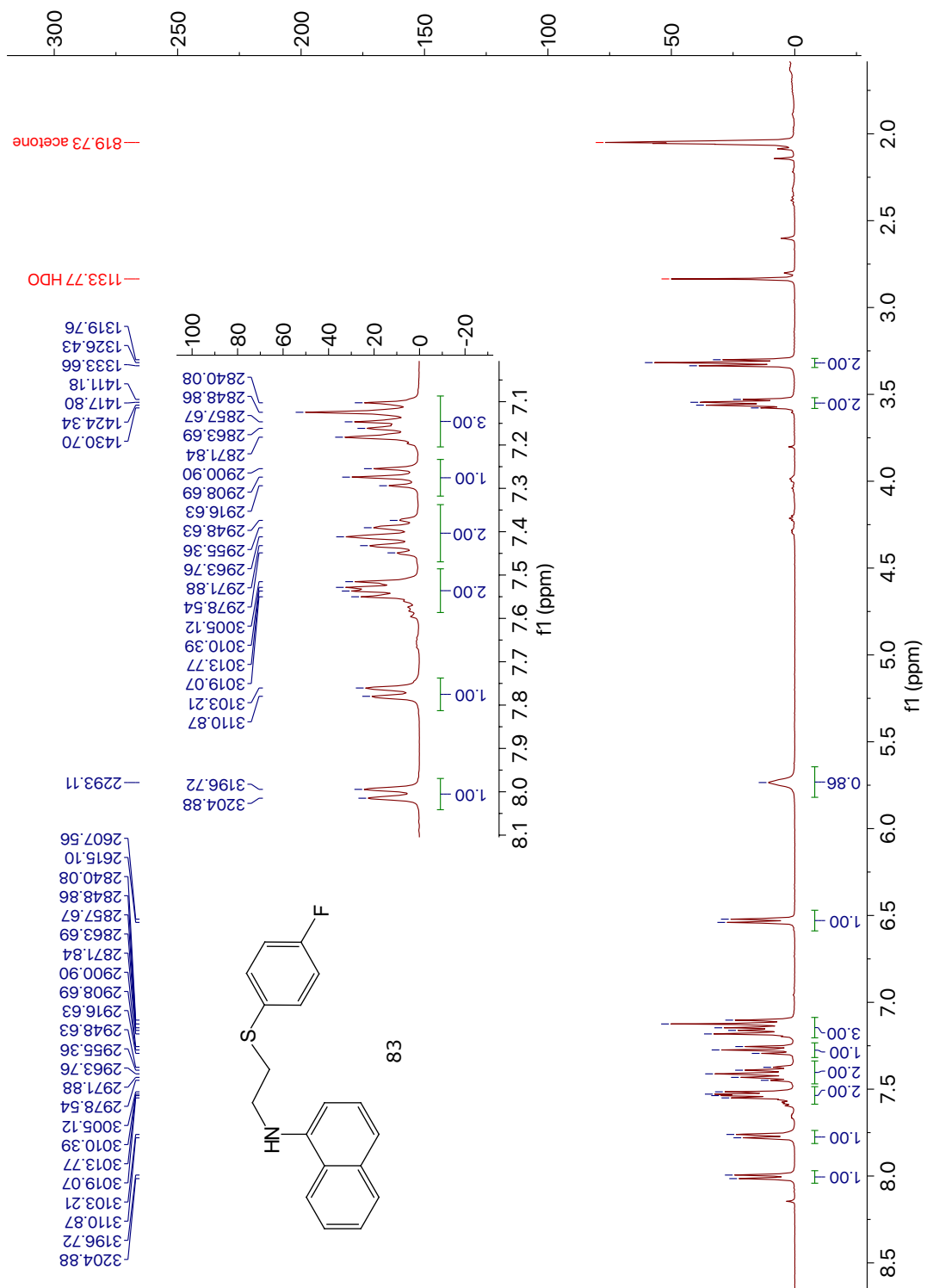


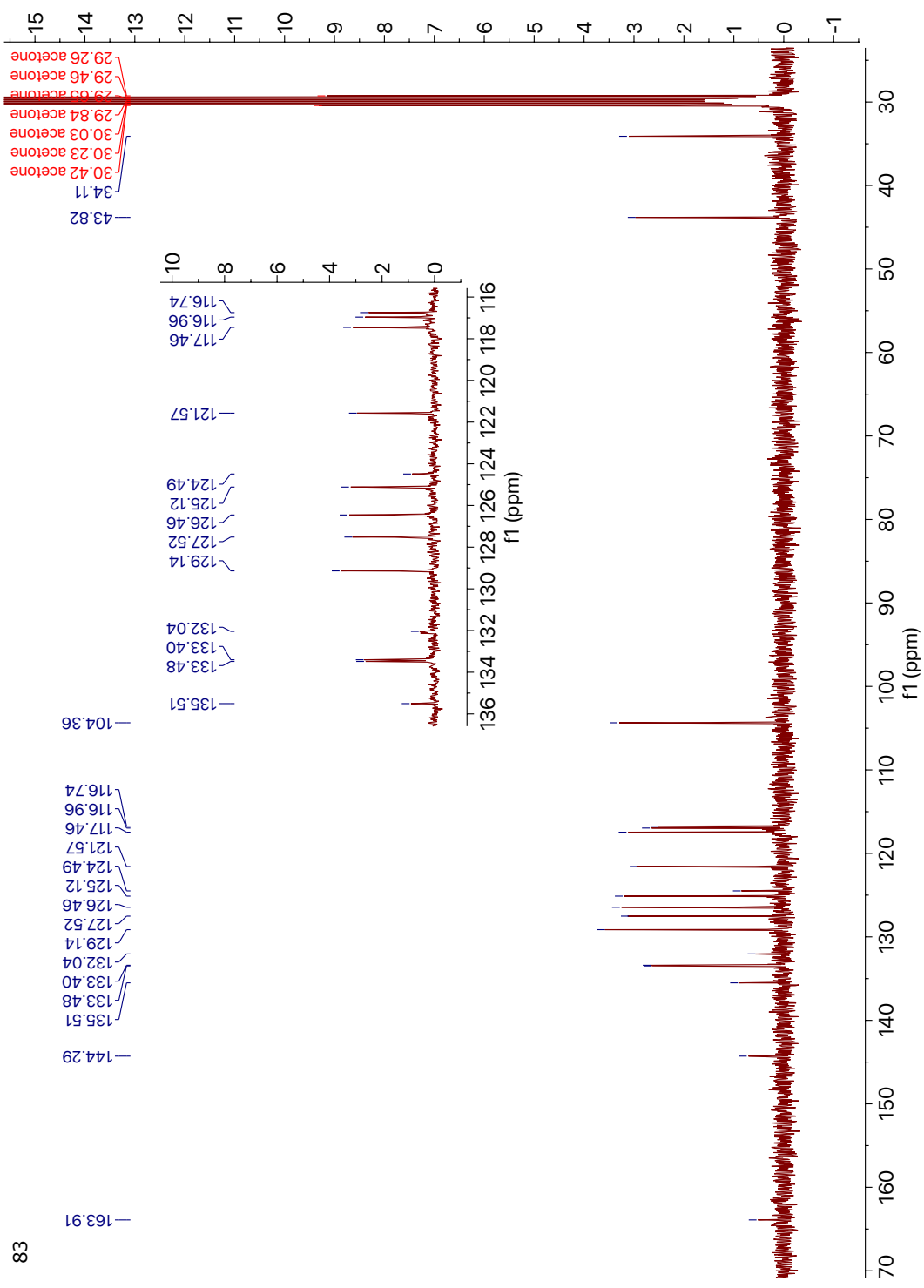
81

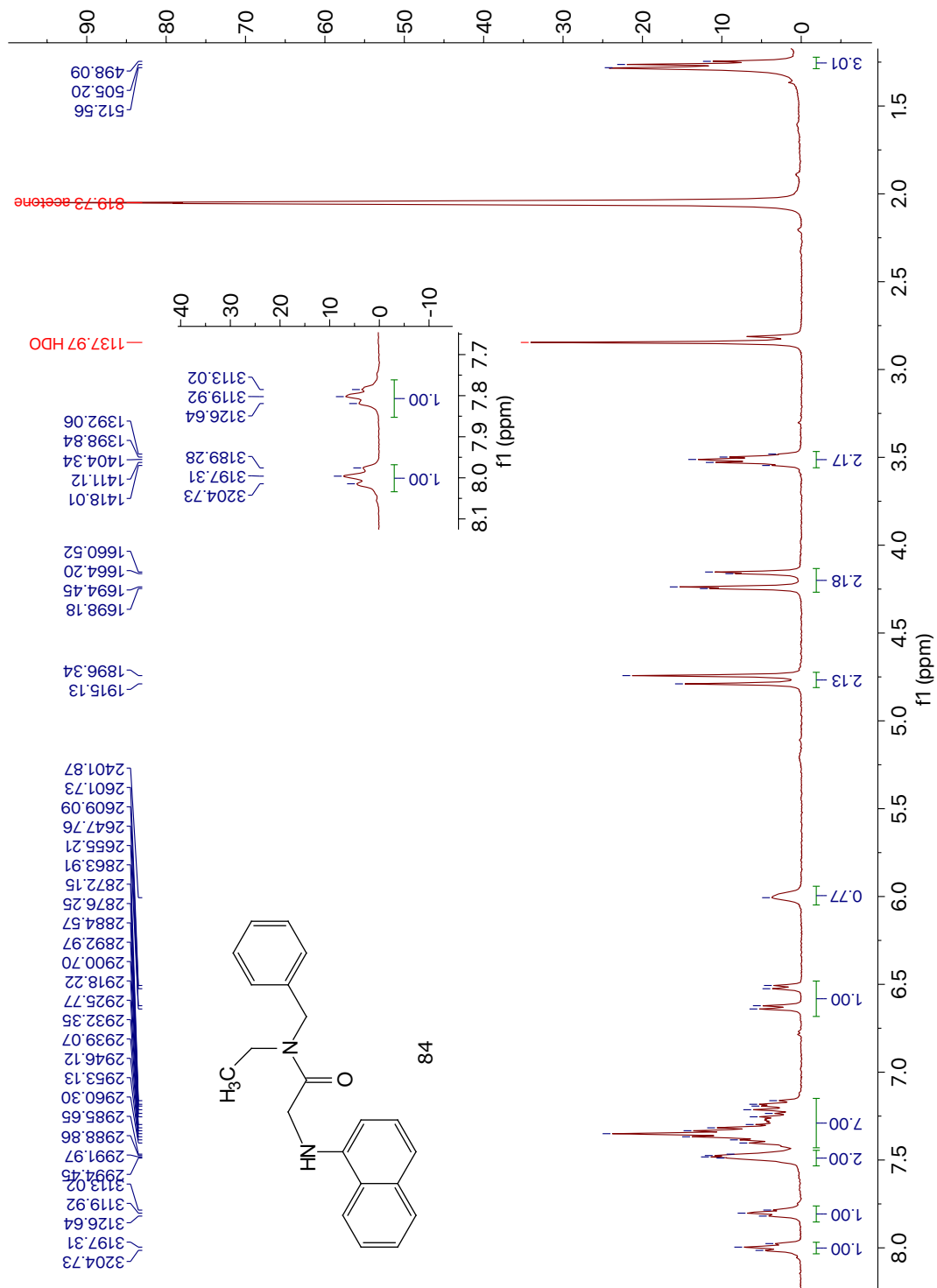


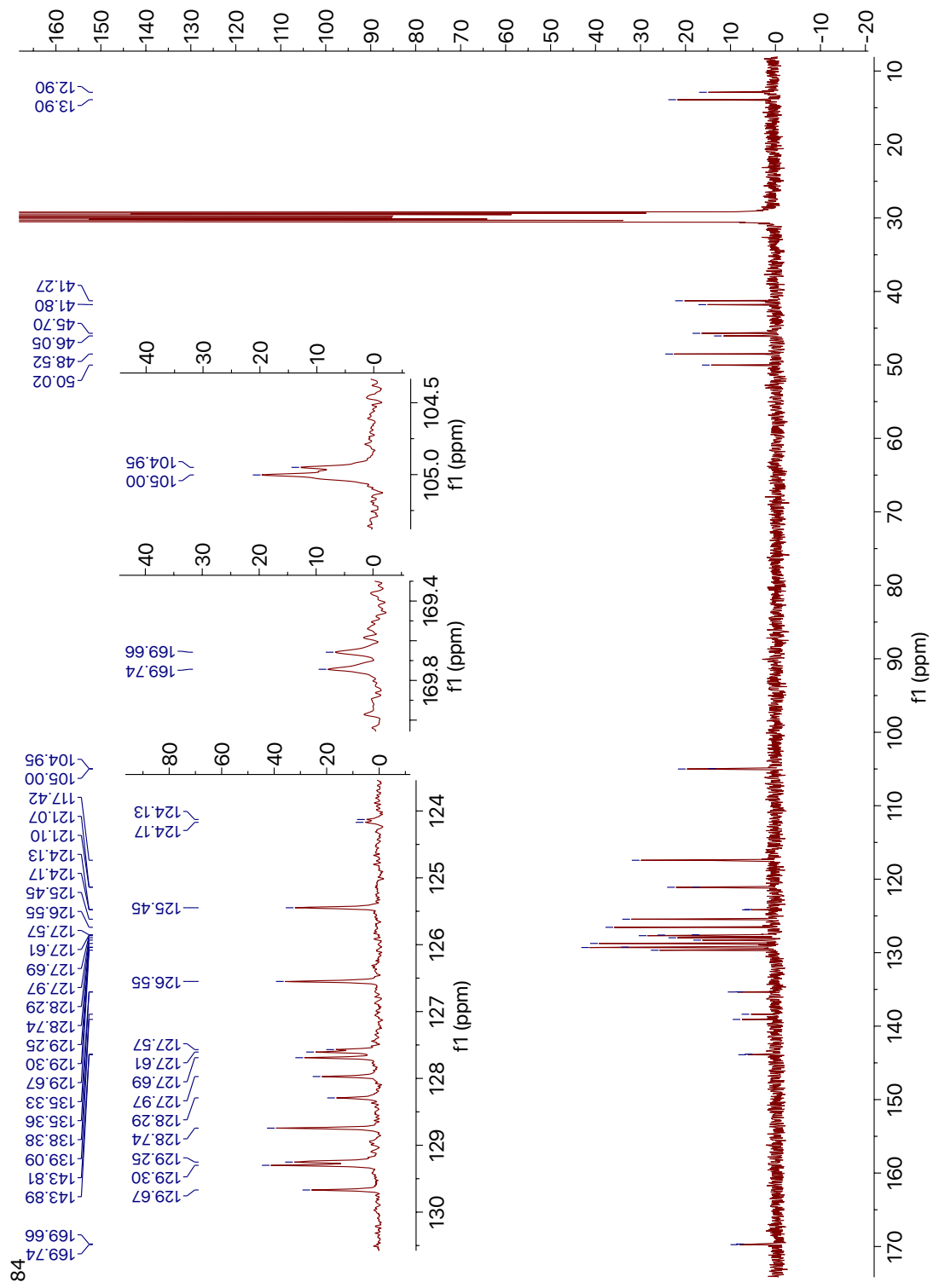


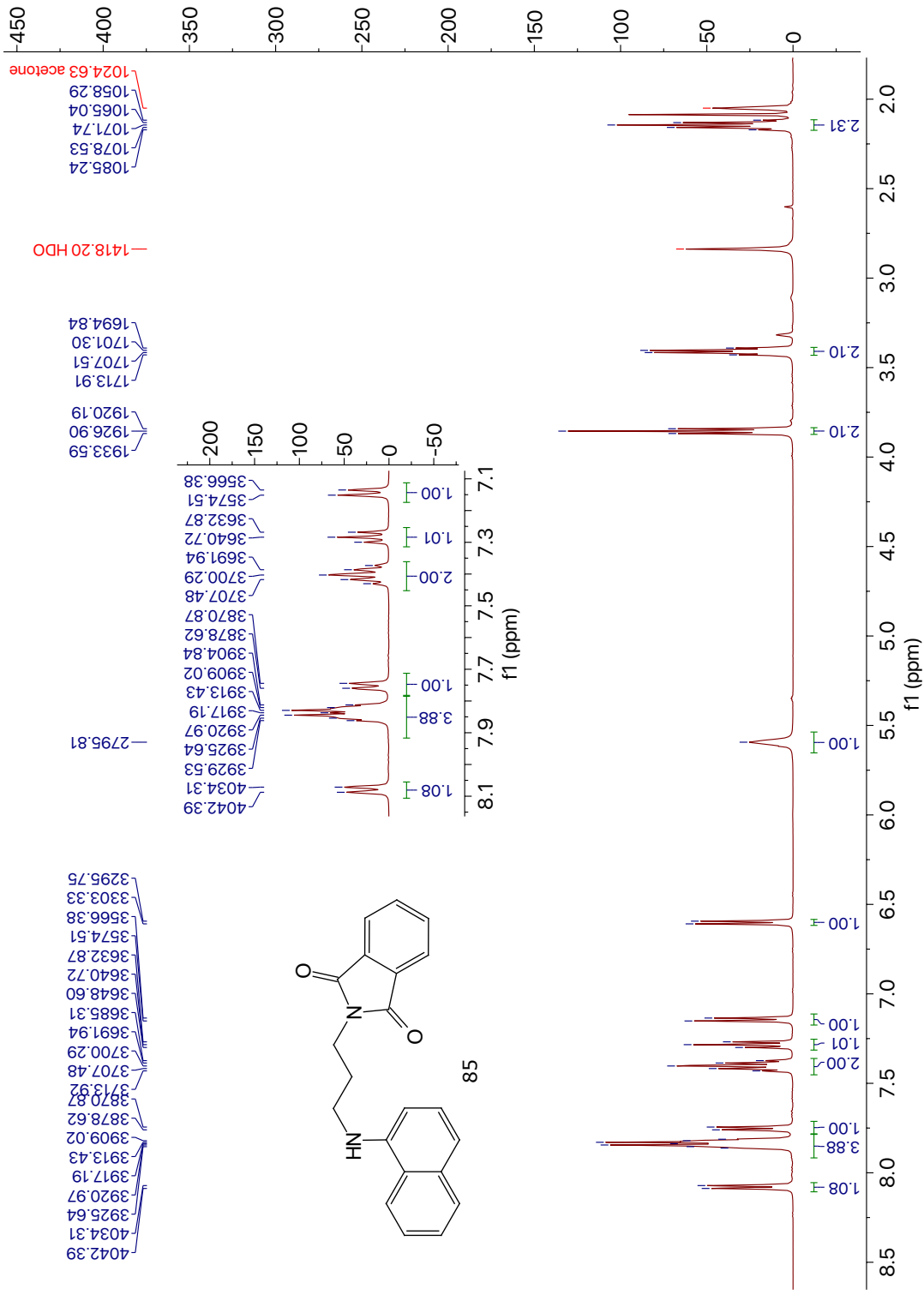
82

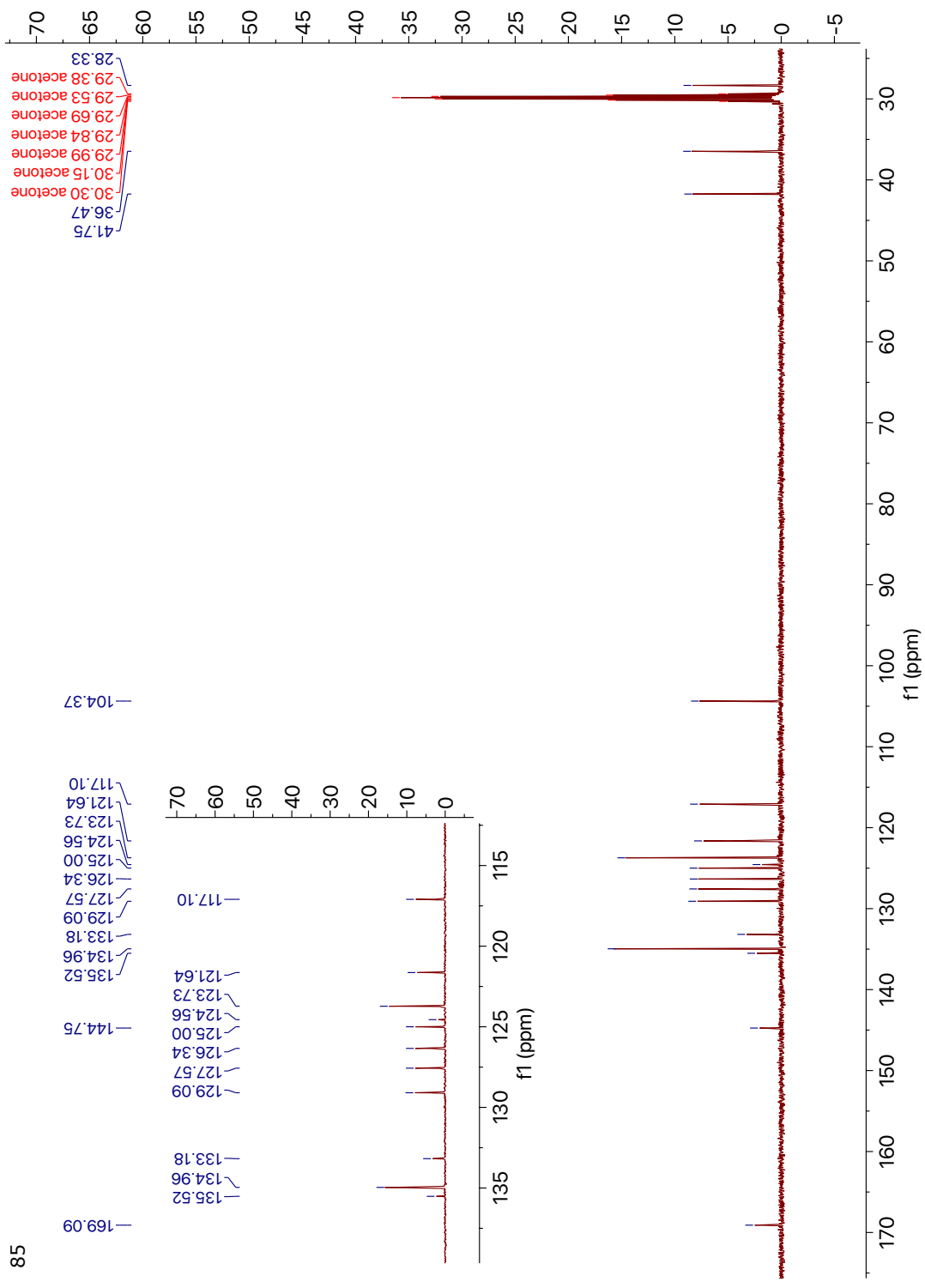




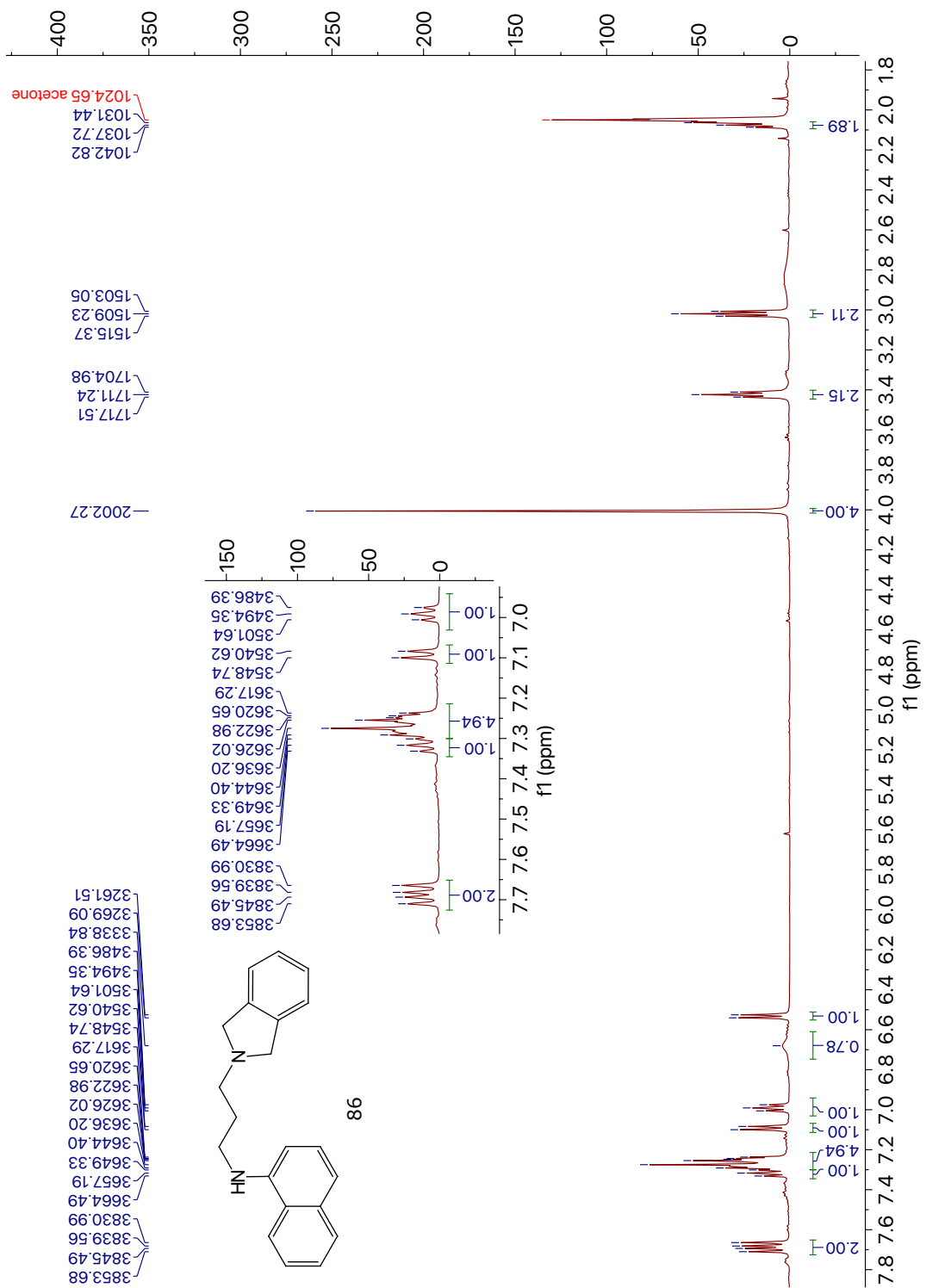


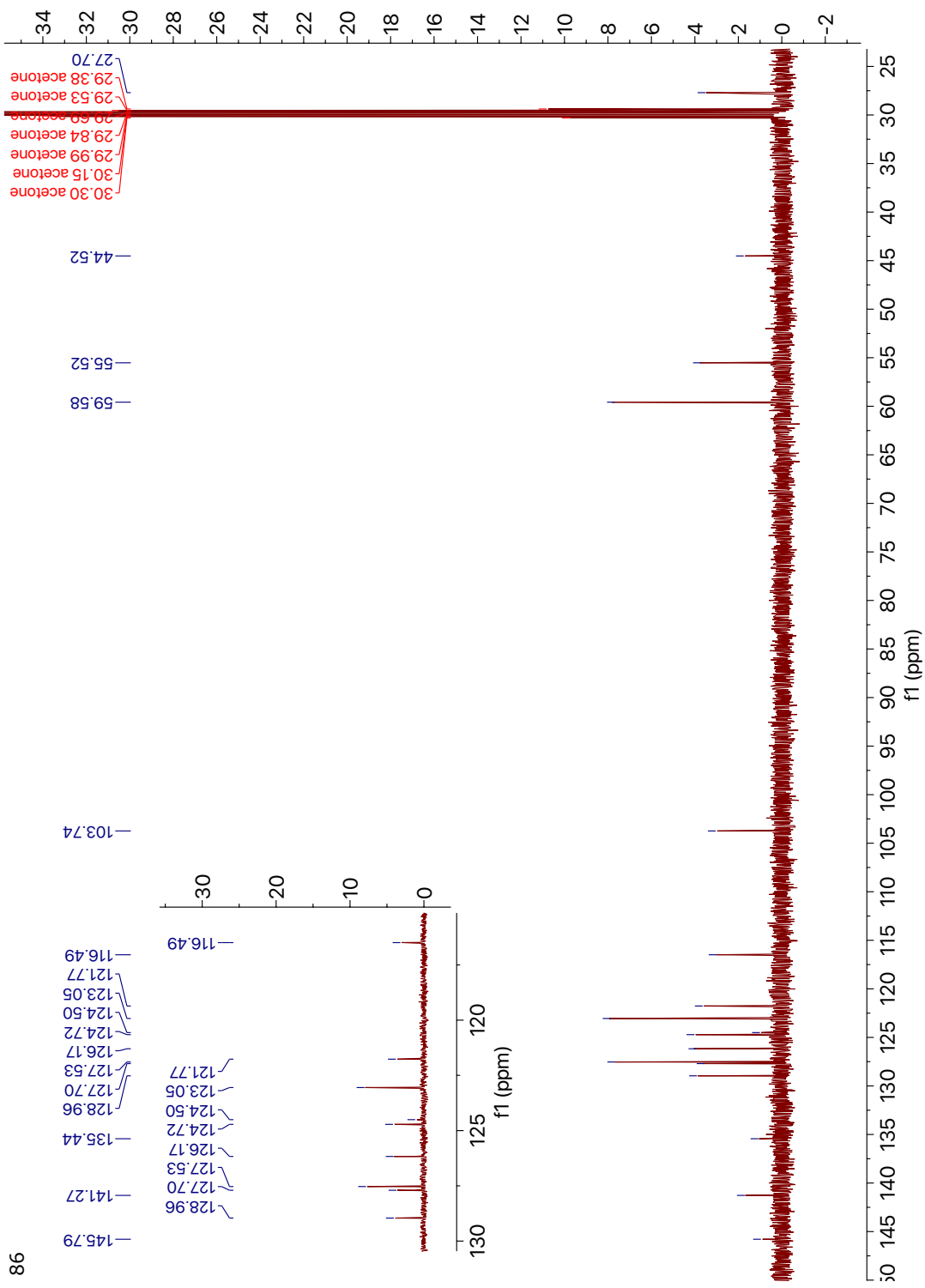




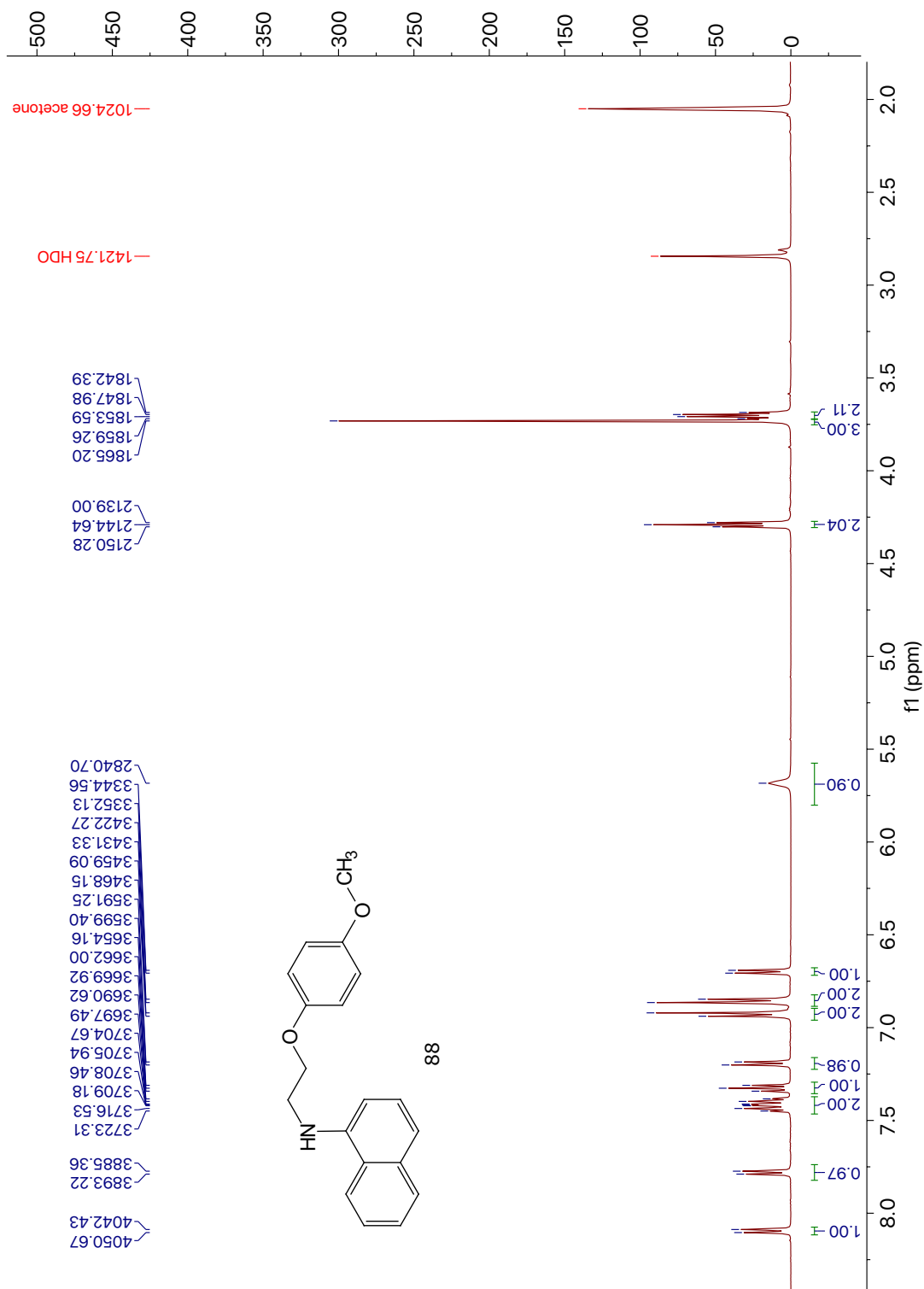


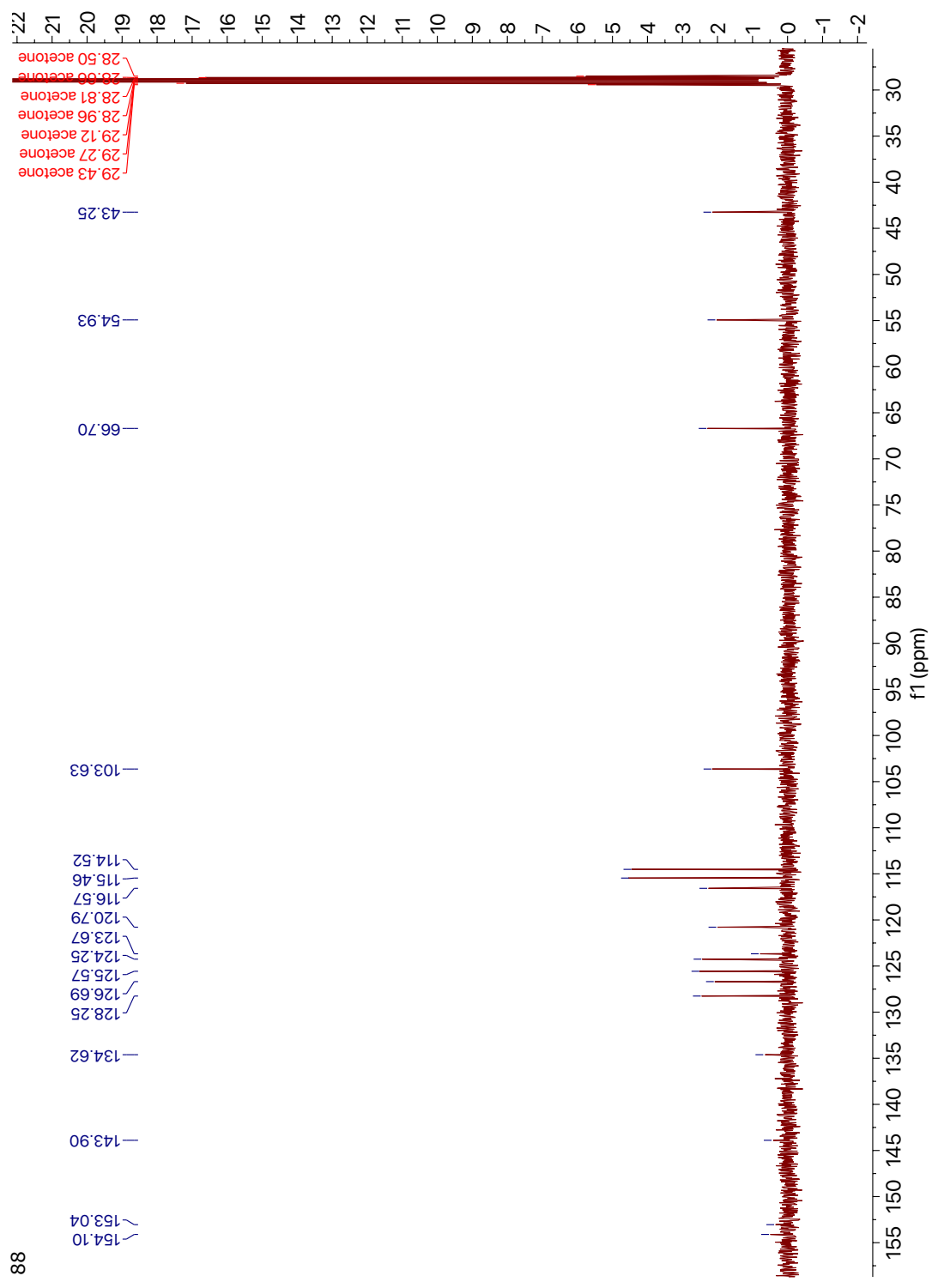
85



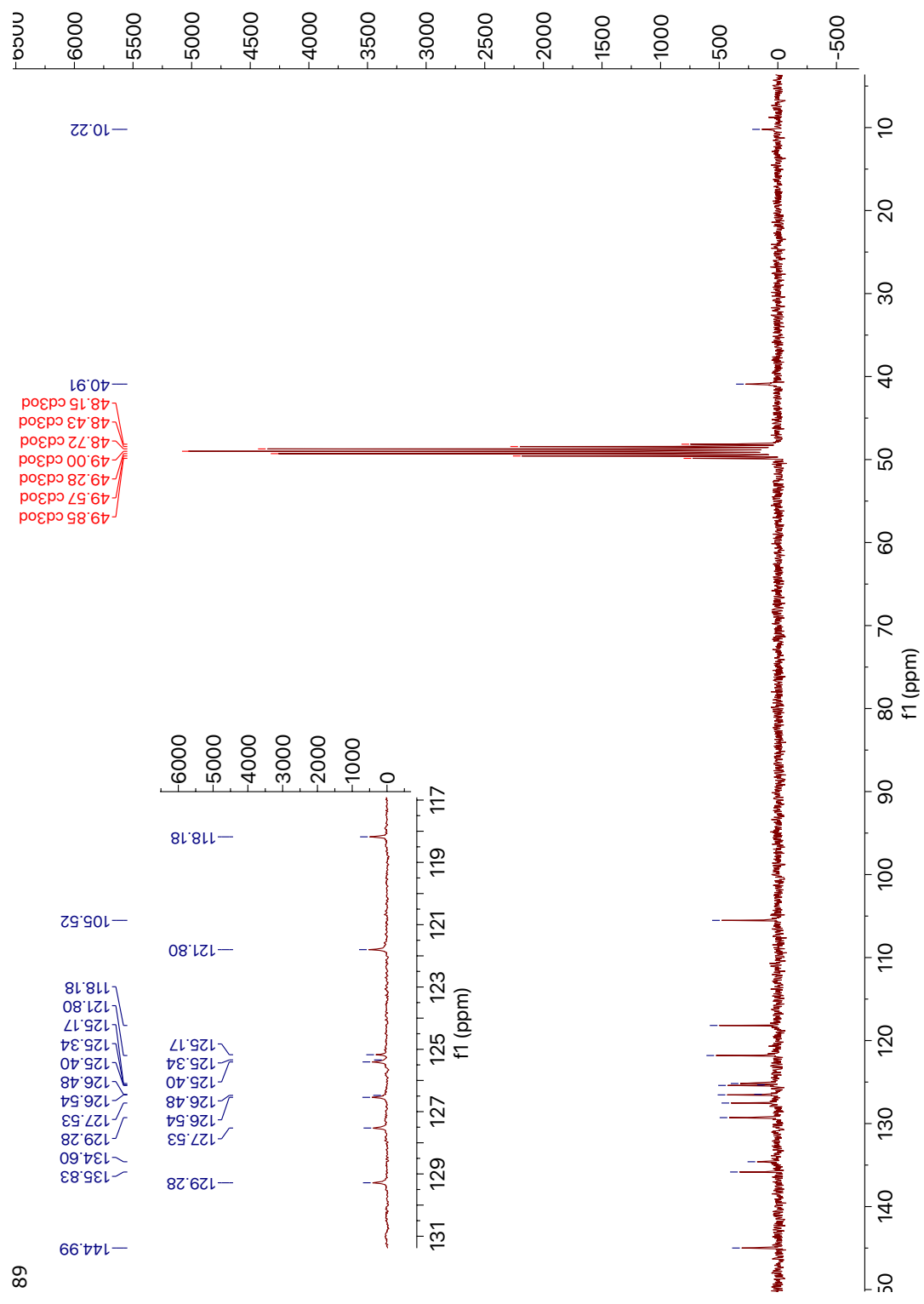


86

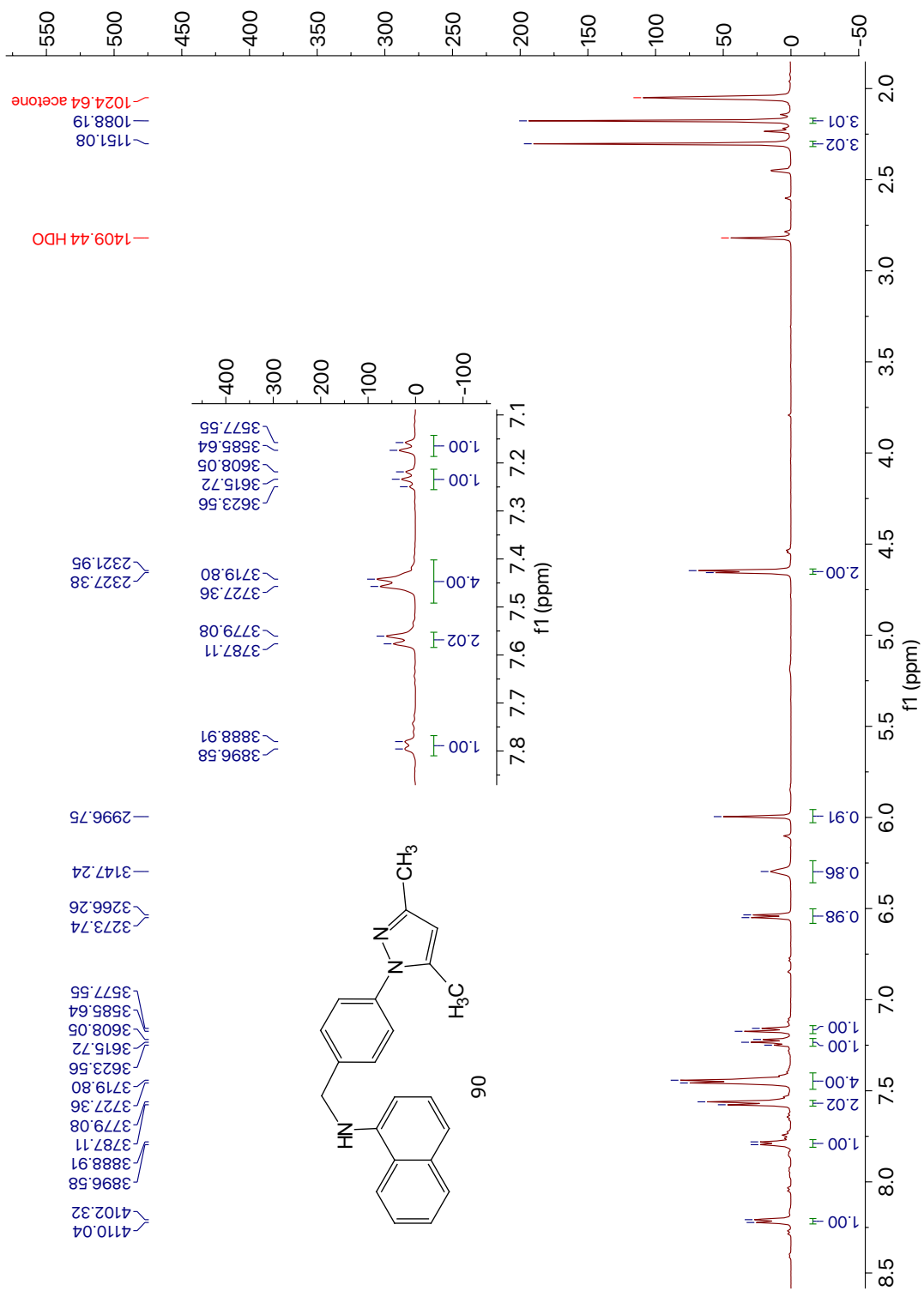


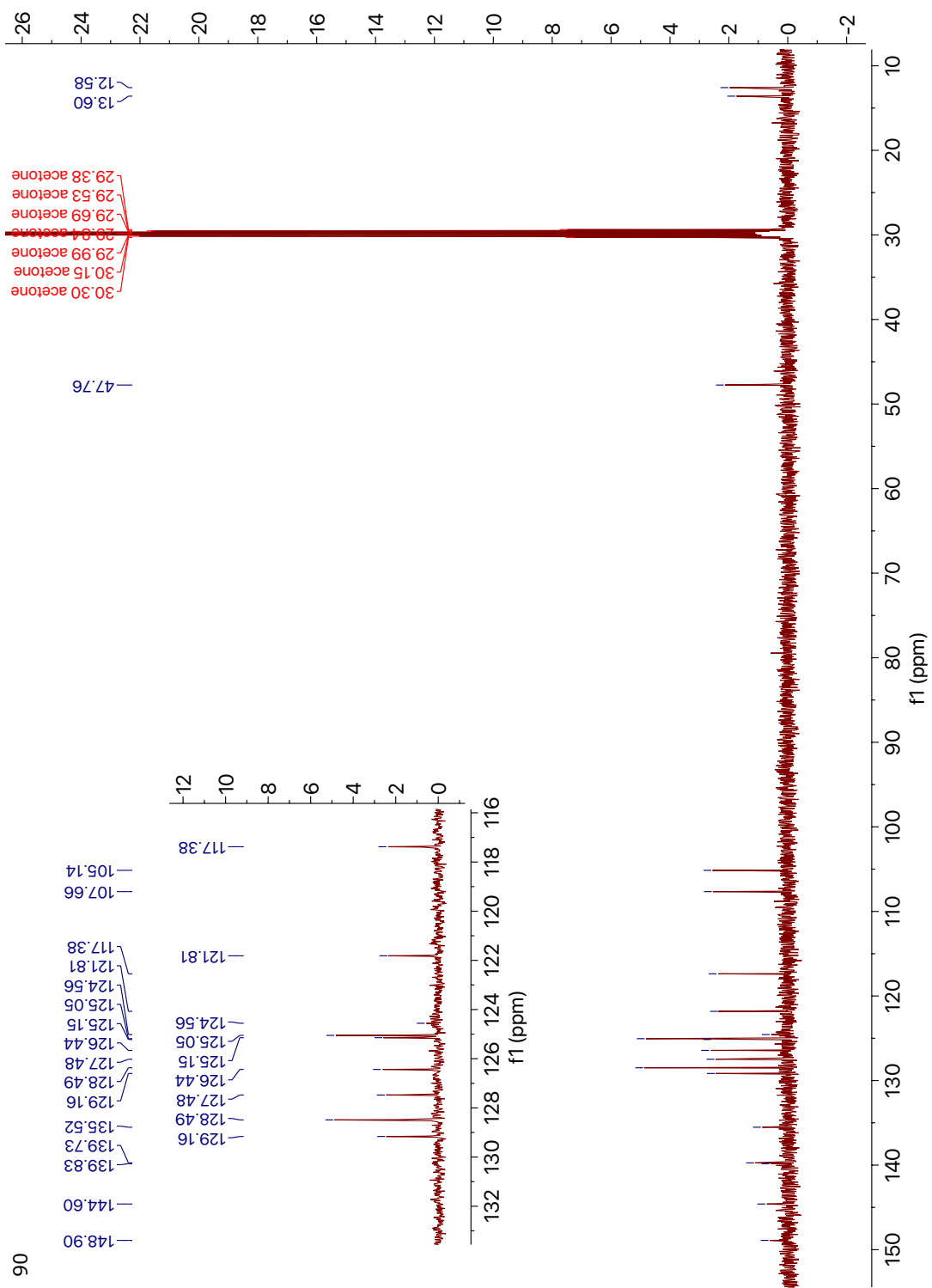


88

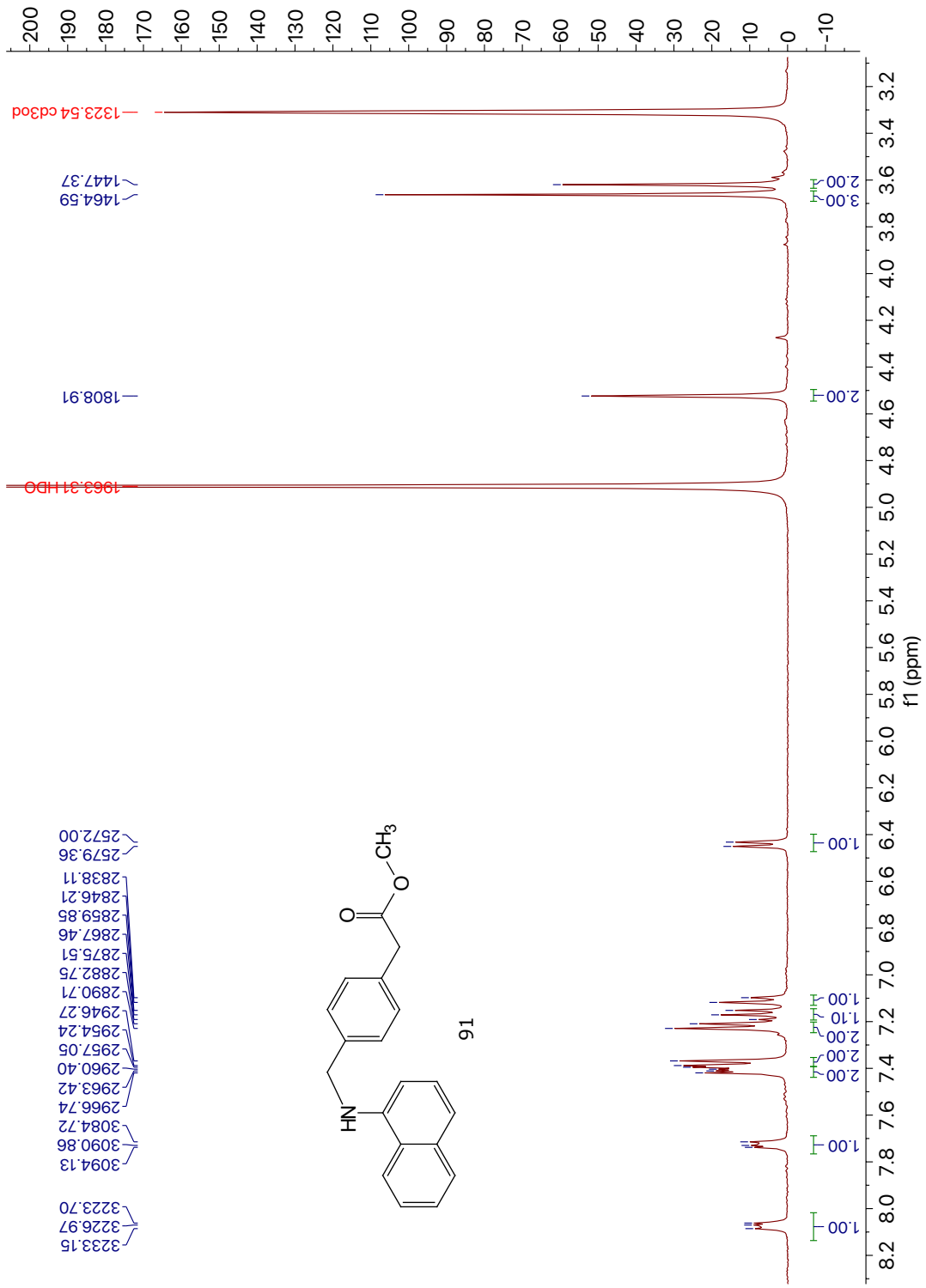


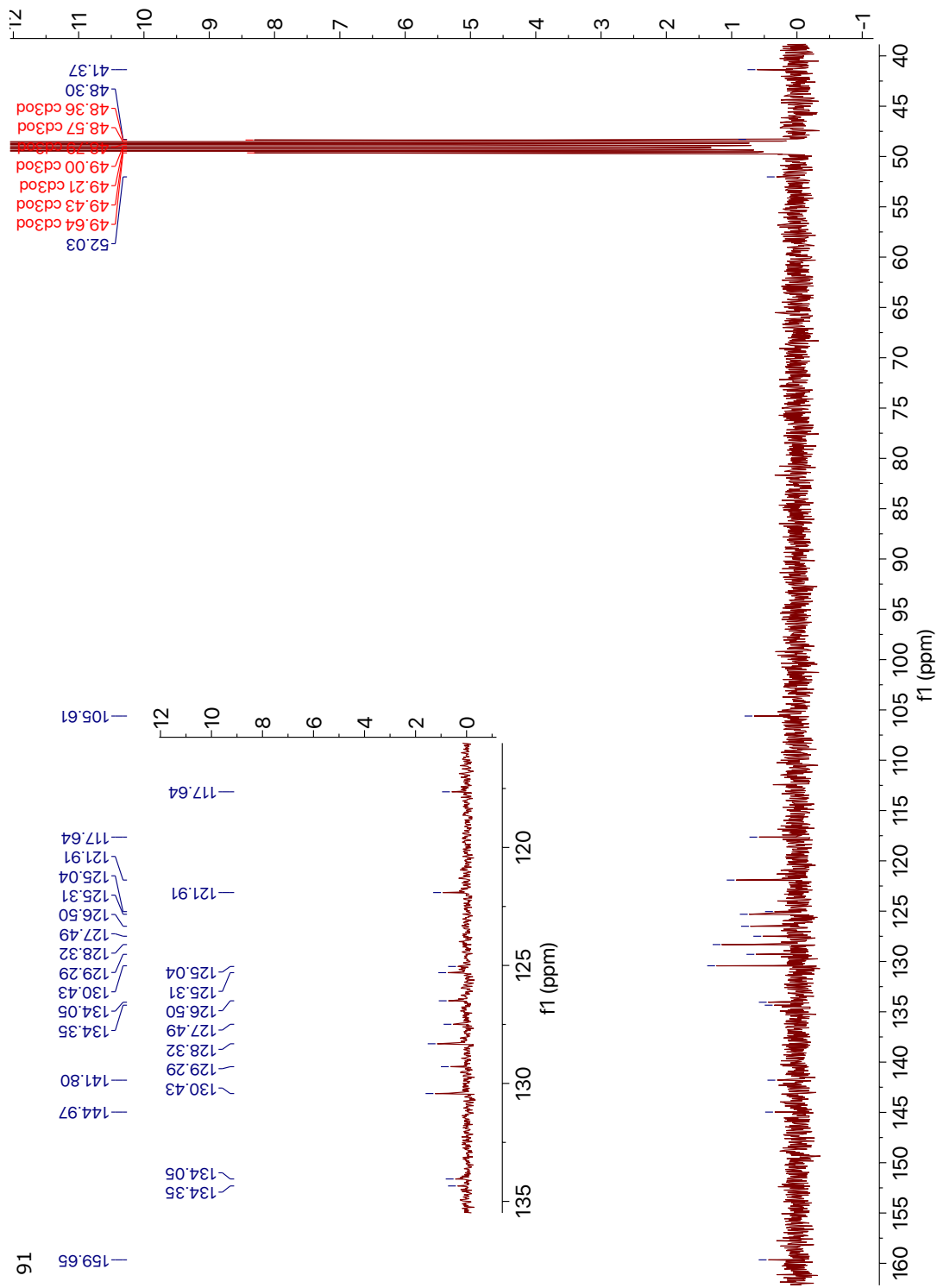
89

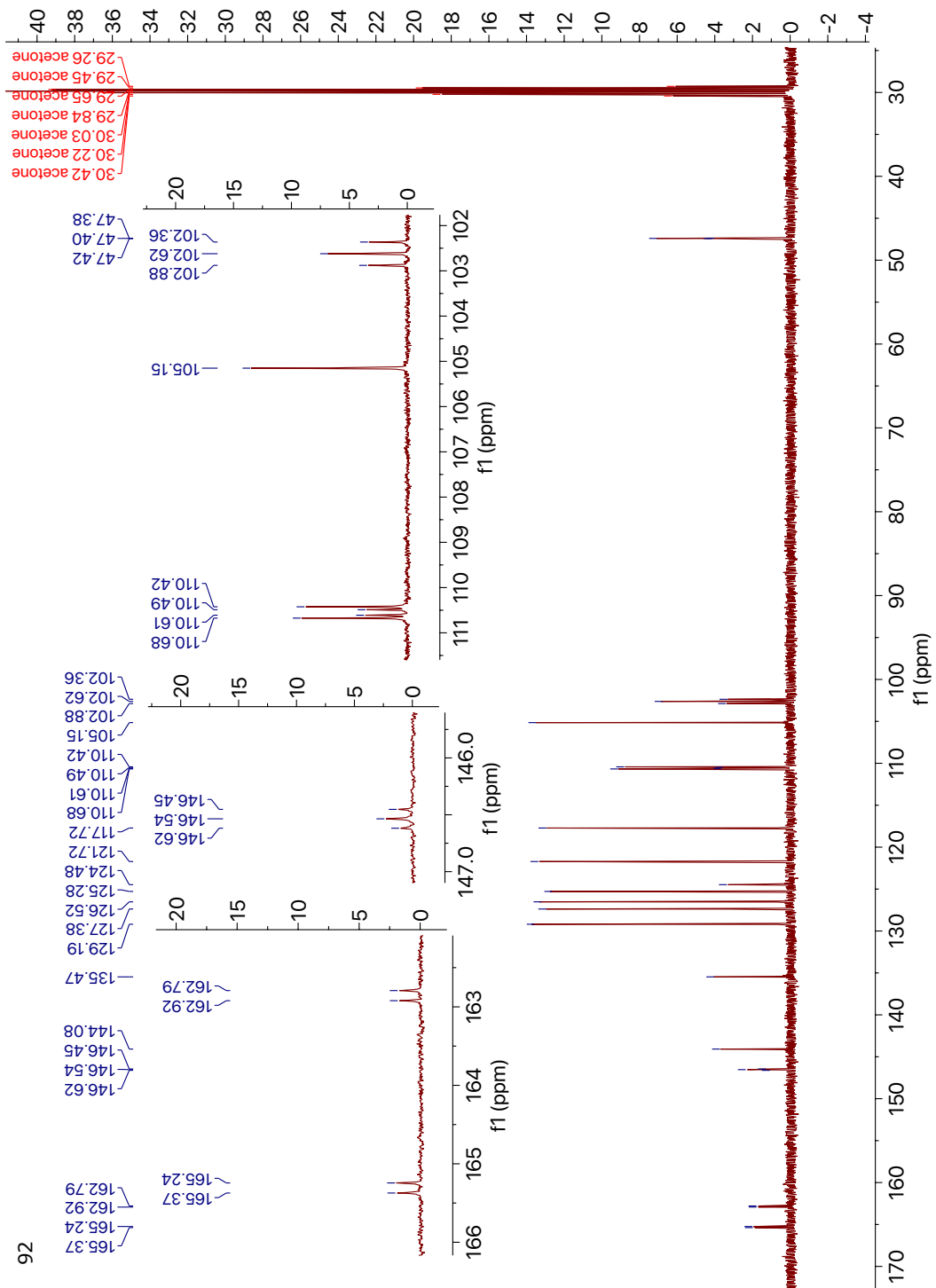




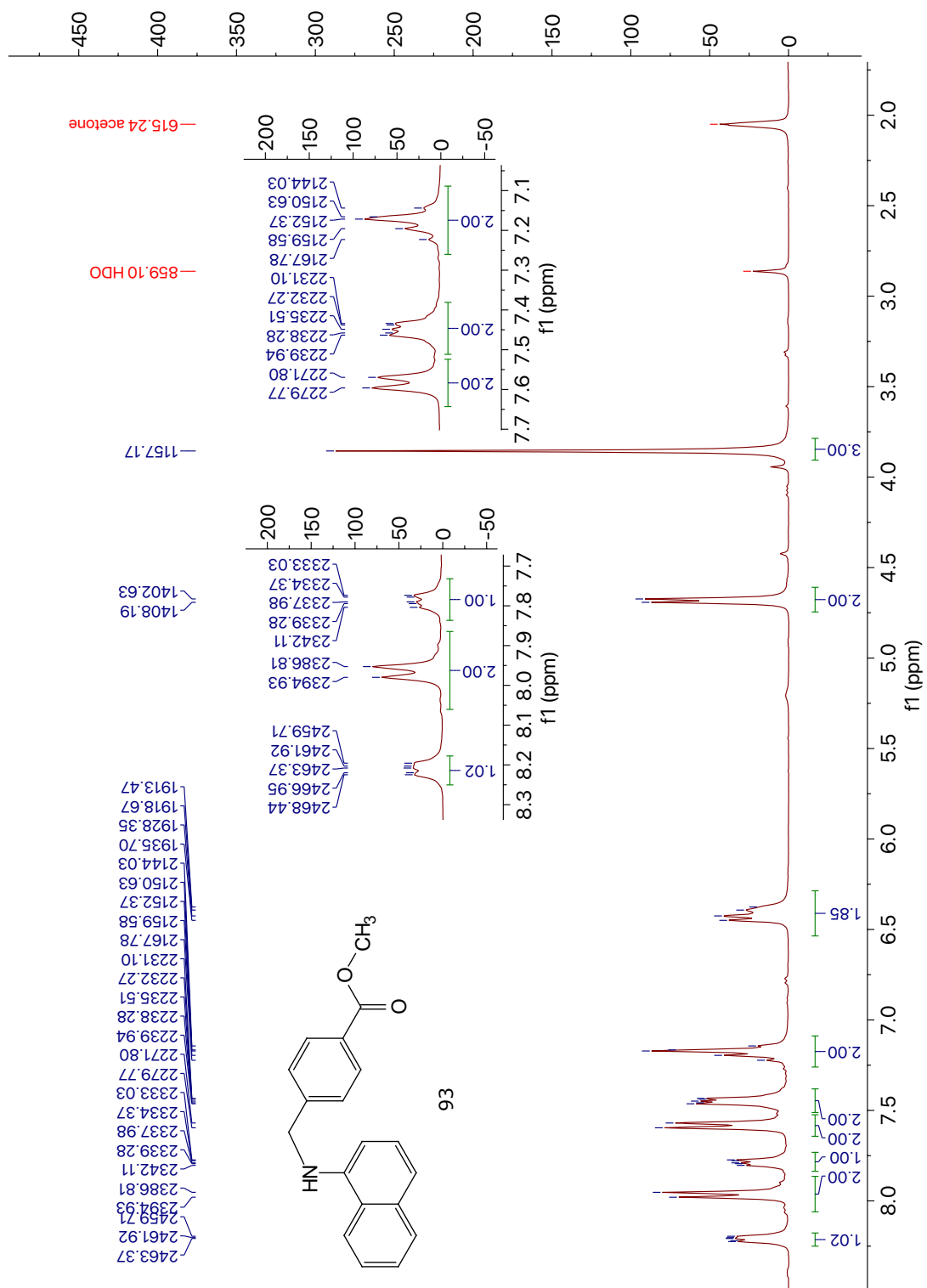
90

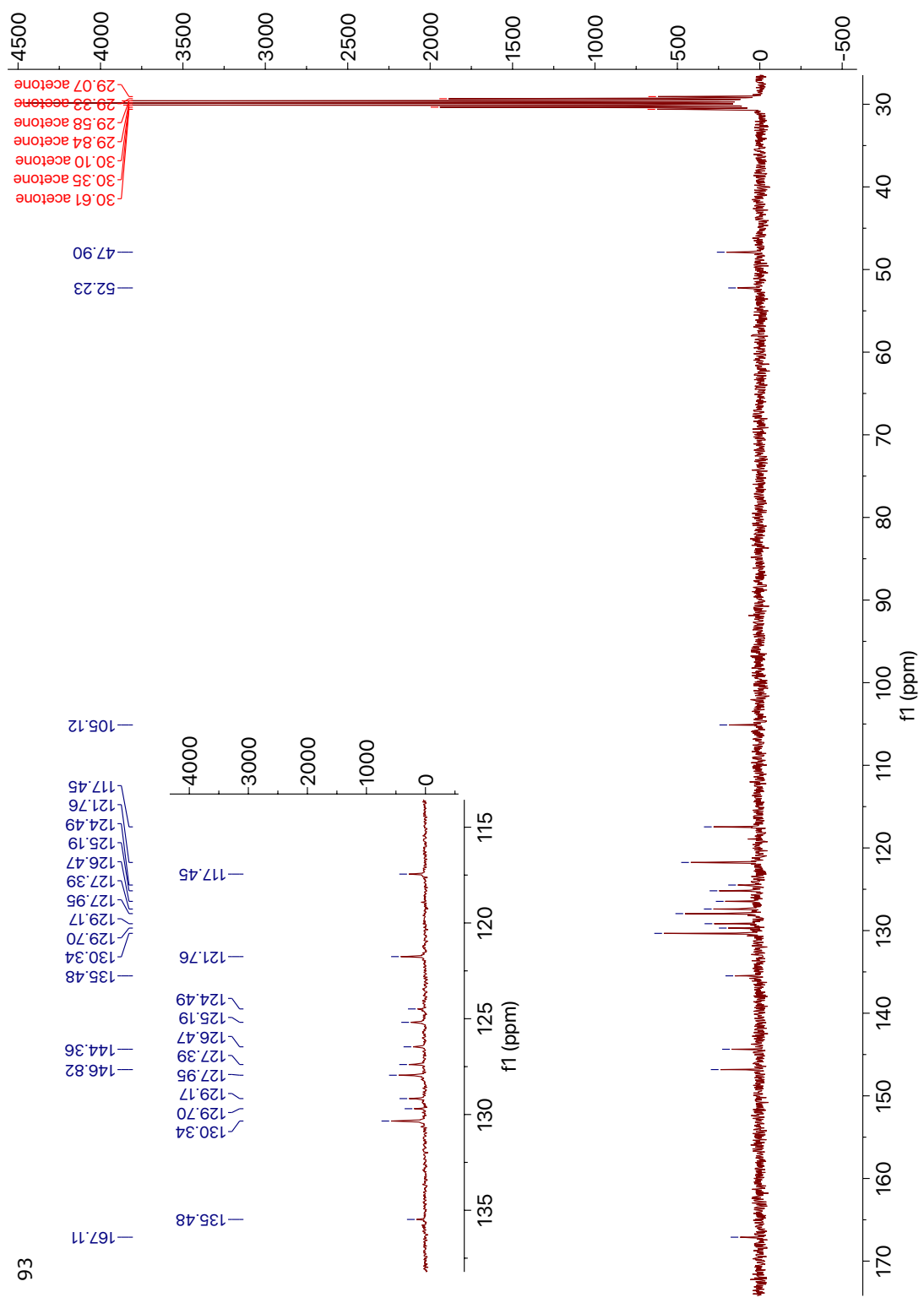




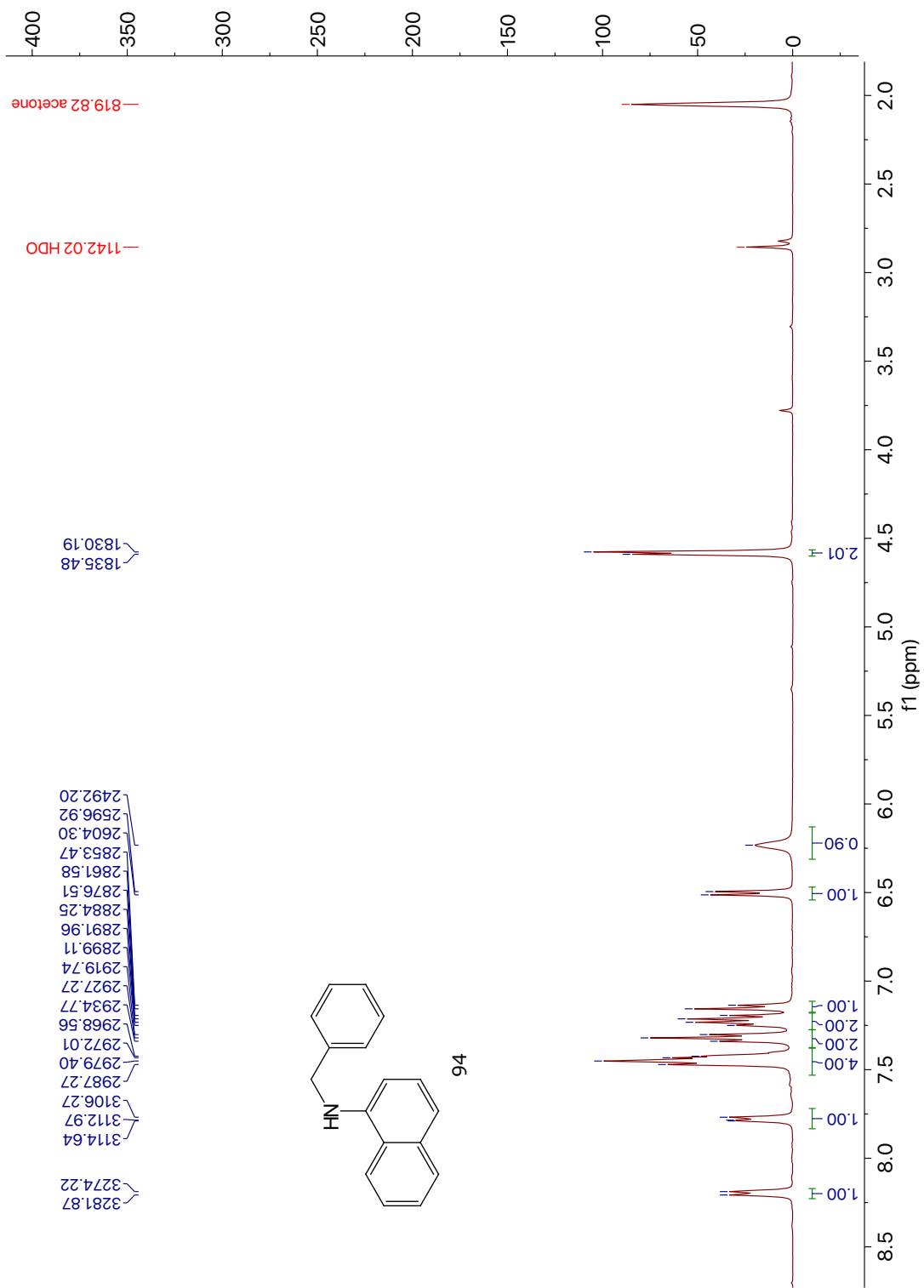


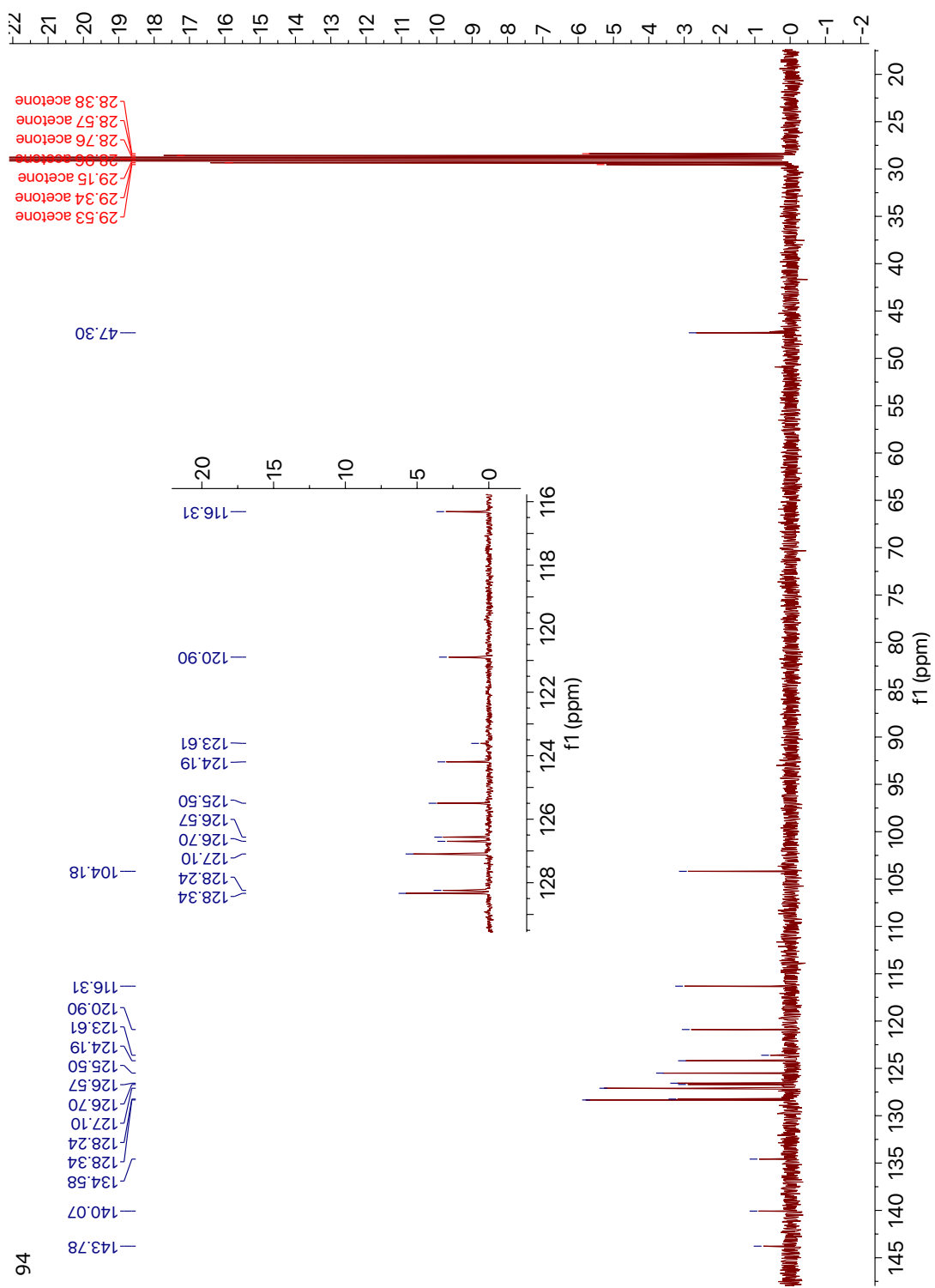
92



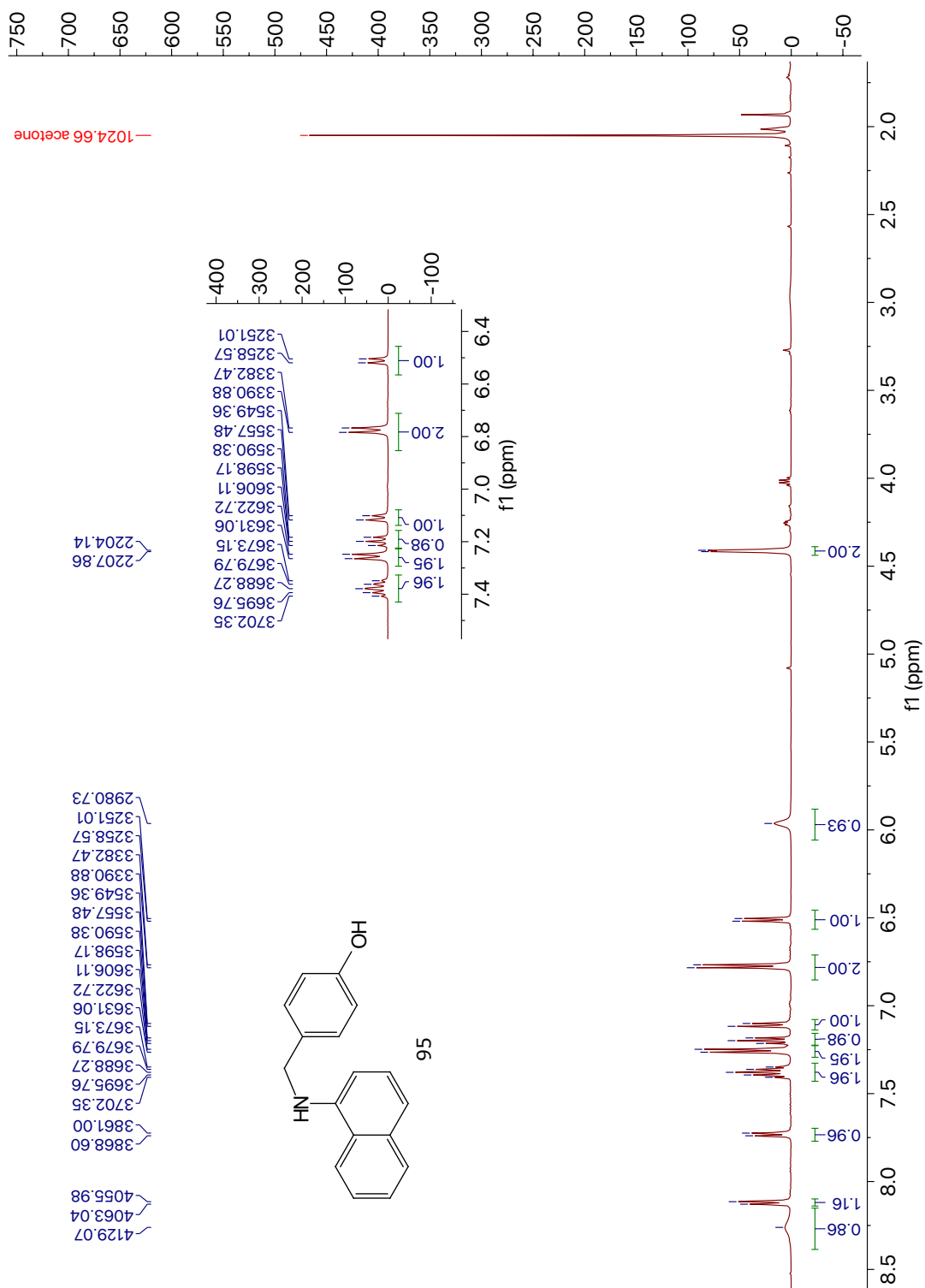


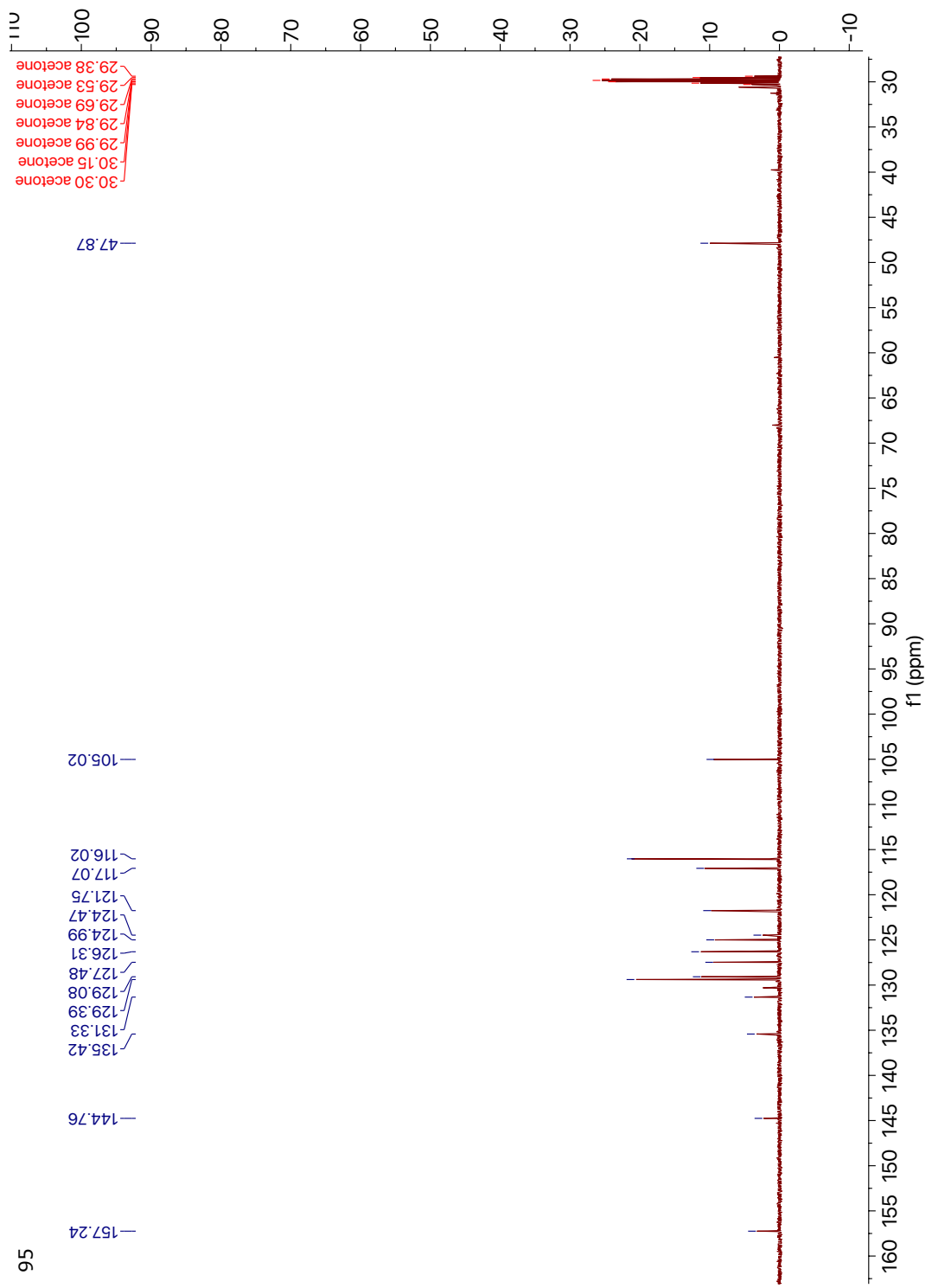
93



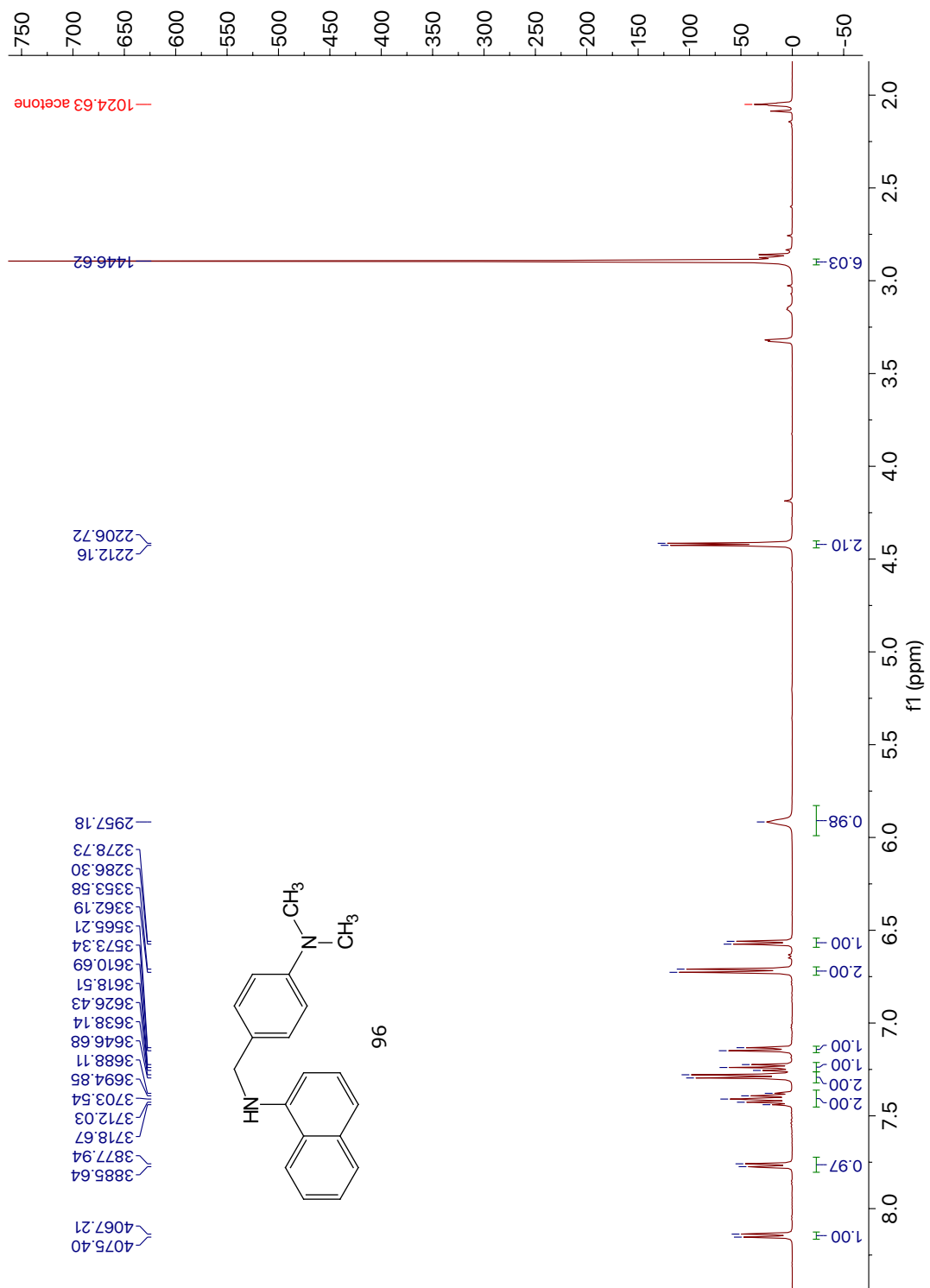


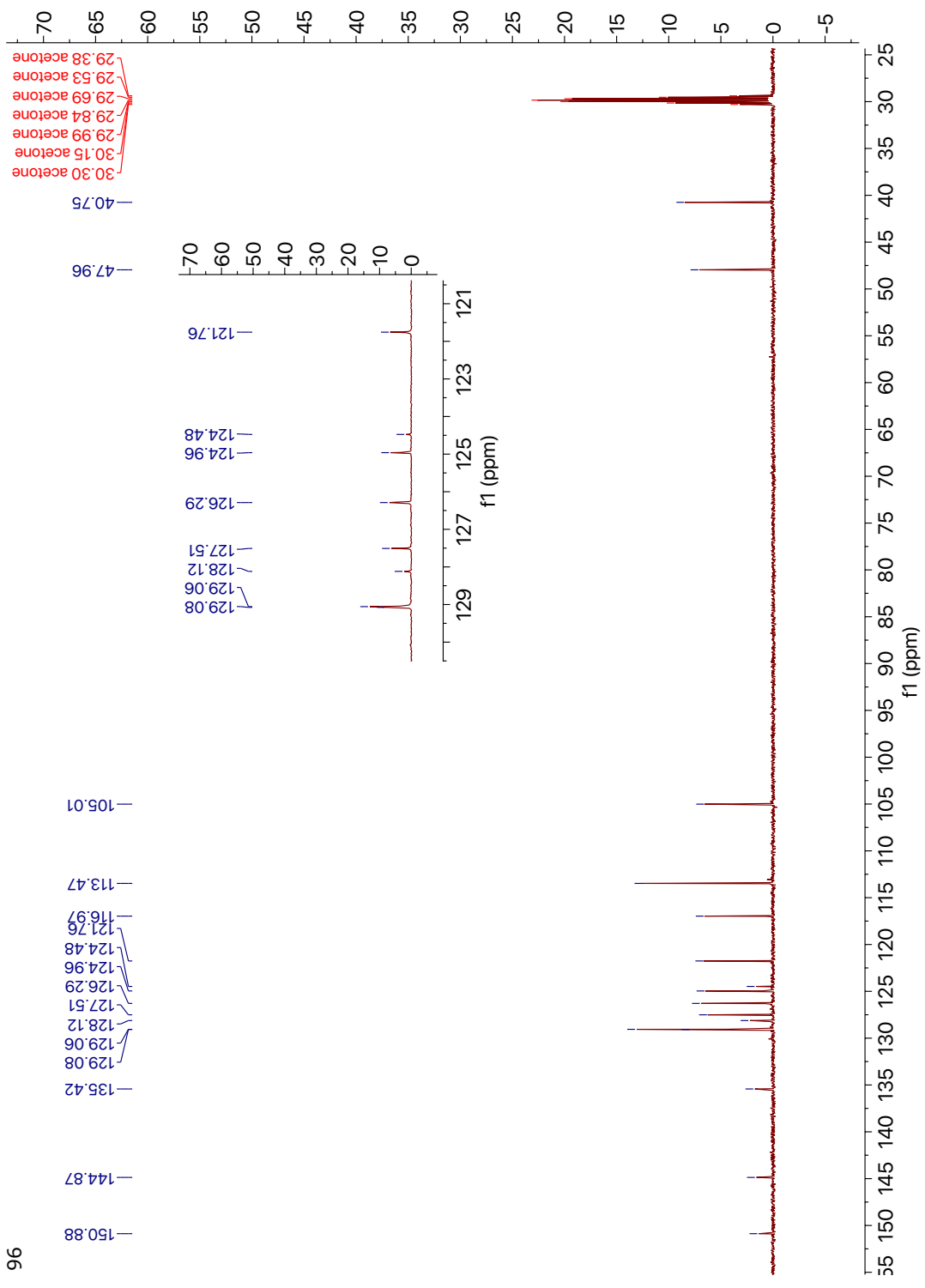
94

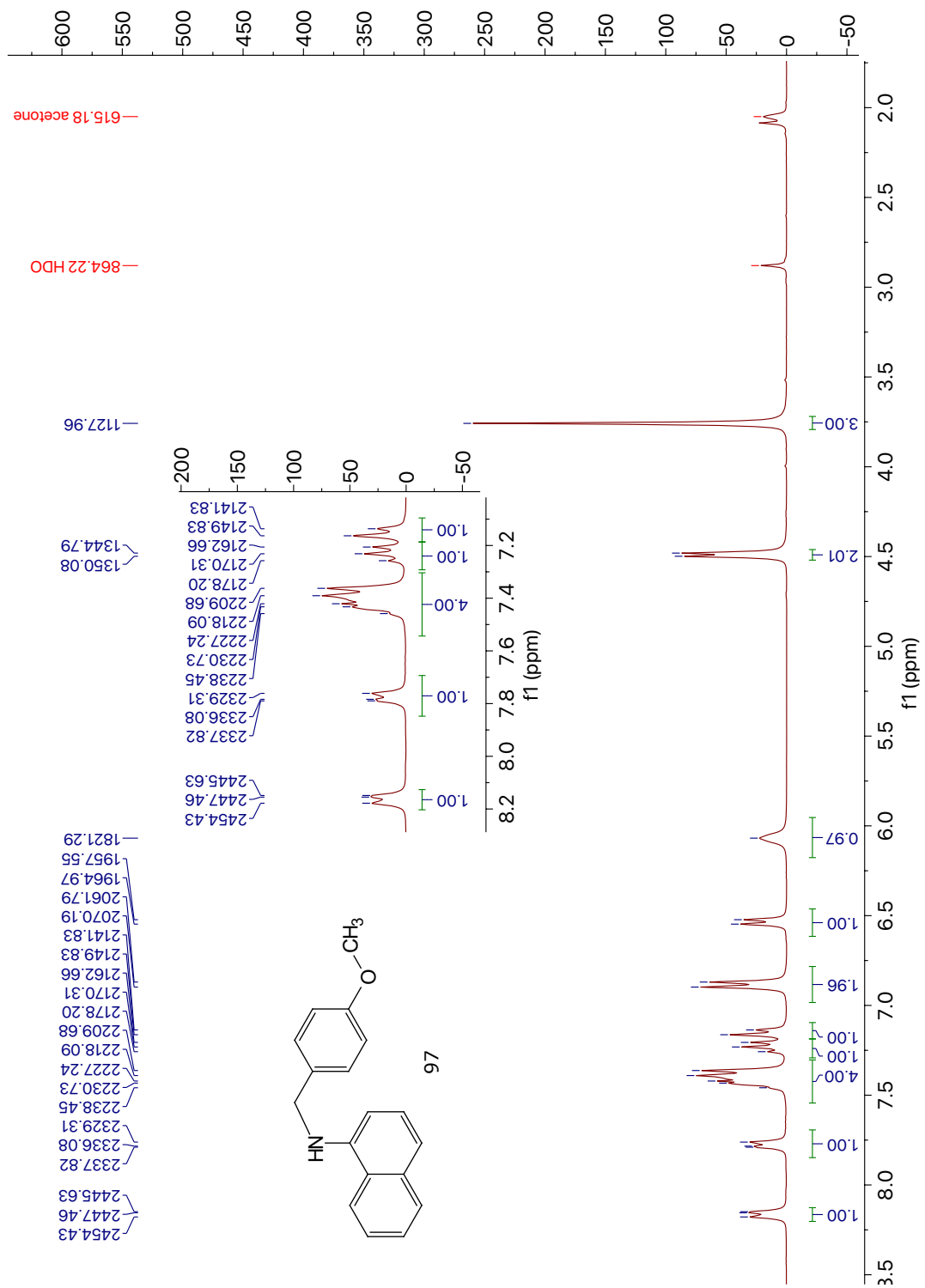


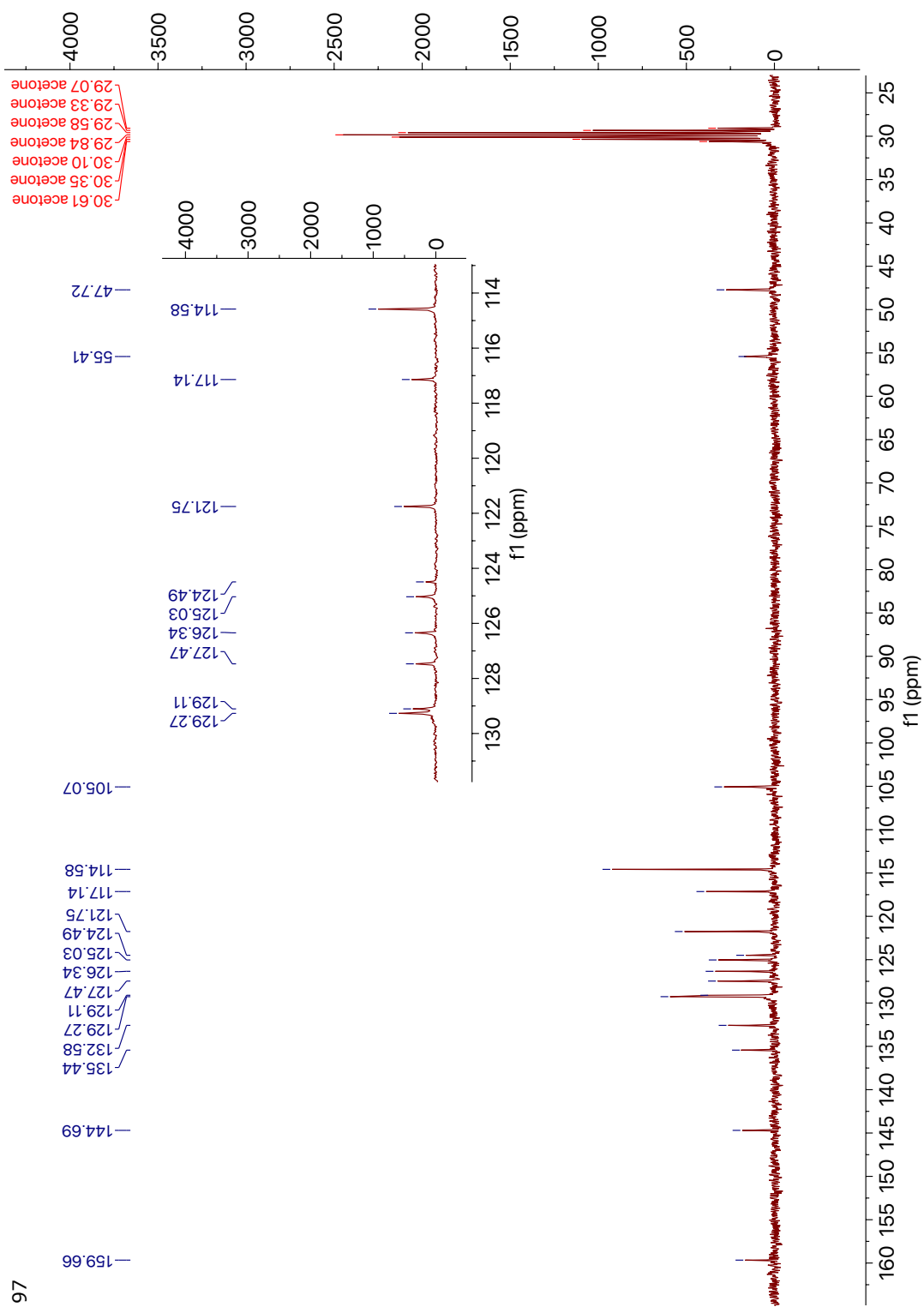


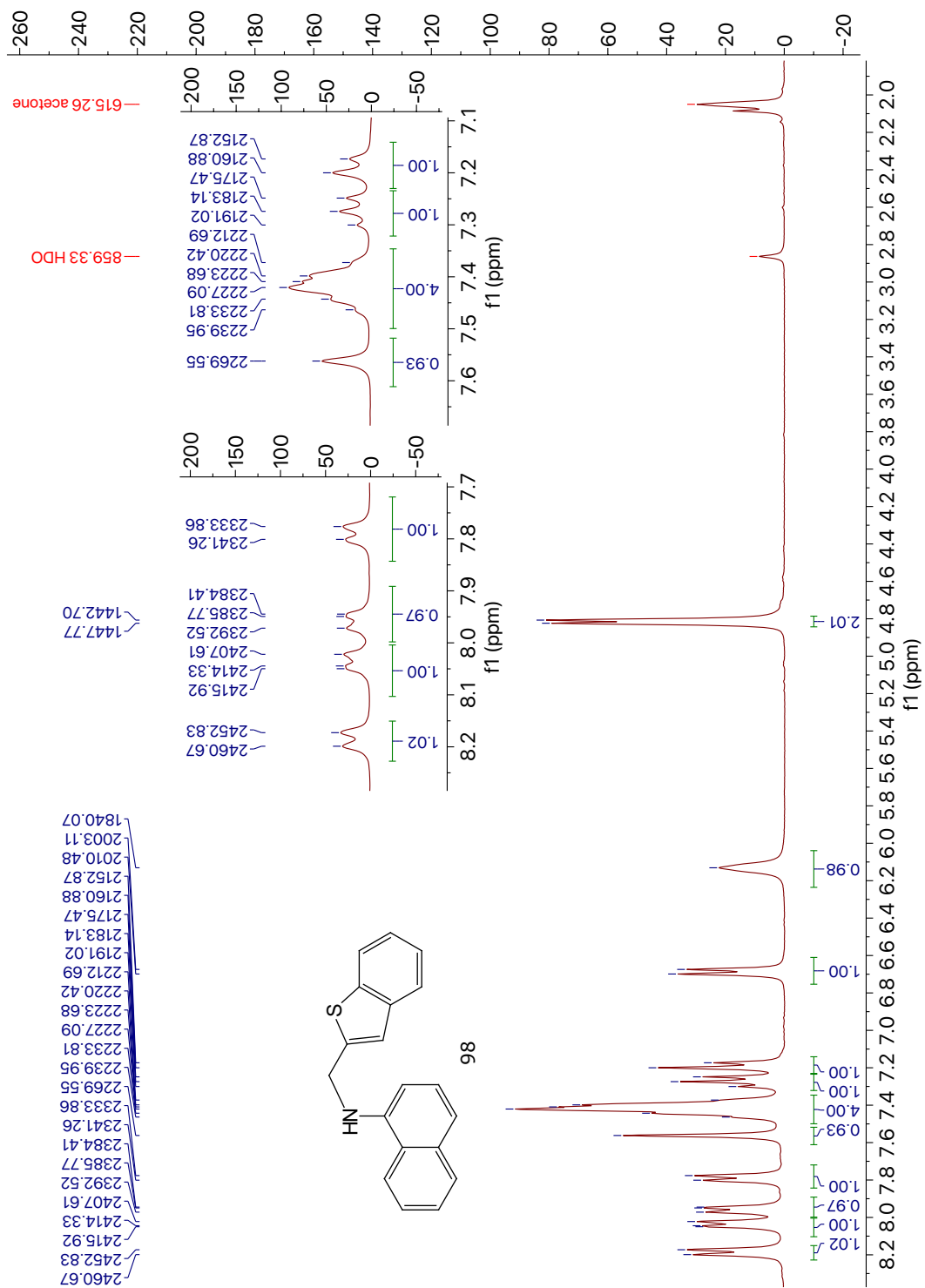
95

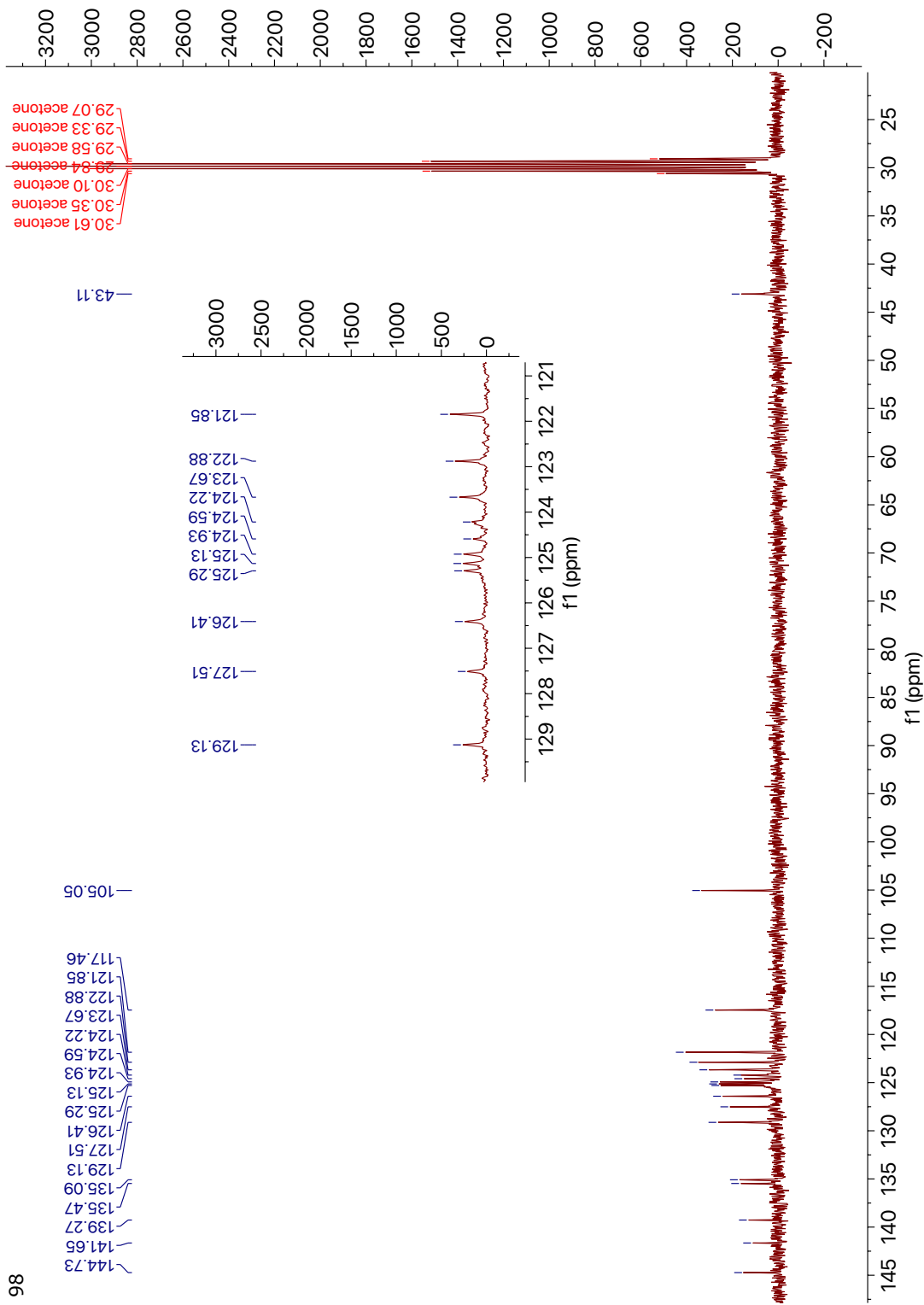


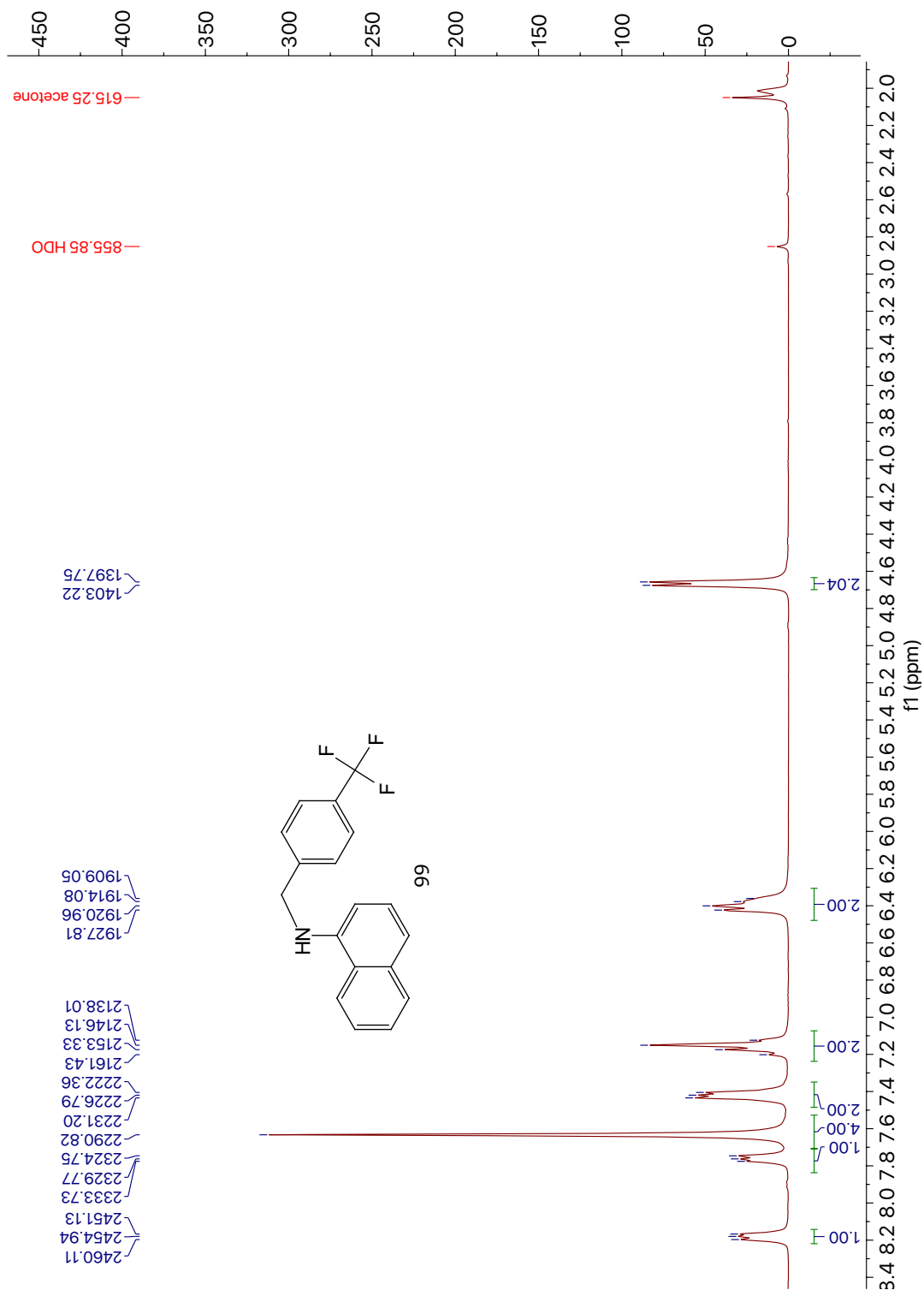


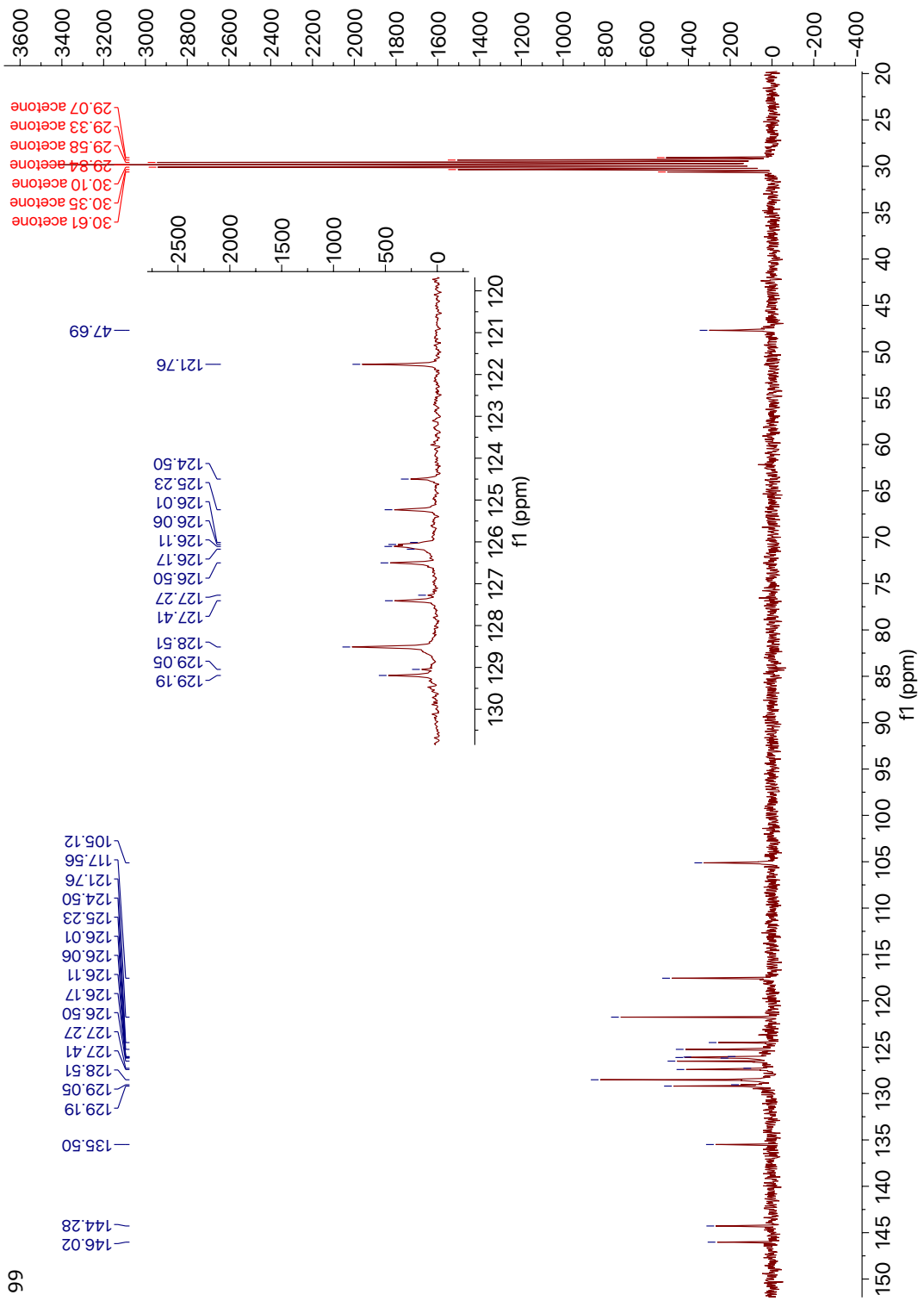


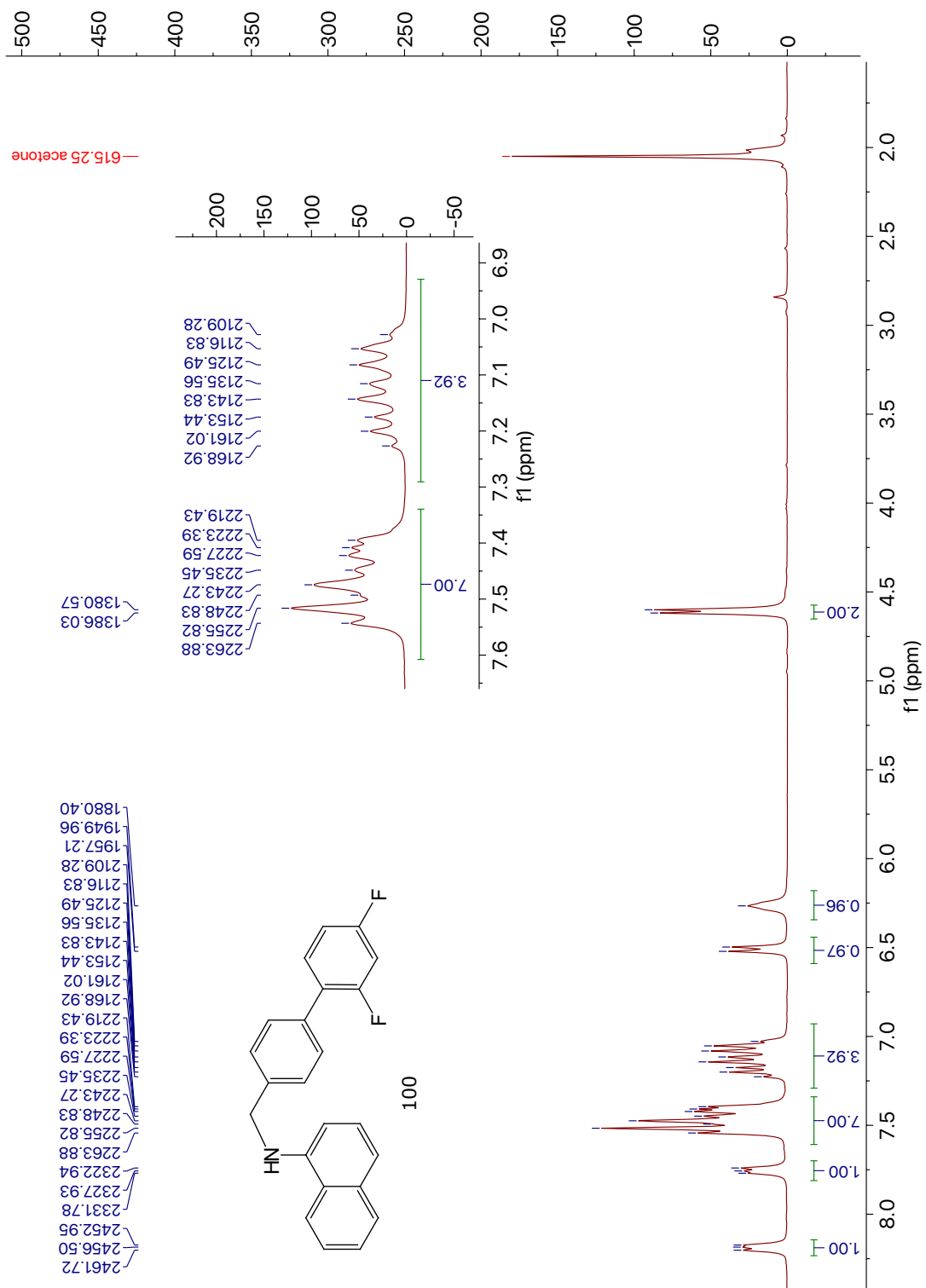


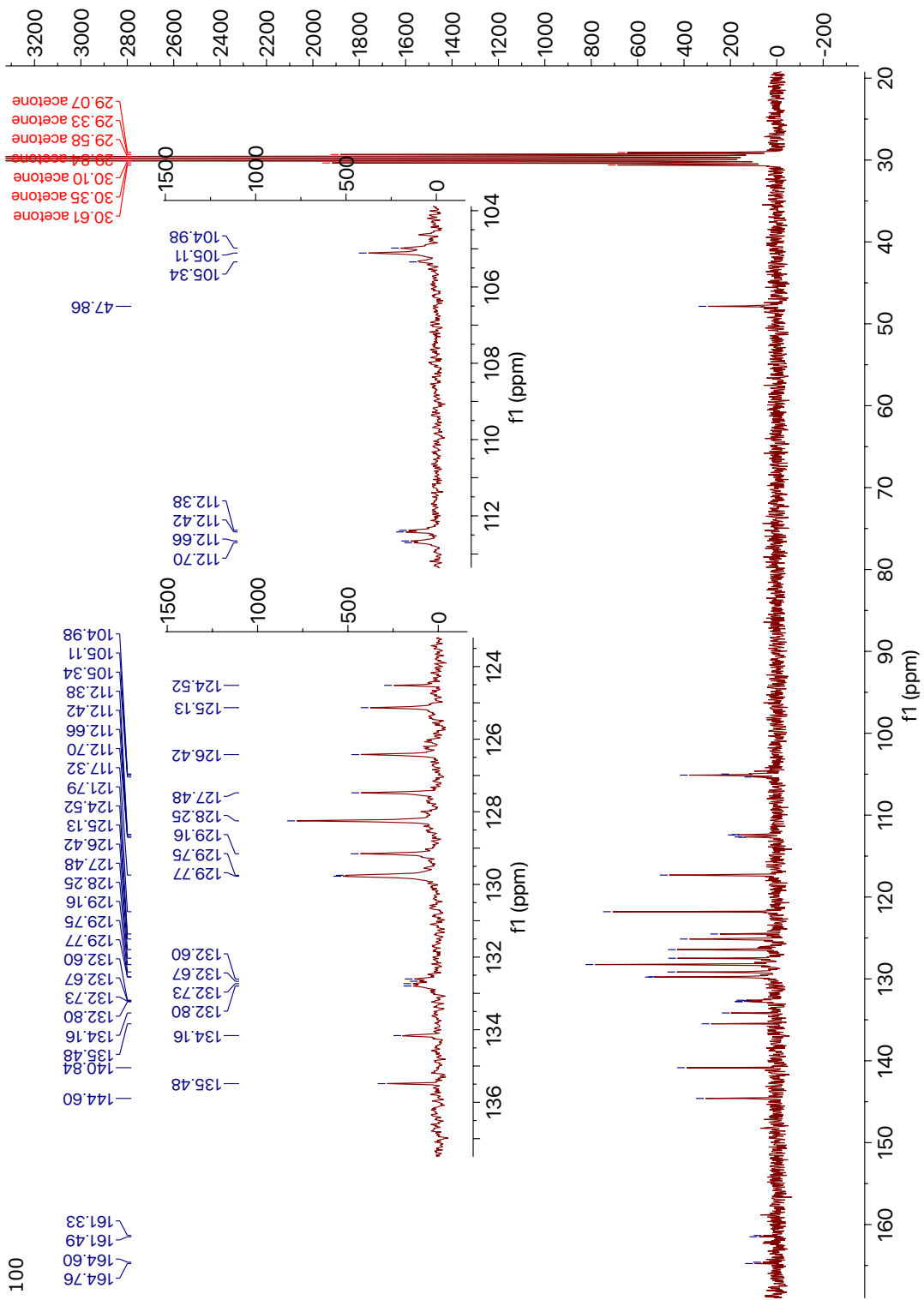


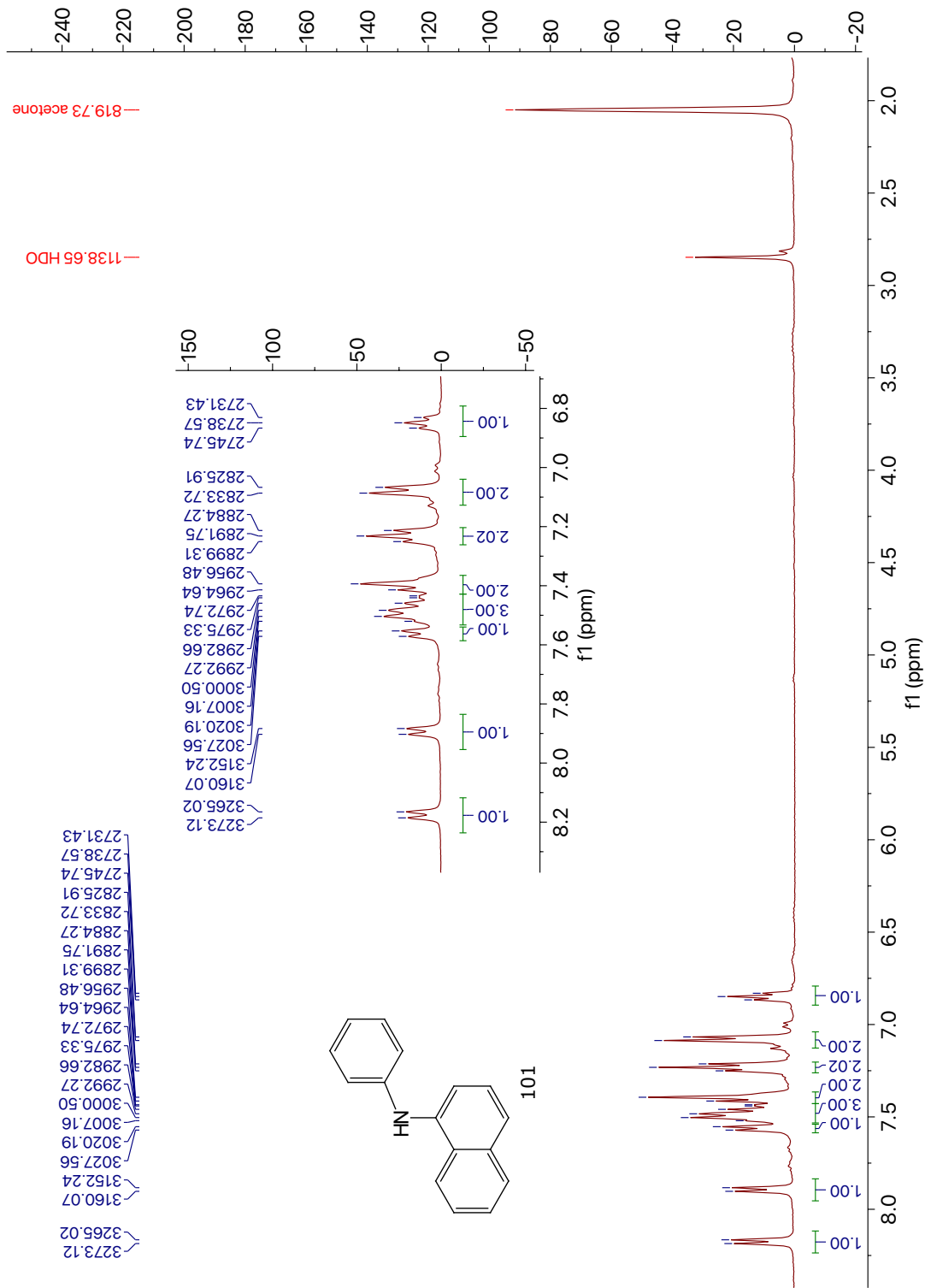


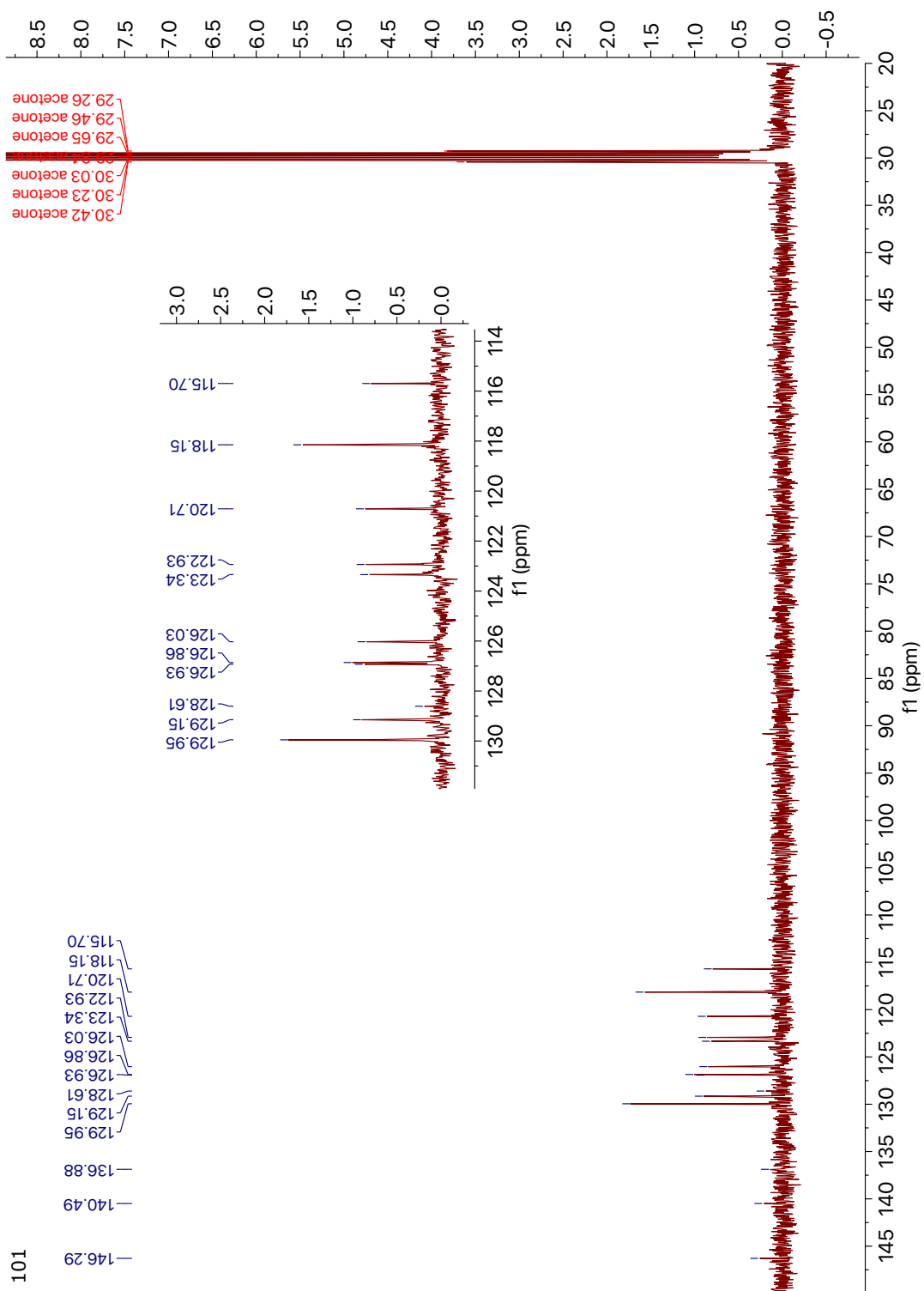




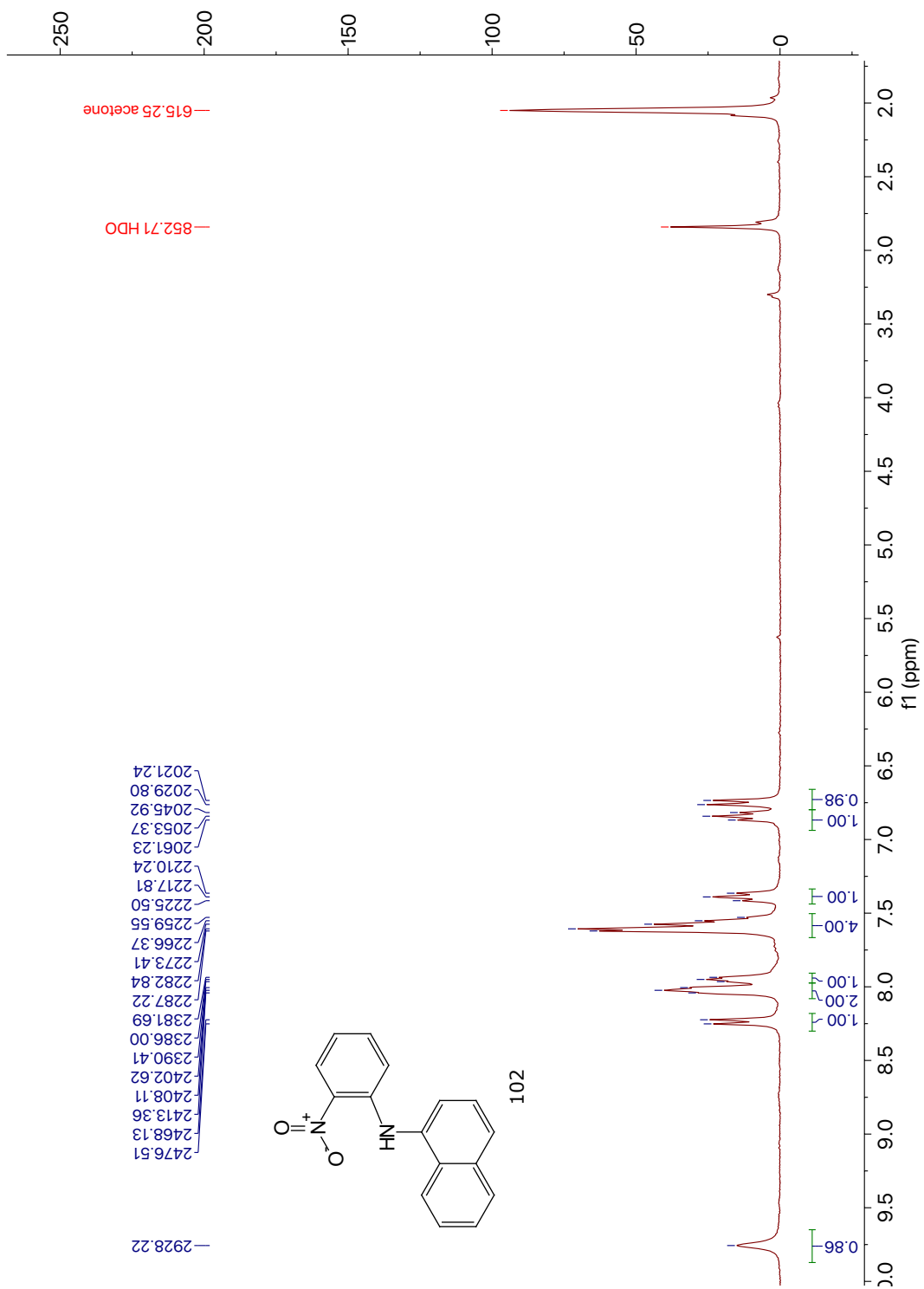


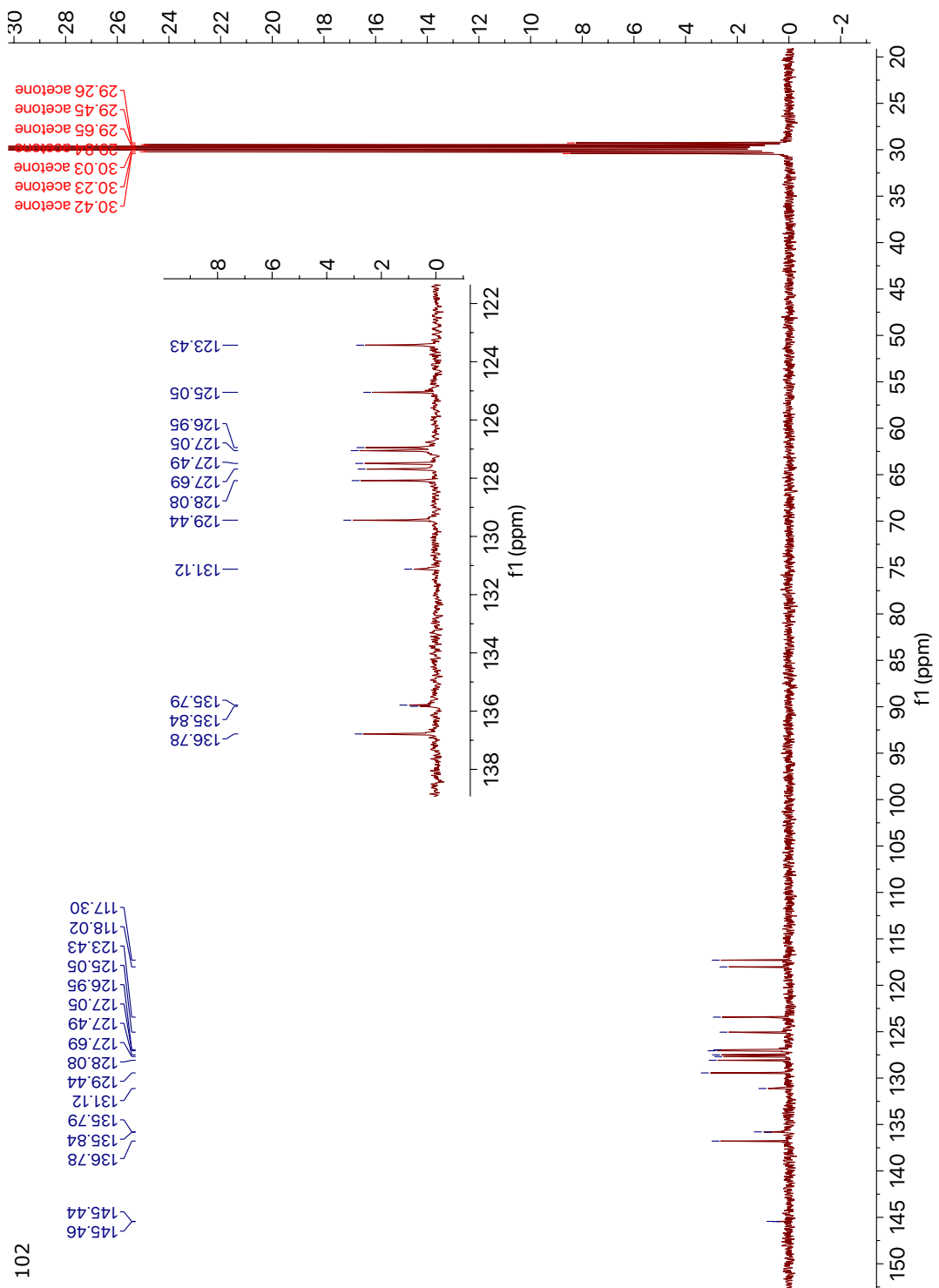




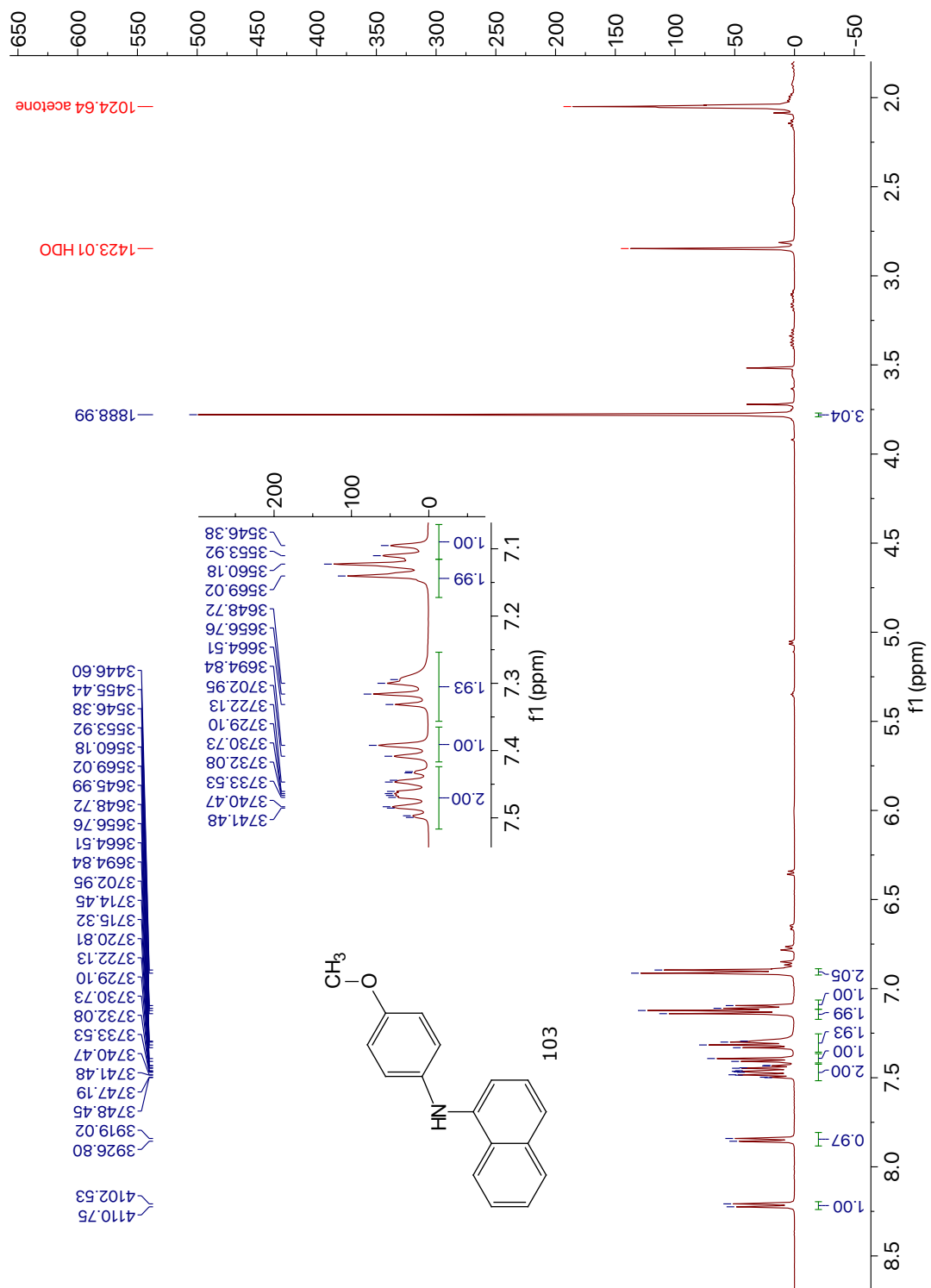


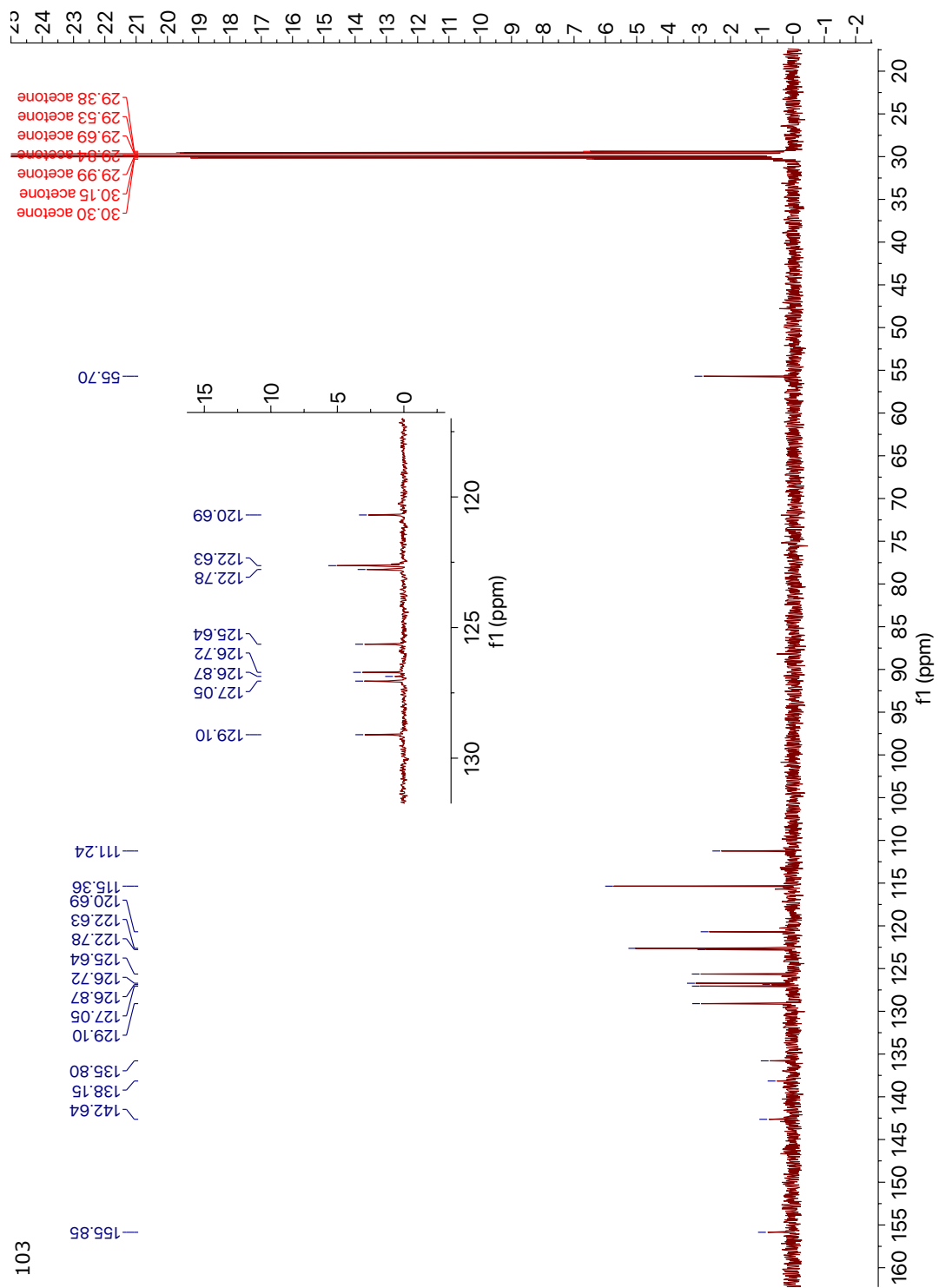
101



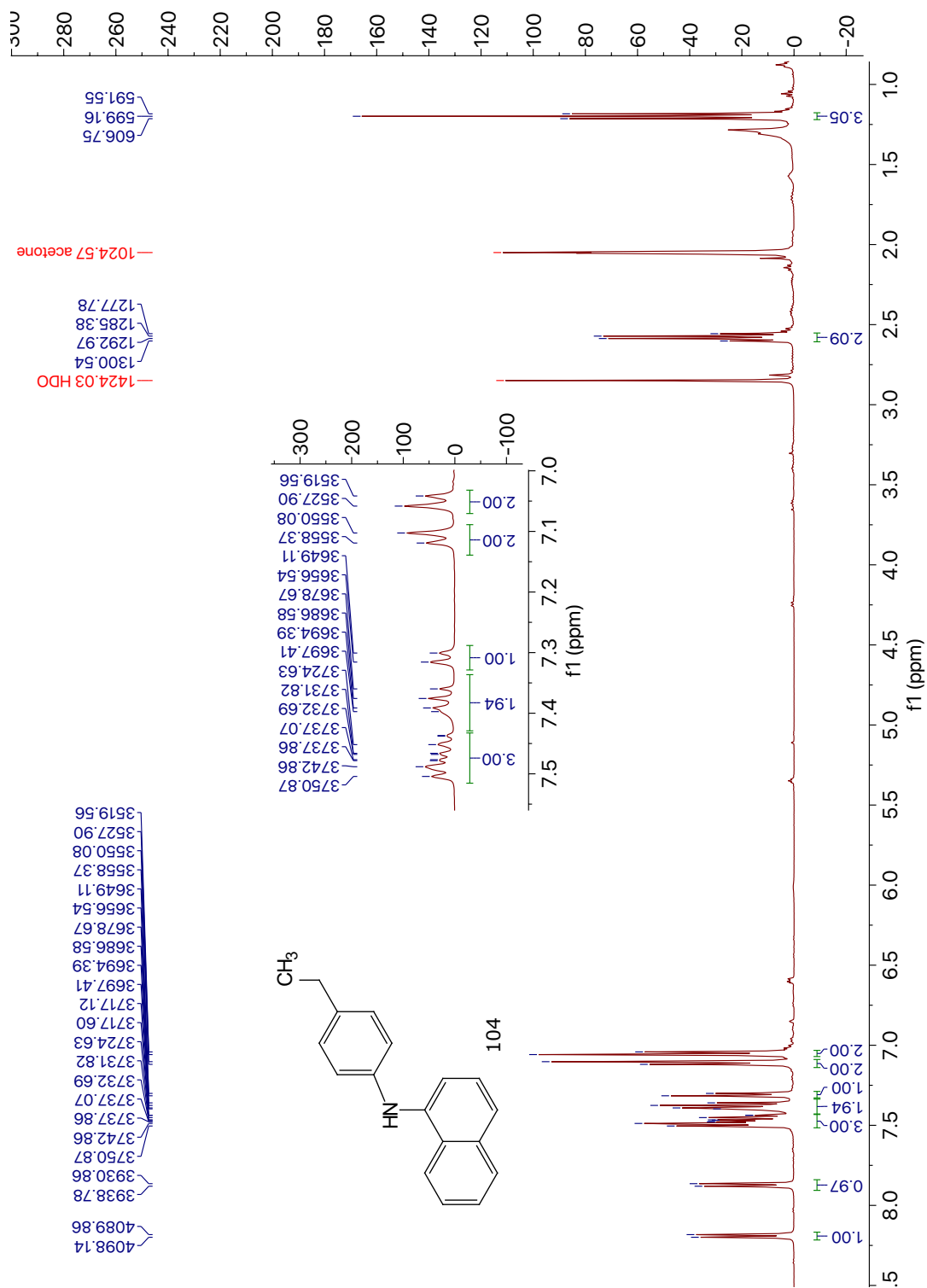


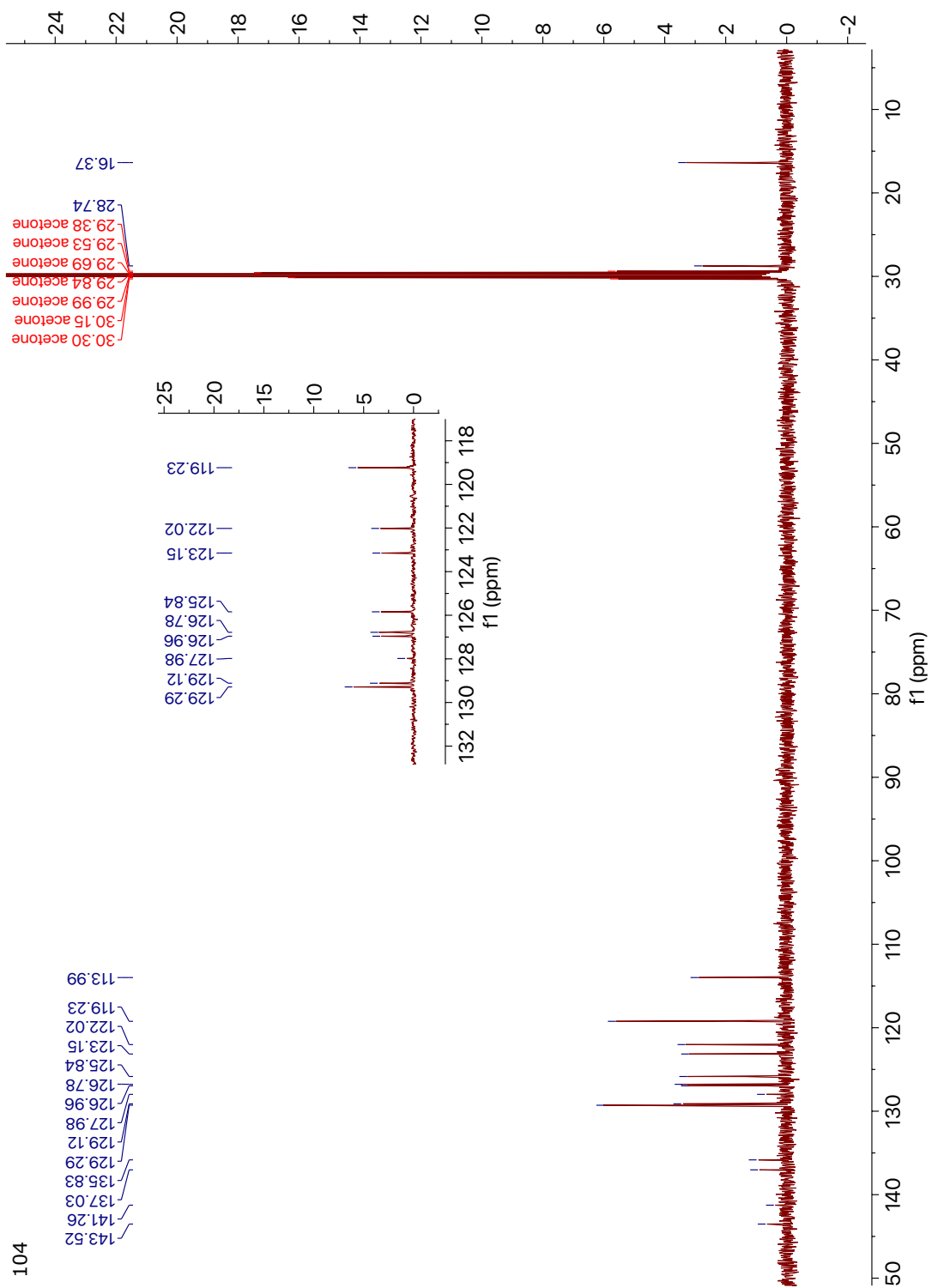
102





103





104